frontiers | Research Topics

Meeting the Triple-H challenge: advanced crop-soil-fertilizer management strategies to maximize crop yield, quality, and nutrient efficiency

Edited by
Laichao Luo and Muhammad Farooq

Published in
Frontiers in Plant Science

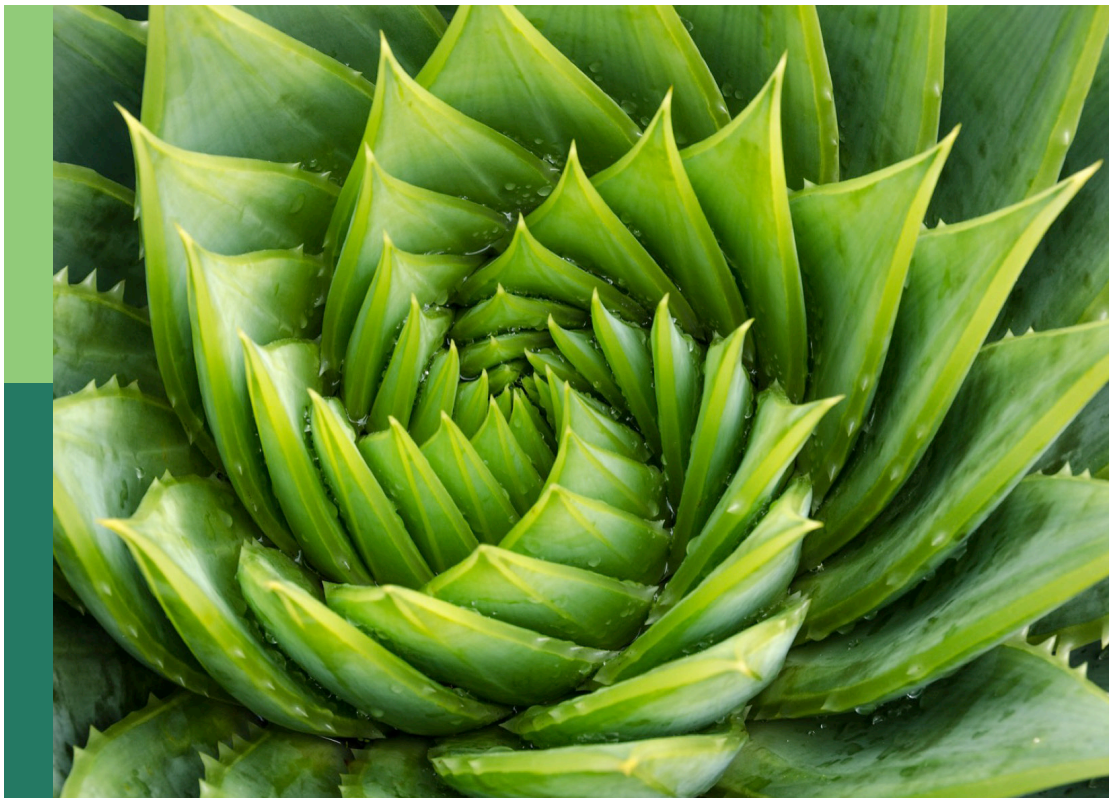

ISSN 1664-8714
ISBN 978-2-8325-6028-0
DOI 10.3389/978-2-8325-6028-0

About Frontiers

Frontiers is more than just an open access publisher of scholarly articles: it is a pioneering approach to the world of academia, radically improving the way scholarly research is managed. The grand vision of Frontiers is a world where all people have an equal opportunity to seek, share and generate knowledge. Frontiers provides immediate and permanent online open access to all its publications, but this alone is not enough to realize our grand goals.

Frontiers journal series

The Frontiers journal series is a multi-tier and interdisciplinary set of open-access, online journals, promising a paradigm shift from the current review, selection and dissemination processes in academic publishing. All Frontiers journals are driven by researchers for researchers; therefore, they constitute a service to the scholarly community. At the same time, the *Frontiers journal series* operates on a revolutionary invention, the tiered publishing system, initially addressing specific communities of scholars, and gradually climbing up to broader public understanding, thus serving the interests of the lay society, too.

Dedication to quality

Each Frontiers article is a landmark of the highest quality, thanks to genuinely collaborative interactions between authors and review editors, who include some of the world's best academicians. Research must be certified by peers before entering a stream of knowledge that may eventually reach the public - and shape society; therefore, Frontiers only applies the most rigorous and unbiased reviews. Frontiers revolutionizes research publishing by freely delivering the most outstanding research, evaluated with no bias from both the academic and social point of view. By applying the most advanced information technologies, Frontiers is catapulting scholarly publishing into a new generation.

What are Frontiers Research Topics?

Frontiers Research Topics are very popular trademarks of the *Frontiers journals series*: they are collections of at least ten articles, all centered on a particular subject. With their unique mix of varied contributions from Original Research to Review Articles, Frontiers Research Topics unify the most influential researchers, the latest key findings and historical advances in a hot research area.

Find out more on how to host your own Frontiers Research Topic or contribute to one as an author by contacting the Frontiers editorial office: frontiersin.org/about/contact

Meeting the Triple-H challenge: advanced crop-soil-fertilizer management strategies to maximize crop yield, quality, and nutrient efficiency

Topic editors

Laichao Luo — Anhui Agricultural University, China

Muhammad Farooq — Sultan Qaboos University, Oman

Citation

Luo, L., Farooq, M., eds. (2025). *Meeting the Triple-H challenge: advanced crop-soil-fertilizer management strategies to maximize crop yield, quality, and nutrient efficiency*. Lausanne: Frontiers Media SA. doi: 10.3389/978-2-8325-6028-0

Table of contents

frontiers | Frontiers in Plant Science

TYPE Review
PUBLISHED 24 October 2023
DOI 10.3389/fpls.2023.1285512

OPEN ACCESS

EDITED BY
Laichao Luo,
Anhui Agricultural University, China

REVIEWED BY
Xiaohui Chen,
Fujian Agriculture and Forestry University, China
Viabhav Kumar Upadhayay,
Dr. Rajendra Prasad Central Agricultural University, India

*CORRESPONDENCE
Panfeng Tu
tupanfeng@163.com

†These authors have contributed equally to this work

RECEIVED 30 August 2023
ACCEPTED 09 October 2023
PUBLISHED 24 October 2023

CITATION
Ahmed N, Zhang B, Bozdar B, Chachar S, Rai M, Li J, Li Y, Hayat F, Chachar Z and Tu P (2023) The power of magnesium: unlocking the potential for increased yield, quality, and stress tolerance of horticultural crops.
Front. Plant Sci. 14:1285512.
doi: 10.3389/fpls.2023.1285512

The power of magnesium: unlocking the potential for increased yield, quality, and stress tolerance of horticultural crops

Nazir Ahmed[1†], Baige Zhang[2†], Bilquees Bozdar[3], Sadaruddin Chachar[1], Mehtab Rai[3], Juan Li[1], Yongquan Li[1], Faisal Hayat[1], Zaid Chachar[4] and Panfeng Tu[1*]

[1]College of Horticulture and Landscape Architecture, Zhongkai University of Agriculture and Engineering, Guangzhou, Guangdong, China, [2]Key Laboratory for New Technology Research of Vegetable, Vegetable Research Institute, Guangdong Academy of Agricultural Science, Guangzhou, China, [3]Department of Crop Physiology, Faculty of Crop Production, Sindh Agriculture University, Tandojam, Pakistan, [4]College of Agriculture and Biology, Zhongkai University of Agriculture and Engineering, Guangzhou, Guangdong, China

Magnesium (Mg^{2+}) is pivotal for the vitality, yield, and quality of horticultural crops. Central to plant physiology, Mg^{2+} powers photosynthesis as an integral component of chlorophyll, bolstering growth and biomass accumulation. Beyond basic growth, it critically affects crop quality factors, from chlorophyll synthesis to taste, texture, and shelf life. However, Mg2 + deficiency can cripple yields and impede plant development. Magnesium Transporters (MGTs) orchestrate Mg^{2+} dynamics, with notable variations observed in horticultural species such as *Cucumis sativus, Citrullus lanatus*, and *Citrus sinensis*. Furthermore, Mg^{2+} is key in fortifying plants against environmental stressors and diseases by reinforcing cell walls and spurring the synthesis of defense substances. A burgeoning area of research is the application of magnesium oxide nanoparticles (MgO-NPs), which, owing to their nanoscale size and high reactivity, optimize nutrient uptake, and enhance plant growth and stress resilience. Concurrently, modern breeding techniques provide insights into Mg^{2+} dynamics to develop crops with improved Mg^{2+} efficiency and resilience to deficiency. Effective Mg^{2+} management through soil tests, balanced fertilization, and pH adjustments holds promise for maximizing crop health, productivity, and sustainability. This review unravels the nuanced intricacies of Mg^{2+} in plant physiology and genetics, and its interplay with external factors, serving as a cornerstone for those keen on harnessing its potential for horticultural excellence.

KEYWORDS

biofortification, Mg^{2+} transporter, photosynthesis, absorption, stress tolerance, plant nutrition, deficiency and toxicity, nanocompoiste

1 Introduction

Magnesium (Mg^{2+}) is not only a quintessential macronutrient but also a cornerstone for the vitality and quality of horticultural crops. Its importance stretches across a broad spectrum of plant physiology, governing photosynthesis, nutrient metabolism, cell membrane stability, enzyme activation, and, notably, its resilience against various environmental stresses (Chen et al., 2018; Tian et al., 2021; Kumari et al., 2022). While its influence on agronomic plants has been meticulously explored in previous research, the depth of knowledge regarding horticultural crops remains comparatively shallow (Crusciol et al., 2019; Qin et al., 2020; Heidari et al., 2021; Sharma et al., 2022). This gap is surprising given the pronounced impact of Mg^{2+} on pivotal horticultural crop attributes, from enhancing flavor to influencing texture and extending shelf life (Zhang H, et al., 2020; Adnan et al., 2021). It is becoming apparent that the intricate interplay of Mg^{2+} with flavor nuances, texture modulation, and postharvest durability in horticultural crops is a fertile ground for exploration. In today's context, where consumers exhibit an escalating appetite for premium-quality produce, unraveling the depth of Mg^{2+}'s role is not just a scientific endeavor but also an economic imperative (Gelli et al., 2015; Adaskaveg and Blanco-Ulate, 2023). Addressing this will not merely align with market aspirations, but will also carve a competitive edge for growers. Moreover, although the qualitative advantages of Mg^{2+} are evident, its quantitative contribution to crop yields cannot be understood. Proper management of Mg^{2+} is not a luxury but a necessity for the economic viability and sustainability of horticultural enterprises (Adnan et al., 2021; He et al., 2022). The tapestry of horticultural crops, with their unique characteristics and demands, presents a compelling case for a more exhaustive examination of the role of Mg^{2+}. By illuminating the myriad ways in which Mg^{2+} shapes the growth, development, and quality of these crops, we can equip growers with a refined toolkit for nutrient management, aligning scientific insight with on-ground farming practices.

2 The critical role of magnesium in horticultural crop physiology and productivity

Magnesium although present in plant tissues at relatively modest concentrations, is an indispensable macronutrient. It plays a multitude of pivotal roles in plant physiology, growth, development, productivity, and resilience to environmental stresses (Tang and Luan, 2020; Hamedeh et al., 2022; Bin et al., 2023). Despite its seemingly small presence, the myriad functions that Mg^{2+} undertakes within plant physiology affirms its critical importance for maintaining plant health and securing high yields. Mg^{2+} plays an indispensable role in plant physiology; from its key role as the central atom in the chlorophyll molecule, crucial for photosynthesis (Tang et al., 2023), to its function as an activator of myriad enzymes. This dual capacity not only underscores its importance in fundamental photosynthetic processes but also highlights its pervasive influence across a broad spectrum of plant metabolic activities, including nutrient uptake, energy transfer, and regulation of cellular processes (Morozova, 2022; Kleczkowski and Igamberdiev, 2023). Moreover, Mg^{2+} plays a significant role in transporting carbohydrates from leaves to other developing tissues (Jiao et al., 2023). In addition to its metabolic role, Mg^{2+} contributes to the maintenance of structural stability in plant cells. It aids in stabilizing cell structures, particularly cell membranes, ribosomes, mitochondria, chloroplasts, and nucleic acids, ensuring both the structural integrity and functional efficiency of plant cells (Rengel et al., 2015; Kleczkowski and Igamberdiev, 2023). Furthermore, an emerging body of research has underscored the importance of Mg^{2+} in bolstering plant resilience against diverse environmental stressors (Rengel et al., 2015; Silva et al., 2017).

2.1 Role in photosynthesis and energy metabolism

Mg^{2+} is a paramount macronutrient that serves as a linchpin for numerous aspects of plant growth, development, and function (Figure 1). Its role in photosynthesis is multifaceted and its presence can significantly influence this process, directly affecting plant productivity (Li et al., 2023b). The efficacy of photosynthetic processes depends heavily on Mg^{2+} availability (Peng et al., 2019). Its interaction with the chlorophyll absorption spectrum aligns with specific light wavelengths (Ma et al., 2023), primarily in red and blue ranges. Within the chlorophyll molecule, Mg^{2+} ions play a vital role in photon capture and the subsequent transfer of energy to the photosynthetic machinery of plants (Igamberdiev and Kleczkowski, 2011; Sun T. et al., 2023). Specifically, within the thylakoid membranes of chloroplasts, Mg^{2+}-containing chlorophyll molecules assemble into photosystems I and II (Rankelytė et al., 2023). These structures orchestrate the light-dependent photosynthetic reactions. When chlorophyll absorbs light energy, Mg^{2+} ions are pivotal in initiating electron transfer and the formation of energy-rich molecules such as adenosine triphosphate (ATP) and nicotinamide adenine dinucleotide phosphate (NADPH) (Tang and Luan, 2017; Kleczkowski and Igamberdiev, 2023). This electron flow is vital for synthesizing ATP and fueling a myriad of cellular processes, including the conversion of carbon dioxide into organic compounds (Figure 2) (Jiao et al., 2023). Furthermore, Mg^{2+}'s significance in photosynthesis permeates dark reactions, most notably in its role with the enzyme RuBisCO (ribulose-1,5-bisphosphate carboxylase/oxygenase), which catalyzes the fixation of carbon dioxide (CO_2) and the subsequent formation of carbohydrates (Douglas-Gallardo et al., 2022). As an essential cofactor, Mg^{2+} empowers RuBisCO activation and optimization, facilitating the transformation of CO_2 into organic molecules (Douglas-Gallardo et al., 2022). Conclusively, Mg^{2+} central position within the chlorophyll molecule is indispensable for light energy absorption and the onset of photosynthesis (Tang et al., 2023). Through electron transfer, ATP synthesis, CO_2 fixation, and carbohydrate synthesis, Mg^{2+} acts as an underlying catalyst, nurturing plant growth, development, and productivity. Its strategic and multifunctional roles underscore its importance, reinforcing the necessity of recognizing and harnessing its potential within horticulture.

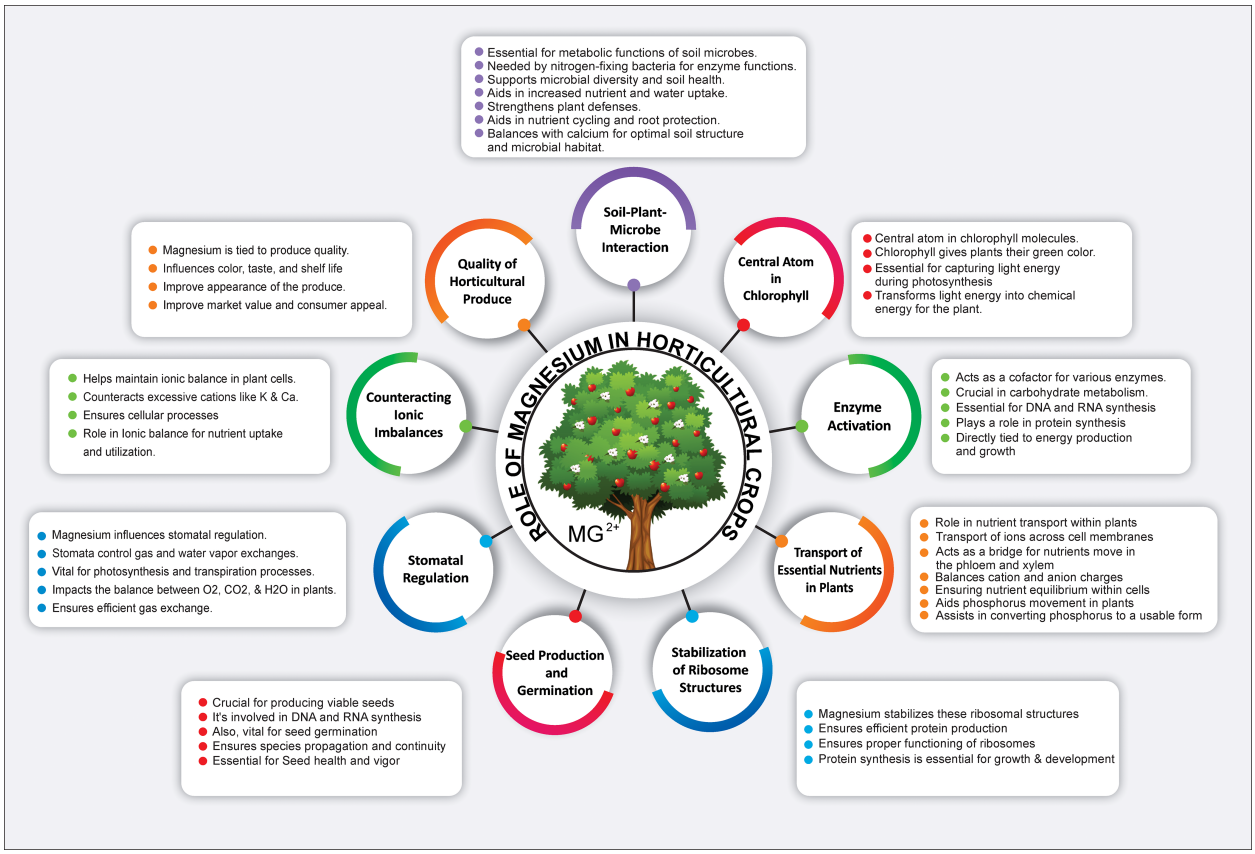

FIGURE 1
Role of magnesium in plant physiology: Central atom in chlorophyll, Enzymatic cofactor, Nutrient transporter, Ribosomal stabilizer, Seed production enhancer, Stomatal regulator, Ionic balance maintainer, and Influencer of horticultural quality and soil-microbe interactions.

Mg^{2+} serves as a multifunctional catalyst in plant physiology, playing a critical role in various aspects of enzyme activation and metabolism (Figure 1). Its function as a cofactor in numerous enzymatic reactions emphasizes its significance in the synthesis and metabolism of carbohydrates, proteins, and nucleic acids (Farhat et al., 2016; Douglas-Gallardo et al., 2022; Tang et al., 2022a). The influence of Mg^{2+} extends to essential processes such as protein synthesis, cell division, and DNA replication, reflecting its pervasive impact on plant metabolism (Gerendás and Führs, 2013; Wang et al., 2020; Zhang B, et al., 2020). Specifically, Mg^{2+} is fundamental in activating key enzymes such as pyruvate kinase, which catalyzes the conversion of phosphoenolpyruvate (PEP) to pyruvate during glycolysis (Schormann et al., 2019). Moreover, Mg^{2+} affects the activity of enzymes in the tricarboxylic acid (TCA) cycle, such as isocitrate dehydrogenase and α-ketoglutarate dehydrogenase (Yang et al., 2013; Jin et al., 2023), which are both crucial for energy production and the synthesis of metabolic intermediates. Moreover, Mg^{2+} is indispensable for protein synthesis in plants as it contributes to the structure and function of ribosomes (Figure 2). By interacting with ribosomal subunits, Mg^{2+} adds stability and aids in binding messenger RNA (mRNA) and transfer RNA (tRNA), ensuring the accurate translation of genetic information into functional proteins (Yu et al., 2023). In terms of nucleic acid metabolism, Mg^{2+} is actively involved in DNA replication and repair. It influences the function of enzymes, such as DNA polymerase and DNA ligase (Adhikari et al., 2006; Romani, 2011), as well as RNA synthesis and processing, affecting the activity of RNA polymerases and ribonucleases in transcription and RNA maturation (Yu et al., 2023).

Furthermore, Mg^{2+} plays a role in phosphate transport and metabolism by activating ATPases and phosphatases (Cakmak and Yazici, 2010). This helps to regulate the transition of phosphate ions across membranes and the conversion of organic phosphates into accessible inorganic forms for cellular use. In energy metabolism, Mg^{2+} is involved in the synthesis and utilization of adenosine triphosphate (ATP). Acting as a cofactor for ATP synthase, ATP synthesis is observed during oxidative phosphorylation in mitochondria (Cakmak and Kirkby, 2008; Igamberdiev and Kleczkowski, 2011). Additionally, Mg^{2+} affects the activity of enzymes that break down ATP, such as ATPases, thereby releasing energy for various cellular functions (Ma et al., 2023). Mg^{2+} serves as an essential cofactor in plant enzymatic reactions and plays a pivotal role in various metabolic pathways, which in turn influences plant physiology, growth, and overall development.

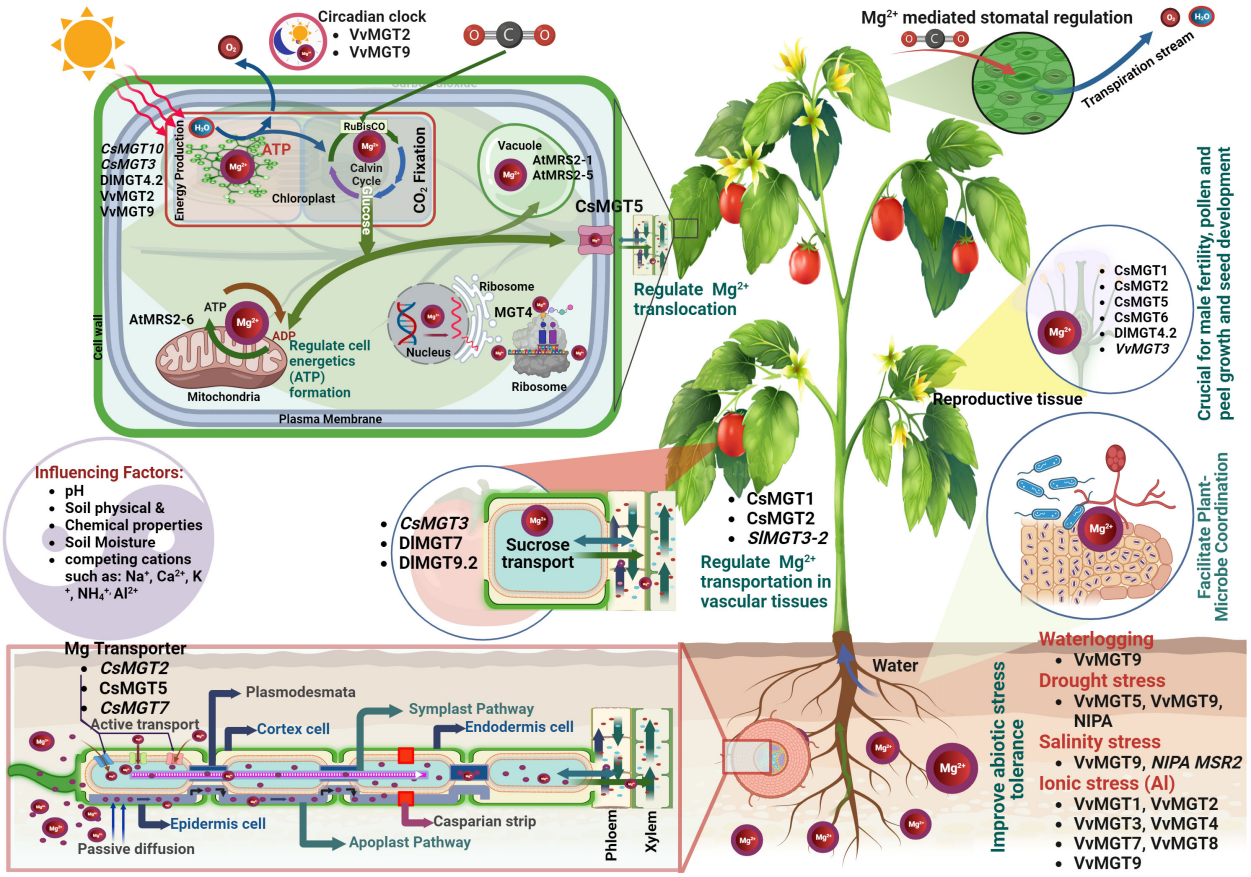

FIGURE 2
Roles of Mg^{2+} and Magnesium Transporters (MGTs) in plants: (Upon entry into the root stele, Mg^{2+} ions are shuttled into xylem vessels by transport proteins, aiding their distribution to the aerial parts. Mg^{2+} is central to photosynthesis because of its position in the chlorophyll. It catalyses ATP synthesis, CO2 fixation, and carbohydrate production, thereby fostering plant growth. Inside the cells, Mg^{2+} supports protein synthesis, DNA replication, and ATP utilization. These ions are essential for chlorophyll synthesis, enzyme activation and nucleic acid production. MGTs are also vital for Mg^{2+} absorption, transport, and utilization in reproductive organs, influencing pollen development, fruit quality, and stress tolerance).

2.2 Protein synthesis

Mg^{2+} serves as a cornerstone in the intricate process of protein synthesis, which is a critical aspect of plant growth and development. Their involvement spans several stages of protein formation, all of which collectively contribute to the synthesis of functional proteins (Petrov et al., 2012). Mg^{2+} is integral to the structural formation and function of ribosomes, which are the cell organelles responsible for protein synthesis. Mg^{2+} aids in the stability of ribosomal subunits and promotes the binding of messenger RNA (mRNA) and transfer RNA (tRNA), thereby ensuring accurate translation of genetic information into proteins (Petrov et al., 2012; Verbruggen and Hermans, 2013; Yu et al., 2023). Furthermore, Mg^{2+} influences gene expression by modulating multiple phases of transcription and RNA processing. It activates and regulates enzymes and proteins essential for DNA replication, transcription, and RNA maturation, such as DNA and RNA polymerases (Adhikari et al., 2006; Andreadelli et al., 2021; El-Sharkawy et al., 2022). By interacting with various enzymes involved in DNA repair, Mg^{2+} enhances their activity and ensures the effective transcription of genetic information. Mg^{2+} also contributes to the stability and integrity of RNA by preventing its degradation by ribonucleases (RNases). Its involvement in pre-mRNA splicing is vital for the formation of mature and functional mRNA molecules (Adhikari et al., 2006). This precise splicing process, facilitated by Mg^{2+}, ensures the proper removal of introns and retention of exons, leading to the synthesis of functional proteins (Johansson and Jacobson, 2010). The influence of Mg^{2+} extends to the compaction and packaging of DNA, where it plays a role in shaping the structure and organization of chromatin (Hartwig, 2001). Mg^{2+} interacts with histone proteins that bind to DNA, thereby facilitating the formation of nucleosomes and higher-order chromatin structures (Ohyama, 2019). These interactions help maintain chromatin stability and integrity, influencing gene accessibility and the regulation of transcription and translation. Mg^{2+} is essential for protein synthesis, weaving its way through various processes to ensure the accurate and effective production of proteins. From influencing ribosome structure to regulating gene expression and RNA splicing, the role of Mg^{2+} is multifaceted and crucial. It even extends to the structural components of DNA, maintaining its stability and integrity.

2.3 Magnesium in the transport of essential nutrients in plants

Mg^{2+} plays a pivotal role in the uptake and transport of vital nutrients within plants, ensuring proper growth, development, and metabolic function. This multifaceted role can be understood by exploring its influence on various nutrient transport systems. Mg^{2+} is pivotal in the regulation of phosphorus uptake and transport by modulating the activity of P transporters and channels. Mg^{2+} ensures the efficient movement of phosphate ions from the soil into plant roots, thus maintaining optimal intracellular P levels (Verbruggen and Hermans, 2013; Assunção et al., 2022). Mg^{2+} also plays a vital role in the regulation of K + transporters and channels, orchestrating the proper movement of K^+ ions across cell membranes (Hermans et al., 2013). A deficiency in Mg^{2+} can disrupt K^+ uptake, leading to an imbalance that affects physiological processes, such as osmoregulation, enzymatic activity, and stomatal function (Verbruggen and Hermans, 2013). Similarly, Mg^{2+} is involved in the regulation of Ca^{2+} transporters and channels, thereby controlling the influx of Ca^{2+} across membranes (Cakmak and Yazici, 2010). Imbalances in Ca^{2+}, often stemming from Mg^{2+} deficiency, can affect essential functions, such as cell division, cell wall synthesis, and signal transduction. Moreover, Mg^{2+} has broad effects on the uptake and distribution of other essential nutrients including nitrogen (N), iron (Fe^{2+}), and zinc (Zn^{2+}). The interactions of Mg^{2+} with other nutrients are summarized in Table 1. Deficiencies in Mg^{2+} can lead to inadequate uptake and utilization of Fe^{2+} and Zn^{2+}, resulting in micronutrient imbalances that can hinder plant growth and development (Cakmak and Yazici, 2010). Mg^{2+} establishes a delicate balance within the plant by interacting with and regulating various nutrient transport systems. This balance ensures proper nutrient distribution and supports various physiological processes (Cakmak and Yazici, 2010; Ye et al., 2019). Delving deeper into the intricate relationship between Mg^{2+} and nutrient transport, as explored in studies like those by Assunção et al. (2022), unveils promising avenues to bolster plant health and productivity. Tailoring fertilization strategies to include optimal levels of Mg^{2+} could mitigate nutrient deficiencies and enhance overall crop yields.

2.4 Magnesium in maintaining cellular functions

Mg^{2+} is a critical element that permeates various cellular functions within plants, acts as a catalyst in enzymatic reactions, stabilizes cell membranes, and contributes to ion homeostasis (Farhat et al., 2016; Tian et al., 2022). Its diverse roles are essential for the optimal growth, development, and productivity of horticultural crops (Andreadelli et al., 2021). Recognizing the paramount importance of Mg^{2+} in plants, the following sections will delve into the multifaceted roles of Mg^{2+}, exploring how it orchestrates and supports essential cellular functions, from energy metabolism to structural stability and resilience.

In plants, Mg^{2+} plays an important role in maintaining cell membrane stability and in regulating ion homeostasis. Their presence influences the structure and function of cell membranes, thereby ensuring proper cellular processes and overall plant health (Li et al., 2023b). Mg^{2+} interacts with phospholipids, which are the main components of cell membranes, helping to maintain their fluidity and stability (Cakmak and Yazici, 2010; Li et al., 2023b). Mg^{2+} also plays a crucial role in preventing the destruction of lipid bilayers and maintaining the structural integrity of cell membranes under various environmental conditions (Kobayashi and Tanoi, 2015). It interacts with ion channels, modulates their activity, and controls the movement of ions, including potassium (K^+), calcium (Ca^{2+}), and other cations, across membranes (Hermans et al., 2013; Verma et al., 2021). Hence, it helps regulate the balance of important ions such as K^+, Ca^{2+}, and Na^+ (Verma et al., 2021). Mg^{2+} ions interact with ion transporters and pumps, influencing the movement and distribution of ions across cell membranes, which is crucial for physiological processes, such as nutrient uptake, osmoregulation, and cellular signaling (Yang et al., 2012; Hermans et al., 2013; Ye et al., 2019). Mg^{2+} also contributes to the regulation of the cytoplasmic pH in plants. It influences the activity of proton pumps and ion channels involved in pH regulation, maintains an optimal pH environment within plant cells, and is essential for the proper functioning of enzymes and metabolic processes (Bose et al., 2011). The stability of the cell membrane is pivotal in protecting cells from various environmental stresses, such as drought, heat, cold, photooxidative damage,

TABLE 1 Interactions of magnesium with other nutrients in horticultural cropping systems.

Nutrient	Type of interaction	Effects on crops	Strategies to address nutrient imbalances	References
Calcium	Antagonistic	Lower magnesium intake	Adjust calcium-magnesium ratio	(Tang and Luan, 2017)
Phosphorus	Positive/Competitive	Lower availability of magnesium	Optimisation of phosphorus application rates	(Marschner, 2011)
Potassium	Synergistic	Improved magnesium absorption	Maintain balanced K to Mg^{2+} ratio	(Xie et al., 2021)
Nitrogen	Interaction/ Competition	Altered magnesium distribution	Adjust nitrogen-magnesium ratio	(Fageria and Oliveira, 2014; Peng et al., 2020; Potarzycki et al., 2022)
Zinc	Interaction/ Competition	Impaired magnesium absorption	Optimise the zinc output quantities	(Sadeghi et al., 2021)
Iron	Interaction/ Competition	Lower magnesium intake	Optimise the application of iron	(Sadeghi et al., 2021)

salinity, and heavy metal stress (Cakmak and Kirkby, 2008; Rengel et al., 2015; Silva et al., 2017; Adnan et al., 2021; Hamedeh et al., 2022; Li et al., 2023b). The role of Mg^{2+} in maintaining membrane stability helps preserve the viability and functionality of cells under adverse conditions (Rehman et al., 2018).

Mg^{2+} interacts with various negatively charged molecules, such as nucleotides and chlorophyll, thereby stabilizing their structure (Tang and Luan, 2017; Tränkner et al., 2018). This stabilization helps in maintaining the electrochemical gradient across cell membranes, which is essential for cellular activities (Bose et al., 2011). Mg^{2+} participates in controlling the activity of ionic channels in many tissues. Its mechanism of action relies on direct interaction with the channel, indirect modification of channel function through other proteins (e.g., enzymes or G proteins), or via membrane surface charges and phospholipids (Marschner, 2011). It also acts as a cofactor for several transport proteins and channels responsible for the movement of ions across membranes (Allen, 2013; Chen and Ma, 2013). It regulates the activity of these channels, thereby controlling the passage of vital ions such as K^+ and Ca^{2+}, which are crucial in various cellular signaling pathways (Hermans et al., 2013; Tang and Luan, 2017; Ge H. et al., 2022). A deficiency or imbalance in Mg^{2+} affects ion homeostasis, leading to dysfunctions in various cellular processes. The symptoms include poor plant growth, chlorosis, and increased susceptibility to stress (Yang et al., 2013; Peng et al., 2019; Ye et al., 2019). Continued research in this area can provide insights into maximizing crop yield and quality through proper Mg management (Yang et al., 2012; He et al., 2022). Therefore, Mg^{2+} is pivotal in regulating plant cellular ion balance, influencing overall health and development. Its connection with ion homeostasis provides insights into plant nutrition and potential agricultural advancements.

2.5 Role of magnesium in soil-plant-microbe interaction

The role of Mg^{2+} in soil-plant-microbe interactions is multifaceted and essential for sustainable horticultural crop production. Adequate Mg^{2+} levels in the soil promote the growth of beneficial microorganisms, improve nutrient availability, and enhance the overall health and resilience of horticultural crops (Yang et al., 2021; Nikolaou et al., 2023; Yang et al., 2023). Mg^{2+} availability in the soil not only affects plant growth and development but also has profound implications for the composition and activity of soil microbial communities. Mg^{2+} availability in the soil can modulate the abundance and diversity of soil microbial communities (Yang et al., 2023). Studies have shown that sufficient Mg^{2+} levels promote the growth of beneficial microorganisms such as mycorrhizal fungi (Hou et al., 2021; Yang et al., 2023). These mycorrhizal associations form symbiotic relationships with plant roots, facilitating nutrient uptake and promoting plant growth and stress tolerance (Qin et al., 2020; Liu et al., 2023). Mg^{2+} availability in the rhizosphere can also influence soil pH, nutrient solubility, and availability to plants. Adequate Mg^{2+} levels help to maintain optimal rhizosphere pH and enhance nutrient availability for plant uptake (Wang et al., 2020). It also influences the activity of plant growth-promoting rhizobacteria (PGPR) (Nikolaou et al., 2023). These beneficial bacteria colonize the rhizosphere and promote plant growth by facilitating nutrient acquisition, disease resistance, and stress tolerance (Kumar et al., 2021; Tahiri et al., 2022). Research has shown that Mg^{2+} availability can modulate the production of certain plant growth-promoting substances by PGPR, leading to beneficial effects on horticultural crop growth and yield (Yang et al., 2021; Tahiri et al., 2022; Yang et al., 2023). Mg^{2+} also plays a role in nutrient cycling within the soil, affecting the decomposition of organic matter, mineralization of nutrients, and nutrient availability to plants. Proper Mg^{2+} management helps to maintain soil fertility and nutrient balance, ensuring that essential nutrients are readily available for plant uptake (Ye et al., 2019; Nikolaou et al., 2023). Understanding these intricate interactions between Mg, soil, plants, and microbes can guide effective Mg^{2+} management practices, ultimately leading to optimized crop productivity and improved agricultural sustainability.

2.6 Magnesium in reproductive development

Magnesium, an essential macronutrient, plays a significant role in the reproductive development of plants, directly affecting yield quality and quantity. The role of Mg^{2+} has been underscored in numerous studies, particularly during the flowering and fruit development phases. These studies illustrate that Mg^{2+} deficiency can lead to suboptimal fruit and seed sets, thereby contributing to a significant reduction in crop yields (Gransee and Führs, 2013; Setiawati et al., 2020; Wang et al., 2020; Zhang H. et al., 2020). A crucial aspect of plant reproduction is the development of pollen, the primary vehicle for fertilization in plants. A recent study demonstrated that an insufficient Mg^{2+} supply adversely affects pollen development, thereby decreasing overall plant fertility (Xu X.F. et al., 2021). Consequently, poor fruit set is observed, which directly affects crop yield by reducing the number of fruits produced (Ceylan et al., 2016; Kanjana, 2020; Zhang et al., 2020; Zhang S. et al., 2021). Mg^{2+} deficiency can impede seed formation and maturation, resulting in fewer and poor-quality seeds (Ceylan et al., 2016; Kanjana, 2020). Such subpar seed formation contributes to yield reduction and can compromise the viability of future plant generations (Zhang et al., 2020). Importantly, the role of Mg^{2+} extends beyond immediate crop yield. Research suggests that Mg^{2+} deficiency can also lead to a long-term decline in plant fertility, thereby affecting the plant's yield potential in successive growing seasons (Tang and Luan, 2017; Zhang B, et al., 2020). Furthermore, Mg^{2+} plays a pivotal role in both chlorophyll synthesis and photosynthesis, which directly influence plant growth and reproduction (Shaul, 2002; Hamedeh et al., 2022). An inadequate Mg^{2+} supply can impede these processes, thus indirectly affecting plant fertility and yield. Understanding the vital role of Mg^{2+} in plant reproductive development provides insights into maximizing crop yield and quality. Careful management of Mg^{2+} can enhance fertility and fruit and seed development, thereby supporting the sustainable growth of horticultural crops.

3 Impact of magnesium on crop development

3.1 Effects of magnesium on crop quality

Magnesium is an essential macronutrient vital for various physiological processes in plants, including growth, development, reproduction, and quality enhancement (Xu J. et al., 2021; Li et al., 2023c; Tian et al., 2023b). Its importance extends to influencing the taste, texture, shelf life, and nutritional content of fruits and vegetables, thereby driving consumer preferences and market value (Petrescu et al., 2020; Yousaf et al., 2021; Zhang S. et al., 2021; Mullins and Wolt, 2022). In recent years, extensive research has illuminated the complex roles of Mg^{2+}, contributing to a nuanced understanding of its effects on horticultural products (Bashir et al., 2019; Zhang H, et al., 2020; Quddus et al., 2022). This study synthesizes these findings and offers a comprehensive examination of the multifaceted effects of Mg^{2+}. Mg^{2+} has a profound effect on the taste and aroma of horticultural crops. Liu et al. (2022) demonstrated a positive correlation between Mg^{2+} content and sugar accumulation in navel oranges, substantiating the role of Mg^{2+} in sugar synthesis. Furthermore, Li et al. (2021) investigated *Camellia sinensis* and revealed that adequate Mg^{2+} levels enhance the production of volatile compounds, thus improving the quality constituents of Hydroponic-Cultivated Tea. In a study on oolong tea gardens, He et al. (2023) found that application of Mg^{2+} fertilizer significantly enhanced tea yield, improved tea quality, and boosted nitrogen use efficiency. In addition, Du et al. (2021) investigated the impact of Mg^{2+} stress on lemon varieties with a special focus on taste and aroma. Under Mg^{2+} stress, all varieties showed a decline in Mg^{2+} content, particularly in leaves, roots, fruits, and stems. Although the external appearance of the fruit remained largely unaffected, there were discernible reductions in juice yield, total soluble solids, total acid, and vitamin C content. Such changes, intimately tied to the lemon's taste and aroma, are correlated with the fruit's Mg^{2+} levels. Additionally, the taste profile was further influenced by an increase in nutrients, such as K, Ca, and Mn. These findings underscore the essential role of Mg^{2+} in preserving the taste and aroma characteristics of lemons. Texture is a significant determinant of crop quality, and Mg^{2+} plays an indispensable role in shaping it. Quddus et al. (2022) conducted research on tomato and found that Mg^{2+}-supplemented fruits retained firmness for a more extended period, indicating Mg^{2+}'s influence on cell wall composition. Preciado-Mongui et al. (2023) delved into lettuce and observed that Mg^{2+} levels enhanced the crispness and appeal, thereby boosting market value. A related study by Zheng and Moreira (2020) demonstrated Mg^{2+} ion impregnation in potato slices to improve cell integrity, reduce oil absorption during frying, and increase crispness. Extensive research underscores the multifaceted benefits of Mg^{2+} fertilizers in agriculture. Tan et al. (2000) highlighted its positive effects on a range of crops. Building on this foundation, recent studies have delved deeper into specific advantages. For instance, Djabou et al. (2018) found that Mg^{2+} delayed post-harvest deterioration in cassava. Similarly, kenaf plants exhibited enhanced growth when exposed to Mg^{2+}, as documented by Salih et al. (2023). Watermelon genetics were also affected, with a distinct gene expression pattern in response to Mg^{2+}, according to Heidari et al. (2022). Morales-Payan (2022) pinpointed optimal pineapple yields when magnesium sulfate was employed as the Mg^{2+} source. Zhang et al. (2022) identified variations in Soybean and Pomelo yields depending on the type of Mg^{2+} fertilizer used. The importance of Mg^{2+} is further emphasized by Mengutay et al. (2013), who reported that a deficiency in maize plants increased their susceptibility to heat stress. Moreira et al. (2015) established that a higher concentration of Mg^{2+} results in reduced disease severity and improved photosynthesis. Rajitha et al. (2019) documented Mg^{2+} positive influence on groundnuts, while Tan et al. (2000) acknowledged its role in optimizing the yields of sweet potatoes, sugarcane, and various vegetables.

The effects of Mg^{2+} go beyond immediate sensory qualities, extending the postharvest shelf life and quality. Aghofack and Yambou (2006) reported that Ca^{2+} and Mg^{2+} may play a role in stabilizing cell membranes, maintaining cell wall firmness, and inhibiting chlorophyll-degrading enzymes in climacteric banana fruits and non-climacteric pineapple fruits, as well as in inhibiting respiration and the breakdown of membrane lipids in climacteric banana fruits. Kumar et al. (2020) demonstrated that passive modified atmosphere packaging (PMAP) using a pectin-based bionanocomposite film reinforced with Mg^{2+} hydroxide nanoparticles effectively preserved the quality of cherry tomatoes at low temperatures (10°C), prolonging shelf life up to 24 days, offering a sustainable, biodegradable alternative to traditional synthetic packaging materials like low density polyethylene and polypropylene. A study by Aghofack-Nguemezi et al. (2014) demonstrated that the use of calcium- and magnesium-based fertilizers significantly reduced the incidence and severity of fungal diseases in tomato plants, promoted growth and yield, and extended the shelf life of fruits in the three most cultivated varieties of tomatoes in the Western Highlands of Cameroon. Mg^{2+} has consistently emerged as a pivotal element in determining nutrient content across a diverse range of crops, signifying its vital role in agricultural practices. Ye et al. (2019) highlighted this in their research on *Citrus sinensis* seedlings, where it was discovered that Mg^{2+} application considerably augmented the nutrient content of the leaf blades. Specifically, while Mg2 + deficiency resulted in a decrease in the concentrations of N, P, and Mg^{2+}, it influenced the levels of other nutrients such as K, Ca, Mn, Fe, Cu, and Zn in different ways depending on the leaf's position and age. This emphasizes the complex yet crucial interplay between Mg^{2+} and other nutrients in plant growth. Highlighting the broad influence of Mg^{2+}, Nikolaou et al. (2023) reported that organic fertilization rich in Ca^{2+} and Mg^{2+} significantly boosted the plant's bioactive compounds, notably acemannan and total phenolic content in Aloe vera. This not only underscores the role of Mg^{2+} in nutrient enhancement but also hints at its potential influence on the therapeutic properties of medicinal plants. Yousaf et al. (2021) broadened this perspective with their work on radishes, demonstrating that specific nitrogen and Mg^{2+} treatments distinctly impacted soluble protein, sugar, and ascorbic acid contents. This further supports the idea that the role of Mg^{2+} in

nutrient enhancement is not limited to fruits or medicinal plants but extends across the vegetable spectrum. In a recent study on tomatoes, Quddus et al. (2022) highlighted the significance of precise application of Mg^{2+}. A dose of 12 kg·ha^{-1} Mg^{2+} yielded not only the most abundant tomatoes but also tomatoes of superior nutritional quality, enriched with vitamin C, β-carotene, and protein. Collectively, these studies underscore Mg^{2+} pivotal role in enriching the nutrient profile of various crops, ranging from fruits to vegetables and medicinal plants, highlighting its significant impact on agriculture.

3.2 Magnesium and crop yield

Mg^{2+} is a fundamental macronutrient pivotal to various physiological and metabolic processes in horticultural crops, profoundly influencing the yield and quality of fruits, vegetables, and root crops. For instance, Tian et al. (2023b) revealed that Mg^{2+} supplementation in 'Red Fuji' apple trees bolstered nitrogen utilization, enhanced photosynthesis, and encouraged anthocyanin biosynthesis, thereby elevating fruit size, weight, and yield. Quddus et al. (2022) demonstrated that tomatoes benefited substantially from Mg^{2+} application. Specifically, 12 kg·ha^{-1} of Mg^{2+} notably improved photosynthetic efficiency, carbohydrate translocation, and overall yield, resulting in heavier, more nutritious fruits. Similarly, El-Sharkawy et al. (2022) found that spraying grapevines with 3% magnesium carbonate ($MgCO_3$) amplified crop yield by 20% and enhanced berry biochemical properties, suggesting its role in strengthening plant defense mechanisms and optimizing grape growth and yield. Root crops such as potatoes also benefit from Mg^{2+} supplementation. A two-season study by El-Metwaly and Mansour (2019) showed that using $MgSO_4$ combined with calcium chloride foliar application optimized growth characteristics, leading to significant improvements in tuber yield, dry matter, and starch content. The combined treatment resulted in yield spikes of approximately 42%. Leafy vegetables such as spinach and lettuce are also responsive to Mg^{2+}. Jamali Jaghdani et al. (2021) found that Mg^{2+} deficiency in spinach reduces CO_2 assimilation. Preciado-Mongui et al. (2023) highlighted an ideal fertilization combo for lettuce, optimizing yield while emphasizing the significance of balanced nutrient application. Zhang et al. (2022) further emphasized that slow-release Mg^{2+} fertilizers, predominantly MgO, outperform their fast-release counterparts in boosting soybean and pomelo yields in acidic soils. In studies on peppers and cucumbers, researchers observed that while Mg^{2+} supplementation significantly improved yields, its influence on nutrient composition and interactions with factors like irrigation and nitrogen was equally critical. A study by Li et al. (2023a) on cucumbers pinpointed the optimal fertilization combination, leveraging factors like yield, quality, and efficiency. Researchers have also explored the complex interplay between Mg^{2+} and other nutrients in horticultural crops. Findings by Li et al. (2023b), El-Metwaly and Mansour (2019) underscore the intricate relationship between these nutrients, highlighting the importance of a comprehensive nutrient-management strategy. Finally, reinforcing the necessity of Mg^{2+}, Chen et al. (2023) discovered that while China's soils are replete with N, P, and K, there is a glaring deficiency of Mg^{2+} in 73% of them, prompting the recommendation to curtail NPK usage and elevate Mg^{2+} supplementation to further sustainable agriculture. The interrelationship between Mg^{2+} and other nutrients underscores the importance of a holistic nutrient management strategy.

3.3 Magnesium and abiotic stress tolerance

Many environmental and intracellular factors affect Mg^{2+} homeostasis in plants, including Mg^{2+} deficiency and toxicity, high temperature, drought, high light irradiance, low or high pH, and antagonistic ions (Guo, 2017; Tariq Aftab, 2020). However, recent research has highlighted another critical aspect of Mg^{2+}; its role in bolstering the resilience of horticultural crops to various abiotic stresses such as drought, heat, cold, high irradiance, salinity, and heavy metal toxicity (Boaretto et al., 2020; Jamali Jaghdani et al., 2021; Li et al., 2023b). Understanding the influence of Mg^{2+} on stress tolerance in horticultural crops provides key insights for the development of effective agricultural practices and supports sustainable horticulture in the face of a changing climate (Hamedeh et al., 2022; Li et al., 2023b). Drought is a significant abiotic stress factor that affects the growth and yield of horticultural crops. In a study by Hamedeh et al. (2022) The biostimulant EnNuVi® ALPAN®, rich in magnesium, was found to enhance drought tolerance in tomato plants by modulating molecular pathways associated with carbohydrate metabolism, stomatal regulation, and cellular homeostasis. This Mg^{2+}-rich formulation mitigated the adverse effects of drought by preserving the photosynthetic pigment levels and reducing cellular oxidative damage. Heat stress is another principal concern in horticultural crop production, particularly given ongoing global warming. Recent studies on lemon trees and tea have demonstrated the beneficial effects of Mg^{2+} in mitigating the adverse impacts of heat stress (Du et al., 2021; Zhang Q. et al., 2021). In a study by Boaretto et al. (2020), young lemon trees supplemented with extra Mg^{2+} and/or nitrogen (N) displayed increased resilience to elevated irradiance and air temperature commonly associated with heatwaves. The trees maintained optimal photosynthetic and transpiration rates and Mg^{2+} enhanced the activity of the antioxidant enzyme system, thereby decreasing oxidative stress. Similarly, Silva et al. (2017) highlighted the importance of Mg^{2+} nutrition in mitigating the adverse effects of heat stress in coffee seedlings. Adequate Mg^{2+} nutrition is essential for maintaining lower hydrogen peroxide production and preventing lipid peroxidation and protein degradation under heat stress, emphasizing its indispensable role in preserving cellular integrity and enhancing antioxidant responses during temperature extremes.

Cold stress, particularly in temperate regions, can severely affect the yield of horticultural crops. A study by Li et al. (2023b) on tobacco (*Nicotiana tabacum* L.) demonstrated that under cold stress

conditions, Mg^{2+} supplementation led to notable improvements in plant morphology, nutrient uptake, and photosynthetic attributes. Notably, tobacco plants treated with Mg^{2+} under cold stress exhibited significant increases in biomass, nutrient uptake, photosynthetic activity, and chlorophyll content. Furthermore, Mg^{2+} application positively influenced tobacco quality, including increased starch and sucrose content. These findings highlight that Mg^{2+} application can mitigate the adverse effects of cold stress and promote better growth and quality of tobacco plants. Mg^{2+} supplementation has been identified as a vital factor for improving the resilience of pepper plants to salinity stress. Zirek and Uzal (2020) investigated the effects of varying Mg^{2+} doses on pepper plants under salt-induced stress and discovered that higher Mg^{2+} doses led to increased plant growth, as demonstrated by greater total plant weights, especially in the exogenous application of Mg^{2+} @98.56 ppm + salt treatments. Additionally, elevated Mg^{2+} levels resulted in augmented chlorophyll content and heightened antioxidant enzyme activities, which play a role in combating oxidative stress. Simultaneously, there was a reduction in malondialdehyde (MDA) levels, an indicator of cellular damage. These findings suggest that increasing Mg^{2+} doses can mitigate the detrimental effects of salinity stress on pepper plants, thereby enhancing their growth and physiological health.

The growing concern over heavy metal toxicity in soils has sparked research into $Mg^{2\ the}$ potential role in alleviating these toxic effects in horticultural crops. Lu et al. (2021a) explored the impact of Mg^{2+} on field-grown Chinese cabbage and discovered that it significantly enhanced the cabbage's nutritional profile, with noticeable increases in vitamin C and water-soluble protein content. Most notably, Mg^{2+} reduced the uptake and accumulation of heavy metals, such as cadmium and nickel, in plant tissues, thereby minimizing their adverse health effects. Cr uptake increased, but the health risks posed by Cr were substantially lower than those posed by Cd and Ni. Therefore, soil-applied Mg^{2+}, particularly in the range of 22.5–45 kg ha^{-1}, can notably enhance the nutritional qualities of Chinese cabbage, while alleviating the potential health risks from heavy metal consumption. Luo et al. (2020) investigated the effects of nanometer magnesium hydroxide on the growth of Chinese cabbage and its ability to uptake cadmium (Cd) from polluted soil. These findings revealed that low doses of nanometer-sized magnesium hydroxide boosted the biomass of Chinese cabbage, whereas higher doses had toxic effects. Crucially, the presence of magnesium hydroxide, especially in its nanometer form, effectively decreased the concentration of Cd in various parts of the cabbage, especially under low Cd stress. This Mg^{2+} treatment also transformed the soil Cd into less bioavailable forms, reducing the exchangeable Cd content and increasing other bound Cd forms. This means that magnesium hydroxide, particularly in its nanometer form, can act as an effective agent in reducing harmful Cd concentrations in crops grown in contaminated soils, offering a potential avenue for mitigating heavy metal stress in agricultural settings. In a separate investigation by Faizan et al. (2022), it was reported that increasing the accumulation of metalloids, such as arsenic, poses significant threats to crop growth and yield. This study revealed that MgO-NPs could bolster plant growth and fortify plant resistance to metal/metalloid toxicity. When soybean plants were treated with MgO-NPs under arsenic-containing conditions, there was a marked improvement in various growth parameters, photosynthetic functions, and nutrient uptake. The nanoparticles also reduced arsenic uptake and associated oxidative damage. These findings highlight that Mg^{2+} supplementation could reduce the uptake and accumulation of these heavy metals, thus protecting plants from oxidative damage and preserving their growth and productivity. These findings underscore the crucial role of Mg^{2+} in bolstering the resilience of horticultural crops to various abiotic stresses and maintaining their productivity and quality. Nonetheless, further research is necessary to elucidate the precise mechanisms of Mg^{2+}-mediated stress tolerance and to develop tailored Mg^{2+}-based strategies for mitigating different types of abiotic stress in horticulture. In order to provide a comprehensive overview of the effects of magnesium supplementation on the tolerance of crops to environmental stresses, we have summarized recent research findings in Table 2.

3.4 Magnesium and its multifaceted role in biotic stress tolerance

Magnesium stands out as more than just an essential macronutrient for plants; its impact permeates deep into the physiological and biochemical frameworks of plants, steering their resistance against biotic stresses, and affirming its crucial role in modern agriculture (Huber and Jones, 2013). Central to the effect of Mg^{2+} on plant physiology is its role in photosynthesis. Their integral position in chlorophyll molecules resonates with the vitality of plants and their combined resistance to biotic threats (Tang and Luan, 2020). Mg^{2+} is a linchpin in the biosynthesis of salicylic acid (SA), which is a cornerstone of plant defense. In its nanoparticle form, Mg^{2+} amplifies the function of phenylalanine ammonia-lyase (PAL), a significant driver of SA production (Setiawati et al., 2020). As SA is fundamental to pathogen defense (Lefevere et al., 2020; Zhong et al., 2021), the interplay between Mg^{2+} and SA assumes colossal significance. This SA-mediated defense is multifaceted; it orchestrates immediate counteractions against biotrophic pathogens, while simultaneously harmonizing defense and growth via interactions with other hormones, particularly auxins (Zhong et al., 2021). Some plants, such as *Fritillaria unibracteata*, have demonstrated a role for Mg^{2+} influenced PAL in mediating drought tolerance by enhancing SA accumulation (Qin et al., 2022). However, SA is not a lone warrior in plant defenses. Other hormones, such as jasmonic acid (JA) and ethylene (ET), have distinctive roles in countering different threats, from (hemo) biotrophic pathogens to herbivorous pests (Huang et al., 2020; Wu and Ye, 2020). The versatility of Mg^{2+} has been highlighted by the mediation of these diverse pathways. For instance, when Arabidopsis

TABLE 2 Influence of magnesium supplementation on crop tolerance to various environmental stresses: a summary of recent studies.

Crop	Stress Type	Key Findings related to Stress Tolerance	Reference
Apple	Low Mg^{2+} & N availability	Mg^{2+} promotes sorbitol synthesis & transport, leading to upregulation of nitrate transporters and increased nitrate absorption.	(Tian et al., 2023a)
Pomelo	Soil acidification (Low pH)	Lime+Mg^{2+} treatment in acidic soils of pomelo orchards mitigated soil acidification, enhanced nutrient availability, and significantly improved fruit yield and quality	(Zhang S. et al., 2021)
Vicia faba L.	Heat Stress (HS)	Mg^{2+} supplementation bolstered growth, enhanced photosynthetic pigment synthesis, and improved enzyme activities, promoting accumulation of organic solutes and strengthening antioxidant responses, thereby suppressing damage from ROS, while mitigating oxidative damage	(Siddiqui et al., 2018)
Daucus carota	Lead (Pb) Stress	Mg^{2+} oxide nanoparticles reduce Pb stress, enhance antioxidant activity, and improve mineral nutrient uptake.	(Faiz et al., 2022)
Soybean & Maize	Nutrient stress	Foliar Mg^{2+} supplementation leads to increased photosynthesis, sugar concentration, and overall metabolism, boosting grain yields and environmental stress tolerance.	(Rodrigues et al., 2021)
Apple	Aluminum (Al) Stress	Mg^{2+} counters Al-induced growth inhibition by boosting photosynthesis, enhancing antioxidant capacity, improving sucrose transport, and optimizing nitrogen metabolism in apple seedlings.	(Lyu et al., 2023)
Tomato	Water stress	ALPAN®, a biostimulant rich in Mg^{2+} content, enhances carbohydrate metabolism and translocation, promotes stomatal closure, and preserves cellular homeostasis. It stabilizes photosynthetic pigments, regulates osmo-protectants, and reduces lipid oxidation, thus supporting plant health under water stress.	(Hamedeh et al., 2022)
Chinese Cabbage	Heavy metal stress	Mg^{2+} improved its nutritional quality, increasing vitamin C and water-soluble protein contents, decreased the accumulation of Cd and Ni. Overall, improve nutritional content and reduce potential health risks from heavy metals	(Lu et al., 2021a)
Coffee	Heat stress	Adequate Mg^{2+} nutrition in coffee seedlings reduces oxidative damage by enhancing antioxidant metabolism and osmoprotectants, subsequently decreasing hydrogen peroxide production, lipid peroxidation, and protein degradation.	(Silva et al., 2017)
Citrus (Lemon)	Light and temperature stress	Extra nutrient supply (Mg, N, Mg+N) increased plant tolerance, maintaining high photosynthetic rates, enhancing antioxidant enzyme activity, and reducing oxidative stress.	(Boaretto et al., 2020)

plants were treated with MgO, SA content increased, boosting resistance against *Ralstonia solanacearum*, a pattern mediated by both SA biosynthesis and ROS production (Ota et al., 2019). However, in another instance, Mg^{2+}'s influence pivoted towards JA signaling, which is critical for tomato plants to ward off *Fusarium* wilt (Fujikawa et al., 2021). In addition to hormones, Mg^{2+} tendrils influence various biochemical aspects of plant defence. It modulates metabolic pathways and shapes the production of secondary metabolites that are vital for defense (Guo et al., 2016). However, the influence of Mg^{2+} spans even further. It has a symbiotic relationship with the cell wall, fortifying plant cells against pathogen infiltration, while ensuring the optimal function of defense-signaling proteins (Ye et al., 2021; Hamedeh et al., 2022). Within this cellular symphony, Mg^{2+} guarantees the stability of RNA and the timely synthesis of defense-related proteins in the face of pathogenic threats, a response greatly amplified by its availability (Liang et al., 2017; Andreadelli et al., 2021). Additionally, as a co-factor for an array of enzymes, Mg^{2+} oversees reactive oxygen species detoxification and the synthesis of defence compounds, forming an immediate shield against biotic stressors (Faizan et al., 2022). Mg^{2+} also intricately modulates metabolic pathways governing secondary metabolite production, many of which underpin plant defense mechanisms (Guo et al., 2016). Another dimension of the Mg^{2+} defense strategy has emerged from studies pointing to the antimicrobial properties of MgO nanoparticles. These nanoparticles have shown efficacy against a spectrum of bacterial and fungal plant diseases (Liao et al., 2019; Liao et al., 2021). Copper (Cu) bactericides, which are extensively used in agriculture, pose environmental risks and foster Cu-tolerant pathogens such as *Xanthomonas perforins*. Recent research has found that MgO-NPs effectively reduced tomato bacterial spot disease severity without negative yield impacts or significant soil accumulation of metals, suggesting it as a potential environmentally friendly alternative to Cu bactericides (Liao et al., 2021). However, determining whether antimicrobial efficacy is attributed to the inherent properties of MgO or the unique characteristics of nanoparticles remains a compelling question. However, although the contribution of Mg^{2+} to plant defense is monumental, there is a balancing act at play. Extreme Mg^{2+} deprivation can induce stress in plants, leading to chlorophyll degradation and increased ROS generation, thus underscoring the nuanced role of Mg^{2+} in plant health (Peng et al., 2019).These

insights present revolutionary prospects for enhancing plant defense and yield in contemporary agricultural landscapes, emphasizing the pivotal role of Mg^{2+} in the narrative of plant resilience.

4 Mechanisms and dynamics of magnesium in plants

4.1 Mechanisms of magnesium absorption

Plants absorb Mg^{2+} from their surrounding environment primarily through their roots via intricate and highly regulated mechanisms. These absorption processes are governed by various environmental factors and operate passively, following a concentration gradient, and actively against it (Hermans et al., 2013). When the Mg^{2+} content in the soil solution is high, passive diffusion primarily drives uptake (Figure 2). Mg^{2+} ions permeate the root epidermis and cortex from areas of higher concentration in the soil solution to areas of lower concentration within the roots. However, when soil Mg^{2+} levels are low, active transport mechanisms become crucial. This involves specialized proteins, known as Mg^{2+} transporters or channels, which are present in the membranes of root cells. Among these, the CorA, MRS2, and MGT family members have been identified as key players in this process (Li et al., 2016). These transporters facilitate the movement of Mg^{2+} ions against the concentration gradient into the root cells, an energy-dependent process that requires ATP. The root epidermis, which is the outermost cell layer of the root, acts as the primary site for Mg^{2+} uptake, with epidermal cells orchestrating the initial contact and uptake of Mg^{2+} ions from the soil solution (Figure 2). Once these ions infiltrate the root cortex, they traverse the plasma membrane of the root cells, a process assisted by membrane transport proteins including Mg^{2+} transporters or channels. Upon entering the cytoplasm of root cells, Mg^{2+} ions can either opt for a symplastic or apoplastic pathway. In the symplastic pathway, Mg^{2+} ions are transferred from one cell to another through plasmodesmata, the cytoplasmic connections between neighboring cells. Conversely, the apoplastic pathway enables Mg^{2+} ions to traverse through the cell walls and extracellular spaces between cells (Ishfaq et al., 2022). Following this, Mg^{2+} ions are transported towards the central root stele housing the xylem vessels, which serve as the primary highway for long-distance nutrient transport. Both the symplastic and apoplastic pathways participate in this movement. Once within the root stele, Mg^{2+} ions are actively loaded into the xylem vessels and transported upward to the aerial parts of the plant, a process facilitated by specific transport proteins in the plasma membrane of the xylem parenchyma cells (Ishfaq et al., 2022). This upward movement or xylem loading is heavily influenced by transpiration rates and can also be affected by the plant's Mg^{2+} nutritional status. The phloem also plays a significant role in redistributing Mg^{2+} to areas of higher demand, particularly younger leaves and reproductive tissues (Koch et al., 2020). Once in the leaves, Mg^{2+} ions are vital for several physiological processes, including chlorophyll synthesis and operation of the photosystem II complex. Mg^{2+} also plays a pivotal role in the activation of numerous enzymes, assisting in carbohydrate partitioning and the synthesis of nucleic acids and proteins (Chen et al., 2018). Therefore, the journey of Mg^{2+} within a plant from root absorption to leaf utilization is an intricate, multifaceted process, as shown in Figure 2. Understanding these mechanisms offers profound insights into how to optimize the Mg^{2+} nutritional status of plants, which has implications for improving crop yield and overall plant health.

4.2 Factors affecting magnesium availability and intake

The availability of Mg^{2+} in the soil and its subsequent intake by plants depends on a variety of factors, such as soil pH, cation exchange capacity (CEC), soil organic matter, soil texture and structure, moisture and drainage, presence of other nutrients, and ambient temperature (Chen and Ma, 2013; Gransee and Führs, 2013; Mengutay et al., 2013; Sun et al., 2013). The availability of Mg^{2+} in the soil is significantly influenced by the pH level. When the soil is acidic (pH < 6.0), the solubility of Mg^{2+} decreases because it binds more readily to the soil particles, leading to less accessibility for plant uptake. Conversely, in alkaline soils (pH > 7.0), Mg^{2+} can become limited owing to the excessive precipitation of Ca and Mg carbonates (Koyama et al., 2001; Kobayashi et al., 2013). The CEC of a soil refers to its capacity to bind and exchange cations, including Mg^{2+}. High CEC soils are advantageous because they have greater Mg^{2+} retention, thus promoting their availability for plant uptake (Mayland and Wilkinson, 1989). The organic matter content of soil can affect Mg^{2+} availability. This is because organic matter enhances the soil structure, facilitates cation exchange, and aids the release of Mg^{2+} from organic matter as it decomposes (Mayland and Wilkinson, 1989). Soil texture and structure also play crucial roles in determining Mg^{2+} availability. For instance, sandy soils, which have larger particles and low water-holding capacity, are susceptible to Mg^{2+} leaching, thereby reducing their accessibility to plants. In contrast, clay soils can retain Mg^{2+} better but may limit their accessibility due to poor drainage and limited root penetration (Senbayram et al., 2015).

The moisture content and drainage of soil can also affect the availability of Mg^{2+}. If the soil is excessively wet or waterlogged, roots may be deprived of oxygen, leading to reduced Mg^{2+} uptake (Grzebisz, 2011; Gransee and Führs, 2013). The presence and concentration of other nutrients can also influence Mg^{2+} uptake. For instance, excessive Ca^{2+} can compete with Mg^{2+} for uptake by plant roots, potentially reducing Mg^{2+} availability. Similarly, an imbalance or excessive levels of other nutrients such as K^+ or NH_4^+ can also affect Mg^{2+} uptake (Fageria, 2001; Römheld and Kirkby, 2009; Cakmak and Yazici, 2010). Mg^{2+} absorption rates are typically higher in warmer soil temperatures, which facilitates root activity and nutrient uptake. Conversely, cold temperatures can limit root activity and nutrient uptake, potentially affecting Mg^{2+} uptake during colder seasons (Jin et al., 2022). In conclusion, the availability and absorption of Mg^{2+} in plants are complex processes that are affected by various environmental and soil factors. Effective management of these factors through appropriate soil amendments, irrigation practices, and nutrient management strategies is critical to ensure optimal Mg^{2+} uptake and to meet the physiological needs of plants.

5 Magnesium transporters and their importance

5.1 Molecular insights into magnesium transporters: their pivotal roles in plant development and stress responses

Navigating these Mg^{2+} dynamics are Mg^{2+} transporter (MGTs) proteins, whose functionalities are garnering increasing research attention. It meticulously orchestrates the absorption, transportation, and storage of Mg^{2+} within plant cells, ensuring optimal growth and stress responses (Heidari et al., 2022; Bin et al., 2023; Tang et al., 2023). In the horticulture domain, the pertinence of these transporters is evident. *Cucumis sativus* and *Citrullus lanatus*, members of the *Cucurbitaceae* family, house 19 and 20 MGT genes, respectively, predominantly stationed in their root tissues (Heidari et al., 2022). In contrast, *Citrus sinensis* responds to Mg^{2+} deficiency with altered CO_2 assimilation patterns and heightened expression of specific MGT genes, notably *CsMGT3* (Yang et al., 2019; Ye et al., 2019). Furthermore, the intracellular Mg^{2+} ion dynamics of grapes can be mapped through the structure and function of their MGTs (Ge M. et al., 2022). Remarkably, despite its undeniable importance, Mg^{2+}'s prominence in academia and agriculture often falls into shadow. Historically, cereal seeds have witnessed a decline in their Mg^{2+} content (Guo et al., 2016). However, with evolving research, especially concerning horticultural crops, the imperative to uncover and understand the molecular transport mechanisms of Mg^{2+} has surged to the forefront. This chapter ventures into this molecular journey, embarking from the roots, coursing through the xylem, navigating the leaves, and arriving at the blossoms and fruits, shedding light on the nuances of Mg^{2+} dynamics in these pivotal plant structures.

5.2 Mg^{2+} absorption in roots: unraveling the transporters and mechanisms

Magnesium, a pivotal nutrient in plant physiology, relies on specialized proteins (MGTs) for its uptake and transportation across plant tissues. Recent research on MGTs in horticultural crops is summarized in Table 3. The role of MGTs is particularly pronounced in the root system, the primary gateway for nutrients from the soil to the plant. Roots serve as linchpins in plant nutrient acquisition, with Mg^{2+} absorption being central to a myriad of biological processes. As the primary interface between the plant and its soil environment, roots are equipped with an array of transporters to facilitate Mg^{2+} uptake (Tian et al., 2023a). The morphology of the roots is directly influenced by the Mg^{2+} levels they encounter. Studies such as those by Regon et al. (2019) highlight how low Mg^{2+} concentrations result in slender roots sprouting numerous hairs, whereas an abundance of Mg^{2+} produces thicker, nearly hairless roots. Diving deeper into molecular intricacies, MGTs in roots exhibit an array of functionalities. For instance, Arabidopsis leans on its *MGT6* transporter under Mg^{2+}-limited conditions, thereby ensuring high-affinity Mg^{2+} uptake (Yan et al., 2018). However, the narrative is more nuanced in varied crops. In *Citrus sinensis*, a host of MGTs, such as *CsMGT2* and *CsMGT7*, modulates their activities according to soil Mg^{2+} levels. They ramp up expression during scarcity, working overtime to ensure the plant does not starve of this crucial nutrient (Yang et al., 2019; Bin et al., 2023). The tea plant story *Camellia sinensis* L. adds another chapter to the tale. Here, *CsMGT5* stands out, especially during Mg^{2+} crunch times, to ensure sustained uptake (Bin et al., 2023). Similar to Arabidopsis *MGT6*, *CsMGT5* exhibits evolutionary convergence of function across plant species (Li et al., 2023a). The subcellular localization of these transporters further unravels the depths of their intricacies. For instance, *CsMGT5* localizes to the plasma membrane, positioning it perfectly for high-affinity Mg^{2+} transportation (Li et al., 2023a). When faced with challenging environments, *CsMGT5* manifests resilience, emphasizing the transporter's prowess (Li et al., 2023a; Tang et al., 2021). Moreover, its heterologous expression in Arabidopsis led to enhanced Mg^{2+} retention not only in the roots but also in the above-ground parts, underscoring its comprehensive role in Mg^{2+} dynamics (Li et al., 2023a). In conclusion, the multifaceted world of Mg^{2+} transporters in roots provides a picture of evolutionary brilliance. Their diverse functionalities, adaptive expression patterns, and strategic subcellular positioning collectively ensure that plants thrive, even when faced with fluctuating soil Mg^{2+} levels. Their role is a testament to the intricate the regulation of plant nutrition, adaptation, and survival.

5.3 Magnesium transport in shoots and leaves

Upon absorption from the soil, Mg^{2+} is transported via the xylem from the roots to the shoots and is particularly mobile within the phloem. This mobility facilitates the redistribution from mature to younger tissues, ensuring that newer tissues receive adequate Mg^{2+} levels (Tang and Luan, 2017). Specific transporters such as *MGT-1* and *MGT-2* in *Arabidopsis thaliana* play a pivotal role, especially under Mg^{2+} stress, aiding in the mobilization of Mg^{2+} from vacuoles (Meng et al., 2022; Tang et al., 2022b). This action ensures a balanced Mg^{2+} equilibrium within the plant, even when the external Mg^{2+} supply is limited (Tang et al., 2022b). Transporter expression is a dynamic process. During Mg^{2+} deficiency, there is an increase in the expression of specific *MGT* genes in various crops, such as *CsMGT3* and *CsMGT7*, to maintain adequate internal Mg^{2+} levels (Tang et al., 2021). Furthermore, diverse plants, such as *Dimocarpus longan* and tomato (*Solanum lycopersicum*), display unique patterns. In *Dimocarpus longan*, MGT genes like *DlMGT4.2* are expressed across various organs, suggesting a universal role in Mg^{2+} management (Lv et al., 2023). In contrast, tomato plants under Mg^{2+} stress exhibit heightened expression of genes such as *SlMGT1-1* and *SlMGT3-2* across roots and shoots (Regon et al., 2019). Delving into the subcellular localization of these transporters offers profound insights into their respective functionalities. Specifically, *AtMGT2* and *MGT3* are pivotal in channeling Mg^{2+} into mesophyll vacuoles (Tang and Luan, 2017). The suspected involvement of *MGT10* in shuttling Mg^{2+} into the chloroplast envelope remains a riveting research topic (Tang and Luan, 2017).

Further highlighting the myriad roles of these transporters, the overexpression of *AtMRS2-10* in tobacco was observed to enhance Mg^{2+} concentration within the plants, thereby conferring tolerance to low-Mg^{2+} and even aluminum stress (Deng et al., 2006). Functionality assays utilizing a Mg^{2+}-deficient strain of *Salmonella typhimurium* (*MM281*) have indicated distinct transport capacities among different transporters (Tang et al., 2021). Notably, while *CsMGT1* demonstrated a robust Mg^{2+} transport capacity, surpassing that of *CsMGT2*, both *CsMGT2.1* and *CsMGT3* exhibited negligible Mg^{2+} transport functions (Tang et al., 2021). These findings shed light on the diverse functionalities of the *CsMGT* family in *Camellia sinensis*, thereby providing a foundation for future endeavors aimed at optimizing Mg^{2+} utilization in these plants (Tang et al., 2021). In addition to their functions in cellular homeostasis, Mg^{2+} transporters also facilitate critical biochemical processes. ATP synthesis, a product of oxidative and photosynthetic phosphorylation occurring in mitochondria and chloroplasts, respectively, underscores the role of Mg^{2+} in maintaining electron transport and generating membrane potential (Tang and Luan, 2017; Kleczkowski and Igamberdiev, 2021). Intriguingly, Mg^{2+} transporters manifest in diverse cellular locations, including the plasma membrane, tonoplast, plastids, mitochondria, and ER (Tang and Luan, 2017; Chen et al., 2018). Some transporters, such as the Arabidopsis mitochondrial *MGT5*, display tissue specificity; it is expressed exclusively in anthers during the early stages of flower development, highlighting its potential involvement in pollen development and male fertility (Li et al., 2008). Conclusively, the Mg^{2+} transporter/mitochondrial RNA splicing 2 (MGT/MRS2) family stands out as a linchpin in maintaining Mg^{2+} homeostasis, thereby underpinning the plant's growth and developmental trajectories (Li et al., 2023a; Yang et al., 2022; Lv et al., 2023). Beyond its role in photosynthesis, Mg^{2+} is also pivotal for enzymes such as Mg^{2+} chelatase (MgCh) in chlorophyll biosynthesis. Disruptions in this process, as observed in the strawberry species *Fragaria pentaphylla*, manifest as phenotypic changes, such as yellow-green leaves, underlining the importance of Mg^{2+} in plant health (Ma et al., 2023). In summary, the sophisticated interplay between Mg^{2+} transporters and their modulated expression in different plants highlights the critical role of Mg^{2+} in plant physiology and health (Figure 2).

5.4 Magnesium dynamics in reproductive parts

Magnesium transporters play crucial roles across plants, with significant functions detected in the reproductive parts, ensuring successful pollen development, male fertility, and fruit quality (Li et al., 2015; Xu X. F. et al., 2021; Tian et al., 2023b). Several members of the MGT family, including *MGT4, MGT5*, and *MGT9*, are vital for pollen development and male fertility. *MGT4*, which is situated in the endoplasmic reticulum, and *MGT9*, which is localized in the plasma membrane, are integral to pollen maturation processes (Tang and Luan, 2017; Chen et al., 2018). A comprehensive study of tea plants (*Camellia sinensis* L.) sheds light on four key MGT genes: *CsMGT1*, *CsMGT2, CsMGT2.1*, and *CsMGT3*. These genes were expressed across roots, stems, leaves, and flowers, with varying responses to Mg^{2+} levels. Intriguingly, while *CsMGT1* and *CsMGT2* have evident Mg^{2+} transport functionality (Figure 3), *CsMGT2.1* and *CsMGT3* showed negligible transport action. This discovery underscores the varied roles of these transporters in Mg^{2+} management within tea plants, with potential ramifications for agricultural utilization and Mg^{2+} enhancement in such crops (Bin et al., 2023; Tang et al., 2023).

Diverse expression patterns have also been observed in tomatoes (*Solanum lycopersicum*). Liu et al. (2023) pinpointed differential tissue-specific activity among SlMGT genes. *SlMGT1-1*, for instance, was more dynamically expressed in stems, leaves, and flowers, while genes like *SlMGT3-1* and *SlMGT5-1* showed minuscule transcript levels in stems and flowers. Such variations hint at the unique roles that each transporter plays in plant growth and physiological metabolism. Viticulture is another arena in which Mg^{2+} plays a vital role. Recent observations have highlighted increasing Mg^{2+} deficiencies in vineyards in southern China, which have adverse consequences for grape growth and fruit quality (Ge M. et al., 2022). In grapevines, *VvMGT3* was prominently expressed only in pollen and rachis PFS, elucidating its potential role in the growth and development of these specific tissues (Ge M. et al., 2022). Additionally, the application of Mg^{2+} was found to promote fruit coloring in apples, with a marked upregulation in genes associated with anthocyanin synthesis in the fruit peel, underscoring the intertwined nature of Mg^{2+} with fruit quality (Tian et al., 2023b). Citrus is another domain in which Mg^{2+} transporters have unique roles. In citrus fruit pulp and peels, the expression of *CsMGT3* outshone others, while *CsMGT5*'s presence was almost negligible (Bin et al., 2023; Tang et al., 2023). Such tissue-specific expression of *CsMGT* genes suggests their diverse functions during citrus plant growth and development phases. In summary, Mg^{2+} transporters, particularly the MGT family, demonstrate a plethora of roles across plant reproductive parts. These transporters not only ensure successful reproduction but also influence fruit development and quality, with implications for agricultural productivity and crop enhancement.

5.5 Magnesium transporters in plants: deciphering roles in biotic and abiotic stress responses and adaptation

Recent studies have significantly expanded our understanding of the role of MGTs in abiotic stress tolerance in plants. In grapes (*Vitis vinifera*), the *VvMGT9* gene is notably upregulated under waterlogging, suggesting a key role in waterlogging resistance (Ge M. et al., 2022). The same gene, along with *VvMGT5*, also showed marked upregulation during drought stress, emphasizing its potential in drought tolerance (Ge M. et al., 2022). This was further corroborated by findings in watermelon (*Citrullus lanatus*), where two *NIPA* genes were found to be responsive to drought stress (Heidari et al., 2022). The role of MGTs in the salinity response has been highlighted in cucumber (*Cucumis sativus*). Here, *NIPA* and *MSR2* genes exhibited upregulated expression when exposed to NaCl stress (Heidari et al., 2022). Metal stress, particularly from copper, magnesium, and aluminum, presents another dimension of the MGTs function. In grapes, several *VvMGT* genes show varied expression patterns under

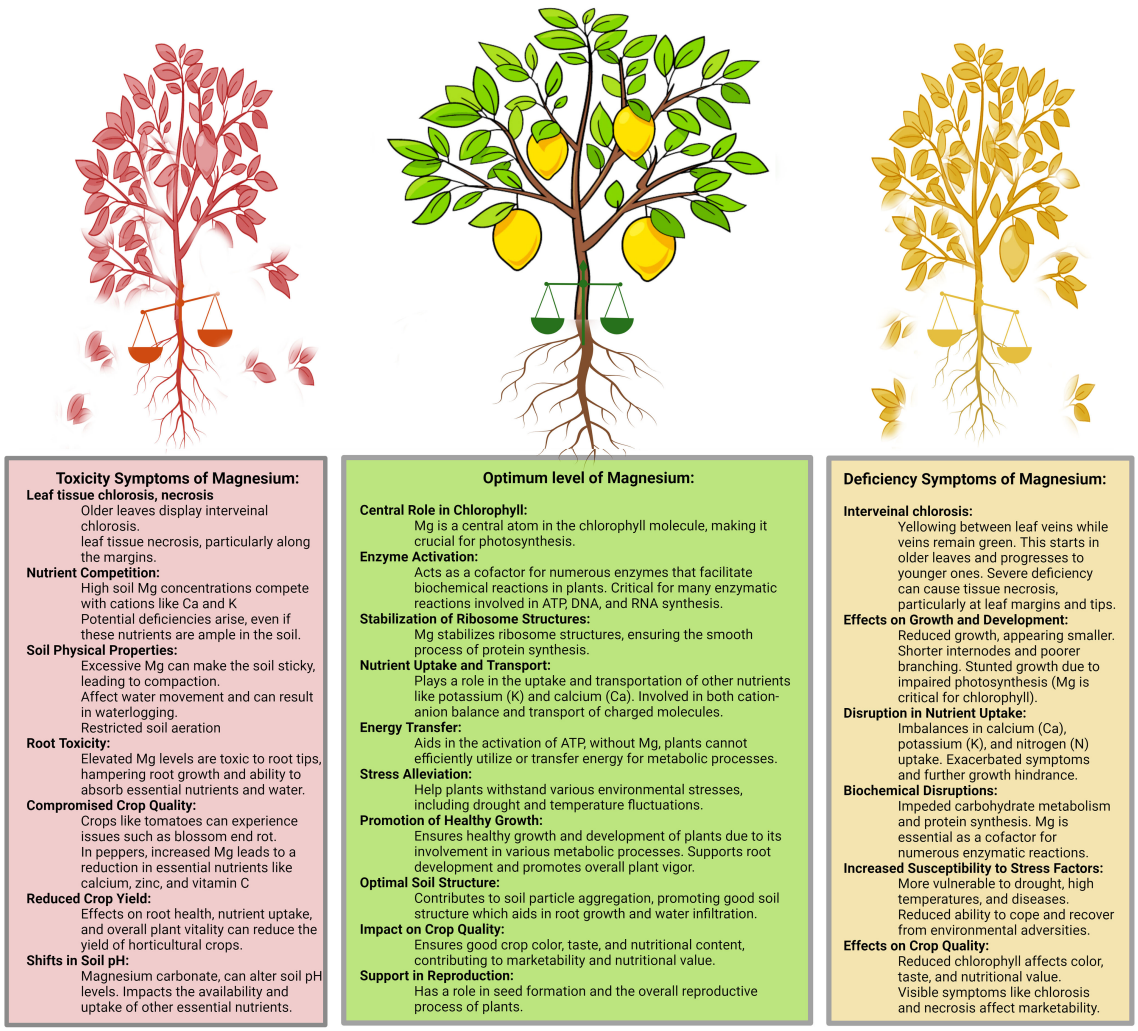

FIGURE 3
The triphasic impact of magnesium levels in plants: toxicity, optimum, and deficiency.

these stresses. Intriguingly, while magnesium treatment led to a peak in the expression of numerous *VvMGT* genes at 24 h, aluminum exposure mostly resulted in up-regulation, except for *VvMGT2*. This divergence in the response to aluminum hints at the unique mechanisms at play (Ge M. et al., 2022).

Furthermore, the potential of magnesium to mitigate aluminum toxicity has been recognized. Specifically, certain concentrations of Mg^{2+} alleviate the toxic effects of aluminum, coinciding with increased Al-induced citrate exudation and enhanced plasma membrane H^+ ATPase activity (Chen et al., 2014). The regulatory role of Mg^{2+} is not limited to stress responses. Evidence from a study on potatoes suggests that the "plant hormone signal transduction pathway" may be influenced by Mg-ONPs without any detrimental effects (Wang et al., 2022). Additionally, watermelons show a particular response to melatonin treatment and low leaf nitrogen content, with two NIPA genes being more highly induced (Heidari et al., 2022). In terms of protection, MgONPs were identified as potential agents to shield potatoes against the detrimental effects of Phytophthora infestans at specific dosages (Wang et al., 2022). In *Citrus sinensis*, an intricate response is observed under Mg^{2+} deficiency, which is characterized by decreased CO_2 assimilation and fluctuations in multiple compounds. RNA-Seq analyses from various studies have revealed the differential expression of a plethora of genes. Remarkably, among the seven identified *CsMGTs, CsMGT3* showed the highest expression across diverse tissues (Bin et al., 2023; Tang et al., 2023). Collectively, these studies underscore the multifunctional role of MGTs in abiotic stress responses. Their varied and sometimes tissue-specific expression patterns in different plant species, from grapes to citrus, highlight their potential as prime targets for enhancing stress tolerance in crop plants.Highlighting the journey of Mg^{2+} within horticultural crops, this chapter traces its path from soil uptake to its integral functions within the fruit. Key transporters, particularly MGTs, ensure its optimal distribution, which is crucial not only for basic cellular operations but also for the plant's critical reproductive stages. The adaptability of these transporters against both biotic and abiotic stresses emphasize their evolutionary importance and suggests

potential pathways for crop enhancement. As global agriculture grapples with increasing challenges, a deep understanding of Mg^{2+} roles and its transport systems can guide us towards more sustainable and robust cropping paradigms.

6 Adverse effects of magnesium deficiency and toxicity

6.1 The consequences of magnesium deficiency

Mg^{2+} deficiency in plants can lead to a range of negative effects on growth, productivity, and general plant health. Recent research findings are summarized in Table 4 (Cakmak and Yazici, 2010; Yang et al., 2012; Verbruggen and Hermans, 2013). A key symptom of Mg^{2+} deficiency in plants is interveinal chlorosis, where the tissues between the leaf veins turn yellow, while the veins remain green. This typically starts in older leaves before progressing to younger ones (Figure 3). Severe deficiency can lead to necrosis or tissue death, particularly at the leaf margins and tips (Hermans and Verbruggen, 2005; Hermans et al., 2005; Hermans et al., 2010a). Plants lacking Mg^{2+} often exhibit reduced growth and development. They might appear smaller, with shorter internodes and poorer branching. This is because Mg^{2+} is a critical component of the chlorophyll molecule, and without sufficient Mg^{2+}, plants cannot perform photosynthesis effectively, leading to reduced energy production and subsequently stunted growth (Hermans and Verbruggen, 2005; Cakmak and Yazici, 2010; Yang et al., 2012). Mg^{2+} deficiency can disrupt the uptake of other essential nutrients such as Ca^{2+}, K^{+}, and N. This can lead to an imbalance of these nutrients

TABLE 3 Comparative expression and response of MGT genes in horticultural crops.

Crop Name	Gene/Transporter	Tissue Expression	Key Findings	Reference
Cucumber (*Cucumis sativus*)	CsMGT1, CsMGT2, CsMGT3, CsMGT5, CsMGT6	High expression in flowers; CsMGT3 high in fruit pulp and peels	Essential for Mg^{2+} transport, tissue-specific expression	Bin et al., 2023
Tea (*Camellia sinensis*)	CsMGT1, CsMGT2, CsMGT2.1, CsMGT3	Expressed in roots, stems, leaves, and flowers	CsMGT1 and CsMGT2 have Mg^{2+} transport function; CsMGT1 better than CsMGT2	Bin et al., 2023
Tomato (*Solanum lycopersicum*)	SlMGT3-2, SlMGT5-2, SlMGT4-1, SlMGT1-1, SlMGT2-1, SlMGT3-1, SlMGT5-1	Varies by gene; e.g., SlMGT4-1 is dominant in leaves and flowers	Different family members regulate plant growth and physiological metabolism	Liu et al., 2023
Grape (*Vitis vinifera*)	VvMGT3, VvMGT6	VvMGT3 in pollen and rachis PFS; VvMGT6 low in tissue senescence and organs	Tissue-specific and spatiotemporal expression; VvMGT3 might participate in pollen and peel signal transduction	Ge M. et al., 2022
Citrus (*Citrus* spp.)	CsMGT3, CsMGT5	CsMGT3 high in fruit pulp and peels	Tissue-specific expression suggests diverse roles in development and growth	Bin et al., 2023
Potato (*Solanum tuberosum*)	DEGs (Differentially Expressed Genes)	leaves and tubers	Mg^{2+}O NPs inhibit P. infestans, attenuating potato late blight, while promoting potential disease resistance and growth in potatoes.	Wang et al., 2022
Apple (*Malus domestica*)	MdSOT1, MdSOT3, MdSUT1, MdSUT4, MdCHS, MdF3H, MdMYB1, MdbZIP44	Leaves, fruit stalk, fruit flesh, apple peel	Mg^{2+} application enhances N and C metabolism, promotes photosynthesis, boosts sugar transport to fruits, and increases anthocyanin content in apple peel.	Tian et al., 2023b
longan (*Dimocarpus*)	DlMGT9.2	High in fruit; low in flowers and leaves	Specific Mg^{2+} transport function	Lv et al., 2023
Strawberry (*Fragaria pentaphylla*)	CHLI, CHLD, CHLH	Leaves	Mutation in CHLI Glu186 affects chlorophyll biosynthesis and ATPase activity, leading to yellow-green leaves and alterations in nitrogen and carbon metabolism.	(Ma et al., 2023)
Pepper (*Capsicum annuum*)	WRKY1, bZIP	Shoots and Roots	nMg^{2+} and bMg^{2+} enhance biomass accumulation and upregulate expression of WRKY1 and bZIP transcription factors involved in defense/stress responses and secondary metabolism.	Sotoodehnia-Korani et al., 2023
Cucumber *(Cucumis sativus)*	MSR2 (Csa_2G225310, Csa_2G19910, Csa_7G070800) & NIPAs (Csa_7G291140, Csa_5G586580, Csa_3G251940)	High in shoot tissues	MSR2 gene, Csa_2G225310, upregulated in response to nematode; NIPA, Csa_3G129750, and MSR2, Csa_1G138280, upregulated under NaCl stress; NIPA, Csa_4G646200, upregulated 1 dai by PC	(Heidari et al., 2022)
Watermelon (*Citrullus lanatus*)	NIPAs (Cla97C05G083800, Cla97C03G063010, Cla97C02G031120) & MSR2 (Cla97C02G033950)	High in roots; MSR2 (Cla97C02G033950) across all tissues	Two NIPAs upregulated under drought and mosaic virus stress; further NIPA genes induced in response to melatonin treatment and under low nitrogen content in leaves	(Heidari et al., 2022)

TABLE 4 Effects of magnesium deficiency on crop yield and quality.

Crops	Yield parameters	Quality attributes	References
Tomatoes	Reduced size and weight of the fruit	Less flavour intensity	(Kashinath et al., 2013)
Spinach	Lower biomass production	Reduced nutrient content	(Borowski and Michalek, 2010; Jamali Jaghdani et al., 2021)
Carrots	Stunted root growth	Increased nitrate accumulation	(Villeneuve and Geoffriau, 2020)
Apples	Reduced fruit yield	Impaired colour development	(Tian et al., 2023b)
Broccoli	Smaller head size and lighter weight	Lower vitamin C content	(Almeida et al., 2020)
Strawberries	Lower yield and smaller size of the fruits	Reduced sweetness	(Trejo-Téllez and Gómez-Merino, 2014)
Pickles	Lower fruit set and yield	Impaired crispness and texture	(Aparna and Singh, 2018)
Lettuce	Reduced head formation	Lower antioxidant capacity	(Pacumbaba and Beyl, 2011; Preciado-Mongui et al., 2023)
Paprika	Lower fruit yield and smaller size	Decreased vitamin content	(Massimi and Radocz, 2021)
Green beans	Lower pod production	Less tenderness and poorer taste	(Shehata et al., 2015; Salcido-Martinez et al., 2020)

within the plant, which can exacerbate symptoms of Mg^{2+} deficiency and further hinder plant growth (Hermans and Verbruggen, 2005; Cakmak and Yazici, 2010; Malvi, 2011). As a cofactor for numerous enzymatic reactions, Mg^{2+} plays a key role in many plant metabolic processes. Therefore, Mg^{2+} deficiency can disrupt these functions and impede essential biochemical processes, such as carbohydrate metabolism and protein synthesis (Hermans and Verbruggen, 2005; Hermans et al., 2005; Farhat et al., 2014). Mg^{2+} deficiency can also weaken plants, making them more susceptible to various stress factors, such as drought, high temperatures, and diseases. This compromises the ability of plants to withstand and recover from adverse environmental conditions, leading to potential yield losses (Hermans and Verbruggen, 2005; Hermans et al., 2005; Ceppi et al., 2012). In addition to affecting yield, Mg^{2+} deficiency can negatively affect crop quality. With reduced chlorophyll content, the color, taste, and nutritional value of crops can be adversely affected (Hermans and Verbruggen, 2005; Nedim and Damla, 2015; Wang et al., 2020). Furthermore, visible symptoms such as chlorosis and necrosis can negatively impact the marketability and consumer acceptance of the produce (Hermans and Verbruggen, 2005; Cakmak and Yazici, 2010). To minimize these negative effects, it is critical to detect and rectify Mg^{2+} deficiencies in a timely manner. Soil and plant tissue analyses can be used to identify deficiencies, and appropriate fertilization strategies can be implemented to correct them. By addressing Mg^{2+} deficiency, farmers can not only improve plant health and maximize productivity, but also enhance the quality of their crops.

6.2 The consequences of magnesium toxicity

Mg^{2+} is integral to the plant physiology. Adequate levels are vital for numerous metabolic processes, particularly in horticultural crops. However, excessive levels can lead to toxicity and multiple adverse effects (Marschner, 2011; Römheld, 2012). Numerous studies have investigated the nuances of the role of Mg^{2+} and its impacts when present in excess. Older leaves can show interveinal chlorosis, a distinct yellowing between the veins (Figure 3). As toxicity progresses, leaf tissues, especially along the margins, can undergo necrosis or death (Römheld, 2012). High Mg^{2+} concentrations in the soil can compete with other cations, such as Ca^{2+} and K^{+}, at the root uptake sites (Figure 2), potentially leading to deficiencies, even if the soil has ample amounts of these nutrients (Fageria, 2001; Römheld and Kirkby, 2009). An overabundance of Mg^{2+} can alter the physical properties of soil, making it sticky when wet, leading to compaction. These conditions hinder water movement and can lead to waterlogging. Additionally, compacted soil restricts aeration, thereby affecting root health and function (Kopittke and Menzies, 2007; Damm et al., 2013). Elevated Mg^{2+} levels can be toxic to root tips, stifling root growth, which in turn diminishes the plant's ability to effectively absorb essential nutrients and water (Sun L. et al., 2023). Crops such as tomatoes exposed to excessive Mg^{2+} can experience compromised fruit quality, including blossom end rot (Kwon et al., 2019). Increased Mg^{2+} concentrations in peppers were correlated with a notable reduction in essential nutrients, such as calcium, zinc, and vitamin C. This decrease in nutritional value is believed to elevate health risks for Chinese adults consuming these peppers, especially due to lowered calcium and vitamin C levels (Lu et al., 2021b). The amalgamation of effects on root health, nutrient uptake, and general plant vitality can culminate in the reduced yield of horticultural crops (Marschner, 2011). Magnesium, particularly magnesium carbonate, can alter soil pH levels, indirectly influencing the availability and uptake of other essential nutrients (Machin and Navas, 2000). To manage Mg^{2+} toxicity, a multi-pronged approach involving reduced Mg input, improved soil drainage, and the use of soil amendments is recommended. Continuous research in this domain is vital to understand the evolving challenges and mitigation strategies related to Mg^{2+} toxicity in horticulture.

6.3 Factors influencing MGTs functionality in plants

Mg^{2+} is a fundamental nutrient that plays a critical role in many plants physiological processes, including chlorophyll biosynthesis, enzyme activation, and energy metabolism. However, the uptake and homeostasis of Mg^{2+} are not isolated events; they are influenced by a

multitude of internal and external factors. Transcriptional regulators, hormonal cues, inter-nutrient dynamics, and environmental stresses converge to determine the function of MGTs in plants. These MGTs, in turn, dictate how well plants adapt to fluctuating soil Mg^{2+} levels and optimize their growth and development (Hermans et al., 2010b; Chaudhry et al., 2021; Ishfaq et al., 2022).

6.3.1 Hormonal interactions influencing MGTs expression in plants

Ethylene, a key phytohormone, plays a crucial role in modulating numerous growth and developmental processes in plants, including responses to Mg^{2+} starvation. This is exemplified by the induction of specific isoforms of the 1-aminocyclopropane-1-carboxylic acid synthase (ACS) family under Mg-deficient conditions. Notably, the *ACS11* gene becomes active in both roots and leaves, whereas *ACS2, ACS7*, and *ACS8* are primarily expressed in leaves, underscoring the profound role of ethylene in the Mg^{2+} starvation response (Hermans et al., 2010b). In addition to ethylene, other hormones also intersect with Mg^{2+} regulation. For instance, MGT has been identified as being under the control of JA (Chen et al., 2010). There is also evidence that hormones such as ABA and GA are responsive to Mg^{2+} toxicity. In particular, signaling factors, such as DELLA and ABI1, associated with ABA and GA, have been implicated in reactions to Mg^{2+} toxicity (Guo et al., 2014). Delving into specific genes, the *AtMHX* gene in *Arabidopsis thaliana* is noteworthy. This gene encodes a vacuolar transporter that is crucial for maintaining the metal and proton balance within cells, an essential process for photosynthesis. While both auxin and ABA influence *AtMHX's* expression, it is especially active in tissues with photosynthetic potential. However, Mg toxicity can suppress its expression, although the exact upstream regulators in response to Mg levels have yet to be identified (David-Assael et al., 2006; Guo et al., 2014).

6.3.2 Interactions between Mg^{2+} and other nutrients in plant physiology

Mg^{2+} uptake and MGT expression are not only influenced by Mg^{2+} availability but also by interactions with other nutrients. The balance between Mg^{2+} and other elements, particularly calcium, is pivotal for maintaining nutrient homeostasis in plants (Lenz et al., 2013). Soil factors, such as type, pH, and temperature, play instrumental roles in nutrient uptake. For instance, high availability of K^+ in the soil can potentially limit Mg^{2+} uptake because some MGTs also transport K^+. In such cases, K^+ may compete for transporter-binding sites, thereby reducing Mg^{2+} uptake. However, this interference is not reciprocal; elevated levels of Mg^{2+} do not typically hinder K^+ uptake owing to the specificity of K^+ transporters (Gransee and Führs, 2013). The importance of these interactions is further highlighted under specific environmental stresses. In rice, the Mg^{2+} transporter *OsMGT1* not only aids in Mg^{2+} uptake but also plays a pivotal role in salt stress tolerance. It is believed to modulate the transport activity of the *OsHKT1;5* sodium transporter, thus preventing excessive sodium accumulation in the plant shoots, which could otherwise be detrimental (Chen et al., 2017). Moreover, the influence of other nutrients on Mg uptake and MGT expression extends beyond that of K^+. For example, the *AtMGT1* transporter, while primarily responsible for Mg^{2+} transport, also has the capacity to transport other divalent cations, albeit at non-typical physiological concentrations (Li et al., 2001).

6.3.3 Genetic influences on MGT expression and function in plants

MGTs expression in plants is intricately regulated by a complex network of genetic factors. Key transcription factors such as the MYB and WRKY families have been identified as significant players in this regulatory matrix. For instance, distinct genes, such as *MYB108* and *WRKY75*, which display differential expression under Mg^{2+} deficiency (MD) in banana seedlings, have revealed an essential role in root hair development under MD conditions. *MYB108*'s function appears multifaceted, as it is also implicated in processes such as wound healing, and potentially in the regulation of genes linked to chlorophyll catabolism (Cui et al., 2013; Xu X. F. et al., 2021). The differential MGT activities observed across plant genotypes could be rooted in genetic polymorphisms within the regulatory regions of these genes. Highlighting the importance of individual MGTs, overexpression of *PtrMGT5* in Arabidopsis demonstrated enhanced tolerance to MD, as evidenced by increased plant weight and Mg^{2+} content (Liu et al., 2019). Further emphasizing the importance of proper MGT regulation, combined knockouts of specific Arabidopsis genes, *AtMRS2-1* and *AtMRS2-5*, led to pronounced developmental delays when exposed to low Mg^{2+} conditions (Lenz et al., 2013). The intricate connection between Mg^{2+} and other elements, particularly Ca^{2+}, indicates a delicate balance in plant nutrient homeostasis. Under Mg^{2+} scarcity conditions, reducing calcium concentrations can ameliorate adverse growth effects, underscoring the tight link between these divalent cations (Lenz et al., 2013).

6.3.4 Internal Mg^{2+} status and nutrient homeostasis

A balanced mineral supply is vital for plant growth. Plants have evolved mechanisms to manage ion concentrations either by preventing excess ion entry or by sequestering them in vacuoles. *MRS2* transporters are central to maintaining Mg^{2+} homeostasis under various conditions. Some *MRS2* transporters, such as *MRS2-2* and *MRS2-7*, have been identified with innate polymorphisms; MGTs functionality in plants is influenced by a web of interconnected factors, spanning from environmental to genetic scales (Turner et al., 2010; Oda et al., 2016). Given that Mg2 + plays a central role in plant physiology, understanding these influencing factors offers a roadmap for improving plant health and productivity in various and often challenging environments.

7 Strategies for magnesium management in horticulture

Effective management of Mg^{2+} is pivotal for optimal plant nutrition and prevention of deficiency symptoms in horticultural crops. Accordingly, strategies such as regular soil testing, appropriate

fertilization, and vigilant plant monitoring are essential to ensure sufficient Mg^{2+} levels for crop growth and productivity. Effective management of Mg^{2+} is paramount for ensuring the optimal nutrition of plants and preventing deficiency symptoms in horticultural crops. Some of the strategies to manage Mg^{2+} levels in the soil include conducting regular soil tests, which can provide insights into the Mg^{2+} content of the soil as well as the soil pH, both of which can guide decisions about nutrient management. Regular testing of plant tissues can provide an accurate representation of the Mg^{2+} status within plants, allowing for the early detection of deficiencies or imbalances (Cakmak and Yazici, 2010; Gransee and Führs, 2013). Adjusting the soil pH is vital for optimal Mg^{2+} availability. In acidic soils (pH below 6.0), liming with materials such as dolomitic lime can help increase pH and Mg^{2+} availability. In alkaline soils, pH must be reduced using acidifiers to increase Mg^{2+} availability. Furthermore, chelated Mg can be used effectively in alkaline soils, as it is more soluble and available to plants than inorganic sources at higher pH levels (Gransee and Führs, 2013). Incorporating Mg^{2+}-containing fertilizers, such as magnesium sulfate (Epsom salt) or magnesium oxide, into a balanced fertilization program can help provide Mg^{2+} to plants. While Epsom salt is highly soluble and provides an immediate source of Mg^{2+}, magnesium oxide is a slow-release fertilizer that provides Mg^{2+} over an extended period (Cakmak and Yazici, 2010; Gransee and Führs, 2013).

In cases of severe Mg^{2+} deficiency, the foliar application of Mg^{2+} may be an effective strategy. Spraying soluble sources of Mg^{2+}, such as magnesium sulfate, directly onto the leaves can quickly correct this deficiency (He et al., 2022). In a study on pomelo orchards in South China, adding Mg^{2+} to optimized fertilization significantly boosted yield, fruit quality, and economic benefits by up to 15% compared to traditional practices, while reducing greenhouse gas emissions and energy inputs by over 20%. This suggests that optimized fertilization can enhance productivity and sustainability under acidic soil conditions (Chen et al., 2022). Incorporating organic matter, such as compost or well-rotted manure, into the soil can help improve soil structure, cation exchange capacity, and nutrient storage, thereby improving the availability of Mg^{2+} in the soil (Gransee and Führs, 2013). Moreover, proper irrigation management is essential to ensure Mg^{2+} availability. Maintaining optimal soil moisture levels aids the efficient uptake of Mg^{2+} by plants (Marschner, 2011). Crop rotation and use of cover crops can also contribute to the management of Mg^{2+} in the soil. Different crops have different Mg^{2+} requirements, which can help to avoid excessive nutrient depletion or imbalances (Mauro et al., 2015). Regular review and refinement of management practices are also necessary to ensure the optimization of Mg^{2+} availability and utilization (Yeh et al., 2000; Verbruggen and Hermans, 2013). Implementing these strategies, while considering the specific requirements of the crop and soil conditions, can effectively manage Mg^{2+} levels in horticultural crops and support optimal growth, nutrition, and productivity.

7.1 Breeding and genetic engineering strategies to improve magnesium uptake and utilization in crop plants

Mg^{2+} is a pivotal nutrient that is integral to many physiological processes in plants, including photosynthesis and various cellular functions. Proper absorption and utilization in horticultural crops are vital for achieving desirable yield and quality (Adnan et al., 2021). Recently, the interplay of molecular and genetic studies has opened avenues for the development of robust strategies to enhance magnesium uptake in crops. Traditional breeding methods have capitalized on vast natural genetic variations associated with Mg^{2+} absorption and utilization. Diverse germplasm collections serve as a rich reservoir, where researchers have identified genotypes exhibiting superior nutrient uptake or resilience under nutrient-deficient scenarios (Kudapa et al., 2023). Complementing this approach is Quantitative Trait Locus (QTL) Mapping. This powerful technique identifies genomic regions intrinsically linked to magnesium-related traits, paving the way for the rapid marker-assisted breeding of magnesium-optimized plants (Zhi et al., 2023). Delving deeper, studies centered on the Malvaceae family, particularly Theobroma cacao and Gossypium hirsutum, have been revelatory. They have uncovered key MGT genes that regulate Mg^{2+} transport, offering invaluable insights for breeding not only within Malvaceae but extending to other families such as Cucurbitaceae (Heidari et al., 2021; Heidari et al., 2022). Concurrently, the realm of genetic engineering has seen remarkable advancements, presenting precise mechanisms for optimizing Mg^{2+} in crops. One such strategy involves the introduction and silencing of specific genes. For instance, the introduction of genes like *AtMGT1* into *Nicotiana benthamiana* has showcased enhanced magnesium absorption and resilience against adversities like aluminum toxicity (Deng et al., 2006). In contrast, silencing genes, such as *MGT6* in *Arabidopsis thaliana*, have been shown to have indispensable roles in magnesium uptake (Yan et al., 2018). Further magnification of the genetic precision was performed using the CRISPR-Cas9 system. Its application in editing the MgCh gene in sugarcane, pivotal for chlorophyll synthesis, is a testament to its transformative potential (Eid et al., 2021). In addition, the fascinating symbiotic relationship between plants and mycorrhizal fungi can be harnessed to enhance Mg^{2+} uptake. Beneficial fungi, in particular, have demonstrated their capability to amplify magnesium absorption in specific crops under stress, such as the salt affected Sesbania species (Giri and Mukerji, 2004).

Merging traditional breeding with advanced genomic tools can capture selection precision. In-depth genomic analyses of crops such as *Vitis vinifera* have unearthed SNPs intricately tied to Mg^{2+} uptake, offering refined markers for breeding programs (Eid et al., 2021). In addition, discoveries in *Camellia sinensis* and *Vitis vinifera* have highlighted pivotal Mg^{2+} transporter genes, enriching our understanding of Mg^{2+} uptake and adaptive stress responses (Tang et al., 2021; Ge M. et al., 2022). The combined efforts of breeding and genetic engineering present a bright future for enhancing Mg^{2+} utilization in crops. As our understanding of the crucial role of Mg^{2+} in plant health deepens, it is essential to weave these insights into practical agricultural techniques. As we venture further into this pioneering domain, thorough assessments of altered crops remain imperative for maintaining both environmental balance and food safety. Together, grounded in comprehensive research, these methods promise a sustainable agricultural future, particularly for areas with Mg^{2+} deficiencies, reinforcing the pillars of global food security.

7.2 Nano-Mg and integrated approaches: pioneering advances in horticultural crops

At the crossroads of food security and sustainable agriculture, nanotechnology has become an innovative solution. The application of Mg^{2+} nanoparticles stands out in this field, especially when addressing plant nutrition challenges (Singh and Shukla, 2020; Hayat et al., 2023). Although Mg^{2+} is a vital macronutrient, its occasional scarcity poses challenges. Nanofertilizers are lauded for their exceptional physicochemical traits, such as heightened reactivity and extensive surface area, and are a promising alternative to their traditional counterparts. By offering increased agricultural yields and acting as a protective shield against both biotic and abiotic stresses, they pave the way for a sustainable agricultural future by minimizing ecological impacts. In particular, magnesium oxide nanoparticles (MgO NPs) have garnered significant attention. Their biodegradability and non-toxicity coupled with their diverse applications make them indispensable. Fernandes et al. (2020) spotlighted their versatility, highlighting their role in areas ranging from environmental waste treatment to advanced medical applications, like anti-cancer treatments. Further accentuating the role of nanotechnology in agriculture is its potential to revolutionize plant breeding and genetic transformation processes. As Singh and Shukla (2020) posited, this cutting-edge technology is set to anchor future agricultural advancements. One of its most prominent manifestations is the rise of nanofertilizers. These advanced fertilizers, characterized by their vast surface areas and consistent nutrient release, have been championed by researchers, such as Yaseen Aljanabi (2021), as the next step in optimizing crop yields while mitigating environmental concerns associated with excessive agrochemical usage. Furthermore, bean plants showed optimized biomass and photosynthetic pigment production when treated with precise dosages of Mg NPs, as documented by Salcido-Martinez et al. (2020).

Luo et al. (2020) added another dimension to this burgeoning field by demonstrating the positive effects of nanometer MgOH on Chinese cabbage, especially under the stress of cadmium pollution, a common agricultural concern. Addressing another critical environmental concern in agriculture, the contamination by metalloids like arsenic, Faizan et al. (2022) explored the potential of MgOH. Their study highlighted the dual role of NPs in promoting plant growth in contaminated environments and simultaneously mitigating the oxidative stress induced by such pollutants. As for disease control, the versatility of Mg-NPs are noteworthy. Liao et al., in a series of studies from 2019 and 2021, brought to light the significant bactericidal activity of nano-sized MgO particles, suggesting them as potent, eco-friendly alternatives to traditional copper-based bactericides. Their findings are particularly timely given the increasing global challenges posed by Cu-tolerant pathogens in agriculture. Andreadelli et al. (2021) highlighted that hydrated MgO NPs sprays resulted in a profound alteration of the tomato phylloplane microbiota. This modification strengthens their immune systems, leading to a 70% reduction in fungal infestation. However, tomatoes are not the only beneficiaries. In a groundbreaking study by Wang et al. (2022), it was revealed that potatoes treated with MgO NPs garnered a protective layer against the notorious pathogen Phytophthora infestans. Beyond crop health, the sustainability wave driven by nanotechnology is reshaping agricultural packaging. Kumar et al. (2020) introduced a sustainable solution by developing a biodegradable pectin-based bionanocomposite film integrated with MgOH NPs. These films are not just environmentally friendly, but also compare favorably with conventional packaging materials in terms of performance. In essence, the confluence of nanotechnology and Mg-NPs holds the promise to usher in a new era in horticulture. From fortifying crops against pests and diseases to optimizing growth and even addressing broader environmental concerns, this innovative approach paves the way for sustainable, efficient, and resilient future practices in horticulture.

8 Future directions and research needs

Although significant progress has been made in understanding the role of Mg^{2+} in horticulture, certain knowledge gaps and areas require further exploration. Addressing these gaps could guide future research and enhance our understanding of the role of Mg^{2+} in crop production. Some potential research directions and needs include the following.

Comprehensive genomic and transcriptomic studies to identify Mg^{2+}-responsive genes and transcription factors in horticultural plants. Better knowledge of the genetic regulation of Mg^{2+} uptake, transport, and utilization can pave the way for targeted breeding programs and genetic engineering strategies. Employing omics approaches such as metabolomics and proteomics to decipher the metabolic and biochemical pathways influenced by Mg^{2+} deficiency or excess (Yang et al., 2019; Cao et al., 2021). By monitoring changes in associated metabolites and proteins, researchers can unearth the underlying mechanisms and metabolic adaptations of plants to Mg^{2+} stress. Extensive research into the molecular mechanisms of Mg^{2+} transport in plants, from root uptake to distribution in various tissues and organs, is required to understand the role of transporters, channels, and regulatory factors involved in Mg^{2+} uptake, long-distance transport, and compartmentalization, which will further enhance our understanding of Mg^{2+} homeostasis in plants. Investigating the interactions between Mg^{2+} and other vital nutrients, such as calcium, potassium, and phosphorus, is essential to comprehend their synergistic and antagonistic effects on plant growth and development. Developing precise nutrient management strategies that affect spatial and temporal variations in Mg^{2+} availability and crop nutrient requirements (Chen et al., 2009). Remote sensing technologies, soil sensors, and predictive models can also be used to optimize the rates and timing of Mg^{2+} application to ensure that a precise nutrient supply meets crop needs. Probing the genetic regulation of Mg^{2+} homeostasis in horticultural crops is critical for the evolution of plant varieties with improved Mg^{2+} utilization (Hermans et al., 2013). Further studies are needed to identify and characterize the crucial genes,

transcription factors, and signaling pathways involved in Mg^{2+} recognition, transport, and distribution. Studying Mg^{2+} dynamics in different soil types, including their interactions with soil pH, organic matter, and nutrient availability, is crucial for effective nutrient management (Mikkelsen, 2010; Neina, 2019). Further research should focus on Mg^{2+} availability, mobility, and transformation in diverse soil environments under various management practices. Designing sustainable Mg^{2+} management strategies that balance nutrient availability with minimal environmental impacts is crucial (Tully and Ryals, 2017). Future research should explore innovative approaches, such as precise nutrient management, using Mg^{2+}-efficient plant genotypes, and optimizing fertilization techniques to enhance Mg^{2+} utilization and minimize nutrient losses. Examining the role of rhizosphere microbiome in regulating Mg^{2+} availability and uptake by plants is a promising research direction (Lazcano et al., 2021). Understanding the interactions between plant roots, soil microorganisms, and the Mg^{2+} cycle can provide insights into potential microbial strategies to improve Mg^{2+} uptake and nutrient acquisition. Furthermore, studies focusing on Mg^{2+} management under specific growing conditions, such as hydroponics, greenhouse cultivation, or controlled environments, would help optimize nutrient supply and crop performance. Integrating Mg^{2+} management practices with other sustainable cropping strategies, such as conservation agriculture, organic farming, and cover cropping, could provide holistic solutions (Altieri et al., 2017). The combined effects of these practices on Mg^{2+} availability, soil health, and crop performance should be evaluated to develop comprehensive approaches for improving nutrient use efficiency and sustainability. By addressing these research needs, we aim to refine our understanding of the role of Mg^{2+} in horticultural crops, improve Mg^{2+} management practices, develop nutrient-efficient crop varieties, and promote sustainable and resilient agriculture. This could fuel innovation in crop management, breeding programs, and nutrient optimization strategies, ultimately enhancing the efficiency, sustainability, and nutritional value of horticultural production.

9 Conclusion

In summary, this study emphasized the significant role of Mg^{2+} in the production and quality of horticultural crops. As a vital macronutrient, it is implicated in several physiological functions such as chlorophyll synthesis, enzyme activation, nutrient uptake, protein synthesis, and gene expression. Ensuring appropriate levels of Mg^{2+} contributes to higher quality plants by enhancing chlorophyll production, leading to vibrant leaf coloration and more efficient photosynthesis. Beyond mere aesthetics, Mg^{2+} also affects the nutrient content, flavor, texture, and shelf life of horticultural produce, increasing their consumer appeal. Conversely, Mg^{2+} deficiency can restrict plant growth, impair reproductive development, and lead to yield losses, underlining the importance of nutrients in crop yield potential. Another crucial aspect of Mg^{2+} is its role in bolstering stress tolerance, disease resistance, and pest defence mechanisms in plants. These factors can significantly affect the resilience and overall health of horticultural crops, thereby affecting their productivity and profitability. Interactions among Mg^{2+}, plants, and soil microbiomes also require mention. The role of MGTs from various cellular levels to different organ levels and compartmentalization, and their role in Mg^{2+} homeostasis are also highlighted. Mg^{2+} availability can influence the rhizosphere microbiome composition, which in turn can affect plant health and nutrient acquisition. Microbial activities in the rhizosphere can also affect Mg^{2+} availability and form, which can affect plant uptake and utilization. Efficient Mg^{2+} management strategies, including soil testing, balanced fertilization, and precise nutrient management, are integral to ensuring optimal Mg^{2+} availability and utilization in horticultural cropping systems. Emphasizing the importance of Mg^{2+} and implementing effective management practices can enhance crop quality, yield, stress tolerance, and disease resistance. Ultimately, this can optimize horticultural productivity and profitability, underscoring the need for continued research and innovation in Mg^{2+} management in horticulture.

Author contributions

NA: Conceptualization, Formal Analysis, Investigation, Methodology, Software, Visualization, Writing – original draft, Writing – review & editing. BZ: Funding acquisition, Supervision, Writing – review & editing. BB: Investigation, Writing – review & editing. SC: Investigation, Visualization, Writing – review & editing. MR: Investigation, Writing – review & editing. JL: Conceptualization, Writing – review & editing. YL: Project administration, Writing – review & editing. FH: Methodology, Writing – review & editing. ZC: Formal Analysis, Writing – review & editing. PT: Funding acquisition, Project administration, Resources, Supervision, Writing – review & editing.

Funding

The author(s) declare financial support was received for the research, authorship, and/or publication of this article. Funding was jointly provided by the GuangDong Basic and Applied Basic Research Foundation (2023A1515030283), Agricultural Competitive Industry Discipline Team Building Project of Guangdong Academy of Agricultural Sciences (202103TD), Scarce and Quality Economic Forest Engineering Technology Research Center (2022GCZX002), and Meizhou Science and Technology Project (2021A0304001).

Conflict of interest

The authors declare that the research was conducted in the absence of any commercial or financial relationships that could be construed as a potential conflict of interest.

Publisher's note

References

Adaskaveg, J. A., and Blanco-Ulate, B. (2023). Targeting ripening regulators to develop fruit with high quality and extended shelf life. *Curr. Opin. Biotechnol.* 79, 102872. doi: 10.1016/j.copbio.2022.102872

Adhikari, S., Toretsky, J. A., Yuan, L., and Roy, R. (2006). Magnesium, essential for base excision repair enzymes, inhibits substrate binding of N-methylpurine-DNA glycosylase. *J. Biol. Chem.* 281, 29525–29532. doi: 10.1074/jbc.M602673200

Adnan, M., Tampubolon, K., Ur Rehman, F., Saeed, M. S., Hayyat, M. S., Imran, M., et al. (2021). Influence of foliar application of magnesium on horticultural crops: A review. *Agrinula: Jurnal Agroteknologi dan Perkebunan* 4, 13–21. doi: 10.36490/agri.v4i1.109

Aghofack, J. N., and Yambou, T. N. (2006). Effects of Calcium chloride and magnesium sulphate treatments on the shelf-life of climacteric banana and non-climacteric pineapple fruits. *Cameroon J. Exp. Biol.* 1, 34–38. doi: 10.4314/cajeb.v1i1.37923

Aghofack-Nguemezi, J., Noumbo, G., and Nkumbe, C. (2014). Influence of calcium and magnesium based fertilizers on fungal diseases, plant growth parameters and fruit quality of three varieties of tomato (*Solanum lycopersicum*). *J. Sci. Technol. (Ghana)* 34, 9–20. doi: 10.4314/just.v34i1.2

Allen, L. H. (2013). Magnesium. *Encyclopedia Hum. Nutr.* 3–4, 131–135. doi: 10.1016/B978-0-12-375083-9.00177-X

Almeida, H. J. d., Carmona, V. M. V., Cavalcante, V. S., Filho, A. B. C., Prado, R.d. M., Flores, R. A., et al. (2020). Nutritional and visual diagnosis in broccoli (Brassica oleracea var. italica L.) Plants: disorders in physiological activity, nutritional efficiency and metabolism of carbohydrates. *Agronomy* 10, 1572.

Altieri, M. A., Nicholls, C. I., and Montalba, R. (2017). Technological approaches to sustainable agriculture at a crossroads: An agroecological perspective. *Sustainability* 9, 349. doi: 10.3390/su9030349

Andreadelli, A., Petrakis, S., Tsoureki, A., Tsiolas, G., Michailidou, S., Baltzopoulou, P., et al. (2021). Effects of magnesium oxide and magnesium hydroxide microparticle foliar treatment on tomato pr gene expression and leaf microbiome. *Microorganisms* 9, 1217. doi: 10.3390/microorganisms9061217

Aparna, C. A. K., and Singh, P. K. (2018). Estimation of toxic, trace and essential metals (Pb, cd, Fe, Zn, Mn, Cu, Mg, K) in fruit and vegetable product (jam, ketchup, pickles) by atomic absorption spectrophotometer. *Pharm. Innov.* 7, 313–317.

Assunção, A. G. L., Cakmak, I., Clemens, S., González-Guerrero, M., Nawrocki, A., and Thomine, S. (2022). Micronutrient homeostasis in plants for more sustainable agriculture and healthier human nutrition. *J. Exp. Bot.* 73, 1789–1799. doi: 10.1093/jxb/erac014

Bashir, M. A., Noreen, A., Ikhlaq, M., Shabir, K., Altaf, F., and Akhtar, N. (2019). Effect of Boric acid, Potassium nitrate and Magnesium sulphate on Managing Fruit Cracking and Improving Fruit Yield and Quality of Pomegranate. *J. Hortic. Sci. Technol.* 2, 49–53. doi: 10.46653/jhst190202049

Bin, M., Yi, G., and Zhang, X. (2023). Discovery and characterization of magnesium transporter (MGT) gene family in Citrus sinensis and their role in magnesium deficiency stress. *Plant Growth Regul.* 100, 733–746. doi: 10.1007/s10725-023-00973-7

Boaretto, R. M., Hippler, F. W. R., Ferreira, G. A., Azevedo, R. A., Quaggio, J. A., and Mattos, D. (2020). The possible role of extra magnesium and nitrogen supply to alleviate stress caused by high irradiation and temperature in lemon trees. *Plant Soil* 457, 57–70. doi: 10.1007/s11104-020-04597-y

Borowski, E., and Michalek, S. (2010). The effect of foliar nutrition of spinach (Spinacia oleracea L.) with magnesium salts and urea on gas exchange, leaf yield and quality. *Acta Agrobot* 63.

Bose, J., Babourina, O., and Rengel, Z. (2011). Role of magnesium in alleviation of aluminium toxicity in plants. *J. Exp. Bot.* 62, 2251–2264. doi: 10.1093/jxb/erq456

Cakmak, I., and Kirkby, E. A. (2008). Role of magnesium in carbon partitioning and alleviating photooxidative damage. *Physiol. Plant* 133, 692–704. doi: 10.1111/J.1399-3054.2007.01042.X

Cakmak, I., and Yazici, A. M. (2010). Magnesium: A forgotten element in crop production. *Better Crops* 94, 23–25.

Cao, Q., Li, L., Yang, Z., Wang, Y., Li, J., Chen, W., et al. (2021). Transcriptome analysis of genes in response to magnesium nitrate stress on cucumber leaf. *Sci. Hortic.* 288, 110391. doi: 10.1016/j.scienta.2021.110391

Ceppi, M. G., Oukarroum, A., Çiçek, N., Strasser, R. J., and Schansker, G. (2012). The IP amplitude of the fluorescence rise OJIP is sensitive to changes in the photosystem I content of leaves: a study on plants exposed to magnesium and sulfate deficiencies, drought stress and salt stress. *Physiol. Plant* 144, 277–288. doi: 10.1111/j.1399-3054.2011.01549.x

Ceylan, Y., Kutman, U. B., Mengutay, M., and Cakmak, I. (2016). Magnesium applications to growth medium and foliage affect the starch distribution, increase the grain size and improve the seed germination in wheat. *Plant Soil* 406, 145–156. doi: 10.1007/s11104-016-2871-8

Chaudhry, A. H., Nayab, S., Hussain, S. B., Ali, M., and Pan, Z. (2021). Current understandings on magnesium deficiency and future outlooks for sustainable agriculture. *Int. J. Mol. Sci.* doi: 10.3390/ijms22041819

Chen, W., Bell, R. W., Brennan, R. F., Bowden, J. W., Dobermann, A., Rengel, Z., et al. (2009). Key crop nutrient management issues in the Western Australia grains industry: a review. *Soil Res.* 47, 1–18. doi: 10.1071/SR08097

Chen, Y., Hoehenwarter, W., and Weckwerth, W. (2010). Comparative analysis of phytohormone-responsive phosphoproteins in Arabidopsis thaliana using TiO2-phosphopeptide enrichment and mass accuracy precursor alignment. *Plant J.* 63, 1–17. doi: 10.1111/j.1365-313X.2010.04218.x

Chen, Q., Kan, Q., Wang, P., Yu, W., Yu, Y., Zhao, Y., et al. (2014). Phosphorylation and interaction with the 14-3-3 protein of the plasma membrane H+-ATPase are involved in the regulation of magnesium-mediated increases in aluminum-induced citrate exudation in broad bean (Vicia faba. L). *Plant Cell Physiol.* 56, 1144–1153. doi: 10.1093/pcp/pcv038

Chen, Z. C., and Ma, J. F. (2013). Magnesium transporters and their role in Al tolerance in plants. *Plant Soil* 368, 51–56. doi: 10.1007/s11104-012-1433-y

Chen, Z. C., Peng, W. T., Li, J., and Liao, H. (2018). Functional dissection and transport mechanism of magnesium in plants. *Semin. Cell Dev. Biol.* 74, 142–152. doi: 10.1016/j.semcdb.2017.08.005

Chen, X., Wang, Z., Muneer, M. A., Ma, C., He, D., White, P. J., et al. (2023). Short planks in the crop nutrient barrel theory of China are changing: Evidence from 15 crops in 13 provinces. *Food Energy Secur* 12, e389. doi: 10.1002/fes3.389

Chen, Z. C., Yamaji, N., Horie, T., Che, J., Li, J., An, G., et al. (2017). A magnesium transporter OsMGT1 plays a critical role in salt tolerance in rice. *Plant Physiol.* 174, 1837–1849. doi: 10.1104/pp.17.00532

Chen, X., Yan, X., Muneer, M. A., Weng, X., Cai, Y., Ma, C., et al. (2022). Pomelo green production on acidic soil: reduce traditional fertilizers, but do not ignore magnesium. *Front. Sustain Food Syst.* 6. doi: 10.3389/fsufs.2022.948810

Crusciol, C. A. C., Moretti, L. G., Bossolani, J. W., Moreira, A., Micheri, P. H., and Rossi, R. (2019). Can dunite promote physiological changes, magnesium nutrition and increased corn grain yield? *Commun. Soil Sci. Plant Anal.* 50, 2343–2353. doi: 10.1080/00103624.2019.1659304

Cui, F., Brosché, M., Sipari, N., Tang, S., and Overmyer, K. (2013). Regulation of ABA dependent wound induced spreading cell death by MYB108. *New Phytol.* 200, 634–640. doi: 10.1111/nph.12456

Damm, S., Hofmann, B., Gransee, A., and Christen, O. (2013). Zur Wirkung von Kalium auf ausgewählte bodenphysikalische Eigenschaften und den Wurzeltiefgang landwirtschaftlicher Kulturpflanzen. *Arch. Agron. Soil Sci.* 59, 1–19. doi: 10.1080/03650340.2011.596827

David-Assael, O., Berezin, I., Shoshani-Knaani, N., Saul, H., Mizrachy-Dagri, T., Chen, J., et al. (2006). AtMHX is an auxin and ABA-regulated transporter whose expression pattern suggests a role in metal homeostasis in tissues with photosynthetic potential. *Funct. Plant Biol.* 33, 661–672. doi: 10.1071/FP05295

Deng, W., Luo, K., Li, D., Zheng, X., Wei, X., Smith, W., et al. (2006). Overexpression of an Arabidopsis magnesium transport gene, AtMGT1, in Nicotiana benthamiana confers Al tolerance. *J. Exp. Bot.* 57, 4235–4243. doi: 10.1093/jxb/erl201

Djabou, A. S. M., Qin, Y., Thaddee, B., Figueiredo, P. G., Feifei, A., Carvalho, L. J. C. B., et al. (2018). Effects of calcium and magnesium fertilization on antioxidant activities during cassava postharvest physiological deterioration. *Crop Sci.* 58, 1385–1392. doi: 10.2135/cropsci2017.09.0526

Douglas-Gallardo, O. A., Murillo-López, J. A., Oller, J., Mulholland, A. J., and Vöhringer-Martinez, E. (2022). Carbon dioxide fixation in ruBisCO is protonation-state-dependent and irreversible. *ACS Catal* 12, 9418–9429. doi: 10.1021/acscatal.2c01677

Du, Y., Li, J., Cun, D., Zhu, C., Liu, H., Li, D., et al. (2021). Effect of low magnesium stress on mineral element contents in various organs, yield and fruit quality in different lemon varieties. *J. Fruit Sci.* 38, 1330–1339. doi: 10.13925/j.cnki.gsxb.20200213

Eid, A., Mohan, C., Sanchez, S., Wang, D., and Altpeter, F. (2021). Multiallelic, targeted mutagenesis of magnesium chelatase with CRISPR/cas9 provides a rapidly scorable phenotype in highly polyploid sugarcane. *Front. Genome Ed* 3. doi: 10.3389/fgeed.2021.654996

El-Metwaly, H. M. B., and Mansour, F. Y. O. (2019). Effect of addition methods of magnesium and calcium foliar application on productivity and quality of potato crop in winter plantation. *Fayoum J. Agric. Res. Dev.* 33, 148–158. doi: 10.21608/fjard.2019.190242

El-Sharkawy, H. H. A., Rashad, Y. M., El-kenawy, M. A., and Galilah, D. A. (2022). Magnesium carbonate elicits defense-related genes in King Ruby grapevines against downy mildew and improves its growth, yield, and berries quality. *Pestic Biochem. Physiol.* 184. doi: 10.1016/j.pestbp.2022.105075

Fageria, V. D. (2001). Nutrient interactions in crop plants. *J. Plant Nutr.* 24, 1269–1290. doi: 10.1081/PLN-100106981

Fageria, N. K., and Oliveira, J. P. (2014). Nitrogen, phosphorus and potassium interactions in upland rice. *J. Plant Nutr.* 37, 1586–1600. doi: 10.1080/01904167.2014.920362

Faiz, S., Yasin, N. A., Khan, W. U., Shah, A. A., Akram, W., Ahmad, A., et al. (2022). Role of magnesium oxide nanoparticles in the mitigation of lead-induced stress in Daucus carota: modulation in polyamines and antioxidant enzymes. *Int. J. Phytoremediation* 24, 364–372. doi: 10.1080/15226514.2021.1949263

Faizan, M., Bhat, J. A., El-Serehy, H. A., Moustakas, M., and Ahmad, P. (2022). Magnesium oxide nanoparticles (MgO-NPs) alleviate arsenic toxicity in soybean by modulating photosynthetic function, nutrient uptake and antioxidant potential. *Metals (Basel)* 12. doi: 10.3390/met12122030

Farhat, N., Elkhouni, A., Zorrig, W., Smaoui, A., Abdelly, C., and Rabhi, M. (2016). Effects of magnesium deficiency on photosynthesis and carbohydrate partitioning. *Acta Physiol. Plant* 38, 145. doi: 10.1007/S11738-016-2165-Z

Farhat, N., Rabhi, M., Krol, M., Barhoumi, Z., Ivanov, A. G., McCarthy, A., et al. (2014). Starch and sugar accumulation in Sulla carnosa leaves upon Mg 2+ starvation. *Acta Physiol. Plant* 36, 2157–2165. doi: 10.1007/s11738-014-1592-y

Fernandes, M., Singh, R. B., Sarkar, T., Singh, P., and Pratap Singh, R. (2020). Recent Applications of Magnesium Oxide (MgO) Nanoparticles in various domains. *Adv. Mater Lett.* 11, 1–10. doi: 10.5185/amlett.2020.081543

Fujikawa, I., Takehara, Y., Ota, M., Imada, K., Sasaki, K., Kajihara, H., et al. (2021). Magnesium oxide induces immunity against Fusarium wilt by triggering the jasmonic acid signaling pathway in tomato. *J. Biotechnol.* 325, 100–108. doi: 10.1016/j.jbiotec.2020.11.012

Ge, H., Shao, Q., Chen, J., Chen, J., Li, X., Tan, Y., et al. (2022). A metal tolerance protein, MTP10, is required for the calcium and magnesium homeostasis in Arabidopsis. *Plant Signal Behav.* 17, 2025322. doi: 10.1080/15592324.2021.2025322

Ge, M., Zhong, R., Sadeghnezhad, E., Hakeem, A., Xiao, X., Wang, P., et al. (2022). Genome-wide identification and expression analysis of magnesium transporter gene family in grape (Vitis vinifera). *BMC Plant Biol.* 22, 680. doi: 10.1186/s12870-022-03599-5

Gelli, A., Hawkes, C., Donovan, J., Harris, J., Allen, S. L., de Brauw, A., et al. (2015). Value chains and nutrition: A framework to support the identification, design, and evaluation of interventions. *SSRN Electronic J.* doi: 10.2139/ssrn.2564541

Gerendás, J., and Führs, H. (2013). The significance of magnesium for crop quality. *Plant Soil* 368, 101–128. doi: 10.1007/s11104-012-1555-2

Giri, B., and Mukerji, K. G. (2004). Mycorrhizal inoculant alleviates salt stress in Sesbania aEgyptiaca and Sesbania grandiflora under field conditions: Evidence for reduced sodium and improved magnesium uptake. *Mycorrhiza* 14, 307–312. doi: 10.1007/s00572-003-0274-1

Gransee, A., and Führs, H. (2013). Magnesium mobility in soils as a challenge for soil and plant analysis, magnesium fertilization and root uptake under adverse growth conditions. *Plant Soil* 368, 5–21. doi: 10.1007/S11104-012-1567-Y/FIGURES/5

Grzebisz, W. (2011). Magnesium–food and human health. *J. Elem* 16. doi: 10.5601/jelem.2011.16.2.13

Guo, W. (2017). Magnesium homeostasis mechanisms and magnesium use efficiency in plants, in: Mohammad Anwar Hossain, Takehiro Kamiya, D.J. B., Lam-Son Phan Tran and Toru Fujiwara (Eds.), *Plant Macronutrient Use Efficiency: Molecular and Genomic Perspectives in Crop Plants. Academic Press* 197–213. doi: 10.1016/B978-0-12-811308-0.00011-9

Guo, W., Cong, Y., Hussain, N., Wang, Y., Liu, Z., Jiang, L., et al. (2014). The remodeling of seedling development in response to long-term magnesium toxicity and regulation by ABA-DELLA signaling in Arabidopsis. *Plant Cell Physiol.* 55, 1713–1726. doi: 10.1093/pcp/pcu102

Guo, W., Nazim, H., Liang, Z., and Yang, D. (2016). Magnesium deficiency in plants: An urgent problem. *Crop J.* 4, 83–91. doi: 10.1016/j.cj.2015.11.003

Hamedeh, H., Antoni, S., Cocciaglia, L., and Ciccolini, V. (2022). Molecular and physiological effects of magnesium–polyphenolic compound as biostimulant in drought stress mitigation in tomato. *Plants* 11, 586. doi: 10.3390/plants11050586

Hartwig, A. (2001). Role of magnesium in genomic stability. *Mutat. Res. - Fundam. Mol. Mech. Mutagenesis*. doi: 10.1016/S0027-5107(01)00074-4

Hayat, F., Khanum, F., Li, J., Iqbal, S., Khan, U., Javed, H. U., et al. (2023). Nanoparticles and their potential role in plant adaptation to abiotic stress in horticultural crops: A review. *Sci. Hortic.* 321, 112285. doi: 10.1016/j.scienta.2023.112285

He, D., Chen, X., Zhang, Y., Huang, Z., Yin, J., Weng, X., et al. (2023). Magnesium is a nutritional tool for the yield and quality of oolong tea (Camellia sinensis L.) and reduces reactive nitrogen loss. *Sci. Hortic.* 308, 111590. doi: 10.1016/j.scienta.2022.111590

He, H., Khan, S., Deng, Y., Hu, H., Yin, L., and Huang, J. (2022). Supplemental foliar-applied magnesium reverted photosynthetic inhibition and improved biomass partitioning in magnesium-deficient banana. *Horticulturae* 8, 1050. doi: 10.3390/horticulturae8111050

Heidari, P., Abdullah, F., and Poczai, P. (2021). Magnesium transporter gene family: Genome-wide identification and characterization in theobroma cacao, corchorus capsularis, and gossypium hirsutum of family malvaceae. *Agronomy* 11, 1651. doi: 10.3390/agronomy11081651

Heidari, P., Puresmaeli, F., and Mora-Poblete, F. (2022). Genome-Wide Identification and Molecular Evolution of the Magnesium Transporter (MGT) Gene Family in Citrullus lanatus and Cucumis sativus. *Agronomy* 12, 2253. doi: 10.3390/agronomy12102253

Hermans, C., Bourgis, F., Faucher, M., Strasser, R. J., Delrot, S., and Verbruggen, N. (2005). Magnesium deficiency in sugar beets alters sugar partitioning and phloem loading in young mature leaves. *Planta* 220, 541–549. doi: 10.1007/s00425-004-1376-5

Hermans, C., Conn, S. J., Chen, J., Xiao, Q., and Verbruggen, N. (2013). An update on magnesium homeostasis mechanisms in plants. *Metallomics*. 5, 1170–1183. doi: 10.1039/c3mt20223b

Hermans, C., and Verbruggen, N. (2005). Physiological characterization of Mg deficiency in Arabidopsis thaliana. *J. Exp. Bot.* 56, 2153–2161. doi: 10.1093/jxb/eri215

Hermans, C., Vuylsteke, M., Coppens, F., Craciun, A., Inzé, D., and Verbruggen, N. (2010a). Early transcriptomic changes induced by magnesium deficiency in Arabidopsis thaliana reveal the alteration of circadian clock gene expression in roots and the triggering of abscisic acid-responsive genes. *New Phytol.* 187, 119–131. doi: 10.1111/j.1469-8137.2010.03258.x

Hermans, C., Vuylsteke, M., Coppens, F., Cristescu, S. M., Harren, F. J. M., Inzé, D., et al. (2010b). Systems analysis of the responses to long-term magnesium deficiency and restoration in Arabidopsis thaliana. *New Phytol.* 187, 132–144. doi: 10.1111/j.1469-8137.2010.03257.x

Hou, J., Cheng, X., Li, J., and Dong, Y. (2021). Magnesium and nitrogen drive soil bacterial community structure under long-term apple orchard cultivation systems. *Appl. Soil Ecol.* 167, 104103. doi: 10.1016/J.APSOIL.2021.104103

Huang, S., Zhang, X., and Fernando, W. G. D. (2020). Directing trophic divergence in plant-pathogen interactions: antagonistic phytohormones with NO doubt? *Front. Plant Sci* 11, 600063. doi: 10.3389/fpls.2020.600063

Huber, D. M., and Jones, J. B. (2013). The role of magnesium in plant disease. *Plant Soil* 368, 73–85. doi: 10.1007/s11104-012-1476-0

Igamberdiev, A. U., and Kleczkowski, L. A. (2011). Magnesium and cell energetics in plants under anoxia. *Biochem. J.* doi: 10.1042/BJ20110213

Ishfaq, M., Wang, Y., Yan, M., Wang, Z., Wu, L., Li, C., et al. (2022). Physiological essence of magnesium in plants and its widespread deficiency in the farming system of China. *Front. Plant Sci.* 13. doi: 10.3389/fpls.2022.802274

Jamali Jaghdani, S., Jahns, P., and Tränkner, M. (2021). The impact of magnesium deficiency on photosynthesis and photoprotection in Spinacia oleracea. *Plant Stress* 2, 100040. doi: 10.1016/j.stress.2021.100040

Jiao, J., Li, J., Chang, J., Li, J., Chen, X., Li, Z., et al. (2023). Magnesium effects on carbohydrate characters in leaves, phloem sap and mesocarp in wax gourd (Benincasa hispida (Thunb.) cogn.). *Agronomy* 13, 455. doi: 10.3390/agronomy13020455

Jin, X., Ackah, M., Wang, L., Amoako, F. K., Shi, Y., Essoh, L. G., et al. (2023). Magnesium nutrient application induces metabolomics and physiological responses in mulberry (Morus alba) plants. *Int. J. Mol. Sci.* 24, 9650. doi: 10.3390/IJMS24119650/S1

Jin, S., Zhou, W., Meng, L., Chen, Q., and Li, J. (2022). Magnesium fertilizer application and soil warming increases tomato yield by increasing magnesium uptake under PE-film covered greenhouse. *Agronomy* 12, 940. doi: 10.3390/agronomy12040940

Johansson, M. J. O., and Jacobson, A. (2010). Nonsense-mediated mRNA decay maintains translational fidelity by limiting magnesium uptake. *Genes Dev.* 24, 1491–1495. doi: 10.1101/gad.1930710

Kanjana, D. (2020). Foliar application of magnesium oxide nanoparticles on nutrient element concentrations, growth, physiological, and yield parameters of cotton. *J. Plant Nutr.* 43, 3035–3049. doi: 10.1080/01904167.2020.1799001

Kashinath, B. L., Murthy, A. N. G., Senthivel, T., Pitchai, G. J., and Sadashiva, A. T. (2013). Effect of applied magnesium on yield and quality of tomato in Alfisols of Karnataka. *J. Hortic. Sci.* 8, 55–59. doi: 10.24154/jhs.v8i1.335

Kleczkowski, L. A., and Igamberdiev, A. U. (2021). Magnesium signaling in plants. *Int. J. Mol. Sci.* 22, 1159.22. doi: 10.3390/IJMS22031159

Kleczkowski, L. A., and Igamberdiev, A. U. (2023). Magnesium and cell energetics: At the junction of metabolism of adenylate and non-adenylate nucleotides. *J. Plant Physiol.* 280, 53901. doi: 10.1016/J.JPLPH.2022.153901

Kobayashi, N. I., Iwata, N., Saito, T., Suzuki, H., Iwata, R., Tanoi, K., et al. (2013). Application of 28 Mg for characterization of Mg uptake in rice seedling under different pH conditions. *J. Radioanal Nucl. Chem.* 296, 531–534. doi: 10.1007/s10967-012-2010-9

Kobayashi, N. I., and Tanoi, K. (2015). Critical issues in the study of magnesium transport systems and magnesium deficiency symptoms in plants. *Int. J. Mol. Sci.* 16, 23076–23093. doi: 10.3390/ijms160923076

Koch, M., Winkelmann, M. K., Hasler, M., Pawelzik, E., and Naumann, M. (2020). Root growth in light of changing magnesium distribution and transport between source and sink tissues in potato (Solanum tuberosum L.). *Sci. Rep.* 10, 8796. doi: 10.1038/s41598-020-65896-z

Kopittke, P. M., and Menzies, N. W. (2007). A review of the use of the basic cation saturation ratio and the "ideal". *soil. Soil Sci. Soc. America J.* 71, 259–265. doi: 10.2136/sssaj2006.0186

Koyama, H., Toda, T., and Hara, T. (2001). Brief exposure to low-pH stress causes irreversible damage to the growing root in Arabidopsis thaliana: pectin–Ca interaction may play an important role in proton rhizotoxicity. *J. Exp. Bot.* 52, 361–368.

Kudapa, H., Barmukh, R., Vemuri, H., Gorthy, S., Pinnamaneni, R., Vetriventhan, M., et al. (2023). Genetic and genomic interventions in crop biofortification: Examples in millets. *Front. Plant Sci* 14, 1123655. doi: 10.3389/fpls.2023.1123655

Kumar, M., Giri, V. P., Pandey, S., Gupta, A., Patel, M. K., Bajpai, A. B., et al. (2021). Plant-growth-promoting rhizobacteria emerging as an effective bioinoculant to improve the growth, production and stress tolerance of vegetable crops. *Int. J. Mol. Sci.* 22, 12245. doi: 10.3390/ijms222212245

Kumar, N., Kaur, P., Devgan, K., and Attkan, A. K. (2020). Shelf life prolongation of cherry tomato using magnesium hydroxide reinforced bio-nanocomposite and conventional plastic films. *J. Food Process Preserv* 44, e14379. doi: 10.1111/jfpp.14379

Kumari, V. V., Banerjee, P., Verma, V. C., Sukumaran, S., Chandran, M. A. S., Gopinath, K. A., et al. (2022). Plant nutrition: an effective way to alleviate abiotic stress in agricultural crops. *Int. J. Mol. Sci.* 23, 8519. doi: 10.3390/ijms23158519

Kwon, M. C., Kim, Y. X., Lee, S., Jung, E. S., Singh, D., Sung, J., et al. (2019). Comparative metabolomics unravel the effect of magnesium oversupply on tomato fruit quality and associated plant metabolism. *Metabolites* 9, 231. doi: 10.3390/metabo9100231

Lazcano, C., Boyd, E., Holmes, G., Hewavitharana, S., Pasulka, A., and Ivors, K. (2021). The rhizosphere microbiome plays a role in the resistance to soil-borne pathogens and nutrient uptake of strawberry cultivars under field conditions. *Sci. Rep.* 11, 3188. doi: 10.1038/s41598-021-82768-2

Lefevere, H., Bauters, L., and Gheysen, G. (2020). Salicylic acid biosynthesis in plants. *Front. Plant Sci* 11, 338. doi: 10.3389/fpls.2020.00338

Lenz, H., Dombinov, V., Dreistein, J., Reinhard, M. R., Gebert, M., and Knoop, V. (2013). Magnesium deficiency phenotypes upon multiple knockout of arabidopsis thaliana MRS2 clade B genes can be ameliorated by concomitantly reduced calcium supply. *Plant Cell Physiol.* 54. doi: 10.1093/pcp/pct062

Li, H., Du, H., Huang, K., Chen, X., Liu, T., Gao, S., et al. (2016). Identification, and functional and expression analyses of the CorA/MRS2/MGT-type magnesium transporter family in maize. *Plant Cell Physiol.* 57, 1153–1168. doi: 10.1093/pcp/pcw064

Li, J., Hu, X., Zhang, R., Li, Q., Xu, W., Zhang, L., et al. (2023a). The plasma membrane magnesium transporter CsMGT5 mediates magnesium uptake and translocation under magnesium limitation in tea plants (Camellia sinensis L.). *Sci. Hortic.* 310. doi: 10.1016/j.scienta.2022.111711

Li, J., Huang, Y., Tan, H., Yang, X., Tian, L., Luan, S., et al. (2015). An endoplasmic reticulum magnesium transporter is essential for pollen development in Arabidopsis. *Plant Sci.* 231, 212–220. doi: 10.1016/j.plantsci.2014.12.008

Li, J., Li, Q. H., Zhang, X. Y., Zhang, L. Y., Zhao, P. L., Wen, T., et al. (2021). Exploring the effects of magnesium deficiency on the quality constituents of hydroponic-cultivated tea (Camellia sinensis L.) leaves. *J. Agric. Food Chem.* 69, 14278–14286. doi: 10.1021/ACS.JAFC.1C05141

Li, J., Muneer, M. A., Sun, A., Guo, Q., Wang, Y., Huang, Z., et al. (2023b). Magnesium application improves the morphology, nutrients uptake, photosynthetic traits, and quality of tobacco (Nicotiana tabacum L.) under cold stress. *Front. Plant Sci.* 14, 1078128. doi: 10.3389/FPLS.2023.1078128/BIBTEX

Li, L. G., Sokolov, L. N., Yang, Y. H., Li, D. P., Ting, J., Pandy, G. K., et al. (2008). A mitochondrial magnesium transporter functions in Arabidopsis pollen development. *Mol. Plant* 1, 675–685. doi: 10.1093/mp/ssn031

Li, L., Tutone, A. F., Drummond, R. S. M., Gardner, R. C., and Luan, S. (2001). A novel family of magnesium transport genes in arabidopsis. *Plant Cell* 13, 2761–2775. doi: 10.1105/tpc.010352

Li, J., Yang, X., Zhang, M., Li, D., Jiang, Y., Yao, W., et al. (2023c). Yield, quality, and water and fertilizer partial productivity of cucumber as influenced by the interaction of water, nitrogen, and magnesium. *Agronomy* 13, 772. doi: 10.3390/agronomy13030772

Liang, W. W., Huang, J. H., Li, C. P., Yang, L. T., Ye, X., Lin, D., et al. (2017). MicroRNA-mediated responses to long-term magnesium-deficiency in Citrus sinensis roots revealed by Illumina sequencing. *BMC Genomics* 18, 1–16. doi: 10.1186/s12864-017-3999-5

Liao, Y. Y., Huang, Y., Carvalho, R., Choudhary, M., Da Silva, S., Colee, J., et al. (2021). Magnesium oxide nanomaterial, an alternative for commercial copper bactericides: field-scale tomato bacterial spot disease management and total and bioavailable metal accumulation in soil. *Environ. Sci. Technol.* 55, 13561–13570. doi: 10.1021/acs.est.1c00804

Liao, Y. Y., Strayer-Scherer, A., White, J. C., de la Torre-Roche, R., Ritchie, L., Colee, J., et al. (2019). Particle-size dependent bactericidal activity of magnesium oxide against Xanthomonas perforans and bacterial spot of tomato. *Sci. Rep.* 9, 18530. doi: 10.1038/s41598-019-54717-7

Liu, J., Fang, L., Pei, W., Li, F., and Zhao, J. (2023). Effects of magnesium application on the arbuscular mycorrhizal symbiosis in tomato. *Symbiosis* 89, 73–82. doi: 10.1007/s13199-022-00862-z

Liu, X., Guo, L. X., Luo, L. J., Liu, Y. Z., and Peng, S. A. (2019). Identification of the magnesium transport (MGT) family in Poncirus trifoliata and functional characterization of PtrMGT5 in magnesium deficiency stress. *Plant Mol. Biol.* 101, 551–560. doi: 10.1007/s11103-019-00924-9

Liu, X., Hu, C., Liu, X., Riaz, M., Liu, Y., Dong, Z., et al. (2022). Effect of magnesium application on the fruit coloration and sugar accumulation of navel orange (Citrus sinensis Osb.). *Sci. Hortic.* 304. doi: 10.1016/j.scienta.2022.111282

Lu, M., Liang, Y., Lakshmanan, P., Guan, X., Liu, D., and Chen, X. (2021a). Magnesium application reduced heavy metal-associated health risks and improved nutritional quality of field-grown Chinese cabbage. *Environ. pollut.* 289, 117881. doi: 10.1016/j.envpol.2021.117881

Lu, M., Liu, D., Shi, Z., Gao, X., Liang, Y., Yao, Z., et al. (2021b). Nutritional quality and health risk of pepper fruit as affected by magnesium fertilization. *J. Sci. Food Agric.* 101, 582–592. doi: 10.1002/jsfa.10670

Luo, X., Zhang, C., Xu, W., Peng, Q., Jiao, L., and Deng, J. (2020). Effects of nanometer magnesium hydroxide on growth, cadmium (Cd) uptake of Chinese cabbage (Brassica campestris) and soil cd form. *Int. J. Agric. Biol.* 24, 1006–1016. doi: 10.17957/IJAB/15.1527

Lv, X., Huang, S., Wang, J., Han, D., Li, J., Guo, D., et al. (2023). Genome-wide identification of Mg2+ transporters and functional characteristics of DlMGT1 in Dimocarpus longan. *Front. Plant Sci.* 14. doi: 10.3389/fpls.2023.1110005

Lyu, M., Liu, J., Xu, X., Liu, C., Qin, H., Zhang, X., et al. (2023). Magnesium alleviates aluminum-induced growth inhibition by enhancing antioxidant enzyme activity and carbon–nitrogen metabolism in apple seedlings. *Ecotoxicol Environ. Saf.* 249, 114421. doi: 10.1016/j.ecoenv.2022.114421

Ma, Y.-Y., Shi, J.-C., Wang, D.-J., Liang, X., Wei, F., Gong, C.-M., et al. (2023). A point mutation in the gene encoding magnesium chelatase I subunit influences strawberry leaf color and metabolism. *Plant Physiol.* 192, 2737–2755. doi: 10.1093/PLPHYS/KIAD247

Machin, J., and Navas, A. (2000). Soil pH changes induced by contamination by magnesium oxides dust. *Land Degrad Dev.* 11, 37–50. doi: 10.1002/(SICI)1099-145X(200001/02)11:1<37::AID-LDR366>3.0.CO;2-8

Malvi, U. R. (2011). Interaction of micronutrients with major nutrients with special reference to potassium. *Karnataka J. Agric. Sci.* 24 (1), 106–109.

Marschner, P. (2011). *Marschner's Mineral Nutrition of Higher Plants, 3rd ed. Marschner's Mineral Nutrition of Higher Plants: Third Edition*. London: Academic press. doi: 10.1016/C2009-0-63043-9

Massimi, M., and Radocz, L. (2021). The Action of Nutrients Deficiency on Growth Biometrics, Physiological Traits, Production Indicators, and Disease Development in Pepper (Capsicum annuum L.) Plant: A review. *AMERICAN-EURASIAN J. OF Sustain. Agric.* 15, 1–19.

Mauro, R. P., Anastasi, U., Lombardo, S., Pandino, G., Pesce, R., Alessia, R., et al. (2015). Cover crops for managing weeds, soil chemical fertility and nutritional status of organically grown orange orchard in Sicily. *Ital. J. Agron.* 10, 101–104. doi: 10.4081/ija.2015.641

Mayland, H. F., and Wilkinson, S. R. (1989). Soil factors affecting magnesium availability in plant-animal systems: a review. *J. Anim. Sci.* 67, 3437–3444. doi: 10.2527/jas1989.67123437x

Meng, S. F., Zhang, B., Tang, R. J., Zheng, X. J., Chen, R., Liu, C. G., et al. (2022). Four plasma membrane-localized MGR transporters mediate xylem Mg2+ loading for root-to-shoot Mg2+ translocation in Arabidopsis. *Mol. Plant* 15, 805–819. doi: 10.1016/j.molp.2022.01.011

Mengutay, M., Ceylan, Y., Kutman, U. B., and Cakmak, I. (2013). Adequate magnesium nutrition mitigates adverse effects of heat stress on maize and wheat. *Plant Soil* 368, 57–72. doi: 10.1007/s11104-013-1761-6

Mikkelsen, R. (2010). Soil and fertilizer magnesium. *Better Crops* 94, 26–28.

Morales-Payan, J. P. (2022). Performance of 'MD-2' pineapple as affected by magnesium source and rate. *Acta Hortic.*, 367–372. doi: 10.17660/ActaHortic.2022.1333.49

Moreira, W. R., da Silva Bispo, W. M., Rios, J. A., Debona, D., Nascimento, C. W. A., and Rodrigues, F.Á. (2015). Magnesium-induced alterations in the photosynthetic performance and resistance of rice plants infected with bipolaris oryzae. *Sci. Agric.* 72, 328–333. doi: 10.1590/0103-9016-2014-0312

Morozova, L. (2022). The role of magnesium ions for the growth and development of tomatoes when growing in protected soil conditions. *Balanced Nat. using.* 10, 112–118. doi: 10.33730/2310-4678.4.2022.275039

Mullins, C. A., and Wolt, J. D. (2022). Effects of calcium and magnesium lime sources on yield, fruit quality, and elemental uptake of tomato. *J. Am. Soc. Hortic. Sci.* 108, 850–854. doi: 10.21273/jashs.108.5.850

Nedim, O., and Damla, B. O. (2015). Effect of magnesium fertilization on some plant nutrient interactions and nut quality properties in Turkish hazelnut (Corylus avellana L.). *Sci. Res. Essays* 10, 465–470. doi: 10.5897/sre2014.5811

Neina, D. (2019). The role of soil pH in plant nutrition and soil remediation. *Appl. Environ. Soil Sci.* 2019, 1–9. doi: 10.1155/2019/5794869

Nikolaou, C. N., Chatziartemiou, A., Tsiknia, M., Karyda, A. G., Ehaliotis, C., and Gasparatos, D. (2023). Calcium- and Magnesium-Enriched Organic Fertilizer and Plant Growth-Promoting Rhizobacteria Affect Soil Nutrient Availability, Plant Nutrient Uptake, and Secondary Metabolite Production in Aloe vera (Aloe barbadensis Miller) Grown under Field Conditions. *Agronomy* 13, 1–14. doi: 10.3390/agronomy13020482

Oda, K., Kamiya, T., Shikanai, Y., Shigenobu, S., Yamaguchi, K., and Fujiwara, T. (2016). The arabidopsis Mg transporter, MRS2-4, is essential for Mg homeostasis under both low and high Mg conditions. *Plant Cell Physiol.* 57, 754–763. doi: 10.1093/pcp/pcv196

Ohyama, T. (2019). New aspects of magnesium function: A key regulator in nucleosome self-assembly, chromatin folding and phase separation. *Int. J. Mol. Sci.* 20, 4232. doi: 10.3390/ijms20174232

Ota, M., Imada, K., Sasaki, K., Kajihara, H., Sakai, S., and Ito, S. (2019). MgO-induced defence against bacterial wilt disease in Arabidopsis thaliana. *Plant Pathol.* 68, 323–333. doi: 10.1111/ppa.12939

Pacumbaba, R. O. Jr., and Beyl, C. A. (2011). Changes in hyperspectral reflectance signatures of lettuce leaves in response to macronutrient deficiencies. *Adv. Space Res.* 48, 32–42. doi: 10.1016/j.asr.2011.02.020

Peng, Y. Y., Liao, L. L., Liu, S., Nie, M. M., Li, J., Zhang, L. D., et al. (2019). Magnesium deficiency triggers sgr-mediated chlorophyll degradation for magnesium remobilization. *Plant Physiol.* 181, 262–275. doi: 10.1104/PP.19.00610

Peng, W. T., Qi, W. L., Nie, M. M., Xiao, Y. B., Liao, H., and Chen, Z. C. (2020). Magnesium supports nitrogen uptake through regulating NRT2. 1/2.2 in soybean. *Plant Soil* 457, 97–111. doi: 10.1007/s11104-019-04157-z

Petrescu, D. C., Vermeir, I., and Petrescu-Mag, R. M. (2020). Consumer understanding of food quality, healthiness, and environmental impact: A cross-national perspective. *Int. J. Environ. Res. Public Health* 17. doi: 10.3390/ijerph17010169

Petrov, A. S., Bernier, C. R., Hsiao, C., Okafor, C. D., Tannenbaum, E., Stern, J., et al. (2012). RNA-magnesium-protein interactions in large ribosomal subunit. *J. Phys. Chem.* 116. doi: 10.1021/jp304723w

Potarzycki, J., Grzebisz, W., and Szczepaniak, W. (2022). Magnesium fertilization increases nitrogen use efficiency in winter wheat (Triticum aestivum L.). *Plants* 11, 2600. doi: 10.3390/plants11192600

Preciado-Mongui, I. M., Reyes-Medina, A. J., Romero-Barrera, Y., Álvarez-Herrera, J. G., and Jaime-Guerrero, M. (2023). Growth and production of crisp lettuce (Lactuca sativa L.) using different doses of nitrogen and magnesium. *Rev. Colombiana Cienc. Hortícolas* 17, e15706. doi: 10.17584/RCCH.2023V17I1.15706

Qin, Y., Li, Q., An, Q., Li, D., Huang, S., Zhao, Y., et al. (2022). A phenylalanine ammonia lyase from Fritillaria unibracteata promotes drought tolerance by regulating lignin biosynthesis and SA signaling pathway. *Int. J. Biol. Macromol* 213, 574–588. doi: 10.1016/j.ijbiomac.2022.05.161

Qin, J., Wang, H., Cao, H., Chen, K., and Wang, X. (2020). Combined effects of phosphorus and magnesium on mycorrhizal symbiosis through altering metabolism and transport of photosynthates in soybean. *Mycorrhiza* 30, 285–298. doi: 10.1007/s00572-020-00955-x

Quddus, M. A., Siddiky, M. A., Hussain, M. J., Rahman, M. A., Ali, M. R., and Masud, M. A. T. (2022). Magnesium influences growth, yield, nutrient uptake, and fruit quality of tomato. *Int. J. Vegetable Sci.* 28, 441–464. doi: 10.1080/19315260.2021.2014614

Rajitha, G., Reddy, M. S., Ramesh Babu, P. V., and Maheshwari, V. U. (2019). Influence of secondary and micronutrients on primary nutrient uptake by groundnut (Arachis hypogaea L.). *Agric. Sci. Digest - A Res. J.* 38, 285–288. doi: 10.18805/ag.d-4798

Rankelytė, G., Chmeliov, J., Gelžinis, A., and Valkūnas, L. (2023). "Excited states of chlorophyll molecules in light-harvesting antenna of PSI," in Chemistry and chemical technology: international conference CCT-2023, Vilnius: *Conference Book. Vilnius university press*. March 10, 2023. doi: 10.15388/CCT.2023

Regon, P., Chowra, U., Awasthi, J. P., Borgohain, P., and Panda, S. K. (2019). Genome-wide analysis of magnesium transporter genes in Solanum lycopersicum. *Comput. Biol. Chem.* 80, 498–511. doi: 10.1016/j.compbiolchem.2019.05.014

Rehman, H., Alharby, H. F., Alzahrani, Y., and Rady, M. M. (2018). Magnesium and organic biostimulant integrative application induces physiological and biochemical changes in sunflower plants and its harvested progeny on sandy soil. *Plant Physiol. Biochem.* 126, 97–105. doi: 10.1016/J.PLAPHY.2018.02.031

Rengel, Z., Bose, J., Chen, Q., and Tripathi, B. N. (2015). Magnesium alleviates plant toxicity of aluminium and heavy metals. *Crop Pasture Sci.* 66, 1298–1307. doi: 10.1071/CP15284

Rodrigues, V. A., Crusciol, C. A. C., Bossolani, J. W., Moretti, L. G., Portugal, J. R., Mundt, T. T., et al. (2021). Magnesium foliar supplementation increases grain yield of soybean and maize by improving photosynthetic carbon metabolism and antioxidant metabolism. *Plants* 10, 797. doi: 10.3390/plants10040797

Romani, A. M. P. (2011). Cellular magnesium homeostasis. *Arch. Biochem. Biophys.* 512, 1–23. doi: 10.1016/j.abb.2011.05.010

Römheld, V. (2012). *Diagnosis of deficiency and toxicity of nutrients, in: Marschner's Mineral Nutrition of Higher Plants, 3rd edn*. San Diego: Elsevier/Academic Press, 299–312.

Römheld, V., and Kirkby, E. A. (2009). Magnesium functions in crop nutrition and yield. *Nawozy i Nawożenie (Fertilisers Fertilization)* 34, 163–182.

Sadeghi, F., Rezeizad, A., and Rahimi, M. (2021). Effect of zinc and magnesium fertilizers on the yield and some characteristics of wheat (Triticum aestivum L.) seeds in two years. *Int. J. Agron.* 2021, 1–6. doi: 10.1155/2021/8857222

Salcido-Martinez, A., Sanchez, E., Licon-Trillo, L. P., Perez-Alvarez, S., Palacio-Marquez, A., Amaya-Olivas, N. I., et al. (2020). Impact of the foliar application of magnesium nanofertilizer on physiological and biochemical parameters and yield in green beans. *Not Bot. Horti Agrobot Cluj Napoca* 48, 2167–2181. doi: 10.15835/48412090

Salih, R. F., Ismail, T. N., and Hamad, E. M. (2023). Foliar application of NPK improves growth, yield and fiber morphological properties of some kenaf (Hibiscus cannabunus L.) varieties. *Passer J. Basic Appl. Sci.* 5, 183–190. doi: 10.24271/PSR.2023.387988.1267

Schormann, N., Hayden, K. L., Lee, P., Banerjee, S., and Chattopadhyay, D. (2019). An overview of structure, function, and regulation of pyruvate kinases. *Protein Sci.* 28, 1771–1784. doi: 10.1002/pro.3691

Senbayram, M., Gransee, A., Wahle, V., and Thiel, H. (2015). Role of magnesium fertilisers in agriculture: plant–soil continuum. *Crop Pasture Sci.* 66, 1219–1229. doi: 10.1071/CP15104

Setiawati, W., Hasyim, A., Udiarto, B. K., and Hudayya, A. (2020). Pengaruh Magnesium, Boron, dan Pupuk Hayati terhadap Produktivitas Cabai serta Serangan Hama dan Penyakit (Effect of Magnesium, Boron, and Biofertilizers on Chili Pepper Productivity and Impact of Pests and Diseases). *Jurnal Hortikultura* 30, 65–74. doi: 10.21082/jhort.v30n1.2020.p65-74

Sharma, P., Gautam, A., Kumar, V., and Guleria, P. (2022). *In vitro* exposed magnesium oxide nanoparticles enhanced the growth of legume Macrotyloma uniflorum. *Environ. Sci. pollut. Res.* 29, 13635–13645. doi: 10.1007/s11356-021-16828-5

Shaul, O. (2002). Magnesium transport and function in plants: The tip of the iceberg. *BioMetals*. 15, 307–321. doi: 10.1023/A:1016091118585

Shehata, S. A., ZA, S., M Attia, M., and Rageh, M. A. (2015). Effect of foliar application of micronutrients, magnesium and wrapping films on yield, quality and storability of green bean pods. *Fayoum J. Agric. Res. Dev.* 29, 121–138. doi: 10.21608/fjard.2015.192992

Siddiqui, M. H., Alamri, S. A., Al-Khaishany, M. Y. Y., Al-Qutami, M. A., Ali, H. M., Al-Whaibi, M. H., et al. (2018). Mitigation of adverse effects of heat stress on Vicia faba by exogenous application of magnesium. *Saudi J. Biol. Sci.* 25, 1393–1401. doi: 10.1016/j.sjbs.2016.09.022

Silva, D. M. d., Souza, K., Vilas Boas, L. V., Alves, Y. S., and Alves, J. D. (2017). The effect of magnesium nutrition on the antioxidant response of coffee seedlings under heat stress. *Sci. Hortic.* 224, 115–125. doi: 10.1016/j.scienta.2017.04.029

Singh, N., and Shukla, S. (2020). Nano technology for increasing productivity in agriculture. *Vivechan Int. J. Res.* 11, 2020.

Sotoodehnia-Korani, S., Iranbakhsh, A., and Ebadi, M. (2020). Efficacy of magnesium nanoparticles in modifying growth, antioxidant activity, nitrogen status, and expression of wrky1 and bzip transcription factors in pepper (Capsicum annuum); an in vitro biological assessment. *Russ J Plant Physiol* 70, 39. doi: 10.1134/S1021443723600186

Sun, X., Kay, A. D., Kang, H., Small, G. E., Liu, G., Zhou, X., et al. (2013). Correlated biogeographic variation of magnesium across trophic levels in a terrestrial food chain. *PloS One* 8, e78444. doi: 10.1371/journal.pone.0078444

Sun, T., Wang, P., Rao, S., Zhou, X., Wrightstone, E., Lu, S., et al. (2023). Co-chaperoning of chlorophyll and carotenoid biosynthesis by ORANGE family proteins in plants. *Mol. Plant* 16, 1048–1065. doi: 10.1016/j.molp.2023.05.006

Sun, L., Zhang, P., Xing, M., Li, R., Yu, H., Ju, Q., et al. (2023). NAC32 alleviates magnesium toxicity-induced cell death through positive regulation of XIPOTL1 expression. *Plant Physiol.* 191, 849–853. doi: 10.1093/plphys/kiac562

Tahiri, A., Meddich, A., Raklami, A., Alahmad, A., Bechtaoui, N., Anli, M., et al. (2022). Assessing the potential role of compost, PGPR, and AMF in improving tomato plant growth, yield, fruit quality, and water stress tolerance. *J. Soil Sci. Plant Nutr.* 22, 1–22. doi: 10.1007/s42729-021-00684-w

Tan, H., Du, C., and Zhou, L. (2000). Effect of magnesium fertilizer on sustaining upland agricultural development in Guangxi province. *Better Crops Int.* 14, 13–15.

Tang, R. J., and Luan, S. (2017). Regulation of calcium and magnesium homeostasis in plants: from transporters to signaling network. *Curr. Opin. Plant Biol.* 39, 97–105. doi: 10.1016/j.pbi.2017.06.009

Tang, R. J., and Luan, S. (2020). Rhythms of magnesium. *Nat. Plants*. 6, 742–743. doi: 10.1038/s41477-020-0706-3

Tang, R. J., Meng, S. F., Zheng, X. J., Zhang, B., Yang, Y., Wang, C., et al. (2022a). Conserved mechanism for vacuolar magnesium sequestration in yeast and plant cells. *Nat. Plants* 8, 181–190. doi: 10.1038/s41477-021-01087-6

Tang, L., Xiao, L., Chen, E., Lei, X., Ren, J., Yang, Y., et al. (2023). Magnesium transporter CsMGT10 of tea plants plays a key role in chlorosis leaf vein greening. *Plant Physiol. Biochem.* 201, 107842. doi: 10.1016/j.plaphy.2023.107842

Tang, L., Xiao, L., Huang, Y., Xiao, B., and Gong, C. (2021). Cloning and magnesium transport function analysis of csMGTs genes in tea plants (Camellia sinensis). *J. Tea Sci.* 41, 761–776.

Tang, R. J., Yang, Y., Yan, Y. W., Mao, D. D., Yuan, H. M., Wang, C., et al. (2022b). Two transporters mobilize magnesium from vacuolar stores to enable plant acclimation to magnesium deficiency. *Plant Physiol.* 190, 1307–1320. doi: 10.1093/plphys/kiac330

Tariq Aftab, K. R. H. (2020). *Plant Micronutrients: Deficiency and Toxicity Management* (Springer: Springer Nature, Cham). doi: 10.1007/978-3-030-49856-6

Tian, X. Y., He, D. D., Bai, S., Zeng, W. Z., Wang, Z., Wang, M., et al. (2021). Physiological and molecular advances in magnesium nutrition of plants. *Plant Soil.* doi: 10.1007/s11104-021-05139-w

Tian, G., Liu, C., Xu, X., Xing, Y., Liu, J., Lyu, M., et al. (2022). Magnesium promotes nitrate uptake by increasing shoot-to-root translocation of sorbitol in apple seedlings. *SSRN Electronic J.* 19, 1–27. doi: 10.2139/ssrn.4290413

Tian, G., Liu, C., Xu, X., Xing, Y., Liu, J., Lyu, M., et al. (2023a). Effects of Magnesium on nitrate uptake and sorbitol synthesis and translocation in apple seedlings. *Plant Physiol. Biochem.* 196, 139–151. doi: 10.1016/j.plaphy.2023.01.033

Tian, G., Qin, H., Liu, C., Xing, Y., Feng, Z., Xu, X., et al. (2023b). Magnesium improved fruit quality by regulating photosynthetic nitrogen use efficiency, carbon–nitrogen metabolism, and anthocyanin biosynthesis in 'Red Fuji' apple. *Front. Plant Sci.* 14. doi: 10.3389/fpls.2023.1136179

Tränkner, M., Tavakol, E., and Jákli, B. (2018). Functioning of potassium and magnesium in photosynthesis, photosynthate translocation and photoprotection. *Physiol. Plant* 163, 414–431. doi: 10.1111/ppl.12747

Trejo-Téllez, L. I., and Gómez-Merino, F. C. (2014). Nutrient management in strawberry: Effects on yield, quality and plant health. *Strawberries: Cultivation antioxidant properties Health benefits*, 239–267.

Tully, K., and Ryals, R. (2017). Nutrient cycling in agroecosystems: Balancing food and environmental objectives. *Agroecol Sustain. Food Syst.* 41, 761–798. doi: 10.1080/21683565.2017.1336149

Turner, T. L., Bourne, E. C., Von Wettberg, E. J., Hu, T. T., and Nuzhdin, S. V. (2010). Population resequencing reveals local adaptation of Arabidopsis lyrata to serpentine soils. *Nat. Genet.* 42, 260–263. doi: 10.1038/ng.515

Verbruggen, N., and Hermans, C. (2013). Physiological and molecular responses to magnesium nutritional imbalance in plants. *Plant Soil* 368, 87–99. doi: 10.1007/s11104-013-1589-0

Verma, P., Sanyal, S. K., and Pandey, G. K. (2021). Ca2+–CBL–CIPK: a modulator system for efficient nutrient acquisition. *Plant Cell Rep.* 40, 2111–2122. doi: 10.1007/S00299-021-02772-8/FIGURES/3

Villeneuve, F., and Geoffriau, E. (2020). "Carrot physiological disorders and crop adaptation to stress," in *Carrots and Related Apiaceae Crops* Cabi, Wallingford, 156–170. doi: 10.1079/9781789240955.0156

Wang, Z., Hassan, M. U., Nadeem, F., Wu, L., Zhang, F., and Li, X. (2020). Magnesium fertilization improves crop yield in most production systems: A meta-analysis. *Front. Plant Sci* 10, 1727. doi: 10.3389/fpls.2019.01727

Wang, Z., Zhang, X., Fan, G. J., Que, Y., Xue, F., and Liu, Y. H. (2022). Toxicity Effects and Mechanisms of MgO Nanoparticles on the Oomycete Pathogen Phytophthora infestans and Its Host Solanum tuberosum. *Toxics* 10, 553. doi: 10.3390/toxics10100553

Wu, X., and Ye, J. (2020). Manipulation of jasmonate signaling by plant viruses and their insect vectors. *Viruses*. 12, 1–16. doi: 10.3390/v12020148

Xie, K., Cakmak, I., Wang, S., Zhang, F., and Guo, S. (2021). Synergistic and antagonistic interactions between potassium and magnesium in higher plants. *Crop J.* 9, 249–256. doi: 10.1016/j.cj.2020.10.005

Xu, X. F., Qian, X. X., Wang, K. Q., Yu, Y. H., Guo, Y. Y., Zhao, X., et al. (2021). Slowing development facilitates arabidopsis mgt mutants to accumulate enough magnesium for pollen formation and fertility restoration. *Front. Plant Sci.* 11. doi: 10.3389/FPLS.2020.621338/BIBTEX

Xu, J., Wu, L., Tong, B., Yin, J., Huang, Z., Li, W., et al. (2021). Magnesium supplementation alters leaf metabolic pathways for higher flavor quality of oolong tea. *Agriculture (Switzerland)* 11 (2), 1–12. doi: 10.3390/agriculture11020120

Yan, Y. W., Mao, D. D., Yang, L., Qi, J. L., Zhang, X. X., Tang, Q. L., et al. (2018). Magnesium transporter MGT6 plays an essential role in maintaining magnesium homeostasis and regulating high magnesium tolerance in Arabidopsis. *Front. Plant Sci.* 9. doi: 10.3389/fpls.2018.00274

Yang, W., Ji, Z., Wu, A., He, D., Rensing, C., Chen, Y., et al. (2023). Inconsistent responses of soil bacterial and fungal community's diversity and network to magnesium fertilization in tea (Camellia sinensis) plantation soils. *Appl. Soil Ecol.* 191, 105055. doi: 10.1016/J.APSOIL.2023.105055

Yang, X., Kobayashi, N. I., Hayashi, Y., Ito, K., Moriwaki, Y., Terada, T., et al. (2022). Mutagenesis analysis of GMN motif in Arabidopsis thaliana Mg2+transporter MRS2-1. *Biosci. Biotechnol. Biochem.* 86, 870–874. doi: 10.1093/bbb/zbac064

Yang, G. H., Yang, L. T., Jiang, H. X., Li, Y., Wang, P., and Chen, L. S. (2012). Physiological impacts of magnesium-deficiency in Citrus seedlings: Photosynthesis, antioxidant system and carbohydrates. *Trees - Structure Funct.* 26, 1237–1250. doi: 10.1007/S00468-012-0699-2

Yang, L. T., Yang, G. H., You, X., Zhou, C. P., Lu, Y. B., and Chen, L. S. (2013). Magnesium deficiency-induced changes in organic acid metabolism of Citrus sinensis roots and leaves. *Biol. Plant* 57, 481–486. doi: 10.1007/s10535-013-0313-5

Yang, W., Zhang, X., Wu, L., Rensing, C., and Xing, S. (2021). Short-term application of magnesium fertilizer affected soil microbial biomass, activity, and community structure. *J. Soil Sci. Plant Nutr.* 21, 675–689. doi: 10.1007/s42729-020-00392-x

Yang, L. T., Zhou, Y. F., Wang, Y. Y., Wu, Y. M., Ye, X., Guo, J. X., et al. (2019). Magnesium deficiency induced global transcriptome change in citrus sinensis leaves revealed by RNA-seq. *Int. J. Mol. Sci.* 20, 3129. doi: 10.3390/ijms20133129

Yaseen Aljanabi, H. A. (2021). Effects of nano fertilizers technology on agriculture production. *Ann. Rom Soc. Cell Biol.* 25, 6728–6739.

Ye, X., Chen, X. F., Deng, C. L., Yang, L. T., Lai, N. W., Guo, J. X., et al. (2019). Magnesium-deficiency effects on pigments, photosynthesis and photosynthetic electron transport of leaves, and nutrients of leaf blades and veins in citrus sinensis seedlings. *Plants* 8, 389. doi: 10.3390/plants8100389

Ye, X., Huang, H. Y., Wu, F. L., Cai, L. Y., Lai, N. W., Deng, C. L., et al. (2021). Molecular mechanisms for magnesium-deficiency-induced leaf vein lignification, enlargement and cracking in Citrus sinensis revealed by RNA-Seq. *Tree Physiol.* 41, 280–301. doi: 10.1093/treephys/tpaa128

Yeh, D.-M., Lin, L., and Wright, C. J. (2000). Effects of mineral nutrient deficiencies on leaf development, visual symptoms and shoot–root ratio of Spathiphyllum. *Sci. Hortic.* 86, 223–233. doi: 10.1016/S0304-4238(00)00152-7

Yousaf, M., Bashir, S., Raza, H., Shah, A. N., Iqbal, J., Arif, M., et al. (2021). Role of nitrogen and magnesium for growth, yield and nutritional quality of radish. *Saudi J. Biol. Sci.* 28, 3021–3030. doi: 10.1016/j.sjbs.2021.02.043

Yu, T., Jiang, J., Yu, Q., Li, X., and Zeng, F. (2023). Structural Insights into the Distortion of the Ribosomal Small Subunit at Different Magnesium Concentrations. *Biomolecules* 13, 566. doi: 10.3390/biom13030566

Zhang, B., Cakmak, I., Feng, J., Yu, C., Chen, X., Xie, D., et al. (2020). Magnesium deficiency reduced the yield and seed germination in wax gourd by affecting the carbohydrate translocation. *Front. Plant Sci.* 11, 797. doi: 10.3389/fpls.2020.00797

Zhang, W., Liu, Y., Muneer, M. A., Jin, D., Zhang, H., Cai, Y., et al. (2022). Characterization of different magnesium fertilizers and their effect on yield and quality of soybean and pomelo. *Agronomy* 12, 2693. doi: 10.3390/agronomy12112693

Zhang, Q., Ni, K., Yi, X., Liu, M., and Ruan, J. (2021). Advances of magnesium nutrition in tea plant. *J. Tea Sci.* 41, 19–27.

Zhang, S., Yang, W., Muneer, M. A., Ji, Z., Tong, L., Zhang, X., et al. (2021). Integrated use of lime with Mg fertilizer significantly improves the pomelo yield, quality, economic returns and soil physicochemical properties under acidic soil of southern China. *Sci. Hortic.* 290, 110502. doi: 10.1016/j.scienta.2021.110502

Zhang, H., Zhao, D., Yan, S., Xu, K., and Zhang, Y. (2020). Effect of potassium-magnesium ratio on "Zaosu" pear fruit quality. *J. Fruit Sci.* 37, 1667–1675. doi: 10.13925/j.cnki.gsxb.20200183

Zheng, T., and Moreira, R. G. (2020). Magnesium ion impregnation in potato slices to improve cell integrity and reduce oil absorption in potato chips during frying. *Heliyon* 6, e05834. doi: 10.1016/j.heliyon.2020.e05834

Zhi, S., Zou, W., Li, J., Meng, L., Liu, J., Chen, J., et al. (2023). Mapping QTLs and gene validation studies for Mg2+ uptake and translocation using a MAGIC population in rice. *Front. Plant Sci.* 14. doi: 10.3389/fpls.2023.1131064

Zhong, Q., Hu, H., Fan, B., Zhu, C., and Chen, Z. (2021). Biosynthesis and roles of salicylic acid in balancing stress response and growth in plants. *Int. J. Mol. Sci.* 22, 1–14. doi: 10.3390/ijms222111672

Zirek, N. S., and Uzal, O. (2020). The developmental and metabolic effects of different magnesium dozes in pepper plants under salt stress. *Not Bot. Horti Agrobot Cluj Napoca* 48, 967–977. doi: 10.15835/nbha48211943

frontiers | Frontiers in Plant Science

TYPE Original Research
PUBLISHED 28 February 2024
DOI 10.3389/fpls.2024.1351843

OPEN ACCESS

EDITED BY
Xiaoli Hui,
Northwest A&F University, China

REVIEWED BY
Esmaeil Rezaei-Chiyaneh,
Urmia University, Iran
Debasis Mitra,
National Rice Research Institute (ICAR), India

*CORRESPONDENCE
Xiangyi Li
lixy@ms.xjb.ac.cn
Lei Li
lilei@ms.xjb.ac.cn

RECEIVED 07 December 2023
ACCEPTED 29 January 2024
PUBLISHED 28 February 2024

CITATION
Shen X, Liu Y, Li X and Li L (2024) Effect of intercropping with legumes at different rates on the yield and soil physicochemical properties of *Cyperus esculentus* L. in arid land.
Front. Plant Sci. 15:1351843.
doi: 10.3389/fpls.2024.1351843

Effect of intercropping with legumes at different rates on the yield and soil physicochemical properties of *Cyperus esculentus* L. in arid land

Xin Shen[1,2,3,4], Yalan Liu[1,2,3,4], Xiangyi Li[1,2,3,4]* and Lei Li[1,2,3,4]*

[1]State Key Laboratory of Desert and Oasis Ecology, Xinjiang Institute of Ecology and Geography, Chinese Academy of Sciences, Urumqi, China, [2]Xinjiang Key Laboratory of Desert Plant Roots Ecology and Vegetation Restoration, Xinjiang Institute of Ecology and Geography, Chinese Academy of Sciences, Urumqi, China, [3]Cele National Station of Observation and Research for Desert-Grassland Ecosystems, Cele, China, [4]University of Chinese Academy of Sciences, Beijing, China

Intercropping has the potential to enhance yields and nutrient availability in resource-limited agricultural systems. However, the effects on crop yield nutrients and soil properties can vary considerably depending on the specific plant combinations and intercropping ratios used. In this study, the advantages and impacts of intercropping *C. esculentus* with legumes were investigated by measuring their biomass, nutrient content, and soil properties. The experiment included five intercropping treatments: monoculture of *C. esculentus* (MC), intercropping of *C. esculentus* with *Medicago sativa* L. (alfalfa) at row spacing ratios of 4:4 (4:4CM) and 8:4 (8:4CM), and intercropping of *C. esculentus* with *Glycine max* (L.) Merr. (soybean), also at row spacing ratios of 4:4 (4:4CG) and 8:4 (8:4CG). Our results demonstrated that all four intercropping treatments (4:4CM, 4:4CG, 8:4CM, and 8:4CG) significantly increased the biomass of *C. esculentus* by approximately 41.05%, 41.73%, 16.08%, and 18.43%, respectively, compared with monoculture cultivation alone, among which the 4:4CG treatment was optimum. However, no significant differences were observed in alfalfa or soybean biomass across different intercropping ratios. A notable increase was found in the total nitrogen (TN) and total phosphorus (TP) contents in the leaves, roots, and tubers of *C. esculentus* under intercropping, along with increased soil organic carbon (SOC), alkaline-hydrolyzed nitrogen (AN), available phosphorus (AP), microbial biomass carbon (MBC), microbial biomass nitrogen (MBN), and soil water content (SWC), and significantly reduced the soil pH. Among the intercropping treatments, the 4:4CG treatment also exhibited the most favorable soil properties. In particular, compared with MC, the 4:4CG treatment resulted in significant increases of 163.8%, 394.6%, and 716.8% in SOC, AN, and AP contents, respectively. The same treatment also led to significant increases of 48.34%, 46.40%, and 208.65% in MBC, MBN, and SWC, respectively. Overall, the findings suggest that the use of 4:4CG intercropping is an effective approach for sustainable farming management in Xinjiang.

KEYWORDS

***Cyperus esculentus* L., legumes, intercropping, biomass, plant nutrients, soil properties**

1 Introduction

Approximately 45% of the Earth's land area comprises drylands (Prăvălie, 2016), and with the ongoing climate warming, these global drylands are projected to expand in the forthcoming decades (Zhang et al., 2021). However, such an expansion poses a remarkable threat to food security, thus underscoring the urgent need to identify suitable crops and cultivation methods for these dry regions. *C. esculentus*, commonly known as tiger nut and belonging to the family *Cyperaceae Juss.*, is indigenous to the Mediterranean region of Africa (Follak et al., 2016). It is widely distributed in many northern temperate regions and is becoming increasingly popular as an energy crop in China, India, Egypt, and the United States (Ayeni, 2022). *C. esculentus* possesses exceptional traits, such as drought resistance and salinity tolerance (Duan et al., 2022; Zhang et al., 2023; Zhu et al., 2023). The tubers of *C. esculentus* are rich in fats, proteins, sugars, other nutrients, and a wide range of active compounds, making it a high-quality, high-yield, and high-value crop (Coskuner et al., 2002). In addition, the above-ground leafy part of *C. esculentus*, which has a growing period of around 120 days, is usually harvested for animal fodder, while the underground tuber part can be used as high-quality fodder, making it an ecologically vital cash crop (Kizzie-Hayford et al., 2015).

Intercropping, which refers to the concurrent cultivation of two or more crops on the same plot (Willey, 1990), offers heightened crop yield and stability compared with monocropping (Lan et al., 2023; Parvin et al., 2023). This agricultural practice mitigates the adverse environmental impacts associated with modern farming methods while simultaneously optimizing soil nutrient, water, and resource utilization (Chen et al., 2017). Various common species can be utilized for intercropping (Qu et al., 2023), and studies have demonstrated notable advantages when legumes are included—for instance, Qu et al. (2022) revealed that rape with common vetch significantly increased biomass, reduced soil pH, and increased soil organic carbon (SOC) and soil available phosphorus (AP). Similarly, Huang et al. (2022) demonstrated that the intercropping of tea plant with both soybean and zoysia significantly increased SOC, total nitrogen (TN), and tea quality. These findings can be attributed to the ability of legumes to alleviate nutrient stress and enhance nutrient availability through nitrogen (N) fixation or transfer to non-leguminous plants (Hobbie and Högberg, 2012; Shao et al., 2020). In addition, legumes serve as nutrient suppliers by delivering nutrients to non-leguminous plants via root secretions or arbuscular mycorrhizal fungal networks (Hauggaard-Nielsen and Jensen, 2005; Li et al., 2008; Adomako et al., 2022). Together with the root exudates, the legume-based intercropping system also promotes a beneficial rhizobacterial community, thereby improving soil quality and the rhizosphere soil environment for better resource uptake (Duchene et al., 2017; Chamkhi et al., 2022; Zhao et al., 2022). This synergistic effect on nutrient acquisition contributes to the growth of both intercropped species, ultimately leading to increased crop yield (Lu et al., 2024).

In addition, Black and Ong (2000) reported that, compared with monocropping, intercropping reduced crop water consumption (WC) without affecting total biomass production. Rezig et al. (2013) also showed that intercropping led to WC reduction in potato and sulla, resulting in increased water use efficiency of both crops. This phenomenon can be attributed to two factors. First, intercropping systems can improve water use efficiency and land occupancy by significantly developing canopy and reducing soil evapotranspiration. Second, the proportion of evapotranspiration flow is higher in intercropping than in monoculture, resulting in an expansion of the vegetation cover area and a subsequent increase in evapotranspiration. In turn, this reduces soil evapotranspiration in intercropping systems and increases soil water content (SWC). Therefore, it is important to study different intercropping treatments to increase crop yield and plant nutrients, improve soil nutrients, reduce soil pH, and increase SWC in arid areas.

In intercropping systems, the growth and resource capture of crops are determined by both intraspecific and interspecific competition among plants (Vandermeer, 1989). Therefore, maintaining appropriate ratios in intercropping systems is crucial to mitigate plant competition and optimize environmental resource uptake (Koocheki et al., 2016). Typically, a higher proportion of legumes can enhance atmospheric N fixation through symbiotic interactions with rhizobia, thus mitigating competition with non-leguminous plants for soil N resources; however, increasing proportions of intercropped plants may lead to reduced yields from the main crop (Andersen et al., 2005; Viaud et al., 2023). In addition, legumes possess the ability to enhance N availability in intercropping systems by fixing N, minimizing N leaching, and supplying N to neighboring crops (Vrignon-Brenas et al., 2016), yet whether this increased N availability offsets the competitive effects of higher proportions remains unclear from existing findings. Therefore, different intercropping proportions were also explored in the current study to investigate whether increased N availability from intercropping with legumes could counteract the competitive nature of high proportions of *C. esculentus* and whether it could improve *C. esculentus* yields and nutrients.

The southern fringe of the Taklamakan Desert in Xinjiang is located within the arid and semiarid belt of Asia and Europe, which features a typical temperate continental arid climate (Mazdiyasni and AghaKouchak, 2015). Xinjiang's predominant sandy soil, coupled with the snakeberry's robust root system and vigorous tillering capacity, contributes to sand fixation, soil stabilization, and wind protection (Aydar et al., 2020). *Medicago sativa* L. (alfalfa) and *Glycine max* (L.) Merr. (soybean) are both major legume crops in this region, which can significantly enhance the fertility and physicochemical properties of soil, thus establishing a mutually beneficial relationship between utilization and conservation (Rau et al., 2023). Alfalfa and soybean are sensitive to drought, with limited growth and lower yields in dry areas. However, some studies have demonstrated that intercropping with other crops can reduce the drought sensitivity of alfalfa and soybean, reduce water consumption, and increase yields (Ouda et al., 2007; Mao et al., 2012; Zhang et al., 2021; Jamali et al., 2023). In view of the limited research on intercropping *C. esculentus*, an emerging oilseed crop, the present study presents an innovative approach to intercropping *C. esculentus* with alfalfa and soybean in different proportions to assess the effects on their yield, nutrients, and soil properties. The

goal of the current work is to fully utilize the economic and ecological potential of *C. esculentus* and to understand the key methods of growing oil salsa bean in such drylands. Furthermore, this study aims to determine whether intercropping two legumes can alleviate the competitive effects caused by the high rates of *C. esculentus*. To this end, two hypotheses were formulated: (1) intercropping significantly enhances the yield and nutrients of *C. esculentus* and enriches soil nutrient content and (2) legumes effectively counteract the competitive effects among *C. esculentus* when intercropped with high proportions of *C. esculentus*.

2 Material and methods

2.1 Site description

This experiment was conducted in June 2021 in the *C. esculentus* planting area (81°06′18″ E, 37°25′99″ N) located in Tuan Jie New Village in the Hotan Prefecture of the Xinjiang Uygur Autonomous Region, China (Figure 1). The area is a newly reclaimed sandy land located in the Taklamakan Desert that features a temperate continental desert climate, with an average annual temperature of approximately 13.1°C, an average annual precipitation of 43.8 mm, and a total evapotranspiration of 2,624.4 mm. The initial soil indicators were collected from the area at depths of 0–20 cm, air-dried, and sieved through a 2-mm sieve to remove rhizomes and debris. Next, the physical and chemical properties of the soils were determined with three replicates for all measurements, thereby yielding the following results: soil capacity (1.54 g·cm^{-3}), pH (8.72), SOC (2.11 g·kg^{-1}), AN (1.86 mg·kg^{-1}), AP (1.23 mg·kg^{-1}), MBC (23.09 mg·kg^{-1}), and MBN (2.16 mg·kg^{-1}).

2.2 Experimental design

The experimental variety of *C. esculentus* used in this study was "XinKe No. 1." The experiment followed a one-way randomized design, including the following five treatments: *C. esculentus* monoculture (MC), *C. esculentus* and alfalfa according to a 4:4 intercropping (4:4CM), *C. esculentus* and soybean according to a 4:4 intercropping (4:4CG), *C. esculentus* and alfalfa according to an 8:4 intercropping (8:4CM), and *C. esculentus* and soybean according to an 8:4 intercropping (8:4CG). All rows were uniformly spaced at intervals of 30 cm, and each row strip measured 60 cm in width (Figure 2). Each treatment plant was planted in a one-hectare experimental plot. A base fertilizer comprising 300 kg·hm^{-2} urea ($N \geq 18\%$), 300 kg·hm^{-2} diammonium phosphate ($P_2O \geq 48\%$), and 300 kg·hm^{-2} humic acid was applied, while water application amounted to 2,025 m^3·hm^{-2}.

The sowing process took place on June 10, 2021 using mechanically opened furrows and strip planting techniques. The

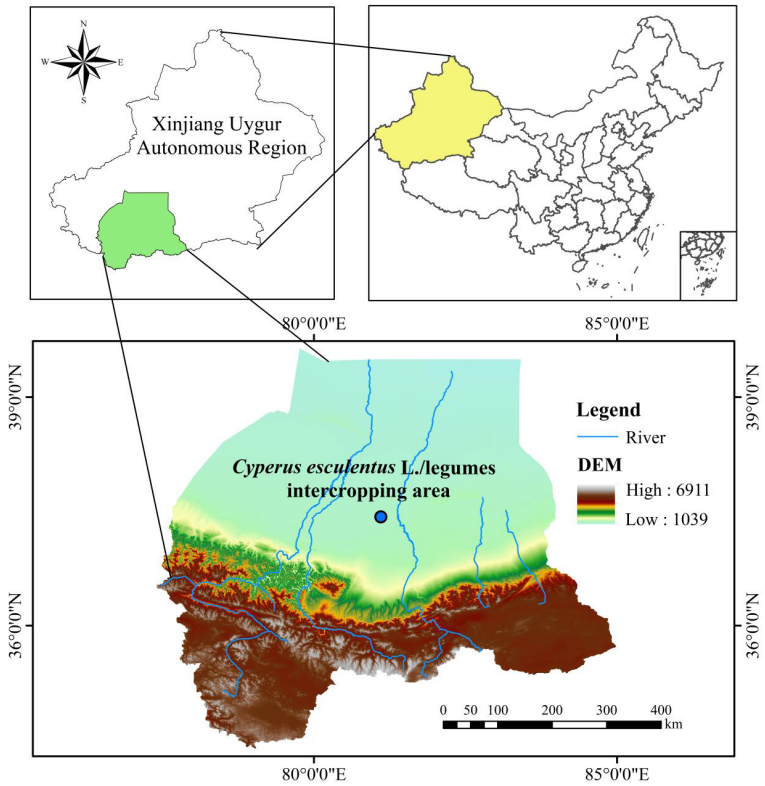

FIGURE 1
Location of the *C. esculentus* planting demonstration area in Hotan Prefecture, Xinjiang, China.

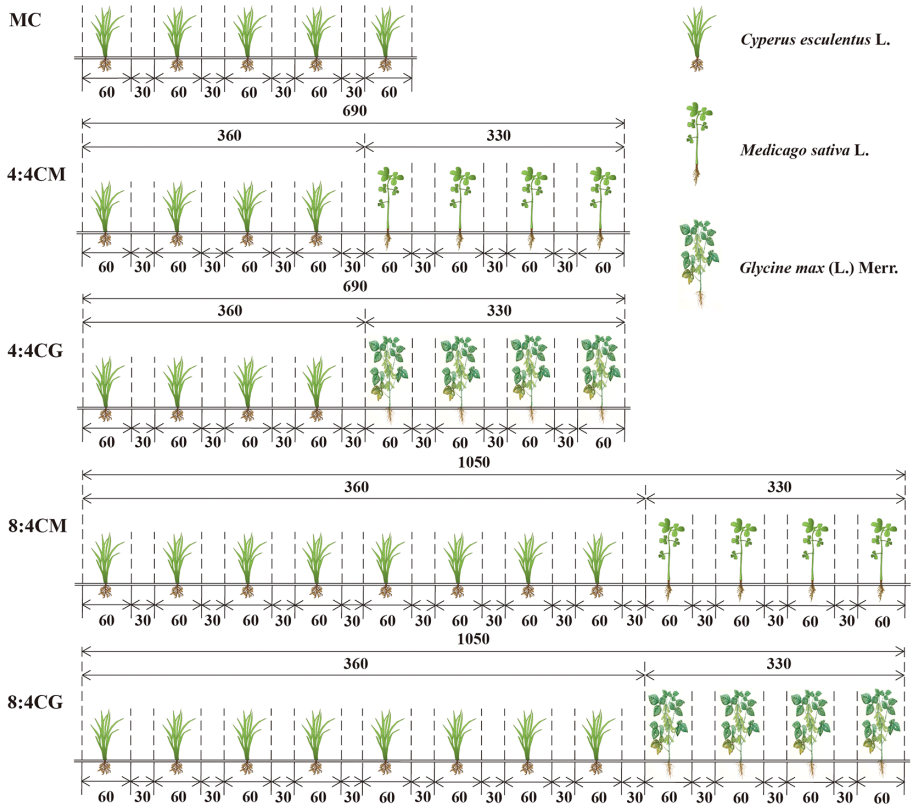

FIGURE 2
Diagram of different intercropping treatments of *C. esculentus* with alfalfa and soybean (the numbers indicate the distance in centimeters). MC, 4:4CM, 4:4CG, 8:4CM, and 8:4CG represent monocropping *C. esculentus*, 4:4 *C. esculentus*/Medicago sativa L. intercropping, 4:4 *C. esculentus*/*Glycine max* (L.) Merr., 8:4 *C. esculentus*/*Medicago sativa* L., and 8:4 *C. esculentus* L./*Glycine max* (L.) Merr. intercropping, respectively.

sowing rate for the planting treatments remained constant at 300 kg·hm^{-2}. Throughout the growing season, fertilizers and water were administered via drip irrigation, with each drip irrigation strip spaced at intervals of 30 cm apart. In the early growth stage of *C. esculentus* (July), water was dripped four times, with a total volume of approximately 9.38 m^3·hm^{-2}, along with an application of approximately 1.69 m^3·hm^{-2} urea and 0.75 kg·hm^{-2} potassium sulfate ($K \geq 52\%$). During the middle stage of irrigation (from August to the end of September), water was applied 12 times, followed by additional four applications during the late stage of irrigation (from the end of September to the beginning of October), using identical quantities for both water and fertilizer inputs. Using appropriate herbicides and pesticides, weed and pest control measures were implemented at regular monthly intervals.

The resulting plants were harvested on October 10, 2021. Three 10 × 5-m plots were set up at 5 m apart. Three designated sampling points were selected in each plot, and plant samples (leaves, roots, and tubers) were collected from the central areas (0.5 m × 0.5 m) of these points, with 10 plants randomly selected from each point to record above- and below-ground biomass. Next, soil samples were collected from three random points in each plot using a soil sampler; each point had a 2-cm diameter and a depth range of 0–20 cm. All soil samples were thoroughly mixed to form a uniform sample and then passed through a 2-mm sieve to remove roots and debris.

2.3 Sampling and measurements

The plant samples were washed with water, purified, and dried at 75°C for 48 h until the biomass was constant and then subjected to the determination of indicators. Subsequently, the dry matter was ground using a vibrating disc mill (RS200, Retsch GmbH Inc., Haan, Germany). After passing through a 1-mm sieve, the nutrient content and quality of the different organs were assessed. Organic carbon (OC) and total nitrogen (TN) concentrations were measured using a CN autoanalyzer (Eurovector, Milan, Italy), and total phosphorus (TP) concentrations were analyzed by using Mo–Sb colorimetric method after persulphate oxidation (Lu et al., 2015).

The soil samples were passed through a 2-mm sieve to eliminate rhizomes and debris. Subsequently, the samples were air-dried at 105° C for 48 h. The soil pH was determined using a pH meter (PHS-3C, China), while soil organic carbon (SOC) content was assessed using the potassium dichromate oxidation-heating method (Jiang et al., 2017). Soil alkali-hydrolyzable nitrogen (AN) concentration was quantified through the Kjeldahl method (Bremner and Mulvaney, 1982), while AP content was measured using the ammonium molybdate method after completing the H_2SO_4 digestion of the samples (Liu et al., 2021). Soil microbial biomass carbon (MBC) and microbial biomass nitrogen (MBN) were quantified via fumigation extraction (Vance et al., 1987). The soil samples were weighed and measured both before and after being air-dried in an

oven at 105°C to determine the SWC and soil bulk density (Chehab et al., 2020). The particle size distribution of the soil was analyzed using the pipette method (Chen et al., 1991). Following the guidelines of the International System of Soil Classification (ISSC), the particle sizes were classified into four categories: clay (0–0.002 mm), silt (0.002–0.02 mm), very fine sands (Vfs, 0.02–0.2 mm), and medium and coarse sands (Macs, 0.2–2 mm).

2.4 Statistical analysis

The effects of intercropping on the nutrients, above- and below-ground biomass, and soil properties of *C. esculentus* were tested using one-way analysis of variance (ANOVA). Tukey's test was employed to compare differences among intercropping treatments. All statistical analyses were performed using R v4.1.0 (R Core Team, 2018) and SPSS 23.0 software (SPSS Inc., Chicago, IL, USA), with the significance level set at $P < 0.05$. Pearson correlation analysis with the corrplot software package was utilized to investigate and visualize plant–soil relationships.

3 Results

3.1 Effect of different intercropping treatments on the biomass of *C. esculentus*

The biomass obtained from the 4:4CM and 4:4CG treatments of oilseed bean was significantly higher ($P < 0.05$) than that obtained via the MC treatment, with increases of 41.05% and 41.73%, respectively (Table 1). The biomass of oilseed bean in the 8:4CM and 8:4CG treatments was not significantly different ($P > 0.05$) from that of the MC treatment. Furthermore, the biomass of alfalfa and soybean did not differ significantly ($P > 0.05$) among different intercropping treatments. The *C. esculentus* leaf biomass, produced by the 4:4CM treatment, was significantly higher than that produced by MC at 56.85% ($P < 0.05$), while those produced by the 4:4CG, 8:4CM, and 8:4CG treatments were not significantly different from that produced by the MC treatment ($P > 0.05$) (Table 2). Regarding the root biomass of *C. esculentus*, the 4:4CG treatment yielded significantly higher biomass by 78.41% ($P < 0.05$) than MC. In addition, for tuber biomass, both 4:4CM and 4:4CG treatments yielded significantly higher tuber biomass than the MC treatment by 29.77% and 39.01% ($P < 0.05$), respectively, while the 8:4CM and 8:4CG treatments did not have any significant ($P > 0.05$) difference from MC.

3.2 Effects of different intercropping treatments on the nutrient concentrations of *C. esculentus*

The OC contents in leaves, roots, and tubers of *C. esculentus* were not significantly different ($P > 0.05$) in all treatments (Figure 3A). In comparison, the TN contents in the leaves and roots of *C. esculentus* were significantly higher ($P < 0.05$) in all the intercropping treatments compared with MC (Figure 3B), although there were no significant differences ($P > 0.05$) among the intercropping treatments. The highest TN contents were found in the leaves and roots of aubergine under the 8:4CM treatment, which increased by 149.08% and 295.03%, respectively, compared with the MC treatment. The TP content of *C. esculentus* leaves and roots was significantly higher in the 8:4CM treatment than in MC (Figure 3C), with increases of 258.3% and 258.3%, respectively. However, there were no significant differences ($P > 0.05$) among the various intercropping treatments. Furthermore, the TN and TP contents of *C. esculentus* tubers did not show significant differences ($P > 0.05$) among all treatments.

TABLE 1 Total biomass of *C. esculentus*, alfalfa, and soybean under different intercropping treatments (kg·acre^{-2}/g).

Treatment	Biomass		
	C. esculentus	*Medicago sativa* L.	*Glycine max* (L.) Merr.
MC	272.98 ± 28.61 b	–	–
4:4CM	385.04 ± 39.11 a	198.68 ± 41.33 a	–
4:4CG	386.89 ± 58.28 a	–	217.40 ± 35.87 a
8:4CM	316.88 ± 10.18 ab	187.29 ± 54.54 a	–
8:4CG	334.65 ± 42.65 ab	–	200.63 ± 29.22 a

The different lowercase letters indicate significant differences between intercropping treatments ($P < 0.05$). MC, 4:4CM, 4:4CG, 8:4CM, and 8:4CG represent monocropping *C. esculentus*, 4:4 *C. esculentus/Medicago sativa* L. intercropping, 4:4 C. esculentus/Glycine max (L.) Merr., 8:4 *C. esculentus/Medicago sativa* L., and 8:4 *C. esculentus/Glycine max* (L.) Merr. intercropping, respectively. In addition, there were no data for *Medicago sativa* L. and *Glycine max* (L.) Merr. because MC represents monoculture *C. esculentus*, no data for *Glycine max* (L.) Merr. because 4:4CM and 8:4CM represent an intercropping of *C. esculentus* and *Medicago sativa* L., and no data for *Medicago sativa* L. because 4:4CG and 8:4CG represent an intercropping of *C. esculentus* and *Glycine max* (L.) Merr. The symbol "-" in the table means no data.

3.3 Effect of different intercropping treatments on the soil properties of *C. esculentus*

All intercropping treatments showed a significant increase in the SOC, with the 4:4CG treatment being the most significant ($P < 0.05$) (Figure 4A). In particular, the 4:4CG treatment increased the SOC by 163.89% compared with the MC treatment. In terms of the AN content, the 4:4CM, 4:4CG, and 8:4CG treatments showed significant ($P < 0.05$) increases compared with MC (Figure 4B), with the 4:4CG treatment showing the most significant increase of 163.89% compared with the MC. Meanwhile, there was no significant difference ($P > 0.05$) between the 8:4CM treatment and MC. For the AP, all intercropping treatments showed significant ($P < 0.05$) increases compared with MC (Figure 4C), with the 4:4CG treatment being the most significant, increasing the AP by 163.89% compared with the MC treatment.

The soil pH values of all four intercropping patterns were significantly lower than those of the monocropping treatments (Figure 5A), with the lowest pH value in the 4:4CG treatment

10.3389/fpls.2024.1351843

TABLE 2 Biomass of the separate components of *C. esculentus* under various intercropping treatments (kg·acre^{-2}/g).

Organ	Treatment				
	MC	4:4CM	4:4CG	8:4CM	8:4CG
Leaf	101.60 ± 19.02 b	159.36 ± 32.15 a	137.01 ± 36.61 ab	126.18 ± 26.72 ab	128.44 ± 24.02 ab
Root	29.51 ± 3.48 d	41.56 ± 6.19 bc	52.65 ± 5.38 a	33.79 ± 3.33 cd	43.51 ± 3.51 b
Tuber	141.87 ± 7.81 c	184.11 ± 16.98 ab	197.22 ± 27.09 a	156.91 ± 27.32 bc	162.70 ± 17.17 abc

The different lowercase letters indicate significant differences between intercropping treatments at P < 0.05. MC, 4:4CM, 4:4CG, 8:4CM, and 8:4CG represent monocropping *C. esculentus*, 4:4 *C. esculentus*/*Medicago sativa* L. intercropping, 4:4 *C. esculentus*/*Glycine max* (L.) Merr., 8:4 *C. esculentus*/*Medicago sativa* L., and 8:4 *C. esculentus*/*Glycine max* (L.) Merr. intercropping, respectively.

($P < 0.05$), which was reduced by 5.78%, 3.18%, 4.51%, and 4.01% compared with the MC, 4:4CM, 8:4CM, and 8:4CG treatments, respectively. In addition, SWC was significantly higher ($P < 0.05$) in the intercropping treatments than in the monocropping treatments, with 4:4CG averaging the highest with an increase of 212.07% compared with the MC treatment (Figure 5B). MBC was significantly higher ($P < 0.05$) in both the 4:4CM and 4:4CG treatments than MC (Figure 5C), with the former being the highest on average, showing an increase of 93.57% compared with MC. However, there was no significant difference between the 8:4CM and 8:4CG intercrop treatments and MC ($P > 0.05$). Moreover, MBN was significantly higher ($P < 0.05$) in the 4:4CM, 4:4CG, 8:4CM, and 8:4CG treatments than in the MC treatment (Figure 5D), with increases of 75.09%, 86.57%, 61.25%, and 74.68%, respectively. There were no significant differences ($P > 0.05$) among the intercrop treatments.

The MC and intercropping treatments significantly altered the proportion of grain size in the initial soil (IS, Figure 6). In the IS, the largest proportion of Vfs was 45%, while the smallest proportion of clay was 9%. However, after the MC and intercropping treatments, the percentage of grain size in the soil changed significantly ($P < 0.05$). There was also a significant decrease in Macs and a significant increase in the percentage of clay particles in the MC and all intercropping treatment soils ($P < 0.05$), with Macs having the smallest percentage of soil particle size, while the percentages of clay, silt, and Vfs in the soils were roughly similar.

3.4 Plant–soil relationship

The SOC, AN, and AP were significantly and positively correlated with the total biomass of *C. esculentus* ($P < 0.05$, Figure 7). The MBC and MBN were significantly and positively correlated with the total biomass, TN and TP in leaves, TN and TP in roots, and SOC in *C. esculentus* ($P < 0.05$). Similarly, the SWC was significantly and positively correlated with the TN and TP in leaves and roots, soil nutrients, the MBC, and MBN ($P < 0.05$). At the same time, significant negative correlations were observed between pH and total biomass and between soil nutrients and SWC ($P < 0.05$). In terms of soil particle size, a significant negative correlation was found between clay and Vfs, Macs, and the SOC and between AN and AP ($P < 0.05$).

4 Discussion

4.1 Plant growth response to different intercropping treatments

Intercropping, especially with legumes, confers substantial advantages in crop yield compared with monocropping (Qu et al., 2022; Lan et al., 2023; Parvin et al., 2023). This finding aligns with that of the present study, demonstrating higher *C. esculentus* biomass in intercropping treatments than in MC. This increase

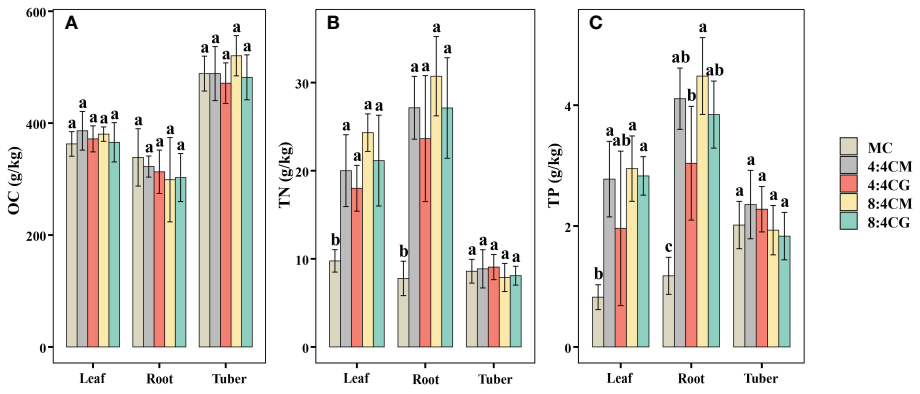

FIGURE 3
Effect of different intercropping treatments on **(A)** organic carbon content, **(B)** total nitrogen content, and **(C)** total phosphorus content of the leaves, roots, and tubers of *C. esculentus*. The different small letters indicate significant differences among the four treatments ($P < 0.05$). MC, 4:4CM, 4:4CG, 8:4CM, and 8:4CG represent monocropping *C. esculentus*, 4:4 *C. esculentus*/*Medicago sativa* L. intercropping, 4:4 *C. esculentus*/*Glycine max* (L.) Merr., 8:4 *C. esculentus*/*Medicago sativa* L., and 8:4 *C. esculentus*/*Glycine max* (L.) Merr. intercropping, respectively.

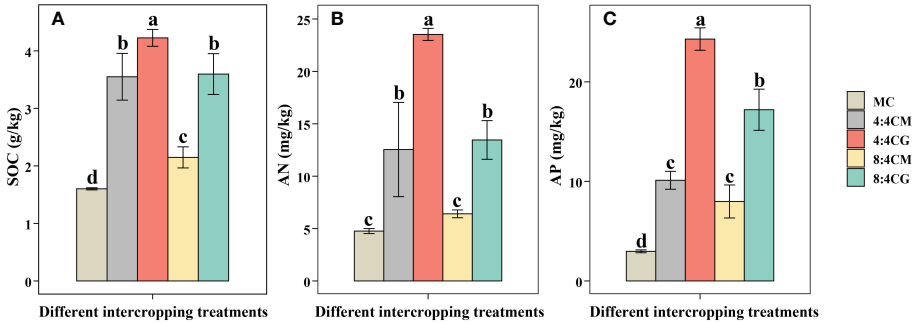

FIGURE 4
Effects of different intercropping treatments on **(A)** soil organic carbon content, **(B)** soil alkali-hydrolyzable nitrogen content, and **(C)** soil available phosphorus content. The different small letters indicate significant differences among the five treatments ($P < 0.05$). MC, 4:4CM, 4:4CG, 8:4CM, and 8:4CG represent monocropping *C. esculentus*, 4:4 *C. esculentus*/*Medicago sativa* L. intercropping, 4:4 *C. esculentus*/*Glycine max* (L.) Merr., 8:4 *C. esculentus*/*Medicago sativa* L., and 8:4 *C. esculentus*/*Glycine max* (L.) Merr. intercropping, respectively.

can be attributed to the legumes' ability to achieve biological N fixation, thus alleviating N limitations in crops and fostering enhanced plant growth and development (Zhao et al., 2022). Moreover, intercropping optimizes soil nutrient management and fortifies crop nutrient supply, ultimately augmenting plant biomass (Zhang et al., 2016; Eusun et al., 2022; Lu et al., 2024). Conventionally, a higher proportion of the main crop correlates with increased yield (Tehulie and Nigatie, 2023). However, the present study revealed no significant differences in *C. esculentus*, alfalfa, and soybean yields among treatments with varying intercropping proportions. This finding suggests that the competitive effect of *C. esculentus* may outweigh the promoting effect of legumes in high-proportion cropping practices.

Beyond yield enhancements, intercropping with legumes increases the essential nutrient content in plants, particularly N and P (Schwerdtner and Spohn, 2022; Zhao et al., 2022). Furthermore, our results showed that the TN and TP contents of *C. esculentus* leaves and roots were significantly increased compared with the MC treatment. This study thus presents findings that are consistent with previous results—for example, the research of Li et al. (2022) on corn–soybean intercropping demonstrated significantly higher TN and TP contents in corn leaves compared with MC or corn–millet intercropping. Similarly, Li et al. (2010) observed a 9%–30% increase in maize's N uptake in intercropping scenarios compared with MC. This increased N content in *C. esculentus* may be attributed to the process of legumes transferring nutrients to non-legumes (Chu et al., 2004; Rau et al., 2023). At the same time, the improvement in P nutrition in *C. esculentus* through intercropping may be attributed to P uptake released during legume root residue decomposition (Li et al., 2003). Furthermore, the enhanced N uptake promotes root growth and spatial distribution while delaying root senescence at the same time. Thus, the resulting boost in root uptake capacity contributes to the increased N content in *C. esculentus* (Zheng et al., 2021). These factors collectively underscore the multifaceted benefits of intercropping strategies involving legumes.

4.2 Response of soil properties to different intercropping treatments

Intercropping increases soil nutrients, thereby boosting crop yield and nutrient uptake capacity (Liu et al., 2014; Chamkhi et al., 2022). In particular, Lu et al. (2023) demonstrated that

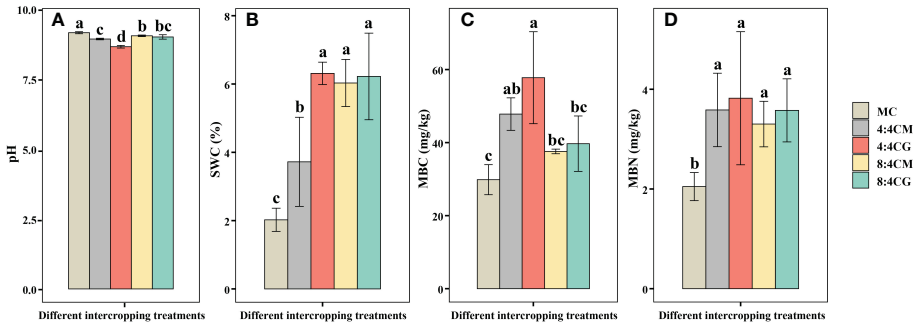

FIGURE 5
Effects of different intercropping treatments on **(A)** soil pH, **(B)** soil water content (SWC), **(C)** soil microbiomass carbon, and **(D)** soil microbiomass nitrogen content. The different small letters indicate significant differences among the four treatments ($P < 0.05$). MC, 4:4CM, 4:4CG, 8:4CM, and 8:4CG represent monocropping *C. esculentus*, 4:4 *C. esculentus*/*Medicago sativa* L. intercropping, 4:4 *C. esculentus*/*Glycine max* (L.) Merr., 8:4 *C. esculentus*/*Medicago sativa* L., and 8:4 *C. esculentus*/*Glycine max* (L.) Merr. intercropping, respectively.

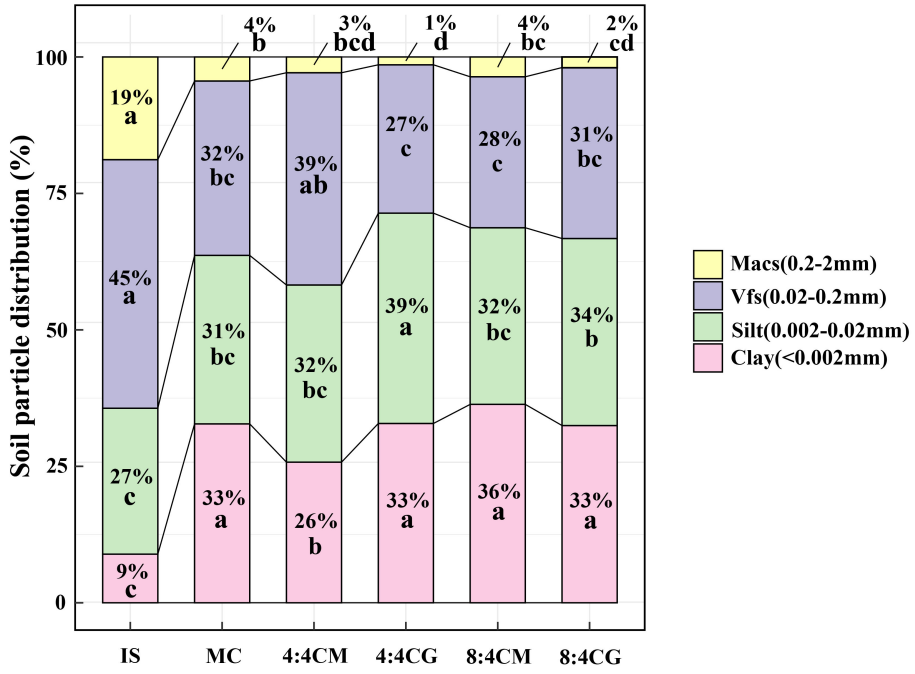

FIGURE 6
A comparison of original soil samples, monocropping, and intercropping treatments was analyzed to characterize soil particle size distribution. The different small letters indicate significant differences among the four treatments ($P < 0.05$). Vfs and Macs represent very fine sand and medium and coarse sand, respectively. IS, MC, 4:4CM, 4:4CG, 8:4CM, and 8:4CG represent initial soil, monocropping *C. esculentus*, 4:4 *C. esculentus*/*Medicago sativa* L. intercropping, 4:4 *C. esculentus*/*Glycine max* (L.) Merr., 8:4 *C. esculentus*/*Medicago sativa* L., and 8:4 *C. esculentus*/*Glycine max* (L.) Merr. intercropping, respectively.

intercropping maize and soya bean increased AN and AP in inter-root soils. Similarly, Cuartero et al. (2022) concluded that the intercropping of melon with cowpea significantly increased the TC, TN, and AP levels in the soil compared with monocropping. Consistent with previous studies, our study revealed that intercropping *C. esculentus* with legumes significantly increased SOC, AN, and AP, thus enriching soil nutrients. This enhancement may be attributed to the increased populations of bacteria involved in soil nutrient cycling, such as rhizobia, phosphate-solubilizing, and potassium-solubilizing bacteria (Duchene et al., 2017; Zhang et al., 2018).

Moreover, distinct differences were observed among various intercropping practices (Qu et al., 2023), with the SOC, AN, and AP contents being significantly higher in *C. esculentus* and soybean intercropping treatments than in *C. esculentus* and alfalfa intercropping treatments. This finding may be attributed to the fact that the intercropping of *C. esculentus* with soybean increases the relative abundance of proteobacteria, which may potentially enhance N_2 fixation (Rahav et al., 2016; Li et al., 2018; Huang et al., 2022; Jamali et al., 2023) and promote soil fertility. Among the intercropping of *C. esculentus* and soybean, soil nutrients were again significantly higher in the 4:4 intercropping treatment than in the 8:4 treatment. This is because the reduced competition intensity stemming from the low-proportion planting density of *C. esculentus* (Edmeades and Daynard, 1979; Tetio-Kagho and Gardner, 1988) decreases the competition for soil nutrient resources (Hara, 1986; Weiner, 1990; Schwinn and Weiner, 1998; Hara, 2005). In addition, the competition between *C. esculentus* and soybean may be lower than that with alfalfa, thus appearing to be significantly highest in the SOC, AN, and AP levels under the 4:4CG treatment.

The results of our study also showed a significant decrease in the pH level and a significant increase in the SWC of soil when *C. esculentus* was intercropped with legumes. These results are supported by previous studies, such as that of Wang et al. (2023), who observed a considerable decrease in soil pH after intercropping tea with legumes compared with monocropping. Shen et al. (2023) reported increased SWC when intercropping maize and soybean. These findings can be explained by the fact that intercropping with legumes can increase N fixation and decrease pH by increasing N accumulation (Chen et al., 2023; Liu et al., 2023). In addition, acidic metabolites are produced by intercropping plants with alfalfa and soybeans, resulting in a decrease in pH. These acids act as main osmotic pressure regulators, contributing to the increased SWC in intercropping (Rezig et al., 2013). Our results also showed that intercropping with legumes increases soil SWC, which is supported by previous studies indicating that intercropping systems can significantly improve soil physicohydraulic properties and optimize soil structure (Chen et al., 2019; Shen et al., 2023). This finding suggests that the intercropping of oilseed bean with soybean significantly improves adaptation to drought and provides a basis for promoting soybean cultivation in arid regions. The current study also revealed that, unlike the grain size of the IS, monocropping and intercropping both increased the clay percentage and reduced the percentage of Macs compared with

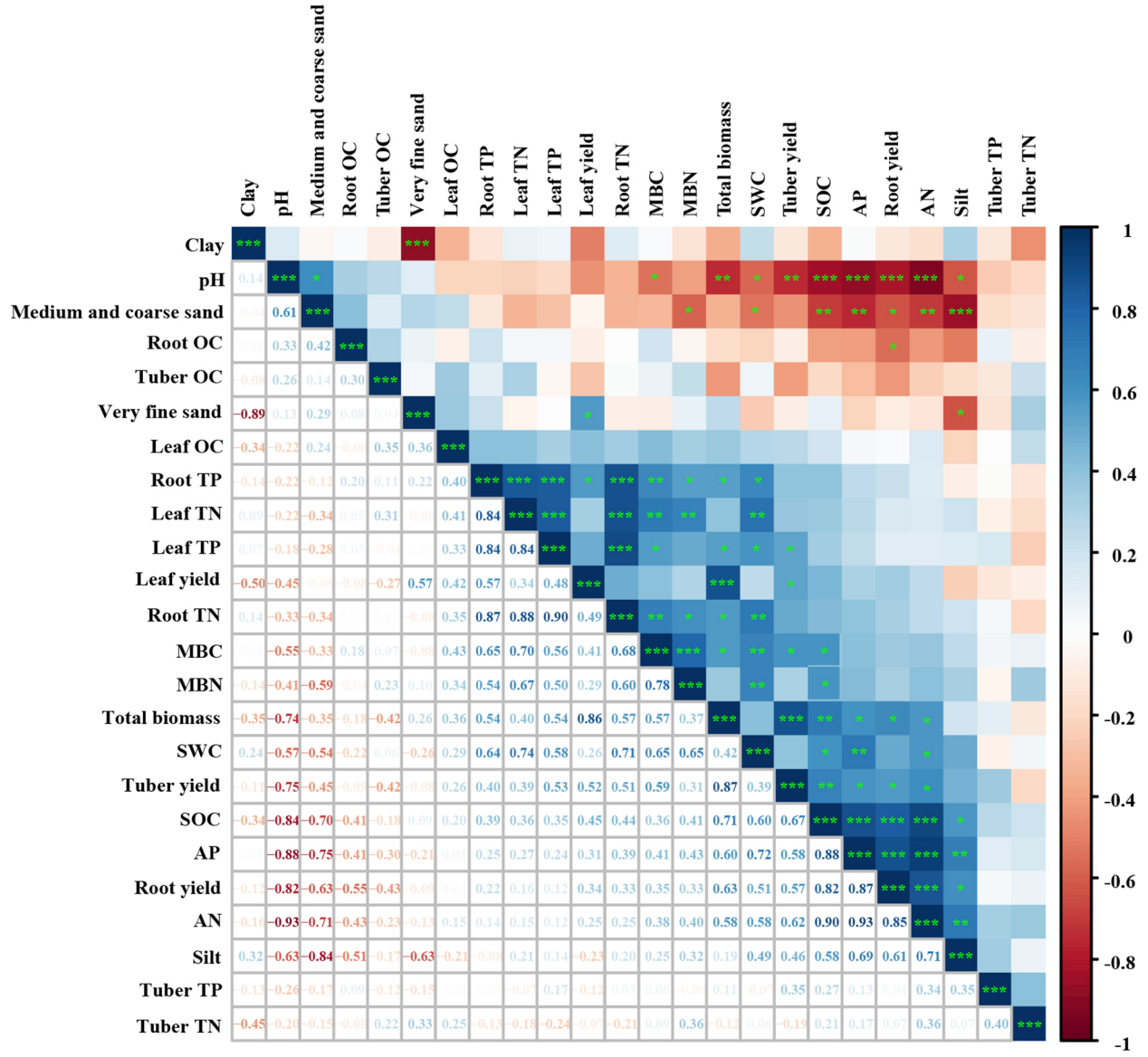

FIGURE 7
Relationships between plant and soil. *$P < 0.05$, **$P < 0.01$, ***$P < 0.001$.

the original soil's grain size. However, no significant difference was observed in soil particle size between the MC and intercropping treatments, possibly due to the study's short duration. Thus, additional experiments with extended durations must be conducted to further delve into this aspect.

Intercropping with legumes notably increased the concentrations of microbial C and N in the soil. This finding aligns with that of Qu et al. (2022), who revealed significant increases in MBC and MBN under intercropping, directly proving the notion that enhanced stimulation of the microbial community can be achieved through intercropping. This enhancement may stem from the strong correlation observed between total microbial biomass and soil C concentration (Goyal et al., 1993; Elfstrand et al., 2007). Notably, 4:4CG intercropping exhibited the highest MBC and MBN contents, which are likely due to the increased soil nutrient concentration that encourages microbial colonization and accumulation, subsequently boosting soil microbial activity (Wu et al., 2016). These alterations in soil properties and the subsequent increase in soil microbial population may have exerted a positive feedback on plant growth and productivity (Hauggaard-Nielsen and Jensen, 2005; Adomako et al., 2022). Therefore, further studies are needed to assess the feedback effects with microorganisms under *C. esculentus* intercropping.

5 Conclusions

The evaluation of *C. esculentus* yield, nutrient content, and soil properties within a *C. esculentus* and legume intercropping system encompassed various intercropping methods and ratios. The study

results showed that intercropping significantly increased the yield and nutrients of *C. esculentus* compared with monocropping, although there were no significant differences between the intercropping treatments. This finding suggests that increasing the proportion of *C. esculentus* in intercropping does not increase the yield and nutrient content of the former. Furthermore, intercropping with legumes was not effective in counteracting the competitive effects of high proportions of *C. esculentus*. Meanwhile compared with monocropping, intercropping had significant positive effects on soil nutrients, with the 4:4CG treatment being the most effective. Therefore, the use of 4:4CG intercropping treatment is important to improve yield, plant nutrients, and soil quality, especially in arid and nutrient-deficient lands, such as Xinjiang. In addition, designing long-term field observations to understand the interaction mechanism of intercropping between oilseed rape and legumes is an important direction for future research.

Data availability statement

The original contributions presented in the study are included in the article/supplementary material. Further inquiries can be directed to the corresponding authors.

Author contributions

XS: Writing – original draft, Writing – review & editing. YL: Writing – review & editing. XL: Writing – review & editing. LL: Writing – review & editing.

Funding

The author(s) declare that financial support was received for the research, authorship, and/or publication of this article. This research was supported funding from the Xinjiang Key Research and Development Programme Project (2022B02040-2).

Acknowledgments

The authors sincerely acknowledge the National Field Scientific Observation and Experimental Station of Celle Desert Grassland Ecosystem, Xinjiang Institute of Ecology and Geography, Chinese Academy of Sciences and the researchers for their assistance.

Conflict of interest

The authors declare that the research was conducted in the absence of any commercial or financial relationships that could be construed as a potential conflict of interest.

Publisher's note

References

Adomako, M. O., Roiloa, S., and Yu, F. H. (2022). Potential roles of soil microorganisms in regulating the effect of soil nutrient heterogeneity on plant performance. *Microorganisms* 10 (12), 2399. doi: 10.3390/microorganisms10122399

Andersen, M. K., Hauggaard-Nielsen, H., Ambus, P., and Jensen, E. S. (2005). Biomass production, symbiotic nitrogen fixation and inorganic N use in dual and tri-component annual intercrops. *Plant Soil* 266, 273–287. doi: 10.1007/s11104-005-0997-1

Aydar, E. F., Tutuncu, S., and Ozcelik, B. (2020). Plant-based milk substitutes: Bioactive compounds, conventional and novel processes, bioavailability studies, and health effects. *J. Funct. Food.* 70, 103975. doi: 10.1016/j.jff.2020.103975

Ayeni, A. O. (2022). Hoop house and field evaluation of tigernut (*Cyperus esculentus* L. var. sativus boeck) selections in new Jersey, USA. *Plants* 11, 897. doi: 10.3390/plants11070897

Black, C. R., and Ong, C. K. (2000). Utilisation of light and water in tropical agriculture. *Agric. For. Meteorol.* 104, 25–47. doi: 10.1016/S0168-1923(00)00145-3

Bremner, J. M., and Mulvaney, C. S. (1982). Nitrogen-total. Methods of soil analysis. Part 2. Chemical and microbiological properties. *Methodsofsoilan* 2, 595–624.

Chamkhi, I., Cheto, S., Geistlinger, J., Zeroual, Y., Kouisni, L., Bargaz, A., et al. (2022). Legume-based intercropping systems promote beneficial rhizobacterial community and crop yield under stressing conditions. *Ind. Crops Prod.* 183, 114985. doi: 10.1016/j.indcrop.2022.114958

Chehab, H., Tekaya, M., Hajlaoui, H., Abdelhamid, S., Gouiaa, M., Sfina, H., et al. (2020). Complementary irrigation with saline water and soil organic amendments modified soil salinity, leaf Na+, productivity and oil phenols of olive trees (*cv. Chemlali*) grown under semiarid conditions. *Agric. Water Manage.* 237, 106183. doi: 10.1016/j.agwat.2020.106183

Chen, C., Liu, W., Wu, J., Jiang, X., and Zhu, X. (2019). Can intercropping with the cash crop help improve the soil physico-chemical properties of rubber plantations? *Geoderma* 335, 149–160. doi: 10.1016/j.geoderma.2018.08.023

Chen, C., Xiao, W., and Chen, H. Y. H. (2023). Mapping global soil acidification under N deposition. *Glob. Change Biol.* 29, 4652–4661. doi: 10.1111/gcb.16813

Chen, J., Wei, F., Zheng, C., Wu, Y. Y., and Adriano, D. C. (1991). Background concentrations of elements in soils of China. *Water Air Soil pollut.* 57, 699–712. doi: 10.1007/BF00282934

Chen, X., Tian, Y., Guo, F., Chen, G., He, H., and Li, H. (2017). The effect of monocropping peanut and cassava/peanut intercropping on physical and chemical properties in peanut rhizosphere soil under the biochar application and straw mulching. *IOP Conf. Ser. Earth Environ. Sci.* 59, 12021. doi: 10.1088/1755-1315/59/1/012021

Chu, G., Shen, Q., and Cao, J. (2004). Nitrogen fixation and N transfer from peanut to rice cultivated in aerobic soil in an intercropping system and its effect on soil N fertility. *Plant Soil* 263, 17–27. doi: 10.1023/B:PLSO.0000047722.49160.9e

Coskuner, Y., Ercan, R., Karababa, E., and Nazlican, A. N. (2002). Physical and chemical properties of chufa (Cyperus esculentus L.) tubers grown in the C, ukurova region of Turkey. *J. Sci. Food Agric.* 82, 625–631. doi: 10.1002/jsfa.1091

Cuartero, J., Pascual, J. A., Vivo, J. M., Özbolat, O., Sánchez-Navarro, V., Egea-Cortines, M., et al. (2022). A first-year melon/cowpea intercropping system improves soil nutrients and changes the soil microbial community. *Agriculture Ecosyst. Environ.* 328, 107856. doi: 10.1016/j.agee.2022.107856

Duan, Y., Ren, W., Zhao, J., Luo, C., and Liu, Y. (2022). Planting Cyperus esculentus augments soil microbial biomass and diversity, but not enzymatic activities. *PeerJ* 10, e14199. doi: 10.7717/peerj.14199

Duchene, O., Vian, J.-F., and Celette, F. (2017). Intercropping with legume for agroecological cropping systems: Complementarity and facilitation processes and the importance of soil microorganisms. A review. *Agric. Ecosyst. Environ.* 240, 148–161. doi: 10.1016/j.agee.2017.02.019

Edmeades, G., and Daynard, T. (1979). The development of plant to-plant variability in maize at different planting densities. *Can. J. Plant Sci.* 59 (3), 561–576. doi: 10.4141/cjps79-095

Elfstrand, S., Hedlund, K., and Mårtensson, A. (2007). Soil enzyme activities, microbial community composition and function after 47 years of continuous green manuring. *Appl. Soil Ecol.* 35, 610–621. doi: 10.1016/j.apsoil.2006.09.011

Eusun, H., Weronika, C., Dorte Bodin, D., and Kristian, T. K. (2022). Exploitation of neighbouring subsoil for nutrient acquisition under annual-perennial strip intercropping systems. *bioRxiv. Plant Biol.* 109, 475–506. doi: 10.1016/j.agee.2022.108106

Follak, S., Belz, R., Bohren, C., De Castro, O., Del Guacchio, E., Pascual-Seva, N., et al. (2016). Biological flora of Central Europe: *Cyperus esculentus* L. *Perspect. Plant Ecol. Evol. Syst.* 23, 33–51. doi: 10.1016/j.ppees.2016.09.003

Goyal, S., Mishra, M., Dhankar, S., Kapoor, K., and Batra, R. (1993). Microbial biomass turnover and enzyme activities following the application of farmyard manure to field soils with and without previous long-term applications. *Biol. Fertil. Soils* 15, 60–64. doi: 10.1007/BF00336290

Hara, T. (1986). Growth of individuals in plant populations. *Ann. Bot.* 57, 55–68. doi: 10.1093/oxfordjournals.aob.a087094

Hara, T. (2005). Mode of competition and size-structure dynamics in plant communities. *Plant Spec. Biol.* 8 (2-3), 75–84. doi: 10.1111/j.1442-1984.1993.tb00059.x

Hauggaard-Nielsen, H., and Jensen, E. S. (2005). Facilitative root interactions in intercrops. *Plant Soil* 274, 237–250. doi: 10.1007/s11104-004-1305-1

Hobbie, E. A., and Högberg, P. (2012). Nitrogen isotopes link mycorrhizal fungi and plants to nitrogen dynamics. *New Phytol.* 196, 367–382. doi: 10.1111/j.1469-8137.2012.04300.x

Huang, Z., Cui, C., Cao, Y., Dai, J., Cheng, X., Hua, S., et al. (2022). Tea plant–legume intercropping simultaneously improves soil fertility and tea quality by changing Bacillus species composition. *Hortic. Res.-England.* 9, uhac046. doi: 10.1093/hr/uhac046

Jamali, Z. H., Ali, S., Qasim, M., Song, C., Anwar, M., Du, J., et al. (2023). Assessment of molybdenum application on soybean physiological characteristics in maize-soybean intercropping. *Front. Plant Sci.* 14. doi: 10.3389/fpls.2023.1240146

Jiang, Y. F., Ye, Y. C., Guo, X., Rao, L., Sun, K., and Li, W. F. (2017). Spatial variability of ecological stoichiometry of soil nitrogen and phosphorus in farmlands of Jiangxi province and its influencing factors. *Acta Pedol. Sin.* 54, 1527–1539.

Kizzie-Hayford, N., Jaros, D., Schneider, Y., and Rohm, H. (2015). Physico-chemical properties of globular tiger nut proteins. *Eur. Food. Res. Technol.* 241, 835–841. doi: 10.1007/s00217-015-2508-9

Koocheki, A., Seyyedi, S. M., and Gharaei, S. (2016). Evaluation of the effects of saffron–cumin intercropping on growth, quality and land equivalent ratio under semi-arid conditions. *Sci. Hortic.* 201, 190–198. doi: 10.1016/j.scienta.2016.02.005

Lan, Y., Zhang, H., He, Y., Jiang, C., Yang, M., and Ye, S. (2023). Legume-bacteria-soil interaction networks linked to improved plant productivity and soil fertility in intercropping systems. *Ind. Crop Prod.* 196, 116504. doi: 10.1016/j.indcrop.2023.116504

Li, L., Duan, R., Li, R., Zou, Y., Liu, J., Chen, F., et al. (2022). Impacts of corn intercropping with soybean, peanut and millet through different planting patterns on population dynamics and community diversity of insects under fertilizer reduction. *Front. Plant Sci.* 13. doi: 10.3389/fpls.2022.936039

Li, L., Zhang, F., Li, X., Christie, P., Sun, J., Yang, S., et al. (2003). Interspecific facilitation of nutrient uptake by intercropped maize and faba bean. *Nutr. Cycl. Agroecosyst.* 65, 61–71. doi: 10.1023/A:1021885032241

Li, Q. Z., Sun, J. H., Wei, X. J., Christie, P., Zhang, F. S., and Li, L. (2010). Overyielding and interspecific interactions mediated by nitrogen fertilization in strip intercropping of maize with faba bean, wheat and barley. *Plant Soil* 339 (1-2), 147–161. doi: 10.1007/s11104-010-0561-5

Li, Y., Pan, F., and Yao, H. (2018). Response of symbiotic and asymbiotic nitrogen-fixing microorganisms to nitrogen fertilizer application. *J. Soils Sediments* 19, 1948–1958. doi: 10.1007/s11368-018-2192-z

Li, Y., Ran, W., Zhang, R., Sun, S., and Xu, G. (2008). Facilitated legume nodulation, phosphate uptake and nitrogen transfer by arbuscular inoculation in an upland rice and mung bean intercropping system. *Plant Soil* 315, 285–296. doi: 10.1007/s11104-008-9751-9

Liu, T., Cheng, Z., Meng, H., Ahmad, I., and Zhao, H. (2014). Growth, yield and quality of spring tomato and physicochemical properties of medium in a tomato/garlic intercropping system under plastic tunnel organic medium cultivation. *Sci. Hortic.* 170, 159–168. doi: 10.1016/j.scienta.2014.02.039

Liu, H. Y., Huang, N., Zhao, C. M., and Li, J. H. (2023). Responses of carbon cycling and soil organic carbon content to nitrogen addition in grasslands globally. *Soil Biol. Biochem.* 186, 109164. doi: 10.1016/j.soilbio.2023.109164

Liu, Q., Yin, R., Tan, B., You, C., Zhang, L., Zhang, J., et al. (2021). Nitrogen addition and plant functional type independently modify soil mesofauna effects on litter decomposition. *Soil Biol. Biochem.* 160, 108340. doi: 10.1016/j.soilbio.2021.108340

Lu, J., Liu, Y., Zou, X., Zhang, X., Yu, X., Wang, Y., et al. (2024). Rotational strip peanut/cotton intercropping improves agricultural production through modulating plant growth, root exudates, and soil microbial communities. *Agric. Ecosyst. Environ.* 359, 108767. doi: 10.1016/j.agee.2023.108767

Lu, X., Yan, Y., Sun, J., Zhang, X., Chen, Y., Wang, X., et al. (2015). Carbon, nitrogen, and phosphorus storage in alpine grassland ecosystems of Tibet: Effects of grazing exclusion. *Ecol. Evol.* 19, 4492–4504. doi: 10.1002/ece3.1732

Lu, M., Zhao, J., Lu, Z., Li, M., Yang, J., Fullen, M., et al. (2023). Maize–soybean intercropping increases soil nutrient availability and aggregate stability. *Plant Soil.* doi: 10.1007/s11104-023-06282-2

Mao, L., Zhang, L., Li, W., van der Werf, W., Sun, J., Spiertz, H., et al. (2012). Yield advantage and water saving in maize/pea intercrop. *Field Crops Res.* 138, 11–20. doi: 10.1016/j.fcr.2012.09.019

Mazdiyasni, O., and AghaKouchak, A. (2015). Substantial increase in concurrent droughts and heatwaves in the United States. *Proc. Natl. Acad. Sci. U.S.A.* 112, 11484–11489. doi: 10.1073/pnas.1422945112

Ouda, S. ,. A., Mesiry, T. ,. E., Adballah, E. ,. F., and Gaballah, M. ,. S. (2007). Effect of water stress on the yield of soybean and maize grown under different intercropping patterns. *Austral. J. basic Appl. Sci.* 1, 578–585.

Parvin, S., Bajwa, A., Uddin, S., Sandral, G., Rose, M. T., Van Zwieten, L., et al. (2023). Impact of wheat-vetch temporary intercropping on soil functions and grain yield in a dryland semi-arid environment. *Plant Soil.* doi: 10.1007/s11104-023-05914-x

Prăvălie, R. (2016). Drylands extent and environmental issues. A global approach. *Earth-Sci. Rev.* 161, 259–278. doi: 10.1016/j.earscirev.2016.08.003

Qu, J., Li, L., Wang, Y, Yang, J., and Zhao, X. (2022). Effects of rape/common vetch intercropping on biomass, soil characteristics, and microbial community diversity. *Front. Environ. Sci.* 10, 947014. doi: 10.3389/fenvs.2022.947014

Qu, J., Li, L., Zhao, P., Zhang, T., Chen, G., Yang, J., et al. (2023). Effects of intercropping oat and common vetch on plant biomass yield and soil nitrogen and phosphorus availability in different soil characteristics. *J. Soil Sci. Plant Nutr.* 23, 3258–3270. doi: 10.1007/s42729-023-01211-9

Rahav, E., Giannetto, M. J., and Bar-Zeev, E. (2016). Contribution of mono and polysaccharides to heterotrophic N2 fixation at the eastern Mediterranean coastline. *Sci. Rep.* 6, (1). doi: 10.1038/srep27858

Rau, A., Zhu, K., Nurlan, B., Mirobit, M., Yessenkul, K., Bek, M. H., et al. (2023). Agronomic and reclamation strategies to enhance soil fertility, productivity and water accessibility. *Front. Sustain. Food Syst.* 7. doi: 10.3389/fsufs.2023.1288481

Rezig, M., Sahli, A., Ben jeddi, F., and Harbaoui, Y. (2013). Potato (*Solanum tuberosum* L.) and Sulla (*Hedysarum coronarium* L.) Intercropping in Tunisia: Effects in Water Consumption and Water Use Efficiency. *J. Aric. Sci.* 5. doi: 10.5539/jas.v5n10p123

Schwerdtner, U., and Spohn, M. (2022). Plant species interactions in the rhizosphere increase maize N and P acquisition and maize yields in intercropping. *J. Soil Sci. Plant Nutr.* 22, 3868–3884. doi: 10.1007/s42729-022-00936-3

Schwinn, S., and Weiner, J. (1998). Mechanisms determining the degree of size asymmetry in competition among plants. *Oecologia* 113, 447–455. doi: 10.1007/s004420050397

Shao, Z., Wang, X., Gao, Q., Zhang, H., Yu, H., Wang, Y., et al. (2020). Root contact between maize and alfalfa facilitates nitrogen transfer and uptake using techniques of foliar 15N-labeling. *Agronomy* 10 (3), 360. doi: 10.3390/agronomy10030360

Shen, L., Wang, X., Liu, T., Wei, W., Zhang, S., Keyhani, A., et al. (2023). Border row effects on the distribution of root and soil resources in maize–soybean strip intercropping systems. *Soil Tillage Res.* 233, 105812. doi: 10.1016/j.still.2023.105812

Tehulie, N. S., and Nigatie, T. Z. (2023). Response of intercropping coffee (Coffea arabica L.) with banana (Musa spp.) on yield, yield components, and quality of coffee. *Crop Sci.* 63, 888–898. doi: 10.1002/csc2.20862

Tetio-Kagho, F., and Gardner, F. P. (1988). Responses of maize to plant population density. II. Reproductive development, yield, and yield adjustments. *Agron. J.* 80, 935–940. doi: 10.2134/agronj1988.00021962008000060019x

Vance, E. D., Brookes, P. C., and Jenkinson, D. S. (1987). An extraction method for measuring soil microbial biomass C. *Soil Biol. Biochem.* 19, 703–707. doi: 10.1016/0038-0717(87)90052-6

Vandermeer, J. H. (1989). *The ecology of intercropping* (Cambridge: Cambridge University Press). doi: 10.1017/CBO9780511623523.

Viaud, P., Heuclin, B., Letourmy, P., Christina, M., Versini, A., Mansuy, A., et al. (2023). Sugarcane yield response to legume intercropped: A meta-analysis. *Field Crop Res.* 295, 108882. doi: 10.1016/j.fcr.2023.108882

Vrignon-Brenas, S., Celette, F., Piquet-Pissaloux, A., Jeuffroy, M. H., and David, C. (2016). Early assessment of ecological services provided by forage legumes in relay intercropping. *Eur. J. Agron.* 75, 89–98. doi: 10.1016/j.eja.2016.01.011

Weiner, J. (1990). Asymmetric competition in plant populations. *Trends Ecol. Evol.* 5, 360–364. doi: 10.1016/0169-5347(90)90095-U

Willey, R. W. (1990). Resource use in intercropping systems. *Agric. Water Manage.* 17, 215–231. doi: 10.1016/0378-3774(90)90069-B

Wu, G. L., Liu, Y., Tian, F. P., and Shi, Z. H. (2016). Legumes functional group promotes soil organic carbon and nitrogen storage by increasing plant diversity. *Land Degrad. Dev.* 28, 1336–1344. doi: 10.1002/ldr.2570

Zhang, R. Y., Liu, C., Chen, P. X., Jiang, M. M., Zhu, W. X., and Liu, H. M. (2023). Sequential extraction of oligosaccharide and polysaccharides from defatted tiger nut (*Cyperus esculentus*) meal for its comprehensive utilization. *J. Food Meas. Charact.* 17, 4357–4370. doi: 10.1007/s11694-023-01978-6

Zhang, W. P., Liu, G. C., Sun, J. H., Fornara, D., Zhang, L. Z., Zhang, F. F., et al. (2016). Temporal dynamics of nutrient uptake by neighbouring plant species: evidence from intercropping. *Funct. Ecol.* 31, 469–479. doi: 10.1111/1365-2435.12732

Zhang, M. M., Wang, N., Hu, Y. B., and Sun, G. Y. (2018). Changes in soil physicochemical properties and soil bacterial community in mulberry (Morus alba L.)/alfalfa (Medicago sativa L.) intercropping system. *Microbiol. Open* 7 (2), e00555. doi: 10.1002/mbo3.555

Zhang, C., Yang, Y., Yang, D., and Wu, X. (2021). Multidimensional assessment of global dryland changes under future warming in climate projections. *J. Hydrol.* 592. doi: 10.1016/j.jhydrol.2020.125618

Zhao, J., Chen, J., Beillouin, D., Lambers, H., Yang, Y., Smith, P., et al. (2022). Global systematic review with meta-analysis reveals yield advantage of legume-based rotations and its drivers. *Nat. Commun.* 13, 4926. doi: 10.1038/s41467-022-32464-0

Zheng, B., Zhang, X., Chen, P., Du, Q., Zhou, Y., Yang, H., et al. (2021). Improving maize's N uptake and N use efficiency by strengthening roots' absorption capacity when intercropped with legumes. *PeerJ* 9, e11658. doi: 10.7717/peerj.11658

Zhu, Y., Wang, Y., Wei, Z., Zhang, X., Jiao, B., Tian, Y., et al. (2023). Analysis of oil synthesis pathway in *Cyperus esculentus* tubers and identification of oleosin and caleosin genes. *J. Plant Physiol.* 284, 153961. doi: 10.1016/j.jplph.2023.153961

frontiers | Frontiers in Plant Science

TYPE Original Research
PUBLISHED 10 May 2024
DOI 10.3389/fpls.2024.1400146

OPEN ACCESS

EDITED BY
Laichao Luo,
Anhui Agricultural University, China

REVIEWED BY
Huabin Zheng,
Hunan Agricultural University, China
Weiyang Zhang,
Yangzhou University, China
Muhammad Ishfaq,
Shenzhen University, China

*CORRESPONDENCE
Yongjian Sun
yongjians1980@163.com

RECEIVED 13 March 2024
ACCEPTED 26 April 2024
PUBLISHED 10 May 2024

CITATION
Sun Y, Xing M, He Z, Sun Y, Deng Y, Luo Y, Chen X, Cao Y, Xiong W, Huang X, Deng P, Luo M, Yang Z, Chen Z and Ma J (2024) Effects of urea topdressing time on yield, nitrogen utilization, and quality of mechanical direct-seeding hybrid *indica* rice under slow-mixed fertilizer base application. *Front. Plant Sci.* 15:1400146. doi: 10.3389/fpls.2024.1400146

Effects of urea topdressing time on yield, nitrogen utilization, and quality of mechanical direct-seeding hybrid *indica* rice under slow-mixed fertilizer base application

Yongjian Sun[1,2]*, Mengwen Xing[2], Ziting He[2], Yuanyuan Sun[3], Yuqian Deng[4], Yongheng Luo[2], Xuefang Chen[2], Yun Cao[2], Wenbo Xiong[4], Xinghai Huang[2], Pengxin Deng[2], Min Luo[4], Zhiyuan Yang[2], Zongkui Chen[2] and Jun Ma[2]

[1]State Key Laboratory of Crop Gene Exploration and Utilization in Southwest China, Sichuan Agricultural University, Chengdu, China, [2]Ecophysiology and Cultivation Key Laboratory of Sichuan Province, Sichuan Agricultural University, Chengdu, China, [3]Sichuan Agricultural Meteorological Center, Sichuan Meteorological Bureau, Chengdu, China, [4]Rongxian Agricultural Technology Extension Center, Rongxian Agricultural and Rural Bureau, Rongxian, China

Introduction: The use of controlled-release nitrogen (N) fertilizers has been shown to improve yield and N-use efficiency (NUE) in mechanical transplanted rice. However, the fertilizer requirements for mechanical direct-seeding rice differ from those for mechanical transplanted rice. The effects of controlled-release fertilizers on yield, NUE, and quality in mechanical direct-seeding rice are still unknown.

Methods: Hybrid *indica* rice varieties Yixiangyou 2115 and Fyou 498 were used as test materials, and slow-mixed N fertilizer (120 kg hm^{-2}) as a base (N_1), N_1+urea-N (30 kg hm^{-2}) once as a base (N_2), N_1+urea-N (30 kg hm^{-2}) topdressing at the tillering stage (N_3), N_1+urea-N (30 kg hm^{-2}) topdressing at the booting stage (N_4) four N fertilizer management to study their impact on the yield, NUE and quality of mechanical direct-seeding rice.

Results and discussion: Compared with Yixiangyou 2115, Fyou 498 significantly increased photosynthetic potential, population growth rate, root vigor, and N transport rate by 3.34–23.88%. This increase further resulted in a significant improvement in the yield and NUE of urea-N topdressing by 1.73–5.95 kg kg^{-1}. However, Fyou 498 showed a significant decrease in the head rice rate and taste value by 3.34–7.67%. All varieties were treated with N_4 that significantly increase photosynthetic potential and population growth rate by 15.41–62.72%, reduce the decay rate of root vigor by 5.01–21.39%, promote the N transport amount in stem-sheaths (leaves) by 13.54–59.96%, and then significantly increase the yields by 4.45–20.98% and NUE of urea-N topdressing by 5.20–45.56 kg kg^{-1}. Moreover, the rice processing and taste values were optimized using this model. Correlation analysis revealed to achieve synergistic enhancement of high-yield, high-quality, and high-NUE in rice, it is crucial to focus on

increasing photosynthetic potential, population growth rate, and promoting leaf N transport. Specifically, increasing the contribution rate of N transport in stem-sheaths is the most important. These findings offer an effective N management strategy for 4R nutrient stewardship (right source, right method, right rate and right timing) of mechanical direct-seeding hybrid *indica* rice.

KEYWORDS

slow-mixed fertilizer, urea-N topdressing, direct-seeding rice, yield, rice quality

1 Introduction

China is currently undergoing critical transformation from traditional to modern agriculture (Cheng et al., 2023). Although the mechanization rate for plowing and harvesting is high, the rice (*Oryza sativa* L.) machine planting segment lags behind at a rate of less than 50% (National Bureau of Statistics of China, 2022). To improve this situation, China has increased its support for mechanical transplanted rice. However, although machine transplanting technology has significant advantages over traditional seedling raising and hand transplanting, the laborious process of seedling raising and management for mechanical transplanted rice, coupled with the high labor intensity of centralized seedling transport and transplanting, still results in high overall cost (Zhong et al., 2021; He et al., 2023). For large-scale production, direct seeding using rice machines is the most convenient method for rice cultivation (Guo et al., 2023a). Mechanical direct-seeding eliminates the need for raising, transporting, and transplanting seedlings, resulting in improved production efficiency (Farooq et al., 2011). This approach also boosts mechanized planting and is an efficient method for large-scale rice production (Farooq et al., 2011; Yang et al., 2023). However, rice varieties suitable for mechanical direct-seeding in China's major rice-producing regions are not appropriate (Sun et al., 2022; Guo et al., 2023a). To achieve high-yield and high-efficiency cultivation, it is further essential to integrate agricultural machinery and agronomy deeply (Yang et al., 2022). However, research on the theory of high-quality and high-yield cultivation of mechanically direct-seeding rice is still relatively inadequate.

Nitrogen (N) fertilizers are key for boosting rice production. However, N fertilizers are prone to volatilization and leakage. In China, the N use efficiency (NUE) of rice is low at approximately 30–35%, which is considerably lower than the global average in developed countries (46%) (Peng et al., 2009; Sun et al., 2023a). The primary cause is excessive fertilizer application, which results in diminishing returns. Nitrification and denitrification are significant contributors to low NUE (Chen et al., 2022). To address these issues, measures such as the 4R nutrient stewardship concept (right source, right rate, right time, right place) (IPNI, 2012) promoted by the International Plant Nutrition Institute (IPNI), N fertilizer management (Yokamo et al., 2023; Sun et al., 2023a; Sun et al., 2023b), soil testing and formulated fertilizer application (Chen et al., 2021), and leaf color diagnosis of SPAD meter (Peng et al., 1996) have been implemented by numerous scholars, resulting in positive outcomes. It is crucial to adopt practices to ensure that the N release rate aligns with the crop fertilizer requirements. The development and application of controlled-release fertilizers have garnered increased interest and research due to their potential to enhance N use and production efficiency, while saving time and labor (Ke et al., 2018; Lyu et al., 2021a; He et al., 2023). This area remains a focus of research, with the literature predominantly focusing on hand- and machine-transplanted rice (Ke et al., 2018; Lyu et al., 2021a; Yu et al., 2022). However, there is limited research on the effects of controlled-release fertilizers in mechanically direct-seeding rice. This study primarily examined the various types, optimal application amounts, and methods of side deep fertilization, as well as the use of slow-mixed fertilizers and other relevant factors related to slow-controlled-release fertilizers (Ke et al., 2018; Wu et al., 2021; Sun et al., 2023b). These factors were investigated under a onetime basal application. However, inconsistencies were observed in the study due to variations in controlled-release fertilizers (Wu et al., 2021; Lyu et al., 2021a), nutrient release timing (Cheng et al., 2022), and supporting application techniques (Hou et al., 2021; He et al., 2023). During the later stages, the rate and intensity of controlled-release fertilizers did not meet the immediate requirements of the heavy panicle hybrid rice and super rice varieties. These varieties require increased tillers, grains per panicle, 1000-grain weight, and single panicle weight (Jiang et al., 2016; Sun et al., 2022; Li et al., 2023). Currently, there is limited research on the optimal period for applying N fertilizer during the grain-filling stage of mechanical direct-seeding of heavy panicle hybrid rice. It is uncertain whether adjusting the timing of N fertilizer topdressing to match the growth and development characteristics of the plant will cause improved yield, NUE, and rice quality compared with the basal application of a controlled-release fertilizer.

Based on our previous research (Sun et al., 2022; Guo et al., 2023a; Sun et al., 2023b), we selected heavy panicle super-hybrid rice varieties for this study. We investigated the effects of base

application of slow-mixed fertilizer and topdressing of conventional N fertilizer on photosynthetic production and N-use characteristics under the condition of mechanical direct seeding. This study systematically examined the yield and quality of direct-seeding rice, along with its physiological mechanisms. This study proposes an optimal management mode for combining controlled-release N fertilizers with mechanical direct-seeding rice. It also suggests technical regulations for improving quality, yield, and NUE. These findings provide a theoretical and practical basis for implementing high-quality, high-yield, and high-efficiency 4R nutrient stewardship (right source, right method, right rate and right timing) technologies for heavy panicle mechanical direct-seeding hybrid *indica* rice.

2 Materials and methods

2.1 Study site and materials

Field experiments were conducted in Chongzhou (103°38′E, 30° 33′N), Sichuan Province, China, in 2021 and 2022. The soils samples (0–20 cm) were analyzed physicochemical characteristics before initiation of the experiments (Table 1). The study site has a subtropical monsoon humid climate, and the rainfall, sunshine hours, and average temperature, during the rice growing season (May to October) were 924.10 mm, 836.05 h, and 22.77°C in 2021 and 894.20 mm, 762.41 h, and 23.02°C in 2022, respectively. This study used Yixiangyou 2115 (growth periods 145.2 d, female parent Yixiang 1A and male parent Yahui 2115) and Fyou 498 (growth periods 144.5 d, female parent FS3A and male parent Shuhui 498), two representative hybrid *indica* rice cultivars bred by Sichuan Agricultural University that are widely planted in South China. A slow-mixed basal fertilizer was applied, including 120 kg hm^{-2} N fertilizer comprising polymer-coated controlled-release urea-N (90 kg hm^{-2}) and conventional urea-N (30 kg hm^{-2}), 75 kg hm^{-2} P_2O_5, and 150 kg hm^{-2} K_2O, provided by Yantai Longdeng Fertilizer Co., Ltd. The N-release characteristics of the controlled-release N immersed in water at pH 7 and 25°C and the cumulative release rate of N reached 87.67% within 78 d shown in Figure 1 as described by Tomaszewska and Jarosiewicz, 2002.

2.2 Experimental design and field management

The experiments used a randomized design with two varieties and four strategies for managing N fertilizer. The comprehensive N fertilizer management mode (Table 2) were as follows: (1) slow-mixed N fertilizer (120 kg hm^{-2}) as a base (N_1, as control, in order to further calculate the NUE of urea-N topdressing); (2) N_1+urea-N (30 kg hm^{-2}) once as a base (N_2); (3) N_1+urea-N (30 kg hm^{-2}) topdressing on 32d after sowing at the tillering stage (N_3); (4) N_1 +urea-N (30 kg hm^{-2}) topdressing on 93d after sowing at the booting stage (N_4). Rice seeds were sown directly using a 2BDS-6 hand-held rice precision hill-direct-seeding machine (Guilin High-tech Zone Kefeng Machinery Co., Ltd.) on May 14th for both years. The row spacing and plant spacing were 25 cm and 20 cm, respectively, with a sowing amount of 30.0 kg hm^{-2} (4–6 seeds per hole) and density of 200,000 holes hm^{-2}. Each treatment had three replicates, with a plot area of 40.8 m^2 (8.5 m length and 4.8 m width). To prevent water and fertilizer from mixing, the plastic film was wrapped around ridges (40 cm wide and 30 cm high) constructed between the plots. All treatments used a high-efficiency alternation-irrigation technique (Sun et al., 2012). Chemical pesticides have been used to prevent yield loss and experimental errors caused by insects, diseases, and weeds.

2.3 Measurement terms and methods

2.3.1 Leaf area index

At the jointing, heading, and maturity stages, we obtained five holes from the representative rice plants in each plot based on the average number of tillers. We measured the leaf area of the rice plants at each growth stage using a CID-203 leaf area analyzer (CID Company, USA). The leaf area index (LAI) was calculated using the method reported by Liu et al. (2022).

2.3.2 Biomass accumulation

Five holes were sampled from each plot, representing rice plants with average tillers at the heading and maturity stages. The samples were divided into four parts: the stem sheaths, leaves, panicles, and roots. The samples were then exposed to 105°C for 40 min and subsequently dried at 80°C until they reached a constant weight (Guo et al., 2023a). The total biomass accumulation was calculated as the sum of the dry matter accumulation of the four plant parts.

2.3.3 Root vigor

As mentioned in Section 2.3.2, the method of Ramasamy et al. (1997) was used. Fresh roots (2.0 g) from each plot sample were transferred into a 100 mL flask. Then, 25.0 mL of 50.0 mg L^{-1}α-NA and 25.0 mL of phosphate buffer (0.1 mol L^{-1}, pH 7.0) were added. After filtration for 2h at 25°C in a closed shaker, 2.0 mL of $NaNO_2$ (100.0 mg L^{-1}) and 1.0mL of sulfonamide (1.0%) were added to the

TABLE 1 Average values for selected soil characteristics of composite topsoil samples in the field experiments.

Year	Organic matter (g kg^{-1})	Total N (g kg^{-1})	Available nutrient (mg kg^{-1})			pH	Bulk density (g cm^{-3})
			N	P	K		
2021	18.63	1.48	90.51	21.46	111.72	6.39	1.27
2022	19.64	1.52	89.71	21.98	104.35	6.42	1.28

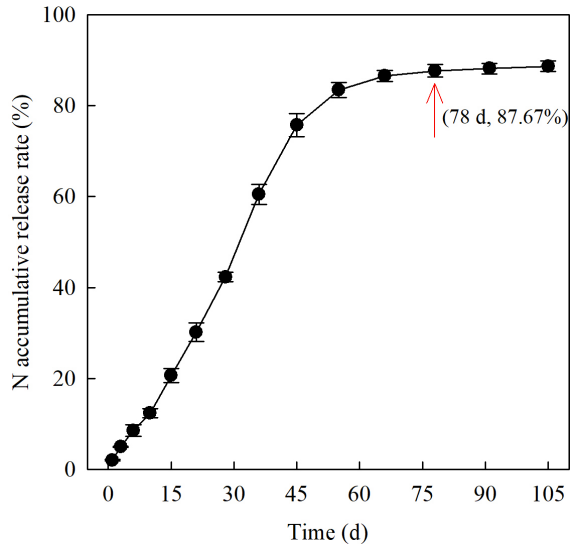

FIGURE 1
N cumulative release rate curve of controlled-release N fertilizer.

filtrate. Color was determined using a Shimadzu-1700 spectrophotometer (Japan) at 510 nm. The results were expressed as mg α-NA g^{-1}DW h^{-1}.

2.3.4 Nitrogen content

As stated in Section 2.3.2, each part was crushed and sieved separately through an 80-mesh sieve. The N content of each part was determined using the Kjeldahl method (Kjeltec-8400; FOSS, Hillerd, Denmark), as described by Yoshida et al. (1976).

2.3.5 Grain yield and its components

The number of effective panicles per plant was determined by examining 50 holes in rice plants in each plot at maturity. From each plot, 10 holes of rice plants were selected based on the average tillers to examine the total grains per panicle, number of full grains, and 1000-grain weight. The seed-setting percentages were also calculated (Guo et al., 2023a). The grain yield was determined by harvesting each 12.0 m^2 plot without border plants and adjusting it to a standard moisture content of 13.5% using a grain moisture meter (PM-8188-A, Kett Electric Laboratory, Tokyo, Japan).

2.3.6 Grain quality measurements

Approximately 1000 g of grains were harvested from each plot and naturally dried in the shade for three months to stabilize their physicochemical properties. The grains were then analyzed for quality after being passed through a dehusker and polished. A 250-gram sample was separated into broken and unbroken grains, and the brown rice, milled rice, and head rice rates were expressed as percentages of the total 250-gram rice grains (Zhang et al., 2008). For each sample, 1000 whole milled rice grains were randomly selected and scanned to create a digital image. This process was repeated three times. Image analysis software (JMWT-12, Dongfujiuheng Instrument Technology Co., Ltd., Beijing, China) was used to determine the rates of chalky grains and the degree of chalkiness (Guo et al., 2023b). The taste of cooked rice was measured using a Satake Rice Taste Analyzer (STA1A type, Satake, Japan) (Shi et al., 2022). 30.0 g of milled rice were weighed and placed in a stainless steel tank. Water was added at a rice-to-water ratio of 1:1.4, and the mixture was soaked for 30 min. The mouth of the tank was wrapped with filter paper and the tank was placed in a steam electric rice cooker. The rice was steamed for 30 min and then cooled for 2 h. After cooling, 7.0 g of rice was weighed at 25°C and placed into a special rice press instrument to form a rice cake. The rice cakes were then placed in a taste analyzer for testing.

2.4 Indicator calculation

As mentioned in Section 2.3 measurement terms, the calculation and definition of the following parameters are based on the method of Sun et al. (2023a).

Population photosynthetic potential from jointing to heading stage (PP; $\times 10^4$ m^2 d hm^{-2}) = 1/2 (the leaf area at the jointing stage + the leaf area at the heading stage) × (the time at the heading stage-the time at the jointing stage)

Dry matter transport rate in stem sheaths (DTR; %) = (dry matter weight in stem sheaths at the maturity stage-dry matter weight in stem sheaths at the heading stage)/dry matter weight in stem sheaths at the heading stage × 100

Dry matter transport contribution rate in stem sheaths (DCR; %) = (dry matter weight in stem sheaths at the maturity

TABLE 2 The comprehensive N fertilizer management mode (kg hm^{-2}).

Treatments	Total N amount	Basal N fertilizer (1d before sowing)		N topdressing of conventional urea	
		Slow-mixed N	Conventional urea N	Tiller fertilizer (32d after sowing)	Booting fertilizer (93d after sowing)
N_1	120	120	0	0	0
N_2	150	120	30	0	0
N_3	150	120	0	30	0
N_4	150	120	0	0	30

N_1: slow-mixed N fertilizer (120 kg hm^{-2}) as a base; N_2: N_1+urea-N (30 kg hm^{-2}) one-time as a base; N_3: N_1+urea-N (30 kg hm^{-2}) topdressing at tillering stage (32d after sowing); N_4: N_1+urea-N (30 kg hm^{-2}) topdressing at booting stage (93d after sowing).

stage-dry matter weight in stem sheaths at the heading stage)/grain weigh at the maturity stage × 100

Population growth rate (PGR; $g \cdot m^{-2} \cdot d^{-1}$) = (dry matter weight in plants at the maturity stage-dry matter weight in plants at the heading stage)/(the time at the maturity stage-the time at the heading stage)

Root vigor of decay rate from heading to maturity stage (DCRT; %) = (root vigor at the maturity stage-root vigor at the heading stage)/root vigor at the heading stage ×100

N transport amount in leaves or stem sheaths from heading to maturity stage (NTA; kg hm^{-2}) = N accumulation amount in leaves or stem sheaths at the heading stage-N accumulation amount in leaves or stem sheaths at the maturity stage

N transport rate in leaves or stem sheaths from heading to the maturity stage (NTR; %) = NTA in leaves or stem sheaths/N accumulation amount in leaves or stem sheaths at the heading stage

N transport contribution rate in leaves or stem sheaths from heading to the maturity stage (NCR; %) = NTA in leaves or stem sheaths/N accumulation amount in panicles at the maturity stage

N agronomic efficiency of urea-N topdressing (NAE; kg kg^{-1}) = (grain yield in urea-N topdressing supply-grain yield in zero urea-N topdressing supply)/urea-N topdressing supply amount

N recovery efficiency of urea-N topdressing (NPE; kg kg^{-1}) = (grain yield in urea-N topdressing supply-grain yield in zero urea-N topdressing supply)/(total N accumulation in urea-N topdressing supply at the maturity stage-total N accumulation in zero urea-N topdressing supply at the maturity stage)

2.5 Statistical analysis

Data were analyzed using Microsoft Excel 2010. Analysis of variance (ANOVA) was performed using the statistical program SPSS 18.0 (SPSS Statistics, SPSS Inc., Chicago, IL, USA). Graphs were generated using SigmaPlot 10.0 (Systat Software Inc., Chicago, IL, USA). The treatment means were tested using the least significant difference (LSD) test ($P < 0.05$). Principal component analysis was conducted using Origin 2021 (OriginLab Corp., Northampton, MA, USA).

3 Results

3.1 Yield and yield components

The impact of varying N fertilizer management on grain yield and its components in mechanical direct-seeding hybrid *indica* rice is significant. The interaction effect of the two factors on grain yield, filled spikelets, total spikelets, and seed-setting rate was also significant. The trend observed in the two-year experiments was consistent (Table 3). Under different varieties and N fertilizer management, the impact of N fertilizer on yield was significantly greater than variety. The yields of the N_2, N_3, and N_4 treatments increased by 4.45%, 13.29%, and 20.98%, respectively, compared to the N_1 treatment, with the highest yield observed in the N_4 treatment. Fyou 498 showed a greater increase under N_2 and N_3 treatments compared to Yixiangyou 2115. This suggests that varieties with a large panicle type and high sink capacity, such as Fyou 498, should be treated with late booting fertilizer besides the base application of slow-mixed fertilizer to exploit their high-yield potential.

Table 3 show that N fertilizer management resulted in higher numbers of filled spikelets, total spikelets, and filled grains than the effects of variety differences. However, the number of effective panicles and 1000-grain weight showed opposite trends. This suggests that a suitable combination of variety and N fertilizer regulation can adjust the yield components of mechanical direct-seeding hybrid *indica* rice, ultimately promoting yield. The mean values of the yield components for Fyou 498 were significantly higher than those for Yixiangyou 2115 among the different varieties, except for the number of effective panicles and 1000-grain weight. Under the application of slow-release fertilizer combined with urea-N topdressing, the number of effective panicles initially increased and then decreased with a delay in the urea-N fertilizer application time. The yield components of different varieties also increased with the delay in the urea-N fertilizer application time. The filled spikelets, total spikelets, filled grains, and 1000-grain weight of the two varieties under N_4 treatment were higher than those under the other treatments. This compensated for the deficiency of the effective panicle number and was a significant factor in achieving a high yield under N_4 treatment.

3.2 Leaf area index and population photosynthetic potential

At both the jointing and heading stages, the LAI of Fyou 498 was significantly higher than Yixiangyou 2115 by 9.61–13.91% and 8.67–13.35%, respectively. This trend was consistent across both years of experimentation (Figures 2A, B, D, E). For the same variety under different N fertilizer management, LAI at the jointing and heading stages showed an initial increase, followed by a decrease. Compared to the N_1 treatment, the average values of the N_2, N_3, and N_4 treatments for the two varieties during the jointing stage (N_4 treatment without topdressing urea-N fertilizer during this time) were significantly higher by 22.62%, 30.15%, and 20.63%, respectively. At the heading stage, the LAI of the N_2, N_3, and N_4 treatments increased significantly by 21.45%, 31.03%, and 26.20%, respectively. The LAI in the N_4 treatment showed the most significant increase. From the jointing to heading stage, the population photosynthetic potential of Fyou 498 was 5.01%–10.49% higher than Yixiangyou 2115 (Figures 2C, F). The photosynthetic potential of the population under the same variety

10.3389/fpls.2024.1400146

TABLE 3 Effects of slow-mixed fertilizer base application combined with urea topdressing time on yield and its components of mechanical direct-seeding hybrid *indica* rice.

Year	Cultivar	N treatments	Effective panicles ($\times10^4$·hm^{-2})	Filled spikelets (No. panicle^{-1})	Total spikelets ($\times10^6$·hm^{-2})	Filled grains (%)	1000-grain weight (g)	Grain yield (kg·hm^{-2})
2021	Yixiangyou2115	N_1	229.83c	116.60c	267.94c	81.14b	36.00b	8100.85c
		N_2	239.00b	122.15bc	291.15b	78.67c	36.06b	8458.75c
		N_3	252.66a	128.10b	323.73a	81.95b	36.06b	9169.85b
		N_4	234.23bc	140.00a	327.94a	83.55a	36.87a	9825.54a
	Average		**238.93**	**126.71**	**302.70**	**81.33**	**36.25**	**8888.75**
	Fyou 498	N_1	220.00c	145.28c	319.74c	81.53c	32.06ab	8297.75c
		N_2	228.70b	150.06bc	343.15b	80.67c	31.66b	8746.28c
		N_3	236.80a	156.44b	370.36a	83.25b	31.93ab	9494.78b
		N_4	227.61bc	167.41a	381.05a	84.83a	32.18a	10090.28a
	Average		**228.28**	**154.80**	**353.58**	**82.57**	**31.96**	**9157.27**
	F value	V	54.91**	367.03**	113.51**	19.03**	4457.63**	5.16*
		N	33.28**	44.67**	34.33**	42.43**	13.39**	43.57**
		V×N	1.74	6.04*	4.92*	4.23*	2.23	4.45*
2022	Yixiangyou2115	N_1	223.02c	114.44c	267.79c	76.12bc	35.33b	8004.75c
		N_2	234.00b	121.04b	269.94c	74.18c	35.60b	8239.32c
		N_3	257.67a	122.52b	299.60b	79.76b	36.25ab	8949.53b
		N_4	234.17b	127.94a	315.69a	84.73a	36.88a	9556.51a
	Average		**237.21**	**121.48**	**288.25**	**78.70**	**36.01**	**8687.52**
	Fyou 498	N_1	220.00c	144.21c	329.75c	72.33b	32.05b	8075.86d
		N_2	228.67b	146.11c	346.03b	70.76b	32.13ab	8481.72c
		N_3	236.83a	152.23b	354.35a	79.79a	32.15ab	9187.14b
		N_4	233.57ab	161.07a	355.57a	80.52a	32.49a	9825.58a
	Average		**229.77**	**150.90**	**346.42**	**75.85**	**32.20**	**8892.58**
	F value	V	54.69**	52.04**	31.46**	50.71**	412.88**	6.99*
		N	33.17**	21.64*	6.59*	49.24**	6.77*	38.78**
		V×N	1.77	7.02*	5.21*	6.47*	1.25	7.15*

N_1: slow-mixed N fertilizer (120 kg hm^{-2}) as a base; N_2: N_1+urea-N (30 kg hm^{-2}) one-time as a base; N_3: N_1+urea-N (30 kg hm^{-2}) topdressing at the tillering stage (32d after sowing); N_4: N_1+urea-N (30 kg hm^{-2}) topdressing at the booting stage (93d after sowing). V, Variety; N, N fertilizer treatment; V×N, cultivar and N fertilizer treatment interaction.*, $P < 0.05$; **, $P < 0.01$. Different lowercase letters indicate significant ($P < 0.05$) differences among N fertilizer treatments under the same variety.

increased significantly from the jointing to the heading stage with the postponement of urea-N fertilizer application. Compared with the N_1 treatment, the N_2, N_3, and N_4 treatments increased significantly by 15.07%, 35.43%, and 47.09%, respectively.

3.3 Dry matter accumulation and translocation and population growth rate

The impact of variety and N fertilizer on the indices of dry matter accumulation and transport, as well as the population growth rate from the heading to the maturity stage, was significant. The interaction effect of the two factors on the amount of dry matter accumulation, transport rate, and contribution rate in stem sheaths, as well as the population growth rate, was also significant (Table 4). Furthermore, the accumulation and translocation of dry matter, as well as the population growth rate from the heading to maturity stage, were significantly more affected by the management of N fertilizer than by the differences between the varieties. The amount of dry matter accumulated in the stem sheaths of Fyou 498 was 4.46% higher than Yixiangyou 2115 at the heading stage, and 2.42% higher at the maturity stage. The dry matter accumulation, dry matter transport rate, dry matter transport contribution rate, and population growth rate of Fyou 498 from the heading to maturity stage were 8.83%, 5.48%, 7.09%, and 8.40% higher than those of Yixiangyou 2115,

10.3389/fpls.2024.1400146

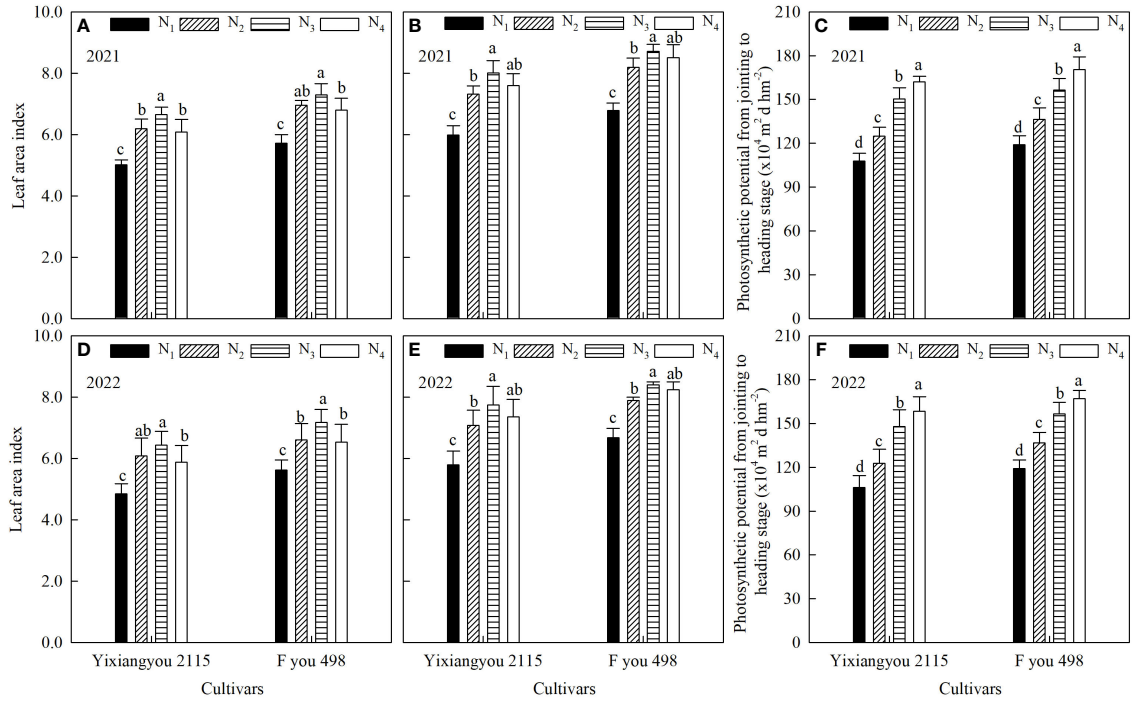

FIGURE 2
Effects of slow-mixed fertilizer base application combined with urea topdressing time on LAI at the jointing stage **(A, D)**, LAI at the heading stage **(B, E)** and photosynthetic potential **(C, F)** from the jointing to heading stage of mechanical direct-seeding hybrid *indica* rice. N_1: slow-mixed N fertilizer (120 kg hm^{-2}) as a base; N_2: N_1+urea-N (30 kg hm^{-2}) one-time as a base; N_3: N_1+urea-N (30 kg hm^{-2}) topdressing at the tillering stage (32 d after sowing); N_4: N_1+urea-N (30 kg hm^{-2}) topdressing at the booting stage (93 d after sowing). Different lowercase letters indicate significant ($P < 0.05$) differences among N fertilizer treatments under the same variety.

TABLE 4 Effects of slow-mixed fertilizer base application combined with urea topdressing time on dry matter accumulation and translocation and population growth rate from the heading to maturity stage of mechanical direct-seeding hybrid *indica* rice.

Cultivar	N treatments	DASH ($kg·hm^{-2}$)	DASM ($kg·hm^{-2}$)	From heading to maturity stage			
				DAP ($kg·hm^{-2}$)	DTR (%)	DCR (%)	PGR ($g·m^{-2}·d^{-1}$)
Yixiangyou 2115	N_1	5900.27b	3899.34d	3002.20d	33.91a	24.69a	10.00d
	N_2	6079.29b	4574.95c	3818.40c	24.75c	17.78c	12.73c
	N_3	7453.23a	5545.42b	4564.10b	25.60b	20.81b	15.21b
	N_4	7849.36a	5800.19a	5012.60a	26.11b	20.86b	16.71a
	Average	**6820.54**	**4954.98**	**4099.33**	**27.59**	**21.04**	**13.66**
Fyou498	N_1	5948.65d	3904.58d	3146.80d	34.36a	24.71a	10.49d
	N_2	6480.93c	4797.13c	3986.30c	25.98d	19.25d	13.29c
	N_3	7749.27b	5618.85b	5122.10b	27.49c	22.44c	17.07b
	N_4	8354.37a	5993.65a	5618.90a	28.26b	23.40b	18.73a
	Average	**7133.31**	**5078.55**	**4468.53**	**29.02**	**22.45**	**14.90**
F value	V	13.17**	3.98*	47.47**	16.77**	27.11**	47.79**
	N	145.77**	210.84**	346.57**	128.43**	89.13**	348.01**
	V×N	1.29	0.67	5.31**	4.82*	4.10*	5.29**

N_1: slow-mixed N fertilizer (120 $kg·hm^{-2}$) as a base; N_2: N_1+urea-N (30 $kg·hm^{-2}$) one-time as a base; N_3: N_1+urea-N (30 $kg·hm^{-2}$) topdressing at the tillering stage (32d after sowing); N_4: N_1+urea-N (30 $kg·hm^{-2}$) topdressing at the booting stage (93d after sowing). V, Variety; N, N fertilizer treatment; V×N, cultivar and N fertilizer treatment interaction. DASH, dry matter accumulation amount in stem-sheath at the heading stage; DASM, dry matter accumulation amount in stem sheaths at the maturity stage; DAP, dry matter accumulation amount in plants; DTR, dry matter transport rate in stem sheaths; DCR, dry matter transport contribution rate in stem sheaths; PGR, population growth rate. *, $P < 0.05$; **, $P < 0.01$. Different lowercase letters indicate significant ($P < 0.05$) differences among N fertilizer treatments under the same variety.

respectively. The indices of dry matter accumulation and population growth rate increased to varying degrees with the postponement of the urea-N topdressing time under the same variety. Compared to the N_1 treatment, the N_2, N_3, and N_4 treatments significantly increased the dry matter accumulation in stem sheaths during the heading and maturity stages by 3.04–40.43% and 17.31–53.50%, respectively. Furthermore, the dry matter accumulation in plants and population growth rate from the heading to maturity stage were significantly increased by 27.18–78.55% and 26.69–62.72%, respectively. Compared with the N_1 treatment, the dry matter transport rate and contribution rate in stem sheaths from heading to maturity among the N_2, N_3, and N_4 treatments were significantly reduced by 6.95–8.77% and 2.57–6.18%. However, the dry matter transport rate and contribution rate in stem sheaths from heading to maturity increased by 1.18–1.82% and 3.11–3.62% with the postponement of the urea-N fertilizer application time in the N_2, N_3, and N_4 treatments.

3.4 Root vigor

The root vigor of Fyou 498 was significantly higher than Yixiangyou 2115 at both the heading (Figures 3A, D) and maturity stages (Figures 3B, E), with differences ranging from 4.80% to 18.15% and 8.76% to 23.88%, respectively. Furthermore, the root vigor decay rate from the heading to maturity stage (Figures 3C, F) was 1.76–7.08% lower in Fyou 498 than in Yixiangyou 2115. The results of the 2-year experiments showed consistent trends. In the same variety, postponing the application time of urea-N resulted in a significant increase in root vigor during the heading and maturity stages. Compared with the N_1 treatment, the root vigor at the heading stage increased significantly by 12.05–27.04%, 39.07–53.36%, and 77.89–80.09% in the N_2, N_3, and N_4 treatments, respectively. At the maturity stage, root vigor increased significantly by 27.60–40.42%, 65.91–76.26%, and 118.52–126.18% in the N_2, N_3, and N_4 treatments, respectively. Moreover, the decay rate of root vigor from the heading to maturity stage decreased with postponement of the urea-N fertilizer application time. Compared to the N_1 treatment, root vigor decay rate decreased significantly by 7.91–10.72%, 11.05- 15.07%, and 16.05–21.39% in the N_2, N_3, and N_4 treatments, respectively, from the heading to maturity stage.

3.5 Nitrogen transport and utilization

Table 5 shows that the effect of variety on the N transport contribution rate in stem sheaths from the heading to the maturity stage was not significant. However, the effects of variety and N fertilizer management on N translocation in stem sheaths (leaves) from heading to maturity and NUE (NAE and NPE) were significant. Furthermore, the interaction effect of these two factors on N transport in stem sheaths and leaves, as well as the transport rate from heading to maturity, was significant. Compared to Yixiangyou 2115, Fyou 498 exhibited an increase of 1.03–9.38% in the N transport rate and N transport contribution rate in stem sheaths from heading to maturity. Moreover, Fyou 498 showed an

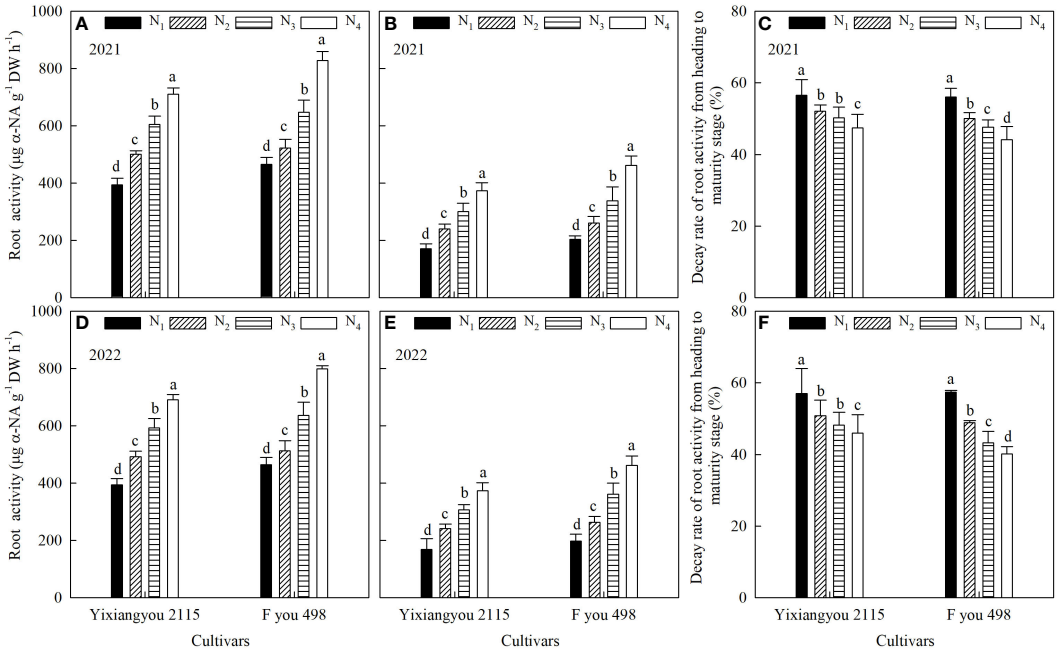

FIGURE 3
Effects of slow-mixed fertilizer base application combined with urea topdressing time on root vigor at the heading stage **(A, D)**, root vigor at the maturity stage **(B, E)** and root vigor decay rate **(C, F)** from the heading to maturity stage of mechanical direct-seeding hybrid *indica* rice. N_1: slow-mixed N fertilizer (120 kg hm^{-2}) as a base; N_2: N_1+urea-N (30 kg hm^{-2}) one-time as a base; N_3: N_1+urea-N (30 kg hm^{-2}) topdressing at the tillering stage (32 d after sowing); N_4: N_1+urea-N (30 kg hm^{-2}) topdressing at the booting stage (93 d after sowing). Different lowercase letters indicate significant ($P < 0.05$) differences among N fertilizer treatments under the same variety.

10.3389/fpls.2024.1400146

TABLE 5 Effects of slow-mixed fertilizer base application combined with urea topdressing time on N translocation in stem-sheaths and leaves from the heading to maturity stage and NUE of mechanical direct-seeding hybrid *indica* rice.

Cultivar	N treat-ments	NSTA (kg·hm^{-2})	NSTR (%)	NSCR (%)	NLTA (kg·hm^{-2})	NLTR (%)	NLCR (%)	NAE (kg kg^{-1})		NPE (kg kg^{-1})	
								2021	2022	2021	2022
Yixiangyou 2115	N_1	10.37d	28.88a	10.04b	28.35d	69.08a	27.45b	–	–	–	–
	N_2	11.94c	26.39b	10.22b	32.19c	53.88b	27.57b	11.93c	7.82c	9.91c	6.50c
	N_3	14.40b	26.16bc	10.86a	36.76b	52.63bc	27.74b	35.63b	31.49b	16.52b	14.60b
	N_4	16.25a	25.06c	11.60a	39.70a	51.62c	28.33a	57.49a	51.73a	20.43a	18.38a
	Average	**13.24**	**26.62**	**10.68**	**34.25**	**56.80**	**27.77**	**35.02**	**30.35**	**15.62**	**14.16**
Fyou 498	N_1	11.34d	30.03a	10.18c	30.74d	69.64a	27.60c	–	–	–	–
	N_2	12.95c	29.39a	10.21c	36.24c	57.30b	28.56b	14.95c	13.53c	13.13c	11.88c
	N_3	15.50b	26.86b	10.91b	41.44b	56.42bc	29.18a	39.90b	37.04b	18.40b	17.08b
	N_4	18.14a	26.77b	11.86a	45.04a	55.25c	29.46a	59.75a	58.32a	20.53a	20.04a
	Average	**14.48**	**28.26**	**10.79**	**38.36**	**59.65**	**28.70**	**38.20**	**36.30**	**17.35**	**16.33**
F value	V	52.03**	19.95**	0.68	83.93**	15.76**	4.08*	46.81**	40.21**	53.11**	65.37**
	N	261.91**	23.76**	31.54**	156.40*	87.95**	7.18*	240.87**	163.59**	132.32**	142.57**
	V×N	3.85*	4.34*	0.20	3.98*	3.89*	0.63	4.93*	5.07*	4.44*	4.01*

N_1: slow-mixed N fertilizer (120 kg·hm^{-2}) as a base; N_2: N_1+urea-N (30 kg·hm^{-2}) one-time as a base; N_3: N_1+urea-N (30 kg·hm^{-2}) topdressing at the tillering stage (32d after sowing); N_4: N_1+urea-N (30 kg·hm^{-2}) topdressing at the booting stage (93d after sowing). V: Variety; N: N fertilizer treatment; V×N: cultivar and N fertilizer treatment interaction. NSTA, N transport amount in stem sheaths; NSTR, N transport rate in stem sheaths; NSCR, N transport contribution rate in stem sheaths; NLTA, N transport amount in leaves; NLTR, N transport rate in leaves; NLCR, N transport contribution rate in leaves; NAE, N agronomic efficiency of urea-N topdressing; NPE, N recovery efficiency of urea-N topdressing. *, $P < 0.05$; **, $P < 0.01$. Different lowercase letters indicate significant ($P < 0.05$) differences among N fertilizer treatments under the same variety.

increase of 3.34–12.01% in the N transport rate and N transport contribution rate in leaves from heading to maturity. The NAE and NPE of Fyou 498 were significantly higher than those of Yixiangyou 2115, by 13.98% and 15.44%, respectively. For the same variety, the amount of N transported in stem sheaths (leaves) and the contribution rate of N transport in stem sheaths (leaves) increased to varying degrees from the heading to maturity stage, with a delay in the urea-N topdressing time. Compared to the N_1 treatment, the N_2, N_3, and N_4 treatments significantly increased the amount of N transported in stem sheaths (leaves) from the heading to maturity stage by 13.54–59.96%. Furthermore, the N transport contribution rate in stem sheaths (leaves) increased by 0.29–16.50%. However, the rate of N transport in stem sheaths (leaves) from the heading to maturity stage decreased by 2.13–25.27% when the urea-N topdressing was postponed. Moreover, both NAE and NPE increased significantly with a delay in the urea-N topdressing.

3.6 Rice quality

The 2-year experiments showed significant effects of variety and N fertilizer management on rice quality indicators. The interaction effect of the two factors only had a significant impact on chalkiness and chalky kernel rate (Table 6). Regarding the treatment of varieties and N fertilizer management, the rice quality indicators of the variety differences were significantly higher than those of N fertilizer management, except for the brown rice rate. Compared with Yixiangyou 2115, Fyou 498 exhibited a decrease in brown rice rate, milled rice rate, head rice rate, and taste value by 0.52–5.51%, 1.53–3.40%, 3.73–6.64%, and 5.05–7.67%, respectively. Furthermore, the chalkiness and chalky kernel rates increased by 1.63–4.91% and 4.37–13.17%, respectively. When comparing the same variety, brown rice, milled rice, head rice, chalkiness, and chalky grain rates increased to varying degrees with the postponement of the urea-N topdressing time. Compared to the N_1 treatment, the brown rice, milled rice, head rice, chalkiness, and chalky grain rates increased by 0.65–5.09%, 0.67–3.75%, 1.17–6.44%, 0.21–3.48%, and 0.52–12.77% in the N_2, N_3, and N_4 treatments, respectively. Compared to the N_1 treatment, the taste values of the N_2, N_3, and N_4 treatments decreased significantly by 1.16–5.88%. However, the taste value increased significantly when the urea-N topdressing time was delayed.

3.7 Relationships between photosynthetic production, root vigor, N transport, yield, rice quality, and NUE

Principal component analysis (PCA) was conducted to analyze the relationship between photosynthetic production, root vigor, and N translocation and grain yield, total spikelets, NUE, head rice rate, and taste value under different varieties and N application management (Figure 4). Under various N fertilizer treatments, Yixiangyou 2115 and Fyou 498 had principal components 1 and 2, explaining 92.2% and 93.1% of the total changes in grain yield, total spikelets, NAE, NPE, head rice rate, and taste value,

10.3389/fpls.2024.1400146

TABLE 6 Effects of slow-mixed fertilizer base application combined with urea topdressing time on rice quality of mechanical direct-seeding hybrid *indica* rice.

Year	Cultivar	N treatments	Brown rice (%)	Milled rice (%)	Head rice (%)	Chalkiness (%)	Chalky kernel (%)	Taste value
2021	Yixiangyou 2115	N_1	75.00c	64.64c	55.33b	3.11c	12.11c	87.33a
		N_2	77.41b	66.26b	56.50b	3.32bc	12.63b	84.00c
		N_3	77.99ab	66.32b	58.26a	3.69ab	14.19a	84.20c
		N_4	78.06a	67.58a	58.44a	4.00a	14.52a	86.10b
		Average	**77.12**	**66.20**	**57.13**	**3.53**	**13.36**	**85.41**
	Fyou 498	N_1	74.21d	63.11c	48.17c	4.74c	16.48c	82.21a
		N_2	74.86c	63.78bc	51.02b	6.59b	20.23b	76.33d
		N_3	76.41b	63.89b	51.91b	7.28a	24.39a	79.00c
		N_4	77.54a	65.80a	54.61a	7.35a	24.53a	81.05b
		Average	**75.76**	**64.15**	**51.57**	**6.49**	**21.41**	**79.65**
	F value	V	4.75*	14.87**	52.41**	99.29**	84.20**	72.99**
		N	5.94*	4.71*	8.72*	26.70**	20.52**	9.12**
		V×N	0.53	0.20	1.91	7.88**	6.23**	0.89
2022	Yixiangyou 2115	N_1	76.29c	63.92c	54.22b	3.47c	12.01b	85.83a
		N_2	77.71b	65.76b	55.61b	4.14bc	12.97b	81.10c
		N_3	78.93a	66.42b	57.04a	4.50b	15.51a	83.00b
		N_4	78.96a	67.67a	58.34a	5.85a	16.87a	85.05a
		Average	**77.97**	**65.94**	**56.30**	**4.49**	**14.34**	**83.75**
	Fyou 498	N_1	70.77d	61.28c	48.69c	8.28c	18.26d	80.71a
		N_2	72.32c	62.49b	50.95b	8.95c	21.73c	74.50d
		N_3	74.80b	63.65a	51.62b	10.58b	27.90b	76.67c
		N_4	75.86a	64.27a	55.03a	11.76a	31.03a	78.69b
		Average	**73.44**	**62.92**	**51.43**	**9.64**	**24.73**	**77.64**
	F value	V	5.83*	10.14**	47.82**	87.34**	98.04**	54.12**
		N	6.44*	5.22*	6.94*	21.23**	27.11**	10.76**
		V×N	0.24	0.79	3.02	9.01**	7.95**	3.13

N_1: slow-mixed N fertilizer (120 kg·hm^{-2}) as a base; N_2: N_1+urea-N (30 kg·hm^{-2}) one-time as a base; N_3: N_1+urea-N (30 kg·hm^{-2}) topdressing at the tillering stage (32d after sowing); N_4: N_1+urea-N (30 kg·hm^{-2}) topdressing at the booting stage (93d after sowing). V, Variety; N, N fertilizer treatment; V×N, cultivar and N fertilizer treatment interaction. *, $P < 0.05$; **, $P < 0.01$. Different lowercase letters indicate significant ($P < 0.05$) differences among N fertilizer treatments under the same variety.

respectively. The relationship between these variables suggested that grain yield, NAE, NPE, and taste value of the two varieties were correlated positively with LAI at the jointing stage, LAI at the heading stage, photosynthetic potential from the jointing to heading stage, root vigor at the maturity stage, dry matter transport rate and dry matter transport contribution rate in stem sheaths from the heading to maturity stage, population growth rate from the heading to maturity stage, N transport amount and N transport contribution rate in stem sheaths from the heading to maturity stage, N transport amount and N transport contribution rate in leaves from the heading to maturity stage (Figure 4). However, they correlated negatively with the root vigor of decay rate from the heading to maturity stage, N transport rate in stem sheaths from heading to maturity stage, and N transport rate in leaves from heading to maturity stage (Figure 4). The total explained amount of the two rice varieties under different N fertilizer treatments (Figure 4), compared to Yixiangyou 2115, can better explain the synergistic enhancement of high yield, good quality, and high NUE in rice, including grain yield, rice quality, and NUE for Fyou 498.

The correlation analysis in Figure 5 indicates that the grain yield, total spikelets, NAE, NPE, head rice rate, and taste value of both varieties were significantly positively correlated with the photosynthetic potential from the jointing to heading stage, dry matter transport contribution rate in stem sheaths from the heading to maturity stage, N transport contribution rate in stem sheaths from the heading to maturity stage, and N transport amount in

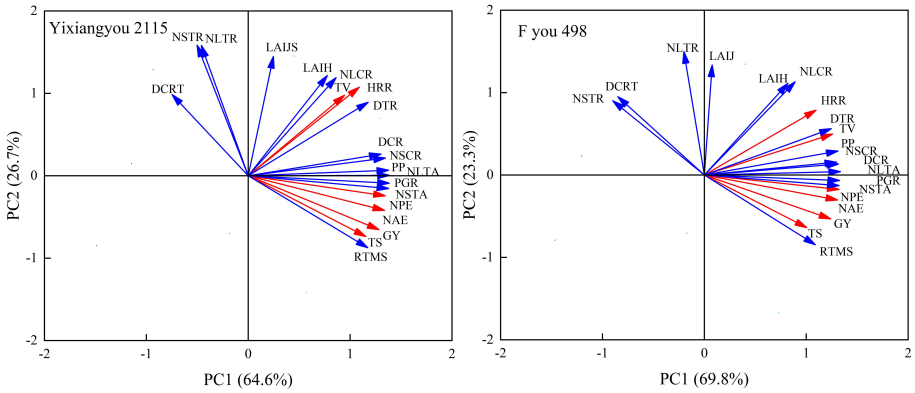

FIGURE 4
Principal component analysis of grain yield, rice quality and NUE with photosynthetic production, root vigor and N transport. The number of samples is 24 in the analysis of each indicator under every variety. GY, grain yield; TS, total spikelets; NAE, N agronomic efficiency of urea-N topdressing; NPE, N recovery efficiency of urea-N topdressing; HRR, head rice rate; TV, taste value; LAIJ, LAI at the jointing stage; LAIH, LAI at the heading stage; PP, photosynthetic potential from the jointing to heading stage; RTMS, root vigor at the maturity stage; DCRT, root vigor of decay rate from the heading to maturity stage; DTR, dry matter transport rate in stem sheaths from the heading to maturity stage; DCR, dry matter transport contribution rate in stem sheaths from the heading to maturity stage; PGR, population growth rate from heading to maturity stage; NSTA, N transport amount in stem sheaths from the heading to maturity stage; NSTR, N transport rate in stem sheaths from heading to maturity stage; NSCR, N transport contribution rate in stem sheaths from the heading to maturity stage; NLTA, N transport amount in leaves from the heading to maturity stage; NSTR, N transport rate in leaves from the heading to maturity stage; NSCR, N transport contribution rate in leaves from the heading to maturity stage.

leaves from the heading to maturity stage. The correlations between the N transport contribution rate in stem sheaths from the heading to maturity stage and the photosynthetic potential from the jointing to heading stage, population growth rate from the heading to maturity stage, and N transport amount in leaves from the heading to maturity stage were highly significant. This indicates that increasing the N transport contribution rate in stem sheaths from the heading to maturity stage can synergistically enhance the high yield, high quality, and high NUE of mechanical direct-seeding hybrid *indica* rice. Furthermore, when considering each variety, the effects of different N fertilizer management on the taste regulation of the high taste value Yixiangyou 2115 were significantly less

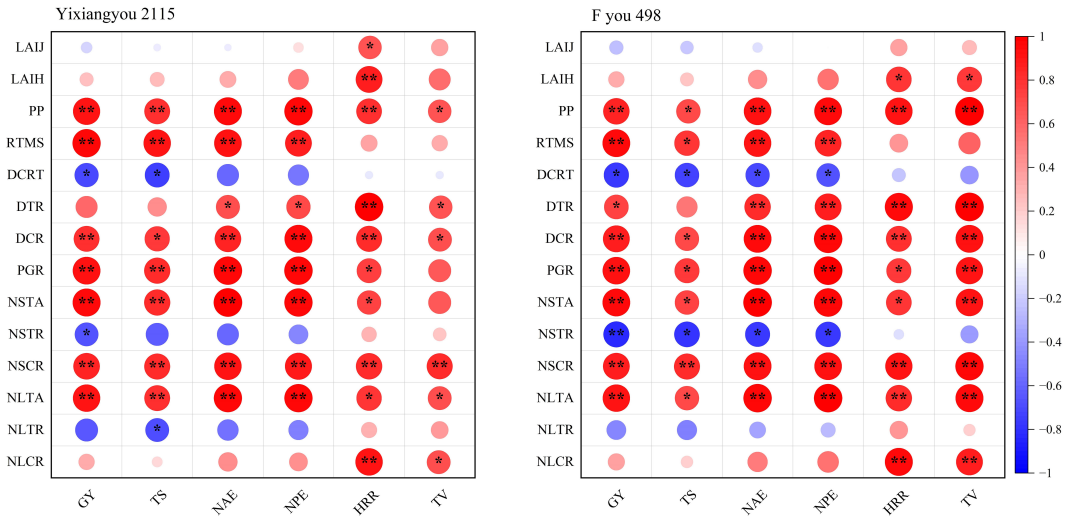

FIGURE 5
Heat map of person correlation in grain yield, rice quality and NUE with photosynthetic production, root vigor and N transport. The number of samples is 24 in the analysis of each indicator under every variety. GY, grain yield; TS, total spikelets; NAE, N agronomic efficiency of urea-N topdressing; NPE, N recovery efficiency of urea-N topdressing; HRR, head rice rate; TV, taste value; LAIJ, LAI at the jointing stage; LAIH, LAI at the heading stage; PP, photosynthetic potential from the jointing to heading stage; RTMS, root vigor at the maturity stage; DCRT, root vigor of decay rate from the heading to maturity stage; DTR, dry matter transport rate in stem sheaths from the heading to maturity stage; DCR, dry matter transport contribution rate in stem sheaths from the heading to maturity stage; PGR, population growth rate from the heading to maturity stage; NSTA, N transport amount in stem sheaths from the heading to maturity stage; NSTR, N transport rate in stem sheaths from heading to maturity stage; NSCR, N transport contribution rate in stem sheaths from the heading to maturity stage; NLTA, N transport amount in leaves from the heading to maturity stage; NSTR, N transport rate in leaves from heading to maturity stage; NSCR, N transport contribution rate in leaves from the heading to maturity stage. *, $P < 0.05$; **, $P < 0.01$.

pronounced than those of the low-taste value Fyou 498. This suggests that there is significant potential for improving the taste value of low-taste value varieties through urea-N topdressing under slow-mixed fertilizer-based application.

4 Discussion

4.1 Effect of slow-mixed fertilizer base application combined with available N fertilizer on rice yield formation

Selecting appropriate rice varieties and optimizing N fertilizer management are crucial for regulating rice yield (Jiang et al., 2016; Li et al., 2023). The most important factors affecting yield were the number of effective panicles, number of filled spikelets, and 1000-grain weight. Different conclusions have been drawn regarding how to balance the relationships between these factors under varying cultivation conditions (Guo et al., 2023a; Sun et al., 2023a). Previous studies have shown that the productivity of rice varieties primarily depends on the total number of spikelets, which is the product of the number of effective panicles and number of grains per panicle (Wei et al., 2016; Lyu et al., 2021a; Li et al., 2023). The study results indicate that the N_1 treatment, which involves using urea-N fertilizer as a base fertilizer without topdressing in the later stage and varieties with excessive total spikelets, can lead to issues such as unfilled grains, decreased seed-setting rate, and reduced 1000-grain weight. This is compared to the N_3 and N_4 treatments (Table 3). Previous studies have suggested that onetime basal application of controlled-release fertilizers and formulations can increase rice yield and efficiency. This method is effective for increasing rice yield and efficiency. This method also regulates the amount of fertilizer used (Deng et al., 2021; Hou et al., 2021; He et al., 2023). However, this study suggests that slow-release fertilizers should be applied as a single basal application. If combined with urea-N in the later stage, the 'sink' capacity of the variety should be taken into consideration. In this study, Fyou 498 had a significantly higher total spikelet count than Yixiangyou 2115, but Yixiangyou 2115 had a 1000-grain weight >36.0 g (grain length 7.60 mm, grain width 2.65 mm, and length-width ratio 2.87 of single grain). The 1000-grain weight indirectly reflects the rice's 'sink' capacity based on a certain amount of total spikelets. Both varieties in this study had a large 'sink' capacity. Therefore, to promote a significant increase in grain yield (Table 3), it is necessary to consider the combined application of urea-N fertilizer in the later stage, based on the application of slow-mixed fertilizer.

Rice yield is closely related to the dynamics of population tillers, photosynthetic characteristics, material accumulation, and transport capacity (Sun et al., 2012; Guo et al., 2023a). Super-high-yield rice is characterized by a lower number of tillers in the early growth stage but a higher percentage of productive tillers. LAI and dry matter accumulation exhibited slow growth in the early stage, moderate growth during the heading stage, and a significant increase after the heading stage. The population growth rate was high, and 70–80% of the grain yield was achieved during the late growth stage (Cheng et al., 2022; Liu et al., 2022; Li et al., 2023). The study showed that using slow-mixed fertilizer combined with urea-N fertilizer N_3 treatment can increase the photosynthetic potential from the jointing to heading stage and the root vigor decay rate from the heading to maturity stage. This is important for ensuring a high population growth rate and dry matter quality in the late growth stage, resulting in a high yield and efficiency of direct-seeding rice. These findings further enriched and improved the results of previous studies (Wang et al., 2021; Cheng et al., 2022; Liu et al., 2022; Guo et al., 2023a). This study confirmed that rice varieties can contribute to high yield and efficiency (Meng et al., 2022). The study found that Fyou 498 had a significantly higher population photosynthetic potential, population growth rate, and root vigor than Yixiangyou 2115 during the main growth stages (Figures 2, 3; Table 4). This study found that rice varieties and slow-mixed fertilizer base application with urea-N topdressing had significant effects on the photosynthetic characteristics, dry matter accumulation, and transport, and root vigor of mechanical direct-seeding rice. When applying controlled-release fertilizer, it is important to consider the combination of improved varieties and cultivation methods. This study was conducted based on a previous study that found the optimal amount of topdressing N fertilizer for direct-seeding rice in the latter stage to be 20% of the total N application. Increasing the proportion of postponed N fertilizer beyond 20% to 40–60% of the total amount significantly reduces the population quality of direct-seeding rice and increases the lodging index, resulting in yield reduction (Wu et al., 2020; Sun et al., 2022). Therefore, this study did not consider increasing the amount of N fertilizer postponement.

4.2 Effect of slow-mixed fertilizer base application combined with available N fertilizer on NUE and rice quality

High-NUE rice varieties, types of N fertilizer, and N fertilizer management practices are closely related to improving both NUE and rice quality (Li et al., 2023; Sun et al., 2023b). In this study, different varieties and slow-mixed basal fertilizer application with urea-N fertilizer management were compared. It was found that Fyou 498 significantly increased the transport of N and the contribution of stem sheaths (leaves) from heading to maturity compared to Yixiangyou 2115. Furthermore, Fyou 498 showed higher NAE and NPE values (Table 5), indicating synergistic characteristics of high yield and NUE (Koutroubas and Ntanos, 2003; Sun et al., 2017). However, the head rice rate and taste value of Fyou 498 were significantly lower than those of Yixiangyou 2115, and the chalky kernel rate significantly increased. This study found that the genetic difference in rice quality among varieties was significantly higher than N fertilizer (Table 6). This suggests that although the varieties were high yielding and highly efficient, they were not necessarily of high quality. Therefore, it is necessary to increase the screening of high-quality, high-yield, and high-efficiency varieties suitable for mechanization. This finding complements the previous and our research results (Li et al., 2023; Yuan et al., 2023). Previous studies have concluded that the application of controlled-release N fertilizer and optimal N fertilizer operation can increase the N transport rate in

plants, promoting N absorption and utilization in rice (Deng et al., 2021; Lyu et al., 2021a; Cheng et al., 2022). However, this study demonstrates that the N transport rate in stem sheaths (leaves) decreases to varying degrees with the delay of the N-topdressing period under the slow-mixed fertilizer base application. This finding is in contrast with the results of previous studies (Deng et al., 2021; Cheng et al., 2022). Although the amount of N transported in the stem sheaths (leaves) and the contribution rate of N transport in the stem sheaths (leaves) increased significantly during the topdressing time with N fertilizer in the experiments, the effect of urea-N fertilizer was significantly improved. However, the proportion of N retained in the stem sheaths (leaves) remained relatively high (Table 5). Further research is needed to improve the rate of N transport in vegetative organs during the filling stage of slow-mixed fertilizer combined with urea-N application.

Research findings on rice quality differences between varieties are more consistent due to their genetic background (Lin et al., 2011). However, the effect of N fertilizer management on rice quality characteristics remains a topic of debate (Cao et al., 2017; Shi et al., 2022; Guo et al., 2023b). Some studies have suggested that using controlled-release N fertilizer, increasing the N application amount, or delaying the application of N fertilizer under the same N application rate can reduce chalkiness and improve the overall eating quality of rice (Yuan et al., 2023; Guo et al., 2023b). Some studies have shown that increasing or delaying the application of N fertilizer can increase the chalkiness of rice (Cao et al., 2017). However, this study found that the effect of combined urea-N on the quality characteristics of direct-seeding rice under slow-mixed fertilizer-based application contradicted previous research (Zhang et al., 2008; Cao et al., 2017; Lyu et al., 2021b). The brown rice, milled rice, head rice, and taste values of direct-seeding rice improved with a delay in the N-topdressing period. The combined application of urea-N under slow-mixed fertilizer-based application may moderately increase grain plumpness (Sun et al., 2017; Sun et al., 2023b). However, delaying the application of urea-N under slow-mixed fertilizer base application worsens the degree of chalkiness and increases the rate of chalky grains. Further research is needed to determine whether the delayed release rate of controlled-release N fertilizer (Cheng et al., 2022) or the moderate delay of urea-N application affects the grain-filling rate (Sun et al., 2023b), starch anabolism (Yuan et al., 2023), and amylopectin chain length distribution (Guo et al., 2023b).

4.3 Mechanism of slow-mixed fertilizer base application combined with available N fertilizer synergistic improvement of grain yield, rice quality, and NUE

Previous studies have shown the types and release rates of controlled-release N fertilizers as well as their effectiveness in increasing rice yield through one time basal application (Ke et al., 2018; Wu et al., 2021). These studies also investigated the physiological regulatory mechanisms under different soil types, varieties, and planting methods (Lyu et al., 2021b; Cheng et al., 2022; Meng et al., 2022; Ishfaq et al., 2023). However, there are few studies on the combined application of urea-N fertilizers under slow-mixed fertilizer base applications, especially in mechanical direct-seeding rice. This study aimed to investigate the synergistic effects of urea-N fertilizers on yield, rice quality, and NUE. However, the mechanism underlying this process has rarely been reported. The mechanism for the synergistic improvement of yield, rice quality, and NUE in direct-directing rice by slow-mixed fertilizer basal application with urea-N fertilizer (N_3 treatment) in this experiment is as follows: different varieties can improve the photosynthetic potential from the jointing to heading stage, optimize the LAI of the population, promote dry matter accumulation and transport during the grain-filling stage, improve the population growth rate from the heading to the maturity stage, and then optimize the yield components, which is an important reason for the final increase in yield. Applying urea-N fertilizer during the booting stage is optimal for slow-mixed fertilizer application. This application can increase the root vigor decay rate from heading to maturity and promote N transport from the stem sheath (leaves) to the panicle during the filling stage. This is the main reason for improving the NUE of urea-N topdressing and enhancing the rice processing and eating quality. It can be used as an important method to achieve high NUE and high-quality coordination in mechanical direct-seeding hybrid *indica* rice.

Selecting appropriate indicators to evaluate grain yield, rice quality, and NUE is crucial for evaluating the physiological ecology of high-yield, high-quality, and NUE crops (Zhang et al., 2013; Sun et al., 2017; Sun et al., 2023b). The use of principal components and correlation analysis is shown in Figures 4, 5. This study suggests that increasing the population's photosynthetic potential from the jointing to heading stage, promoting N transport in leaves from the heading to maturity stage, and increasing the N transport contribution rate in stem sheaths from the heading to maturity stage, can be used as an evaluation index for the simultaneous improvement of high yield, high quality, and NUE in direct-seeding rice. These findings provide another important way to achieve coordination and unification of high yield, high quality, and NUE in direct-seeding rice.

5 Conclusions

The effects of different varieties and slow-mixed fertilizer basal application with urea-N topdressing on the photosynthetic characteristics, dry matter accumulation, and transport, root vigor, NUE, yield, and rice quality of mechanical direct-seeded rice were significant. In this experiment, under the N application level of 150 kg hm^{-2}, the combination of slow-mixed fertilizer (N 120 kg hm^{-2}) basal application and booting stage urea-N fertilizer (N 30 kg hm^{-2}) topdressing significantly improved the photosynthetic potential of different varieties from the jointing to heading stage, the population growth rate and the N transport amount of leaves from the heading to maturity stage. It especially improved the N transport contribution rate in the stem sheaths, achieving the effect of increasing yield. Simultaneously, it improved the NUE of the N fertilizer topdressing and the processing and eating quality of rice synergistically. The best slow-mixed fertilizer

basal application with urea-N fertilizer topdressing achieved a synergistic improvement in grain quality, yield, and NUE of direct-seeding rice.

Data availability statement

The original contributions presented in the study are included in the article/Supplementary Material. Further inquiries can be directed to the corresponding author.

Author contributions

YJS: Data curation, Funding acquisition, Project administration, Writing – original draft. MX: Data curation, Investigation, Writing – review & editing. ZH: Formal analysis, Investigation, Writing – review & editing. YYS: Formal analysis, Methodology, Software, Writing – review & editing. YD: Validation, Visualization, Writing – review & editing. YL: Investigation, Writing – review & editing. XC: Investigation, Software, Writing – review & editing. YC: Investigation, Methodology, Writing – review & editing. WX: Visualization, Writing – review & editing. XH: Data curation, Investigation, Writing – review & editing. PD: Software, Writing – review & editing, Investigation, Methodology. ML: Writing – review & editing, Formal analysis, Software. ZY: Writing – review & editing, Resources, Validation. ZC: Writing – review & editing, Investigation. JM: Supervision, Writing – review & editing.

Funding

The author(s) declare financial support was received for the research, authorship, and/or publication of this article. This work was Supported by the National Key Research and Development Program Foundation of Ministry of Science and Technology of China (Grant No. 2023YFD2301903); the Sichuan Natural Science Foundation Project (Grant No. 24NSFSC0081); the Project Foundation of the State Key Laboratory of Crop Gene Exploration and Utilization in Southwest China (Grant No. SKL-ZY202228); the Research Program Foundation of Key Laboratory of Sichuan Province, China, the Cultivation of Green and Efficient Super Rice Varieties (Grant No. 2022ZDZX0012); the Rice Breeding Project Foundation of Sichuan Provincial Science and Technology Department (Grant No. 2021YFYZ0005).

Conflict of interest

The authors declare that the research was conducted in the absence of any commercial or financial relationships that could be construed as a potential conflict of interest.

Publisher's note

All claims expressed in this article are solely those of the authors and do not necessarily represent those of their affiliated organizations, or those of the publisher, the editors and the reviewers. Any product that may be evaluated in this article, or claim that may be made by its manufacturer, is not guaranteed or endorsed by the publisher.

Supplementary material

The Supplementary Material for this article can be found online at: https://www.frontiersin.org/articles/10.3389/fpls.2024.1400146/full#supplementary-material

References

Cao, X. M., Sun, H. Y., Wang, C. G., Ren, X. J., Liu, H. F., and Zhang, Z. J. (2017). Effects of late-stage nitrogen fertilizer application on the starch structure and cooking quality of rice. *J. Sci. Food Agr.* 98, 2332–2340. doi: 10.1002/jsfa.8723

Chen, A. L., Zhang, W. Z., Sheng, R., Liu, Y., Hou, H. J., Liu, F., et al. (2021). Long-term partial replacement of mineral fertilizer with *in situ* crop residues ensures continued rice yields and soil fertility: A case study of a 27-year field experiment in subtropical China. *Sci. Total Environ.* 787, 147523. doi: 10.1016/j.scitotenv.2021.147523

Chen, Z. M., Wang, Q., Ma, J. C., Zhao, J., Huai, Y., Ma, J. W., et al. (2022). Combing mechanical side-deep fertilization and controlled-release nitrogen fertilizer to increase nitrogen use efficiency by reducing ammonia volatilization in a double rice cropping system. *Front. Environ. Sci.* 10. doi: 10.3389/fenvs.2022.1006606

Cheng, Q. Y., Li, L. Y., Liao, Q., Fu, H., Nie, J. X., Luo, Y. H., et al. (2023). Is scale production more advantageous than smallholders for Chinese rice production? *Energy* 283, 128753. doi: 10.1016/j.energy.2023.128753

Cheng, S., Xing, Z. P., Tian, C., Li, S. P., Tian, J. Y., Liu, Q. Y., et al. (2022). Effects of controlled release urea formula and conventional urea ratio on grain yield and nitrogen use efficiency of direct-seeded rice. *Agriculture* 12, 1230. doi: 10.3390/agriculture12081230

Deng, F., Li, W., Wang, L., Hu, H., Liao, S., Pu, S. L., et al. (2021). Effect of controlled-release fertilizers on leaf characteristics, grain yield, and nitrogen use efficiency of machine-transplanted rice in southwest China. *Arch. Agron. Soil Sci.* 67, 1739–1753. doi: 10.1080/03650340.2020.1807519

Farooq, M., Siddique, K. H. M., Rehman, H., Aziz, T., Lee, D. J., and Wahid, A. (2011). Rice direct seeding: experiences, challenges and opportunities. *Soil Tillage Res.* 111, 87–98. doi: 10.1016/j.still.2010.10.008

Guo, C. C., Wuza, R. Q., Tao, Z. L., Yuan, X. J., Luo, Y. H., Li, F. J., et al. (2023b). Effects of elevated nitrogen fertilizer on the multi-level structure and thermal properties of rice starch granules and their relationship with chalkiness traits. *J. Sci. Food Agric.* 103, 12886. doi: 10.1002/jsfa.12886

Guo, C. C., Yuan, X. J., Wen, Y. F., Yang, Y. G., Ma, Y. M., Yan, F. J., et al. (2023a). Common population characteristics of direct-seeded hybrid *indica* rice for high yield. *Agron. J.* 115, 1606–1621. doi: 10.1002/agj2.21359

He, W. J., He, B., Wu, B. Y., Wang, Y. H., Yan, F. Y., Ding, Y. F., et al. (2023). Growth of tandem long-mat rice seedlings using controlled release fertilizers: mechanical transplantation could be more economical and high yielding. *J. Integr. Agr* 22, 3652–3666. doi: 10.1016/j.jia.2023.05.007

Hou, P. F., Yuan, W. S., Li, G. H., Petropoulos, E., Xue, L. X., Feng, Y. F., et al. (2021). Deep fertilization with controlled-release fertilizer for higher cereal yield and N utilization in paddies: the optimal fertilization depth. *Agron. J.* 113, 5027–5039. doi: 10.1002/agj2.20772

IPNI (2012). *4R plant nutrition manual: A manual for improving the management of plant nutrition*. Eds. T. W. Bruulsema, P. E. Fixen and G. D. Sulewski (GA, USA: IPNI, Norcross), 140. Available at: http://www.ipni.net/article/IPNI-3255.

Ishfaq, M., Wang, Y. Q., Xu, J. L., Hassan, M., Yuan, H., Liu, L. L., et al. (2023). Improvement of nutritional quality of food crops with fertilizer: a global meta-analysis. *Agron. Sustain. Dev.* 43, 74. doi: 10.1007/s13593-023-00923-7

Jiang, Q., Du, Y., Tian, X., Wang, Q., Xiong, R., Xu, G., et al. (2016). Effect of panicle nitrogen on grain filling characteristics of high-yielding rice cultivars. *Eur. J. Agron.* 74, 185–192. doi: 10.1016/j.eja.2015.11.006

Ke, J., He, R. C., Hou, P. F., Ding, C., Ding, Y. F., Wang, S. H., et al. (2018). Combined controlled- released nitrogen fertilizers and deep placement effects of N leaching, rice yield and N recovery in machine-transplanted rice. *Agr Ecosyst. Environ.* 265, 402–412. doi: 10.1016/j.agee.2018.06.023

Koutroubas, S. D., and Ntanos, D. A. (2003). Genotypic differences for grain yield and nitrogen utilization in *indica* and *japonica* rice under Mediterranean conditions. *Field Crops Res.* 83, 251–260. doi: 10.1016/S0378-4290(03)00067-4

Li, M., Zhu, D. W., Jiang, M. J., Luo, D. Q., Jiang, X. H., Ji, G. M., et al. (2023). Dry matter production and panicle characteristics of high yield and good taste *indica* hybrid rice varieties. *J. Integr. Agr* 22, 1338–1350. doi: 10.1016/j.jia.2022.08.033

Lin, J. H., Singh, H., Chang, Y. T., and Chang, Y. H. (2011). Factor analysis of the functional properties of rice flours from mutant genotypes. *Food Chem.* 126, 1108–1114. doi: 10.1016/j.foodchem.2010.11.140

Liu, Q. Y., Chen, S., Zhou, L., Tao, Y., Tian, J. Y., Xing, Z. P., et al. (2022). Characteristics of population quality and rice quality of *semi-waxy* japonica rice varieties with different grain yields. *Agriculture* 12, 241. doi: 10.3390/agriculture12020241

Lyu, T. F., Shen, J., Ma, J., Ma, P., Yang, Z. Y., Dai, Z., et al. (2021a). Hybrid rice yield response to potted-seedling machine transplanting and slow-release nitrogen fertilizer application combined with urea topdressing. *Crop J.* 9, 915–923. doi: 10.1016/j.cj.2020.08.013

Lyu, Y. F., Yang, X. D., Pan, H. Y., Zhang, X. H., Cao, H. X., Ulgiati, S., et al. (2021b). Impact of fertilization schemes with different ratios of urea to controlled release nitrogen fertilizer on environmental sustainability, nitrogen use efficiency and economic benefit of rice production: A study case from Southwest China. *J. Clean. Pro* 293, 126198. doi: 10.1016/j.jclepro.2021.126198

Meng, T. Y., Zhang, X. B., Ge, J. L., Chen, X., Zhu, G. L., Chen, Y. L., et al. (2022). Improvements in grain yield and nutrient utilization efficiency of japonica inbred rice released since the 1980s in eastern China. *Field Crops Res.* 277, 108427. doi: 10.1016/j.fcr.2021.108427

National Bureau of Statistics of China (NBSC). (2022). *China statistical yearbook* (Beijing: China Statistics Press).

Peng, S. B., Garcia, F. V., Laza, R. C., Sanico, A. L., Visperas, R. M., and Cassman, K. G. (1996). Increased N-use efficiency using a chlorophyll meter on high yielding irrigated rice. *Field Crops Res.* 47, 243–252. doi: 10.1016/0378-4290(96)00018-4

Peng, S. B., Tang, Q. Y., and Zou, Y. B. (2009). Current status and challenges of rice production in China. *Plant Prod Sci.* 12, 3–8. doi: 10.1626/pps.12.3

Ramasamy, S., ten Berge, H. F. M., and Purushothaman, S. (1997). Yield formation in rice in response to drainage and nitrogen application. *Field Crops Res.* 51, 65–82. doi: 10.1016/S0378-4290(96)01039-8

Shi, S. J., Pan, K. Q., Yu, M., Li, L. N., Tang, J. C., Cheng, B., et al. (2022). Differences in starch multi-layer structure, pasting, and rice eating quality between fresh rice and 7 years stored rice. *Curr. Res. Food Sci.* 5, 1379–1385. doi: 10.1016/j.crfs.2022.08.013

Sun, Y. J., Lin, D., Sun, Y. Y., Yan, F. J., Ma, P., Guo, C. C., et al. (2023a). Improving yield and nitrogen use efficiency of hybrid *indica* rice through optimizing nitrogen application strategies in the rice season under different rotation patterns. *Paddy Water Environ.* 21, 99–113. doi: 10.1007/s10333-022-00916-4

Sun, Y. J., Ma, J., Sun, Y. Y., Xu, H., Yang, Z. Y., Liu, S. J., et al. (2012). The effects of different water and nitrogen managements on yield and nitrogen use efficiency in hybrid rice of China. *Field Crops Res.* 127, 85–98. doi: 10.1016/j.fcr.2011.11.015

Sun, Y. J., Sun, Y. Y., Yan, F. J., Yang, Z. Y., Xu, H., Li, Y., et al. (2017). Effects of postponing nitrogen topdressing on post-anthesis carbon and nitrogen metabolism in rice cultivars with different nitrogen use efficiencies. *Acta Agron. Sin.* 3, 407–419. doi: 10.3724/SP.J.1006.2017.00407

Sun, Y. J., Wu, Y. X., Sun, Y., Luo, Y. H., Guo, C., Li, B., et al. (2022). Effects of water and nitrogen on grain filling characteristics, canopy microclimate with chalkiness of directly seeded rice. *Agriculture* 12, 122. doi: 10.3390/agriculture12010122

Sun, Y. Y., Yuan, X. J., Chen, K. R., Wang, H. Y., Luo, Y. H., Guo, C. C., et al. (2023b). Improving the yield and nitrogen use efficiency of hybrid rice through rational use of controlled-release nitrogen fertilizer and urea topdressing. *Front. Plant Sci.* 14. doi: 10.3389/fpls.2023.1240238

Tomaszewska, M., and Jarosiewicz, A. (2002). Use of polysulfone in controlled-release NPK fertilizer formulations. *J. Agr Food Chem.* 50, 4634. doi: 10.1021/jf0116808

Wang, W. X., Jie, D. U., Zhou, Y. Z., Zeng, Y. J., Tan, X. M., Pan, X. H., et al. (2021). Effects of different mechanical direct seeding methods on grain yield and lodging resistance of early *indica* rice in South China. *J. Integr. Agr* 20, 1204–1215. doi: 10.1016/S2095-3119(20)63191-4

Wei, H. Y., Zhang, H. C., Blumwald, E., Li, H. L., Cheng, J. Q., Dai, Q. G., et al. (2016). Different characteristics of high yield formation between inbred japonica super rice and intersub-specific hybrid super rice. *Field Crops Res.* 198, 179–187. doi: 10.1016/j.fcr.2016.09.009

Wu, Q., Wang, Y. H., Ding, Y. F., Tao, W. K., Gao, S., Li, Q. X., et al. (2021). Effects of different types of slow-and controlled-release fertilizers on rice yield. *J. Integr. Agr* 20, 1503–1514. doi: 10.1016/S2095-3119(20)63406-2

Wu, Y. X., Guo, C. C., Sun, Y. J., Liu, F. Y., Zhang, Q., Xiang, K. H., et al. (2020). Relationship of population quality and nitrogen fertlizer utlization characteristics of direct seedling rice under water-nitrogen interaction. *Chin. J. Appl. Ecol.* 31, 899–908. doi: 10.13287/j.1001–9332.202003.022

Yang, Z. Y., Cheng, Q. Y., Liao, Q., Fu, H., Zhang, J. Y., Zhu, Y. M., et al. (2022). Can reduced-input direct seeding improve resource use efficiencies and profitability of hybrid rice in China? *Sci. Total Environ.* 833, 155186. doi: 10.1016/j.scitotenv.2022.155186

Yang, Z. Y., Zhu, Y. M., Zhang, X. L., Liao, Q., Fu, H., Cheng, Q. Y., et al. (2023). Unmanned aerial vehicle direct seeding or integrated mechanical transplanting, which will be the next step for mechanized rice production in China? —A comparison based on energy use efficiency and economic benefits. *Energy* 273, 127223. doi: 10.1016/j.energy.2023.127223

Yokamo, S., Irfan, M., Huan, W. W., Wang, B., Wang, Y. L., Ishfaq, M., et al. (2023). Global evaluation of key factors influencing nitrogen fertilization efficiency in wheat: a recent meta-analysis, (2000–2022). *Front. Plant Sci.* 14. doi: 10.3389/fpls.2023.1272098

Yoshida, S., Forno, D. A., Cock, J. H., and Gomez, K. A. (1976). *Laboratory manual for physiological studies of rice. 3rd ed* (Los Baños, Philippines: International Rice Research Institute), 83.

Yu, Z. X., Shen, Z. Y., Xu, L., Yu, J., Zhang, L., Wang, X. K., et al. (2022). Effect of combined application of slow-release and conventional urea on yield and nitrogen use efficiency of rice and wheat under full straw return. *Agronomy* 12, 998. doi: 10.3390/agronomy12050998

Yuan, X. J., Luo, Y. H., Yang, Y. G., Chen, K. R., Wen, Y. F., Luo, Y. H., et al. (2023). Effects of postponing nitrogen topdressing on starch structural properties of superior and inferior grains in hybrid *indica* rice cultivars with different taste values. *Front. Plant Sci.* 14. doi: 10.3389/fpls.2023.1251505

Zhang, H., Chen, T. T., Liu, L. J., Wang, Z. Q., Yang, J. C., and Zhang, J. H. (2013). Performance in grain yield and physiological traits of rice in the Yangtze River Basin of China during the last 60yr. *J. Integr. Agr* 12, 57–66. doi: 10.1016/S2095-3119(13)60205-1

Zhang, Z. C., Zhang, S. F., Yang, J. C., and Zhang, J. H. (2008). Yield, grain quality and water use efficiency of rice under non-flooded mulching cultivation. *Field Crops Res.* 108, 71–81. doi: 10.1016/j.fcr.2008.03.004

Zhong, X. M., Peng, J. W., Kang, X. R., Wu, Y. F., Luo, G. W., Hu, W. F., et al. (2021). Optimizing agronomic traits and increasing economic returns of machine-transplanted rice with side-deep fertilization of double-cropping rice system in southern China. *Field Crops Res.* 270, 108191. doi: 10.1016/j.fcr.2021.108191

frontiers | Frontiers in Plant Science

TYPE Original Research
PUBLISHED 28 May 2024
DOI 10.3389/fpls.2024.1372385

OPEN ACCESS

EDITED BY
Xiaoli Hui,
Northwest A&F University, China

REVIEWED BY
Jiameng Guo,
Henan Agricultural University, China
Lv Xiaokang,
Hebei Agricultural University, China
Lina Jiang,
Henan Normal University, China
Hafeez Ur Rehman,
University of Agriculture Faisalabad, Pakistan

*CORRESPONDENCE
Youjun Li
lyj@haust.edu.cn
Guoqiang Li
gqli@hnagri.org.cn

RECEIVED 18 January 2024
ACCEPTED 09 May 2024
PUBLISHED 28 May 2024

CITATION
Huang M, Li W, Hu C, Wu J, Wang H, Fu G, Shaaban M, Li Y and Li G (2024) Coupled one-off alternate furrow irrigation with nitrogen topdressing at jointing optimizes soil nitrate-N distribution and wheat nitrogen productivity in dryland.
Front. Plant Sci. 15:1372385.
doi: 10.3389/fpls.2024.1372385

Coupled one-off alternate furrow irrigation with nitrogen topdressing at jointing optimizes soil nitrate-N distribution and wheat nitrogen productivity in dryland

Ming Huang[1], Wenna Li[1], Chuan Hu[1], Jinzhi Wu[1], Hezheng Wang[1], Guozhan Fu[1], Muhammad Shaaban[1], Youjun Li[1]* and Guoqiang Li[2,3]*

[1]College of Agriculture, Henan University of Science and Technology, Luoyang, China, [2]Key Laboratory of Huang-Huai-Hai Smart Agricultural Technology, Ministry of Agriculture and Rural Affairs, Zhengzhou, China, [3]Institute of Agricultural Information Technology, Henan Academy of Agricultural Sciences, Zhengzhou, China

The judicious management of water and nitrogen (N) is pivotal for augmenting crop productivity and N use efficiency, while also mitigating environmental concerns. With the advent of the High–Farmland Construction Program in China, one–off irrigation has become feasible for most dryland fields, presenting a novel opportunity to explore the synergistic strategies of water and N management. This study delves into the impact of one–off alternate furrow irrigation (AFI) and topdressing N fertilizer (TN) on soil nitrate–N distribution, and N productivity—including plant N accumulation, translocation, and allocation, and grain yield, protein content, N use efficiency of winter wheat (Triticum aestivum L.) in 2018–2019 and 2019–2020. Experimental treatments administered at the jointing stage comprised of two irrigation methods—every (EFI) and alternative (AFI) furrow irrigation at 75 mm, and two topdressing N rates—0 (NTN) and 60 (TN) kg N ha^{-1}. Additionally, a conventional local farmer practice featuring no irrigation and no topdressing N (NINTN) was served as control. Compared to NINTN, EFINTN substantially increased aboveground N accumulation, grain yield, and protein yield, albeit with a reduction in grain protein content by 8.1%–10.6%. AFI, in turn, led to higher nitrate–N accumulation in the 60–160 cm soil depth at booting and anthesis, but diminished levels at maturity, resulting in a significant surge in N accumulation from anthesis to maturity and its contribution to grain, N fertilizer partial factor productivity (PFPN), and N uptake efficiency (NUPE), thereby promoting grain yield by 9.9% and preserving grain protein content. Likewise, TN enhanced soil nitrate–N at key growth stages, reflected in marked improvements in N accumulation both from booting to anthesis and from anthesis to maturity, as well as in grain yield, protein content, and protein yield. The combination of AFI and TN (AFITN) yielded the highest grain yield,

protein content, with PFPN, NUPE, and N internal efficiency outstripping those of EFINTN, but not AFINTN. In essence, one–off AFI coupled with TN at the jointing stage is a promising strategy for optimizing soil nitrate–N and enhancing wheat N productivity in dryland where one–off irrigation is assured.

KEYWORDS

one-off alternate furrow irrigation, topdressing N, dryland winter wheat, soil nitrate-N, grain yield, N use efficiency

1 Introduction

Wheat stands as the cornerstone of nutrition and vegetable protein in the human diet, occupying over 20% of the world's arable territory and feeds about 30% of the world population (Zhang et al., 2019; Liu et al., 2020). Despite this, around 75% of wheat production emanates from drylands area in world—regions mainly characterized by aridity, semi–aridity, and semi–humid drought–prone (Khan et al., 2017; Zhang et al., 2019). Water scarcity and nutrient shortfalls impose significant constraints on the pursuit of enhanced and consistent wheat yields in these regions (Luo et al., 2021). Soil moisture deficits not only curtail nutrient uptake efficiency but also compromise the productivity of both water and nutrients, leading to low and unstable wheat yields (Gan et al., 2013; Zhang et al., 2020). Nonetheless, the swift progression of the High–Standard Farmland Construction Program in China, culminating in 66.7 million hectares of high–caliber farmland by 2022 and plans for an additional 13.3 million hectares during the 14th Five–Year Plan, has cemented the provision of one–off irrigation for wheat growth across numerous dryland areas—locales previously bereft of irrigation (Wang et al., 2022; Zhao et al., 2023b). However, management strategies that leverage this one–off irrigation are still underdeveloped, it is a urgent necessity to refine water and nutrient management tactics to grasp this one-off irrigation opportunity to bolster wheat productivity.

Nitrogen (N), a linchpin for crop physiological and agronomic health, is crucial for robust plant growth and development (Wang et al., 2014). An adequate water regimen enhances grain N uptake and overall crop productivity (Kumari et al., 2017); conversely, water imbalances can precipitate N inefficiencies (Sarker et al., 2020; Zhao et al., 2023b). Research by Jia et al. (2021) acknowledged that alternate furrow irrigation (AFI) targets the root zone with precision, thereby optimizing water provisioning, bolstering shoot N accumulation, and augmenting N use efficiency (NUE), ultimately yielding richer wheat harvests. However, instances under low rainfall condition have shown AFI to be detrimental to N uptake, leading to decreased crop yields when contrasted with conventional every furrow irrigation (EFI) due to diminished irrigation volumes (Benjamin et al., 1997; Sepaskhah and Hosseini, 2008). Yet, combining AFI with other approaches, such as N management and planting modes, has been demonstrated to enhance NUE in wheat crops (Ghasemi-Aghbolaghi and Sepaskhah, 2018). Topdressing nitrogen (TN), a strategic intervention for crop yield improvement, furnishes N nutrition vital for subsequent growth stages, particularly when soil N content is suboptimal (Li et al., 2020; Ji et al., 2021; Fu et al., 2022). Zain et al. (2021) discovered that TN applied at the jointing stage syncs with wheat's N demands, optimizing NUE in China North Plain. In drought–prone zones, a one-off irrigation based on 0–40 cm soil moisture levels at the regreening stage and coupled with a 50% N fertilizer topdressing, has proven to increase shoot N accumulation, NUE, and grain yield while minimizing soil nitrate-N residue at harvest (Zhao et al., 2023b). These insights suggest that judicious irrigation paired with TN at the proper stage are pivotal for elevating grain yield and NUE, enabling an environmentally congenial wheat production system. However, farmers usually apply all N fertilizers before sowing due to irrigation and labor constraints, which lead to a misalignment between the wheat's water and N requirements and result in some environmental issues (Wang and Li, 2019). Thus, this condition reinforce the need for AFI and TN protocols in enhancing winter wheat productivity in drylands.

The presence of nitrate–N in soil is integral for plant N uptake; however, if it exceeds safety thresholds, it is at risk of leaching, denitrification, and emissions in winter wheat production systems (Zhou and Buterbach-Bahl, 2014; Dai et al., 2015; Huang et al., 2017; Zhao et al., 2023a). Notably, dryland farms in China often exhibit substantial soil nitrate–N concentrations, such as 601 kg ha^{-1} in 100–180 cm (Dai et al., 2015), 1065 kg ha^{-1} in 0–300 cm (Guo et al., 2010), and a staggering 708–1500 kg ha^{-1} within a 0–380 cm soil profile (Zhao et al., 2023a)—figures that underscore the urgency for agro–operations focused on optimizing soil nitrate–N to favor crop uptake and minimize environmental risks (Adel et al., 2019; Wang and Li, 2019).

The furrow-seeded (FS) framework, is widely applied in drylands for the purpose to increase crop yields and N use efficiency (Sharma et al., 2012; Gan et al., 2013; Mehdi et al., 2017; Ali et al., 2018; Zhang et al., 2020; Yang et al., 2021). In FS system, the ridges in the field alternate with the corresponding furrows, which made irrigation more conveniently and precisely (Jia et al., 2021). Previous studies have demonstrated that, under RF, the winter wheat yield in dryland could be significantly increased via irrigation (Ali et al., 2018; Li et al., 2019). For example, Li et al. (2019) found that a total amount of irrigation of 165 mm during the growth stage increased wheat yield by 46.1%. Luo et al. (2020)

reported that the irrigation of 7.8–11.8 mm at wintering and jointing increased wheat yield by 10.0–27.1%. However, these researches mainly focus on optimizing amount and/or its technology of irrigation, but not pay attention in one-off irrigation. Moreover, the influence of coupled FI and TN techniques on soil nitrate–N and N productivity in FS winter wheat remains elusive. This gap inhibits the full utilization of water resources, which come from High–Standard Farmland Construction efforts, to boost wheat productivity.

Within this context, our study proposed that coupled AFI with TN could optimize soil nitrate–N and maximize N productivity in winter wheat. Employing AFI and TN at the jointing stage of winter wheat in a semi–humid and drought–prone region, this research aims to: (1) elucidate the effects of FI, AFI, and TN, as well as their interactions, on soil nitrate–N accumulation; (2) evaluate their impact on aboveground N accumulation, translocation, allocation, grain yield, grain protein content, protein yield, and N use efficiency; and (3) identify an optimal agronomic strategy that synergizes soil nitrate–N, crop yield, quality, and efficiency within the FS system in drylands where one–off irrigation is assured.

2 Materials and methods

2.1 Study site description

From October 2018 and June 2020, a two–year field experiment was carried out at Nandasu village, located in Xiaolangdi town, Mengjin district, Luoyang, Henan province—one of typical dryland winter wheat producing regions in China. The study site was characterized by an average annual air temperature of 13.7°C and a mean annual frost–free period of 210 days, the area enjoys an average annual sunshine duration of 2196 hours and receives an average annual precipitation of 650 mm. Notably, around 60% of this rainfall occurs from June to September, which marginally overlaps with the winter wheat year. The predominant cropping system in this locale is the winter wheat–summer maize rotation, with winter wheat typically sown in early to mid–October and harvested at the beginning of June the following year.

During the two experimental years, the recorded annual precipitation was 602.1 mm in 2018–2019 and 692.7 mm in 2019–2020, with 16.5% and 38.0% of this, respectively, occurring during the winter wheat season (Figure 1). The experimental site's soil, formed from cinnamon–colored parent material and classified as a calcareous Eum–Orthic Anthrosol according to Chinese soil taxonomy, displayed consistent baseline properties at the initiation of the experiment for both years. Within the upper 0–20 cm soil layer, assessments revealed a soil field capacity ranging from 27.3% to 27.4%, bulk density between 1.35 and 1.36 g cm^{-3}, pH of 8.2, organic matter content averaging 13.1–13.2 g kg^{-1}, total N content fixed at 0.81 g kg^{-1}, available phosphorus contents ranging from 12.1 to 13.2 mg kg^{-1}, and available potassium levels between 121.6 and 125.4 mg kg^{-1}.

2.2 Experimental design and field management

Our study incorporated a two–factor experimental design beyond the control treatment, focusing on furrow irrigation (FI) techniques and topdressing nitrogen (TN) rates. The primary treatments involved two FI techniques: every furrow irrigation (EFI) and alternate furrow irrigation (AFI), each with 75 mm of water applied at the jointing stage. For the secondary treatments, we employed two TN rates: a Zero–N topdressing (NTN) at 0 kg ha^{-1}, and a N topdressing (TN) at 60 kg ha^{-1}, administered concurrently with the irrigation. Additionally, the traditional local farmer planting practice featuring no irrigation and no topdressing N (NINTN) was served as control. Consequently, the experimental framework encompassed five distinct treatments:

1. Conventional no irrigation and no topdressing N (NINTN).
2. Every furrow irrigation without topdressing N (EFINTN).
3. Alternate furrow irrigation without topdressing N (AFINTN).
4. Every furrow irrigation with topdressing N (EFITN).

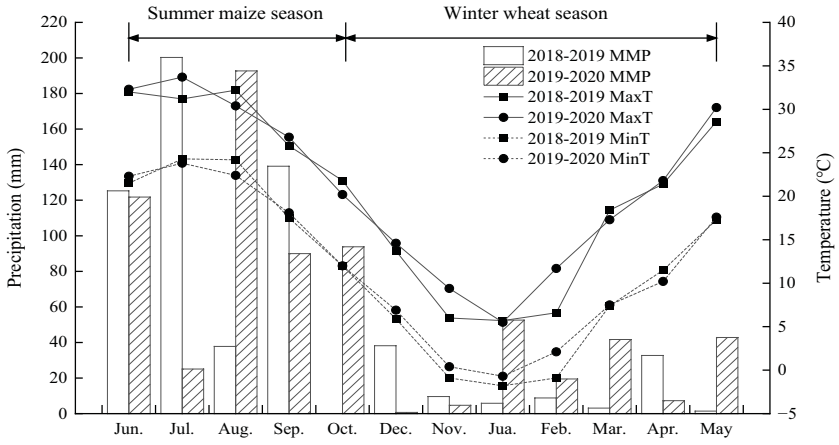

FIGURE 1
Monthly precipitation at the experimental site from June 2018 to May 2020.

5. Alternate furrow irrigation with topdressing N (AFITN).

The application amount of basal fertilizer is set according to local farmer' practice, and both the application amount of irrigation and N fertilizer topdressing are recommended by local agricultural experts. The specific amounts for irrigation and fertilizer application are detailed in Table 1.

Our study utilized a completely randomized plot design with three replications for each treatment. Each plot measured 20 meters in length and 6.12 meters in width, and all were situated within the same field with a 1–meter buffer between each. Upon sowing, we utilized a no–till fertilizer seeder (model 2BMQF–6/12A, produced by Luoyang Xinle Machinery Co., Ltd) to apply compound fertilizers (N:P_2O_5:K_2O ratio of 23:10:6) at a rate of 750 kg per hectare as the base fertilizer.

The 2BMQF–6/12A no–till seeder is designed to perform multiple tasks—including furrowing, ridging, fertilizing, sowing, and soil repacking—simultaneously. Post–sowing, the equipment was adjusted to create ridges 20 cm wide and 10 cm high, with furrows that were 14 cm wide. Consequently, the spacing for wheat plants in the wider rows was 20 cm, compared to 14 cm in the narrower rows, averaging to 17 cm overall (Figure 2).

Winter wheat variety Zhoumai36 was sown using a seeding rate of 187.5 kg per hectare, at a depth of 3–5 cm within the furrows. The base fertilizers were precisely drilled between two seed rows at a depth of 10 cm. Sowing dates were October 13, 2018, and October 15, 2019, with respective harvest dates of May 30, 2019, and June 2, 2020. The previous crop in the both two years were summer maize (Zhengdan958), which harvest at early-October. Irrigation conducted at the jointing stage (Zadoks 31) on March 19, 2019, and March 22, 2020, with both the AFI and EFI treatments receiving 75 mm, calibrated for the entire plot area and regulated using a mechanical water meter (with 0.01m^3 accuracy and operating at outlet valve pressures between 0.10–0.12 MPa). Specifically, each plot received 9.18 m^3 of water, and the irrigation space per furrow was 2.8 m^2 (20 m × 0.14 m). Under EFI treatment, the total irrigated area per plot was 50.4 m^2 (20 m × 2.52 m), with 0.51 m^3 of water for each irrigated furrow. Conversely, under AFI treatment, the irrigated area per plot was halved to 25.2 m^2 (20 m × 1.26 m), with 1.02 m^3 of water for each irrigated furrow—effectively doubling the irrigation volume per furrow compared to EFI (Figure 2).

For TN treatments, a uniform rate of 60 kg N per hectare was hand–broadcast in the watering furrows just before the irrigation event. To manage weeds, pests, and diseases, we employed the same herbicides and pesticides used by local farmers.

2.3 Measurements and methods

2.3.1 Soil nitrate–N

During the 2018–2019 and 2019–2020 years, soil core samples were collected randomly at key phenological stages: booting (Zadoks 43), anthesis (Zadoks 65), and maturity (Zadoks 94). We sampled these using a soil auger with an internal diameter of 4.0 cm, extracting cores from 0 to 200 cm soil depths in 20 cm intervals. For NINTN and EFI treatments, we randomly took three soil cores from the center between two plant rows within a furrow. In the case of AFI treatments, we collected three soil cores from the center of irrigated furrows and another three from the center of non–irrigated furrows. The individual soil samples from identical depths and the same plot were combined, yielding round 300 grams after a homogeneous mix. This composite sample was immediately sealed in a labeled plastic bag to preserve it for further laboratory analysis. In the laboratory, the nitrate-N was quantified with the method described by Huang et al. (2017), fresh soil samples weighing 5.0 g were extracted with 50 mL of a 1.0 mol L^{-1} KCl after shaking it continuously for 1h. We then filtered the resultant mixture and promptly measured the nitrate–N concentration within the filtrate using a high–resolution digital colorimeter, the AutoAnalyzer 3 (AA3) from SEAL Company in Germany.

The soil nitrate–N accumulation (SNA, kg N ha^{-1}) in the 0–200 cm soil profile was calculated as follows (Dai et al., 2015; Huang et al., 2017):

$$SNA = Ti \times Di \times Ci \times 0.1 \quad (1)$$

where T_i is the soil layer thickness (cm), D_i is the soil bulk density (g cm^{-3}), C_i is the soil nitrate concentration (mg kg^{-1}), i.e., i = 20, 40, 60, 80, 100, 120, 140, 160, 180, 200. The soil bulk density of 1.32, 1.34 and 1.38 g cm^{-3} was used in 0–20, 20–40, and 40–200 cm according to the average value of local field, and 0.1 is the conversion coefficient.

2.3.2 Plant N

At the jointing (Zadoks 31) stage, we collected four 0.5 m–long samples of winter wheat from random locations within the experimental field. Additional samples were harvested from each

TABLE 1 The irrigation amount and fertilizer application rates in different treatments in 2018–2019 and 2019–2020.

Treatments	Irrigation (mm)	Fertilizer application rates(kg ha^{-1})			
		Basal N	Basal P_2O_5	Basal K_2O	Topdressing N
NINTN	0	172.5	75	45	0
EFINTN	75	172.5	75	45	0
AFINTN	75	172.5	75	45	0
EFITN	75	172.5	75	45	60
AFITN	75	172.5	75	45	60

NINTN, no irrigation with no topdressing N; EFINTN, every furrow irrigation with no topdressing N; AFINTN, alternate furrow irrigation with no topdressing N; EFITN, every furrow irrigation with topdressing N; AFITN, alternate furrow irrigation with topdressing N.

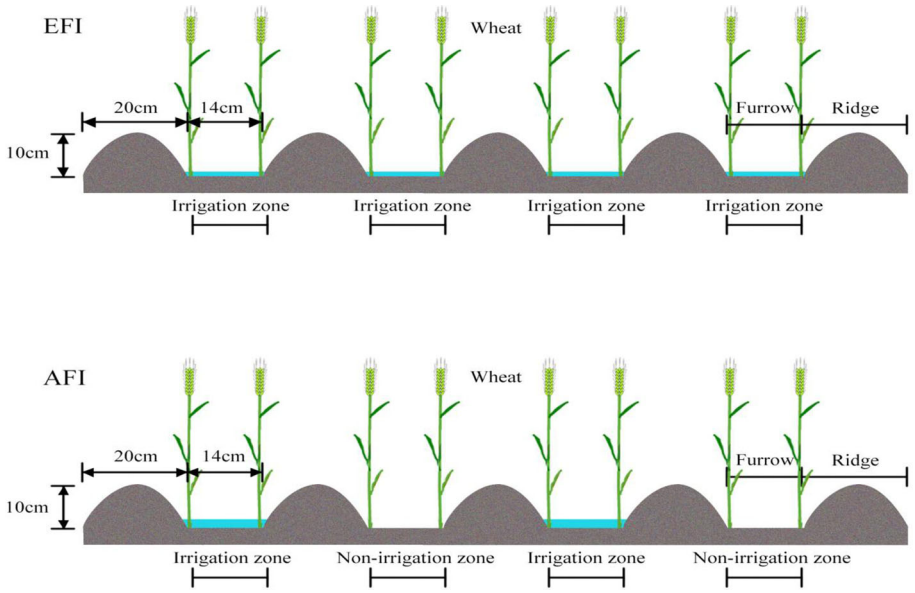

FIGURE 2
A schematic diagram of EFI and AFI system.

plot at anthesis (Zadoks 65) and maturity (Zadoks 94) stages. The process involved counting the tillers and removing the roots using scissors where the stem intersected with the root system. The aboveground biomass at both anthesis and maturity stages was categorized into stem, leaves, sheath, and ear components. Specifically, at maturity, the ear was further divided into grain and chaff (glume + rachis). Subsequently, the biomass was oven–dried at 105°C for 30 minutes, followed by drying at 65°C for 24 hours to establish the dry weight. The oven–dried samples, encompassing grain, straw, and glume, were finely ground in preparation for chemical analysis. Utilizing a mixture of sulfuric acid and hydrogen peroxide (H_2SO_4–H_2O_2), the samples were digested, allowing us to determine N concentrations in the digestion solution with an AutoAnalyzer 3 (AA3, SEAL Company, Germany) using the method prescribed by Huang et al. (2017). The N accumulation in each plant organ was calculated by multiplying the organ's dry weight (expressed in kg per hectare) by its respective total N concentration (in g kg^{-1}). The total aboveground N accumulation (NA, in kg ha^{-1}) was then computed by aggregating the N accumulation figures for each organ. Further, we calculated various N–related parameters including accumulation, translocation, and allocation based on the Equations 2-7 (Huang et al. 2021).

$$\begin{aligned}&\text{Aboveground N accumulation from jointing to anthesis}\\&(NA_{JTA}, \text{kg ha}^{-1})\\&= \text{Aboveground N accumulation at anthesis}\\&- \text{Aboveground N accumulation at jointing}\end{aligned} \quad (2)$$

$$\begin{aligned}&\text{Aboveground N accumulation from anthesis to maturity}\\&(NA_{ATM}, \text{kg ha}^{-1})\\&= \text{Aboveground N accumulation at maturity} -\\&\text{Aboveground N accumulation at anthesis}\end{aligned} \quad (3)$$

$$\begin{aligned}&\text{Rate of periodical N accumulation to total N accumulation}(\%)\\&= \text{Periodical aboveground N accumulation}\\&\div \text{Aboveground N accumulation at maturity}\end{aligned} \quad (3)$$

$$\begin{aligned}&\text{Pre–anthesis N translocation amount}(TA_{PRN}, \text{kg ha}^{-1})\\&= \text{Aboveground N accumulation of vegetable organ at anthesis}\\&- \text{Aboveground N accumulation of vegetable organ at maturity}\end{aligned} \quad (4)$$

$$\begin{aligned}&\text{Translocation rate } (TR_{PRN}, \%)\\&= \text{Pre–anthesis N translocation}\\&\div \text{Aboveground N accumulation at anthesis} \times 100\end{aligned} \quad (5)$$

$$\begin{aligned}&\text{Contribution rate of pre–anthesis N translocation to grain N}\\&(CR_{PRN}, \%)\\&= \text{Pre–anthesis N translocation}\\&\div \text{Grain N accumulation at maturity} \times 100\end{aligned} \quad (6)$$

$$\text{Contribution rate of post–anthesis N accumulation to grain N}(CR_{ATM}, \%) = (\text{Post–anthesis N accumulation}) \div \text{Grain N accumulation at maturity} \times 100 \quad (7)$$

2.3.3 Grain yield, protein content and protein yield

At the maturity stage, four representative sampling areas, each measuring 2 m by 1.36 m, were randomly selected within each plot. The wheat plants within these areas were manually harvested to assess grain yield. Following harvest, the plants were air–dried, threshed, and the grain obtained was weighed. To accurately determine grain moisture content and dry weight, 100 g samples of the air–dried grain were further oven–dried at 90°C for 30 minutes and then at a reduced temperature of 65°C for a duration of 24 hours. Grain yield calculations for each plot were standardized to a uniform moisture content of 12.5%, using the air–dried grain weight and its determined water content to adjust the figures accordingly. The grain protein content was then calculated by multiplying the grain's total N content, expressed in g kg^{-1}, by the factor 0.57—which is specific to cereal grains. Lastly,the protein yield, expressed in kilograms per hectare (kg ha^{-1}), was calculated using the Equation 8, as documented by Huang et al. (2021):

$$\text{Protein yield}(kg\ ha^{-1}) = 0.875 \times \text{Grain yield} \times \text{Grain protein content} \div 100, \text{ where 0.875 and 100 were the conversion coefficients .} \quad (8)$$

2.3.4 N use efficiency

The N fertilizer partial factor productivity, N internal efficiency, N uptake efficiency and N harvest index were calculated using the Equations 9-12, respectively (Huang et al. 2017):

$$\text{N fertilizer partial factor productivity}(PFPN, kg\ kg^{-1}) = Y_g \div F_N \quad (9)$$

$$\text{N uptake efficiency}(NUPE, kg\ kg^{-1}) = NA_M \div F_r \quad (10)$$

$$\text{N internal efficiency}(NIE, kg\ kg^{-1}) = Y_g \div NA_M \quad (11)$$

$$\text{N harvest index}(NHI, \%) = NA_g \div NA_M \times 100 \quad (12)$$

where Y_g is the grain yield (kg ha^{-1}); and F_N is the fertilizer rate for N (kg N ha^{-1}); NA_M is the total N accumulation in aboveground parts at maturity (kg ha^{-1}); NA_g is the N accumulation in grain at maturity (kg ha^{-1}).

2.4 Statistical analysis

The means of the data for each treatment were computed by averaging the values across all plots. Differences between these means were assessed using analysis of variance (ANOVA) followed by the Least Significant Difference (LSD) test at a significance level of $P = 0.05$. These statistical analyses were conducted using the SPSS statistical software (version 18, IBM Corp., Chicago, IL, USA). Graphical representations of the data were created with Microsoft Excel 2010.

3 Results

3.1 Soil nitrate–N

Significant differences in soil nitrate–N accumulation were observed among the treatments at the booting, anthesis, and maturity stages in both years, as shown in Table 2 and Figure 3.

TABLE 2 Soil nitrate–N accumulation kg N ha^{-1}) at booting, anthesis and maturity stages affected by the FI, AFI and TN techniques in 2018–2019 and 2019–2020.

Treatment	Booting stage		Anthesis stage		Maturity stage	
	2018–2019	2019–2020	2018–2019	2019–2020	2018–2019	2019–2020
NINTN	160.5 c	163.8 cd	144.0 c	129.3 c	128.6 a	122.2 a
EFINTN	161.5 c	160.4 d	130.5 e	120.3 d	113.1 bc	113.3 b
AFINTN	173.5 b	169.0 c	136.0 d	122.7 d	105.5 d	102.3 c
EFITN	210.6 a	202.7 b	161.2 b	151.2 b	117.4 b	112.1 b
AFITN	216.2 a	210.6 a	169.9 a	157.0 a	109.3 cd	104.9 c
F–value						
Year (Y)	4.0ns		8.2*		23.7**	
Treatment(T)	201.3**		322.5**		82.3**	
Y*T	1.5ns		0.7ns		2.7ns	

NINTN, no irrigation with no topdressing N; EFINTN, every furrow irrigation with no topdressing N; AFINTN, alternate furrow irrigation with no topdressing N; EFITN, every furrow irrigation with topdressing N; AFITN, alternate furrow irrigation with topdressing N. Means in a column followed by the different lowercase letters within a year are significantly different at P<0.05. The symbol *, ** and ns indicated that the P are< 0.05,< 0.01 and > 0.05.

10.3389/fpls.2024.1372385

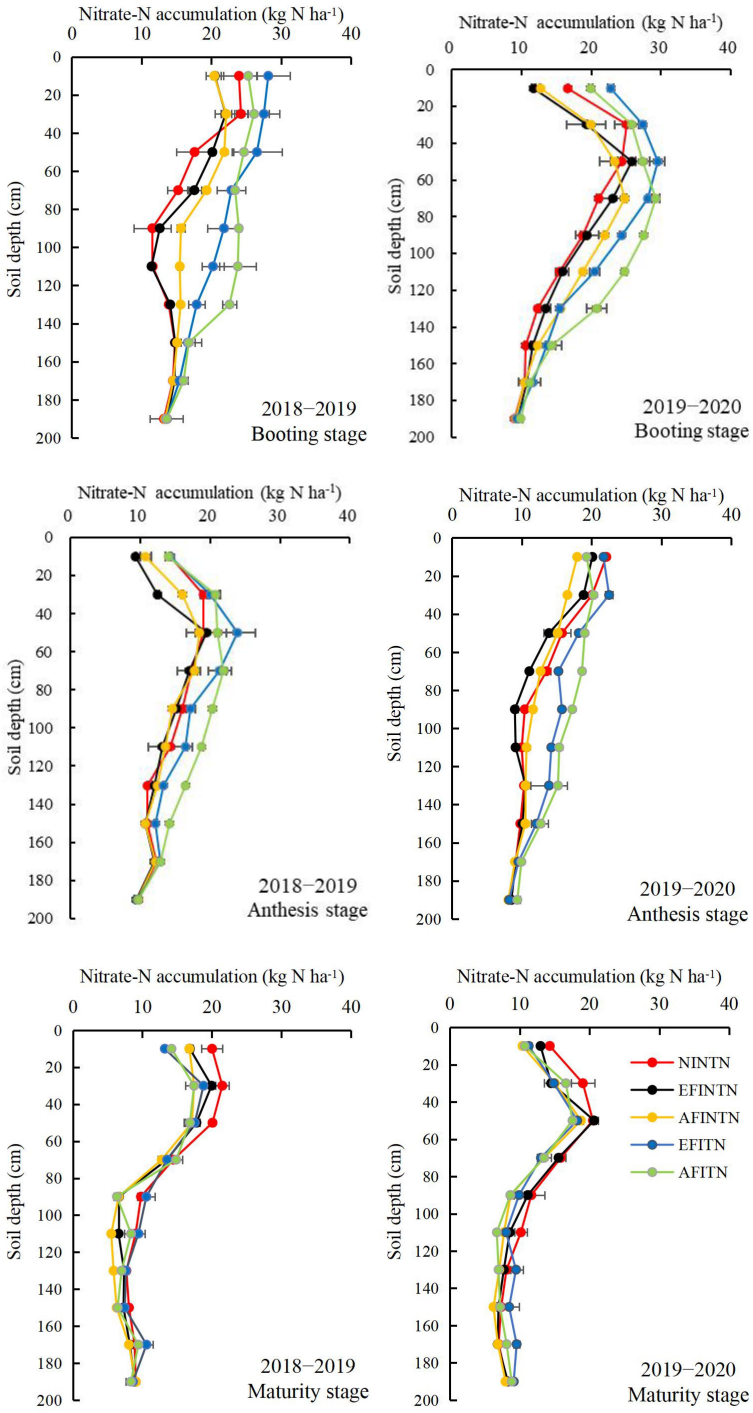

FIGURE 3
Soil nitrate–N accumulation at the different soil depths affected by the FI, AFI and TN techniques in 2018–2019 and 2019–2020. NINTN, no irrigation with no topdressing N; EFINTN, every furrow irrigation with no topdressing N; AFINTN, alternate furrow irrigation with no topdressing N; EFITN, every furrow irrigation with topdressing N; AFITN, alternate furrow irrigation with topdressing N. Bars indicated standard deviation.

Compared to NINTN treatment, the EFINTN treatment did not alter the soil nitrate–N accumulation at the booting stage. However, it resulted in a notable reduction in soil nitrate–N accumulation by 7.0–9.4% at the anthesis stage and 7.3–12.1% at the maturity stage, respectively. These reductions suggest that furrow irrigation at the jointing stage enhanced the uptake of soil nitrate–N by the wheat crop. In contrast, when compared to the every furrow irrigation (EFI) treatments, the alternate furrow irrigation (AFI) treatments showed increased soil nitrate–N accumulation levels at booting and anthesis stages, with a marked decrease in the upper soil layer but a significant increase in the 80–140 cm soil layer. Nevertheless, at the maturity stage, AFI treatments exhibited a significant reduction in

soil nitrate–N accumulation, ranging from 6.8–8.1%. Irrespective of the irrigation method, the topdressing nitrogen (TN) treatments exhibited a significant increase in soil nitrate–N accumulation at booting (28.3%) and anthesis (24.6%) stages when compared to the no topdressing nitrogen (NTN) treatments. However, the TN treatments did not show a significant effect on the soil nitrate–N accumulation at maturity. The findings suggest that employing both AFI and TN techniques at the jointing stage could enhance soil N availability during the middle growth stages of winter wheat but had no beneficial impact at maturity. Across the two years, the soil nitrate–N accumulation at the maturity stage was observed to be AFITN = AFINTN< EFITN = EFINNT< NINTN and the AFITN, AFINTN, EFITN, and EFINNT treatments reduced the soil nitrate–N accumulation by 9.7%, 17.1%, 8.5%, and 14.6%, respectively, compared to the NINTN treatment. These results indicated that implementing the AFINTN technique effectively decreased the risk of nitrate–N accumulation, even with an application of 60 kg N ha^{-1} at the jointing stage.

3.2 Plant N accumulation, translocation, and allocation

3.2.1 Periodical N accumulation during various growth stages and its rate to aboveground N at maturity

Aboveground N accumulation during different growth stages, as well as its proportion of aboveground total N accumulation at maturity, were influenced by the furrow irrigation (FI), AFI, and TN techniques over the two years, as detailed in Table 3. Compared to the NINTN treatment, the EFINTN treatment significantly boosted both the overall N accumulation, specifically the N accumulation from jointing to anthesis and from anthesis to maturity. Consequentially, the N accumulation at anthesis was increased by 14.8% and the aboveground N accumulation at maturity by 22.8%. Compared to the EFI treatments, AFI treatments under the same TN rates decreased both the N accumulation from jointing to anthesis and its rate to aboveground N accumulation at maturity. Nevertheless, they significantly raised N accumulation from anthesis to maturity by 63.2% and its rate to aboveground total N accumulation at maturity by 48.9%, culminating in a 9.4–10.1% increase in aboveground N accumulation at maturity across the two years. Additionally, within the same FI technique, TN treatments markedly raised the N accumulation from jointing to anthesis by 42.9–50.0% and the rate of periodical N accumulation from jointing to anthesis to aboveground N accumulation at maturity by 12.9–18.0%, as well as the N accumulation from anthesis to maturity by 63.5–97.9% and the rate of periodical N accumulation from anthesis to maturity to aboveground N accumulation at maturity by 29.5–56.1%, ultimately enhancing the aboveground N accumulation at maturity by 23.1–29.5%, averaged across the two years. These findings demonstrate that both AFI and TN techniques have the potential to promote aboveground N accumulation during the mid and late growth periods and its rate to aboveground total N accumulation at maturity in dryland winter wheat.

3.2.2 Pre–anthesis N translocation and its contribution to grain

Table 4 illustrates the translocation amount and translocation rate of pre–anthesis N from vegetative organs to grains, which can be ranked as follows: the TN treatments exhibited higher values than NTN treatments, and the EFI treatments showed higher values than AFI treatments. Conversely, the contribution rates of pre–anthesis N to grain N were higher for the NTN treatments than TN treatments, and for the AFI treatments than EFI treatments. Consequently, the optimized values for pre–anthesis N translocation amount and its rate were achieved under the EFITN treatment. However, the contribution rates of pre–anthesis N translocation to grain N was most substantially recorded under the NINTN treatment over the two years.

Both AFI and TN treatments, when compared within the same TN rate or FI technique, significantly enhanced the contribution rate of aboveground N accumulation from anthesis to maturity to grain N. The highest values for aboveground N accumulation from anthesis to maturity to grain N were observed under the AFITN treatment, followed by EFITN or AFINTN, then enhanced compared to EFINTN, and, finally, NINTN. This descending order of effectiveness was consistent in the two years. Notably, the differences in aboveground N accumulation from anthesis to maturity to grain N among treatments were statistically significant, with the exception of no significant difference discerned between EFITN and AFINTN.

3.2.3 N allocation in various organs at maturity

Table 5 presents data indicating that the EFINTN treatment significantly increased N allocation in different winter wheat organs in both years when compared with the NINTN treatment, with the exception of the glume + rachis in 2018–2019. Furthermore, when compared to the EFI treatments, the AFI treatments boosted grain N allocation by 11.6% averaged across the years and TN techniques. In comparison to the NTN treatments, the TN treatments significantly increased N allocation: 28.5% in grain, 21.2% in the glume + rachis, and 19.8% in the stem + leaf + sheath, averaged across the years and FI techniques. Finally, the AFITN treatment yielded the greatest N allocation in grain, which increased by 80.2%, 44.1%, 28.6%, and 11.4% when compared to the NINTN, EFINTN, AFINTN, and EFITN respectively, averaged across the two years. These findings underscore that N allocation in various organs of winter wheat at maturity is significantly influenced by both FI and AFI, as well as TN techniques. Moreover, the data suggest that the synergistic interaction between AFI and TN is a major determinant of N distribution patterns in winter wheat.

3.3 Grain yield, protein content, and protein yield

Table 6 reveals significant variances among treatments in terms of grain yield, protein content, and protein yield. The AFITN treatment achieved the highest grain and protein yields, followed by EFITN, AFINTN, EFINTN, and lastly, NINTN, all in descending order with statistical significance ($P< 0.05$) over the two years.

10.3389/fpls.2024.1372385

TABLE 3 Periodical N accumulation amount and its rate to aboveground N accumulation at maturity affected by the FI, AFI and TN techniques in 2018–2019 and 2019–2020.

Year	Treatment	NA_{JTA} (kg ha^{-1})	NA_{A} (kg ha^{-1})	NA_{ATM} (kg ha^{-1})	NA_{M} (kg ha^{-1})	R_{JTA} (%)	R_{ATM} (%)
2018–2019	NINTN	33.1 d	127.1 d	18.3 d	145.3 e	22.8 b	12.5 d
2018–2019	EFINTN	49.9 bc	143.8 bc	29.6 c	173.4 d	28.8 a	17.1 c
2018–2019	AFINTN	45.0 c	139.0 c	51.0 b	190.0 c	23.7 b	26.9 b
2018–2019	EFITN	63.5 a	157.4 a	56.5 b	213.8 b	29.7 a	26.4 b
2018–2019	AFITN	53.6 b	147.5 b	86.3 a	233.8 a	22.9 b	36.9 a
2019–2020	NINTN	17.6 c	117.2 c	8.6 d	125.8 e	13.9 c	6.9 d
2019–2020	EFINTN	37.2 b	136.7 b	24.5 c	161.2 d	23.0 b	15.2 c
2019–2020	AFINTN	32.4 b	132.0 b	45.4 b	177.4 c	18.3 c	25.6 b
2019–2020	EFITN	59.0 a	158.5 a	50.2 b	208.7 b	28.2 a	24.0 b
2019–2020	AFITN	58.6 a	158.1 a	71.6 a	229.8 a	25.5 ab	31.2 a
F–value							
Year (Y)		29.0**	3.7ns	28.6**	3.7ns	16.1**	20.4**
Treatment(T)		72.4**	100.4**	214.5**	100.4**	15.5**	129.6**
Y*T		6.3**	8.7**	1.4ns	8.7**	4.3*	1.7 ns

NINTN, no irrigation with no topdressing N; EFINTN, every furrow irrigation with no topdressing N; AFINTN, alternate furrow irrigation with no topdressing N; EFITN, every furrow irrigation with topdressing N; AFITN, alternate furrow irrigation with topdressing N. NAJTA, the aboveground N accumulation from jointing to anthesis; NAA, the aboveground N accumulation at anthesis; NAATM, the aboveground N accumulation from anthesis to maturity; NAM, the aboveground N accumulation at maturity; RJTA, the rate of NAJTA to NAM; RATM, the rate of NAATM to NAM. Means in a column followed by the different lowercase letters within a year are significantly different at $P < 0.05$. The symbol *, ** and ns indicated that the P are < 0.05, < 0.01 and > 0.05.

TABLE 4 N translocation from vegetative organ to grain, and contribution rate of post–anthesis N accumulation to grain of winter wheat affected by the FI, AFI and TN techniques in 2018–2019 and 2019–2020.

Year	Treatment	TA_{PRN} (kg ha^{-1})	TR_{PRN} (%)	CR_{PRN} (%)	CR_{ATM} (%)
2018–2019	NINTN	91.9 b	72.3 a	83.5 a	16.5 d
2018–2019	EFINTN	99.7 a	69.3 b	77.1 b	22.9 c
2018–2019	AFINTN	92.8 b	66.8 bc	64.5 c	35.5 b
2018–2019	EFITN	104.2 a	66.2 c	64.9 c	35.1 b
2018–2019	AFITN	91.1 b	61.8 d	51.3 d	48.7 a
2019–2020	NINTN	73.6 c	62.7 a	89.5 a	10.5 d
2019–2020	EFINTN	84.0 b	61.5 a	77.4 b	22.6 c
2019–2020	AFINTN	77.0 c	58.3 b	62.9 c	37.1 b
2019–2020	EFITN	95.8 a	60.4 ab	65.6 c	34.4 b
2019–2020	AFITN	92.4 a	58.4 b	56.4 d	43.6 a
F–value					
Year (Y)		60.8**	168.2**	3.9ns	3.9ns
Treatment(T)		17.1**	21.9**	118.6**	118.6**
Y*T		6.0**	4.1*	1.9ns	1.9ns

NINTN, no irrigation with no topdressing N; EFINTN, every furrow irrigation with no topdressing N; AFINTN, alternate furrow irrigation with no topdressing N; EFITN, every furrow irrigation with topdressing N; AFITN, alternate furrow irrigation with topdressing N. TA_{PRN}, the translocation amount of pre–anthesis N; TR_{PRN}, the translocation rate of pre–anthesis N; CR_{PRN}, the contribution rates of pre–anthesis N translocation to grain N; CR_{ATM}, the contribution rate of NA_{ATM} to grain N. Means in a column followed by the different lowercase letters within a year are significantly different at $P< 0.05$. The symbol *, ** and ns indicated that the P are< 0.05,< 0.01 and > 0.05.

10.3389/fpls.2024.1372385

TABLE 5 N allocation (kg ha^{-1}) in various organs of wheat at maturity affected by the FI, AFI and TN techniques in 2018–2019 and 2019–2020.

Treatment	Grain		Glume + rachis		Stem + leaf + sheath	
	2018–2019	2019–2020	2018–2019	2019–2020	2018–2019	2019–2020
NINTN	110.2 e	82.2 e	13.3 c	13.1 c	21.8 d	30.5 d
EFINTN	129.3 d	108.6 d	13.7 c	15.5 b	30.5 c	37.2 c
AFINTN	143.9 c	122.4 c	13.3 c	15.6 b	32.8 b	39.4 c
EFITN	160.6 b	145.9 b	16.0 b	18.4 a	37.2 a	44.3 b
AFITN	177.4 a	164.0 a	17.5 a	18.5 a	38.9 a	47.2 a
F–value						
Year (Y)	259.9**		69.7**		226.9**	
Treatment(T)	454.3**		106.8**		141.0**	
Y*T	4.6**		7.1**		0.7ns	

NINTN, no irrigation with no topdressing N; EFINTN, every furrow irrigation with no topdressing N; AFINTN, alternate furrow irrigation with no topdressing N; EFITN, every furrow irrigation with topdressing N; AFITN, alternate furrow irrigation with topdressing N. Means in a column followed by the different lowercase letters within a year are significantly different at P< 0.05. *Significant at P< 0.05; ** significant at P< 0.01; ns, not significant.

Regarding grain protein content, there was no statistical difference was detected between EFINTN and AFINTN treatments; but there was a respective decrease of 8.8% and 10.7% when compared to the NINTN treatment, averaged across the two seasons. TN treatments under same furrow irrigation (FI) technique exhibited significant increases in grain protein content—ranging from 4.4% to 14.9%—when compared to the NTN treatments. Of note, the enhancements under AFI were higher than those under EFI. Furthermore, in comparison to the NINTN treatment, the grain protein content under the EFITN treatment diminished significantly by 2.7% to 4.1%, whereas it did not decrease under the AFITN treatment and in fact exhibited an increase of 2.7% in 2019–2020. These results conclusively indicates that the strategic coupled application of AFI and TN techqiue at the jointing stage can substantially enhance grain yield and either sustain or potentially increase the protein content, thereby significantly elevating the protein yield of dryland winter wheat.

3.4 N use efficiency

Across both years, a significant divergence in N fertilizer partial factor productivity (PFPN), N uptake efficiency (NUPE), and N internal efficiency (NIE) was observed among the different treatments, generally ordered as AFINTN > EFINTN > AFITN > EFITN > NINTN (Table 7). Specifically, the PFPN under the AFINTN treatment surpassed EFINTN, AFITN, EFITN, and NINTN by 13.4%, 17.3%, 25.6%, and 53.9%, respectively, as well as NUPE by 9.8%, 6.5%, 17.0%, and 35.7%, while NIE showed improvements of 3.4%, 9.8%, 7.0%, and 13.9%, averaged across the two years. These results suggest that both FI and AFI techniques bolster N use efficiency, whereas the TN technique had a diminishing effect. In 2018–2019 year, the differences in the N harvest index (NHI) among treatments were not statistically significant. Nonetheless, in 2019–2020, the NHI was ranked as AFITN > EFITN > AFINTN > EFINTN > NINTN, with significant differences among all treatments exception between EFITN and AFINTN or AFITN.

TABLE 6 Grain yield, protein content, protein yield of winter wheat affected by the FI, AFI and TN techniques in 2018–2019 and 2019–2020.

Treatment	Grain yield (kg ha^{-1})		Protein content (%)		Protein yield (kg ha^{-1})	
	2018–2019	2019–2020	2018–2019	2019–2020	2018–2019	2019–2020
NINTN	4853 e	3571 e	14.8 a	15.0 b	628.1 e	468.6 e
EFINTN	6202 d	5209 d	13.6 c	13.4 d	736.9 d	618.9 d
AFINTN	6999 c	5953 c	13.4 c	13.4 d	820.1 c	697.8 c
EFITN	7392 b	6515 b	14.2 b	14.6 c	915.6 b	831.8 b
AFITN	7918 a	6943 a	14.6 a	15.4 a	1011.2 a	934.8 a
F–value						
Year (Y)	625.5**		13.3**		260.0**	
Treatment(T)	759.7**		94.1**		454.4**	
Y*T	3.1*		5.7**		4.6**	

NINTN, no irrigation with no topdressing N; EFINTN, every furrow irrigation with no topdressing N; AFINTN, alternate furrow irrigation with no topdressing N; EFITN, every furrow irrigation with topdressing N; AFITN, alternate furrow irrigation with topdressing N. Means in a column followed by the different lowercase letters within a year are significantly different at P< 0.05. The symbol * and ** indicated that the P are< 0.05,< 0.01 and > 0.05.

10.3389/fpls.2024.1372385

TABLE 7 N use efficiency of winter wheat affected by the FI, AFI and TN techniques in 2018–2019 and 2019–2020.

Treatment	PFPN (kg kg^{-1})		NUPE (kg kg^{-1})		NIE (kg kg^{-1})		NHI (%)	
	2018–2019	2019–2020	2018–2019	2019–2020	2018–2019	2019–2020	2018–2019	2019 –2020
NINTN	28.1 e	20.7 e	0.84 d	0.73 e	33.4 d	28.4 e	75.8 a	65.3 d
EFINTN	36.0 b	30.2 b	1.01 b	0.93 c	35.8 b	32.3 b	74.6 a	67.3 c
AFINTN	40.6 a	34.5 a	1.10 a	1.03 a	36.8 a	33.6 a	75.7 a	69.0 b
EFITN	31.8 d	28.0 d	0.92 c	0.90 d	34.6 c	31.2 c	75.1 a	69.9 ab
AFITN	34.1 c	29.9 c	1.01 b	0.99 b	33.9 cd	30.2 d	75.9 a	71.4 a
F–value								
Year (Y)	642.0**		88.1**		379.0**		374.4**	
Treatment(T)	398.3**		224.8**		60.9**		10.0**	
Y*T	9.5**		8.3**		2.8ns		8.7**	

NINTN, no irrigation with no topdressing N; EFINTN, every furrow irrigation with no topdressing N; AFINTN, alternate furrow irrigation with no topdressing N; EFITN, every furrow irrigation with topdressing N; AFITN, alternate furrow irrigation with topdressing N. PFPN: N fertilizer partial factor productively; NUPE: N uptake efficiency, NIE: N internal efficiency; NHI: N harvest index. Means in a column followed by the different lowercase letters within a year are significantly different at P<0.05. The symbol * and ** indicated that the P are< 0.05,< 0.01 and > 0.05.

4 Discussion

4.1 Impact of FI, AFI, and TN at jointing on soil nitrate–N

Soil nitrate–N, the predominant form of N absorbed by crops in dry farming regions, is influenced by a myriad of factors including N fertilizer application, plant uptake and utilization, soil water penetration, and leaching processes (Zhou and Buterbach-Bahl, 2014; Wang and Li, 2019). Our study found that compared to the NINTN treatment, the EFINTN treatment resulted in lower soil nitrate–N accumulation at both the anthesis and maturity stages, suggesting that furrow irrigation (FI) reduced soil nitrate–N accumulation in dryland winter wheat farming systems. This reduction was primarily attributed to the improved N uptake by the crop due to better soil moisture from irrigation (Table 2, Adel et al., 2019). When comparing irrigation methods, alternate furrow irrigation (AFI) elevated soil nitrate–N accumulation at the booting and anthesis stages, particularly within the 80–140 cm soil layer, compared to every furrow irrigation (EFI). This enhancement, however, diminished progressively with wheat growth, especially from anthesis to maturity, leading to lower soil nitrate–N accumulation under AFI than under EFI at the maturity stage (Table 2, Figure 3). These findings suggest that AFI enhances subsoil nitrate–N accumulation in the mid–growth stages but reduces it at maturity stage of wheat, potentially due to the dual role of water movement and plant N uptake. Firstly, soil nitrate–N is prone to download leaching with irrigation water, more irrigation amount in the irrigated furrow resulted in less nitrate–N in the upper and more nitrate–N in the deeper soil layers (Khan et al., 2020). Secondly, AFI's moist environment is known to improve plant N requirement (Jia et al., 2021) and the distribution, density, and activity of crop root (Liang et al., 2000; Wang et al., 2014), all of these would help to increase soil nitrate-N absorption by wheat (Jia et al., 2021).

Previous research demonstrated that N fertilizer topdressing can modulate soil nitrate–N accumulation, and its effects influenced by water management strategies (Zhao and Yu, 2006; Shi et al., 2012; Li et al., 2020). Han et al. (2014) compared AFI and N topdressing paired to conventional irrigation and fertilization, noting that the former increased nitrate–N in the upper soil (0–60 cm) by 30–60% while reducing it in the deeper layers (60–200 cm) by 8–44% in summer maize farmland, mainly due to the enhancement of N requirement and root morphology from the optimized moisture introduced by AFI. In our investigation, TN treatments with 60 kg N ha^{-1} topdressing at the jointing stage consistently improved the soil nitrate–N accumulation in most soil layers at the booting and anthesis stages, regardless of the irrigation techqiue employed, although the differences waned as the wheat matured. Notably, the combination of AFI and TN synergistically increased the soil nitrate–N accumulation, leading to the AFITN treatment exhibiting the highest soil nitrate–N accumulation during the booting and anthesis stages (Table 2, Figure 3). This implies that integrating AFI with TN at the jointing stage can bolster the soil nitrate–N accumulation and providing a favorable N supply in wheat's middle growth phase. This soil nitrate–N accumulation enhancement mainly ascribed the N from topdressing and soil N mineralization. The greater moisture in the irrigated furrow and the partially dry soils under AFI system has strong air permeability, which generate favorable conditions for microbial activity, thus enhancing soil N mineralization and affecting the nitrate-N distribution in soil (Tian et al., 2016; Pu et al., 2022).

In terms of environmental risk, less residual nitrate–N at wheat maturity is preferable for reducing N loss and water pollution (Huang et al., 2017; Lu et al., 2019). Researches have indicated

that FI technique can contribute significantly to nitrate–N leaching and groundwater contamination within agricultural systems, potentially leaching up to 40% of the nitrate–N in the root development zone (Siyal et al., 2012; Iqbal et al., 2019). Luo et al. (2020) observed that supplemental irrigation under rainfed systems could substantially increase soil nitrate–N concentration. However, studies like those by Skinner et al. (1999) have shown that AFI may lessen the risk of nitrate–N leaching when irrigation water is weekly applied, similar to EFI techniques throughout crop growth stages. Optimal irrigation and fertilization under furrow irrigation system shown by Adel et al. (2019) was also found to increase root water and N uptake while reducing nitrate–N losses, compared to conventional practices. Variations in experimental conditions may account for differences in study outcomes. In our case, FI treatments exhibited a substantial reduction in the soil nitrate–N accumulation at the maturity stage of wheat, especially under AFI treatments, meaning that AFI at jointing is prone to reduce the soil nitrate–N accumulation at maturity in wheat cropping system (Table 2, Figure 3). This aligns with Jia et al. (2021), who found that AFI with 180 mm of water reduced nitrate–N leaching by an average of 8.3% and 16.6% compared to flood irrigation with 180 mm and 270 mm, respectively. In turn, TN treatments did not show a discernible effect on the soil nitrate–N accumulation at maturity stage of winter wheat (Table 2, Figure 3). This showed that the 60 kg N ha^{-1} topdressing under one-off furrow irrigation did not increase the environment risk from nitrate–N. Moreover, all combinations of FI and TN techniques decreased soil nitrate–N accumulation at the maturity stage of winter wheat when compared to NINTN, particularly highlighting the effectiveness of AFITN in minimizing the risk of nitrate–N leaching (Table 2, Figure 3). These results indicated that at the maturity stage of winter wheat, the effectiveness of TN-introduced soil nitrate–N accumulation increase was lower than the FI-introduced soil nitrate–N accumulation decrease, leading to a marked decrease of soil nitrate–N accumulation, and thus alleviating the environmental risk.

4.2 Influence of FI, AFI and TN at jointing on winter wheat grain yield and protein content

Boosting grain yield remains a primary driver in wheat production, particularly in dryland regions where the potential for yield increases eclipses that of more infertile areas (Wang and Li, 2019). Our research reveals that the techniques of furrow irrigation (FI), alternative furrow irrigation (AFI), and topdressing nitrogen (TN) all contributed to a significant upsurge in winter wheat's grain yield. This mainly ascribe to the improvement of soil moisture (Wu et al., 2023) and N supply (Table 2, Figure 3). Notably, the AFITN treatment outperformed the NINTN by 63.2–94.4% in the two years, indicating a substantial margin for yield enhancement in dryland furrow–seeded (FS) wheat systems provided by a coupled application of one-off AFI and TN at the jointing stage.

Evolving living standards have ramped up demand for high–quality grain and wheat flour (Lin et al., 2015). Grain protein content is a critical quality parameter for winter wheat, vital for both food and non–food applications (Luo et al., 2018; Hu et al., 2021). In our study, compared to the NINTN treatment, the FI technique under NTN (EFINTN and AFINTN) treatments decreased grain protein content by 8.1–10.6%. This reduction is often linked to the dilutive effect on N concentration due to the increased grain yield (Sissons et al., 2014; Hu et al., 2021), as supported by Luo et al. (2020), who documented a 5.4% drop in protein content in FI–treated winter wheat. Similarly, Sarker et al. (2020) found that AFI maintained yield and grain N content in maize despite a 37.0% reduction in irrigation water in a sub–tropical South Asian climate.

The interplay of plant N requirement, accumulation, translocation, and allocation, and the N supply-demand relationships in various wheat growth stages greatly dictates variations in wheat yield and grain protein content, all of which can be refined through judicious irrigation and N management (Aziz et al., 2018; Jia et al., 2021; Damme et al., 2022). An Iranian field experiment illustrated AFI's superiority over EFI in bolstering shoot N uptake and grain protein content in the FS barley system (Ghasemi-Aghbolaghi and Sepaskhah, 2018). Similarly, in China's Huang–Huai–Hai Plain, AFI distributed at wintering and grain filling stage outpaced EFI treatments at anthesis stage with the same irrigation amount, improving both grain yield and grain N accumulation (Jia et al., 2021). Our investigation further corroborates that, AFI did not significantly alter wheat grain protein content under NTN while increased by 2.8–5.5% under TN (Table 6), indicating the TN treatments could minimized N dilution under AFI system despite the augmented yield. The reason being, although AFI did not noticeably alter the N accumulation at anthesis and the translocation amount of pre–anthesis N, it considerably enhanced the N accumulation from anthesis to maturity, and its contribution to grain N in winter wheat, supporting the significant increase of grain N accumulation at maturity (Table 4). Four potential reasons are discernible: (1) AFITN's promotion of robust root systems (Wang et al., 2012) and supply-demand status (Zhang et al., 2012), leading to heightened N uptake and assimilation (Jia et al., 2021; Yang et al., 2021); (2) the improved soil moisture and soil nitrate–N accumulation enhancing the N accumulation from anthesis to maturity and its contribution to grain N, resulting in the enhancement of grain protein content (Table 6); (3) the 2–folds irrigation volume within the irrigated furrow under AFI allowing the deep soil deposition of fertilizer N, which eluded fertilizer N loss via volatilization, favored root development and N uptake during later growth phases (Wang et al., 2014). (4) the moderate moisture levels under AFI assist N cycle phases, improving N availability and leading to amplified grain N storage (Ashraf et al., 2016).

Optimized N supply at key growth stages is often used to improve plant N characteristics, increase crop yield and grain protein content (Aziz et al., 2018; Damme et al., 2022). Wang et al. (2021) found that employing topdressing N technique at the jointing stage significantly or extremely significantly enhanced the N accumulation, yield, protein content of all the tested wheat. Similar results were also obtained in this study, employed the 60 kg N kg^{-1} topdressing at the jointing stage show significant advantages in N accumulation at

anthesis, N transloctaion amout of pre-anthesis N, N accumulation from anthesis to maturity and its contribution to grain N (Tables 3, 4), grain N allocation (Table 5) and consequently boosting grain yield and protein content (Table 6), thereby addressing the grain protein content reduction caused by FI and AFI. As a result, the AFITN combination yielded top levels in grain yield, and protein content, culminating in an optimal protein yield. These results illustrated that, the topdressing N may employ to balance the N supply-demand for simultaneously increasing grain protein quality and the FI-introduced increase of N requirement.

4.3 Enhancement of N use efficiency by FI, AFI, and TN at jointing

Enhancing N use efficiency (NUE) is crucial for sustainable and environmentally friendly wheat production (Zhang et al., 2020; Zhao et al., 2023b). Studies, such as Jia et al. (2021), found that alternate furrow irrigation (AFI), with an equivalent water volume of 150 mm, significantly increased winter wheat's N uptake efficiency (NUPE) by 8.0% compared to the flood irrigation. Han et al. (2014) also demonstrated that AFI combined with separated N fertilizer applications, improved N agronomic efficiency by 36–56% in summer maize compared to conventional irrigation methods. Comparable enhancements in N use efficiency (NUE) of AFI under the same irrigation quantities were recorded with sugar beets in Turkey (Mon et al., 2016) and safflower in Iran (Shahrokhnia and Sepaskhah, 2016). Conducted under semi–humid, drought–prone conditions, our study shows that implementing furrow irrigation (FI) with 75 mm at the jointing stage significantly enhances the partial factor productivity of nitrogen (PFPN), NUPE, and N internal efficiency (NIE) by 24.2–55.6%, 16.4–36.0%, and 3.9–14.2% respectively across the two years. Herein, the gains under the AFI treatments surpassed those under the EFI treatments, whereas improvements under the TN treatments fell short of the NTN treatments. These outcomes suggest that NUE in winter wheat can be markedly augmented through FI and AFI, particularly for AFI under both NTN and TN conditions. The enhancement results chiefly from FI and AFI's significant increase in soil moisture content (Wu et al., 2023) and the optimized nitrate–N distribution from booting to maturity (Table 2, Figure 3), thus balancing the plant N requirement and soil N supply, finally elevating the plant N absorption, accumulation, and utilization proficiency (Chen et al., 2020; Jia et al., 2021). Contrastingly, there have been instances where AFI was associated with reduced NUE in winter wheat (Sepaskhah and Hosseini, 2008) and plant N uptake for sugar beets in Iran (Mehdi et al., 2017). Ghasemi-Aghbolaghi and Sepaskhah (2018) also reported a decrease in both N internal efficiency (NIE) and NAE for barley using AFI in Iran. Variations in experimental conditions such as climate, soil properties, and cultivation managements may account for differences in study outcomes. In this study, although the precipitation amount in whole year and wheat growing season is higher, the N uptake efficiency in 2019–2020 was obviously lower than 2018–2019, which mainly because the consecutively extreme high temperature (from2 May to 4 May, over 40°C) occurred during early grain filling stage in 2020–2021, thus resulting in a marked decrease in grains per spike and 1000-grain weight (Wu et al., 2023), and finally decreasing the grain yield (Table 6) and grain N accumulation (Table 5). Ru et al. (2022) also reported that short-term extreme heat stress after anthesis resulted in a pronounced decrease in yield and NUE by reducing grain number per spike and thousand kernel weight. Hence, the effects of climate such as temperature should be considered in wheat production to enhance wheat yield and nutrient use efficiency.

N management remains a pivotal influence on N use efficiency in winter wheat, and the effectiveness relates to water conditions (Ji et al., 2021; Zain et al., 2021; Zhao et al., 2023b). In our study, compared to NTN, TN treatments of 60 kg ha^{-1} topdressing at the jointing stage has a dampening impact on PFPN, NUE, and NIE under both EFI and AFI, but these efficiencies still register significantly higher than that under the traditional NINTN treatment. This maybe ascribe to FI's promotion of N uptake and assimilation (Jia et al., 2021; Yang et al., 2021). In our case, the decrease of soil nitrate–N accumulation (Figure 3, Table 2) at different growth stages among treatments can also provide an evidence for the marked difference of soil nitrate–N uptake by wheat This reveals that the potential negative influence of TN on N use efficiency can be mitigated by FI and AFI strategies, especially in dryland where at least one-off irrigation is assured.

5 Conclusion

The obtained results indicate that under the furrow seeding system, when implemented the furrow irrigation (FI), alternate furrow irrigation (AFI), and topdressing nitrogen (TN) techniques, significantly enhances nitrate–N levels at the booting and anthesis stages. This elevation leads to increased aboveground N accumulation, particularly post–anthesis, which contributes considerably to grain yield and protein yield. Concurrently, TN treatment notably enhances grain protein content, while AFI markedly improves N use efficiency. Therefore, the coupled application of AFI and TN not only boosts yield, quality, and efficiency but also mitigates soil nitrate–N residues at the maturity stage of winter wheat production. This coupled strategy holds great promise for dryland regions where a one–off irrigation event is assured during the growth stages of winter wheat.

Data availability statement

The raw data supporting the conclusions of this article will be made available by the authors, without undue reservation.

Author contributions

MH: Data curation, Formal analysis, Investigation, Writing – original draft, Writing – review & editing, Software. WL: Data

curation, Formal analysis, Writing – review & editing. CH: Data curation, Formal analysis, Writing – review & editing. JW: Conceptualization, Investigation, Project administration, Writing – review & editing. HW: Conceptualization, Investigation, Project administration, Writing – review & editing. GF: Conceptualization, Project administration, Writing – review & editing. MS: Writing – review & editing. YL: Conceptualization, Funding acquisition, Project administration, Writing – review & editing, Investigation. GL: Conceptualization, Funding acquisition, Project administration, Software, Writing – review & editing.

Funding

The author(s) declare financial support was received for the research, authorship, and/or publication of this article. This study was financially supported by National Key Research and Development Program of China (under Grant No. 2022YFD2300800; 2022YFD2001005), the Science and Technology Research Project of Henan, China (under Grant No. 222102110087; 232102111009; 232102110051).

Acknowledgments

The author would like to thank the reviewers for their valuable comments and suggestions for this work.

Conflict of interest

The authors declare that the research was conducted in the absence of any commercial or financial relationships that could be construed as a potential conflict of interest.

Publisher's note

References

Adel, M., Sina, B., and Fariborz, A. (2019). Effects of irrigation and fertilization management on reducing nitrogen losses and increasing corn yield under furrow irrigation. *Agric. Water Manage.* 213, 1116–1129. doi: 10.1016/j.agwat.2018.11.007

Ali, S., Xu, Y. Y., Jia, Q., Irshad, A., Wei, T., Ren, X. L., et al. (2018). Cultivation techniques combined with deficit irrigation improves winter wheat photosynthetic characteristics, dry matter translocation and water use efficiency under simulated rainfall conditions. *Agric. Water Manage.* 201, 207–218. doi: 10.1016/j.agwat.2018.01.017

Ashraf, U., Salim, M. N., Sher, A., Sabir, S. U. R., Khan, A., Pan, S. G., et al. (2016). Maize growth, yield formation and water-nitrogen usage in response to varied irrigation and nitrogen supply under semi-arid climate. *Turk. J. Field Crops* 21, 88–96. doi: 10.17557/tjfc.93898

Aziz, O., Hussain, S., Rizwan, M., Riaz, M., Bashir, S., Lin, L. R., et al. (2018). Increasing water productivity, nitrogen economy, and grain yield of rice by water saving irrigation and fertilizer–N management. *Environ. Sci. pollut. Res.* 25, 16601–16615. doi: 10.1007/s11356-018-1855-z

Benjamin, J. G., Porter, L. K., Duke, H. R., and Ahuja, L. R. (1997). Corn growth and nitrogen uptake with furrow irrigation and fertilizer bands. *Agron. J.* 89, 609–612. doi: 10.2134/agronj1997.00021962008900040012x

Chen, X. W., Zhao, H. B., Liu, J. F., and Mao, A. R. (2020). Winter wheat nitrogen utilization under different mulching techniques on the Loess Plateau. *Agron. J.* 112, 1391–1405. doi: 10.1002/agj2.20105

Dai, J., Wang, Z. H., Li, F. C., He, G., Wang, S., Li, Q., et al. (2015). Optimizing nitrogen input by balancing winter wheat yield and residual nitrate in soil in a long–term dryland field experiment in the Loess Plateau of China. *Field Crops Res.* 181, 32–41. doi: 10.1016/j.fcr.2015.06.014

Damme, L., Jing, S. X., Montcalm, A. M., Jepson, M., Andersen, M. N., and Hansen, E. M. (2022). Proper management of irrigation and nitrogen–application increases crop N–uptake efficiency and reduces nitrate leaching. *Acta Agric. Scand. B Soil Plant Sci.* 72, 913–922. doi: 10.1080/09064710.2022.2122864

Fu, X., Wang, J., Peng, Z. P., Yang, X. N., and Zhang, S. H. (2022). Late topdressing can sustain wheat grain yield under straw mulching in the Loess Plateau of China. *Agron. J.* 114, 3487–3497. doi: 10.1002/agj2.21200

Gan, Y. T., Siddique, K. H. M., Turner, N. C., Li, X. G., Niu, J. Y., Yang, C., et al. (2013). Ridge furrow mulching systems—an innovative technique for boosting crop productivity in semiarid rain–fed environments. *Adv. Agron.* 125, 429–476. doi: 10.1016/B978-0-12-405942-9.00007-4

Ghasemi-Aghbolaghi, S., and Sepaskhah, A. R. (2018). Barley (Hordeum vulgare L.) response to partial root drying irrigation, planting method and nitrogen application rates. *Int. J. Plant Prod.* 12 (1), 13–24. doi: 10.1007/s42106–017-0002-y

Guo, S. L., Wu, J. S., Dang, T. H., Liu, W. Z., Li, Y., Wei, W. X., et al. (2010). Impacts of fertilizer practices on environmental risk of nitrate in semiarid farmlands in the Loess Plateau of China. *Plant Soil.* 330, 1–13. doi: 10.1007/s11104-009-0204-x

Han, K., Yang, Y., Zhou, C. J., Shangguan, Y. X., Zhang, L., Li, N., et al. (2014). Management of furrow irrigation and nitrogen application on summer maize. *Agronomy* 106, 1402–1410. doi: 10.2134/agronj13.0367

Hu, C. L., Sadras, V. O., Lu, G. Y., Zhang, P. X., Han, Y., Liu, L., et al. (2021). A global meta–analysis of split nitrogen application for improved wheat yield and grain protein content. *Soil Till Res.* 213, 105111. doi: 10.1016/j.still.2021.105111

Huang, M., Wang, Z. H., Luo, L. C., Wang, S., Hui, X. L., He, G., et al. (2017). Soil testing at harvest to enhance productivity and reduce nitrate residues in dryland wheat production. *Field Crops Res.* 212, 153–164. doi: 10.1016/j.fcr.2017.07.011

Huang, M., Wu, J. Z., Li, Y. J., Fu, G. Z., Zhao, K. N., Zhang, Z. W., et al. (2021). Effects of tillage practices and nitrogen fertilizer application rates on grain yield, protein content in winter wheat and soil nitrate residue in dryland. *Sci. Agric. Sin.* 54, 5206–5219. doi: 10.3864/j.issn.0578–1752.2021.24.004

Iqbal, S., Arif, M., Thierfelder, C., Yasmeen, T., and Li, T. (2019). Reducing nitrogen losses and increasing maize productivity in organic manures amending soils by increasing the ridge to furrow production. *Exp. Agric.* 55, 428–442. doi: 10.1017/S0014479718000091

Ji, J. C., Liu, J. L., Chen, J. J., Niu, Y. J., Xuan, K. F., Jiang, Y. F., et al. (2021). Optimization of topdressing for winter wheat by accurate growth monitoring and improved production estimation. *Remote Sens.* 13, 2349. doi: 10.3390/rs13122349

Jia, D. Y., Dai, X. L., Xie, Y. Y., and He, M. R. (2021). Alternate furrow irrigation improves grain yield and nitrogen use efficiency in winter wheat. *Agric. Water Manage.* 244, 106606. doi: 10.1016/j.agwat.2020.106606

Khan, S., Abbas, S. K., Irshad, S., Mazhar, S. A., and Batool, S. (2020). Impact of various irrigation practices on nitrate movement in soil profile and wheat productivity. *Appl. Water Sci.* 10, 6. doi: 10.1007/s13201-020-01238-8

Khan, Z. I., Ahmad, K., Rehman, S., Siddique, S., Bashir, H., Zafar, A., et al. (2017). Health risk assessment of heavy metals in wheat using different water qualities: implication for human health. *Environ. Sci. Pollut. Res.* 24, 947e955. doi: 10.1007/s11356-016-7865-9

Kumari, K., Dass, A., Sudhishri, S., Kaur, D., and Rani, A. (2017). Yield components, yield and nutrient uptake pattern in maize (Zea mays) under varying irrigation and nitrogen levels. *Indian J. Agron.* 62, 104–107. doi: 10.59797/ija.v62i1.4265

Li, W. W., Xiong, L., Wang, C. J., Liao, Y. C., and Wu, W. (2019). Optimized ridge-furrow with plastic film mulching system to use precipitation efficiently for winter wheat production in dry semi-humid areas. *Agric. Water Manage.* 218, 211–221. doi: 10.1016/j.agwat.2019.03.048

Li, X. X., Shi, Z. L., Wang, J. C., Wang, F., and Jiang, R. F. (2020). Economical nitrogen application rate of winter wheat under rice–wheat rotation in the Yangtze River basin of China. *Chin. J. Appl. Ecol.* 31, 3015–3022. doi: 10.13287/j.1001–9332.202009.027

Liang, Z. S., Kang, S. Z., Shi, P. Z., Pan, Y. H., and He, L. J. (2000). Effect of alternate furrow irrigation on maize production, root density and water–saving benefit. *Sci. Agric. Sin.* 33, 26–32.

Lin, Z., Chang, X. H., Wang, D. M., Zhao, G. C., and Zhao, B. Q. (2015). Long–term fertilization effects on processing quality of wheat grain in the North China Plain. *Field Crops Res.* 174, 55–60. doi: 10.1016/j.fcr.2015.01.008

Liu, Y., Zhang, X. L., Xi, L. Y., Liao, Y. C., and Han, J. (2020). Ridge–furrow planting promotes wheat grain yield and water productivity in the irrigated sub–humid region of China. *Agric. Water Manage.* 231, 105935. doi: 10.1016/j.agwat.2019.105935

Lu, J., Bai, Z. H., Velthof, G. L., Wu, Z. G., Chadwick, D., and Ma, L. (2019). Accumulation and leaching of nitrate in soils in wheat–maize production in China. *Agric. Water Manage.* 212, 407–415. doi: 10.1016/j.agwat.2018.08.039

Luo, J., Liang, Z. M., Xi, L. Y., Liao, Y. C., and Liu, Y. (2020). Plastic–covered ridge–furrow planting combined with supplemental irrigation based on measuring soil moisture promotes wheat grain yield and irrigation water use efficiency in irrigated fields on the loess plateau, China. *Agronomy* 10 (7), 1010. doi: 10.3390/agronomy10071010

Luo, L. C., Wang, Z. H., Huang, M., Hui, X. L., Wang, S., Zhao, Y., et al. (2018). Plastic film mulch increased winter wheat grain yield but reduced its protein content in dryland of Northwest China. *Field Crops Res.* 218, 69–77. doi: 10.1016/j.fcr.2018.01.005

Luo, C. L., Zhang, X. F., Duan, H. X., Zhou, R., Mo, F., Mburu, D. M., et al. (2021). Responses of rainfed wheat productivity to varying ridge–furrow size and rate in semiarid eastern African Plateau. *Agric. Water Manage.* 249, 106813. doi: 10.1016/j.agwat.2021.106813

Mehdi, B., Ali, R. S., and Seyed, H. A. (2017). Irrigation and nitrogen managements affect nitrogen leaching and root yield of sugar beet. *Nutr. Cycl. Agroecosystems* 108, 211–230. doi: 10.1007/s10705-017-9853-y

Mon, J., Bronson, K. F., Hunsaker, D. J., Thorp, K. R., White, J. W., and French, A. N. (2016). Interactive effects of nitrogen fertilization and irrigation on grain yield, canopy temperature, and nitrogen use efficiency in overhead sprinkler–irrigated durum wheat. *Field Crops Res* 191, 54–65. doi: 10.1016/j.fcr.2016.02.011

Pu, J. X., Fan, Y. Q., Feng, X. Y., Liu, Y. H., Qiao, S. T., and Liu, R. H. (2022). Effects of alternate partial root–zone irrigation on soil moisture and nutrient conditions and crop growth. *China Soils Fert.* 9, 209–215. doi: 10.11838/sfsc.1673–6257.21376

Ru, C., Hu, X. T., Chen, D. Y., Song, T. Y., Wang, W. N., Lv, M. W., et al. (2022). Nitrogen modulates the effects of short-term heat, drought and combined stresses after anthesis on photosynthesis, nitrogen metabolism, yield, and water and nitrogen use efficiency of wheat. *Water* 14, 1407. doi: 10.3390/w14091407

Sarker, K. K., Hossain, A., Timsina, J., Biswas, S. K., Malone, S. L., Alam, M. K., et al. (2020). Alternate furrow irrigation can maintain grain yield and nutrient content, and increase crop water productivity in dry season maize in subtropical climate of South Asia. *Agric. Water Manage.* 238, 106229. doi: 10.1016/j.agwat.2020.106229

Sepaskhah, A. R., and Hosseini, S. N. (2008). Effects of alternate furrow irrigation and nitrogen application rates on yield and water–and nitrogen–use efficiency of winter wheat (Triticum aestivum L.). *Plant Prod. Sci.* 11, 250–259. doi: 10.1626/pps.11.250

Shahrokhnia, M. H., and Sepaskhah, A. R. (2016). Effects of irrigation strategies, planting methods and nitrogen fertilization on yield, water and nitrogen efficiencies of safflower. *Agri Water Manage.* 172, 18–30. doi: 10.1016/j.agwat.2016.04.010

Sharma, P., Shukla, M. K., Sammis, T. W., Steiner, R. L., and Mexal, J. G. (2012). Nitrate-nitrogen leaching from three specialty crops of New Mexico under furrow irrigation system. *Agri Water Manage.* 109, 71–80. doi: 10.1016/j.agwat.2012.02.008

Shi, Z. L., Yang, S. J., Zhang, C. H., and Gu, K. J. (2012). Effect of nitrogen application on soil nitrate nitrogen content, root growth and nitrogen utilization of winter wheat in rice–wheat rotation. *J. Soil Water Conserv.* 26, 118–122. doi: 10.13870/j.cnki.stbcxb.2012.05.054

Sissons, M., Ovenden, B., Adorada, D., and Milgate, A. (2014). Durum wheat quality in high input irrigation systems in south–eastern Australia. *Crop Pasture Sci.* 65, 411–422. doi: 10.1071/CP13431

Siyal, A. A., Bristow, K. L., and Simunek, J. (2012). Minimizing nitrogen leaching from furrow irrigation through novel fertilizer placement and soil surface management strategies. *Agric. Water Manage.* 115, 242–251. doi: 10.1016/j.agwat.2012.09.008

Skinner, H., Hanson, J., and Benjamin, J. G. (1999). Nitrogen uptake and partitioning under alternate–and every–furrow irrigation. *Plant Soil.* 210, 11–20. doi: 10.1023/A:1004695301778

Tian, D., Gao, M., and Xue, C. (2016). Effects of soil moisture and nitrogen addition on nitrogen mineralization and soil pH in purple soil of three different textures. *J. Soil Water Conserv.* 30, 256–261. doi: 10.13870/j.cnki.stbcxb.2016.01.046

Wang, Z. H., and Li, S. X. (2019). Nitrate N loss by leaching and surface runoff in agricultural land: a global issue (a review). *Adv. Agron.* 156, 159–217. doi: 10.1016/bs.agron.2019.01.007

Wang, Y., Li, G. Q., Wang, S. W., Zhang, Y. G., Li, D. H., Zhou, H., et al. (2022). A comprehensive evaluation of benefit of high-standard farmland development in China. *Sustainablity* 14, 10361.doi:10.3390/su141610361. doi: 10.3390/su141610361

Wang, Z. C., Liu, F. L., Kang, S. Z., and Jensen, C. R. (2012). Alternate partial root–zone drying irrigation improves nitrogen nutrition in maize (Zea mays L.) leaves. *Environ. Exp. Bot.* 75, 36–40. doi: 10.1016/j.envexpbot.2011.08.015

Wang, C. Y., Liu, W. X., Li, Q. X., Ma, D. Y., Lu, H. F., Feng, W., et al. (2014). Effects of different irrigation and nitrogen regimes on root growth and its correlation with above–ground plant parts in high-yielding wheat under field conditions. *Field Crops Res.* 165, 138–114. doi: 10.1016/j.fcr.2014.04.011

Wang, Y. J., Wang, D. M., Wang, Y. J., Yang, Y. S., Chang, X. H., and Shi, S. B. (2021). Response of yield and quality of winter wheat materials from different ecological regions to nitrogen topdressing rate. *J. Plant Nutri. Ferti.* 27, 719–727. doi: 10.11674/zwyf.20541

Wu, J. Z., Guan, H. Y., Wang, Z. M., Li, Y. J., Fu, G. Z., Huang, M., et al. (2023). Alternative furrow irrigation combined with topdressing nitrogen at jointing help yield formation and water use of winter wheat under no–till ridge furrow planting system in semi–humid drought–prone areas of China. *Agronomy* 13, 1390. doi: 10.3390/agronomy13051390

Yang, Z. S., Wu, J. Z., Huang, M., Li, Y. J., Fu, G. Z., Zhao, K. N., et al. (2021). Effects of furrow planting and fertilization optimization on wheat yield, water and fertilizer use efficiency in dryland. *Acta Agric. Boreali–Sin.* 36, 157–166. doi: 10.7668/hbnxb.20192122

Zain, M., Si, Z. Y., Li, S., Gao, Y., Mehmood, F., Rahman, S. U., et al. (2021). The coupled effects of irrigation scheduling and nitrogen fertilization mode on growth, yield and water use efficiency in drip–irrigated winter wheat. *Sustainability* 13, 1–18. doi: 10.3390/su13052742

Zhang, L. D., Gao, L. H., Zhang, L. X., Wang, S. ,. Z., Sui, X. ,. L., and Zhang, Z. ,. X. (2012). Alternate furrow irrigation and nitrogen level effects on migration of water and nitrate-nitrogen in soil and root growth of cucumber in solar-greenhouse. *Sci. Hortic.* 138, 43–49. doi: 10.1016/j.scienta.2012.02.003

Zhang, X. D., Kamran, M., Li, F. J., Xue, X. K., Jia, Z. K., and Han, Q. F. (2020). Optimizing fertilization under ridge–furrow rainfall harvesting system to improve foxtail millet yield and water use in a semiarid region, China. *Agric. Water Manage.* 227, 105852. doi: 10.1016/j.agwat.2019.105852

Zhang, X., Li, X. H., Luo, L. C., Ma, Q. X., Ma, Q., Hui, X. L., et al. (2019). Monitoring wheat nitrogen requirement and top soil nitrate for nitrate residue controlling in drylands. *J. Clean. Prod.* 241, 118372. doi: 10.1016/j.jclepro.2019.118372

Zhao, K. N., Huang, M., Li, Y. J., Wu, J. Z., Tian, W. Z., Li, J. H., et al. (2023a). Combined organic fertilizer and straw return enhanced summer maize productivity and optimized soil nitrate–N distribution in rainfed summer maize–winter wheat rotation on the Southeast Loess Plateau. *Soil Sci. Plant Nutr.* 23, 938–952. doi: 10.1007/s42729-022-01094-2

Zhao, K. N., Wang, H. T., Wu, J. Z., Liu, A. K., Huang, X. L., Li, G. Q., et al. (2023b). One–off irrigation improves water and nitrogen use efficiency and productivity of wheat as mediated by nitrogen rate and tillage in drought–prone areas. *Field Crops Res.* 295, 108898. doi: 10.1016/j.fcr.2023.108898

Zhao, J. Y., and Yu, Z. W. (2006). Effects of nitrogen rate on nitrogen fertilizer use of winter wheat and content of soil nitrate–N under different fertility condition. *Acta Ecol. Sin.* 26, 815–822.

Zhou, M. H., and Buterbach-Bahl, K. (2014). Assessment of nitrate leaching loss on a yield-scaled basis from maize and wheat cropping systems. *Plant Soil.* 374, 977–991. doi: 10.1007/s11104-013-1876-9

frontiers | Frontiers in Plant Science

TYPE Original Research
PUBLISHED 06 June 2024
DOI 10.3389/fpls.2024.1401287

OPEN ACCESS

EDITED BY
Laichao Luo,
Anhui Agricultural University, China

REVIEWED BY
Hafeez Noor,
Shanxi Agricultural University, China
Shanchao Yue,
Northwest A&F University, China

*CORRESPONDENCE
Ming Huang
huangming_2003@126.com
Youjun Li
lyj@haust.edu.cn

RECEIVED 15 March 2024
ACCEPTED 14 May 2024
PUBLISHED 06 June 2024

CITATION
Wu J, Wang R, Zhao W, Zhao K, Wu S, Zhang J, Wang H, Fu G, Huang M and Li Y (2024) Combined subsoiling and ridge–furrow rainfall harvesting during the summer fallow season improves wheat yield, water and nutrient use efficiency, and quality and reduces soil nitrate-N residue in the dryland summer fallow–winter wheat rotation. *Front. Plant Sci.* 15:1401287. doi: 10.3389/fpls.2024.1401287

Combined subsoiling and ridge–furrow rainfall harvesting during the summer fallow season improves wheat yield, water and nutrient use efficiency, and quality and reduces soil nitrate-N residue in the dryland summer fallow–winter wheat rotation

Jinzhi Wu, Rongrong Wang, Wenxin Zhao, Kainan Zhao, Shanwei Wu, Jun Zhang, Hezheng Wang, Guozhan Fu, Ming Huang* and Youjun Li*

College of Agriculture, Henan University of Science and Technology, Luoyang, China

Both subsoiling tillage (ST) and ridge and furrow rainfall harvesting (RF) are widely implemented and play an important role in boosting wheat productivity. However, information about the effects of ST coupled with RF during the summer fallow season on wheat productivity and environmental issues remains limited. This study aims to explore the effects of ST coupled with RF on water harvesting, wheat productivity–yield traits, water and nutrient use efficiency and quality, and soil nitrate-N residue in dryland winter wheat–summer fallow rotation at the intersection of southern Loess Plateau and western Huang–Huai–Hai Plain in China in 2018–2022. Three tillage practices—deep plowing with straw turnover (PTST), subsoiling with straw mulching (STSM), and STSM coupled with RF (SRFSM)—are conducted during the summer fallow season. The results indicated that tillage practices during the summer fallow season significantly impacted wheat productivity and soil nitrate-N residue. Compared to PTST, STSM significantly enhanced rainfall fallow efficiency and water use efficiency by 7.0% and 14.2%, respectively, as well as N, P, and K uptake efficiency by 16.9%, 16.2%, and 15.3%, and thus increased grain yield by 14.3% and improved most parameters of protein components and processing quality, albeit with an increase in nitrate-N residue in the 0- to 300-cm soil depth by 12.5%. SRFSM, in turn, led to a further increase in water storage at sowing, resulting in an increase of water use efficiency by 6.8%, as well as N, P, and K uptake efficiency and K internal efficiency by 11.8%, 10.4%, 8.8%, and 4.7%, thereby significantly promoting grain yield by 10.2%, and improving the contents of all the protein components and enhancing the processing quality in grain, and simultaneously reducing the nitrate-N residue in the 0- to 300-cm soil layer by 16.1%, compared to STSM. In essence, this study posits that employing subsoiling coupled with ridge–furrow rainfall harvesting (SRFSM) during the summer

fallow season is a promising strategy for enhancing wheat yield, efficiency, and quality, and simultaneously reducing soil nitrate-N residue within the dryland summer fallow–winter wheat rotation system.

KEYWORDS

dryland, wheat, tillage practice during summer fallow season, grain yield, productivity, nitrate-N residue

1 Introduction

Wheat (*Triticum aestivum L.*), which accounts for more than 20% of the world's arable land, contributes to over 45% of the global calorie supply and over 20% of the global protein supply, and feeds approximately 30% of the world population (FAO, 2016), plays a crucial role in food security and people's dietary structure optimization. However, approximately 75% of all the wheat is produced from the dryland including arid, semi-arid, and semi-humid drought-prone areas (Zhang et al., 2019). In these areas, water shortage, infertile soil, and less-advanced cropping technique are the critical limiting factors for sustaining the wheat production (Hartmann et al., 2015; Sun et al., 2018; Wang and Li, 2019; Huang et al., 2021), which not only result in a low and unsustainable yield, efficiency, and quality (Huang et al., 2021), but also lead to environmental issues such as nitrate-N leaching and the emission of nitrous oxide and ammonia due to the high amount of nitrate-N residue in wheat fields (Zhou and Buterbach-Bahl, 2014; Lu et al., 2019; Zhao et al., 2023a, Zhao et al., 2023b). The summer fallow–winter wheat (namely, F–W) is one of the most popular wheat cropping systems in the dryland area of China, where the winter wheat is planted in the beginning of late September to October and harvested in late May to early July in the next year, followed by summer, which is approximately 3–4 months before the next sowing of winter wheat (Wang and Li, 2019). In this system, the annual rainfall is 400–800 mm, with 60%–70% occurring during the summer fallow season, while the rainfall during the wheat growth period is usually approximately 200 mm, which cannot meet the water needs of wheat growth (Shi et al., 2021; You et al., 2022). This situation has led to a lower, unstable grain yield, lower resource efficiency in wheat (Cao et al., 2017; Wang and Li, 2019), and overaccumulation of nitrate-N in soil (Dai et al., 2015; Huang et al., 2017). Therefore, sustainable agricultural practices are required to increase wheat yield, efficiency, and quality (Adel et al., 2019) and reduce the soil nitrate-N residue in the F–W system (Wang and Li, 2019).

Subsoiling tillage [ST, usually combined with straw mulching (STSM)] plays important roles in agricultural production, especially in dryland regions, as it is able to increase rainfall harvest, crop yield, and efficiency (Cai et al., 2014; Arnhold et al., 2023) and address environmental issues (Zhao et al., 2023b). Previous studies have primarily demonstrated that ST can influence crop growth and development by reducing soil bulk density (Ahmad et al., 2009; Lampurlanés et al., 2016; Sun et al., 2018), increasing soil porosity (Xue et al., 2018), enhancing water infiltration (Liang et al., 2019; Qiang et al., 2022), increasing soil water usage (Wang et al., 2022; Yang et al., 2022), optimizing soil physical properties and fertility (He et al., 2019; Wang et al., 2020; Yang et al., 2022), improving root characteristics (Izumi et al., 2009; He et al., 2019; Koch et al., 2021; Arnhold et al., 2023), enhancing tiller density (Lv et al., 2019), delaying senescence (He et al., 2020), promoting plant photosynthesis characteristics (Sang et al., 2016; He et al., 2019), and facilitating dry matter accumulation and remobilization (Zhang et al., 2023). In the Loess Plateau of China, studies of two 2-year experiments showed that ST during the summer fallow season improved soil nutrient characteristics, wheat growth, and N uptake characteristics, thus not only increasing wheat yield and water use efficiency (WUE), but also optimizing the quality of albumin, gliadin, glutenin, total protein, and sedimentation values and wet gluten contents (Sun et al., 2013; Zhao et al., 2017). In the Huang–Huai–Hai Plain in China, a field experiment also showed that ST combined with strip rotary promoted the absorption of nitrate-N by wheat, enhancing N accumulation from jointing to maturity (particularly from anthesis to maturity), thus increasing N accumulation in grains and grain yield (Wang et al., 2015). In the study area, our previous studies found that STSM during the summer fallow season increased the soil water storage during sowing (Wu et al., 2021), enhanced shoot and grain N accumulation, improved grain yield and water and N use efficiency in wheat, and reduced the nitrate-N residue at harvest (Huang et al., 2021).

In addition to ST, the ridge and furrow rainfall harvesting technique (RF) is widely utilized in dryland regions to boost crop yield (Zhang et al., 2016; Ali et al., 2017; Zhang et al., 2018; Wu et al., 2023). In the RF system, the arrangement of alternating parallel ridges and furrows helps to channel rainfall water into the furrows, facilitating easy infiltration into deeper soil layers and aiding in rainwater and runoff collection. Moreover, RF has demonstrated the effective regulation of soil water content, temperature, and nutrients (Li et al., 2012; Li et al., 2013; He et al., 2016a, c; Zhang et al., 2021); enhanced soil enzymatic activity and microbial abundance (Zhang et al., 2022); increased root biomass, root length density, and root surface density in the root concentrated layer (Hu et al., 2020); elevated leaf area index, leaf chlorophyll content, and net photosynthetic rate (Gu et al., 2021); promoted plant growth, nutrient absorption, and dry matter accumulation (Ali et al., 2017; Zhang et al., 2022); and ultimately markedly improved grain yield and WUE in wheat (Gan et al., 2013;

Chen et al., 2022; Zhang et al., 2022). Previous studies have confirmed that employing the FS technique can markedly reduce the soil nitrate-N nitrate content in the growth period for spring maize (Zhang et al., 2021), compared to the flat planting system. Another study showed that an RF soil surface—formed by previous wheat production—during the summer fallow season increased rainfall harvesting and forced nitrate-N leaching into the deep soil layer (He et al., 2016a, He et al., 2016c). In the study area, we also found that the RF soil surface formed by the previous wheat production helps to increase rainfall harvesting, nutrient efficiency, and grain yield of wheat (Yang et al., 2021). In addition, the combined tillage selection and ridge–furrow technique can facilitate root proliferation and increase nitrogen accumulation, translocation, and grain yield of maize in the dryland area (Zhang et al., 2023).

To the best of our knowledge, few studies have focused on the combination of ST and RF during the summer fallow season on crop productivity and soil nitrate-N residue. Therefore, we proposed a novel technique that couples ST and RF with straw mulching (namely, SRFSM) during the summer fallow season and employs deep plowing with straw turnover (PTST), subsoiling with straw mulching (STSM), and SRFSM in a 4-year field experiment in a semi-humid, drought-prone region of China. This research aims to (1) investigate the effects of ST and SRFSM on grain yield, water and fertilizer use efficiency, and grain quality; (2) assess the effects of ST and SRFSM on nitrate-N residues; and (3) identify an optimized adaptive tillage technique during the summer fallow season based on the synergistic effect of crop yield, efficiency, quality, and soil nitrate-N in drylands.

2 Materials and methods

2.1 Study site description

From June 2018 to June 2022, a 4-year field experiment was conducted at Meiyao village (111°71′ E, 34°47′ N) in Xiaojie town of Luoning county, Luoyang, Henan province, which is a typical dryland summer fallow–winter wheat production area at the intersection of the southern Loess Plateau and the western Huang–Huai–Hai Plain of China. The average local annual air temperature is 13.7°C, the mean annual frost-free period is 216 days, the average annual amount of sunshine is 2,218 h, and the average annual precipitation is 577 mm. Approximately 70% of the annual precipitation occurs between June and September, which is slightly misaligned with the winter wheat growing season. The summer fallow–winter wheat is one of the main cropping systems in the study area, which involves planting winter wheat in early to mid-October and harvesting it in early June the following year. The annual precipitation levels were 397.5 mm, 653.2 mm, 580.6 mm, and 805.8 mm, and categorized as dry, normal, normal, and wet for the years 2018–2019, 2019–2020, 2020–2021, and 2021–2022, respectively. During these periods, 73.1%, 68.6%, 52.5%, and 88.8% of the total precipitation were received in the summer fallow season (Figure 1). The soils at the experimental site were formed from cinnamon parent material and classified as calcareous Eum-Orthic Anthrosol according to the Chinese soil taxonomy. A field with uniform fertility was chosen, and consistent soil management practices were implemented to maintain soil fertility balance since October 2016. Upon commencing the experiment in 2018, the basic properties of the 0- to 20-cm soil layer were as follows: pH 8.2, organic matter content 12.5 g·kg^{-1}, total nitrogen content 0.8 g kg^{-1}, alkali–hydrolyzable nitrogen content 15.7 g·kg^{-1}, available phosphorus content 23.2 mg kg^{-1}, and available potassium content 197.33 mg kg^{-1}.

2.2 Experimental design and field management

Because tillage practice is difficult to do in a small plot, a large-area design with three tillage practices was applied during the summer fallow season according to Zhao et al. (2018). Three tillage practices included conventional practice of plowing tillage with straw turnover (PTST), subsoiling with straw mulching (STSM), and STSM coupled with RF (SRFSM), which are shown in Figure 2. For PTST, following local farming practices, the previous wheat crop was harvested with 15–20 cm of stubble, and all the straw was evenly spread on the ground. Subsequently, deep

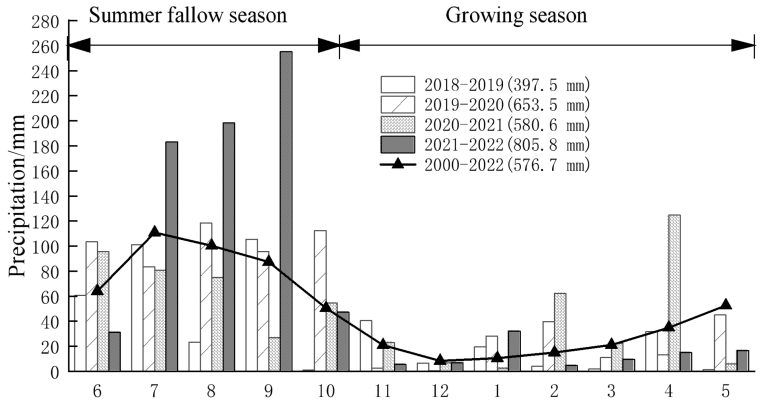

FIGURE 1
Monthly precipitation in the experimental site from June 2018 to June 2022.

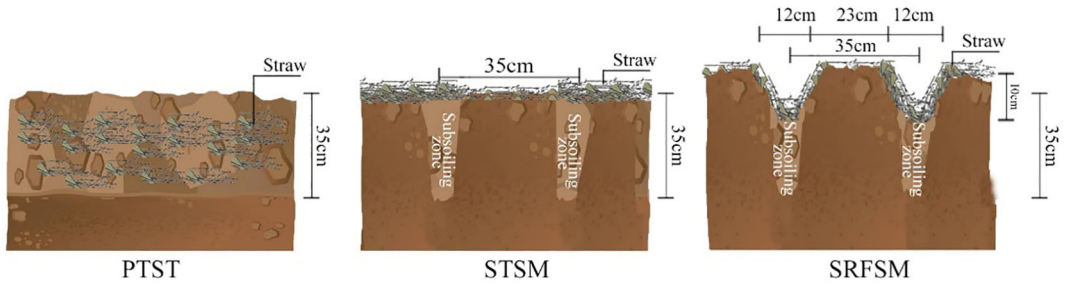

FIGURE 2
Schematic diagram of PTST, STSM, and SRFSM during the summer fallow season.

plowing to a depth of 35 ± 3 cm was carried out after receiving adequate rainfall around late July or early August, incorporating the straw into the soil through plowing tillage. In the case of STSM, similar to PTST, the previous wheat crop was harvested with 15–20 cm of stubble, and the straw was uniformly distributed on the ground. Subsoiling to a depth of 35 ± 3 cm, with a 35-cm interval following conventional practices, was performed approximately 2 weeks after the previous wheat harvest. As for SRFSM, the management practices regarding subsoiling and straw were identical to those of STSM. Additionally, a furrow was created alongside the subsoiled zone, formed during the subsoiling and ridging process, while a ridge was established parallel to the non-subsoiled area. Subsequently, a ridge with a width of 23 ± 2 cm and a height of 10 ± 2 cm, along with a furrow measuring 12 ± 2 cm in width and 10 ± 2 cm in depth, was constructed in the field. Since July 2018, all the treatments have been conducted in the fixed area. The area of each treatment was 420 m^2 (60 m × 7 m). At the four-leaf stage of wheat in each growing season, three 35 m^2 (7 m × 5 m) representative sampling areas were selected for each treatment; thus, there were three replicates in each treatment.

In 2018–2019 and 2019–2020, wheat was drill-planted in furrows spaced 14 cm apart using a ridge and furrow seeder (2BMQF-6/12A, Luoyang Xinle Machinery Co., Ltd., Luoyang, China). Following sowing, ridges and furrows were formed in the field. The ridge had a width of 20 cm and a height of 10 cm, while the furrow was 14 cm wide. This setup resulted in a 20-cm spacing for wheat in the wide rows and a 14-cm spacing in the narrow rows, with an average row spacing of 17 cm. In 2021–2022 and 2022–2023, wheat was drill-planted with an equal row spacing of 20 cm using a conventional flat seeder (2BJM-6, Henan Haofeng Machinery Co., Ltd., Xuchang, China). In all treatments, 750 kg hm^{-2} of compound fertilizer (N:P_2O_5:K_2O = 25:12:8) was evenly broadcast 3 days before sowing and incorporated into the top 0- to 15-cm soil layer as a basal application using a rotary fertilizer seeder. In addition to the changes made to the cultivar and sowing method, wheat cultivation managements were consistent across all treatments except for tillage practices during the summer fallow season. Details regarding the dates of tillage, sowing, and harvest, as well as information on cultivars and seeding amounts, are provided in Table 1. No extra irrigation was supplied in addition to natural precipitation. Weeds, pests, and diseases were controlled with herbicides and pesticides according to the practices employed by local farmers.

2.3 Measurements and methods

2.3.1 Soil water

The soil gravimetric water content (SWC) was determined before the experiment was initiated and periodically at sowing and maturity in 2018–2022. Three random core samples were collected using a handheld soil ferric auger (inner diameter = 4.0 cm) from each sampling plot at a soil depth of 0–200 cm with intervals of 20 cm. The soil samples from the same layer in the same plot were merged, and approximately 300 g of thoroughly mixed soil was sealed immediately in a marked plastic bag for subsequent analysis. The soil water content was determined gravimetrically by drying in an oven at 105°C for 24 h.

Soil water storage (SWS, mm) was calculated using the following equation (Zhao et al., 2023a, b):

$$SWS = \sum_{i=20}^{n} D_i \times H_i \times W_i \times 10 \div 100$$

where D_i is the soil bulk density (g cm^{-3}); H_i is the soil thickness of the i layer (cm); W_i is the soil water content on a gravimetric basis (%); and n is the number of soil layers; i = 20, 40, 60,…, 200. The soil bulk density of 1.32, 1.34, and 1.38 g cm^{-3} was used in the 0- to 20-, >20-to 40-, and >40-cm-deep soil layer, respectively, according to the average value of the local field.

Water harvesting (WH, mm) during the summer fallow season was calculated as (He et al., 2016c):

$$WH = SWS_s - SWS_p$$

where SWS_p and SWS_s are the SWS in the 0- to 200-cm soil layer at maturity of the previous wheat and sowing of the present wheat, respectively.

Evapotranspiration (ET, mm) over the whole winter wheat growing season was calculated as (He et al., 2016c; Zhao et al., 2023b):

$$ET = SWS_s + P + I + U - R - F - SWS_m$$

where SWS_s and SWS_m are the SWS in the 0- to 200-cm soil layer during sowing and at maturity, respectively. P (mm) is the precipitation during wheat growth period; I (mm) is the irrigation amount; U is the upward flow into the root zone; R is the surface runoff; and F is the downward drainage out of the root zone. In our experiment, because the plots are even and no irrigation is applied, the groundwater is below more than 10 m of soil layer. Therefore, I, U, R, and F are zero in this study.

TABLE 1 The date of tillage, sowing, and harvest, and wheat cultivars and seeding amount in 2018–2022.

Year	The date of tillage		Cultivars	Seeding amount (kg ha^{-1})	Sowing date (d-m)	Sowing method	Harvest date (d-m)
	PTST	STSM, SRFSM					
2018–2019	29/7	17/6	ZM175	187.5	9/10	Furrow seeding	7/6
2019–2020	3/8	15/6	LH22	187.5	13/10		7/6
2020–2021	31/7	23/6	LH22	225.0	15/10	Strip seeding	5/6
2021–2022	10/8	19/6	LH22	225.0	29/10		6/6

2.3.2 Soil nitrate-N

Three random core samples were collected from each sampling plot at a soil depth of 0–300 cm with intervals of 20 cm and at 0–60 cm with intervals of 30 cm at maturity in 2020–2021 and 2021–2022. The sample procedures were the same as in Section 2.3.1. A subsample of 5.0 g was extracted with 50 mL of 1 mol L^{-1} KCl by shaking for 1 h (Dai et al., 2015), and the nitrate-N concentrations in the filtrate were determined immediately with a high-resolution digital colorimeter Auto Analyzer 3 (AA3, SEAL Company, Germany).

The soil nitrate-N residue (NR, kg N ha^{-1}) in the 0- to 300-cm soil layer was calculated as follows (Dai et al., 2015):

$$NR = \sum_{i=20\text{ or }30}^{n} D_i \times H_i \times C_i \times 10 \div 100$$

where D_i is the soil bulk density (g cm^{-3}), H_i is the soil layer thickness (cm), and C_i is the soil nitrate concentration (mg kg^{-1}), i.e., i = 20, 40, 60, 90, 120, 150, 180, 210, 240, 270, and 300; 10 and 100 are the conversion coefficients.

2.3.3 Grain yield, yield components, and harvest index

At maturity, three 1 m × 1 m sampling areas were selected randomly in each sample plot and the plants were harvested manually to determine the grain yield. After air drying, the sampled plants were threshed and the grain was weighed. In addition, three 0.5-m-long portions of the winter wheat samples were cut from three different rows in each sampling plot, and the grains per spike and 1,000-grain weight were determined. After cutting off the root, samples were separated into three components (stem + sheath + leaf, rachis + glume, and grain) at maturity. Subsamples of approximately 50 g of air-dried grain and 30 g of air-dried straw or glume were also oven-dried at 60°C to determine the water content. For each sampling plot, the grain yield was expressed at a moisture content of 13.0%, and the biomass yield was expressed on a dry weight basis and calculated according to the air-dried weight and its water content. HI was determined as the ratio of the grain yield relative to the biomass yield.

2.3.4 Plant N, P, and K uptake

In 2020–2021 and 2021–2022, the oven-dried samples of grain, straw, and glume were ground with a ball miller (MM400, RETSCH, Germany) and then digested with H_2SO_4–H_2O_2. The N and P concentrations in the digest solution were determined using an AutoAnalyzer 3 (AA3, Seal Company, Germany) and K concentration was measured using a flame spectrophotometer (Flame Photometer 410, Sherwood Company, England). The nutrient (N, P, and K) uptake levels in each organ were calculated as the dry weight (kg ha^{-1}) multiplied by the corresponding nutrient concentration (g kg^{-1}), and the total nutrient uptake (kg ha^{-1}) in the aboveground biomass was calculated from the summed nutrient uptake by each organ.

2.3.5 Protein composition and processing quality

In 2020–2021 and 2021–2022, protein fractions from whole meal flour were extracted using a sequential extraction procedure based on Luo et al. (2019) with some modifications. Whole meal flour (0.50 g) was weighted to extract the albumin with 5 mL of pure water in a plastic centrifuge tube using the oscillation (20 min) and centrifugation (4,000 rpm for 7 min) method and repeated four times. The extract was collected as albumin after four cycles of oscillation and centrifugation. Similarly, the residue in the tube was extracted with another solution to obtain the fraction of globulin, gliadin, and glutenin using 2% NaCl, 75% ethanol, and 0.2% NaOH solution, respectively, using the same procedure as described above and repeated four times. Afterward, the concentration of protein fraction was determined by the Kjeldahl method (H8750, Haineng Company, China).

In 2020–2021 and 2021–2022, the processing quality including development time (min), stable time (min), sedimentation (mL), wet gluten (%), and extensibility (mm) were determined using a near-infrared analyzer (DA7250, Perten, Stockholm, Sweden).

2.3.6 Resource use efficiency

Rainfall fallow efficiency (RFE, %) was calculated using the following equations (He et al., 2016c):

$$RFE = WH \div P$$

where WH (mm) is the water harvesting during the summer fallow season and P (mm) is the precipitation during the summer fallow season.

WUE (kg ha^{-1} mm^{-1}) was calculated according to Zhao et al. (2023b):

$$WUE = Y \div ET$$

where Y (kg ha^{-1}) is the grain yield and ET (mm) is the evapotranspiration over the whole winter wheat growing season. Because the sampling depth was not uniform between different years, the soil water storage 180- to 200-cm soil layer at maturity is calculated as 2/3 of the 180- to 210-cm soil layer in 2020–2021 and 2021–2022.

The nutrient uptake efficiency and nutrient internal efficiency were calculated using the following equations (Huang et al., 2017):

$$\text{Nutrient uptake efficiency (kgkg}^{-1}) = U_t \div F_P$$

$$\text{Nutrient internal efficiency (kgkg}^{-1}) = Y_g \div U_t$$

where U_t is the total nutrient uptake of N, P, and K in the aboveground biomass (kg ha^{-1}); F_P is the pure fertilizer rate for N, P, and K (kg ha^{-1}); and Y_g is the wheat grain yield (kg ha^{-1}).

2.4 Statistical analysis

Means of the data for each treatment were calculated by averaging the values for each plot. Differences among the means were determined by analysis of variance (ANOVA) and the least significant difference (LSD) test at $p = 0.05$ using the SPSS statistical software package (version 18, IBM Corp., Chicago, IL, USA). The graphs were prepared using Microsoft Excel 2010.

3 Results

3.1 Water harvesting

Table 2 shows tillage practices that significantly affected water harvesting during the fallow season and fallow efficiency except for 2019–2020, while significantly affecting soil water storage at sowing (SWS_s) in all 4 years. Compared to PTST, STSM increased water harvesting during the fallow season (WH) and rainfall fallow efficiency (RFE) in 2018–2019 and 2020–2021 with an increase of 5.0% and 7.0% over the 4 years; in turn, SRFSM significantly increased WH and RFE except for 2019–2020 with an increase of 9.6% and 12.2% over the 4 years. Thus, STSM and SRFSM significantly

TABLE 2 Water harvesting during summer fallow season and soil water storage at sowing under different tillage practices in 2018–2022.

Year	Tillage practice	Water harvesting during fallow season (mm)	Rainfall fallow efficiency (%)	SWS at sowing (mm)
2018–2019	PTST	143.5c	49.4c	522.9c
	STSM	156.5b	53.9b	535.9b
	SRFSM	166.5a	57.3a	545.9a
2019–2020	PTST	206.2a	46.0a	564.5c
	STSM	206.6a	46.1a	571.8b
	SRFSM	208.4a	46.5a	579.8a
2020–2021	PTST	129.4c	42.5c	524.0c
	STSM	153.0b	50.2b	559.2b
	SRFSM	163.5a	53.7a	576.0a
2021–2022	PTST	234.3b	32.8b	638.3c
	STSM	233.0b	32.6b	658.1b
	SRFSM	243.9a	34.1a	677.8a
4-year average	PTST	178.4c	42.7c	562.5c
	STSM	187.3b	45.7b	581.3b
	SRFSM	195.6a	47.9a	594.9a
F value	Year (Y)	2,955.4**	1,830.3**	6,081.2**
	Tillage practice (T)	163.5**	221.7**	722.5**
	Y×T	32.7**	58.2**	50.9**

PTST, plowing tillage with straw turnover; STSM, subsoiling with straw mulching; SRFSM, STSM coupled with RF. Different small letters after the data within the same column and each year indicate significant difference among treatments at $p < 0.05$. ** indicates statistical significance of variance at $p < 0.01$.

10.3389/fpls.2024.1401287

increased the SWS_S in all 4 years with an average increase of 3.3% and 5.8%, respectively. These results indicated that SRFSM increases water harvesting during the fallow season and thereby increasing the soil water storage at sowing in the F–W system.

3.2 Yield components, yield, and harvest index

Both the year and tillage practices had a significant impact on the yield, yield components, and harvest index (HI) of wheat, as shown in Table 3. In comparison to PTST, STSM led to a notable increase in grain yield by 14.3%, with respective increases of 21.5%, 22.4%, and 11.2% in 2018–2019, 2020–2021, and 2021–2022. Similarly, SRFSM resulted in a 25.9% increase in grain yield, with increases of 26.8%, 9.7%, 29.9%, and 37.2% in 2018–2019, 2019–2020, 2020–2021, and 2021–2022. When averaged across the 4 years, both STSM and SRFSM significantly boosted spike numbers, 1,000-grain weight, grain yield, and biomass yield compared to PTST. Additionally, SRFSM showed a significant increase in grains per spike and HI. In comparison to STSM, SRFSM demonstrated significant improvements across all yield traits and achieved a 10.2% increase in grain yield.

3.3 Evapotranspiration and water use efficiency

As shown in Table 4, compared to PTST, STSM did not affect the 4-year average ET with a 2-year increase and a 1-year decrease, but significantly increased the WUE in 3 of 4 years with an average increase of 14.2%; SRFSM significantly increased the ET in all 4 years with an average increase of 3.0%, as well as WUE in all 4 years with an average increase of 22.6%. Compared to STSM, SRFSM significantly increased ET in 2 of 4 years and WUE in all 4 years, respectively, by 2.9% and 6.8% over the 4 years.

3.4 Nutrient use efficiency

Table 5 shows that STSM and SRFSM can increase N, P, and K uptake efficiency and P and K internal efficiency. Compared to PTST, the N, P, and K uptake efficiency were respectively increased by 16.9%, 16.2%, and 15.3% under STSM, as well as 32.5%, 29.7%, and 26.3% under SRFSM over the 2 years, while the P and K internal efficiency were also increased by 3.9% and 6.0% under SRFSM. In comparison to STSM, SRFSM significantly increased N, P, and K uptake efficiency, and K internal efficiency by 11.8%, 10.4%, 8.8%, and 4.7% over the 2 years.

TABLE 3 The yield components, yield, and harvest index of wheat under different tillage practices in 2018–2022.

Year	Tillage practice	Spike numbers ($kg{\cdot}hm^{-2}$)	Grains per spike	1,000-grain weight (g)	Grain yield ($kg{\cdot}hm^{-2}$)	Biomass yield ($kg{\cdot}hm^{-2}$)	Harvest index (%)
2018–2019	PTST	373.8c	31.6b	44.3b	5219c	11894b	49.4c
	STSM	453.6b	31.8b	44.6b	6342b	13915a	51.3b
	SRFSM	469.2a	34.8a	45.9a	6620a	14204a	52.4a
2019–2020	PTST	353.8b	30.5a	44.5c	5052b	12156b	46.8a
	STSM	350.2b	28.9b	47.1a	5049b	12387b	45.9ab
	SRFSM	363.7a	30.1a	45.9b	5544a	13726a	45.4b
2020–2021	PTST	381.7c	37.3b	48.2b	5944c	13562b	49.3a
	STSM	458.0a	36.6c	48.7ab	7277b	17596a	46.5b
	SRFSM	446.3b	38.6a	49.6a	7720a	17871a	48.6a
2021–2022	PTST	365.8c	27.4b	43.3b	4723c	11350c	46.8b
	STSM	420.8b	29.1a	44.7b	5251b	12874b	45.9b
	SRFSM	461.7a	29.6a	45.9a	6481a	15022a	48.5a
4-year average	PTST	368.8c	31.7b	45.1c	5234c	12241c	48.1b
	STSM	420.7b	31.6b	46.3b	5980b	14193b	47.4c
	SRFSM	435.2a	33.3a	46.8a	6591a	15206a	48.8a
F value	Year (Y)	379.7**	859.0**	95.1**	964.0**	608.3**	97.3**
	Tillage practice (T)	488.3**	64.6**	27.5**	972.5**	669.4**	12.9**
	Y×T	59.7**	17.2**	4.1**	79.5**	59.9**	11.4**

PTST, plowing tillage with straw turnover; STSM, subsoiling with straw mulching; SRFSM, STSM coupled with RF. Different small letters after the data within the same column and each year indicate significant difference among treatments at $p < 0.05$. ** indicates statistical significance of variance at $p < 0.01$.

10.3389/fpls.2024.1401287

TABLE 4 The evapotranspiration and water use efficiency of wheat under different tillage practices in 2018–2022.

Tillage practice	Evapotranspiration (mm)					Water use efficiency (kg ha^{-1} mm^{-1})				
	2018–2019	2019–2020	2020–2021	2021–2022	4-year average	2018–2019	2019–2020	2020–2021	2021–2022	4-year average
PTST	271.6b	374.9a	396.1c	332.4b	343.7b	19.2c	13.5b	15.0c	14.2c	15.5c
STSM	277.7a	370.6a	410.0b	313.6c	343.0b	22.8b	13.6b	17.7b	16.7b	17.7b
SRFSM	281.4a	372.4a	418.1a	342.1a	353.5a	23.5a	14.9a	18.5a	18.9a	19.0a
F value										
Year (Y)	2,835.9**					982.1**				
Tillage practice (T)	40.6**					379.8**				
Y×T	22.1**					24.9**				

PTST, plowing tillage with straw turnover; STSM, subsoiling with straw mulching; SRFSM, STSM coupled with RF. Different small letters after the data within the same column and each year indicate significant difference among treatments at $p < 0.05$. ** indicates statistical significance of variance at $p < 0.01$, respectively.

3.5 Contents of protein components and processing quality

Both the year and tillage practices had a significant impact on the contents of protein and protein components in grain of wheat, as shown in Table 6. Averaged across the 2 years, compared to PTST, the contents of albumin, globulin, gliadin, glutenin, and total protein under STSM were increased by 8.6%, 1.7%, 10.4%, 7.6%, and 6.9%, respectively, as well as by 16.0%, 17.8%, 18.0%, 15.2%, and 15.2% under SRFSM. In comparison to STSM, SRFSM significantly increased those by 6.5%, 13.7%, 6.4%, 6.6%, and 7.2%, respectively. These results indicated that STSM and SRFSM during the fallow season increase the contents of grain protein and its components in dryland wheat.

Although they varied yearly, tillage practices significantly affected the processing quality of wheat (Table 7). Considering the 2-year average, with the exception of development time, STSM significantly increased all the measured processing quality of development time, stable time, sedimentation, wet gluten, and extensibility compared with PTST. Likewise, SRFSM significantly increased the processing quality compared with STSM.

3.6 Nitrate-N residue

The nitrate-N residue level varied across soil depth, tillage practices, and years (Figure 3, Table 8). In comparison to PTST, both STSM and SRFSM significantly decreased the nitrate-N residue in the 0- to 60-cm soil layer in both years. However, they

TABLE 5 The N, P, and K uptake and internal efficiency of wheat under different tillage practices in 2020–2022.

Year	Tillage practice	Nutrient uptake efficiency (kg·kg^{-1})			Nutrient internal efficiency (kg·kg^{-1})		
		N	P	K	N	P	K
2020–2021	PTST	0.85c	0.45c	1.93c	37.4a	331.1b	61.8b
	STSM	1.03b	0.53b	2.33b	37.5a	344.8a	62.7ab
	SRFSM	1.09a	0.56a	2.45a	37.7a	345.7a	63.2a
2021–2022	PTST	0.70c	0.30c	1.87c	36.7a	395.3a	51.1b
	STSM	0.77b	0.34b	2.05b	36.3a	393.9a	51.4b
	SRFSM	0.94a	0.41a	2.35a	37.3a	408.8a	56.4a
2-year average	PTST	0.77c	0.37c	1.90c	37.0a	363.2b	56.4b
	STSM	0.90b	0.43b	2.19b	36.9a	369.4a	57.0b
	SRFSM	1.02a	0.48a	2.40a	37.5a	377.3a	59.8a
F value	Year (Y)	9,524.8**	13,883.7**	1,892.3**	107.6**	810.4**	1,660.6**
	Tillage practice (T)	5,334.5**	1,985.5**	7,328.1**	0.5	10.4*	33.1**
	Y×T	385.5**	98.2**	392.3**	1.3	2.1	12.5**

PTST, plowing tillage with straw turnover; STSM, subsoiling with straw mulching; SRFSM, STSM coupled with RF. Different small letters after the data within the same column and each year indicate significant difference among treatments at $p < 0.05$. * and ** indicate statistical significance of variance at $p < 0.05$ and $p < 0.01$, respectively.

10.3389/fpls.2024.1401287

TABLE 6 The content of protein and its components in grain of wheat under different tillage practices in 2020–2022.

Year	Tillage practice	Albumin/%	Globulin/%	Gliadin/%	Glutenin/%	Total protein/%
2020–2021	PTST	2.08c	1.87b	2.43c	3.55c	10.93c
	STSM	2.24b	1.87b	2.80b	3.93b	11.85b
	SRFSM	2.44a	2.24a	2.99a	4.30a	12.98a
2021–2022	PTST	1.67c	1.73b	3.14c	3.30c	10.83c
	STSM	1.82b	1.79b	3.34b	3.46b	11.41b
	SRFSM	1.90a	2.00a	3.57a	3.60a	12.07a
2-year average	PTST	1.87c	1.80b	2.78c	3.43c	10.88c
	STSM	2.03b	1.83b	3.07b	3.69b	11.63b
	SRFSM	2.17a	2.12a	3.28a	3.95a	12.53a
F value	Year (Y)	5,177.4**	3,055.2**	2,044.9**	27,712.9**	1,659.5**
	Tillage practice (T)	767.0**	5,190.5**	459.0**	11,258.7**	6,482.2**
	Y×T	38.6**	293.8**	13.7**	2,068.8**	387.5**

PTST, plowing tillage with straw turnover; STSM, subsoiling with straw mulching; SRFSM, STSM coupled with RF. Different small letters after the data within the same column and each year indicate significant difference among treatments at $p < 0.05$. ** indicates statistical significance of variance at $p < 0.01$.

increased the nitrate-N residue in the 0- to 300-cm and the 60- to 180-cm soil layer in 2020–2021 but decreased in 2021–2022. Compared to PTST, STSM increased the nitrate-N residue by 12.5%, 23.8%, and 20.8% in the 0- to 300-cm, 60- to 180-cm, and 180- to 300-cm soil layer over the 2 years; however, SRFSM did not affect the nitrate-N residue in the 0- to 300-cm soil layer with a decrease of 24.6% in the 0- to 60-cm soil layer and increase of 11.7% in the 60- to 180-cm soil layer. In comparison to STSM, SRFSM significantly reduced the nitrate-N residue in the 0- to 300-cm soil layer by 16.1%, with a decrease of 16.4%, 10.9%, and 23.3% in the 0- to 60-cm, 60- to 180-cm, and 180- to 300-cm soil layer.

4 Discussion

4.1 Soil water, wheat yield, and efficiency affected by ST and RF techniques during the summer fallow season

In dryland regions of China, water shortage is one of the most important factors threatening wheat production, and optimizing the techniques for enhancing soil water and WUE plays an important role in ensuring food security (Gan et al., 2013; Wang et al., 2019). Previous studies have reported that the ST, SM, and RF

TABLE 7 The grain processing quality of wheat under different tillage practices in 2020–2022.

Year	Tillage practice	Development time/min	Stable time/min	Sedimentation/mL	Wet gluten/%	Extensibility/mm
2020–2021	PTST	2.43a	1.40c	25.79c	27.57b	144.5c
	STSM	2.43a	2.10b	27.33b	28.42a	148.9b
	SRFSM	2.57a	2.33a	28.44a	28.74a	151.9a
2021–2022	PTST	3.76b	2.11c	17.95c	24.34c	129.1c
	STSM	3.85b	3.42b	19.41b	25.47b	131.3b
	SRFSM	4.08a	4.32a	20.40a	26.42a	136.4a
2-year average	PTST	3.10b	1.76c	21.87c	25.96c	136.8c
	STSM	3.14b	2.76b	23.37b	26.95b	140.1b
	SRFSM	3.32a	3.33a	24.42a	27.58a	144.1a
F value	Year (Y)	1,523.5**	498.9**	2,347.6**	752.1**	2,270.9**
	Tillage practice (T)	14.4**	235.0**	81.8**	83.6**	155.9**
	Y×T	2.2**	37.7**	0.1**	6.9**	4.4**

PTST, plowing tillage with straw turnover; STSM, subsoiling with straw mulching; SRFSM, STSM coupled with RF. Different small letters after the data within the same column and each year indicate significant difference among treatments at $p < 0.05$. ** indicates statistical significance of variance at $p < 0.01$.

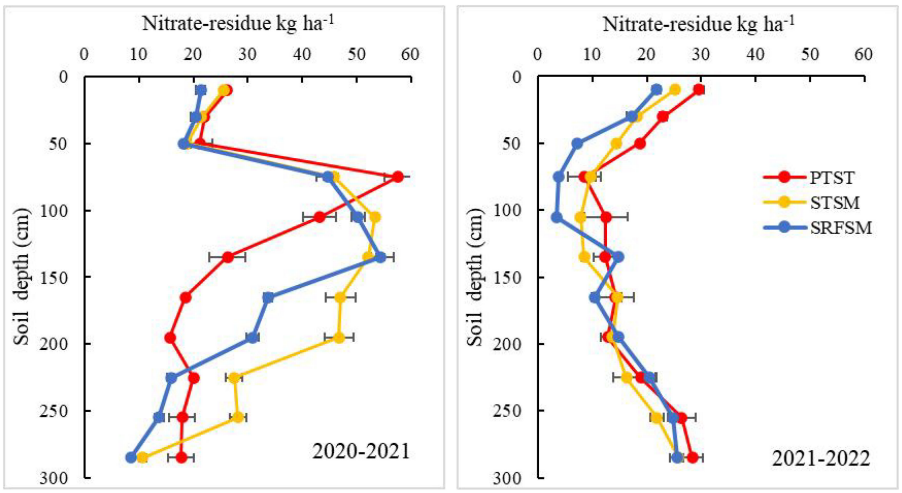

FIGURE 3
Effects of different tillage practices in summer fallow season on soil nitrate residue of wheat field in dryland. PTST, plowing tillage with straw turnover; STSM, subsoiling with straw mulching; SRFSM, STSM coupled with RF.

techniques could increase soil water (Adil et al., 2022), which resulted in an excellent moisture condition for plant growth, tiller differentiation, and dry matter and nutrient accumulation and metabolism, and ultimately achieve the aim of high yield and high efficiency. The studies in drylands of southern Shanxi found that ST during the summer fallow season significantly increased fallow efficiency and soil water storage at sowing, and this could be maintained until the flowering stage, resulting in yield gain and a significant increase in WUE (Sun et al., 2014; Xue et al., 2017; Zhang et al., 2018). Another long-term experiment of He et al. (2016a); He et al. (2016b); He et al. (2016c) showed that RF soil surface with residual plastic film (formed by previous wheat cropping) during the summer season significantly increased rainfall harvesting, thus improving grain yield, WUE, N internal efficiency, and shoot P and K uptake. In our experiment, 4 years of continuous treatment revealed significant variations in grain yield, WUE, and N, P, and K uptake efficiency across different years. Notably, the highest values for these parameters were consistently observed under SRFSM, with STSM following closely behind. This trend suggests that the ST and RF techniques, showing sustainability and stability, are performing well at present. These improvements and sustainability were mainly ascribed to the optimized water harvesting during the fallow season attributed to the STSM and RF techniques, in accordance with the previous studies (Sun et al., 2014; He et al., 2016a, He et al., 2016b, He et al., 2016c; Xue et al., 2017; Zhang et al., 2018). In addition, the improvement in soil

TABLE 8 The nitrate-N residues in the 0- to 300-cm soil layer under different tillage practices in 2020–2022.

Year	Tillage practice	0–300 cm	0–60 cm	60–180 cm	180–300 cm
2020–2021	PTST	286.4c	69.5a	145.4c	71.5b
	STSM	377.4a	65.8b	198.5a	113.2a
	SRFSM	312.1b	60.1c	183.0b	69.0b
2021–2022	PTST	205.5a	71.4a	47.7a	86.4a
	STSM	176.0b	57.8b	40.6ab	77.6b
	SRFSM	164.6b	46.2c	32.7b	85.7ab
2-year average	PTST	245.9b	70.4a	96.5c	79.0b
	STSM	276.7a	61.8b	119.5a	95.4a
	SRFSM	238.3b	53.1c	107.8b	77.4b
F value	Year (Y)	887.4**	126.1**	2,678.6**	0.0
	Tillage practice (T)	23.8**	283.4**	25.8**	0.5
	Y×T	52.5**	60.4**	52.4**	65.5**

PTST, plowing tillage with straw turnover; STSM, subsoiling with straw mulching; SRFSM, STSM coupled with RF. Different small letters after the data within the same column and each year indicate significant difference among treatments at $p < 0.05$. ** indicates statistical significance of variance at $p < 0.01$.

properties by subsoiling and/or straw mulching may explain these increases in grain yield and efficiency (Wang et al., 2015; Zhang et al., 2016). It is important to note that STSM and SRFSM did not significantly increase water harvesting (WH) and rainfall fallow efficiency (RFE), resulting in the lowest yield increase during the normal year of 2019–2020. These findings once again underscore the importance of rainfall harvesting during the summer fallow season for dryland wheat production. Above all, the employment of the combined agronomic techniques of STSM and RF during the summer fallow season could increase rainfall harvesting and dryland wheat productivity such as yield, water, and nutrient efficiency.

4.2 Grain quality affected by ST and RF during the summer fallow season

With the increased standards of living and the development of the food industry, the demand for high-quality grain and flour of wheat has increased rapidly (Lin et al., 2016; Luo et al., 2018; Hu et al., 2021). Proteins and protein components, especially glutenin and gliadin, which serve as multifunctional ingredients in processing and nutritional quality, are the key criteria for assessing the wheat quality in grain (Luo et al., 2019). Previous literature has shown that the effect of subsoiling on wheat quality is inconclusive. A study by Sun et al. (2014) reported that soil water had a positive correlation with grain globulin, gliadin, protein content, and yield. ST during the summer fallow period significantly enhanced soil water, thus increasing grain protein and its components, as well as protein yield in a humid year. A study on the tidal soil areas in China shows that ST significantly increased the protein content of wheat grain by 2.99%–4.90% (Jia et al., 2022). However, another study by Sun et al. (2013) indicated that ST during the summer fallow season decreased the content of albumin, gliadin, and total protein in grains, while increasing the globulin content, glutelin content, and protein yield. Additionally, Xue et al. (2017) reported that ST decreased the grain protein content compared to PT during the summer fallow season. However, a study in Romania by Cociu and Alionte (2017) concluded that ST decreased the protein content of wheat but increased that of maize. In our case, compared to PTST, the contents of protein, albumin, globulin, gliadin, and glutenin in wheat grain under STSM were significantly increased, and the effectiveness was uniform in the two experimental years (Table 6). This result indicated that subsoiling with straw mulching (STSM) during the summer fallow season can increase the content of protein and its components of wheat grain in dryland. The significantly increased N uptake efficiency (Table 4) may explain these results. A field study by Zhang et al. (2017) also found that ST during the summer fallow season significantly increased wheat grain protein by 7%, mainly due to the N uptake improvement caused by the well-water condition induced by ST. Luo et al. (2020) found that, on the basis of soil water management with a target relative content of 100% at wintering and jointing, RF significantly increased the protein and wet gluten content of wheat grain. However, He et al. (2016b) found that the RF soil surface with residual plastic film—formed by previous wheat planting—during the summer fallow season decreased the wheat grain N concentration by 8%, which was associated with the increased N requirement for grain N accumulation and decreased its internal efficiency. In our study, the application of the RF technique within SRFSM during the summer fallow season significantly increased the protein content and protein components of wheat grain. This result was consistent with Luo et al. (2020) but not consistent with He et al. (2016b). Variations in experimental conditions may account for differences in study outcomes.

Commercial value is also determined by the processing quality of wheat. With the gradual increase in bakery flour products, the dough rheological properties, as an important evaluation index of in bakery flour products and wheat processing quality, are being paid more and more attention in nowdays with the improvement of people's living standard. On the Loess Plateau, ST significantly increased sedimentation values and the gluten content of wheat grain (Sun et al., 2013), especially when combined with plastic film mulching (Zhao et al., 2017). Campiglia et al. (2015) reported that ST did not affect the gluten content of durum wheat in the Mediterranean environment of central Italy. However, to the best of our knowledge, few studies focus on how RF affects the processing quality of wheat. In this study, dough rheological properties such as development time, stable time, sedimentation, wet gluten, and extensibility showed the following order: SRFSM>STSM>PTST, with the significant differences between every two treatments, and the impact of different practices on wheat processing quality was the same in the two experimental years (Table 7). The improvement in dough rheological properties is mainly due to the increased protein content and its components (Table 6), as reported by Zhang et al. (2018). These results show that the processing quality of dryland wheat can be improved when STSM and SRFSM are applied during the summer fallow season. Accordingly, the results of this study provide a basis for further investigation and regulation on the quality of wheat in drylands, but further studies are needed to verify our findings in field experiments under varied soil and climatic conditions.

4.3 Soil nitrate-N affected by ST and RF during the summer fallow season

The nitrate-N present in the soil may contribute greatly to the N requirements of crops (Dai et al., 2015), but it is also susceptible to leaching, denitrification, and emission if the level exceeds the safe threshold (López-Bellido et al., 2013; Wang and Li, 2019). In this study, compared to PTST, STSM significantly decreased the nitrate-N residue in the 0- to 60-cm soil layer in both years, but increased it in the 60- to 300-cm soil layer. This is mainly ascribed to the increased N uptake efficiency. Previous studies showed that ST reduced the nitrate-N content in the 0- to 80-cm layer at maturity of winter wheat but increased it in the 120- to 160-cm soil layer in the North China Plain (Zheng et al., 2012; Wang et al., 2015). However, some studies showed that ST helps to increase the nitrate residue in the 0- to 80-cm soil layer but reduced it in the 0- to 380-cm soil layer (Wu et al., 2023). The present study also found that, compared

to STSM, SRFSM significantly reduced the nitrate-N residue in the 0- to 300-cm soil layer by 16.1%, with a decrease of 16.4%, 10.9%, and 23.3% in the 0- to 60-cm, 60- to 180-cm, and 180- to 300-cm soil layers. This was mainly because RF increased soil water and promoted N uptake by wheat plants, and finally reduced nitrate-N residues in the wheat production system (Zhao et al., 2023a). However, another study in the summer maize–winter wheat double cropping system showed that RF planting patterns increased the nitrate-N residue in the 0- to 100-cm layer, but there was no difference in the 0- to 380-cm soil depth (Wu et al., 2023). Above all, the influence of ST and RF during the summer fallow season on nitrate-N residue remains uniform; thus, further studies are needed to verify the influence of ST coupled with RF on nitrate-N residue under varied environmental and cropping conditions.

Our results also showed that nitrate-N residues in soil were closely related to precipitation (Figure 3). In 2020–2021, the nitrate-N residue was 145.4–198.5 kg N ha^{-1} in the 60- to 180-cm soil depth, which surpassed 50% of that in the 0- to 300-cm soil profile. This suggests that the 60- to 180-cm soil layer was the nitrate-N enrichment region. However, the distribution of nitrate-N residue (especially in the 90- to 180-cm soil layer) in 2021–2022 was obviously different from 2020–2021 because of the high amount of precipitation from July to September 2021, where the nitrate-N leached deeper into the soil profile by 90 cm due to heavy rainfall. Most soil N is soluble and easily moves away from upper soil under the conditions of heavy rainfall during the summer season, resulting in the nitrate-N migrating to the even deeper 100- to 200-cm soil layer along the gaps formed by crop roots. In our case, the greater nitrate-N change between 2019–2020 and 2020–2021 was found under STSM and SRFSM compared to PTST. This result demonstrated that STSM and SRFSM have a higher risk of nitrate-N leaching under heavy rainfall conditions due to the increased ability of water infiltration. Zhao et al. (2023b) also reported that heavy rainfall resulted in more nitrate-N leaching in the study area. Hence, the effects of precipitation on the distribution of nitrate-N in soil should be considered in wheat production to effectively utilize soil nitrate-N and reduce nitrate-N leaching to deep soil layers.

5 Conclusion

The obtained results showed that the STSM and RF techniques during the summer fallow season can significantly increase rainfall harvesting during the summer fallow season and soil water storage at sowing. Water improvement under STSM and SRFSM increased water and nutrient uptake efficiency, and ultimately improved grain yield, protein content and its components, and most indicators of processing quality in wheat. In comparison to STSM, rainfall harvesting, grain yield, efficiency, protein content, and processing quality under SRFSM were significantly increased but soil nitrate-N residue was significantly decreased. This study indicated that using the combination of subsoiling and ridge and furrow soil surface during the summer fallow season (SRFSM) is a promising strategy to increase yield, quality, and efficiency, and reduce the soil nitrate-N residue in the dryland summer fallow–winter wheat rotation system.

Data availability statement

The original contributions presented in the study are included in the article/supplementary material. Further inquiries can be directed to the corresponding authors.

Author contributions

JW: Conceptualization, Data curation, Investigation, Writing – original draft, Writing – review & editing. RW: Data curation, Investigation, Visualization, Writing – review & editing. WZ: Data curation, Investigation, Visualization, Writing – review & editing. KZ: Data curation, Investigation, Visualization, Writing – review & editing. SW: Data curation, Investigation, Visualization, Writing – review & editing. JZ: Data curation, Investigation, Visualization, Writing – review & editing. HW: Writing – review & editing. GF: Writing – review & editing. MH: Conceptualization, Funding acquisition, Writing – review & editing. YL: Conceptualization, Funding acquisition, Writing – review & editing.

Funding

The author(s) declare financial support was received for the research, authorship, and/or publication of this article. This study was financially supported by the National Key Research and Development Program of China (under Grant No. 2022YFD2300800) and the Science and Technology Research Project of Henan, China (under Grant Nos. 222102110087 and 232102111009).

Conflict of interest

The authors declare that the research was conducted in the absence of any commercial or financial relationships that could be construed as a potential conflict of interest.

Publisher's note

References

Adel, M., Sina, B., and Fariborz, A. (2019). Effects of irrigation and fertilization management on reducing nitrogen losses and increasing corn yield under furrow irrigation. *Agric. Water Manage.* 213, 1116–1129. doi: 10.1016/j.agwat.2018.11.007

Adil, M., Zhang, S. H., Wang, J., Shah, A. N., Tanveer, M., and Fiaz, S. (2022). Effects of fallow management practices on soil water, crop yield and water use efficiency in winter wheat monoculture system: A Meta-Analysis. *Front. Plant Sci.* 13. doi: 10.3389/fpls.2022.825309

Ahmad, N., Hassan, F. U., and Belford, R. K. (2009). Effects of soil compaction in the sub–humid cropping environment in Pakistan on uptake of NPK and grain yield in wheat (Triticum aestivum): II Alleviation. *Field Crops Res.* 110, 61–68. doi: 10.1016/j.fcr.2008.07.002

Ali, S., Xu, Y., Ma, X., Ahmad, I., Kamran, M., Dong, Z., et al. (2017). Planting patterns and deficit irrigation strategies to improve wheat production and water use efficiency under simulated rainfall conditions. *Front. Plant Sci.* 8. doi: 10.3389/fpls.2017.01408

Arnhold, J., Grunwald, D., Braun-Kiewnick, A., and Koch, H. J. (2023). Effect of crop rotational position and nitrogen supply on root development and yield formation of winter wheat. *Front. Plant Sci.* 14. doi: 10.3389/fpls.2023.1265994

Cai, H. G., Ma, W., Zhang, X. Z., Ping, J. Q., Yan, X. G., and Liu, J. Z. (2014). Effect of subsoil tillage depth on nutrient accumulation, root distribution, and grain yield in spring maize. *Crop J.* 2, 297–307. doi: 10.1016/j.cj.2014.04.006

Campiglia, E., Mancinelli., R., Stefanis, E. D., Pucciarmati, S., and Radicetti, E. (2015). The long–term effects of conventional and organic cropping systems, tillage managements and weather conditions on yield and grain quality of durum wheat (Triticum durum Desf.) in the Mediterranean environment of Central Italy. *Field Crops Res.* 17, 634–644. doi: 10.1016/j.fcr.2015.02.021

Cao, H. B., Wang, Z. H., He, G., Dai, J., Huang, M., Wang, S., et al. (2017). Tailoring NPK fertilizer application to precipitation for dryland winter wheat in the Loess Plateau. *Field Crops Res.* 209, 88–95. doi: 10.1016/j.fcr.2017.04.014

Chen, G. Z., Wu, P., Wang, J. Y., Zhang, P., and Jia, Z. K. (2022). Ridge–furrow rainfall harvesting system helps to improve stability, benefits and precipitation utilization efficiency of maize production in Loess Plateau region of China. *Agric. Water Manage.* 261, 107360. doi: 10.1016/j.agwat.2021.107360

Cociu, A. I., and Alionte, E. (2017). Effect of different tillage systems on grain yield and its quality of winter wheat, maize, and soybean under different weather conditions. *Rom. Agric. Res.* 34, 59–67.

Dai, J., Wang, Z. H., Li, F. C., He, G., Wang, S., Li, Q., et al. (2015). Optimizing nitrogen input by balancing winter wheat yield and residual nitrate in soil in a long–term dryland field experiment in the Loess Plateau of China. *Field Crops Res.* 181, 32–41. doi: 10.1016/j.fcr.2015.06.014

FAO. (2016). Available online at: https://www.fao.org/faostat/en/#data/QC.

Gan, Y. T., Siddique, K. H. M., Turner, N. C., Li, X. G., and Liu, L. P. (2013). Ridge-furrow mulching systems—an innovative technique for boosting crop productivity in semiarid rain-fed environments. *Adv. Agron.* 118, 429–476. doi: 10.1016/B978-0-12-405942-9.00007-4

Gu, X. B., Cai, H. J., Chen, P. P., Li, Y. P., Fang, H., and Li, Y. N. (2021). Ridge-furrow film mulching improves water and nitrogen use efficiencies under reduced irrigation and nitrogen applications in wheat field. *Field Crops Res.* 270, 108214. doi: 10.1016/j.fcr.2021.108214

Hartmann, T. E., Yue, S. C., Schulz, R., He, X., Chen, X. P., Zhang, F. S., et al. (2015). Yield and N use efficiency of a maize–wheat cropping system as affected by different fertilizer management strategies in a farmer's field of the North China Plain. *Field Crops Res.* 174, 30–39. doi: 10.1016/j.fcr.2015.01.006

He, J. N., Shi, Y., Zhao, J. Y., and Yu, Z. W. (2019). Strip rotary tillage with a two-year subsoiling interval enhances root growth and yield in wheat. *Sci. Rep.* 9, 11678. doi: 10.1038/s41598–019-48159–4

He, J. N., Shi, Y., Zhao, J. Y., and Yu, Z. W. (2020). Strip rotary tillage with subsoiling increases winter wheat yield by alleviating leaf senescence and increasing grain filling. *Crop J.* 8, 327–340. doi: 10.1016/j.cj.2019.08.007

He, G., Wang, Z. H., Li, F. C., Dai, J., Li, Q., Xue, C., et al. (2016a). Soil water storage and winter wheat productivity affected by soil surface management and precipitation in dryland of the Loess Plateau, China. *Agric. Water Manage.* 171, 1–9. doi: 10.1016/j.agwat.2016.03.005

He, G., Wang, Z. H., Li, F. C., Dai, J., Li, Q., Xue, C., et al. (2016b). Nitrogen, phosphorus and potassium requirement and their physiological efficiency for winter wheat affected by soil surface managements in dryland. *Sci. Agric. Sin.* 49, 1657–1671. doi: 10.3864/j.issn.0578–1752.2016.09.003

He, G., Wang, Z. H., Li, F. C., Dai, J., and Malhi, S. S. (2016c). Soil nitrate-N residue, loss and accumulation affected by soil surface management and precipitation in a winter wheat-summer fallow system on dryland. *Nutr. Cycling Agroecosyst.* 106, 31–46. doi: 10.1007/s10705-016-9787-9

Hu, Y. J., Ma, P. H., Wu, S. F., Sun, B. H., Feng, H., Pan, X. L., et al. (2020). Spatial-temporal distribution of winter wheat (Triticum aestivum L.) roots and water use efficiency under ridge-furrow dual mulching. *Agric. Water Manage.* 240, 106301. doi: 10.1016/j.agwat.2020.106301

Hu, C. L., Sadras, V. O., Lu, G. Y., Zhang, P. X., Han, Y., Liu, L., et al. (2021). A global meta–analysis of split nitrogen application for improved wheat yield and grain protein content. *Soil Till Res.* 213, 105111. doi: 10.1016/j.still.2021.105111

Huang, M., Wang, Z. H., Luo, L. C., Wang, S., Hui, X. L., He, G., et al. (2017). Soil testing at harvest to enhance productivity and reduce nitrate residues in dryland wheat production. *Field Crops Res.* 212, 153–164. doi: 10.1016/j.fcr.2017.07.011

Huang, M., Wu, J. Z., Li, Y. J., Fu, G. Z., Zhao, K. N., Zhang, Z. W., et al. (2021). Effects of tillage practices and nitrogen fertilizer application rates on grain yield, protein content in winter wheat and soil nitrate residue in dryland. *Sci. Agric. Sin.* 54, 5206–5219. doi: 10.3864/j.issn.0578–1752.2021.24.004

Izumi, Y., Yoshida, T., and Iijima, M. (2009). Effects of subsoiling to the non-tilled field of wheat-Soybean rotation on the root system development, water uptake, and yield. *Plant Prod. Sci.* 12, 327–335. doi: 10.1626/pps.12.327

Jia, M. Y., Huang, L. M., LI, Q. C., Zhao, J. N., Zhang, Y. J., Yang, D., et al. (2022). Effects of tillage methods on physico-chemical and microbial characteristics of farmland soil and nutritional quality of wheat. *J. Plant Resour. Environ.* 28, 1964–1976. doi: 10.11674/zwyf.2022082

Koch, M., Boselli, R., Hasler, M., Zörb, C., Athmann, M., and Kautz, T. (2021). Root and shoot growth of spring wheat (Triticum aestivum L.) are differently affected by increasing subsoil biopore density when grown under different subsoil moisture. *Biol. Fertil.* 57, 1155–1169. doi: 10.1007/s00374-021-01597-7

Lampurlanés, J., Plaza-Bonilla, D., Alvaro-Fuentes, J., and Cantero-Martínez, C. (2016). Long-term analysis of soil water conservation and crop yield under different tillage systems in mediterranean rainfed conditions. *Field Crops Res.* 189, 59–67. doi: 10.1016/j.fcr.2016.02.010

Li, R., Hou, X. Q., Jia, Z. K., Han, Q. F., Ren, X. L., and Yang, B. P. (2013). Effects on soil temperature, moisture, and maize yield of cultivation with ridge and furrow mulching in the rainfed area of the Loess Plateau, China. *Agric. Water Manage.* 116, 101–109. doi: 10.1016/j.agwat.2012.10.001

Li, R., Hou, X. Q., Jia, Z. K., Han, Q. F., and Yang, B. P. (2012). Effects of rainfall harvesting and mulching technologies on soil water, temperature, and maize yield in Loess Plateau region of China. *Soil Res.* 50, 105–113. doi: 10.1071/SR11331

Liang, Y. F., Khan, S., Ren, A. X., Lin, W., Anwar, S., Sun, M., et al. (2019). Subsoiling and sowing time influence soil water content, nitrogen translocation and yield of dryland winter wheat. *Agronomy.* 9 (1), 37. doi: 10.3390/agronomy9010037

Lin, Z. A., Chang, X. H., Wang, D. M., Zhao, G. C., and Zhao, B. Q. (2016). Long–term fertilization effects on processing quality of wheat grain in the North China Plain. *Field Crops Res.* 174, 55–60. doi: 10.1016/j.fcr.2015.01.008

López-Bellido, L., Muñoz-Romero, V., and López-Bellido, R. J. (2013). Nitrate accumulation in the soil profile: Long-term effects of tillage, rotation and N rate in a Mediterranean Vertisol. *Soil Till. Res.* 130, 18–23. doi: 10.1016/j.still.2013.02.002

Lu, J., Bai, Z. H., Velthof, G. L., Wu, Z. G., Chadwick, D., and Ma, L. (2019). Accumulation and leaching of nitrate in soils in wheat–maize production in China. *Agric. Water Manage.* 212, 407–415. doi: 10.1016/j.agwat.2018.08.039

Luo, L. C., Hui, X. L., Wang, Z. H., Zhang, X., Xie, Y. H., Gao, Z. Q., et al. (2019). Multi-site evaluation of plastic film mulch and nitrogen fertilization for wheat grain yield, protein content and its components in semiarid areas of China. *Field Crops Res.* 240, 86–94. doi: 10.1016/j.fcr.2019.06.002

Luo, J., Liang, Z. M., Xi, L. Y., Liao, Y. C., and Liu, Y. (2020). Plastic–covered ridge–furrow planting combined with supplemental irrigation based on measuring soil moisture promotes wheat grain yield and irrigation water use efficiency in irrigated fields on the Loess Plateau, China. *Agronomy.* 10, 1010. doi: 10.3390/agronomy10071010

Luo, L. C., Wang, Z. H., Huang, M., Hui, X. L., Wang, S., Zhao, Y., et al. (2018). Plastic film mulch increased winter wheat grain yield but reduced its protein content in dryland of northwest China. *Field Crops Res.* 218, 69–77. doi: 10.1016/j.fcr.2018.01.005

Lv, G. H., Han, W., Wang, H. B., Bai, W. B., and Song, J. Q. (2019). Effect of subsoiling on tillers, root density and nitrogen use efficiency of winter wheat in loessal soil. *Plant Soil Environ.* 65, 456–462. doi: 10.17221/311/2019-PSE

Qiang, X. M., Sun, J. S., and Ning, H. F. (2022). Impact of subsoiling on cultivated horizon construction and grain yield of winter wheat in the North China Plain. *Agriculture* 12, 2: 236. doi: 10.3390/agriculture12020236

Sang, X. G., Wang, D., and Lin, X. (2016). Effects of tillage practices on water consumption characteristics and grain yield of winter wheat under different soil moisture conditions. *Soil Till Res.* 163, 185–194. doi: 10.1016/j.still.2016.06.003

Shi, Z. J., Liu, D. H., Liu, M., Hafeez, M. B., Wen, P. F., Wang, X. L., et al. (2021). Optimized fertilizer recommendation method for nitrate residue control in a wheat–maize double cropping system in dryland farming. *Field Crops Res.* 271, 108258. doi: 10.1016/j.fcr.2021.108258

Sun, M., Gao, Z. Q., Zhao, W. F., Deng, L. F., Deng, Y., Zhao, H. M., et al. (2013). Effect of subsoiling in fallow period on soil water storage and grain protein accumulation of dryland wheat and its regulatory effect by nitrogen application. *PloS One* 8, e75191. doi: 10.1371/journal.pone.0075191

Sun, M., Ge, X. M., Gao, Z. Q., Ren, A. X., Deng, Y., Zhao, W. F., et al. (2014). Relationship between water storage conservation in fallow period and grains protein formation in dryland wheat in different precipitation years. *Sci. Agric. Sin.* 47, 1692–1704. doi: 10.3864/j.issn.0578–1752.2014.09.004

Sun, M., Ren, A. X., Gao, Z. Q., Wang, P. R., Mo, F., and Xue, L. (2018). Long-term evaluation of tillage methods in fallow season for soil water storage, wheat yield and water use efficiency in semiarid southeast of the Loess Plateau. *Field Crops Res.* 218, 24–32. doi: 10.1016/j.fcr.2017.12.021

Wang, H. G., Guo, Z. J., Shi, Y., Zhang, Y. L., and Yu, Z. W. (2015). Impact of tillage practices on nitrogen accumulation and translocation in wheat and soil nitrate-nitrogen leaching in drylands. *Soil Till Res.* 153, 20–27. doi: 10.1016/j.still.2015.03.006

Wang, Z. H., and Li, S. X. (2019). Nitrate N loss by leaching and surface runoff in agricultural land: a global issue (a review). *Adv. Agron.* 156, 159–217. doi: 10.1016/bs.agron.2019.01.007

Wang, S. L., Wang, H., Hafeez, M. B., Zhang, Q., Yu, Q., Wang, R., et al. (2022). No-tillage and subsoiling increased maize yields and soil water storage under varied rainfall distribution: A 9-year site-specific study in a semi-arid environment. *Field Crops Res.* 255, 107867. doi: 10.1016/j.fcr.2020.107867

Wang, H. G., Yu, Z. W., Shi, Y., and Zhang, Y. L. (2020). Effects of tillage practices on grain yield formation of wheat and the physiological mechanism in rainfed areas. *Soil Till Res.* 202, 104675. doi: 10.1016/j.still.2020.104675

Wang, Q., Zhang, D. K., Zhou, X. J., Liu, J. R., Liu, Q. L., Li, X. L., et al. (2019). Comparing yield, quality, water use efficiency, and value between fodder and grain produced using ridge–furrow rainwater harvesting in a semiarid region. *Crop Sci.* 59, 2214–2226. doi: 10.2135/cropsci2019.03.0180

Wu, J. Z., Huang, M., Li, Y. J., Fu, G. Z., Zhao, K. N., Hou, Y. Q., et al. (2021). Effects of tillage practice and nitrogen rates on grain yield of winter wheat in dryland. *J. Soil Water Conserv.* 35, 264–271. doi: 10.13870/j.cnki.stbcxb.2021.05.036

Wu, J. Z., Wang, H. T., Hou, Y. Q., Tian, W. Z., Li, J. H., Zhang, J., et al. (2023). Optimum tillage pattern with high crop productivity and soil nitrate-N accumulation in rain-fed summer maize and winter wheat double cropping system. *Plant Nutr. Fert. Sci.* 29, 614–627. doi: 10.11674/zwyf.2022472

Xue, J. F., Ren, A. X., Li, H., Gao, Z. Q., and Du, T. Q. (2018). Soil physical properties response to tillage practices during summer fallow of dryland winter wheat field on the loess plateau. *Environ. Sci. Pollut. Res.* 25 (2), 1070–1078. doi: 10.1007/s11356-017-0684-9

Xue, L. Z., Sun, M., Gao, Z. Q., Wang, P. R., Ren, A. X., Lei, M. M., et al. (2017). Effects of incremental seeding rate under sub-soiling during the fallow period on nitrogen absorption and utilization, yield and grain protein content in dryland wheat. *Sci. Agric. Sin.* 50, 2451–2462. doi: 10.3864/j.issn.0578–1752.2017.13.005

Yang, Y. H., Li, M. J., Wu, J. C., Pan, X. Y., Gao, C. M., and Tang, D. W. S. (2022). Impact of combining long-term subsoiling and organic fertilizer on soil microbial biomass carbon and nitrogen, soil enzyme activity, and water use of winter wheat. *Front. Plant Sci.* 12, 788651. doi: 10.3389/fpls.2021.788651

Yang, Z. S., Wu, J. Z., Huang, M., Li, Y. J., Fu, G. Z., Zhao, K. N., et al. (2021). Effects of furrow planting and fertilization optimization on wheat yield, water and fertilizer use efficiency in dryland. *Acta Agric. Boreali–Sin.* 36, 157–166. doi: 10.7668/hbnxb.20192122

You, Y., Song, P., Yang, X., Zheng, Y., Dong, L., and Chen, J. (2022). Optimizing irrigation for winter wheat to maximize yield and maintain high-efficient water use in a semi-arid environment. *Agric. Water Manage.* 273. doi: 10.3389/fpls.2021.788651

Zhang, T. J., Ali, S., Xi, Y. L., Ma, X. C., and Sun, L. F. (2022). Cultivation models and mulching strategies to improve root-bleeding sap, nutrients uptake and wheat production in semi-arid regions. *Agric. Water Manage.* 260, 107302. doi: 10.1016/j.agwat.2021.107302

Zhang, X., Li, X. H., Luo, L. C., Ma, Q. X., Ma, Q., Hui, X. L., et al. (2019). Monitoring wheat nitrogen requirement and top soil nitrate for nitrate residue controlling in drylands. *Clean Prod.* 241, 118372–118372. doi: 10.1016/j.jclepro.2019.118372

Zhang, D., Li, D. X., Wang, H. G., Li, H. R., Li, R. Q., Batchelor, W. D., et al. (2023). Tillage practices offset wheat yield reductions under limited irrigation regime in the North China Plain. *Soil Till Res.* 230, 105687. doi: 10.1016/j.still.2023.105687

Zhang, Y., Liu, D. H., Jia, Z. K., and Zhang, P. (2021). Ridge and furrow rainfall harvesting can significantly reduce N_2O emissions from spring maize fields in semiarid regions of China. *Soil Till Res.* 209, 104971. doi: 10.1016/j.still.2021.104971

Zhang, G. X., Mo, F., Shah, F., Meng, W. H., Liao, Y. C., and Han, J. (2021). Ridge-furrow configuration significantly improves soil water availability, crop water use efficiency, and grain yield in dryland agroecosystems of the Loess Plateau. *Agric. Water Manage.* 245, 106657. doi: 10.1016/j.agwat.2020.106657

Zhang, H. Y., Sun, M., Gao, Z. Q., Liang, Y. F., Yang, Q. S., Zhang, J., et al. (2018). Relationship between soil water variation, wheat yield and grain protein and its components contents under sub-soiling during the fallow period plus mulched-sowing. *Sci. Agric. Sin.* 51, 2860–2871. doi: 10.3864/j.issn.0578–1752.2018.15.003

Zhang, D. Q., Yue, J. Q., Li, X. D., Wang, H. F., Shao, Y. H., Fang, B. T., et al. (2016). Effects of tillage regimes on soil micro-environments and yield of winter wheat in rainfed areas in southern Henan province, China. *Trans. Chin. Soc Agric. Eng.* 32, 32–38. doi: 10.11975/j.issn.1002–6819.2016.z2.005

Zhang, L. J., Zhang, Y. H., Lu, Q. L., Bai, Y. L., Zhou, G., and Wang, H. X. (2017). Effect of tillage model and nitrogen rate on grain quality of dryland winter wheat. *Acta Agric.Nucl. Sin.* 31, 1567–1575. doi: 10.11869/j.issn.100–8551.2017.08.1567

Zhao, K. N., Huang, M., Li, Y. J., Wu, J. Z., Tian, W. Z., Li, J. H., et al. (2023a). Combined organic fertilizer and straw return enhanced summer maize productivity and optimized soil nitrate–N distribution in rainfed summer maize–winter wheat rotation on the Southeast Loess Plateau. *Soil Sci. Plant Nutr.* 23, 938–952. doi: 10.1007/s42729-022-01094-2

Zhao, Y. L., Liu, W. L., Cheng, S., Zhou, Y. N., Zhou, J. L., Wang, X. L., et al. (2018). Effects of pattern of deep tillage on topsoil features, yield and water use efficiency in lime concretion black soil. *Sci. Agr Sin.* 51, 2489–2503. doi: 10.3864/j.issn.0578–1752.2018.13.005

Zhao, K. N., Wang, H. T., Wu, J. Z., Liu, A. K., Huang, X. L., Li, G. Q., et al. (2023b). One–off irrigation improves water and nitrogen use efficiency and productivity of wheat as mediated by nitrogen rate and tillage in drought–prone areas. *Field Crops Res.* 295, 108898. doi: 10.1016/j.fcr.2023.108898

Zhao, H., Zhang, J., Yang, Y., Li, H., Han, H., Ji, A., et al. (2017). Subsoiling combined with film mulch reduces post–anthesis proline accumulation and improves water storage and grain quality in dryland wheat crop. *Agric. Biol.* 19, 1193–1200. doi: 10.17957/IJAB/15.0412

Zheng, C. Y., Yu, Z. W., Wang, D., Zhang, Y. L., and Shi, Y. (2012). Effects of tillage practices on nitrogen accumulation and translocation in winter wheat and NO_3^-N content in soil. *J. Plant Nutr. Fert. Sci.* 18, 1303–1311.

Zhou, M. H., and Buterbach-Bahl, K. (2014). Assessment of nitrate leaching loss on a yield-scaled basis from maize and wheat cropping systems. *Plant Soil.* 374, 977–991. doi: 10.1007/s11104-013-1876-9

frontiers | Frontiers in Plant Science

TYPE Original Research
PUBLISHED 14 June 2024
DOI 10.3389/fpls.2024.1417504

OPEN ACCESS

EDITED BY
Laichao Luo,
Anhui Agricultural University, China

REVIEWED BY
Songjuan Gao,
Nanjing Agricultural University, China
Guopeng Zhou,
Anhui Agricultural University, China
Amit Anil Shahane,
Central Agricultural University, India

*CORRESPONDENCE
Chi-ming Gu
guchiming@foxmail.com
Lu Qin
qinlu-123@126.com

RECEIVED 15 April 2024
ACCEPTED 30 May 2024
PUBLISHED 14 June 2024

CITATION
Gu C-m, Li Y-s, Yang L, Dai J, Hu W, Yu C-b, Brooks M, Liao X and Qin L (2024) Effects of oilseed rape green manure on phosphorus availability of red soil and rice yield in rice–green manure rotation system.
Front. Plant Sci. 15:1417504.
doi: 10.3389/fpls.2024.1417504

Effects of oilseed rape green manure on phosphorus availability of red soil and rice yield in rice–green manure rotation system

Chi-ming Gu[1*], Yin-shui Li[1], Lu Yang[1], Jing Dai[1], Wenshi Hu[1], Chang-bing Yu[1], Margot Brooks[2], Xing Liao[1] and Lu Qin[1*]

[1]Oil Crops Research Institute of the Chinese Academy of Agricultural Sciences, Key Laboratory of Biology and Genetic Improvement of Oil Crops Ministry of Agriculture of China, Wuhan, Hubei, China, [2]Department of Biochemistry and Microbiology, Rhodes University, Grahamstown, South Africa

Improving the nutrient content of red soils in southern China is a priority for efficient rice production there. To assess the effectiveness of oilseed rape as green manure for the improvement of soil phosphorus nutrient supply and rice yield in red soil areas, a long-term field plot experiment was conducted comparing two species of rape, *Brassica napus* (BN) and *Brassica juncea* (BJ). The effects of returning oilseed rape on soil phosphorus availability, phosphorus absorption, and yield of subsequent rice under rice–green manure rotation mode were analyzed, using data from the seasons of 2020 to 2021. The study found that compared with winter fallow treatment (WT) and no-tillage treatment (NT), the soil available phosphorus content of BN was increased, and that of BJ was significantly increased. The content of water-soluble inorganic phosphorus of BJ increased, and that of BN increased substantially. Compared with the WT, the soil organic matter content and soil total phosphorus content of BN significantly increased, as did the soil available potassium content of BJ, and the soil total phosphorus content of BJ was significantly increased compared with NT. The soil particulate phosphorus content of BJ and BN was significantly increased by 14.00% and 16.00%, respectively. Compared with the WT, the phosphorus activation coefficient of BJ was significantly increased by 11.41%. The rice plant tiller number under the green manure returning treatment was significantly increased by 43.16% compared with the winter fallow treatment. The green manure returning measures increased rice grain yield by promoting rice tiller numbers; BN increased rice grain yield by 9.91% and BJ by 11.68%. Based on these results, returning oilseed rape green manure could augment the phosphorus nutrients of red soil and promote phosphorus availability. Rice–oilseed rape green manure rotation could increase rice grain yield.

KEYWORDS

oilseed rape green manure, phosphorus availability, soil phosphorus components, organic farming, rice production

1 Introduction

Insufficient organic fertilizer, the lack of biological fertilization measures, and single planting systems as well as improper use of chemical fertilizer will lead to the decrease of soil organic matter content and deterioration of soil physical and chemical properties and soil structure. The consequence in the arable layer of farmland is the reduction in soil sustainable production capacity (Li et al., 2021). A lack of bioavailable phosphorus in soil restricts rice yield and has become a hot point for rice production research in red soil areas (Xie et al., 2022; Gu et al., 2023). As a high-quality organic fertilizer, green manure can not only effectively enable the utilization of fallow fields but also significantly decrease the soil degradation caused by the long-term application of chemical fertilizers and monocropping (Asghar and Kataoka, 2022). The pressure from demand for staple foods due to increasing population means the area used for summer crops is constantly expanding, especially in rice-growing regions, leaving insufficient time for normal winter crop production. At the same time, great importance is attributed, globally, to the protection of cultivated land and the improvement of arable land quality. Thus, the planting of green manure in winter to fertilize the soil and improve the quality and efficiency of subsequent crops has become a common choice and has attracted more and more attention (Lyu et al., 2024; Ren et al., 2024). Studies have shown that the application of green manure in different rotations has a significant effect on soil physical and chemical properties and the yield of subsequent crops (Gu et al., 2021; Lyu et al., 2024; Ren et al., 2024). Green manure is a general term for the use of plants grown specifically to be plowed back into the soil as fertilizer for subsequent crops. Green manure is a high-quality, clean organic fertilizer that is a renewable biological resource. It has a significant effect on improving and fertilizing soil and can lay a foundation for the high yield and high quality of crops (Xie et al., 2016). Planting green manure can reduce weeds in the field and reduce soil nutrient loss (Yu et al., 2014). Root exudates of green manure crops can enhance soil microbial and soil biochemical activity, dissolve and utilize insoluble phosphorus in the soil, and increase soil available phosphorus levels (Gu et al., 2023; Yuan et al., 2023).

Existing research has shown that oilseed rape as green manure could increase soil organic matter and soil bioavailable phosphorus nutrient content and improve soil fertility. Compared with common leguminous green manure, oilseed rape green manure has the characteristics of wide adaptability and low cost and functions as a biological control (Fu et al., 2012; Srivastava and Ghatak, 2017). In addition, it can increase the total porosity of paddy soil, reduce bulk density, improve soil physical properties, and increase the activity of soil urease and acid phosphatase (Tang et al., 2017). The results of intercropping potato with spring rape as green manure showed that the application of green manure could reduce the application rate of potato fertilizer by 15%–20% without reducing the yield (Jing et al., 2007). After oilseed rape was returned to the field as green manure in another rice–rape rotation study, the leaf area index, flag leaf length, leaf width, chlorophyll content, and photosynthetic rate of subsequent rice plants were increased to a certain extent, and the dry matter accumulation of rice was increased, thereby increasing the subsequent rice yield (Xie et al., 2016). In addition, the surface coverage of green manure crops planted in winter will affect the soil moisture conditions of the farmland and change the activity of soil microorganisms and permeability and redox potential of the soil, affecting the cycle of phosphorus in the soil, thereby affecting the absorption and utilization of phosphorus by subsequent crops (LeBlanc, 2022).

However, the current research on rice–oilseed rape rotation is mainly grain-oriented. There are relatively few studies that focus on the effect of oilseed rape green manure returning on soil phosphorus availability and then on rice phosphorus absorption, which are known to restrict the development of green organic sustainable agriculture in red soil, and thus affect rice yield. To analyze and compare the differences in the effect of the application of different species of oilseed rape green manure on soil phosphorus availability, rice phosphorus uptake, and rice yield after returning in rice production, a positioning field experiment was carried out in Zhanggong Town, Jinxian County, Jiangxi Province. The objective of this study is to demonstrate the effects of oilseed rape green manure amendment on the bioactivity of phosphorus and rice yield in the red soil area, providing practical bases for both the improvement of paddy soil quality and green production of rice by the application of oilseed rape green manure (Figure 1).

2 Materials and methods

2.1 Experimental site

This study was initiated in September 2017 at the field experimental base of the Chinese Academy of Agricultural Science in Hongrang Village, Zhanggong Town, Jinxian City, Jiangxi Province, China. The base is at 28°21′10″N, 116°11′6″E and has an altitude of 26.7 m. It has a typical humid subtropical monsoon climate, with abundant water and heat resources. The rainfall is mainly concentrated from April to August. The annual average rainfall is 1,858 mm, the annual average evaporation is 1,150 mm, the annual average temperature is 17.92°C, the annual effective radiation is 660.42 MJ m^{-2}, and the frost-free period is 262 days. The soil texture is sandy loam with the following chemical characteristics: soil total organic matter (SOM) was 17.42 g kg^{-1}, pH (H_2O:soil = 5:1) was 5.34, alkali-hydrolyzable nitrogen (AN) was 98.98 mg kg^{-1}, available phosphorus (AP) was 6.50 mg kg^{-1}, and available potassium (AK) was 55.53 mg kg^{-1}. Rice is one of the primary crops in the region, with Jiangxi Province being one of the main red soil areas of China. Data in this manuscript were collected from October 2020 to September 2021.

2.2 Experimental design and field management

The experimental design was based on the random block design. The planting mode was rice (*Oryza sativa* L., variety name: Shenliangyou 5814)–green manure rotation, with four treatments: brassica rape (*Brassica napus* L., BN) (variety name: Zhongyoufei No. 1), mustard rape (*Brassica juncea*, BJ) (variety name: Zhongjieyou No. 1), winter fallow (WT), and no tillage (NT), with three replicates each, spanning a total of 12 plots. All the green

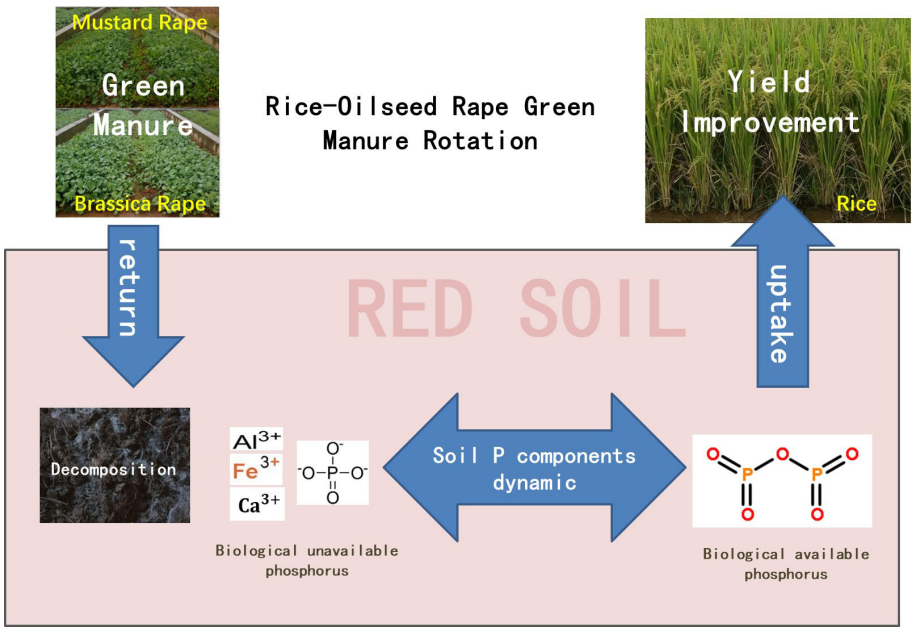

FIGURE 1
Rice–oilseed rape green manure rotation modes.

manure was sown in the second week of October of each year. The aboveground biomass was cut to 10–20 cm at the stage of flowering in the middle of March and returned into the 15–30-cm soil layer by grubbing and using a rotary tiller machine. Rice was sown 25 days before green manure return at a seedling bed in another field. Ten days after green manure incorporation, the field was plowed, irrigated, and soaked to prepare for rice transplanting. Then, rice seedlings were transplanted into each plot with a density of 30,000 plants per hectare and harvested in the middle of September. The chemical fertilizer used in the experiment comprised urea (46% N), superphosphate (12% P_2O_5), and potassium oxide (60% K_2O). An equal amount of fertilizer was applied as base fertilizer in all plots in the green manure season (N:P_2O_5:K_2O was 15:0:0 kg ha^{-1}). In the rice season, the application rate of N, P_2O_5, and K_2O fertilizer in all plots was 195, 90, and 135 kg ha^{-1}, respectively. The full standard quantities of phosphorus and potassium fertilizers of the rice season were used as base fertilizer, while 50% of standard nitrogen fertilizer was used as base fertilizer, with 20% applied as topdressing in the tillering stage and 30% applied as topdressing in the earing stage. In the green manure season, irrigation was done after sowing and artificial weed control was performed during the seedling stage. In the rice season, herbicides were sprayed after plowing, and irrigation and drainage were carried out at the tillering and ear-filling stages of rice, respectively. During the growth periods of green manure and rice, pest prevention and control measures were carried out as necessary.

2.3 Sampling and analysis

Before green manure returning, three representative areas of 0.5 m^2 were chosen in each plot and cut level with the ground in order to weigh the yield of green manure and sample for nutrient testing at the same time. At the rice tillering stage, three representative 0.5 m^2 quadrats were selected to investigate the tillering of rice. Rice plant samples were taken during the harvest stage for yield calculation and nutrient testing. All plant samples were separated into leaf, seed, or root, after which they were air-dried, ground, sieved, and then digested with H_2SO_4-H_2O_2 for nutrient testing. For plant nutrient testing, the total nitrogen (TN) concentration of the samples was determined by the Kjeldahl method, and total phosphorus (TP) and total potassium (TK) were tested by ICP (Germany) after extraction by heating digestion with H_2SO_4-H_2O_2 (Bao, 2000).

Mixed soil samples were collected right before the fertilizer application when rice was transplanted. They were taken from the soil surface layer (0–20 cm) from 5 points in each plot using a soil borer. After removing animal and plant residues and pebbles, the soil samples were air-dried and put through a 100- or 200-mesh sieve for further analysis. SOM was measured by the $K_2Cr_2O_7$ oxidation method, available N (AN) was measured by the alkaline diffusion method, available phosphorus (AP) concentration of the samples was determined by the Olsen method after extraction with 0.03 mol L^{-1} of NH_4F and 0.025 mol L^{-1} of HCl, available K (AK) was measured by flame photometry after extraction with 1 mol L^{-1} of NH_4OAc, and pH (1:10, soil to water rate) was determined with a pH meter (Bao, 2000). For soil total phosphorus (STP), dry soil (2 g) was heated with 0.2 g of sodium hydroxide at 720°C for 20 min. After cooling, the soil was washed with distilled water. Then, 10 mL of 4.5 M H_2SO_4 was added to the combined liquids and made up to 100 mL by adding distilled water. The extract was used for spectrophotometric analysis (Bao, 2000). Total water-soluble phosphorus (TWSP) was determined by placing 2 g of dry soil sample into 20 mL of distilled water, oscillating under 250 r min^{-1} for 1 h, filtering through a 0.45-μm filter, and digesting the filtrate with potassium

persulfate. The extract was used for spectrophotometric analysis. Soil total phosphorus (STP) minus total water-soluble phosphorus (TWSP) equaled to particulate phosphorus (PP). Water-soluble inorganic phosphorus (WSIP) was determined by placing 2 g of dry soil sample into 20 mL of distilled water, oscillating under 250 r min^{-1} for 1 h, filtering through a 0.45-μm filter, and then using the extract for spectrophotometric analysis (Zhu, 2011). TWSP minus WSIP equaled to water-soluble organic phosphorus (WSOP). Nutrient accumulation of plants (NA) was calculated using the following equation:

$$NA = W_L \times N_L + W_S \times N_S + W_R \times N_R$$

where W_L is the weight of the leaf, W_S is the weight of the seed, W_R is the weight of the roots, N_L is the nutrient content of the leaf, N_S is the nutrient content of the seed, N_R is the phosphorus content of the roots, and NA is the nutrient accumulation.

Total phosphorus and available phosphorus are two important indicators to measure the state of soil phosphorus. The ratio of available phosphorus to total phosphorus is expressed as the soil phosphorus activation coefficient (PAC), which can be used as a relative indicator to characterize the effectiveness of soil phosphorus. PAC was calculated using the following equation:

$$PAC = C_{AP}/C_{TP} \times 100\,\%$$

where C_{AP} is the content of soil available phosphorus, C_{TP} is the content of soil total phosphorus, and PAC is the activation coefficient of soil phosphorus.

2.4 Statistical analysis

All data collected were statistically analyzed as a completely randomized design using ANOVA to test the differences in grain yield, soil nutrient contents, yield, and yield components among treatments. Analysis of variance (ANOVA) was carried out to determine the differences between the measured parameters for different treatments. The least significant difference (LSD) at p = 0.05 was used to elucidate any significant differences. All analyses were conducted using SPSS statistical software (ver. 11.0, SPSS, Chicago, IL, USA).

3 Results

3.1 Differences between yield of oilseed rape green manure species

The difference in yield of different oilseed rape green manure species is shown in Figure 2. Comparing the yield of two types of green manure rape, it was found that the yield of BN green manure rape was higher than that of BJ. The average fresh plant yields of BJ and BN in the two species were 56.36 and 60.35 t ha^{-1}, respectively.

The accumulation of nitrogen, phosphorus, and potassium nutrients in different oilseed rape green manure is shown in Table 1. It was found that the amount of nitrogen and phosphorus accumulation of BN was significantly higher than that in BJ, with an average increase of 43.52% and 23.86%, respectively. There was no significant difference in the cumulative amount of potassium between the two species.

3.2 Effects of different treatments on soil physical and chemical properties

The results showed that compared with WT, the oilseed rape green manure returning treatment had a greater impact on soil organic matter and available potassium content (Table 2). The effect of oilseed rape green manure returning on soil organic matter and available potassium content reached a significant level. Compared with the WT, the oilseed rape green manure returning treatments showed a trend of increased contents of soil organic matter and available potassium, and the soil organic matter in BN was significantly increased by 17.16%. The soil available potassium content of BJ was significantly increased by 7.28%.

3.3 Effects of different treatments on phosphorus content in red soil

Compared with WT and NT, the soil total phosphorus content of BN was significantly increased by 5.26% and 17.65%, respectively, while the soil total phosphorus content of BJ was significantly increased by 13.73% compared with NT, but the differences did not reach a significant level compared with WT (Table 3). The content of soil particulate phosphorus in BJ and BN was significantly increased by 14.00% and 16.00% compared with the NT, respectively, but the difference between the two and the WT was not significant. Compared with WT and NT, the soil available phosphorus content of BJ and BN showed an increasing trend. The soil available phosphorus content of BJ was significantly higher than that of WT and NT by 11.12% and 13.01%, respectively, while in BN, it increased by 7.56% and 9.39%, respectively, without

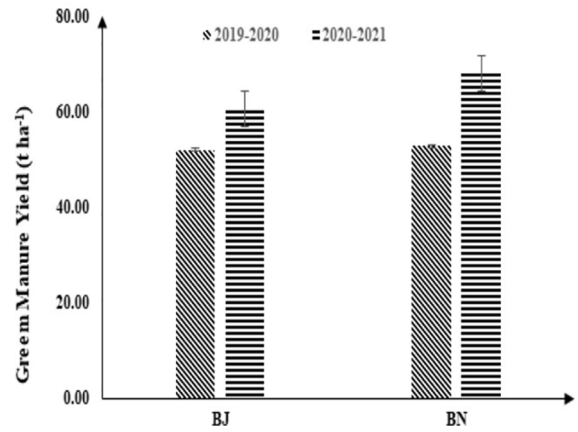

FIGURE 2
Comparison of oilseed rape green manure yield over two growth seasons. BJ represents mustard oilseed rape green manure, and BN represents brassica oilseed rape green manure.

10.3389/fpls.2024.1417504

TABLE 1 Differences in nutrient accumulation of green manure in different rotation modes (kg ha^{-1}).

	Treatments	Nitrogen returning	Phosphorus returning	Potassium returning
2019–2020	BJ	93.28 ± 4.05b	16.03 ± 0.33b	160.08 ± 25.85a
	BN	127.04 ± 9.53a	21.83 ± 0.91a	180.33 ± 70.35a
2020–2021	BJ	108.72 ± 4.72b	20.14 ± 0.87b	201.14 ± 32.47a
	BN	163.99 ± 0.53a	25.29 ± 1.62a	232.77 ± 90.81a

BJ represents *Brassica juncea* oilseed rape green manure, and BN represents *Brassica napus* oilseed rape green manure. Different lowercase letters represent significant differences between different green manure treatments.

significant differences. Compared with WT and NT, the content of water-soluble inorganic phosphorus in the soil of BN significantly increased by 96.97% and 94.03%, respectively, while in BN, it increased by 13.64% and 11.94%, respectively, without significant differences. There was no significant difference between the contents of soil water-soluble total phosphorus and soil water-soluble organic phosphorus in all treatments.

In this study, the phosphorus activation coefficients of experimental soil under different treatments were distributed between 1.49% and 1.77% (Figure 3). Compared with the WT, the phosphorus activation coefficient of BJ was significantly increased by 11.41%. Both BJ and BN showed no significant differences compared with NT.

3.4 Effects of different treatments on the growth and yield of subsequent crops

The results showed that compared with the WT, planting and returning oilseed rape green manure in winter could increase the tillering of rice to varying degrees (Table 4). The results of the two years showed that the tiller number of rice of BJ increased by 14.06% and 26.48%, respectively. The tiller number of rice in BN was increased by 4.29% and 21.62%, respectively, and the increase in BJ reached a significant level in 2020. The oilseed rape green manure returning to the field tended to increase the ear length of rice, but the difference compared with no return was not significant, and the effect on the grain number per panicle was not obvious in the two years reported here.

The effects of different treatments on rice yield are shown in Table 4. The results showed that the measures of oilseed rape green manure returning to the field had a significant effect on rice grain yield. Compared with the WT treatment, the grain yield of rice in BJ was significantly increased by 5.51% and 17.84% in the respective two years, and the grain yield of rice in BN was significantly increased by 6.10% in 2020 and 13.71% in 2021 without a significant difference. Compared with WT, the biomass of rice (straw) in BJ and BN showed an increasing trend by 8.53% and 8.10% on average higher than that in the WT, respectively, but the difference was not significant.

The effects of different treatments on phosphorus accumulation in rice plants are shown in Figure 4. The results showed that the phosphorus accumulation in rice grain after the green manure returning treatments was higher than that of WT. The phosphorus accumulation in rice grain of BN was significantly higher than that of WT for both 2020 and 2021 by 11.21% and 14.82%, respectively. The phosphorus accumulation of rice grain treated with BJ increased by 6.56% and 11.98%, respectively, but only reached a significant level in 2021.

TABLE 2 Effects of oilseed rape green manure return on soil basic properties.

Treatments	pH	SOM g kg^{-1}	AN mg kg^{-1}	AK mg kg^{-1}
BJ	5.70 ± 0.21a	20.59 ± 2.19ab	102.76 ± 10.53a	56.89 ± 5.52a
BN	5.66 ± 0.08a	21.78 ± 0.74a	109.92 ± 25.63a	55.07 ± 2.01ab
WT	5.76 ± 0.24a	18.59 ± 1.30b	108.72 ± 16.03a	53.03 ± 3.18b
NT	5.95 ± 0.27a	22.00 ± 3.04a	120.65 ± 13.13a	78.90 ± 10.30b

SOM is soil organic matter, AN is available nitrogen, AK is available potassium, BJ represents *Brassica juncea* oilseed rape green manure, BN represents *Brassica napus* oilseed rape green manure, WT represents winter fallow, and NT represents no tillage. Different lowercase letters represent significant differences between different treatments.

TABLE 3 Effects of oilseed rape green manure return on components of soil P.

Treatments	STP g kg^{-1}	TWSP mg kg^{-1}	PP g kg^{-1}	WSIP mg kg^{-1}	WSOP mg kg^{-1}	AP mg kg^{-1}
BJ	0.58 ± 0.03ab	4.30 ± 1.97a	0.57 ± 0.03a	0.15 ± 0.03ab	4.22 ± 1.91a	9.99 ± 0.42a
BN	0.60 ± 0.02a	4.12 ± 0.64a	0.58 ± 0.03a	0.26 ± 0.11a	3.99 ± 0.84a	9.67 ± 0.66ab
WT	0.57 ± 0.03b	5.62 ± 2.22a	0.56 ± 0.03a	0.13 ± 0.03b	5.48 ± 1.61a	8.99 ± 0.79b
NT	0.51 ± 0.03c	4.32 ± 2.99a	0.50 ± 0.01b	0.13 ± 0.07b	4.22 ± 0.82a	8.84 ± 3.20b

STP is soil total phosphorus, TWSP is total water-soluble phosphorus, PP is particulate phosphorus, WSIP is water-soluble inorganic phosphorus, WSOP is water-soluble organic phosphorus, AP is available phosphorus, BJ represents *Brassica juncea* oilseed rape green manure, BN represents *Brassica napus* oilseed rape green manure, WT represents winter fallow, and NT represents no tillage. Different lowercase letters represent significant differences between different treatments.

10.3389/fpls.2024.1417504

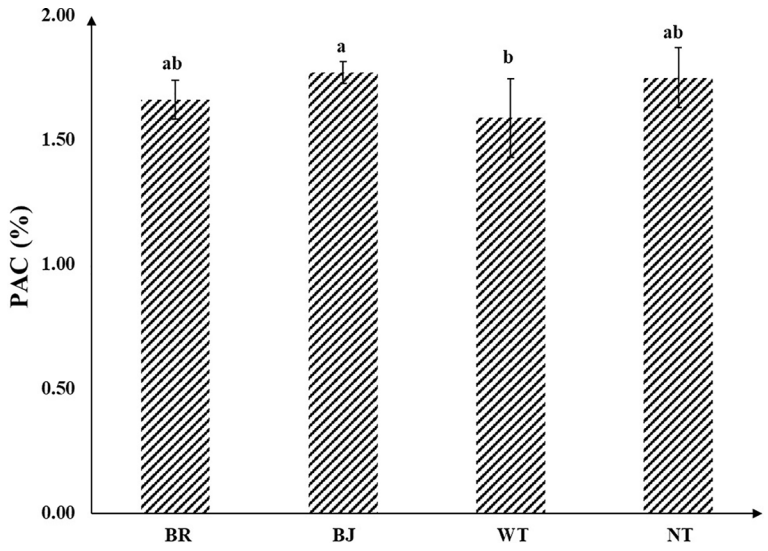

FIGURE 3
Effects of different treatments on soil PAC. PAC represents the activation coefficient of soil phosphorus, BJ represents mustard oilseed rape green manure, BN represents brassica oilseed rape green manure, WT represents winter fallow, and NT represents no tillage. Different lowercase letters represent significant differences between different treatments.

4 Discussion

4.1 Effects of different oilseed rape green manure returning on soil nutrients

After the oilseed rape green manure is returned to the field, the flowers and leaves decompose first, followed by the stems, with the roots last to decompose. This process effectively provides a continuous source of nutrients for the subsequent crops (Talgre et al., 2014; Gu et al., 2019). The decomposition rate of oilseed rape green manure was faster than leguminous green manure, with the decomposition rate of dry matter exceeding 80% 43 days after plowing (Gu et al., 2019). This could significantly increase the organic matter content of the topsoil, especially the increase of organic matter in the 0–20-cm soil layer, which could reach 161.5%–167.7% (Poeplau and Don, 2015). Therefore, the dry matter of the oilseed rape green manure plant itself can significantly increase the soil organic matter and nutrient content after decomposition (Fu et al., 2012). Zhou et al. (2023) found that the organic matter content of rice–rice–rape soil significantly increased by 7.3%–11.6% after 3 years of duplicated cultivation. In this experiment, both types of oilseed rape species in the rice–rape green manure rotation mode had a trend of increasing soil organic matter, and the BN significantly increased the soil organic matter content by 17.16%. This shows that different species of rape green manure returned to the field have different effects on soil organic matter. In the paddy field, the effect of BN on soil organic matter was more obvious than BJ. The higher biomass of BN was the main reason for this (Figure 2).

Studies have shown that planting oilseed rape can reduce the conversion of soil available phosphorus into O–P and make Ca–P in acidic soil more bioavailable and improve the effectiveness of soil phosphorus (Gu et al., 2023; Yuan et al., 2023). During the growth of oilseed rape green manure, root exudates can activate insoluble nutrients in the soil and increase the concentration of available nutrients in the soil, including phosphorus (Vives-Peris et al., 2020; Chen et al., 2023). In this study, the soil available phosphorus content of the two oilseed rape green manure treatments was higher than that of the WT, and the BJ was significantly higher than the WT by 11.12%.

TABLE 4 Effects of oilseed rape green manure return on the growth of subsequent crop.

Treatments		Tiller number	Ear length cm	Grain number per spike	Yield kg ha^{-1}	Biomass kg ha^{-1}
2020	BJ	16.22 ± 1.86a	27.31 ± 0.98a	232 ± 22.70a	8,153 ± 1,085a	14,055 ± 1,092a
	BN	14.83 ± 2.55ab	27.22 ± 2.26a	226 ± 35.40a	8,198 ± 376a	14,233 ± 985a
	WT	14.22 ± 2.05b	26.26 ± 1.99a	247 ± 10.89a	7,727 ± 13b	13,936 ± 505a
2021	BJ	14.33 ± 2.06a	27.10 ± 1.09a	239 ± 24.93a	7,161 ± 40a	13,614 ± 439a
	BN	13.78 ± 2.64a	27.03 ± 2.05a	227 ± 38.93a	6,910 ± 13ab	13,364 ± 13a
	WT	11.33 ± 3.43a	26.13 ± 1.83a	248 ± 5.74a	6,077 ± 1,063b	11,716 ± 2,259a

BJ represents *Brassica juncea* oilseed rape green manure, BN represents *Brassica napus* oilseed rape green manure, and WT represents winter fallow. Different lowercase letters represent significant differences between different treatments.

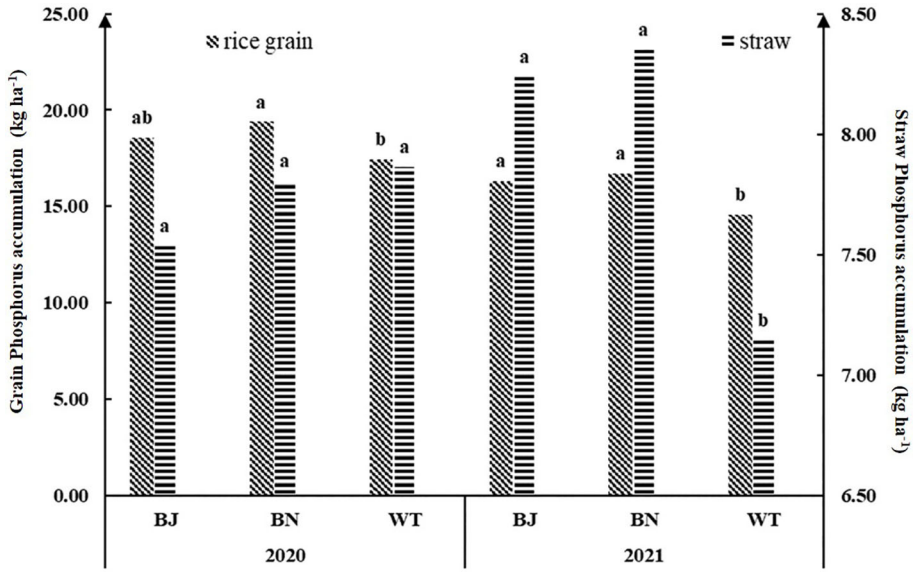

FIGURE 4
Effects of different treatments on the phosphorus accumulation of rice. BJ represents mustard oilseed rape green manure, BN represents brassica oilseed rape green manure, WT represents winter fallow, and NT represents no tillage. Different lowercase letters represent significant differences between different treatments.

In addition, the returning of green manure of different oilseed rape species in this study also had a significant effect on available potassium in the red soil of the experimental site. The content of available potassium in the soil of BJ increased significantly by 7.28%, indicating that the oilseed rape green manure returning measures had a significant positive effect on the soil nutrient availability in the paddy field of the experimental site. Differences may be related to the differences between treatments in the green manure species, green manure decomposition process, and products of organic materials carried into the soil (Fu et al., 2012; Gu et al., 2019) during the growth of the oilseed rape green manures. The red soil of the experimental site contains a large amount of clay minerals, and both the growth and decomposition processes of oilseed rape green manure will promote the release of nutrients from clay minerals. More than 18.09 kg ha^{-1} of phosphorus on average and 170 kg ha^{-1} of potassium on average were accumulated during the oilseed rape green manure growth period (Table 1), and the decomposition rate can exceed 80% in a short time after returning to the field (Fu et al., 2012). Therefore, chemical fertilizers can be appropriately reduced after oilseed rape green manure returning to the field. At present, most of the related research regarding the substitution of chemical fertilizers by green manure has focused on the potential of Chinese milk vetch (Xie et al., 2022). There are few quantitative studies on the potential for reduction of chemical fertilizer application in rice production using oilseed rape green manure returned to the field, which is cheaper and better adapted to the requirements for rotation, justifying amplification in the future.

In addition, planting and returning oilseed rape green manure to the field will also have an effect on soil pH (Pimentel et al., 2023), which will lead directly to changes in bioavailability of soil phosphorus and other nutrients. The study of Li et al. (2012) showed that the application of tropical leguminous green manure affected the pH value of red soil, especially the green manure crops with high ash alkali content, which had a more obvious effect, increasing the pH value. However, no significant difference in soil pH value was observed in the oilseed rape green manure returning treatments in this study. This may be due to the low pH background value of red soil (5.34) in this study and the test time not being long enough, such that the effect of green manure on soil pH value was not significant.

4.2 Effects of different oilseed rape green manure returning on rice growth and yield

At present, there are few studies that focus on the effects of oilseed rape as green manure returned to the field on rice growth and yield in rice–oilseed rape rotation. Oilseed rape is a high-quality green manure with high fertilizer value for rice production due to its large biomass, easy decomposition, and low planting cost (Fu et al., 2012). Returning of oilseed rape green manure to the field has been found to have a significant effect on the production of rice. Researchers found that applying green manure in rice production mainly manifested in significantly increasing leaf area index, flag leaf length and leaf width, chlorophyll content, photosynthetic rate, dry matter accumulation, and effective tiller number (Zhou et al., 2023). The results of this study showed that planting and returning oilseed rape green manure in winter produced a trend of increasing the rice tiller numbers compared with WT. The rice tiller numbers of BJ were significantly increased by 43.16%, one of the main reasons for the significant effect of BJ on rice grain yield in this study.

Earlier studies found that the yield and quality of rice were higher when rice was rotated with oilseed rape rather than other crops, due to an increase in effective panicle number, grain number per panicle, and nitrogen accumulation (Meng et al., 2019; Zhang et al., 2020). The rice–oilseed rape green manure rotation not only

produces high-quality green manure for rice season application but also activates the O–P in the red soil that cannot be directly absorbed and utilized by rice during the oilseed rape growth period. The oilseed rape green manure returning can regulate soil bulk density and soil texture and make the ratio of carbon to nitrogen in the soil conducive to the absorption of soil nutrients by rice (Yu et al., 2014). Confirming the results of earlier studies, this study found that compared with the WT, the oilseed rape green manure treatment showed a trend of increasing the yield of rice. In addition to increasing the effective panicle number and grain number per panicle, the incorporation of oilseed rape green manure can increase the photosynthetic rate and dry matter accumulation of rice, thereby increasing the yield of rice (Zhou et al., 2023; Wang et al., 2012). Green manure returning can effectively delay the senescence of rice leaves by promoting the activity of soil microorganisms, activating the enzyme activities related to nutrient absorption and utilization, and increasing the protease activity in the soil, thus promoting absorption and accumulation by rice plants (Tang et al., 2017). The results of this study showed that the return of oilseed rape green manure to the field had a significant effect on rice yield, and the grain yield of BJ and BN was significantly increased by 5.51% and 6.09%, respectively. Another recent study showed that the yield of early rice increased by 3.5% and that of late rice increased by 2.3% when oilseed rape was used as green manure in red soil paddy fields in rice–rice–rape rotation in southern China (Zhou et al., 2023), which was consistent with the experimental results of this study.

5 Conclusion

Rice–oilseed rape green manure rotation enhanced the phosphorus nutrients of red soil and promoted phosphorus availability. BN increased total phosphorus and water-soluble inorganic phosphorus content, while BJ increased water-soluble inorganic phosphorus content. The phosphorus activation coefficient of BJ increased, and the phosphorus accumulation of subsequent rice increased both in BN and BJ.

Rice–oilseed rape green manure rotation facilitated an increase in rice grain yield, likely due in part to the increase in phosphorus availability, as quantitatively elucidated in this study. These results present an excellent basis for the use of oilseed rape green manure rotation in substitution for harmful chemical fertilizers for productive rice cultivation in red soil areas.

Data availability statement

The original contributions presented in the study are included in the article/supplementary material. Further inquiries can be directed to the corresponding authors.

Author contributions

C-MG: Conceptualization, Data curation, Formal Analysis, Funding acquisition, Investigation, Methodology, Project administration, Resources, Software, Writing – original draft, Supervision, Validation, Visualization, Writing – review & editing. Y-SL: Formal Analysis, Investigation, Writing – review & editing. LY: Formal Analysis, Data curation, Software, Writing – review & editing. JD: Validation, Visualization, Writing – review & editing. WH: Validation, Visualization, Writing – review & editing. C-BY: Conceptualization, Methodology, Writing – review & editing. MB: Resources, Supervision, Writing – review & editing. XL: Conceptualization, Writing – review & editing. LQ: Conceptualization, Project administration, Resources, Supervision, Writing – review & editing.

Funding

The author(s) declare that financial support was received for the research, authorship, and/or publication of this article. This research was funded by the Natural Science Fund Projects of Hubei Province (2021CFB221), China Agriculture Research System of MOF and MARA (CARS-22), and the Agricultural Science and Technology Innovation Program (CAAS-ASTIP-2013-OCRI).

Acknowledgments

We are grateful to all the authors for their support and contribution to the manuscript and to the reviewers for additional refinements.

Conflict of interest

The authors declare that the research was conducted in the absence of any commercial or financial relationships that could be construed as a potential conflict of interest.

Publisher's note

References

Asghar, W., and Kataoka, R. (2022). Green manure incorporation accelerates enzyme activity, plant growth, and changes in the fungal community of soil. *Arch. Microbiol.* 204, 7. doi: 10.1007/s00203–021-02614-x

Bao, S. D. (2000). *Analysis of Soil Agronomy. 3rd ed* (Beijing, China: China Agricultural Press), 34–231.

Chen, S., Yang, D., Wei, Y., He, L., Li, Z., and Yang, S. (2023). Changes in soil phosphorus availability and microbial community structures in rhizospheres of oilseed rapes induced by intercropping with white lupins. *Microorganisms* 11, 326. doi: 10.3390/microorganisms11020326

Fu, T. D., Liang, H. D., and Zhou, G. S. (2012). Advantages and development suggestions of rape green fertilizer in modern agriculture. *China Agric. Tech. Ext.* 28, 37–39. doi: 10.3969/j.issn.1002–381X.2012.08.020

Gu, C., Huang, W., Li, Y., Li, Y., Yu, C., Dai, J., et al. (2021). Green manure amendment can reduce nitrogen fertilizer application rates for oilseed rape in maize–oilseed rape rotation. *plants-Basel* 10, 2640. doi: 10.3390/plants10122640

Gu, C., Li, Y., Xie, L., Hu, X., Liao, X., and Qin, L. (2019). Analysis on application advantages of rapeseed as green manure. *Soil Fertil. Sci. China* 01, 180–183. doi: 10.11838/sfsc.1673–6257.18041

Gu, C., Lv, W., Liao, X., Brooks, M., Li, Y., Yu, C., et al. (2023). Green manure amendment increases soil phosphorus bioavailability and peanut absorption of phosphorus in red soil of south China. *Agronomy-Basel* 13, 2, 376. doi: 10.3390/agronomy13020376

Jing, T. L. (2007). Spring rape green manure turn pressure interplanting potatoes. *China Veg.* 10, 52–53. doi: 10.3969/j.issn.1000-6346.2007.10.023

LeBlanc, N. (2022). Green manures alter taxonomic and functional characteristics of soil bacterial communities. *Microb. Ecol.* 85, 684–697. doi: 10.1007/s00248–022-01975–0

Li, P., Li, Y. B., Xu, L. Y., Zhang, H. J., Shen, X. S., Xu, H. F., et al. (2021). Crop yield soil quality balance in double cropping in China's upland by organic amendments: A meta-analysis. *Geoderma* 403, 115197. doi: 10.1016/j.geoderma.2021.115197

Li, Y., Liu, G. D., Zhang, R. L., Huan, H. F., and Gao, L. (2012). Dynamic effect on Latosol pH value after leguminous green manure application and relevant mechanism. *Soils* 44, 101–106. doi: 10.13758/j.cnki.tr.2012.01.014

Lyu, H., Li, Y., Wang, Y., Wang, P., Shang, Y., Yang, X., et al. (2024). Drive soil nitrogen transformation and improve crop nitrogen absorption and utilization - a review of green manure applications. *Front. Plant Sci.* 14. doi: 10.3389/fpls.2023.1305600

Meng, Y., Jin, W., Dong, Z., Wen, Y., Liang, F., Ding, F., et al. (2019). Comparison of resource utilization efficiency and economic benefit of different paddyupland rotation systems in Jianghuai region. *Chin. J. Ecol.* 38, 3357–3365. doi: 10.13292/j.1000–4890.201911.029

Pimentel, M. L., Reis, I. M. S., Romano, M. L. P. C., Castro, J. S., de Vildoso, C. I. A., Gasparin, E., et al. (2023). Green manure, a sustainable strategy to improve soil quality: a case study in an oxisol from northern Brazil. *Aust. J. Crop Sci.* 17, 488–497. doi: 10.21475/ajcs.23.17.06.p3832

Poeplau, C., and Don, A. (2015). Carbon sequestration in agricultural soils via cultivation of cover crops – a meta-analysis. *Agric. Ecosyst. Environ.* 200, 33–41. doi: 10.1016/j.agee.2014.10.024

Ren, H., Lv, H., Xu, Q., Yao, Z., Yao, P., Zhao, N., et al. (2024). Green manure provides growth benefits for soil mesofauna by promoting soil fertility in agroecosystems. *Soil Till. Res.* 238, 106006. doi: 10.1016/j.still.2024.106006

Srivastava, J. N., and Ghatak, A. (2017). Biofumigation: A control method for the soil-borne diseases. *Int. J. Plant Prot.* 10, 453–460. doi: 10.15740/HAS/IJPP/10.2/453–460

Talgre, L., Lauringson, E., Roostalu, H., and Makke, A. (2014). Phosphorus and potassium release during decomposition of roots and shoots of green manure crops. *Biol. Agric. Hortic.* 30, 264–271. doi: 10.1080/01448765.2014.953582

Tang, H. M., Xiao, X. P., Tang, W. G., Wang, K., Li, C., and Cheng, K. K. (2017). Returning winter cover crop residue influences soil aggregation and humic substances under double-cropped rice fields. *Rev. Bras. Cienc. Solo.* 41, e0160488. doi: 10.1590/18069657rbcs20160488

Vives-Peris, V., de Ollas, C., Gómez-Cadenas, A., and Pérez-Clemente, R. M. (2020). Root exudates: from plant to rhizosphere and beyond. *Plant Cell Rep.* 39, 3–17. doi: 10.1007/s00299–019-02447–5

Wang, D. Y., Peng, J., Xu, C. M., Zhao, F., and Zhang, X. F. (2012). Effects of rape straw manuring on soil fertility and rice growth. *Chin. J. Rice Sci.* 26(1), 85–91. doi: 10.3969/j.issn.1001-7216.2012.01.014

Xie, J., Liang, F., Xie, J. J., Jiang, G., Zhang, X., and Zhang, Q. (2022). Yield variation characteristics of red paddy soil under long-term green manure cultivation and its influencing factors. *Int. J. Environ. Res. Public Health* 19, 2812. doi: 10.3390/ijerph19052812

Xie, Z. J., Tu, S. X., Shah, F., Xu, C. X., Chen, J. R., Han, D., et al. (2016). Substitution of fertilizer-N by green manure improves the sustainability of yield in double-rice cropping system in south China. *Field Crops Res.* 188, 142–149. doi: 10.1016/j.fcr.2016.01.006

Yu, Y. L., Xue, L. H., and Yang, L. Z. (2014). Winter legumes in rice crop rotations reduces nitrogen loss, and improves rice yield and soil nitrogen supply. *Agron. Sustain. Dev.* 34, 633–640. doi: 10.1007/s13593–013-0173–6

Yuan, B., Yu, D., Hu, A., Wang, Y., Sun, Y., and Li, C. (2023). Effects of green manure intercropping on soil nutrient content and bacterial community structure in litchi orchards in China. *Front. Environ. Sci.* 10. doi: 10.3389/fenvs.2022.1059800

Zhang, S. T., Lu, J. W., Cong, R. H., Ren, T., Li, X. K., Liao, S. P., et al. (2020). Effect of rapeseed rotation on the yield of next-stubble crops. *Sci. Agric. Sin.* 53, 2852–2858. doi: 10.3864/j.issn.0578–1752.2020.14.009

Zhou, Q., Zhang, P., Wang, Z., Wang, L., Wang, S., Yang, W., et al. (2023). Winter crop rotation intensification to increase rice yield, soil carbon, and microbial diversity. *Heliyon* 9, e12903. doi: 10.1016/j.heliyon.2023.e12903

Zhu, X. (2011). *Effect of manure application on soil phosphorus components and phosphorus losses of farmland* (Beijing, China: Chinese Academy of Agricultural Sciences).

frontiers | Frontiers in Plant Science

TYPE Original Research
PUBLISHED 21 June 2024
DOI 10.3389/fpls.2024.1373624

OPEN ACCESS

EDITED BY
Laichao Luo,
Anhui Agricultural University, China

REVIEWED BY
Yahui Guo,
Central China Normal University, China
Li Na,
Anhui Agricultural University, China

*CORRESPONDENCE
Xiao-Fang Yu
nmyuxiaofang@imau.edu.cn
Ju-Lin Gao
nmgaojulin@163.com

RECEIVED 20 January 2024
ACCEPTED 30 May 2024
PUBLISHED 21 June 2024

CITATION
Wang L-Q, Yu X-F, Gao J-L, Ma D-L, Liu H-Y and Hu S-P (2024) Regulation of tillage on grain matter accumulation in maize.
Front. Plant Sci. 15:1373624.
doi: 10.3389/fpls.2024.1373624

Regulation of tillage on grain matter accumulation in maize

Li-Qing Wang, Xiao-Fang Yu*, Ju-Lin Gao*, Da-Ling Ma, Hong-Yue Liu and Shu-Ping Hu

College of Agronomy, Inner Mongolia Agricultural University, Hohhot, China

Introduction: To address issues related to shallow soil tillage, low soil nutrient content, and single tillage method in maize production in the Western Inner Mongolia Region, this study implemented various tillage and straw return techniques, including strip cultivation, subsoiling, deep tillage, no-tillage, straw incorporation with strip cultivation, straw incorporation with subsoiling, straw incorporation with deep tillage, and straw incorporation with no tillage, while using conventional shallow spinning by farmers as the control.

Methods: We employed Xianyu 696 (XY696) and Ximeng 6 (XM6) as experimental materials to assess maize 100-grains weight, grain filling rate parameters, and grain nutrient quality. This investigation aimed to elucidate how tillage and straw return influence the accumulation of grain material in different maize varieties.

Results and discussion: The results indicated that proper implementation of tillage and straw return had a significant impact on the 100-grains weight of both varieties. In comparison to CK (farmer's rotary rotation), the most notable rise in 100-grains weight was observed under the DPR treatment (straw incorporation with deep tillage), with a maximum increase of 4.84% for XY696 and 6.28% for XM6. The proper implementation of tillage and straw return in the field resulted in discernible differences in the stages of improving the grain filling rates of different maize varieties. Specifically, XY696 showed a predominant increase in the filling rate during the early stage (V1), while XM6 exhibited an increase in the filling rates during the middle and late stages (V2 and V3). In comparison to CK, V1 increased by 1.54% to 27.56% in XY696, and V2 and V3 increased by 0.41% to 10.42% in XM6 under various tillage and straw return practices. The proper implementation of tillage and straw return had a significant impact on the nutritional quality of the grains in each variety. In comparison to CK, the DPR treatment resulted in the most pronounced decrease in the soluble sugar content of grains by 25.43% and the greatest increase in the crude fat content of grains by 9.67%.

Conclusion: Ultimately, the proper implementation of soil tillage and straw return facilitated an increase in grain crude fat content and significantly boosted grain weight by improving the grouting rate parameters at all stages for various maize varieties. Additionally, the utilization of DPR treatment proved to be more effective. Overall, DPR is the most promising strategy to improve maize yield and the nutritional quality of grain in the long term in the Western Inner Mongolia Region.

KEYWORDS

spring maize, tillage methods, grain weight, grain filling, grain nutritional quality

1 Introduction

The Inner Mongolia Autonomous Region serves as a crucial national grain production base, encompassing 11.5 million hectares of arable land, which represents approximately 9.0% of the country's total arable land. According to statistical data, the aggregate production of grain crops in Inner Mongolia amounted to 3.66 million tonnes in 2021, positioning it as the sixth largest producer in the country (Chen et al., 2021). Nevertheless, the occurrence of issues including diminished soil fertility from prolonged continuous cropping, autotoxicity resulting from plant root secretions, and heightened susceptibility to microbial diseases diminishes crop nutrient absorption and leads to decreased crop yield per unit area (Rubio et al., 2021; Xing et al., 2022), thereby significantly constraining the region's agricultural sustainability. Hence, it is imperative to investigate rational and practical plowing techniques in the region to enhance the soil quality and fertility, thereby safeguarding the national food security.

Prolonged reliance on traditional shallow rotary plowing in farmland in the Western Inner Mongolia Region has led to the formation of a compacted soil tillage layer, elevated soil bulk density, constrained root growth, and hindered nutrient and water absorption, thereby constraining crop growth and yield potential (Liu et al., 2022a; Yu et al., 2023). Deep plowing, no tillage, strip tillage, and other plowing techniques constitute crucial practices in agricultural production. These methods have a direct influence on achieving high and consistent crop yields and promoting sustainable development through alterations in soil structure and physico-chemical properties (Abu-Hamdeh, 2003; Zhang et al., 2021; Wang et al., 2022). Subsoiling enhances soil porosity, facilitating deep rooting and nutrient uptake without causing soil compaction or excessive drying. Deep tilling breaks up the soil crusts and improves the soil permeability, thereby enhancing the exchange of nutrients and gases between soil layers. It also promotes the decomposition of deeply buried straw, resulting in increased soil fertility and the reduction of pests and diseases (He et al., 2021). Conservation tillage methods such as no tillage and minimum tillage mitigate wind and water erosion, reduce evaporation, and contribute to enhancing soil fertility, cost savings, and overall efficiency in land cultivation (Yuan et al., 2018; Pecci et al., 2021). Nevertheless, no tillage contributes to increased soil bulk density and compactness (Blanco-Canqui et al., 2022), lowered soil temperature, and constrained the growth of the maize root system, consequently impacting the nutrient uptake in the deeper soil layers (Li et al., 2022a). Strip rotary tillage improves the photosynthetic efficiency of plant leaves during the late filling stage, enabling enhanced dry matter translocation to the grains and stimulating post-anthesis dry matter accumulation (Chu et al., 2016). Therefore, improvement in soil structure, enhanced crop nutrient uptake, increased grain dry matter accumulation, and enhanced crop yields can be achieved only through the adoption of reasonable plowing measures (Zhai et al., 2021).

The practice of returning straw to the field is an effective method for comprehensively utilizing straw and plays a crucial role in regulating the soil structure, enhancing the crop root structure and function, and safeguarding the ecological environment (Zhang et al., 2014; Qin et al., 2015). Returning straw to the field reduces soil bulk density and enhances total soil porosity, significantly improving soil aeration and facilitating the deeper penetration of crop roots (Yao et al., 2015; Zhang et al., 2015). Upon returning the straw to the field, the decomposition and release of organic matter from the straw enhance the soil's organic matter content and lead to increased levels of available nitrogen, phosphorus, and potassium (Tan et al., 2015). Variations in climatic conditions, soil properties, and tillage management necessitate a judicious combination of straw return methods and tillage practices to notably enhance the efficiency of soil nutrient utilization by the crop root system. Most of the previous studies have focused on the effects of tillage practices on soil and maize plants—for instance, no tillage and straw return safeguard soil structure and protect organic carbon aggregates from microbial degradation, leading to augmented storage of soil organic carbon (SOC), minimized SOC mineralization, and enhanced crop biomass and yield (Sainju et al., 2009; Xu et al., 2019a). Additionally, it has been suggested that deep tilling of straw can effectively address the issues related to delayed straw decomposition and impediments to the emergence of maize seedlings during the process of field straw return. At the same time, it can significantly improve the characteristics of soil structure and increase the soil nutrients (Xu et al., 2019b; Jin et al., 2020; Zhang et al., 2023). Studies investigating the impact of straw return on yield enhancement have found that deep

plowing of returned straw indirectly affects maize yield and its components by directly and preferentially influencing the levels of total and readily available nitrogen in the soil (Wang et al., 2023a). In the realm of intensive maize cultivation, grain weight plays a critical role in enhancing maize yields, with a direct correlation to grain filling characteristics that are significantly impacted by tillage techniques and straw management (Shao et al., 2016; Ren et al., 2021).

A favorable soil micro-environment enhances organic carbon mineralization and stable soil nutrient supply and thus also contributes to improve the grain yield. Therefore, improving soil structure and facilitating maize nutrient uptake through the incorporation of straw into the field, along with appropriate plowing practices, hold a crucial significance for the sustainable utilization of farmland in the Western Inner Mongolia Region. Prior research has extensively studied the impacts of various tillage methodologies on soil conditions and their subsequent ecological advantages. However, comparatively limited studies have endeavored to elucidate the underlying mechanisms of yield variations seen across these tillage techniques from the standpoint of grain filling. Accordingly, this experiment employed a combination of continuous positional tillage and straw return methods in the early stage of the trial to examine the evolving patterns of maize grain filling traits, aiming to establish a theoretical framework for optimizing soil tillage, rational straw resource utilization, and maximizing maize yield in the Western Inner Mongolia Region. The present study hypothesized that DPR (straw incorporation with deep tillage) could effectively ensure the increase of grain weight and the improvement of grain nutritional quality during maize cultivation in Western Inner Mongolia. The objectives of this study were (i) to determine the most suitable tillage practices based on changes in 100-grains weight and grain nutrient quality, (ii) to understand the characteristics of grain filling and the pattern of change in filling rate parameters under different tillage practices, and (iii) to study the relationship between different components of grain nutrient quality and filling rate parameters, elucidating the potential mechanism by which these components respond to 100-grains weight.

2 Materials and methods

2.1 Description of research location

The field experiments took place at the Tumoteyou Qi Experimental Station of Inner Mongolia Agricultural University (40°33′ N, 110°31′ E) in 2020 and 2021. The tillage method testing platform was constructed in autumn 2017 and repeated each year for the previous year's tillage practices. The preceding crop was maize, and the soil type was sandy loam. The nutrient data for the plowed ground (0–30 cm soil layer) before sowing can be found in Table 1. Figure 1 illustrates the primary meteorological factors

TABLE 1 Soil nutrients under different tillage methods in 2020 and 2021.

Tillage method	Year	Alkali-hydrolysable N	Available P	Available K	Organic matter
		(mg kg^{-1})	(mg kg^{-1})	(mg kg^{-1})	(g kg^{-1})
Farmer rotary tillage (CK)	2020	53.44	2.52	64.79	17.36
	2021	53.07	2.57	66.07	17.44
Strip cultivation (SC)	2020	53.20	3.35	71.54	20.13
	2021	54.59	3.34	72.38	19.67
Subsoiling (SS(	2020	55.57	3.01	83.88	22.35
	2021	57.91	3.10	85.81	22.50
Deep tillage (DP)	2020	61.27	2.68	89.98	22.52
	2021	62.58	2.78	90.11	22.80
No-tillage (NT)	2020	65.09	4.42	79.86	20.96
	2021	66.16	4.47	84.26	20.67
Straw incorporation with strip cultivation (SCR)	2020	62.44	3.84	85.85	22.71
	2021	63.12	3.91	87.90	23.18
Straw incorporation with subsoiling (SSR)	2020	72.84	3.32	94.45	23.76
	2021	74.16	3.49	99.02	23.94
Straw incorporation with deep tillage (DPR)	2020	66.77	3.65	113.18	24.86
	2021	70.34	3.83	117.03	25.37
Straw incorporation with no-tillage (NTR)	2020	74.11	4.60	84.28	24.06
	2021	72.90	4.67	89.42	23.98

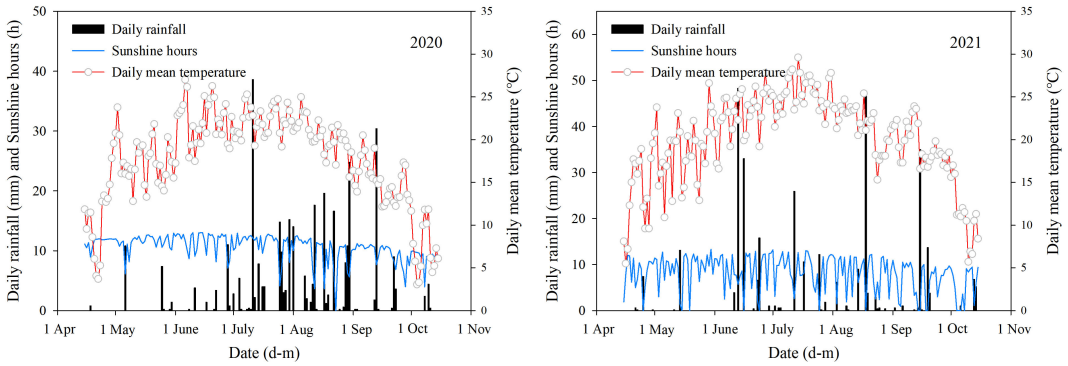

FIGURE 1
Main meteorological factors during the growing period in the experimental area.

that influenced maize growth during the study period. During the maize growing period in 2020 and 2021, the average daily temperature was 18.92°C and 21.19°C, the total rainfall was 328.40 and 310.30 mm, and the total sunshine hours was 1,761.58 and 1,362.02 h, respectively.

2.2 Experimental design

A split-zone experimental design was implemented, where the plowing method was applied in the central zone. The farmer's rotary rotation served as the control (CK). Eight treatments were established for comparison, comprising subsoiling (SS), deep tillage (DP), strip cultivation (SC), no tillage (NT), straw incorporation with strip cultivation (SCR), straw incorporation with subsoiling (SSR), straw incorporation with deep tillage (DPR), and straw incorporation with no tillage (NTR). There was a total of nine tillage treatments. In combination with the tillage methods, two different densely tolerant maize varieties (Xianyu 696 and Ximeng 6) were used, providing a total of 18 treatments, each with three replicates. Xianyu 696 (XY696) and Ximeng 6 (XM6) were provided by Dunhuang Seed Pioneer Variety Co. Ltd., and Inner Mongolia Simon Seed Co. Ltd., which have a fertility period of 125 and 130 days, respectively. Consequently, the experiment consisted of a total of 54 plots, each with an area of 65 m × 6 m. The tillage methods and varieties were assigned to the main plot and subplots, respectively. In subplots, varieties were randomly planted with a row spacing of 60 cm. The nine methods of cultivation are shown in Table 2.

2.3 Crop husbandry

In 2020, maize was sown on April 25 and harvested on October 6; in 2021, maize was sown on 22 April and harvested on 7 October. The planting density was 82,500 plants ha^{-1}. Basal fertilization included the application of ammonium phosphate dibasic and potassium sulfate before seeding. Ammonium dihydrogen phosphate (N 18%; P_2O_5 46%) was applied at a rate of 375 kg ha^{-1}, and potassium sulfate (K_2O 51%) was applied at a rate of 150 kg ha^{-1}. Urea (N, 46%) is utilized as a supplementary fertilizer with application rates of 30% at V6 (sixth leaf), 60% at V12 (12th leaf), and 10% at R2 (blister), with an overall rate of 345 kg ha^{-1}. Annually, during the entire growing cycle of maize, the following fertilizer quantities were utilized: 226.2 kg ha^{-1} of pure nitrogen (N), 76.5 kg ha^{-1} of potassium oxide (K_2O), and 172.5 kg ha^{-1} of phosphorus pentoxide (P_2O_5). Drip irrigation was administered four times throughout the growth stages: at V6, V12, R1 (silking), and R2. Each irrigation event encompassed an area of 750 m^3 ha^{-1}. All other management practices conformed to the standard procedures used in large-scale farming operations.

2.4 Measurement

2.4.1 Determination of 100-grains weight

At physiological maturity, 10 ears were randomly chosen from each plot and air-dried, and then 100 kernels were collected from the middle of each ear, weighed, and subsequently standardized to obtain the 100-grains weight at 14% moisture content.

2.4.2 Determination of grain filling rate

Starting from 15 days post-pollination, samples were collected at 5-day intervals until the end of the filling period. At each sampling point, three ears per plot were collected, and 100 grains were sampled from the middle of each ear. The grains were then weighed, placed into an oven at 105°C for 30 min, dried at 60°C until reaching a constant weight, and subsequently re-weighed.

$$\text{Filling rate(Gmean)} = {}^{(W1-W2)}/_{D}$$

where W1 = 100-grains dry weight of the current sample (g), W2 = 100-grains dry weight of the previous sample (g), and D = number of days between samples (d).

2.4.3 Determination of grain filling characteristics

Since the process of grain dry matter accumulation adheres to the "S" type growth curve, we used the logistic equation to model

TABLE 2 Tillage methods' operating procedures.

Abridge	Tillage methods	Depth (cm)	Methods of tillage practices
CK	Farmer's rotary rotation	15	The straw was removed from the field after being mechanically harvested in autumn, shallowly tilled using a rotary tiller (1BX-4.0, Xinjiang Xinyan Mushin Technology Co., China) in the following spring, and then mechanically sown using a planter (Optina SX-12, Kverneland Group, German).
SC	Strip cultivation	30	The straw had been removed from the field after mechanical harvesting in autumn and subsequently mechanically sown in the following spring using a strip-deep rotary planter (none, Beijing Hehuinong Agricultural Resources Co., China).
SS	Subsoiling	35	After the mechanical harvest in autumn, the straw was removed from the field. Subsequently, subsoiling was conducted using a subsoiler (Sub-tiller, HE-VA Group, Denmark), followed by shallow cultivation with a rotary tiller (1BX-4.0, Xinjiang Xinyan Mushin Technology Co., China). Finally, mechanical (Optina SX-12, Kverneland Group, German) seeding took place in the following spring.
DP	Deep tillage	45	After the mechanical harvest in autumn, the straw was removed from the field. Subsequently, deep tillage was conducted using a deep turner (ILFT550, Xinjiang Xinyan Mushin Technology Co., China), followed by shallow cultivation with a rotary tiller (1BX-4.0, Xinjiang Xinyan Mushin Technology Co., China). Finally, mechanical (Optina SX-12, Kverneland Group, German) seeding took place in the following spring.
NT	No tillage		The straw was removed from the field after mechanical harvesting in autumn and then mechanically (1006NT, Grean Plant Group, USA) sown in the following spring using a no-till planter.
SCR	Straw incorporation with strip cultivation	30	The straw was mechanically (4YZB-5AS, Xinjiang Xinyan Mushin Technology Co., China) harvested in autumn, fully crushed, and returned to the field by covering it on the soil surface. It was then sown in the following spring using a strip deep rotary planter (none, Beijing Hehuinong Agricultural Resources Co., China).
SSR	Straw incorporation with subsoiling	35	After having been mechanically (4YZB-5AS, Xinjiang Xinyan Mushin Technology Co., China) harvested in autumn, the straw was thoroughly crushed and applied as a soil cover to be returned to the field. Simultaneously, subsoiling was performed using a subsoiler (Sub-tiller, HE-VA Group, Denmark), followed by incorporating the straw into the soil with a rotary tiller (1BX-4.0, Xinjiang Xinyan Mushin Technology Co., China). Finally, during the subsequent spring season, seeds were sown utilizing a precision seeder (Optina SX-12, Kverneland Group, German).
DPR	Straw incorporation with deep tillage	45	After the mechanical (4YZB-5AS, Xinjiang Xinyan Mushin Technology Co., China) harvest in autumn, the straw was thoroughly crushed and applied as a soil cover to be returned to the field. Simultaneously, a deep tiller machine (ILFT550, Xinjiang Xinyan Mushin Technology Co., China) was employed to incorporate the straw into the soil, followed by rotary tilling using a rotary tiller (1BX-4.0, Xinjiang Xinyan Mushin Technology Co., China). Finally, in the subsequent spring season, seeds were sown utilizing a planter (Optina SX-12, Kverneland Group, German).
NTR	Straw incorporation with no-tillage		The straw was mechanically (4YZB-5AS, Xinjiang Xinyan Mushin Technology Co., China) harvested in autumn, thoroughly crushed, and covered on the soil surface to be returned to the field. It was then seeded in the following spring using a no-till planter (1006NT, Grean Plant Group, USA).

the process of grain dry matter accumulation. A logistic equation was used to fit the grain filling process, calculate grain filling characteristic parameters, and analyze grain filling growth. The logistic equation was as follows:

$$W = A/(1 + Be^{-Ct})$$

In the equation above, t is the number of days after flowering (blooming day t0 = 0), W is the 100-grains weight after flowering (grain weight on flowering day = w0), A is the theoretical maximum 100-grains weight, and B and C are shape parameters. The filling parameters were derived from the first and second derivatives of the equation.

t1 (the start date of the filling peak period) = (lnB − 1.317)/C, corresponding to the grain weight (w1) at this time: w1=$A/(1 + Be^{-Ct1})$

t2 (the end date of the filling peak period) = (lnB + 1.317)/C, corresponding to the grain weight (w2) at this time: w2=$A/(1 + Be^{-Ct2})$

t3 (the grain weight reaches 99% after flowering, the effective filling period) = (lnB + 4.59512)/C, corresponding to the grain weight (w3) at this time.

The filling duration of the gradually increasing period was calculated as T1 = t1− t0. The increase in grain weight during the rapidly increasing period was calculated as w1 = W1− W0. The mean filling rate of the gradually increasing period was calculated as V1 = w1/T1.

The filling duration of the rapidly increasing period was calculated as T2 = t2− t1. The increase in grain weight during the rapidly increasing period was calculated as w2 = W2 − W1. The mean filling rate of the rapidly increasing stage was calculated as V2 = w2/T2.

The filling duration of the slowly increasing period was calculated as T3 = t3− t2. The increase in grain weight of the slowly increasing period was calculated as w3 = W3− W2. The mean filling rate of the slowly increasing stage was calculated as V3 = w3/T3.

2.4.4 Determination of the nutrient quality components of grains

At physiological maturity, a representative cob was chosen, and the central grains of the cob were oven-dried at 105°C for 30 min, followed by drying to a constant weight at 60°C, and then crushed

for measurement. The total nitrogen content of the grains was determined by employing the semi-micro Kjeldahl method, and the crude protein content was calculated by multiplying the total nitrogen content by a factor of 6.25. The determination of crude fat content utilized the Soxhlet extraction–residue method (Atif and Perveen, 2023), and the total starch and total soluble sugar content were assessed following the method described by Yu et al. (2022).

2.5 Statistical analysis

The data were collected and organized using Microsoft Excel 2019 (Microsoft, Inc., Redmond, WA, USA). Data analysis was conducted using SAS 9.4 (SAS Institute Inc., Raleigh, NC, USA) for variance analysis, correlation analysis, stepwise regression, and principal component analysis. A two-way ANOVA was carried out to explore the impact of tillage methods on the 100-grains weight and nutritional quality components across two varieties. The significance test was performed using LSD (least significant difference) at a significance level of 5%. Correlation analysis was conducted using the Pearson correlation method. Sigmaplot 12.5 (Systat Software, Inc., San Jose, CA, USA) and Origin 2021 (OriginLab Corp., Northampton, MA, USA) were utilized to generate graphs.

3 Results

3.1 Regulatory effects of tillage methods on 100-grains weight of two maize varieties

The ANOVA results (Table 3) indicated highly significant differences in the 100-grains weight among tillage methods or varieties in 2020 ($p< 0.01$). Similarly, in 2021, there were highly significant differences in 100-grains weight among tillage methods or varieties, and significant differences among tillage methods × varieties were observed ($p< 0.05$).

The 100-grains weight of XM6 exceeded that of XY696 under the farmer's rotary tillage treatment (CK) by 3.11% in 2020 and 6.05% in 2021 (Figure 2). Various tillage and straw return methods led to changes in the 100-grains weight of each maize variety, with straw incorporation with subsoiling (SSR) and straw incorporation with deep tillage (DPR) showing superior performance. In 2020, the 100-grains weight of XY696 significantly increased by 4.66% and 4.80% under SSR and DPR treatments, respectively, compared to CK; similarly, XM6's weight increased by 4.73% and 4.84%. In 2021, under similar contrast conditions, the 100-grains weight of XY696 saw a significant increase by 6.05% and 6.28%, while XM6's weight increased by 2.95% and 3.15%.

TABLE 3 Variance analysis of the effect of tillage method and variety on the 100-grains weight.

Sources of variation	2020 year	2021 year
Tillage method (M)	13.08**	19.21**
Error I MS	0.010	0.170
Varieties(V)	113.73**	408.64**
M × V	0.02	2.94*
Error II MS	0.009	0.090

*Significant at p< 0.05.
**Significant at p< 0.01.

3.2 Regulatory effects of tillage methods on the grain filling rate of two maize varieties

Figure 3 illustrates a quadratic trend in the grain filling rate under each treatment, characterized by an initial increase followed by a decrease. In CK, the peak grouting rate of XM6 surpassed that of XY696, and the time of peak grouting rate occurrence was also delayed. In comparison to CK, the peak grouting rate (y) and its occurrence time (x) differed across the other treatments. The peak grouting rate of XY696 under SSR and DPR treatments increased by 9.49% and 11.57% in 2020 and 11.01% and 14.50% in 2021, and the time of occurrence of peak grouting rate was prolonged by 11.18% and 14.04% in 2020 and 10.50% and 14.57% in 2021, in turn, as compared to CK treatment. Under the same comparison conditions, the peak grouting rate of XM6 changed sequentially by -3.04% and 0.12% in 2020 and -4.86% and -1.98% in 2021, and the time of peak grouting rate occurrence changed sequentially by -2.86% and 1.09% in 2020 and -5.91% and -2.57% in 2021.

3.3 Regulatory effects of tillage methods on the parameters of grain filling rate in two maize varieties

The logistic curve equation divided maize grain filling into three periods: gradual increase, fast increase, and slow increase. The duration of filling in each stage followed the order: slow increase period > fast increase period > gradual increase period. The average filling rate in each stage followed the sequence: fast increase period > gradual increase period > slow increase period (Figure 4). In the conditions of farmers' shallow spinning (CK), XM6 exhibited a lower asymptotic grouting duration (T1) and a higher asymptotic grouting rate (V1) than XY696. Nevertheless, the pattern of change in grouting duration (T2, T3) and grouting rate (V2, V3) between varieties during fast and slow growth periods was not consistent across the two growing seasons.

Regarding grouting rate, V1 of XY696 exhibited an increase under SSR and DPR treatments compared to CK: 2.36% and 2.74% in 2020 and 27.56% and 27.55% in 2021, while V2 changed by 1.43% and 1.47% in 2020 and -13.30% and -13.14% in 2021, and V3 changed by 1.43% and 1.47% in 2020 and -13.30% and -13.14% in 2021. In similar contrasting conditions, XM6 exhibited a preference for adjustments in mid- to late-stage grouting rates (V2 and V3), exemplified by V2 increasing by 10.42% and 1.91% in 2020 and by 2.19% and 2.51% in 2021 and V3 exhibiting growth by 10.42% and

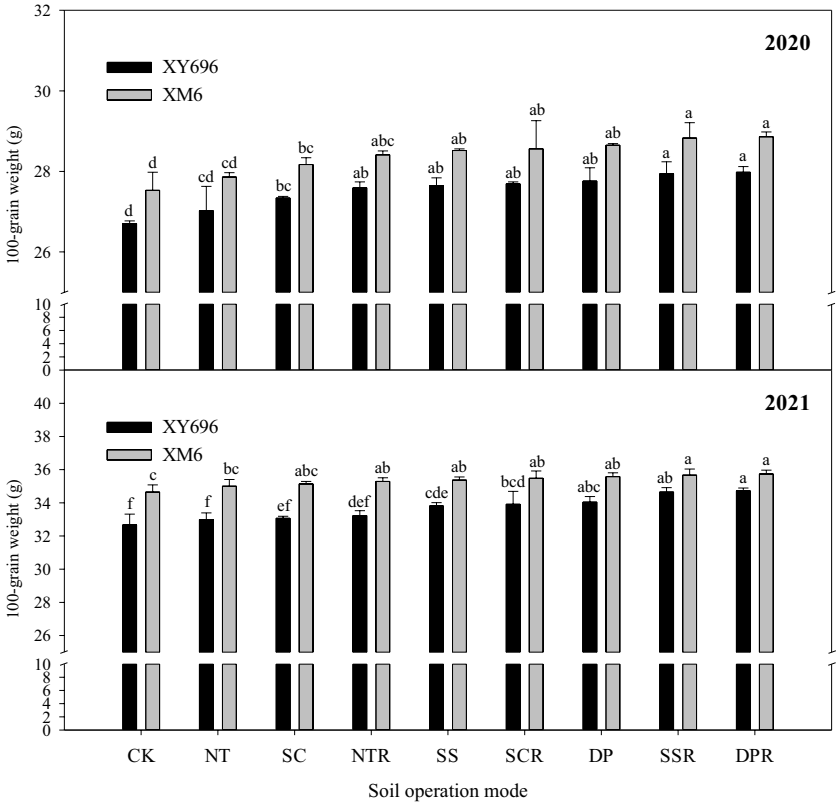

FIGURE 2
Effects of tillage methods on the 100-grains weight of two maize varieties. Different lowercase letters indicate significant differences at the 0.05 level between different tillage methods for the same variety.

1.91% in 2020, followed by 2.19% and 2.51% in 2021. Concerning grouting duration, in comparison to CK, the T1 of XY696 under each SSR and DPR treatment exhibited changes of 7.65% and 8.45% in 2020, and -14.86% and -14.10% in 2021, while T2 increased by 8.63% and 9.80% in 2020 and 25.27% and 26.14% in 2021, and T3 increased by 8.63% and 9.80% in 2020 and 25.27% and 26.14% in 2021 sequentially. Under similar comparison conditions, XM6 demonstrated a preference for alterations in the pre-grouting duration, exemplified by T1 increasing sequentially by 21.40% and 6.40% in 2020 and by 6.21% and 7.11% in 2021.

3.4 Regulatory effects of tillage methods on the nutritional quality of grains of two maize varieties

The ANOVA results (Tables 4, 5) indicated a highly significant difference in grain crude fat content among tillage methods and a highly significant difference in grain total soluble sugar content among tillage methods, varieties, or their interactions in 2020. In 2021, highly significant differences were observed in grain crude fat content between the tillage method and varieties and in grain total soluble sugar content among tillage methods and varieties.

From Figure 5, it can be seen that, compared to CK, the changes in crude protein and total starch content of the grains under the other tillage treatments are relatively small, while there are significant differences in crude fat and soluble sugar content of the grains. In 2020, compared to CK, the crude fat content of XY696 grains only significantly increased under the DPR treatment (4.34%); the soluble total sugar content of the grains showed the largest decrease under the deep tillage (DP) and DPR treatments (22.42% and 17.23%, respectively). Under the same comparative conditions, the crude fat content of XM6 grains showed the largest increase under the SSR and DPR treatments (7.81% and 8.87%, respectively); the soluble total sugar content of the grains also showed the largest decrease under the SSR and DPR treatments (16.04% and 18.01%, respectively). In 2021, compared to CK, the crude fat content of XY696 grains significantly increased under the SSR and DPR treatments (3.49% and 4.71%, respectively); the soluble total sugar content of the grains showed the largest decrease under the SSR and DPR treatments (17.93% and 19.18%, respectively). Under the same comparative conditions, the crude fat content of XM6 grains showed the largest increase under the SSR and DPR treatments (8.52% and 9.67%, respectively); the soluble total sugar content of the grains also showed the largest decrease under the SSR and DPR treatments (23.96% and 25.43%, respectively).

3.5 Correlation between 100-grains dry weight and parameters of grain filling rate

The correlation analyses, as depicted in Figure 6, revealed highly significant, positive correlations (0.87, 0.75, and 0.76, $p< 0.01$)

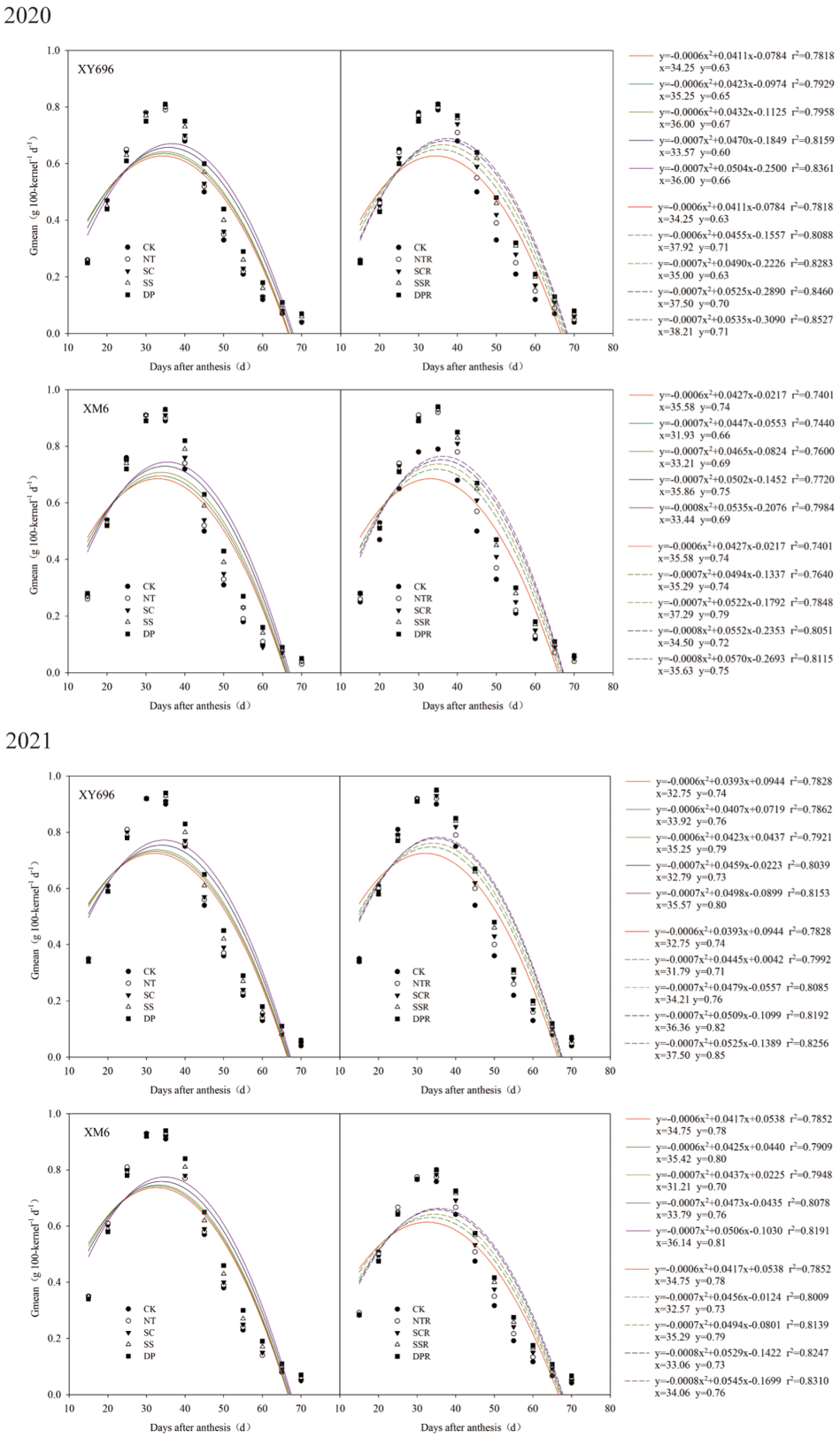

FIGURE 3
Effects of tillage methods on the grain filling rate of two maize varieties.

10.3389/fpls.2024.1373624

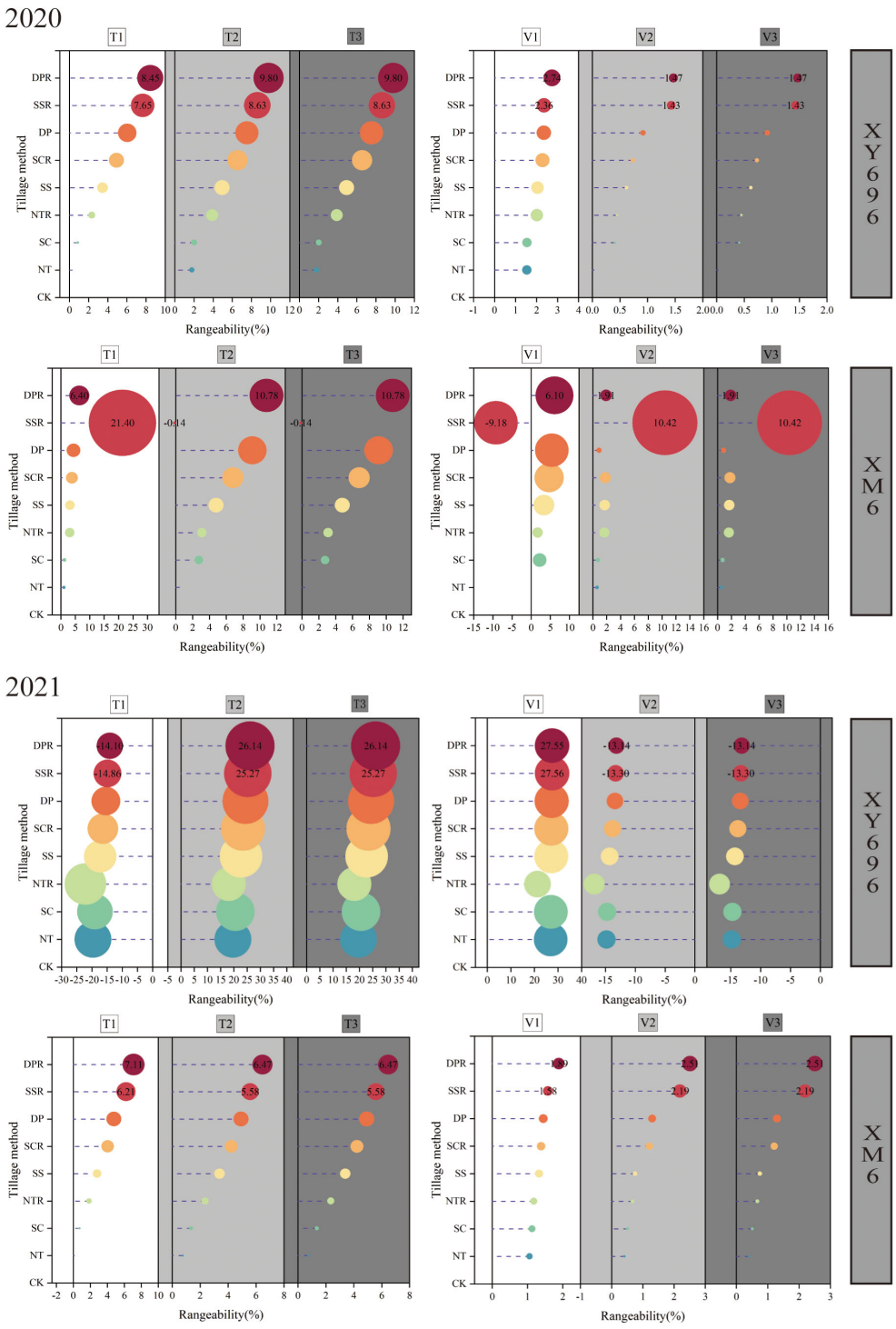

FIGURE 4
Effects of tillage methods on the grain filling rate parameters of two maize varieties.

between the grain dry weight and the rate of grain filling at each stage (V1–V3), with relatively smaller correlations observed with the duration of grain filling at each stage. Significant positive correlations (0.48, 0.49, 0.48, and 0.49, $p< 0.01$) were observed between V1 and V2, T2, V3, and T3. Additionally, V2 exhibited a significant negative correlation (-0.39, $p< 0.05$) with T3 and a highly significant positive correlation (0.99, $p< 0.01$) with V3.

3.6 Correlation between nutritive quality components and 100-grains dry weight of grains

The results of the correlation analysis depicted in Figure 7 indicate highly significant negative correlations between the dry weight of grain and the content of grain crude protein and total

TABLE 4 Variance analysis of the effect of tillage method and variety on the nutritional quality of maize grains in 2020.

Sources of variation	Crude protein content	Total starch content	Crude fat content	Total soluble sugar content
Tillage method (M)	0.46	1.54	13.19**	118.32**
Error I MS	0.012	0.613	0.007	0.017
Varieties(V)	4.25	1.12	0.22	551.63**
M × V	0.01	0.02	1.47	8.01**
Error II MS	0.007	0.884	0.005	0.024

**Significant at $p< 0.01$.

TABLE 5 Variance analysis of the effect of tillage method and variety on the nutritional quality of maize grains in 2021.

Sources of variation	Crude protein content	Total starch content	Crude fat content	Total soluble sugar content
Tillage method (M)	0.34	1.82	27.75**	24.43**
Error I MS	0.008	0.709	0.005	0.085
Varieties (V)	0.25	0.80	63.08**	222.86**
M × V	0.00	0.01	2.12	0.18
Error II MS	0.013	0.855	0.005	0.123

**Significant at $p< 0.01$.

soluble sugar (-0.79 and -0.85, $p< 0.01$) as well as highly significant positive correlations with total starch and crude fat content of grain (0.86 and 0.81, $p< 0.01$).

3.7 Principal component analysis of grain filling rate parameters and grain nutritional quality

The principal component analysis accounted for 81.9% of the total variance, with 53.4% contributed by PCA1 and 28.5% by PCA2 (Figure 8). Notably, the rate of grouting in the tapering stage (V1) exhibited a highly significant and positive correlation with the total starch content of the grain (Starch), whereas the duration of grouting in the fast-growing stage (T2) showed a highly significant and positive correlation with the duration of grouting in the slow-growing stage (T3), resulting in a substantial overlap in the principal component loadings. The contributions of grain crude fat content (Fat), V1, Starch, grain crude protein content (Protein), grain total soluble sugar content (Sugar), and the duration of asymptotic grouting (T1) were higher in the direction of PCA1. Conversely, toward PCA2, the fast-accelerating rate of grouting (V2), slow-accelerating rate of grouting (V3), T2, and T3 made more significant contributions. In relation to grouting rate, the correlations of the grouting rate parameters (V1, V2, and V3) at each stage showed a stronger association with Fat and Starch and a weaker association with Protein and Sugar. Regarding grouting duration, the correlation of T2 and T3 displayed a stronger connection with Fat and Starch, while the correlation of T1 exhibited a stronger association with Protein and Sugar.

3.8 Regression analyses of grain filling rate parameters and grain nutritional quality

Based on the results of the principal component analysis, stepwise regression and multiple linear equations were utilized to fit the grain filling rate (V1, V2, and V3) parameters at each stage with the total starch content and the crude fat content of grain. The analysis revealed that only V1 significantly influenced the total starch content of grain, while V1, V2, and V3 had substantial effects on the crude fat content of grain. The linear function equation for the total grain starch content with V1 from Figure 9 is represented as $y = 65.62 + 10.86x$, showing a positive correlation with the total grain starch content. Additionally, the multivariate linear function equations representing the grain crude fat content and parameters of grain grouting rate at each stage (V1, V2, and V3) were expressed as $y = 2.99 + 2.34x1 - 4.21x2 + 18.43x3$. Notably, V1 and V3 exhibited a positive correlation with grain crude fat content, while V2 showed a negative correlation (Table 6).

4 Discussion

4.1 Effects of ploughing and straw return on grain filling characteristics of different maize varieties

Grain filling is a vital biological process during maize growth and development, significantly influencing the final grain weight and yield. Grouting rate and grouting duration are dynamic traits involved in the formation of grain weight. They respond to the process of grain weight formation, and their interaction collectively

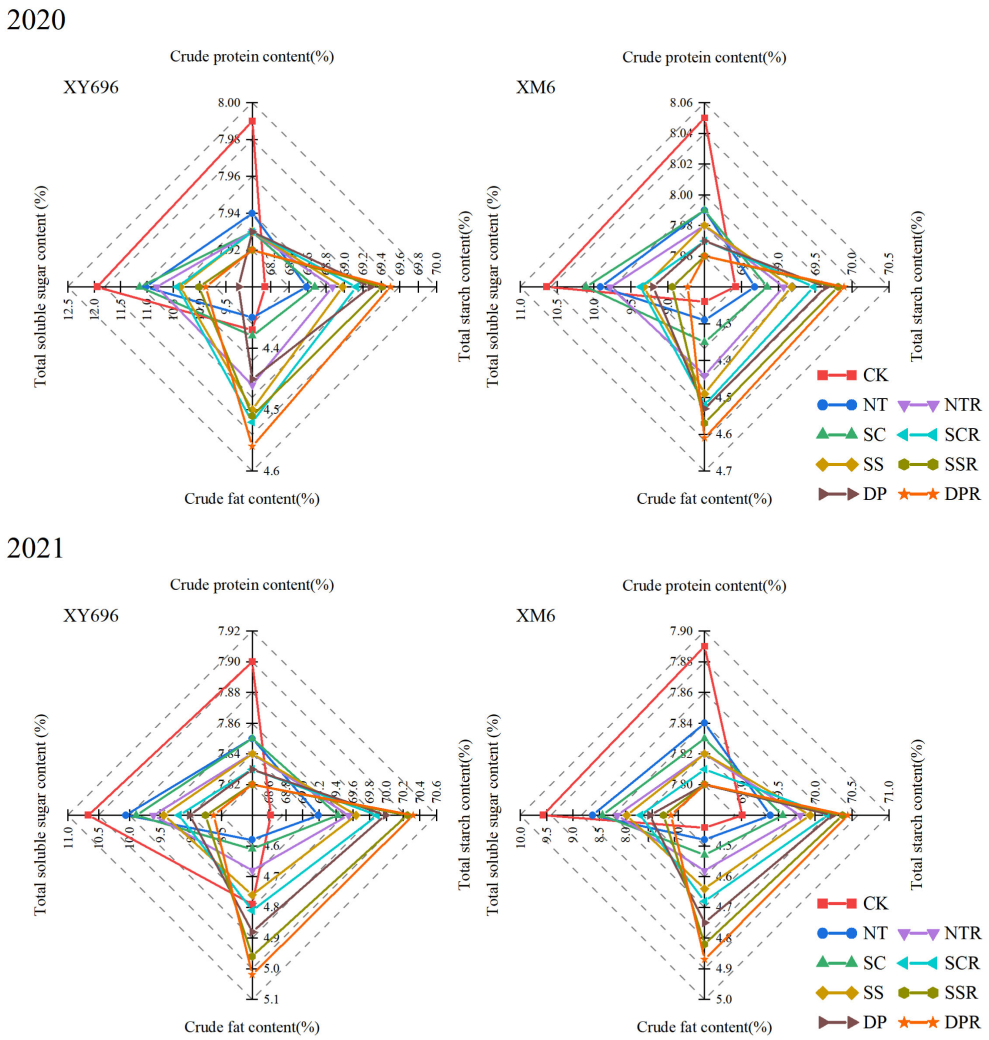

FIGURE 5
Effects of tillage methods on the grain nutrient quality of two maize varieties.

determines the magnitude of grain weight. Fang et al. (2020) demonstrated that the filling rate of maize grain governs the accumulation of dry matter in the grain, consequently impacting the yield at harvest. Moreover, they highlighted that employing proper planting practices can enhance the filling rate of the grain. Daynard et al. (1971) observed that extending the duration of grain filling could lead to an increase in 100-grains dry weight. Gasura et al. (2013) proposed that increasing the average grouting rate while extending the active grouting period is more advantageous for maize grain yield. The characteristics of maize grain filling are influenced by the genotype of the variety and the environmental conditions during growth (Wang et al., 2021; Wang et al., 2023b). Subsequently, Deng et al. (2023) discovered that the grouting duration of DH605 exceeded that of ZD958 across various grouting stages, although the grouting rate exhibited inconsistency. Furthermore, Olmedo and Vyn (2021) indicated that a higher nitrogen supply led to an extension in maize grain filling duration regardless of the timing of nitrogen application and planting density but presented inconsistencies in the effect on effective filling rate. In this study, under CK condition, XM6 exhibited a higher peak grouting rate compared to XY696, and the time of its peak grouting rate appeared to be prolonged. However, the changing pattern of each stage's grouting rate parameter was significantly influenced by the growing season.

In China, soil management and sowing are primarily conducted using small tractors. Without deep plowing, the soil's surface capacity and resistance to water infiltration increase, posing unfavorable conditions for crop growth. Therefore, the plowing method plays a crucial role in influencing the soil system (Godde et al., 2016; He et al., 2021). Straw return significantly influences soil water, fertilizer, air and heat conditions as well as nutrient accumulation and transformation, impacting crop growth and yield formation. Nevertheless, improper straw return can lead to diminished seeding quality and other adverse effects. Therefore, employing suitable tillage practices along with integrated straw return is not only fundamental for efficient farmland production

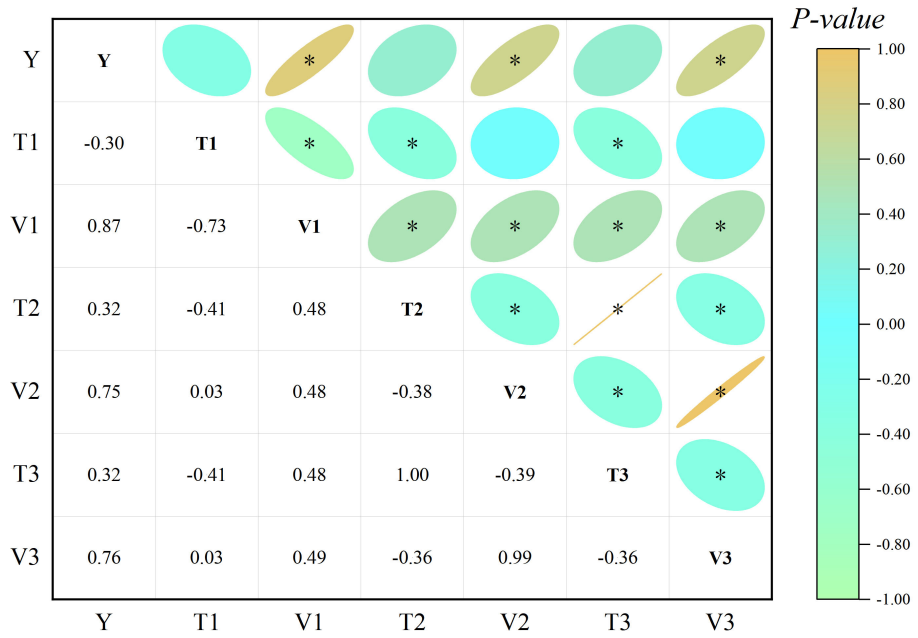

FIGURE 6
Correlation between the 100-grains dry weight and grain filling rate parameters. Y represents the dry weight of 100 grains. *, significant at $p< 0.05$.

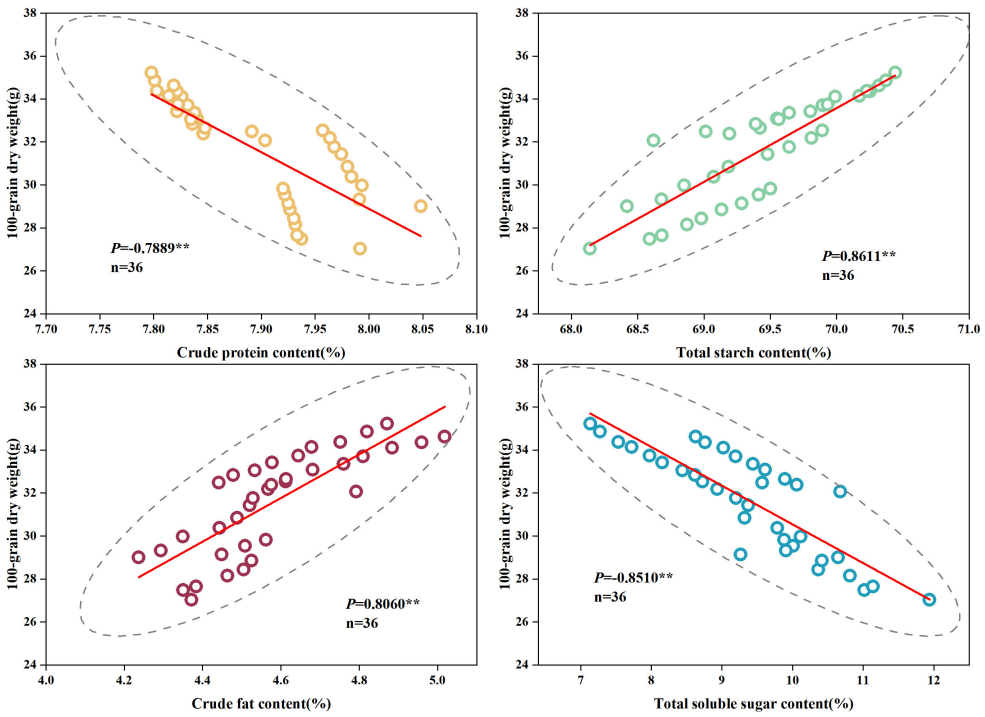

FIGURE 7
Correlation analysis between the nutrient quality components of grain and dry weight of 100-grains. **, significant at $p< 0.01$.

but also a substantial approach for enhancing soil quality (Li et al., 2022a; Li et al., 2022b). Previous research has indicated that employing suitable tillage practices can enhance maize yield by improving the grain filling characteristics (Zhai et al., 2017; Zhai et al., 2021; Yue et al., 2022). The study revealed that compared to shallow rotary tillage, both the peak grouting rate and the time at which the peak grouting rate occurred exhibited varying degrees of change in all deep tillage and no-tillage treatments. Additionally, the grouting rate and duration differed significantly among different maize varieties in response to the stage of tillage and straw return.

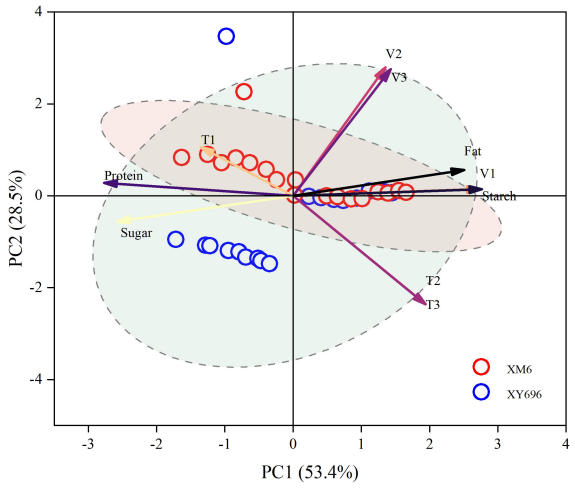

FIGURE 8
Principal component analysis of grain filling rate and grain nutrient quality. "Protein" stands for crude protein content in grains, "Starch" stands for total starch content in grains, "Fat" stands for crude fat content in grains, and "Sugar" stands for total soluble sugar content in grains.

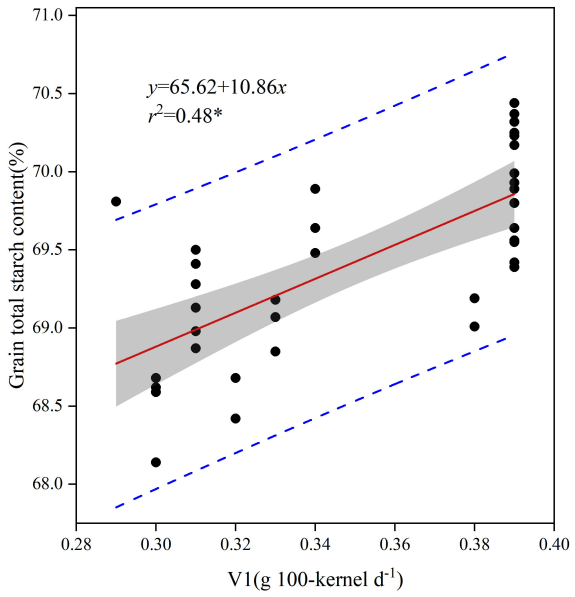

FIGURE 9
Regression analysis of the grain filling rate parameters and total starch content in grains. *, significant at $p < 0.05$.

Specifically, V1 showed an increase of 1.54%–27.56% in XY696, while V2 and V3 increased by 0.41%–10.42% each in XM6 under all other treatments compared to the shallow rotary tillage. Moreover, for grouting duration, T2 and T3 increased by 1.79%–26.14% for XY696 and 0.11%–21.40% for T1 for XM6 under all other treatments compared to CK.

Numerous prior studies have explored the potential mechanisms through which tillage practices affect dry matter accumulation in maize grains—for instance, subsoiling could promote the grain filling of inferior kernel of summer maize by regulating the soil water content, soil water consumption, and photosynthetic capacity (Zhai et al., 2021). Conservation tillage could promote summer maize photosynthetic capacity and grain filling of inferior kernels by regulating the soil water content and root system morphology (Wang et al., 2021). The SRS (strip rotary tillage without subsoiling) treatment resulted in the highest post-anthesis dry matter accumulation and contribution to grain, and such effect was attributed to the high photosynthetic activity at the later grain filling stage (Chu et al., 2016). In our study, we also found that differences in grain filling rate parameters were significant between the various tillage treatments within the different growing seasons—for example, in 2020, the differences in grain filling rate under different tillage treatments for XY696 were relatively small, whereas in 2021, they significantly increased. We believe that this may be related to meteorological resources during the growth season, as longer periods of sunshine are conducive to photosynthesis in leaves. In other words, superior meteorological conditions during the grain filling process will inevitably lead to an increase in the grain filling rate at the current grain filling stage and will also enhance the regulatory role of some appropriate farming practices on the grain filling rate. Therefore, we believe that, in future research, it may be beneficial to pay moderate attention to the allocation of meteorological resources during the grain filling process and achieve efficient utilization of light and heat resources by adjusting the sowing dates or the application of varieties.

TABLE 6 Regression analysis of grain filling rate parameters and grain crude fat content.

Variate	Index	Standard error	*F*-value	Pr > *F*
Intercept	2.99	64.14	89.77	<0.0001
V1 (*x1*)	2.34	1.06	11.53	0.0018
V2 (*x2*)	-4.21	0.74	3.31	0.0782
V3 (*x3*)	18.43	1.20	4.82	0.0355

4.2 Effect of ploughing and straw return on the nutritional quality of grain of different maize varieties

High crop yields have long been the focus of China's agricultural development due to the large population, limited land, and persistent scarcity of agricultural products. However, this focus has overshadowed the attention on agricultural product quality. As China's agricultural production and product availability grow, there will be an increasing demand for higher-quality agricultural products. Crop quality results from both genetic and non-genetic factors. In their study, Wang et al. (2023b) compared high-yielding maize hybrids planted in China over different periods and found that newer varieties exhibited a higher starch content but a lower grain protein content than the older varieties. Our study observed that, under CK treatment, XM6 showed a lower grain crude fat and total soluble sugar content compared to XY696, while

no significant difference was found in grain crude protein and total starch content.

Numerous studies and production practices demonstrate that various cultivation measures implemented during the growth and development of crops can significantly influence the yield and quality, with particular emphasis on crop rotation (Smith et al., 2017), planting density (Zheng et al., 2021), fertilization (Dragicčvic et al., 2022), and irrigation (Hussain et al., 2020). In our study, tillage practices had a significant impact on the crude fat and total soluble sugar content of maize grains, with a lesser influence on crude protein and total starch content. We suggest that this outcome may be attributed to the enhancement of soil moisture through tillage practices and the associated ecological benefits. The tillage effects on the examined traits were generally less pronounced than the effects of environment, variety, and input level and could be demonstrated conclusively in interaction with input levels (Šíp et al., 2013). In this context, our study yielded diverse experimental findings—for instance, the total soluble sugar content of grain exhibited the highest variability of 17.27% among varieties and 25.43% among tillage methods. The tillage method and varietal interaction significantly affected the nutrient quality of maize grains (Harish et al., 2022). Upon comparing to CK, the other tillage methods resulted in varying degrees of changes in the nutrient quality components of the grains, with different patterns observed for different varieties. Upon comparing with CK, the other treatments resulted in varying degrees of changes in the nutrient quality components of the grains, with different patterns observed for different varieties. Tillage and straw return treatments led to a reduction in the crude protein and total soluble sugar content of XY696 and XM6 grains, although the decrease in crude protein content was not significant for both varieties; the total soluble sugar content decreased by 4.98%–25.43% and 5.75%–22.42%, respectively. Additionally, the tillage and straw return treatments increased the grain crude fat content of XY696 and XM6 by 4.34%–8.87% and 3.49%–9.67%, respectively. Notably, XM6 exhibited a higher range of increase of grain crude fat content in response to tillage and straw return treatments compared to XY696.

4.3 Relationship between grain filling characteristics and nutritional quality

The chemical composition and quality of crop grains are shaped during the accumulation of dry matter and the growth, development, and maturation of organs or tissues. The accumulation of nutrients in cereal crop grains does not occur at a uniform rate; there is a slight increase in dry matter at the beginning of grain filling, the fastest accumulation of dry matter at the milk ripening stage, and a slower increase at the wax ripening stage (Sala et al., 2007). During this stage, there is a significant transport of soluble sugars and non-protein nitrogenous compounds (mainly amino acids) from the plant's nutrient organs to the reproductive organs, where they are synthesized into starch and proteins in the grains (Yang et al., 2018; Liu et al., 2022b). During grain filling, the majority of sugars originate from the upper leaves, particularly the flag leaves, while protein accumulation is primarily dependent on nitrogenous compounds transported by the nutrient organs, with minimal reliance on materials absorbed by the root system after flowering (Mu et al., 2018; Sun et al., 2022). The quantity and quality of nitrogen-containing compounds undergo further changes as the seed matures (Zhao et al., 2022). In terms of the relationship between grain filling characteristics and nutritional quality, this study identified a strong correlation between grain crude fat and total starch content and the filling rate parameters at all stages (V1, V2, and V3) as well as a high correlation with the duration of the middle and late filling stages (T2 and T3). The differences in the correlation between grain nutrient quality fractions and filling rate parameters suggest variations in the physiological mechanisms involved in synthesizing nutrient quality fractions, leading to different outcomes. Specifically, under normal ripening conditions, protein synthesis primarily occurs at the beginning of the grain filling period, while starch synthesis is limited. As the milk-to-wax ripening period commences, sugar transport to the grain intensifies, and starch synthesis becomes more dominant than protein synthesis. Toward the end of the grain development period, sugar transport to the grain weakens or ceases, while nitrogen inputs continue (Kim et al., 2020). This study also revealed that certain parameters of the grain filling rate, which exhibited a high correlation with grain crude fat and total starch content, played varying roles in influencing the increase of grain crude fat and total starch content, particularly regarding the degree of influence and the regulatory direction.

In our study, we found that differences in grain nutrient quality components among different tillage treatments did not show significant variations between different growth seasons. Taking into consideration the relationship between grain filling characteristics and the content of grain nutrient quality components, we believe that ripening of the grains may have mitigated the impact of grain filling rate and duration at different stages on the component content of grain nutrients. Furthermore, notable studies have successfully predicted maize yield and grain nutritional quality in the absence of crop damage (Guo et al., 2021, Guo et al., 2022, Guo et al., 2023). As such, we aim to incorporate this research aspect into our forthcoming field trials to achieve efficient and high-throughput acquisition of experimental data.

5 Conclusion

The appropriate application of tillage measures can significantly affect the 100-grains weight of maize and regulate the content of various nutrient components in grains. The change in grain filling rate significantly influences the variation in the content of nutrient components in grains. Among them, the grain filling rate during the gradual increasing phase is the most important parameter affecting the total starch content of grains, while the grain crude fat content is closely related to the grain filling rates during the gradual increasing and slow increasing phases. The DPR tillage method showed greater improvement in the characteristics of grain filling and grain nutrient quality components, so we suggest that the DPR tillage

method should be adopted during maize cultivation in the Western Region of Inner Mongolia. Moreover, we recommend that future research should further investigate the regulation of dry matter accumulation in grains after the long-term implementation of tillage methods. It is advisable to study the effects of proper tillage method implementation on agro-economic aspects.

Data availability statement

The raw data supporting the conclusions of this article will be made available by the authors, without undue reservation.

Author contributions

L-QW: Conceptualization, Data curation, Writing – original draft. X-FY: Data curation, Writing – original draft, Writing – review & editing. J-LG: Conceptualization, Writing – review & editing. D-LM: Data curation, Writing – review & editing. H-YL: Writing – original draft. S-PH: Investigation, Writing – review & editing.

Funding

The author(s) declare financial support was received for the research, authorship, and/or publication of this article. This study was supported by the National Maize Industrial Technology Systems (grant no. CARS-02–50), capacity building project of Key Laboratory of Crop Cultivation and Genetic Improvement of Inner Mongolia Autonomous Region (BR221019), Science and Technology Innovation Projects for High Yield and Efficiency of Grain (grant no. 2017YFD0300804), Key Laboratory of Crop Cultivation and Genetic Improvement of Inner Mongolia Autonomous Region (2021PT0004), Inner Mongolia Science and Technology Major Special Project (2021ZD0003–1), and the Crop Science Observation and Experiment Station in Loess Plateau of North China, Ministry of Agriculture, P.R. of China (grant no. 25204120).

Conflict of interest

The authors declare that the research was conducted in the absence of any commercial or financial relationships that could be construed as a potential conflict of interest.

Publisher's note

All claims expressed in this article are solely those of the authors and do not necessarily represent those of their affiliated organizations, or those of the publisher, the editors and the reviewers. Any product that may be evaluated in this article, or claim that may be made by its manufacturer, is not guaranteed or endorsed by the publisher.

References

Abu-Hamdeh, N. (2003). Compaction and subsoiling effects on corn growth and soil bulk density. *Soil Sci. Soc Am. J.* 67, 1213–1219. doi: 10.2136/sssaj2003.1213

Atif, M., and Perveen, S. (2023). Maize grain nutritional quality amelioration with seed-applied thiamine and indole-3-acetic acid under arsenic toxicity. *Environ. Dev. Sustain.* 26, 7827–7855. doi: 10.1007/s10668-023-03037-y

Blanco-Canqui, H., Hassim, R., Shapiro, C., Jasa, P., and Klopp, H. (2022). How does no-till affect soil-profile compactibility in the long term. *Geoderma* 425, 116016. doi: 10.1016/j.geoderma.2022.116016

Chen, N., Li, X.-Y., Šimůnek, J., Shi, H.-B., Hu, Q., and Zhang, Y.-H. (2021). Evaluating the effects of biodegradable and plastic film mulching on soil temperature in a drip-irrigated field. *Soil Till Res.* 213, 105116. doi: 10.1016/j.still.2021.105116

Chu, P.-F., Zhang, Y.-L., Yu, Z.-W., Gao, Z.-J., and Shi, Y. (2016). Winter wheat grain yield, water use, biomass accumulation and remobilisation under tillage in the North China Plain. *Field Crops Res.* 193, 43–53. doi: 10.1016/j.fcr.2016.03.005

Daynard, T., Tanner, J., and Duncan, W. (1971). Duration of the grain filling period and its relation to grain yield in corn, zed mays L. *Crop Sci.* 11, 45–48. doi: 10.2135/cropsci1971.0011183X001100010015x

Deng, T., Wang, J.-H., Gao, Z., Shen, S., Liang, X.-G., Zhao, X., et al. (2023). Late split-application with reduced nitrogen fertilizer increases yield by mediating source–sink relations during the grain filling stage in summer maize. *Plants* 12, 625. doi: 10.3390/plants12030625

Dragicčvic, V., Brankov, M., Stoiljković, M., Tolimir, M., Kanatas, P., Travlos, I., et al. (2022). Kernel color and fertilization as factors of enhanced maize quality. *Front. Plant Sci.* 13. doi: 10.3389/fpls.2022.1027618

Fang, H., Gu, X.-B., Jiang, T.-C., Yang, J.-Y., Li, Y.-N., Huang, P., et al. (2020). An optimized model for simulating grain-filling of maize and regulating nitrogen application rates under different film mulching and nitrogen fertilizer regimes on the Loess Plateau, China. *Soil Till Res.* 199, 104546. doi: 10.1016/j.still.2019.104546

Gasura, E., Setimela, P., Edema, R., Gibson, P.-T., Okori, P., and Tarekegne, A. (2013). Exploiting grain-filling rate and effective grain-filling duration to improve grain yield of early-maturing maize. *Crop Sci.* 53, 2295–2303. doi: 10.2135/cropsci2013.01.0032

Godde, C.-M., Thorburn, P.-J., Biggs, J.-S., and Meier, E.-A. (2016). Understanding the impacts of soil, climate, and farming practices on soil organic carbon sequestration: A simulation study in Australia. *Front. Plant Sci.* 7. doi: 10.3389/fpls.2016.00661

Guo, Y.-H., Chen, S.-Z., Li, X. X., Cunha, M., Jayavelu, S., Cammarano, D., et al. (2022). Machine learning-based approaches for predicting SPAD values of maize using multi-spectral images. *Remote Sens.* 14, 1337. doi: 10.3390/rs14246290

Guo, Y.-H., Fu, Y.-S., Hao, F.-H., Zhang, X., Wu, W.-X., Jin, X.-L., et al. (2021). Integrated phenology and climate in rice yields prediction using machine learning methods. *Ecol. Indic.* 120, 106935. doi: 10.1016/j.ecolind.2020.106935

Guo, Y.-H., Xiao, Y., Hao, F.-H., Zhang, X., Chen, J.-H., Beurs, K.-D., et al. (2023). Comparison of different machine learning algorithms for predicting maize grain yield using UAV-based hyperspectral images. *Int. J. Appl. Earth Obs. Geoinformation.* 124, 103528. doi: 10.1016/j.jag.2023.103528

Harish, M., Choudhary, A.-K., Kumar, S., Dass, A., Singh, V., Sharma, V., et al. (2022). Double zero tillage and foliar phosphorus fertilization coupled with microbial inoculants enhance maize productivity and quality in a maize–wheat rotation. *Sci. Rep.* 12, 3161. doi: 10.1038/s41598-022-07148-w

He, L.-Y., Lu, S.-X., Wang, C.-G., Mu, J., Zhang, Y.-L., and Wang, X.-D. (2021). Changes in soil organic carbon fractions and enzyme activities in response to tillage practices in the Loess Plateau of China. *Soil Till Res.* 209, 104940. doi: 10.1016/j.still.2021.104940

Hussain, S., Maqsood, M., Ijaz, M., Ul-Allah, S., Sattar, A., Sher, A., et al. (2020). Combined application of potassium and zinc improves water relations, stay green, irrigation water use efficiency, and grain quality of maize under drought stress. *J. Plant Nutr.* 43, 2214–2225. doi: 10.1080/01904167.2020.1765181

Jin, Z.-Q., Shah, T., Zhang, L., Liu, H.-Y., and Peng, S.-B. (2020). Effect of straw returning on soil organic carbon in rice–wheat rotation system: A review. *Food Energy Secur.* 9, 200. doi: 10.1002/fes3.200

Kim, J.-T., Yi, G., Kim, M.-J., Son, B.-Y., Bae, H.-H., Go, Y.-S., et al. (2020). Glycolysis stimulation and storage protein accumulation are hallmarks of maize (Zea mays L.) grain flling. *Appl. Biol. Chem.* 63, 54. doi: 10.1186/s13765-020-00538-6

Li, R.-P., Zhang, J.-Y., Xie, R.-Z., Ming, B., Peng, X.-H., Luo, Y., et al. (2022a). Potential mechanisms of maize yield reduction under short-term no-tillage combined with residue coverage in the semi-humid region of Northeast China. *Soil Till Res.* 217, 105289. doi: 10.1016/j.still.2021.105289

Li, S., Hu, M.-J., Shi, J.-L., and Tian, X.-H. (2022b). Improving long-term crop productivity and soil quality through integrated straw-return and tillage strategies. *Agron. J.* 114, 1500–1511. doi: 10.1002/agj2.20831

Liu, L., Cao, H.-L., Geng, Y.-N., Zhang, Q.-F., Bu, X., and Gao, D.-M. (2022a). Response of soil microecology to different cropping practice under Bupleurum chinense cultivation. *BMC Microbiol.* 22, 223. doi: 10.1186/s12866-022-02638-3

Liu, X.-W., Yu, Y.-H., Huang, S.-B., Xu, C.-C., Wang, X.-Y., Gao, J., et al. (2022b). The impact of drought and heat stress at flowering on maize kernel filling: Insights from the field and laboratory. *Agric. For. Meteorol.* 312, 103733. doi: 10.1016/j.agrformet.2021.108733

Mu, X.-H., Chen, Q.-W., Chen, F.-J., Yuan, L.-X., and Mi, G.-H. (2018). Dynamic remobilization of leaf nitrogen components in relation to photosynthetic rate during grain filling in maize. *Plant Physiol. Biochem.* 129, 27–34. doi: 10.1016/j.plaphy.2018.05.020

Olmedo, P.-L., and Vyn, T.-J. (2021). Dry matter gains in maize kernels are dependent on their nitrogen accumulation rates and duration during grain filling. *Plants* 10, 1222. doi: 10.3390/plants10061222

Pecci, L.-C., Grove, J., Miguez, F., and Poffenbarger, H. (2021). Long-term no-till increases soil nitrogen mineralization but does not affect optimal corn nitrogen fertilization practices relative to inversion tillage. *Soil Till Res.* 213, 105080. doi: 10.1016/j.still.2021.105080

Qin, W., Hu, C.-S., and Oenema, O. (2015). Soil mulching significantly enhances yields and water and nitrogen use efficiencies of maize and wheat: a meta-analysis. *Sci. Rep.* 5, 16210. doi: 10.1038/srep16210

Ren, H., Jiang, Y., Zhao, M., Qi, H., and Li, C.-F. (2021). Nitrogen supply regulates vascular bundle structure and matter transport characteristics of spring maize under high plant density. *Front. Plant Sci.* 11. doi: 10.3389/fpls.2020.602739

Rubio, V., Quincke, A., and Ernst, O. (2021). Deep tillage and nitrogen do not remediate cumulative soil deterioration effects of continuous cropping. *Agron. J.* 113, 5584–5596. doi: 10.1002/agj2.20927

Sainju, U.-M., Lenssen, A.-W., Caesar, T., and Evans, R.-G. (2009). Dryland crop yields and soil organic matter as influenced by long-term tillage and cropping sequence. *Agron. J.* 101, 243–251. doi: 10.2134/agronj2008.0080x

Sala, R.-G., Andrade, F.-H., and Westgate, M.-E. (2007). Maize kernel moisture at physiological maturity as affected by the source–sink relationship during grain filling. *Crop Sci.* 47, 711–714. doi: 10.2135/cropsci2006.06.0381

Shao, Y.-H., Xie, Y.-X., Wang, C.-Y., Yue, J.-Q., Yao, Y.-Q., Li, X.-D., et al. (2016). Effects of different soil conservation tillage approaches on soil nutrients, water use and wheat-maize yield in rainfed dry-land regions of North China. *Eur. J. Agron.* 81, 37–45. doi: 10.1016/j.eja.2016.08.014

Šíp, V., Vavera, R., Chrpová, J., Kusá, H., and Růžek, P. (2013). Winter wheat yield and quality related to tillage practice, input level and environmental conditions. *Soil Till Res.* 132, 77–85. doi: 10.1016/j.still.2013.05.002

Smith, E.-G., Zentner, R.-P., Campbell, C.-A., Lemke, R., and Brandt, K. (2017). Long-term crop rotation effects on production, grain quality, profitability, and risk in the northern great plains. *Agron. J.* 109, 957–967. doi: 10.2134/agronj2016.07.0420

Sun, G.-Y., Meng, Y., Wang, Y., Zhao, M., Wei, S., and Gu, W.-R. (2022). Exogenous hemin optimized maize leaf photosynthesis, root development, grain filling, and resource utilization on alleviating cadmium stress under field condition. *J. Soil Sci. Plant Nutr.* 22, 631–646. doi: 10.1007/s42729-021-00674-y

Tan, C.-J., Cao, X., Yuan, S.-A., Wang, W.-Y., Feng, Y.-Z., and Qiao, B. (2015). Effects of long-term conservation tillage on soil nutrients in sloping fields in regions characterized by water and wind erosion. *Sci. Rep.* 5, 17592. doi: 10.1038/srep17592

Wang, C.-Y., Liang, Y., Liu, J.-Z., Yuan, J.-C., Ren, J., Geng, Y.-D., et al. (2023a). The relationship of soil organic carbon and nutrient contents to maize yield as affected by maize straw return modes. *Appl. Sci.* 13, 12448. doi: 10.3390/app132212448

Wang, Z., Sun, J., Du, Y.-D., and Niu, W.-Q. (2021). Conservation tillage improves the yield of summer maize by regulating soil water, photosynthesis and inferior kernel grain filling on the semiarid Loess Plateau, China. *J. Sci. Food Agric.* 102, 2330–2341. doi: 10.1002/jsfa.11571

Wang, F.-G., Wang, L.-Q., Yu, X.-F., Gao, J.-L., Ma, D.-L., Guo, H.-H., et al. (2023b). Effect of planting density on the nutritional quality of grain in representative high-yielding maize varieties from different eras. *Agriculture* 13, 1835. doi: 10.3390/agriculture13091835

Wang, X.-Z., Zhou, H., Huang, Y.-X., and Ji, J.-T. (2022). Variation of subsoiling effect at wing mounting heights on soil properties and crop growth in wheat–maize cropping system. *Agriculture* 12, 1684. doi: 10.3390/agriculture12101684

Xing, T.-T., Cai, A.-D., Lu, C.-A., Ye, H.-L., Wu, H.-L., Huai, S.-C., et al. (2022). Increasing soil microbial biomass nitrogen in crop rotation systems by improving nitrogen resources under nitrogen application. *J. Integr. Agric.* 21, 1488–1500. doi: 10.1016/S2095-3119(21)63673-0

Xu, X.-R., An, T.-T., Zhang, J.-M., Sun, Z.-H., Schaeffer, S., and Wang, J.-K. (2019b). Transformation and stabilization of straw residue carbon in soil affected by soil types, maize straw addition and fertilized levels of soil. *Geoderma* 337, 622–629. doi: 10.1016/j.geoderma.2018.08.018

Xu, J., Han, H.-F., Ning, T. Y., Li, Z.-J., and Lai, R. (2019a). Long-term effects of tillage and straw management on soil organic carbon, crop yield, and yield stability in a wheat-maize system. *Field Crops Res.* 233, 33–40. doi: 10.1016/j.fcr.2018.12.016

Yang, H., Gu, X.-T., Ding, M.-Q., Lu, W.-P., and Lu, D.-L. (2018). Heat stress during grain filling affects activities of enzymes involved in grain protein and starch synthesis in waxy maize. *Sci. Rep.* 8, 15665. doi: 10.1038/s41598-018-33644-z

Yao, S.-H., Teng, X.-L., and Zhang, B. (2015). Effects of rice straw incorporation and tillage depth on soil puddlability and mechanical properties during rice growth period. *Soil Till Res.* 146, 125–132. doi: 10.1016/j.still.2014.10.007

Yu, B.-G., Chen, X.-X., Zhou, C.-X., Ding, T.-B., Wang, Z.-H., and Zou, C.-Q. (2022). Nutritional composition of maize grain associated with phosphorus and zinc fertilization. *J. Food Compos. Anal.* 114, 104775. doi: 10.1016/j.jfca.2022.104775

Yu, X.-F., Qu, J.-W., Hu, S.-P., Xu, P., Chen, Z.-X., Gao, J.-L., et al. (2023). The effect of tillage methods on soil physical properties and maize yield in Eastern Inner Mongolia. *Eur. J. Agron.* 147, 126852. doi: 10.1016/j.eja.2023.126852

Yuan, M.-W., Greer, K.-D., Nafziger, E.-D., Villamil, M.-B., and Pittelkow, C.-M. (2018). Soil N_2O emissions as affected by long-term residue removal and no-till practices in continuous corn. *GCB Bioenergy.* 10, 972–985. doi: 10.1111/gcbb.12564

Yue, K., Li, L.-L., Xie, J.-H., Wang, L.-L., Liu, Y.-Q., and Anwar, S. (2022). Tillage and nitrogen supply affects maize yield by regulating photosynthetic capacity, hormonal changes and grain filling in the Loess Plateau. *Soil Till Res.* 218, 105317. doi: 10.1016/j.still.2022.105317

Zhai, L.-C., Wang, Z.-B., Song, S.-J., Zhang, L.-H., Zhang, Z.-B., and Jia, X.-L. (2021). Tillage practices affects the grain filling of inferior kernel of summer maize by regulating soil water content and photosynthetic capacity. *Agr Water Manage.* 245, 106600. doi: 10.1016/j.agwat.2020.106600

Zhai, L.-C., Xu, P., Zhang, Z.-B., Li, S.-K., Xie, R.-Z., Zhai, L.-F., et al. (2017). Effects of deep vertical rotary tillage on dry matter accumulation and grain yield of summer maize in the Huang-Huai-Hai Plain of China. *Soil Till Res.* 170, 167–174. doi: 10.1016/j.still.2017.03.013

Zhang, X.-T., Wang, J., Feng, X.-Y., Yang, H.-S., Li, Y.-L., Yakov, K., et al. (2023). Effects of tillage on soil organic carbon and crop yield under straw return. *Agr Ecosyst. Environ.* 354, 108543. doi: 10.1016/j.agee.2023.108543

Zhang, Q., Wang, S.-L., Zhang, Y.-H., Li, H.-Y., Liu, P.-Z., Wang, R., et al. (2021). Effects of subsoiling rotational patterns with residue return systems on soil properties, water use and maize yield on the semiarid Loess Plateau. *Soil Till Res.* 214, 105186. doi: 10.1016/j.still.2021.105186

Zhang, P., Wei, T., Jia, Z.-K., Han, Q.-F., and Ren, X.-L. (2014). Soil aggregate and crop yield changes with different rates of straw incorporation in semiarid areas of northwest China. *Geoderma* 230-231, 41–49. doi: 10.1016/j.geoderma.2014.04.007

Zhang, P., Wei, T., Li, Y.-L., Wang, K., Jia, Z.-K., Han, Q.-F., et al. (2015). Effects of straw incorporation on the stratification of the soil organic C, total N and C:N ratio in a semiarid region of China. *Soil Till Res.* 153, 28–35. doi: 10.1016/j.still.2015.04.008

Zhao, C.-B., Li, Q., Hu, N.-N., Yin, H.-H., Wang, T.-C., Dai, X.-L., et al. (2022). Improvement of structural characteristics and *in vitro* digestion properties of zein by controlling postharvest ripening process of corn. *Food Control.* 142, 109221. doi: 10.1016/j.foodcont.2022.109221

Zheng, B.-Q., Zhang, X.-Q., Wang, Q., Li, W.-Y., Huang, M., Zhou, Q., et al. (2021). Increasing plant density improves grain yield, protein quality and nitrogen agronomic efficiency of soft wheat cultivars with reduced nitrogen rate. *Field Crops Res.* 267, 108145. doi: 10.1016/j.fcr.2021.108145

frontiers | Frontiers in Plant Science

TYPE Original Research
PUBLISHED 26 June 2024
DOI 10.3389/fpls.2024.1414844

OPEN ACCESS

EDITED BY
Xiaoli Hui,
Northwest A&F University, China

REVIEWED BY
Kevin Kosola,
Bayer Crop Science, United States
Lizhen Zhang,
China Agricultural University, China

*CORRESPONDENCE
Haiqiu Yu
yuhaiqiu@syau.edu.cn
Zhanxiang Sun
sunzx67@163.com

†These authors have contributed equally to this work and share first authorship

RECEIVED 09 April 2024
ACCEPTED 03 June 2024
PUBLISHED 26 June 2024

CITATION
Dong Q, Zhao X, Sun Y, Zhou D, Lan G, Pu J, Feng C, Zhang H, Shi X, Liu X, Zhang J, Sun Z and Yu H (2024) Border row effects improved the spatial distributions of maize and peanut roots in an intercropping system, associated with improved yield. *Front. Plant Sci.* 15:1414844. doi: 10.3389/fpls.2024.1414844

Border row effects improved the spatial distributions of maize and peanut roots in an intercropping system, associated with improved yield

Qiqi Dong[1†], Xinhua Zhao[1†], Yuexin Sun[1], Dongying Zhou[1], Guohu Lan[1], Junyu Pu[1], Chen Feng[2,3], He Zhang[1], Xiaolong Shi[1], Xibo Liu[1], Jing Zhang[4], Zhanxiang Sun[2*] and Haiqiu Yu[1,5*]

[1]College of Agronomy, Shenyang Agricultural University, Shenyang, Liaoning, China, [2]Tillage and Cultivation Research Institute, Liaoning Academy of Agricultural Sciences, Shenyang, Liaoning, China, [3]National Agricultural Experimental Station for Agricultural Environment, Fuxin, Liaoning, China, [4]College English Department, Shenyang Agricultural University, Shenyang, Liaoning, China, [5]School of Agriculture and Horticulture, Liaoning Agricultural Vocational and Technical College, Yingkou, Liaoning, China

Background: Border row effects impact the ecosystem functions of intercropping systems, with high direct interactions between neighboring row crops in light, water, and nutrients. However, previous studies have mostly focused on aboveground, whereas the effects of intercropping on the spatial distribution of the root system are poorly understood. Field experiments and planting box experiments were combined to explore the yield, dry matter accumulation, and spatial distribution of root morphological indexes, such as root length density (RLD), root surface area density (RSAD), specific root length (SRL), and root diameter (RD), of maize and peanut and interspecific interactions at different soil depths in an intercropping system.

Results: In the field experiments, the yield of intercropped maize significantly increased by 33.45%; however, the yield of intercropped peanut significantly decreased by 13.40%. The land equivalent ratio (LER) of the maize–peanut intercropping system was greater than 1, and the advantage of intercropping was significant. Maize was highly competitive (A = 0.94, CR=1.54), and the yield advantage is mainly attributed to maize. Intercropped maize had higher RLD, RSAD, and SRL than sole maize, and intercropped peanut had lower RLD, RSAD, and SRL than sole peanut. In the interspecific interaction zone, the increase in RLD, RSAD, SRL, and RD of intercropped maize was greater than that of intercropped peanut, and maize showed greater root morphological plasticity than peanut. A random forest model determined that RSAD significantly impacted yield at 15–60 cm, while SRL had a significant impact at 30–60 cm. Structural equation modeling revealed that root morphology indicators had a greater effect on yield at 30–45 cm, with interactions between indicators being more pronounced at this depth.

Conclusion: These results show that border-row effects mediate the plasticity of root morphology, which could enhance resource use and increase productivity. Therefore, selecting optimal intercropping species and developing sustainable intercropping production systems is of great significance.

KEYWORDS

maize-peanut intercropping, interspecific interaction, root length density, root surface area density, special root length, root diameter

1 Introduction

Intercropping is a sustainable and intensive cropping pattern that has the advantages of improving crop yields (Liu et al., 2020; Zou et al., 2021) and land use efficiency (Yu et al., 2015; Feng et al., 2021), inhibiting weeds, and reducing pests and diseases (Brooker et al., 2015; Beillouin et al., 2021; Chadfield et al., 2022). Many previous studies have confirmed that intercropping of gramineous and leguminous crops has yield advantages, for instance, intercropping of maize and soybean, maize and peanut (Li et al., 2019), and sorghum and soybean (Wang et al., 2021a). Studies have shown that the "solar corridor crop system" or other intercropping designs can open up light access to lower portions of the maize canopy, increasing light interception and light energy efficiency in intercropped maize (Kremer and Deichman, 2014a). When this design is used with peanuts as the intercrop, the content and conversion efficiency of precursors for chlorophyll synthesis are also increased (Lu et al., 2023), thereby improving canopy light energy efficiency and promoting increased yield (Nelson, 2014; Wang et al., 2020; Wang et al., 2021b). In addition, soil quality in this system was improved through increased organic carbon and nitrogen content, efficient nutrient cycling, and increased microbial activity (Kremer and Deichman, 2014b). It was evident that the existence of competitive and complementary roles among intercrops is one of the important factors influencing yield advantage. These are among the reasons why intercropping results in a yield advantage, with the aboveground and underground parts affecting the productivity.

Based on complementary effects, combinations of deep-rooted and shallow-rooted crops are used to obtain soil resources at different depths and alleviate underground competition, which enable sufficient resource use and growth by both species (Hassan et al., 2019; Oburger et al., 2022). It was demonstrated that, in the intercropping system of proso millet and mung bean, the root length density, root surface area density, and root volume density of the dominant crop, proso millet, increased in the top soil layer, which helped to absorb more soil moisture and enhance the water use efficiency of proso millet (Gong et al., 2020). Compared with legumes, intercropped maize had more plasticity in root morphology, with greater variation in root length density, root weight density, and total root surface area. Maize's root system occupied more soil space in the intercropping, which inhibited the lateral distribution of root length density in the legume crop (Yang et al., 2022). The maize/soybean strip intercropping system promoted root growth and distribution in both crops, resulting in 72.15% and 15.72% increase in root length density in maize and soybean, respectively, as well as improved soil water use and productivity (Te et al., 2023).

Our previous study showed that the maize and peanut root interactions improved soil nitrogen utilization, exhibiting a nitrogen utilization advantage for side-row maize (Dong et al., 2022; Zhao et al., 2022a). Side-row maize was larger than the middle-row ones in terms of both above-ground partial light competition and below-ground nitrogen utilization, showing a border-row effects, for example, in a wheat–maize strip intercropping system, the absorbed photosynthetically active radiation of side-row wheat was higher than that of middle-row wheat, and side-row maize did not show an advantage in absorbing photosynthetically active radiation due to interspecific competition (Wang et al., 2017). In the maize–soybean strip intercropping system, the root system of maize extended into the side rows of the soybean rows and was concentrated in the 0–20-cm soil layer. Intercropping also increased the soil moisture and nitrate content of the side-row maize in the 20–60 cm soil layer (Shen et al., 2023). Previous studies have focused on the border-row effect on root distribution, soil nutrient, and water use. However, there are fewer studies on the effects of border-row effect on the spatial distribution characteristics of maize and peanut roots and on exploring the potential effects on crop yields.

We hypothesized that differences in root morphological characteristics and the spatial distribution of roots caused by border-row effects influenced productivity in maize–peanut intercropping systems. This study was conducted with field experiments and planting box experiments to explore the differences in yield, dry matter accumulation, root morphology, and interspecific interactions between maize and peanut under the three planting patterns of sole maize, sole peanut, and maize and

Abbreviations: SM, sole maize; SP, sole peanut; IM, intercropped maize; IP, intercropped peanut; LER, land equivalent ratio; A, aggressivity; CR, competitive ratio; RLD, root length density; RSAD, root surface area density; SRL, specific root length; RD, root diameter.

peanut intercropping. The main purposes are to (1) alter the maize and peanut yields under sole and intercropping planting patterns, (2) determine the differences in the root characteristics and spatial distribution of maize and peanut under sole and intercropping systems, and (3) quantify the correlation between interspecific interactions and root morphological indicators of maize and peanut in intercropping systems. Additionally, this investigation sought to analyze the plasticity of root morphology and spatial distribution in maize–peanut intercropping systems from the point of view of competition and facilitation. The results highlight the border-row effects on the spatial distribution and productivity of the root system of each crop in the intercropping system, which is important for the improvement and promotion of maize–peanut intercropping systems in the future.

2 Materials and methods

2.1 Experimental site

This experiment was carried out in the experimental field of Shenyang Agricultural University at the Crop Cultivation Science Observation Station in Northeast China of the Ministry of Agriculture and Rural Areas (41°82′ N, 123°56′ E) from 2020 to 2021. The monthly average temperature was 19.75°C, and the monthly average precipitation was 120.69 mm in the growing season (Supplementary Figure S1). The soil was brown loam, which was classified according to the Chinese Soil Taxonomy. Before the 2020 experiment, the soil contained 14.59 g·kg^{-1} of organic matter, 178.07 mg·kg^{-1} of available nitrogen, 43.82 mg·kg^{-1} of available phosphorus, and 201.86 mg·kg^{-1} of available potassium, with a pH of 6.5. Before the 2021 experiment, the soil contained 14.85 g·kg^{-1} of organic matter, 199.64 mg·kg^{-1} of available nitrogen, 56.87 mg·kg^{-1} of available phosphorus, and 213.36 mg·kg^{-1} of available potassium, with a pH of 6.5.

2.2 Experimental design

A single-factor randomized block design was used with three planting patterns: sole maize (SM), sole peanut (SP), and an 8:8 rotational strip intercropping of maize and peanut (IMP), with three replications (Figure 1A). Intercropped maize strips and intercropped peanut strips were rotated interannually from 2020 to 2021 to prevent issues related to continuous peanut cropping and maintain soil fertility. The row spacing in the sole maize and intercropped maize strips was 50 cm, the plant spacing was 25 cm, and the plant density was 66,670 plants·hm^{-2}. The row spacing in the sole peanut and intercropped peanut strips was 50 cm, the plant spacing was 12.3 cm, and the density was 271,016 plants·hm^{-2}. Planting proceeded from north to south, covering a length of 10 m. The width of the maize–peanut intercropped strips was 3.5 m, and the band width was 8.0 m. There were 24 rows with only maize and only peanut. The area of the maize and peanut only plots was 120 m^2, and the area of the intercropping plots was 80 m^2.

To better analyze the changes in root spatial distribution at different soil depths, a planting box experiment was carried out (Figure 1B) with three planting patterns (three repetitions): SM, SP, and IMP. To replicate the field conditions and reduce damage to the field soil during destructive harvesting, this experiment was

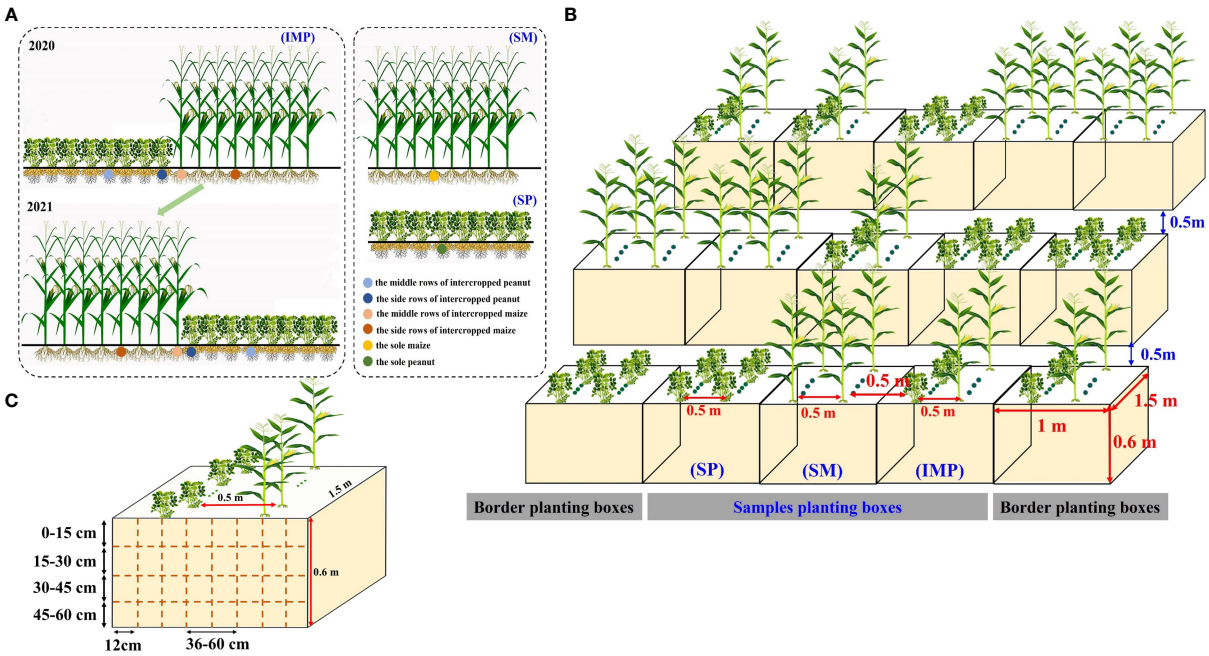

FIGURE 1
Schematic diagram of the planting pattern. **(A)** Row configuration and sampling positions for the field experiment. **(B)** Row configuration for the planting box experiment. **(C)** Sampling positions for the planting box experiment. SM, sole maize; SP, sole peanut; IMP, intercropping of maize and peanut. 0–36 cm: peanut inner row, 36–60 cm: interaction zone, 60–96 cm: maize inner row.

established near the field experiment. Although our planting box experiment may lead to certain limitations (reduced shading of peanuts by maize compared to the field experiment), we ensured consistency with the field experiment, e.g., (1) ensured that the planting direction (north–south) of maize and peanuts was the same as what actually occurred in the field experiment and (2) the planting boxes for each treatment were closely spaced, but the aisle distance between each replication was 0.5 m (Figure 1B). Soil was collected from the 0–20 cm soil layer in the long-term field experiment. After the soil was dried, it was filtered through a 2-mm sieve, and 1,000 kg of soil was placed in each box. One row of maize and one row of peanut were planted in the intercropping box, with a row spacing of 50 cm, maize plant spacing of 25 cm, and peanut plant spacing of 6 cm. The planting boxes with sole maize and sole peanut had two rows of maize and two rows of peanut, respectively, and the row spacing and plant spacing were the same as those in the intercropping system. The amounts of fertilizer applied in the field experiment and planting box experiment are shown in Supplementary Table S1. Other cultivation and management practices were the same as those in conventional field production.

The maize variety was the hybrid Liangyu 99, which was supplied by Dandong Denghai Liangyu Seed Industry Co., Ltd., and the peanut variety was Nonghua 9, which was supplied by the Peanut Research Institute of Agricultural College of Shenyang Agricultural University. Maize and peanut were sown on May 15, 2020 and May 18, 2021 and harvested on September 19, 2020 and September 18, 2021, respectively.

2.3 Sampling

2.3.1 Yield and dry matter accumulation

The yields of maize and peanut were measured at the harvest stage in the 2020–2021 field experiments. In the plots with only maize and only peanut, all the plants in the 2 m long maize or peanut strip within each row for four consecutive rows were harvested. In the maize–peanut intercropped plots, all the plants in the 2 m long maize or peanut strip within each row for four consecutive rows were harvested. The grains were sun-dried and weighed after threshing by hand.

At the harvest stage, three maize plants and three peanut plants were collected in intercropped maize (IM), the middle row of intercropped maize (MIM), intercropped peanut (IP), the middle row of intercropped peanut (MIP), SM, and SP in the field experiments (Figure 1A), and three repetitions of this collection were performed. In the planting box experiment, one maize plant and three peanut plants were collected in IM, IP, SM, and SP, with three repetitions (Figure 1B). The roots, stems, leaves, and grain/pod parts were separated and dried at 105°C for 30 min and 80°C to constant weight for dry matter accumulation.

2.4 Spatial distribution of root morphology

In the flowering and needle setting stage of peanut in 2020–2021, root sampling was conducted for IMP, SM, and SP of the planting box experiment (with three repetitions) to determine the root spatial distribution. A long-bladed knife and an iron plate were used to cut the soil into blocks. The soil samples were taken in layers of 15 cm each and at a volume of $20 \times 12 \times 15$ cm^3 (Figure 1C). The soil samples were placed in mesh bags and washed with water until the roots could be clearly identified. The roots of maize and peanut can be distinguished by color, texture, and branching pattern. Maize roots are white and smooth, while those of peanuts are brown with nodules. The root samples were scanned with an EpsonPerfection V700 root scanner and then analyzed with WinRHIZO root analysis software to determine the root length, root surface area, and average root diameter. Finally, the roots were dried at 80°C in an oven and weighed.

2.5 Calculations

2.5.1 Land equivalent ratio

The land equivalent ratio (LER) was used to assess the advantage of intercropping systems (Ma et al., 2019). LER was calculated as follows:

$$\mathrm{LER} = \frac{\mathrm{Yim} \times \mathrm{Pm}}{\mathrm{Ysm}} + \frac{\mathrm{Yip} \times \mathrm{Pp}}{\mathrm{Ysp}} \quad (1)$$

where Yim and Ysm are the yields of (kg hm^{-2}) intercropped maize and sole maize, respectively. Yip and Ysp are the yields of (kg hm^{-2}) intercropped peanut and sole peanut, respectively. Pm and Pp are the sown proportion of maize and peanut in the intercropping system (Pm = 1/2 and Pp = 1/2), respectively. LER greater than 1.0 indicates interspecific stimulation and a land use advantage from intercropping. Conversely, when LER is less than 1.0, there is no advantage from intercropping.

2.5.2 Interspecies interaction index

Aggressivity (A) is an index that measures interspecies competition in intercropping systems by comparing the yields of intercropping and single cropping as well as their respective land occupancies (Dhima et al., 2007; Yin et al., 2019).

$$A = \frac{\mathrm{Yim}}{\mathrm{Ysm} \times \mathrm{Pm}} - \frac{\mathrm{Yip}}{\mathrm{Ysp} \times \mathrm{Pp}} \quad (2)$$

where A is the aggressiveness of maize relative to peanut in the intercropping systems. If A is greater than 0, the competitiveness of maize is greater than that of peanut in the intercropping system; otherwise, maize is less competitive.

The system productivity (kg hm^{-2}) represents the productivity of the entire intercropping system (Gong et al., 2020).

$$\text{System productivity} = \mathrm{Yim} \times \mathrm{Pm} + \mathrm{Yip} \times \mathrm{Pp} \quad (3)$$

The competitive ratio (CR) is another indicator used to assess the competitiveness of different species in intercropping systems (Liu et al., 2015).

$$\mathrm{CR} = \frac{\mathrm{Yim}}{\mathrm{Ysm} \times \mathrm{Pm}} \Big/ \frac{\mathrm{Yip}}{\mathrm{Ysp} \times \mathrm{Pp}} \quad (4)$$

where CR is the competitiveness of maize relative to peanut. If CR is greater than 1.0, the competitiveness of maize is higher than that of peanut in the intercropping system. Otherwise, the competitiveness is lower than that of peanut.

2.5.3 Root length density

Root length density (RLD) is the root length per unit soil volume (cm cm^{-3}), which was calculated with the following formula (Zhang et al., 2011):

$$RLD = \frac{L}{V} \quad (5)$$

where L is the root length (cm) and V is the volume of the soil sample (3,600 cm^3).

2.5.4 Root surface area density

Root surface area density (RSAD) is the root surface area per unit soil volume (cm^2 cm^{-3}), which was calculated with the following formula (Duan et al., 2017):

$$RSAD = \frac{S}{V} \quad (6)$$

where S is the root surface area (cm^2) and V is the volume of the soil sample (3600 cm^3).

2.5.6 Specific root length

SRL is the ratio of root length to root weight and shows the relationship between root penetration intensity and underground biomass allocation (Wang et al., 2014).

$$SRL = \frac{L}{DW} \quad (7)$$

where L is the root length (cm) and DW is the root weight of the soil sample.

2.6 Statistical analysis

The yield, dry matter accumulation, and interspecific interaction index in field experiments were assessed by one-way analysis of variance (ANOVA) with Duncan's test, and maize and peanut dry matter accumulation in the planting box experiment were assessed by Student's *t*-test using SPSS 26.00 (IBM SPSS Inc., NY, USA). Differences were considered statistically significant at $P< 0.05$. Origin 2023 (Origin Lab Corporation, Northampton, MA, United States) was used to map root length density, root surface area density, specific root length, and root diameter. The yield per plant and the root morphological indexes of maize and peanut were normalized by principal component analysis (PCA). Pearson correlation analysis was performed to examine the potential relationship between the maize and peanut root morphological indexes and the yield per plant of maize and peanut. The random forest model evaluated the significant predictors affecting yield per plant, including root length density, root surface area density, specific root length, and root diameter. These analyses were conducted using the random forest software package. The model significance and predictor importance were verified using the rfUtilities and rfPermute packages in the R software, respectively (Ju et al., 2023; Yuan et al., 2023). Structural equation modeling (SEM) was conducted using the R "piecewiseSEM" package to evaluate the direct and indirect relationships among yield per plant, root length density, root surface area density, specific root length, and root diameter (Jing et al., 2023; Zhao et al., 2023b).

3 Results

3.1 Changes in maize and peanut yields, interspecific interactions, and dry matter accumulation in field experiments

In the field experiments, compared with that of SM, the yield of IM significantly increased by 33.45% (2-year average, Table 1). Compared with that of SP, the yield of intercropped peanut significantly decreased by 13.40% (2-year average, Table 1). In 2020–2021, LER exceeded 1, indicating that intercropping of maize and peanut had advantages and improved the utilization of land resources (Table 1). On average, the 2-year productivity of the system was 8,748.34 kg hm^{-2}. In addition, A exceeded 1, and a significant effect was observed between years (Table 1), indicating that maize was a dominant crop and had a greater competitiveness in the intercropping system. This result was supported by the CR, with a 2-year average greater than 1, and maize had a greater competitiveness than peanuts (Table 1).

In the field experiment, the changes in dry matter accumulation per plant of maize and peanut order was IM > MIM > SM, SP > MIP > IP (Supplementary Figure S2). Compared with those of SM, the roots, stems, leaves, and grain dry matter accumulation of IM

TABLE 1 Changes in maize and peanut yields and interspecies interaction in field experiments.

Planting patterns	2020	2021	2-year average
SM	10,631.39 ± 4.11	10,756.94 ± 4.11	10,694.17 ± 0.42
IM	14,555.56 ± 5.85**	13,986.39 ± 4.19**	14,270.97 ± 5.02
SP	3,796.44 ± 5.67**	3,652.78 ± 0.25**	3,724.61 ± 2.92
IP	3,305.56 ± 1.34	3,145.83 ± 1.67	3,225.69 ± 0.72
LER	1.12	1.08	1.1
System productivity (kg hm^{-2})	8,930.56	8,566.11	8,748.34
Aggressivity (A)	1	0.88	0.94
Competitive ratio (CR)	1.57	1.51	1.54

* and ** indicate significant differences between different planting patterns at $P< 0.05$ and $P< 0.01$, respectively.
SM, sole maize; SP, sole peanut; IM, intercropped maize; IP, intercropped peanut. LER, Land equivalent ratio; based on Equation (1); A, Aggressivity; based on Equation (2); System productivity based on Equation (3); CR, Competitive ratio; based on Equation (4).

significantly increased by 32.42%, 34.52%, 11.78%, and 45.09%, respectively (2-year average, Supplementary Figure S2A). Compared with those of SP, the underground and aboveground dry matter accumulation of IP significantly decreased by 45.23%, 44.36%, 51.61%, and 60.25%, respectively (2-year average, Supplementary Figure S2B).

3.2 Changes in maize and peanut yield per plant and dry matter accumulation in planting box experiments

In the planting box experiments, compared with that of SM, the yield per plant of IM significantly increased by 16.4% (2-year average, Table 2). Compared with that of SP, the yield per plant of IP significantly decreased by 61.65% (2-year average, Table 2). The changes in dry matter accumulation of maize and peanut were consistent with those in the field experiment. Compared with those of SM, the roots, stems, leaves, and grain dry matter accumulation of IM significantly increased by 24.4%, 14.14%, 7.38%, and 20.14%, respectively (2-year average, Supplementary Figure S3A). Compared with those of SP, the roots, stems, leaves, and grain dry matter accumulation of IP significantly decreased by 28.95%, 47.84%, 31.19%, and 60.06%, respectively (2-year average, Supplementary Figure S3B).

3.3 Interspecific interaction alters the spatial distribution of maize and peanut root length density

In general, the RLD of maize and peanut in the maize inner row, peanut inner row, and interaction zone significantly decreased with increasing soil depth. Compared with that of SM, the RLD of IM in the maize inner row increased by 69.01% and 42.67% at the 45–60 and 0–15 cm soil layers, respectively (2-year average, Figures 2A-D). The RLD of IM in the interspecies interactive zone decreased by 7.29% and 9.4% at the 0–15 and 15–30 cm soil layers and increased by 29.42% and 74.74% at the 30–45 and 45–60 cm soil layers, respectively (2-year average, Figures 2A–D). The RLD of IP was higher than that of SP at each soil depth, and the RLD in the peanut inner row increased by 1.65%, 1.76%, 3.86%, and 5.05%, respectively (2-year average, Figures 2E–H). The RLD of IP in the interspecific interaction zone decreased by 4.48%, 10.80%, 7.28%, and 5.66% with increasing soil depth (2-year average, Figures 2E–H).

TABLE 2 Changes in maize and peanut yields in a planting box experiment.

Planting patterns	2020	2021	2-year average
SM	304 ± 4.98*	270 ± 0.72**	287
IM	331 ± 2.34	355 ± 0.36	343
SP	22 ± 1.07**	21 ± 0.81**	21.5
IP	8.50 ± 0.90	8 ± 0.6	8.25

* and ** indicate significant differences between different planting patterns at $P< 0.05$ and $P< 0.01$, respectively.
SM, sole maize; SP, sole peanut; IM, intercropped maize; IP, intercropped peanut.

3.4 Interspecific interaction alters the spatial distribution of maize and peanut root surface area density

The IM root system extended to the area planted with peanut and into deeper soil layers. The root distributions of SP and IP were limited to the space below the peanut plants (Figure 3). In general, the RSAD of maize and peanut in the maize inner row, peanut inner row, and interaction zone decreased significantly with increasing soil depth. Compared with that of SM, the RSAD of IM in the maize inner row increased by 10.3%, 13.71%, and 43.07% at 0–15, 15–30, and 45–60 cm, respectively (Figures 3A, B). The RSAD of IM in the interaction zone increased by 45.54% and 21.12% at 0–15 cm and 15–30 cm, respectively. Compared with that of SP, the RSAD of IP in the peanut inner row decreased by 12.15%, 12.55%, 42.48% and 38.70% at each soil depth, respectively. The RSAD of IP in the interaction zone decreased by 8.70%, 31.81%, 33.89%, and 33.92% at 0–15, 15–30, 30–45, and 45–60 cm, respectively (Figures 3E, F).

3.5 Interspecific interaction alters the spatial distribution of maize and peanut specific root length

Figure 4 represents the spatial distributions of the SRL of maize and peanut under different planting patterns. In general, the SRL of maize and peanut in the maize inner row, peanut inner row, and interaction zone significantly increased with increasing soil depth. Compared with that of SM, the SRL of IM in the maize inner row increased by 22.59% and 113.06% at soil depths of 0–15 and 45–60 cm, respectively (2-year average, Figures 4A–D). In the interspecific interaction zone, the SRL of IM decreased by 9.32% and 12.24% at soil depths of 0–15 and 15–30 cm and increased by 16.91% and 80.65% at soil depths of 30–45 and 45–60 cm, respectively (2-year average, Figures 4A–D). Compared with that of SP, the SRL of IP in the peanut inner row increased by 90.28%, 19.91%, and 74.35% in the 0–15, 15–30, and 30–45 cm soil depths, respectively (2-year average, Figures 4E–G). In the interspecific interaction zone, the SRL of IP increased by 13.98%, 22.27%, 3.90%, and 37.77% at each soil depth (2-year average, Figures 4E–G).

3.6 Interspecific interaction alters the spatial distribution of maize and peanut root diameter

Figure 5 presents the spatial distribution of the RD of maize and peanut under different planting patterns. In general, the RD of

10.3389/fpls.2024.1414844

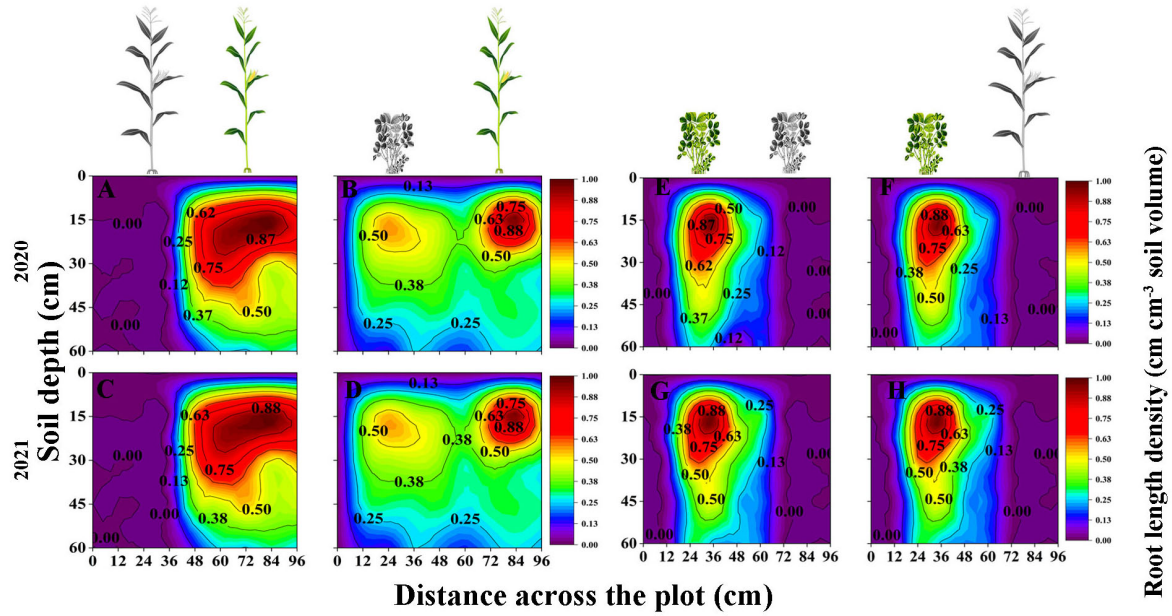

FIGURE 2
Spatial distribution of root length density (RLD, cm cm^{-3}, based on Equation 5) of maize and peanut in different planting patterns. **(A, C)** sole maize (SM), **(B, D)** intercropped maize (IM), **(E, G)** sole peanut (SP), **(F, H)** intercropped peanut (IP), 0-36 cm: peanut inner row, 36-60 cm: interaction zone, 60-96 cm: maize inner row. The colour scale shows the normalized value of root length density (cm cm^{-3}).

maize and peanut in the maize inner row, peanut inner row, and interaction zone significantly decreased with increasing soil depth. Compared with that of SM, the RD of IM in the maize inner row increased by 100.91%, 52.15%, 41.48%, and 33.41% at soil depths of 0–15, 15–30, 30–45, and 45–60 cm, respectively (2-year average, Figures 5A–D). The RD of IM in the interaction zone increased by 66.09%, 14.91%, 7.32%, and 9.33% at soil depths of 0–15, 15–30, 30–45, and 45–60 cm, respectively (2-year average, Figures 5A–D). Compared with that of SP, the RD of IP in the peanut inner row decreased by 9.03%, 10.14%, 13.63%, and 12.63% at soil depths of 0–15, 15–30, 30–45, and 45–60 cm, respectively (2-year average, Figures 5E, F). In the interaction zone, the RD of IP decreased by 11.38%, 24.80%, 10.07%, and 22.32% at soil depths of 0–15, 15–30, 30–45, and 45–60 cm, respectively (2-year average, Figures 5E, F).

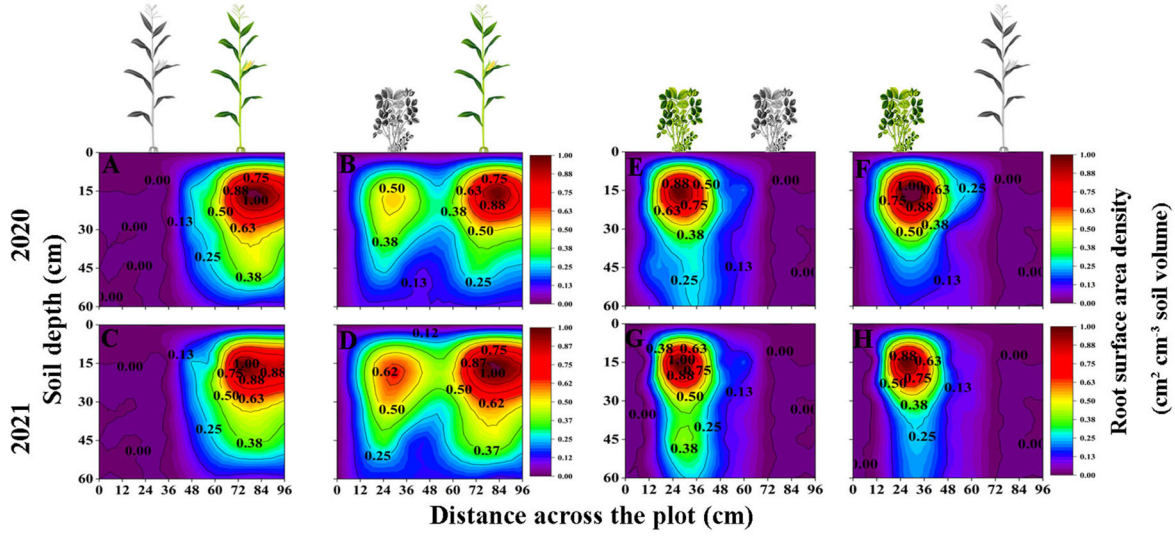

FIGURE 3
Spatial root surface area density (RSAD, cm^2 cm $^{-3}$, based on Equation 6) distributions of maize and peanut in different planting patterns. **(A, C)** sole maize (SM), **(B, D)** intercropped maize (IM), **(E, G)** sole peanut (SP), **(F, H)** intercropped peanut (IP), 0-36 cm: peanut inner row, 36-60 cm: interaction zone, 60-96 cm: maize inner row. The colour scale shows the normalized value of root surface area density (cm^2 cm $^{-3}$).

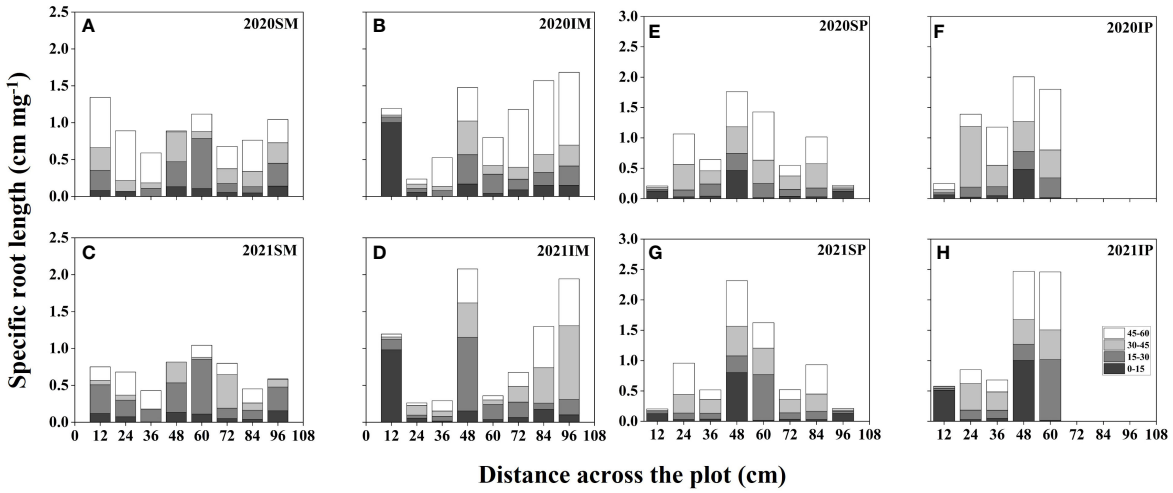

FIGURE 4
Specific root length (SRL, cm mg $^{-1}$, based on Equation 7) spatial distributions of maize and peanut in different planting patterns. **(A, C)** sole maize (SM), **(B, D)** intercropped maize (IM), **(E, G)** sole peanut (SP), **(F, H)** intercropped peanut (IP), SM, sole maize; IM, intercropped maize; SP, sole peanut; IP, intercropped peanut. 0-36 cm: peanut inner row, 36-60 cm: interaction zone, 60-96 cm: maize inner row.

3.7 Correlation analysis of yield, dry matter accumulation, and root morphology

Principal component analysis indicated that there was a positive relationship between maize RD and RSAD at a soil depth of 0–45 cm, between RLD and RSAD at a soil depth of 45–60 cm (Supplementary Figures S4A–D), and between peanut RD and RSAD at a soil depth of 0–60 cm (Supplementary Figures S4E, F). The Pearson correlation analysis revealed that maize RLD, RSAD, SRL, and RD were negatively correlated with maize yield per plant at soil depths of 0–60 cm (Supplementary Figure S5A). RLD, RSAD, SRL, and RD were positively correlated with peanut yield per plant at 0–60 cm soil depth, with RLD having the strongest correlation at 15–45 cm soil depth (Supplementary Figure S5B). A random forest model was used to assess the key factors affecting yield formation, and RSAD significantly affected yield at 15–60 cm. The SRL had a significant impact yield at 30–60 cm (Figures 6A–D). The results of structural equation modeling showed that root morphology indicators had a greater effect on yield with increasing soil depth, with a peak at 30–45 cm. The interaction between root morphology indicators was also more pronounced at 30–45 cm (Figures 6E–G).

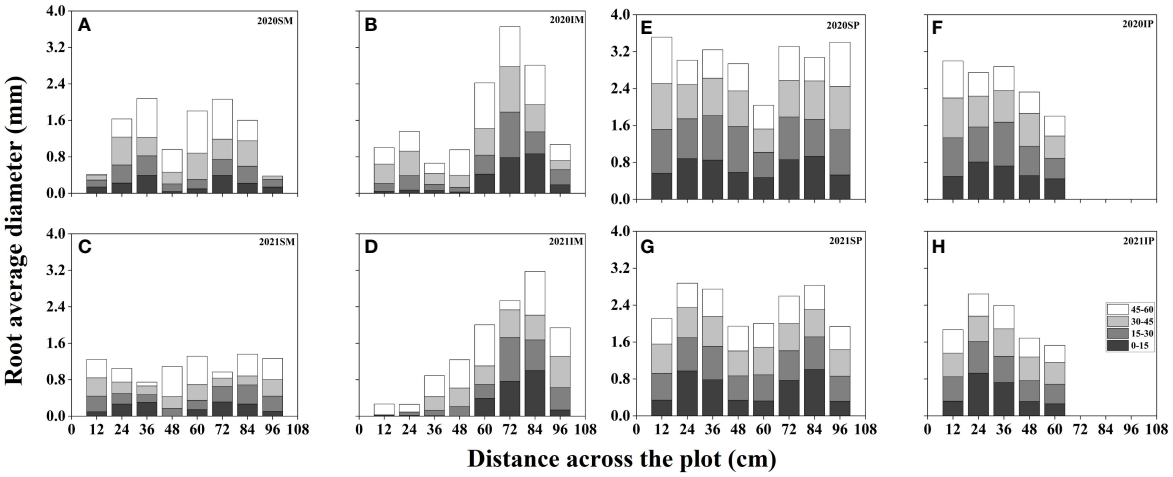

FIGURE 5
Spatial root diameter (RD, mm) distributions of maize and peanut in different planting patterns. **(A, C)** sole maize (SM), **(B, D)** intercropped maize (IM), **(E, G)** sole peanut (SP), **(F, H)** intercropped peanut (IP), SM, sole maize; IM, intercropped maize; SP, sole peanut; IP, intercropped peanut. 0-36 cm: peanut inner row, 36-60 cm: interaction zone, 60-96 cm: maize inner row.

4 Discussion

4.1 Yield and interspecific interactions in maize and peanut intercropping systems

Interactions between intercropping species contribute to intercropping yield advantages. Furthermore, dry matter accumulation is one of the important factors affecting yield (Zhang et al., 2022), which was demonstrated in this study. Similar results in the field experiment and planting box experiment demonstrated that the aboveground and underground dry matter accumulation of intercropped maize was significantly higher than that of sole maize, and the aboveground and underground dry matter accumulation of intercropped peanut was significantly lower than that of sole peanut (Supplementary Figures S2, S3). Importantly, the yield of intercropped maize was significantly higher than that of sole maize, and the yield of intercropped peanut was lower than that of sole peanut (Tables 1, 2), consistent with the results of Li et al. (2019), indicating that the yield advantage of the intercropping system was mainly attributed to maize. This result supports objective 1 and can be explained by border-row effects, with the dominant species (maize) obtaining more resources in a maize–peanut intercropping system, which favors a yield advantage. Previous studies have shown that border row maize yields were on average 48% higher than middle rows, and border row peanut yields were on average 29% lower than middle rows (Wang et al., 2020). This is similar to the findings of this study, where changes in the proportion of border rows significantly affected the relative yield of the crop. This indicated that the intercropping system changes the light environment and promotes dry matter accumulation. Maize, as a C4 crop, not only is characterized by having high rates of photosynthesis but also achieves high levels of light interception and utilization efficiency because of height, which helps to promote sink and source capacities (Gou et al., 2017; Feng et al., 2020). It was observed in a maize alfalfa intercropping study that with a 75–134% increase in nitrogen fixation to give alfalfa the nitrogen it needed for growth, there was a 1.24–

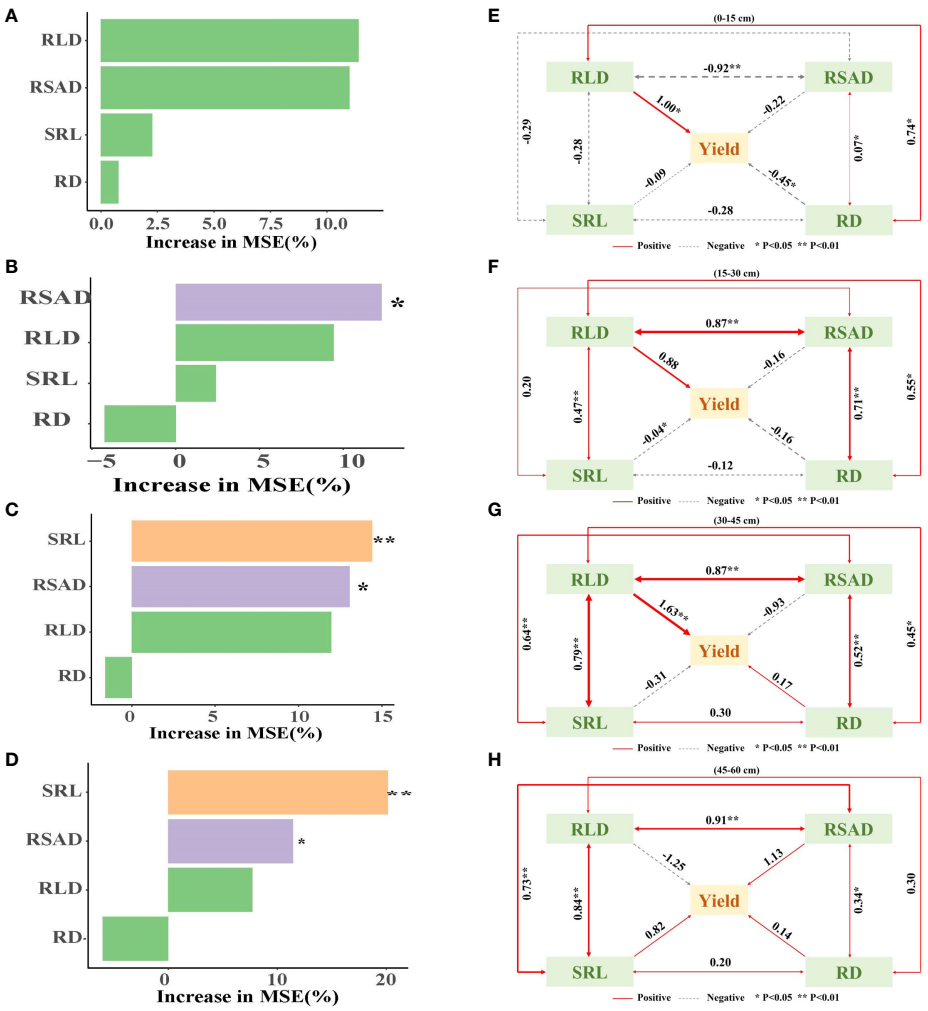

FIGURE 6
Maize and peanut root morphology indexes drive yield formation. **(A–D)** Relationships between yield per plant and root length density, root surface area density, specific root length and root diameter. **(E–H)** Structural equation model (SEM) of direct and indirect effects of the yield per plant, root length density, root surface area density, specific root length and root diameter. RLD, root length density; RSAD, root surface area density; SRL, specific root length; RD, root diameter. *$0.01 < p \leq 0.05$, **$0.001 < p \leq 0.01$.

1.42-fold increase in nitrogen transfer to maize nitrogen (Shao et al., 2021). This is due to the interspecific competition that reduces mineral N in alfalfa rhizosphere soil and increases N fixation, which also supported complementary utilization. Thus, we speculated that in maize–peanut intercropping systems, maize, which has a side-row advantage, receives more light, nutrients, and resources than peanut (Supplementary Figure S6). These results suggested that maize yield was increased and yield advantages were achieved due to the border-row effects in the intercropping system.

The LER is one of the indicators used to assess land use efficiency in intercropping systems (Martin-Guay et al., 2018). We found that the LER was greater than 1 (Table 1). The results of the current study were consistent with the reported productivity of maize and peanut intercropping systems worldwide, i.e., the average LER was 1.31 (Feng et al., 2021). Maize and peanut intercropping has yield advantages and can lead to more efficient use of land resources than sole cropping; plant combinations of species, especially C3/C4 crop combinations, will greatly improve agricultural land use efficiency (Yu et al., 2015; Zhao et al., 2023a). The results were further validated by an analysis of the competitive abilities of the constituent crops. Highly competitive species have access to better ecological niches and gain more resources in intercropping systems, which is one of the reasons for the yield advantage in intercropping systems (Li et al., 2001; Bi et al., 2019; Wu et al., 2023). The *A* (0.94) and CR (1.54) values demonstrate the superior competitiveness of maize over peanuts in the intercropping system (Table 1). The results indicate that maize occupied superior ecological niches and had higher competitiveness than peanut. Conversely, because of the short stature of peanut, intercropping with maize led to a competitive disadvantage (Luo et al., 2021).

The morphological and spatial distribution of roots effectively reflects the ability of crops to compete for nutrients and water in intercropping systems (Ma et al., 2019; Zhao et al., 2022b). The results supported the third objective, that is, the spatial distribution of root length density (Figure 2), root surface area density (Figure 3), and root diameter (Figure 5) promoted the competitiveness of maize, and the spatial distributions of root surface area density and root diameter were suppressed in peanut, which was a weak competitor. Previous studies have shown that in maize–soybean intercropping systems, the root length of intercropped maize and the root length density of intercropped maize increased by 17.97%–44%, while the root length density of intercropped soybean decreased by 30.69%–46.46% (Wei et al., 2022). Maize showed greater root morphological plasticity than legumes, and the changes in root length density, root weight density, and total root surface area in an intercropping system were greater than those in sole cropping (Yang et al., 2022). Consequently, the spatial distribution characteristics of root morphological indexes in response to interspecific interactions can explain the phenomenon of high yields in maize–peanut intercropping (Zhang et al., 2023). This result answers our aim 3, that the dominant species, maize, had higher root length density and root surface area density than peanut in the intercropping system. Differences in the response of root morphological indicators to interspecific effects are a factor in the yield advantage of intercropped maize.

In this study, intercropped maize in the maize inner row had higher RLD, RSAD, and RD than sole maize at each soil depth (Figures 2–5). Compared with sole peanut, intercropped peanut in the peanut inner row had higher RSAD and RD at each soil depth (Figures 3, 5). In addition, the intercropped maize root system extended into the peanut row and below the space occupied by peanut. Additionally, RLD, RSAD, and RD were higher in intercropped maize than in sole maize in the interspecific interaction zone, while RSAD and RD were lower in intercropped peanut than in sole peanut. This result indicated that maize had a competitive advantage in the intercropping system, with optimized root distribution, expanded nutrient absorption area, and increased nutrient acquisition efficiency, resulting in the maximization of the utilization rate of soil resources (Fort et al., 2014; Oram et al., 2018). Thus, well-developed fine roots and an optimized root distribution promote nutrient uptake by crops (Zheng et al., 2022).

Previous studies have shown that temporal or spatial niche differentiation of species influences interspecific competition and resource access (Zhang et al., 2015; Homulle et al., 2021). In the overlapping part of the root system, that is, the interspecific interaction zone, the increase in RLD, RSAD, SRL, and RD of intercropped maize was greater than that of intercropped peanut (Figures 2–5), indicating that maize showed greater root morphological plasticity than peanut. The strong competitiveness of maize optimizes the distribution of root morphology and enhances its ability to compete with neighboring peanuts for water and nutrients (Christina et al., 2023; Wei et al., 2024). Moreover, this explains the decrease in the RSAD and RD of intercropped peanut. Since the root distribution of intercropped maize extends below the peanut plants, occupying a larger soil space, the lateral distribution of peanut roots is reduced. Thus, differences in root morphology between intercropped maize and intercropped peanut lead to less niche overlap and drive positive complementary effects (Yu et al., 2022; Zhao et al., 2022b).

4.2 The correlation between yield and the spatial distribution of root morphology

In this study, the PCA results showed a positive correlation between RLD and RSAD at soil depths of 45–60 cm (Supplementary Figure S4), suggesting an interaction that could impact yield (Gao et al., 2024). Pearson's analysis showed that the effect of root morphological indicators on crop yield varied in soils of different depths (Supplementary Figure S5). The effects of RLD and RSAD on crop yield were gradually revealed with increasing soil depth. In particular, the effect of RSAD on yield has been significant in the 15–60 cm depth range, while SRL also had a significant effect on yield at 30–60 cm. This suggested that there was a positive correlation between root morphological indicators and yield in certain soil depth ranges. For example, Zhang et al. (2014) demonstrated that root length density and root diameter decreased and specific root length increased in intercropped walnut and intercropped wheat compared to sole walnut and sole wheat due to underground root competition, which resulted in lower yields and biomass for both crops. This provides a new

perspective for a deeper understanding of the relationship between root characteristics and crop yield at different soil levels. Moreover, structural equation modeling showed that the correlation of root morphology indicators with yield increased progressively as soil depth increased, reaching its peak at 30–45 cm (Figure 6). Meanwhile, the interaction between root morphology indicators was also more pronounced in the 30-45 cm soil layer, which may have a synergistic effect on yield. These results suggest that the spatial distributions of maize and peanut roots in intercropping systems show great plasticity and importance in regulating maize and peanut productivity in response to interspecific competition. This is also consistent with recent research reports (Yang et al., 2022; Zhang et al., 2023) that plasticity and differences in crop root traits were partly responsible for overproduction in maize–legume intercropping systems. The characteristics of root distribution across varying soil depths to strategically implement cultivation practices, with the goal of enhancing the benefits of root spatial distribution and ultimately increasing crop yield and quality (Dhima et al., 2007). By conducting a comprehensive analysis of the correlation between root morphology and yield, this research can offer a scholarly foundation for agricultural practices and facilitate enhancements in crop yield and production efficiency.

5 Conclusion

Maize–peanut intercropping improves yields and land use efficiency through border-row effects. Compared with that of sole maize, the yield of intercropped maize significantly increased, while the yield of intercropped peanut significantly decreased compared with that of sole peanut. Additionally, intercropped maize showed higher *A* (0.94) and CR (1.55), indicating that maize is the dominant species and has a greater competitive ability than peanut. This also indicates that the yield advantage was mainly due to maize border-row effects. Furthermore, the spatial distribution of intercropped maize roots extended below the space occupied by peanuts, especially in the interspecific interaction zone, where the RLD, RSAD, and RD at each soil depth were higher for intercropped maize than for sole maize and the RLD and RSAD of intercropped peanut were lower than those of sole peanut. It is clear that maize exhibits greater root morphological plasticity than peanut, expanding the nutrient uptake area and thus achieving interspecific complementary effects in intercropping systems. Hence, it is essential to understand the responses of root morphology and spatial distribution plasticity to border-row effects in maize–peanut intercropping systems to achieve sustainable agricultural development and efficient use of limited resources.

Data availability statement

The original contributions presented in the study are included in the article/Supplementary Material. Further inquiries can be directed to the corresponding authors.

Author contributions

QD: Data curation, Formal analysis, Writing – original draft. XZ: Funding acquisition, Supervision, Conceptualization, Visualization, Writing – review & editing. YS: Methodology, Project administration, Validation, Writing – review & editing. DZ: Methodology, Project administration, Writing – review & editing. GL: Project administration, Software, Writing – review & editing. JP: Methodology, Project administration, Writing – review & editing. CF: Supervision, Validation, Visualization, Writing – review & editing. HZ: Supervision, Validation, Visualization, Writing – review & editing. XS: Software, Supervision, Writing – review & editing. XL: Supervision, Validation, Writing – review & editing. JZ: Validation, Visualization, Writing – review & editing. ZS: Supervision, Validation, Visualization, Writing – review & editing. HY: Funding acquisition, Supervision, Writing – review & editing.

Funding

The author(s) declare financial support was received for the research, authorship, and/or publication of this article. This work was jointly supported by the Joint Funds of the National Natural Science Foundation of China (U21A20217) and Liaoning Province Science and Technology Plan Project (2022-MS-263).

Acknowledgments

We thank the editors and reviewers for their comments and constructive suggestions, which have been invaluable in improving the quality of our manuscripts. We thank Dr. Chao Zhong for his help in the manuscript revision process.

Conflict of interest

The authors declare that the research was conducted in the absence of any commercial or financial relationships that could be construed as a potential conflict of interest.

Publisher's note

Supplementary material

The Supplementary Material for this article can be found online at: https://www.frontiersin.org/articles/10.3389/fpls.2024.1414844/full#supplementary-material

References

Beillouin, D., Ben-Ari, T., Malezieux, E., Seufert, V., and Makowski, D. (2021). Positive but variable effects of crop diversification on biodiversity and ecosystem services. *Glob. Change Biol.* 27, 4697–4710. doi: 10.1111/gcb.15747

Bi, Y., Zhou, P., Li, S., Wei, Y., Xiong, X., Shi, Y., et al. (2019). Interspecific interactions contribute to higher forage yield and are affected by phosphorus application in a fully-mixed perennial legume and grass intercropping system. *Field Crop Res.* 244, 107636. doi: 10.1016/j.fcr.2019.107636

Brooker, R. W., Bennett, A. E., Cong, W. F., Daniell, T. J., George, T. S., Hallett, P. D., et al. (2015). Improving intercropping: a synthesis of research in agronomy, plant physiology and ecology. *New Phytol.* 206, 107–117. doi: 10.1111/nph.13132

Chadfield, V. G. A., Hartley, S. E., and Redeker, K. R. (2022). Associational resistance through intercropping reduces yield losses to soil-borne pests and diseases. *New Phytol.* 235, 2393–2405. doi: 10.1111/nph.18302

Christina, M., Chevalier, L., Viaud, P., Schwartz, M., Chetty, J., Ripoche, A., et al. (2023). Intercropping and weed cover reduce sugarcane roots colonization in plant crops as a result of spatial root distribution and the co-occurrence of neighboring plant species. *Plant Soil.* doi: 10.1007/s11104-023-06221-1

Dhima, K. V., Lithourgidis, A. S., Vasilakoglou, I. B., and Dordas, C. A. (2007). Competition indices of common vetch and cereal intercrops in two seeding ratio. *Field Crop Res.* 100, 249–256. doi: 10.1016/j.fcr.2006.07.008

Dong, Q., Zhao, X., Zhou, D., Liu, Z., Shi, X., Yuan, Y., et al. (2022). Maize and peanut intercropping improves the nitrogen accumulation and yield per plant of maize by promoting the secretion of flavonoids and abundance of *Bradyrhizobium* in rhizosphere. *Front. Plant Sci.* 13. doi: 10.3389/fpls.2022.957336

Duan, Z. P., Gan, Y. W., Wang, B. J., Hao, X. D., Xu, W. L., Zhang, W., et al. (2017). Interspecific interaction alters root morphology in young walnut/wheat agroforestry systems in northwest China. *Agrofor. Syst.* 93, 419–434. doi: 10.1007/s10457-017-0133-2

Feng, L., Raza, M. A., Shi, J., Ansar, M., Titriku, J. K., Meraj, T. A., et al. (2020). Delayed maize leaf senescence increases the land equivalent ratio of maize soybean relay intercropping system. *Eur. J. Agron.* 118, 126092. doi: 10.1016/j.eja.2020.126092

Feng, C., Sun, Z., Zhang, L., Feng, L., Zheng, J., Bai, W., et al. (2021). Maize/peanut intercropping increases land productivity: A meta-analysis. *Field Crop Res.* 270, 108208. doi: 10.1016/j.fcr.2021.108208

Fort, F., Cruz, P., Jouany, C., and Field, K. (2014). Hierarchy of root functional trait values and plasticity drive early-stage competition for water and phosphorus among grasses. *Funct. Ecol.* 28, 1030–1040. doi: 10.1111/1365-2435.12217

Gao, J., Zhang, Y., Xu, C., Wang, P., Huang, S., and Lv, Y. (2024). Enhancing spatial and temporal coordination of soil water and root growth to improve maize (*Zea mays* L.) yield. *Agric. Water Manage.* 294, 108728. doi: 10.1016/j.agwat.2024.108728

Gong, X., Dang, K., Lv, S., Zhao, G., Tian, L., Luo, Y., et al. (2020). Interspecific root interactions and water-use efficiency of intercropped proso millet and mung bean. *Eur. J. Agron.* 115, 26034. doi: 10.1016/j.eja.2020.126034

Gou, F., van Ittersum, M. K., Simon, E., Leffelaar, P. A., van der Putten, P. E., Zhang, L., et al. (2017). Intercropping wheat and maize increases total radiation interception and wheat RUE but lowers maize RUE. *Eur. J. Agron.* 84, 125–139. doi: 10.1016/j.eja.2016.10.014

Hassan, A., Dresbøll, D. B., Rasmussen, C. R., Lyhne-Kjærbye, A., Nicolaisen, M. H., Stokholm, M. S., et al. (2019). Root distribution in intercropping systems – a comparison of DNA based methods and visual distinction of roots. *Arch. Agron. Soil Sci.* 67, 15–28. doi: 10.1080/03650340.2019.1675872

Homulle, Z., George, T. S., and Karley, A. J. (2021). Root traits with team benefits: understanding belowground interactions in intercropping systems. *Plant Soil.* 471, 1–26. doi: 10.1007/s11104-021-05165-8

Jing, B., Shi, W., Wang, H., and Lin, F. (2023). ^{15}N labeling technology reveals enhancement of nitrogen uptake and transfer by root interaction in cotton/soybean intercropping. *J. Sci. Food Agric.* 103, 6307–6316. doi: 10.1002/jsfa.12704

Ju, W., Moorhead, D. L., Shen, G., Cui, Y., and Fang, L. (2023). Soil aggregate development and associated microbial metabolic limitations alter grassland carbon storage following livestock removal. *Soil Biol. Biochem.* 177, 108907. doi: 10.1016/j.soilbio.2022.108907

Kremer, R. J., and Deichman, C. L. (2014a). Introduction: the solar corridor concept. *Agron. J.* 106, 1817–1819. doi: 10.2134/agronj14.0291

Kremer, R. J., and Deichman, C. L. (2014b). Soil quality and the solar corridor crop system. *Agron. J.* 106, 1853–1858. doi: 10.2134/agronj13.0508

Li, Y. H., Shi, D. Y., Li, G. H., Zhao, B., Zhang, J. W., Liu, P., et al. (2019). Maize/peanut intercropping increases photosynthetic characteristics, ^{13}C-photosynthate distribution, and grain yield of summer maize. *J. Integr. Agric.* 18, 2219–2229. doi: 10.1016/S2095-3119(19)62616-X

Li, L., Sun, J., Zhang, F., Li, X., Yang, S., and Rengel, Z. (2001). Wheat/maize or wheat/soybean strip intercropping I. Yield advantage and interspecific interactions on nutrients. *Field Crop Res.* 71, 123–137. doi: 10.1016/S0378-4290(01)00156-3

Liu, Z., Gao, F., Li, Y., Zhao, J., Wang, Y., Wang, Z., et al. (2020). Grain yield, and nitrogen uptake and translocation of peanut under different nitrogen management systems in a wheat–peanut rotation. *Agron. J.* 112, 1828–1838. doi: 10.1002/agj2.20065

Liu, Y. X., Zhang, W. P., Sun, J. H., Li, X. F., Christie., P., and Li, L. (2015). High morphological and physiological plasticity of wheat roots is conducive to higher competitive ability of wheat than maize in intercropping systems. *Plant Soil.* 397, 387–399. doi: 10.1007/s11104-015-2654-7

Lu, J., Dong, Q., Lan, G., He, Z., Zhou, D., Zhang, H., et al. (2023). Row ratio increasing improved light distribution, photosynthetic characteristics, and yield of peanut in the maize and peanut strip intercropping system. *Front. Plant Sci.* 14. doi: 10.3389/fpls.2023.1135580

Luo, C., Zhu, J., Ma, L., Guo, Z., Dong, K., and Dong, Y. (2021). Effects of nitrogen regulation and strip intercropping on faba bean biomass, nitrogen accumulation and distribution, and interspecific interactions. *Crop Sci.* 61, 4325–4343. doi: 10.1002/csc2.20556

Ma, L., Li, Y., Wu, P., Zhao, X., Chen, X., and Gao, X. (2019). Effects of varied water regimes on root development and its relations with soil water under wheat/maize intercropping system. *Plant Soil.* 439, 113–130. doi: 10.1007/s11104-018-3800-9

Martin-Guay, M. O., Paquette, A., Dupras, J., and Rivest, D. (2018). The new Green Revolution: Sustainable intensification of agriculture by intercropping. *Sci. Total Environ.* 615, 767–772. doi: 10.1016/j.scitotenv.2017.10.024

Nelson, K. A. (2014). Corn yield response to the solar corridor in upstate Missouri. *Agron. J.* 106, 1847–1852. doi: 10.2134/agronj2012.0326C

Oburger, E., Schmidt, H., and Staudinger, C. (2022). Harnessing belowground processes for sustainable intensification of agricultural systems. *Plant Soil.* 478, 177–209. doi: 10.1007/s11104-022-05508-z

Oram, N. J., Ravenek, J. M., Barry, K. E., Weigelt, A., Chen, H., Gessler, A., et al. (2018). Below-ground complementarity effects in a grassland biodiversity experiment are related to deep-rooting species. *J. Ecol.* 106, 265–277. doi: 10.1111/1365-2745.12877

Shao, Z. Q., Zheng, C. C., Postma, J. A., Lu, W. L., Gao, Q., Gao, Y. Z., et al. (2021). Nitrogen acquisition, fixation and transfer in maize/alfalfa intercrops are increased through root contact and morphological responses to interspecies competition. *J. Integr. Agric.* 20, 2240–2254. doi: 10.1016/S2095-3119(20)63330-5

Shen, L., Wang, X., Liu, T., Wei, W., Zhang, S., Keyhani, A. B., et al. (2023). Border row effects on the distribution of root and soil resources in maize–soybean strip intercropping systems. *Soil Tillage Res.* 233, 105812. doi: 10.1016/j.still.2023.105812

Te, X., Din, A. M. U., Cui, K., Raza, M. A., Fraz-Ali, M., and Xiao, J. (2023). Interspecific root interactions and water use efficiency of maize/soybean relay strip intercropping. *Field Crop Res.* 291, 108793. doi: 10.1016/j.fcr.2022.108793

Wang, R. N., Sun, Z. X., Bai, W., Wang, E. L., Wang, Q., Zhang, D. S., et al. (2021b). Canopy heterogeneity with border-row proportion affects light interception and use efficiency in maize/peanut strip intercropping. *Field Crop.Res.* 271, 108239. doi: 10.1016/j.fcr.2021.108239

Wang, R., Sun, Z., Zhang, L., Yang, N., Feng, L., Bai, W., et al. (2020). Border-row proportion determines strength of interspecific interactions and crop yields in maize/peanut strip intercropping. *Field Crop Res.* 253, 107819. doi: 10.1016/j.fcr.2020.107819

Wang, B. J., Zhang, W., Ahanbieke, P., Gan, Y. W., Xu, W. L., Li, L. H., et al. (2014). Interspecific interactions alter root length density, root diameter and specific root length in jujube/wheat agroforestry systems. *Agrofor. Syst.* 88, 835–850. doi: 10.1007/s10457-014-9729-y

Wang, Z., Zhao, X., Wu, P., Gao, Y., Yang, Q., and Shen, Y. (2017). Border row effects on light interception in wheat/maize strip intercropping systems. *Field Crop Res.* 214, 1–13. doi: 10.1016/j.fcr.2017.08.017

Wang, C., Zhou, L., Zhang, G., Gao, J., Peng, F., Zhang, C., et al. (2021a). Responses of photosynthetic characteristics and dry matter formation in waxy sorghum to row ratio configurations in waxy sorghum-soybean intercropping systems. *Field Crop Res.* 263, 108077. doi: 10.1016/j.fcr.2021.108077

Wei, W., Liu, T., Shen, L., Wang, X., Zhang, S., and Zhang, W. (2022). Effect of maize (*Zeal mays*) and soybean (*Glycine max*) intercropping on yield and root development in Xinjiang, China. *Agriculture-Basel* 12, 996. doi: 10.3390/agriculture12070996

Wei, W., Liu, T., Zhang, S., Shen, L., Wang, X., Li, L., et al. (2024). Root spatial distribution and belowground competition in an apple/ryegrass agroforestry system. *Agric. Syst.* 215, 103869. doi: 10.1016/j.agsy.2024.103869

Wu, J., Bao, X., Zhang, J., Lu, B., Zhang, W., Callaway, R. M., et al. (2023). Temporal stability of productivity is associated with complementarity and competitive intensities in intercropping. *Ecol. Appl.* 33, e2731. doi: 10.1002/eap.2731

Yang, H., Xu, H. S., Zhang, W. P., Li, Z. X., Fan, H. X., Lambers, H., et al. (2022). Overyielding is accounted for partly by plasticity and dissimilarity of crop root traits in maize/legume intercropping systems. *Funct. Ecol.* 36, 2163–2175. doi: 10.1111/1365-2435.14115

Yin, W., Fan, Z., Hu, F., Fan, H., Yu, A., Zhao, C., et al. (2019). Straw and plastic mulching enhances crop productivity via optimizing interspecific interactions of wheat–maize intercropping in arid areas. *Crop Sci.* 59, 2201–2213. doi: 10.2135/cropsci2019.02.0082

Yu, Y., Stomph, T. J., Makowski, D., and van der Werf, W. (2015). Temporal niche differentiation increases the land equivalent ratio of annual intercrops: A meta-analysis. *Field Crop Res.* 184, 133–144. doi: 10.1016/j.fcr.2015.09.010

Yu, R. P., Yang, H., Xing, Y., Zhang, W. P., Lambers, H., and Li, L. (2022). Belowground processes and sustainability in agroecosystems with intercropping. *Plant Soil*. 476, 263–288. doi: 10.1007/s11104-022-05487-1

Yuan, J., Wang, J., Ye, J., Dai, A., Zhang, L., Wang, J., et al. (2023). Long-term organic fertilization enhances potassium uptake and yield of sweet potato by expanding soil aggregates-associated potassium stocks. *Agric. Ecosyst. Environ.* 358, 108701. doi: 10.1016/j.agee.2023.108701

Zhang, W., Ahanbieke, P., Wang, B. J., Gan, Y. W., Li, L. H., Christie, P., et al. (2014). Temporal and spatial distribution of roots as affected by interspecific interactions in a young walnut/wheat alley cropping system in northwest China. *Agrofor. Syst.* 89, 327–343. doi: 10.1007/s10457-014-9770-x

Zhang, W. P., Li, Z. X., Gao, S. N., Yang, H., Xu, H. S., Yang, X., et al. (2023). Resistance vs. surrender: Different responses of functional traits of soybean and peanut to intercropping with maize. *Field Crop Res.* 291, 108779. doi: 10.1016/j.fcr.2022.108779

Zhang, W. P., Liu, G. C., Sun, J. H., Zhang, L. Z., Weiner, J., and Li, L. (2015). Growth trajectories and interspecific competitive dynamics in wheat/maize and barley/maize intercropping. *Plant Soil Environ.* 397, 227–238. doi: 10.1007/s11104-015-2619-x

Zhang, D. S., Sun, Z. X., Feng, L. S., Bai, W., Yang, N., Zhang, Z., et al. (2022). Maize plant density affects yield, growth and source-sink relationship of crops in maize/peanut intercropping. *Field Crop Res.* 257, 107926. doi: 10.1016/j.fcr.2020.107926

Zhang, G., Yang, Z., and Dong, S. (2011). Interspecific competitiveness affects the total biomass yield in an alfalfa and corn intercropping system. *Field Crop Res.* 124, 66–73. doi: 10.1016/j.fcr.2011.06.006

Zhao, J., Bedoussac, L., Sun, J., Chen, W., Li, W., Bao, X., et al. (2023a). Competition-recovery and overyielding of maize in intercropping depend on species temporal complementarity and nitrogen supply. *Field Crop Res.* 292, 108820. doi: 10.1016/j.fcr.2023.108820

Zhao, X., Dong, Q., Han, Y., Zhang, K., Shi, X., Yang, X., et al. (2022a). Maize/peanut intercropping improves nutrient uptake of side-row maize and system microbial community diversity. *BMC Microbiol.* 22, 14. doi: 10.1186/s12866-021-02425-6

Zhao, L., He, N., Wang, J., Siddique, K. H. M., Gao, X., and Zhao, X. (2022b). Plasticity of root traits in a seedling apple intercropping system driven by drought stress on the Loess Plateau of China. *Plant Soil Environ.* 480, 541–560. doi: 10.1007/s11104-022-05603-1

Zhao, M., Shen, H., Zhu, Y., Xing, A., Kang, J., Liu, L., et al. (2023b). Asymmetric responses of abundance and diversity of N-cycling genes to altered precipitation in arid grasslands. *Funct. Ecol.* 37, 2953–2966. doi: 10.1111/1365-2435.14434

Zheng, B. C., Zhou, Y., Chen, P., Zhang, X. N., Du, Q., Yang, H., et al. (2022). Maize–legume intercropping promotes N uptake through changing the root spatial distribution, legume nodulation capacity, and soil N availability. *J. Integr. Agric.* 21, 1755–1771. doi: 10.1016/s2095–3119(21)63730–9

Zou, X. X., Shi, P. X., Zhang, C. J., Si, T., Wang, Y. F., Zhang, X. J., et al. (2021). Rotational strip intercropping of maize and peanuts has multiple benefits for agricultural production in the northern agropastoral ecotone region of China. *Eur. J. Agron.* 129, 26304. doi: 10.1016/j.eja.2021.126304

frontiers | Frontiers in Plant Science

TYPE Original Research
PUBLISHED 14 August 2024
DOI 10.3389/fpls.2024.1451073

OPEN ACCESS

EDITED BY
Xiaoli Hui,
Northwest A&F University, China

REVIEWED BY
Xi Chen,
Chinese Academy of Agricultural Sciences, China
Tao Zhang,
Zhejiang Academy of Agricultural Sciences, China
Vlad Stoian,
University of Agricultural Sciences and Veterinary Medicine of Cluj-Napoca, Romania
Kailou Liu,
Jiangxi Institute of Red Soil, China

*CORRESPONDENCE
Haiqing Gong
haiqinggong@cau.edu.cn

RECEIVED 18 June 2024
ACCEPTED 29 July 2024
PUBLISHED 14 August 2024

CITATION
Chen C, Xiang Y, Jiao X and Gong H (2024) Enhancing maize phosphorus uptake with optimal blends of high and low-concentration phosphorus fertilizers. *Front. Plant Sci.* 15:1451073. doi: 10.3389/fpls.2024.1451073

Enhancing maize phosphorus uptake with optimal blends of high and low-concentration phosphorus fertilizers

Chen Chen[1,2], Yue Xiang[2], Xiaoqiang Jiao[2] and Haiqing Gong[2*]

[1]Ministry of Education Key Laboratory for Biodiversity Science and Ecological Engineering, National Observations and Research Station for Wetland Ecosystems of the Yangtze Estuary, College of Life Sciences, Fudan University, Shanghai, China, [2]College of Resources and Environmental Sciences, National Academy of Agriculture Green Development, Key Laboratory of Plant-Soil Interactions, Ministry of Education, Key Laboratory of Low-carbon Green Agriculture, Ministry of Agriculture and Rural Affairs, China Agricultural University, Beijing, China

High-concentration phosphorus (P) fertilizers are crucial for crop growth. However, fertilizers with lower P concentrations, such as calcium magnesium phosphate (CMP) and single super phosphate (SSP), can also serve as efficient P sources, especially when blended with high-concentration P fertilizers like diammonium phosphate (DAP) or monoammonium phosphate (MAP). In this study, we conducted a 48-day pot experiment to explore how blending low-P fertilizers could optimize maize P utilization, using CMP to replace DAP in acidic soil, and SSP to replace MAP in alkaline soil, with five SSP+MAP and CMP+DAP mixtures tested. Key metrics such as shoot and root biomass, shoot P uptake, root length, and soil P bioavailability were measured. We found that maize biomass and P uptake with 100% DAP were comparable to those with 50% CMP and 50% DAP in acidic soil. Similar results were observed for 100% MAP compared to 50% SSP and 50% DAP in alkaline soil. Root biomass and length were largest with 100% MAP in acidic soil and at 100% DAP in alkaline soil, with no significant differences at 50% SSP or CMP substitutions for MAP and DAP, respectively. Furthermore, 50% SSP or CMP substitutions for MAP and DAP increased the content and proportion of the labile inorganic P (Pi) pool (H_2O-Pi and $NaHCO_3$-Pi), had a direct and positive effect on Olsen-P. Our findings reveal that 1:1 blends of SSP and MAP in acidic soil, and CMP and DAP in alkaline soil, effectively meet maize's P requirements without relying solely on high-concentration P fertilizers. This indicates that strategic blending of fertilizers can optimize P use, which is crucial for sustainable agriculture.

KEYWORDS

phosphorus, maize, inorganic phosphorus pool, alkaline soil, acidic soil

1 Introduction

Phosphorus (P) is an essential limiting nutrient for crop yields in cropping systems (Raymond et al., 2021; Janes-Bassett et al., 2022). P fertilizers have been used to increase plant-available soil P concentrations, enhance crop yields, and develop P fertilizer management strategies to achieve optimal P fertilizer inputs (Gong et al., 2022a; Yan et al., 2022). High-concentration P fertilizers [i.e., monoammonium phosphate (MAP) and diammonium phosphate (DAP)] can readily provide P to soil solutions for plant uptake, owing to their high-water solubilities (Chien et al., 2011). However, previous studies have shown that high P solubility is not always necessary for crop production (Chien et al., 2009). Our previous findings also suggested that fertilizers with low P concentrations can be incorporated into fertilizer blends to improve P use efficiency (Gong et al., 2022a). Researchers have attempted to determine a suitable ratio of low- to high-P fertilizers for crop production. For instance, significant enhancement in P uptake was observed when a mixture of DAP and phosphate rock was applied at a 1:4 P ratio (Bindraban et al., 2020). Wheat P uptake was the highest under 20:80 and 10:90 struvite–DAP blend applications compared with those under 100% struvite and 100% DAP applications, indicating that the optimal fertilizer blend contained less struvite than high water-soluble DAP or MAP (Talboys et al., 2016). Despite these efforts, the suitable ratios of low- to high-P fertilizers to optimize P use and promote plant growth remain unclear. Our research aims to fill this gap by investigating the optimal blend ratios of low- and high-P fertilizers to maximize P use efficiency.

The high concentration P in DAP and MAP has high bioavailability, which can stimulate early root development and seedling growth (Nziguheba et al., 2016; Gong et al., 2022b), and subsequently enhancing enhance the uptake of the acidulated low-concentration P fertilizer (Geissler et al., 2019; Weeks et al., 2023). This P supply over time ensures a continuous supply throughout the plant growth cycle. The transformation of soil P involves significant physicochemical changes, including dissolution, precipitation, adsorption, and desorption (Ghodszad et al., 2022; Zheng et al., 2023), contributing to the complex and dynamic equilibrium of different forms of soil P. Fractionated soil P analysis is typically utilized to understand this equilibrium, helping to evaluate the interconversion among various soil P fractions that reflect the different P pools present in the soil (Kim et al., 2023; Zhang et al., 2020). Soil P availability is expected to increase due to the transformation of stable P into labile P forms during early root development and the subsequent application of acidulated low-concentration P fertilizers (Chen et al., 2021; Joshi et al., 2021). Further research is needed to explore how low- and high-concentration P fertilizer blends interact with different soil P fractions under optimal ratios for crop production. This may lead to more accurate predictions of soil P bioavailability and improve soil P management strategies.

Previous studies have largely depended on mineral P, particularly in high-concentration P fertilizers such as DAP and MAP, to formulate P fertilizer management strategies, however, this reliance may lead to low P use efficiency, and an increased risk of P loss and aquatic environmental pollution (Bindraban et al., 2020; Weeks and Hettiarachchi, 2019). Therefore, it is crucial to develop strategies for managing high-concentration P fertilizers. One effective approach involves blending a high-concentration P fertilizer (e.g., MAP or DAP) with a lower P-concentration fertilizer. This strategy aims to provide sufficient early-season P while reducing pollution risks associated with the rapid solubilization of high-concentration P fertilizers (Everaert et al., 2018), thereby improving P use efficiency. By quantifying crop-specific responses to the proportion of low-P fertilizer in the blend could identify the ratios of low- and high-P fertilizers that maximize crop growth potential. Therefore, the objectives of this pot experiment were to: (i) quantify the effects of different ratios of low- and high-P fertilizer blends on maize biomass and P uptake in soils with different pH levels to determine the optimal ratios for the fertilizer blends; (ii) determine the effects of the optimal fertilizer blends on soil P pool transformation; and (iii) explore potential approaches in which low-P fertilizer is used effectively in fertilizer blends to improve maize P uptake. Our findings can serve as a reference for developing efficient P fertilizer management strategies that ensure optimal use of P resources.

2 Materials and methods

2.1 Experimental setup and design

A pot experiment using maize was conducted from May to July 2022 in a greenhouse at the Quzhou Experimental Station of China Agricultural University in Quzhou County, Hebei Province, China. Alkaline soil was collected from Quzhou (Hebei Province), the basic physical and chemical properties of the soil were as follows: pH, 8.13 (in water); soil organic carbon content, 9.69 g kg^{-1}; total nitrogen content, 1.10 g kg^{-1}; soil Olsen-P content, 2.49 mg kg^{-1}; and soil available potassium content, 183 mg kg^{-1}. Acidic red soil was collected from Yuxi (Yunnan Province), the basic physical and chemical properties of the soil were as follows: pH, 5.34 (in water); soil organic carbon content, 3.85 g kg^{-1}; total nitrogen content, 0.80 g kg^{-1}; soil Olsen-P content, 1.42 mg kg^{-1}; and soil available potassium content, 153 mg kg^{-1}. Both soil types were air-dried and sieved through a 2-mm mesh.

One control group and five treatment groups were established for the acidic red soil: no P (CK), 100% calcium magnesium phosphate (100% CMP), 30% CMP and 70% DAP (30% CMP+70% DAP), 50% CMP and 50% DAP (50% CMP+50% DAP), 70% CMP and 30% DAP (70% CMP+30% DAP), and 100% DAP (100% DAP). Similarly, a control and five treatment groups were established for the alkaline soil: no P (CK), 100% single superphosphate (100% SSP), 30% SSP and 70% MAP (30% SSP+70% MAP), 50% SSP and 50% MAP (50% SSP+50% MAP), 70% SSP and 30% MAP (70% SSP+30% MAP), and 100% MAP (100% MAP). Each of the six treatments had four replicates (for a total of 48 pots), and the pots were arranged based on a completely randomized design. Each pot received 150 kg P ha^{-1} of the corresponding fertilizer blend. In the treatments that received

fertilizer, urea, and muriate of potash were applied as nitrogen and potassium sources, respectively. Both nitrogen (N) and potassium (K_2O) were applied at a rate of 150 kg ha^{-1} (Table 1). All fertilizers were incorporated and mixed completely with the soil during planting.

Maize seeds (*Zea mays L.* cv. Zhengdan958) were surface sterilized using 10% (v/v) H_2O_2 for 30 min, washed three times with deionized water, soaked in a supersaturated calcium sulfate ($CaSO_4$) solution for 1 d, and germinated in a dish lined with wet filter paper and covered with an aerated cover for 3 d at 25°C. Uniformly germinated seeds were selected and sown in the pots. The pots were watered daily to 80% field capacity as measured by weight. The temperature in the glasshouse ranged from 20°C at night to 30°C during the day.

2.2 Plant harvesting and sample analysis

The maize plants were harvested after eight weeks. After separating the shoots and roots, the shoots were oven-dried at 105°C for 0.5 h and then dried at 75°C for 4 d to a constant weight. The dry samples were weighed, crushed, and homogenized. Each fraction was dried, and the milled plant samples were digested in a mixture of sulfuric acid and hydrogen peroxide (H_2SO_4-H_2O_2) as described by Wolf (1982). The P concentrations of the digested samples were determined using the standard vanadomolybdate method (Murphy and Riley, 1962). Shoot P uptake was calculated using the dry weights and P concentrations of the different plant parts.

The roots were carefully separated from the soil and shaken to remove any excess soil. All visible roots in each pot were collected from the soil onto a 2 mm diameter mesh and washed with running water in the lab until they were clean. The root samples were spread onto a transparent tray with water and scanned using an EPSON scanner at 400 dpi (Epson Expression 1600 pro, Model EU-35, Japan). The total root lengths were calculated from the images using the WinRHIZO software package (Pro2004b, version 5.0; Regent Instruments Inc., QC, Canada). The roots were then oven-dried and weighed to obtain the biomass.

The soil samples were dried in the open air and sifted through a 2-mm-mesh sieve. After sample digestion with H_2SO_4 and perchloric acid ($HClO_4$), the soil total P was determined using an ultraviolet spectrometer (UV 2500, Shimadzu, Tokyo, Japan). The Olsen-P levels were assessed in $NaHCO_3$ extracts through molybdenum blue colorimetry. The P fractions were assessed using adapted methodologies adapted from Hedley et al. (1982) and Sui et al. (1999). H_2O-Pi was extracted with deionized water, 0.5 M $NaHCO_3$ was employed for $NaHCO_3$-Pi extraction, 0.1 M NaOH was used for NaOH-Pi extraction, and 1 M HCl was employed for HCl-Pi extraction. Subsequently, any remaining P in the soil following the other extraction procedures was quantified through digestion with H_2SO_4-H_2O_2.

2.3 Statistical analysis

Statistical analyses were conducted using IBM SPSS Statistics 20 (IBM Corp., Armonk, NY, USA). One-way analysis of variance (ANOVA) with Tukey's *post-hoc* test ($p < 0.05$) was employed to evaluate variations in shoot biomass, as well as the shoot P uptake, root biomass, root length, and Pi pools, among P fertilization treatments. Simple path analyses of the indicators affecting shoot biomass were also performed using IBM SPSS Statistics 20.

TABLE 1 Fertilization treatments applied in the present study.

Soil	Treatment	Nitrogen (kg N ha^{-1})	Phosphorus (kg P ha^{-1})	Potassium kg K_2O ha^{-1}
Acidic soil	CK	150	0	150
	100% CMP	150	150	150
	70% CMP+30% DAP	150	150	150
	50% CMP+50% DAP	150	150	150
	30% CMP+70% DAP	150	150	150
	100% DAP	150	150	150
Alkaline soil	CK	150	0	150
	100% SSP	150	150	150
	70% SSP+30% MAP	150	150	150
	50% SSP+50% MAP	150	150	150
	30% SSP+70% MAP	150	150	150
	100% MAP	150	150	150

Sigmaplot 10.0 (version 10.0; Systat Software Inc., San Jose, CA, USA) was used to plot charts.

3 Result

3.1 Shoot biomass and P uptake

There were marked crop-specific biomass responses to the CMP: DAP blends in acidic soil and SSP: MAP blends in alkaline soil (Figure 1). Overall, all P-fertilized plants had higher biomass than those in the CK treatment, confirming that maize was P-limited in the control soil and that the observed biomass responses were influenced by P availability. Shoot biomass was also positively correlated with the MAP and DAP proportions in the fertilizer blends. Specifically, in acidic soil, shoot biomass in the 100% DAP treatment was the highest, and although there were insignificant differences among the 50% CMP+50% DAP and 30% CMP+70% DAP treatments, both treatments exhibited significantly higher biomass than those in the 100% CMP or CK treatments. Similarly, the shoot biomass per plant in the alkaline soil treatments was ranked as follows: 100% MAP > 30% SSP+70% MAP > 50% SSP +50% MAP > 70% SSP+30% MAP > 100% SSP > CK.

Shoot P uptake was similar to shoot biomass across the P treatments (Figure 2). Maize in acidic soil fertilized with 100% DAP had a 77.4% higher total P uptake than maize receiving 100% CMP. In alkaline soil, maize fertilized with 100% MAP had a 42.1% higher total P uptake than maize that received 100% SSP. Interestingly, shoot P uptake in acidic soil was not significantly higher in plants that received 50% CMP + 50% DAP compared to those fertilized with 100% DAP. No difference in total P uptake was observed between maize fertilized with 50% SSP+50% MAP and 100% MAP in alkaline soil. These combined results suggest a strong correlation between P uptake and shoot biomass.

3.2 Root biomass and length

Soil P supply had a significant impact on root morphology regardless of soil type (acidic or alkaline). In acidic soil, the 50% CMP + 50% DAP, 30% CMP + 70% DAP, and 100% DAP treatments resulted in the highest root biomass among all treatments, with increases of 85.4%, 86.0%, and 86.3%, respectively (Figure 3A). These were followed by the 70% CMP + 30% DAP and 100% CMP treatments, which also showed significantly higher biomass compared to the CK treatment. In alkaline soil, the root biomass was significantly higher in the 100% MAP, 30% SSP+70% MAP, and 50% SSP+50% MAP treatments than those in the 70% SSP+30% MAP and 100% SSP treatments, with no significant differences among the 100% MAP, 30% SSP+70% MAP, and 50% SSP+50% MAP treatments (Figure 3B). Moreover, the root biomass in the 50% CMP+50% DAP and 100% DAP treatments in acidic soil were similar, and no significant differences were observed in root biomass between the 50% SSP+50% MAP and 100% MAP treatments in alkaline soil.

Similar to root biomass, the mean root lengths in the 50% CMP+50% DAP, 30% CMP+70% DAP, and 100% DAP treatments in acidic soil were 59.1, 61.4, and 62.7 cm, respectively, which were significantly longer than those in the 70% CMP+30% DAP and 100% CMP treatments. No significant difference in root biomass was observed between the 50% CMP+50% DAP and 100% DAP treatments. In alkaline soil, the maize root length was only 8%

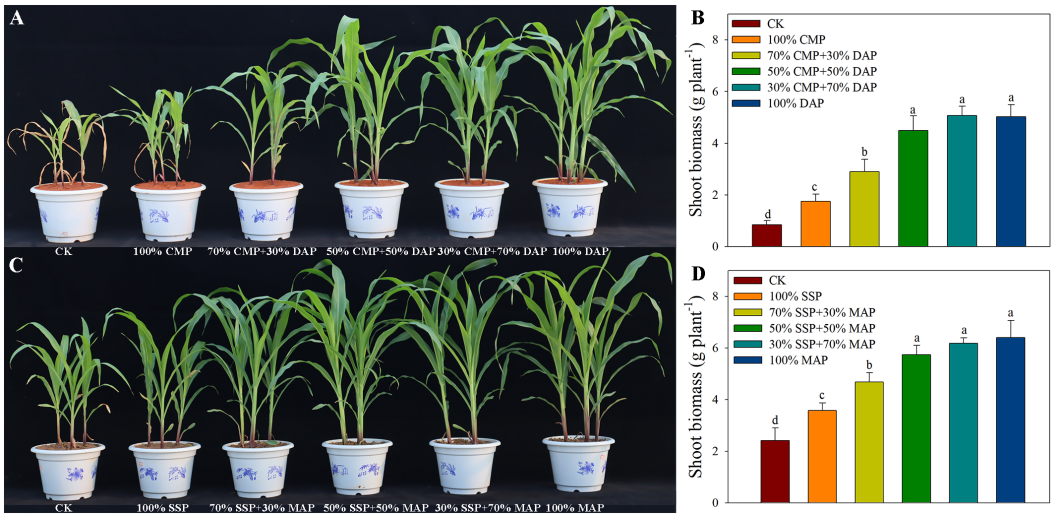

FIGURE 1
Plant growth performance **(A)** and shoot biomass **(B)** under different P fertilizer treatments in acidic soil. Plant growth performance **(C)** and shoot biomass **(D)** under different P fertilizer treatments in alkaline soil. Different lowercase letters indicate significant differences among treatments ($p < 0.05$).

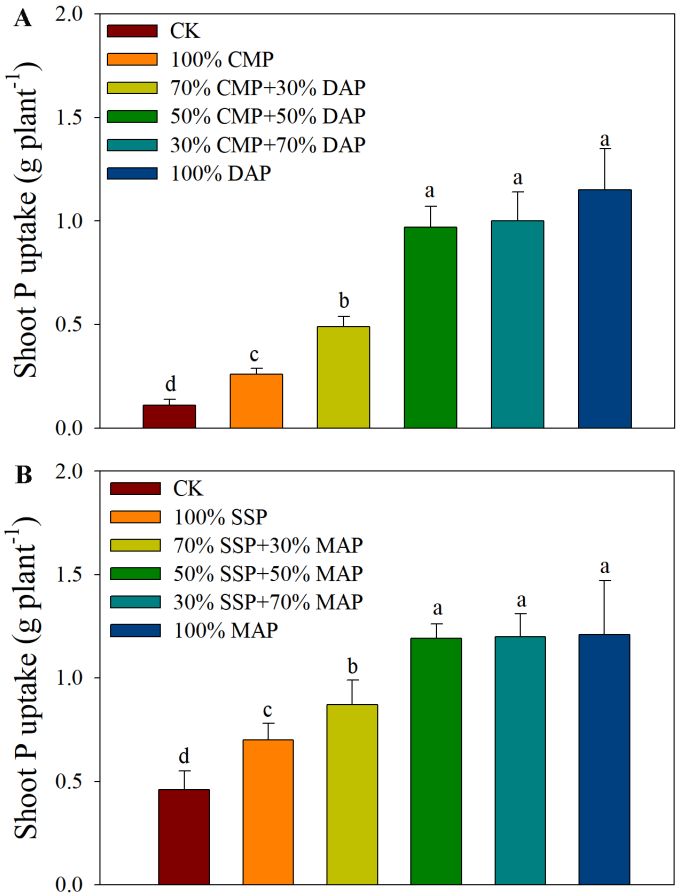

FIGURE 2
Shoot P uptake under different P fertilizer treatments in acidic **(A)** and alkaline **(B)** soil. Different lowercase letters indicate significant differences among treatments according to Duncan's multiple range test following significant one-way ANOVA ($p < 0.05$).

higher in the 100% MAP treatment than that in the 50% SSP+50% MAP treatment; however, no significant difference in length was observed between the 100% MAP and 50% SSP+50% MAP treatments (Figures 3C, D).

3.3 Soil inorganic P fractions

The CMP: DAP blends in acidic soil and SSP: MAP blends in alkaline soil significantly increased the soil H_2O-Pi, $NaHCO_3$-Pi, NaOH-Pi, and HCl-Pi fractions when the percentage of MAP or DAP was greater than 50% (Table 2). In acidic soil, the soil Pi fraction in the 100% DAP treatment was the highest, with insignificant differences between the 50% CMP+50% DAP and 30% CMP+70% DAP treatments, which were significantly higher than those in the CMP and CK treatments. Compared with those in the CK treatment, the soil H_2O-Pi, $NaHCO_3$-Pi, and NaOH-Pi fractions in the 50% CMP +50% DAP treatment increased by 415%, 160.4%, and 82.8%, respectively. Similarly, the alkaline soil inorganic P fraction was the highest in the 100% MAP treatment, but no significant differences were observed between the 100% MAP and 50% SSP+50% MAP treatments. Compared with those in the CK treatment, the soil H_2O-Pi, $NaHCO_3$-Pi, and NaOH-Pi fractions in the 50% SSP+50% MAP treatment increased by 142.8%, 265.8%, and 36.5%, respectively. Figure 4 showed a path coefficient structural model that describes the important relationships among the selected traits. The P fertilizers in both the 50% CMP+50% DAP and 50% SSP+50% MAP treatments enhanced the H_2O-Pi fraction, which subsequently led to an increase in soil P availability. Similarly, the NaOH-Pi fraction was positively influenced by the P fertilizer inputs in the specified treatments. This fraction also contributed significantly to the overall soil P availability (Olsen-P), as indicated by the positive path coefficients.

4 Discussion

4.1 Matching fertilizer properties with soil type for efficient P fertilizer management

Our study indicated a significant increase in total biomass under high proportions of MAP and DAP (Figure 1), consistent with previous studies, emphasizing the importance of balanced fertilization for optimizing crop productivity (Gong et al., 2024). The higher sensitivity of maize growth to MAP or DAP may be attributed to their use as high-concentration P fertilizers, which can provide sufficient P to help sustain early root development (Chien

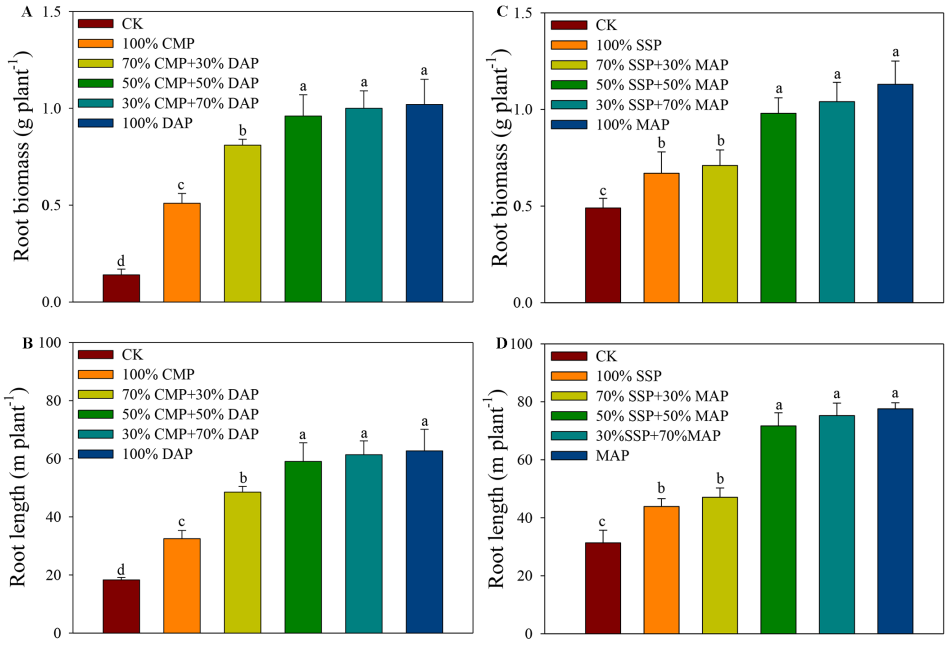

FIGURE 3
Root biomass under different P fertilizer treatments in acidic **(A)** and alkaline **(B)** soil. Root lengths under different P fertilizer treatments in acidic **(C)** and alkaline **(D)** soil. Different lowercase letters indicate significant differences among treatments according to Duncan's multiple range test following significant one-way ANOVA ($p < 0.05$).

et al., 2011). As expected, the highest root biomass and root lengths were observed in plants subjected to the 100% DAP (acidic soil) and 100% MAP (alkaline soil) treatments. This highlights the crucial role of a well-established root system for effective P acquisition and yield potential, given the low mobility of P in the soil (Flaval et al., 2014; Hertzberger et al., 2021). The addition of high-concentration P fertilizers such as MAP or DAP is an efficient way to increase available P concentration in the soil. Moisture initiates the dissolution of fertilizer granules, allowing P to move into the soil solution due to their high water solubility (Weeks and Hettiarachchi, 2019). However, it is important to note that high-P fertilizer application does not necessarily guarantee a sustained increase in maize yield. A previous study showed that the application of low-P fertilizer (i.e., SSP or CMP) at high plant densities resulted in higher yields compared to those with high-P fertilizer applications (i.e., MAP or DAP) (Gong et al., 2022b). The

TABLE 2 Effects of different P fertilizer treatments on soil Pi fractions based on Hedley P fraction in acidic and alkaline soil.

Soil	Treatment	H_2O-Pi (mg kg^{-1})	$NaHCO_3$-Pi (mg kg^{-1})	NaOH-Pi (mg kg^{-1})	HCl-Pi (mg kg^{-1})	Residual-P (mg kg^{-1})
Acidic soil	CK	2.64 ± 0.55c	12.49 ± 2.41b	61.50 ± 9.79c	103.88 ± 3.82c	327.04 ± 13.46b
	100% CMP	6.06 ± 1.37b	16.67 ± 2.89b	76.10 ± 12.70c	114.00 ± 4.80bc	375.58 ± 17.47ab
	70% CMP+30% DAP	9.00 ± 1.46b	21.22 ± 1.01b	86.08 ± 7.77bc	126.81 ± 8.11bc	386.57 ± 32.2ab
	50% CMP+50% DAP	13.60 ± 0.89a	32.52 ± 0.22a	112.42 ± 7.16a	129.76 ± 8.11b	437.64 ± 12.05a
	30% CMP+70% DAP	14.39 ± 1.57a	32.71 ± 2.99a	109.55 ± 5.13ab	137.83 ± 10.99ab	435.67 ± 16.08a
	100% DAP	14.49 ± 1.90a	34.64 ± 0.46a	121.28 ± 9.71a	154.71 ± 12.33a	419.48 ± 34.65a
Alkaline soil	CK	7.94 ± 1.97b	10.30 ± 0.33c	84.85 ± 5.40c	222.09 ± 4.05a	566.93 ± 32.50b
	100% SSP	7.40 ± 1.26b	12.86 ± 2.24b	102.9 ± 2.43b	223.93 ± 1.43a	559.79 ± 40.90b
	70% SSP+30% MAP	8.44 ± 1.28b	17.36 ± 1.57ab	116.08 ± 1.51a	229.09 ± 3.38a	544.58 ± 45.98b
	50% SSP+50% MAP	19.28 ± 1.41a	37.68 ± 1.94a	115.53 ± 3.36a	222.03 ± 5.73a	682.03 ± 9.73a
	30% SSP+70% MAP	19.71 ± 1.86a	36.86 ± 3.09a	113.2 ± 4.27a	222.93 ± 4.56a	684.98 ± 10.89a
	100% MAP	22.24 ± 1.37a	37.14 ± 1.67a	118.52 ± 1.26a	224.92 ± 4.70a	683.7 ± 12.98a

Lowercase letters indicate significant differences between treatments at the $p < 0.05$ level.

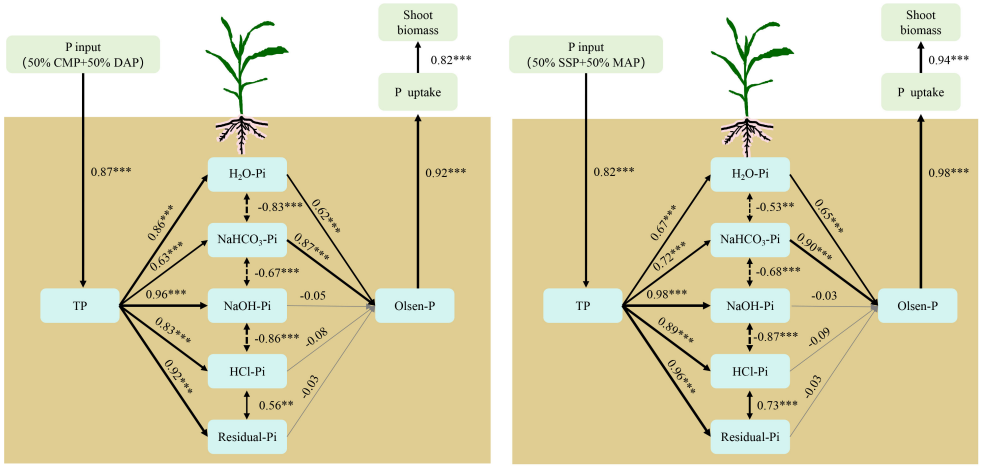

FIGURE 4
Path coefficient structural model of the relationship between shoot biomass and the other variables. Boxes indicate the variable names. Black solid and dotted arrows indicate significant positive and negative effects, respectively. Gray solid arrows indicate nonsignificant effects. Numbers adjacent to the arrows are standardized path coefficients and indicative of the effect size of the relationship. The arrow width is proportional to the strength of the path coefficient. A line with an arrowhead indicates a putative causal link between the cause (arrow base) and effect (arrow tip). ** and *** represent $p < 0.01$ and $p < 0.001$ significance levels, respectively.

high-concentration P fertilizers experience a rapid decline in water solubility due to fixation upon application to soil, limiting their bioavailability (Feng et al., 2019; Maharajan et al., 2021). Therefore, determining the optimal blend of P fertilizer is essential for promoting the conversion of low-solubility P into plant-bioavailable forms and enhancing its efficient utilization by crops.

4.2 The P management strategies for improving P use efficiency

Innovative approaches, such as combining high- and low-P fertilizers, can enhance soil microbial activity and facilitate the conversion of soluble P into plant-bioavailable form. The application of blended fertilizers requires careful consideration of soil properties, crop requirements, and environmental factors to maximize the benefits and promote sustainable agricultural practices. In this study, the pot experiments indicate that the 50% MAP+50% SSP (alkaline soil) and 50% DAP+50% CMP (acidic soil) treatments significantly improved P uptake, which did not differ significantly from the 100% MAP and 100% DAP treatments but were greater than that in the CK treatment, suggesting similar P uptakes as those in the 100% MAP and 100% DAP treatments.

DAP is a high-concentration P fertilizer produced by treating ammonia with phosphoric acid. Factors such as Fe and Al play significant roles in limiting plant P availability in acidic soil. DAP can contribute to higher plant P concentrations during the seedling and tillering stages due to its rapid release of phosphate (Ma et al., 2023; Ning et al., 2023). However, previous studies have shown that this rapid release can lead to P fixation through iron and aluminum oxidation in acidic soil, thereby failing to meet plant P demands during the later stages of crop growth (Chien et al., 2011; Ma et al., 2022). In contrast, MAP is a slow-acting P source that dissolves effectively in acidic soil and provides sufficient P during the later stages of crop growth (Gong et al., 2022b; Qin et al., 2022). Our results show that shoot biomass and P uptake were highest under the 100% DAP treatment but showed no significant differences when compared with the 50% CMP+50% DAP treatment-indicating a notable increase in P uptake owing to the acidulating effect of DAP on CMP.

In alkaline soils, MAP serves as an effective medium-acidity fertilizer that enhances plant P availability. Ammonium ions within MAP decrease pH levels in the rhizosphere zone, reducing phosphate fixation while promoting root proliferation–a vital reaction for improving phosphate uptake (Nunes et al., 2022). Our experimental data revealed consistently lower levels of available P in SSP compared with that of MAP and could not meet plant P demands during the early growth stages. Under similar conditions with respect to P supply, shoot biomass and P uptake in the 100% MAP treatment were significantly higher than those in the 100% SSP treatment. Surprisingly, shoot biomass and P uptake in the 100% DAP treatment did not differ significantly from those in the 50% CMP+50% DAP treatment. Therefore, the coupling of MAP and SSP provides an agronomically and economically effective way to provide the required P, as MAP can initially supply P to plants during their early development, resulting in better plant root development, moreover, the use of lower cost of SSP refers a more cost-effective alternative that could help reduce overall fertilizer expenses while still supplying adequate phosphorous for crop growth, and thus can be employed more effectively in alkaline soils (Gong et al., 2022b).

4.3 Blends of low- and high-P fertilizers increased soil labile and moderately labile Pi fractions

Previous studies have demonstrated the direct impact of P fertilizer inputs on soil Pi fractions (Yan et al., 2017). Our result showed the

addition of chemical P fertilizers increased soil Pi with larger proportions of H_2O-Pi, $NaHCO_3$-Pi, and NaOH-Pi available to plants in the 50% CMP+50% DAP (acidic soil) and 50% SSP+50% MAP (alkaline soil) treatments. Labile P pools such as H_2O-Pi and $NaHCO_3$-Pi are direct sources for crop uptake indicating that the P applied in the 50% CMP +50% DAP (acidic soil) and 50% SSP+50% MAP (alkaline soil) treatments were retained in the more easily extracted fractions (Yan et al., 2022). Furthermore, NaOH-Pi was also a major P pool, which was enhanced by high-P fertilizer applications. Under the conditions used in this study, HCl-P_i was found to be an important P source for maize (in addition to H_2O-Pi, $NaHCO_3$-Pi, and NaOH-Pi) in the 50% CMP+50% DAP (acidic soil) and 50% SSP+50% MAP (alkaline soil) treatments. HCl-Pi and residual P stabilized the P with low use efficiency. Although HCl-Pi and residual P had low use efficiency, plants can enhance P uptake by modulating root morphological and physiological characteristics and by activating insoluble P through microbial activity (Shen et al., 2011; Yan et al., 2022).

In this study, the recommended P fertilizer input met the requirements for optimal crop growth, as soil P bioavailability was enhanced to promote root growth using an appropriate ratio of high- to low-P fertilizers. Enhanced root growth increases organic acid secretion and mediates rhizosphere acidification, which can activate soil P and transform insoluble P into labile P pools (H_2O-Pi and $NaHCO_3$-Pi) (Alamgir et al., 2012; Liu et al., 2023). Therefore, P fertilizer management strategies should better account for soil conditions. Additionally, optimizing soil-plant P nutrition should include a series of strategies for improving crop P uptake, reducing the excessive use of high-concentration P fertilizers, and improving low-P fertilizer concentrations.

5 Conclusion

The SSP: MAP blends and CMP: DAP blends were evaluated for their ability to maximize maize growth. SSP and CMP alone were insufficient to maintain maize growth. However, maize growth was comparable when up to 50% SSP substituted for MAP in acidic soil and up to 50% CMP substituted for DAP in alkaline soil. This indicates that the limitations of higher P-concentration fertilizers (i.e., MAP and DAP) can be mitigated by blending them with low-P fertilizers. Substituting SSP for MAP by up to 50% in acidic soil and CMP for DAP by up to 50% in alkaline, which can meet the crop's P demand. These findings provide a foundation for optimizing P fertilizer types in maize production to enhance P-use efficiency. Further research could focus on optimizing these blend ratios under various soil conditions to meet maize's P demands effectively. This optimization not only enhances P use efficiency in maize production but also promotes sustainable agriculture practices by reducing reliance on high-concentration P fertilizers, which provide a robust foundation for future studies aiming to optimize P fertilizer types in maize production, thereby contributing significantly to sustainable and efficient agricultural practices.

Data availability statement

The original contributions presented in the study are included in the article/Supplementary Material. Further inquiries can be directed to the corresponding author/s.

Author contributions

CC: Conceptualization, Formal Analysis, Methodology, Visualization, Writing – original draft. YX: Writing – review & editing. XJ: Writing – review & editing. HG: Conceptualization, Methodology, Project administration, Writing – review & editing.

Funding

The author(s) declare financial support was received for the research, authorship, and/or publication of this article. This work was supported by the National Key Research and Development Program of China (2023YFD1900100), National Natural Science Foundation of China (NSFC) (32301453), and the China Postdoctoral Science Foundation (2023M730682).

Conflict of interest

The authors declare that the research was conducted in the absence of any commercial or financial relationships that could be construed as a potential conflict of interest.

Publisher's note

Supplementary Material

The Supplementary Material for this article can be found online at: https://www.frontiersin.org/articles/10.3389/fpls.2024.1451073/full#supplementary-material

References

Alamgir, M., McNeill, A., Tang, X., and Marschner, P. (2012). Changes in soil P pools during legume residue decomposition. *Soil Biol. Biochem.* 49, 70–77. doi: 10.1016/j.soilbio.2012.01.031

Bindraban, P., Dimkpa, C., and Pandey, R. (2020). Exploring phosphorus fertilizers and fertilization strategies for improved human and environmental health. *Biol. Fert. Soils.* 56, 299–317. doi: 10.1007/s00374-019-01430-2

Chen, S., Cade-Menun, B., Bainard, L., Luce, M., Hu, Y., and Chen, Q. (2021). The influence of long-term N and P fertilization on soil P forms and cycling in a wheat/fallow cropping system. *Geoderma* 404, 115274. doi: 10.1016/j.geoderma.2021.115274

Chien, S., Prochnow, L., and Cantarella, H. (2009). Recent developments of fertilizer production and use to improve nutrient efficiency and minimize environmental impacts. *Adv. Agron.* 102, 267–322. doi: 10.1016/S0065-2113(09)01008-6

Chien, S., Prochnow, L., Tu, S., and Snyder, C. (2011). Agronomic and environmental aspects of phosphate fertilizers varying in source and solubility: An update review. *Nutr. Cycling Agroecosyst.* 89, 229–255. doi: 10.1007/s10705-010-9390-4

Everaert, M., da Silva, R., Degryse, F., McLaughlin, M., and Smolders, E. (2018). Limited dissolved phosphorus runoff losses from layered double hydroxide and struvite fertilizers in a rainfall simulation study. *J. Environ. Qual.* 47, 371–377. doi: 10.2134/jeq2017.07.0282

Feng, G., Gai, J., Feng, X., Li, H., Zhang, L., Yi, K., et al. (2019). Strategies for improving fertilizer phosphorus use efficiency in Chinese cropping systems. *Front. Agric. Sci. Eng.* 6, 341–347. doi: 10.15302/J-FASE-2019280

Flaval, R., Guppy, C., Tighe, M., Watt, M., and Young, I. (2014). Quantifying the response of wheat (*Triticum aestivym* L) root system architecture to phosphorus in an oxisol. *Plant Soil* 385, 303–310. doi: 10.1007/s11104-014-2191-9

Geissler, B., Mew, M., and Steiner, G. (2019). Phosphate supply security for importing countries: Developments and the current situation. *Sci. Total Environ.* 677, 511–523. doi: 10.1016/j.scitotenv.2019.04.356

Ghodszad, L., Reyhanitabar, A., Oustan, S., and Alidokht, L. (2022). Phosphorus sorption and desorption characteristics of soils as affected by biochar. *Soil Tillage Res.* 216, 105251. doi: 10.1016/j.still.2021.105251

Gong, H., Meng, F., Wang, G., Hartmann, T. E., Feng, G., Wu, J., et al. (2022a). Toward the sustainable use of mineral phosphorus fertilizers for crop production in China: From primary resource demand to final agricultural use. *Sci. Total Environ.* 804, 150183. doi: 10.1016/j.scitotenv.2021.150183

Gong, H., Xiang, Y., Wako, B., and Jiao, X. (2022b). Complementary effects of phosphorus supply and planting density on maize growth and phosphorus use efficiency. *Front. Plant Sci.* 13. doi: 10.3389/fpls.2022.983788

Gong, H., Xing, Y., Wu, J., Luo, L., Chen, X., Jiao., X., et al. (2024). Integrating phosphorus management and cropping technology for sustainable maize production. *J. Integr. Agric.* 23, 1369–1380. doi: 10.1016/j.jia.2023.10.018

Hedley, M., Stewart, J., and Chauhan, B. (1982). Changes in inorganic and organic soil phosphorus fractions induced by cultivation practices and by laboratory incubations. *Soil Sci. Soc Am. J.* 46, 970–976. doi: 10.2136/sssaj1982.03615995004600050017x

Hertzberger, A., Cusick, R., and Margenot, A. (2021). Maize and soybean response to phosphorus fertilization with blends of struvite and monoammonium phosphate. *Plant Soil* 461, 547–563. doi: 10.1007/s11104-021-04830-2

Janes-Bassett, V., Blackwell, M., Blair, G., Davies, J., Haygarth, P., Mezeli, M., et al. (2022). A meta-analysis of phosphatase activity in agricultural settings in response to phosphorus deficiency. *Soil Biol. Biochem.* 165, 108537. doi: 10.1016/j.soilbio.2021.108537

Joshi, S., Morris, J., Tfaily, M., Young, R., and McNear, (2021). Low soil phosphorus availability triggers maize growth stage specific rhizosphere processes leading to mineralization of organic P. *Plant Soil* 459, 423–440. doi: 10.1007/s11104-020-04774-z

Kim, D., Kirschbaum, M., Eichler-Löbermann, B., Gifford, R., and Liáng, L. (2023). The effect of land-use change on soil C, N, P, and their stoichiometries: A global synthesis. *Agric. Ecosyst. Environ.* 348, 108402. doi: 10.1016/j.agee.2023.108402

Liu, C., Ding, T., Liu, W., Tang, Y., and Qiu, R. (2023). Phosphorus mediated rhizosphere mobilization and apoplast precipitation regulate rare earth element accumulation in Phytolacca Americana. *Plant Soil* 483, 697–709. doi: 10.1007/s11104-022-05743-4

Ma, G., Chen, Q., Shi, R., Kong, B., Chen, D., Zhang, Z., et al. (2022). Effect of coated diammonium phosphate combined with *Paecilomyces variotii* extracts on soil available nutrients, photosynthesis-related enzyme activities, endogenous hormones, and maize yield. *ACS omega* 7, 23566–23575. doi: 10.1021/acsomega.2c02102

Ma, S., Wang, G., Su, S., Lu, J., Ren, T., Cong, R., et al. (2023). Effects of optimized nitrogen fertilizer management on the yield, nitrogen uptake, and ammonia volatilization of direct-seeded rice. *J. Sci. Food Agric.* 103, 4553–4561. doi: 10.1002/jsfa.12530

Maharajan, T., Ceasar, S., Krishna, T., and Ignacimuthu, S. (2021). Management of phosphorus nutrient amid climate change for sustainable agriculture. *J. Environ. Qual.* 50, 1303–1324. doi: 10.1002/jeq2.20292

Murphy, J., and Riley, J. (1962). A modified single solution method for the determination of phosphate in natural waters. *Anal. Chim. Acta* 27, 31–36. doi: 10.1016/S0003-2670(00)88444-5

Ning, F., Nkebiwe, P., Hartung, J., Munz, S., Huang, S., Zhou, S., et al. (2023). Phosphate fertilizer type and liming affect the growth and phosphorus uptake of two maize cultivars. *Agriculture* 13, 1771. doi: 10.3390/agriculture13091771

Nunes, A., Santos, C., and Guelfi, D. (2022). Interfaces between biodegradable organic matrices coating and MAP fertilizer for improve use efficiency. *Sci. Total Environ.* 804, 149896. doi: 10.1016/j.scitotenv.2021.149896

Nziguheba, G., Zingore, S., Kihara, J., Merckx, R., Njoroge, S., Otinga, A., et al. (2016). Phosphorus in smallholder farming systems of sub-Saharan Africa: implications for agricultural intensification. *Nutr. Cycling Agroecosyst.* 104, 321–340. doi: 10.1007/s10705-015-9729-y

Qin, P., Hui, H., Song, W., Wu, H., and Li, S. (2022). Characteristics of fused calcium magnesium phosphate fertilizer (FCMP) made from municipal sewage sludge and its properties. *J. Environ. Chem. Eng.* 10, 108563. doi: 10.1016/j.jece.2022.108563

Raymond, N., Gómez-Muñoz, B., van der Bom, F., Nybroe, O., Jensen, L., Müller-Stöver, D., et al. (2021). Phosphate-solubilising microorganisms for improved crop productivity: A critical assessment. *New Phytol.* 229, 1268–1277. doi: 10.1111/nph.16924

Shen, J., Yuan, L., Zhang, J., Li, H., Bai, Z., Chen, X., et al. (2011). Phosphorus dynamics: from soil to plant. *Plant Physiol.* 156, 997–1005. doi: 10.1104/pp.111.175232

Sui, Y., Thompson, M., and Shang, C. (1999). Fractionation of soil phosphorus in a Mollisol amended with biosolids. *Soil Sci. Soc Am. J.* 63, 1174–1180. doi: 10.2136/sssaj1999.6351174x

Talboys, P., Heppell, J., Roose, T., Healey, J., Jones, D., and Withers, P. (2016). Struvite: a slow-release fertiliser for sustainable phosphorus management? *Plant Soil* 401, 109–123. doi: 10.1007/s11104-015-2747-3

Weeks,, and Hettiarachchi, G. (2019). A review of the latest in phosphorus fertilizer technology: Possibilities and pragmatism. *J. Environ. Qual.* 48, 1300–1313. doi: 10.2134/jeq2019.02.0067

Wolf, B. (1982). A comprehensive system of leaf analysis and its use for diagnosing crop nutrients status. Commun. *Commun. Soil Sci. Plant Anal.* 13, 1035–1059. doi: 10.1080/00103628209367332

Yan, J., Ren, T., Wang, K., Li, H., Li, X., Cong, R., et al. (2022). Improved crop yield and phosphorus uptake through the optimization of phosphorus fertilizer rates in an oilseed rape-rice cropping system. *Field Crop Res.* 286, 108614. doi: 10.1016/j.fcr.2022.108614

Yan, X., Wei, Z., Hong, Q., Lu, Z., and Wu, J. (2017). Phosphorus fractions and sorption characteristics in a subtropical paddy soil as influenced by fertilizer sources. *Geoderma* 295, 80–85. doi: 10.1016/j.geoderma.2017.02.012

Zhang, H., Shi, L., Lu, H., Shao, Y., Liu, S., and Fu, S. (2020). Drought promotes soil phosphorus transformation and reduces phosphorus bioavailability in a temperate forest. *Sci. Total Environ.* 732, 139295. doi: 10.1016/j.scitotenv.2020.139295

Zheng, L., Zhao, Q., Lin, G., Hong, X., and Zeng, D. (2023). Nitrogen addition impacts on soil phosphorus transformations depending upon its influences on soil organic carbon and microbial biomass in temperate larch forests across northern China. *Catena* 230, 107252. doi: 10.1016/j.catena.2023.107252

frontiers | Frontiers in Plant Science

TYPE Original Research
PUBLISHED 14 August 2024
DOI 10.3389/fpls.2024.1440859

OPEN ACCESS

EDITED BY
Laichao Luo,
Anhui Agricultural University, China

REVIEWED BY
Puchang Wang,
Guizhou Normal University, China
Shenqiang Lv,
Shandong Academy of Agricultural Sciences, China

*CORRESPONDENCE
Xianyue Li
lixianyue80@126.com

RECEIVED 30 May 2024
ACCEPTED 26 July 2024
PUBLISHED 14 August 2024

CITATION
Ren W, Li X, Liu T, Chen N, Xin M, Liu B, Qi Q and Li G (2024) Impact of fertilization depth on sunflower yield and nitrogen utilization: a perspective on soil nutrient and root system compatibility.
Front. Plant Sci. 15:1440859.
doi: 10.3389/fpls.2024.1440859

Impact of fertilization depth on sunflower yield and nitrogen utilization: a perspective on soil nutrient and root system compatibility

Wenhao Ren[1], Xianyue Li[1,2,3]*, Tingxi Liu[1,2], Ning Chen[1], Maoxin Xin[1], Bin Liu[1], Qian Qi[1] and Gendong Li[4]

[1]College of Water Conservancy and Civil Engineering, Inner Mongolia Agricultural University, Hohhot, China, [2]Collaborative Innovation Center for Integrated Management of Water Resources and Water Environment in the Inner Mongolia Reaches of the Yellow River, Hohhot, China, [3]Research and Development of Efficient Water-saving Technology and Equipment and Research Engineering Center of Soil and Water Environment Effect in Arid Area of Inner Mongolia Autonomous Region, Hohhot, China, [4]Inner Mongolia Hetao Irrigation District Water Conservancy Development Center, Bayannur, China

Introduction: The depth of fertilizer application significantly influences soil nitrate concentration (SNC), sunflower root length density (RLD), sunflower nitrogen uptake (SNU), and yield. However, current studies cannot precisely capture subtle nutrient variations between soil layers and their complex relationships with root growth. They also struggle to assess the impact of different fertilizer application depths on sunflower root development and distribution as well as their response to the spatial and temporal distribution of nutrients.

Methods: The Agricultural Production Systems sIMulator (APSIM) model was employed to explore the spatial and temporal patterns of nitrogen distribution in the soil at three controlled-release fertilizer (CRF) placement depths: 5, 15, and 25 cm. This study investigated the characteristics of the root system regarding nitrogen absorption and utilization and analyzed their correlation with sunflower yield formation. Furthermore, this study introduced the modified Jaccard index (considering the compatibility between soil nitrate and root length density) to analyze soil-root interactions, providing a deeper insight into how changes in CRF placement depth affect crop growth and nitrogen uptake efficiency.

Results: The results indicated that a fertilization depth of 15 cm improved the modified Jaccard index by 6.60% and 7.34% compared to 5 cm and 25 cm depths, respectively, maximizing sunflower yield (an increase of 9.44%) and nitrogen absorption rate (an increase of 5.40%). This depth promoted a greater Root Length Density (RLD), with an increases of 11.95% and 16.42% compared those at 5 cm and 25 cm, respectively, enhancing deeper root growth and improving nitrogen uptake. In contrast, shallow fertilization led to higher nitrate concentrations in the topsoil, whereas deeper fertilization increased the nitrate concentrations in the deeper soil layers.

Discussion: These results provide valuable insights for precision agriculture and sustainable soil management, highlighting the importance of optimizing root nitrogen absorption through tailored fertilization strategies to enhance crop production efficiency and minimize environmental impact.

KEYWORDS

fertilization depth, root growth, nitrogen fertilizer efficiency, sunflower yield, nutrient matching between root and soil

1 Introduction

Nitrogen is crucial for optimal crop yields and is a key nutrient for plant growth (Tabuchi et al., 2007; Heuer et al., 2017). The global utilization rate of nitrogen fertilizers is generally low, often around 40%–53% (Chen et al., 2021b; Wang et al., 2023a), leading to inefficiencies in agricultural practices, where farmers frequently apply excessive nitrogen fertilizer, surpassing the crops' actual growth requirements (Nie et al., 2022; Wang et al., 2022a). Over-application of nitrogen fertilizers increases agricultural costs and causes environmental issues, as reported globally (Chen and Graedel, 2016; Ma et al., 2019; Chen et al., 2021a). Additionally, the excessive application of nitrogen fertilizers can contribute to increased greenhouse gas emissions, such as nitrous oxide (N_2O), which has high global warming potential (Kong et al., 2021; Ren et al., 2021; Wu et al., 2023). Therefore, improving the efficiency of nitrogen fertilizer use is vital for global food security, sustainable economic development, and mitigating the ecological impact of agriculture. Studies have demonstrated that adopting more precise fertilization methods and improved agronomic techniques can significantly enhance nitrogen utilization efficiency (NUE) (Radočaj et al., 2022; Ren et al., 2022; Luo et al., 2023). For example, adjusting fertilization strategies, such as altering the depth of fertilization, can increase nitrogen use efficiency by 38.37%, yield by 13.83%, and reduce nitrogen loss by 70.23% compared with traditional methods (Wu et al., 2021). Changing the timing of fertilization can reduce total nitrogen input by 15% without yield loss (Xie et al., 2007). Controlled-release fertilizers (CRF), a novel type of fertilizer (Haydar et al., 2024), regulate the nitrogen release rate through coating technologies (Sim et al., 2021) and matching crop nitrogen demand (Slafer and Savin, 2018; Vejan et al., 2021). This enhances the nitrogen uptake (Li et al., 2020), lowers soil inorganic nitrogen concentration, and reduces the nitrogen loss (Azeem et al., 2014; Momesso et al., 2022; Zhang et al., 2024). Moreover, strategies to enhance crop NUE include selecting crop varieties that utilize soil nitrogen effectively and reduce nitrogen loss (Ciampitti et al., 2022). This is crucial to sustainable agricultural development. Therefore, adopting a comprehensive approach to nitrogen fertilization management and crop selection is important for improving NUE (Kant et al., 2011; Guo et al., 2020; Geng et al., 2021). Integrating these methods can effectively enhance agricultural production efficiency and reduce environmental impacts, contributing to global food security and sustainable development.

Modern agricultural research has emphasized the importance of matching plant root systems with available soil resources for efficient nutrient absorption (Jin et al., 2017; Gebre and Earl, 2021; Chen et al., 2022c). Root-foraging processes exhibit significant spatiotemporal heterogeneity owing to varying soil resource availability across different layers (Mou et al., 2012; Postma et al., 2014; Hui et al., 2022). Adjusting fertilization depth is a critical agronomic practice that can significantly affect root growth and distribution and optimize nutrient absorption efficiency, especially for nitrogen (Su et al., 2015; Chen et al., 2022a, 2024). Studies have demonstrated that spatially adjusting soil nitrate content under different rainfall conditions enhances deep soil root characteristics, indirectly improving the nitrogen nutrient status of wheat plants (Wang et al., 2022b). In trials with spring maize, increasing fertilization depth compared to conventional methods resulted in significant improvements in root length density: 18% for vertical roots, 14% for inter-row roots, and 24% for intra-row roots at soil depths of 0–1.0m. Similarly, the root surface area density increased by 39%, 17%, and 22%, respectively (Wu et al., 2022b). The application of fertilizer at depths of 15 and 25 cm, rather than 5 cm, increased maize nitrogen absorption by 8.07% and 17.41%, NUE by 17.79% and 38.37%, and maize yield by 5.68% and 13.83%, respectively (Wu et al., 2021). Optimizing the fertilization depth is crucial for improving NUE and regulating crop growth and yield (Jia et al., 2023; Wang et al., 2023b). These practices enable the agricultural production to mitigate environmental impacts while ensuring sufficient crop nutrition and promoting sustainability. This approach is particularly relevant for deep-rooting crops such as sunflowers, maize, and wheat, which can access nutrients from deeper soil layers (Connor and Hall, 1997; Wasson et al., 2012; Lynch, 2013; Zhang et al., 2023).

Sunflower, known for its strong root system adaptability, significantly enhances nitrogen absorption rate, utilization, and crop yield through deep root growth (Kiniry et al., 1992; Ma et al., 2021). Its root system can extend into deeper soil layers, effectively utilizing nutrients beyond the surface layer (Thorup-Kristensen et al., 2020). However, current agricultural research lacks

sufficient analysis of the impact of moderately deep nitrogen fertilization on root distribution and spatiotemporal matching of soil nutrients in sunflower cultivation. In agricultural studies, an accurate understanding of the correlation between soil nitrate content and root length density is crucial to elucidate the interactions between crop roots and soil nutrients (Li et al., 2018; Lopez et al., 2022). This analysis deepens our understanding of how roots adapt to nutrient distribution, thereby affecting growth and yield. Despite their significance, current analytical methods often fail to precisely capture subtle differences between soil layers and their complex relationship with root growth. Therefore, the aim of this study was to develop a refined and comprehensive analytical method to accurately assess the correlation between soil nitrate distribution and root growth. We introduced an improved weighted Jaccard index (Real and Vargas, 1996; Bag et al., 2019), which considers not only the direct match between soil nitrate content and root length density but also the interrelationships among different soil layers, providing a more comprehensive analytical perspective. This method allowed us to reveal the complex interactions between crop roots and soil nutrients more precisely, providing theoretical support for optimizing fertilization strategies and improving crop production efficiency (Duan et al., 2019; Velasco-Muñoz et al., 2021).

The main objectives of this study were to (1) analyze the impact of deep CRF on the growth distribution of the sunflower root system and its role in yield and nutrient use efficiency, (2) investigate the compatibility between deep CRF and root system growth, and (3) determine the ideal CRF depth to promote an adaptive root system structure in sunflowers through more effective fertilization methods, thereby achieving higher yields. Moreover, this experiment can also contribute to refining existing soil and crop models to simulate root growth, crop yield, and nutrient use efficiency.

2 Materials and methods

2.1 Experimental site parameters

The experiment was conducted in the Ganzhaomiao Town experimental field, Linhe District, Bayannaoer City, Inner Mongolia, to investigate the effects of different fertilizer depths over two consecutive growing seasons in 2020 and 2021. The site coordinates are 107°16′42″E and 40°47′54″N, with predominantly silty loam soil (USDA classification). The 0–100 cm soil layer had an average bulk density of 1.41 g/cm^3, an average organic matter mass ratio of 6.19 g/kg, an average hydrolysable nitrogen mass ratio of 34.43 mg/kg, an average available phosphorus mass ratio of 1.84 mg/kg, and an average available potassium mass ratio of 113.04 mg/kg. The soil salt content prior to planting averaged 3.2 g/kg, with an average pH of 8.4. The experimental site experiences an annual average temperature of 6.8 °C, precipitation of 138.8 mm, and total annual sunshine hours of 3229.9 h.

2.2 Experimental design and field practices

The test field comprised 12 plots, each 144 m^2 (14 m×6 m), arranged in triplicate for the four treatments. This study used CRF with a nitrogen application rate of 225 kg/ha. Three depths of fertilizer application were tested: 5 ± 0.5 cm (low), 15 ± 0.5 cm (medium), and 25 ± 0.5 cm (high). Additionally, treatments with TNF at 225 kg/ha and a depth of 5 ± 0.5 cm were included. Plastic films were used between the plots to isolate them and to prevent water, salt, and nitrogen interactions. The CRF was the sixth generation from Luyang, with an N:P:K ratio of 28:12:10. The CRF was applied to the farmland at the corresponding depth through manual trenching before mulching. For the TNF, diammonium phosphate (containing 18% N and 46% P_2O_5) was used as the base fertilizer and was applied at the same depth through manual trenching before mulching, similar to the CRF treatment; topdressing consisted of urea, which was manually spread before irrigation at the bud stage. Diammonium phosphate (1/3 N) was applied before sowing, and urea (2/3 N) was manually applied before irrigation at the budding stage. Sunflowers were irrigated to a depth of 120 mm during their growth period in both 2020 and 2021 using furrow irrigation on July 14th. All the other field management practices were consistent. Sunflower (Xinjiang Sanrui, SH361) was planted using a mechanical film covering and manual planting. The planting pattern involved one film for every two rows, with sunflower plant and row spacing set at 0.4 m and 0.9 m, respectively, resulting in a planting density of approximately 27,777 plants per hectare. Sowing occurred on May 22, 2020, and May 30, 2021, with harvest dates set for September 24 and September 29 of the respective years, resulting in growth periods of 126 and 123 d.

2.3 Observations and measurement methods

Meteorological data (Figure 1), including solar radiation, air temperature, relative humidity, precipitation, and wind speed, were collected at one-hour intervals using an automated meteorological station (Onset Computer Inc., U30, Hobo, USA) located in the experimental field.

Soil water and NO_3-N contents were measured using a soil auger (Beijing New Landmark Soil Equipment Co., Ltd., 0301, XDB, CHN) in covered and exposed areas at vertical depths of 0–10 cm, 10–20 cm, 20–30 cm, 30–40 cm, 40–50 cm, 50–60 cm, 60–80 cm, and 80–100 cm. Samples were collected every 10–15 d, and each sample was replicated three times. The soil samples were divided into two parts: one for measuring soil moisture content and the other air-dried, crushed, and sieved through a 1 mm mesh. Subsequently, 5 g of the sample was soaked in 25 mL of 2 mol/L potassium chloride solution. After stirring and filtering, the NO_3-N concentration was determined using an ultraviolet spectrophotometer (Beijing General Instruments Co., Ltd., TU-1901, Beijing, China).

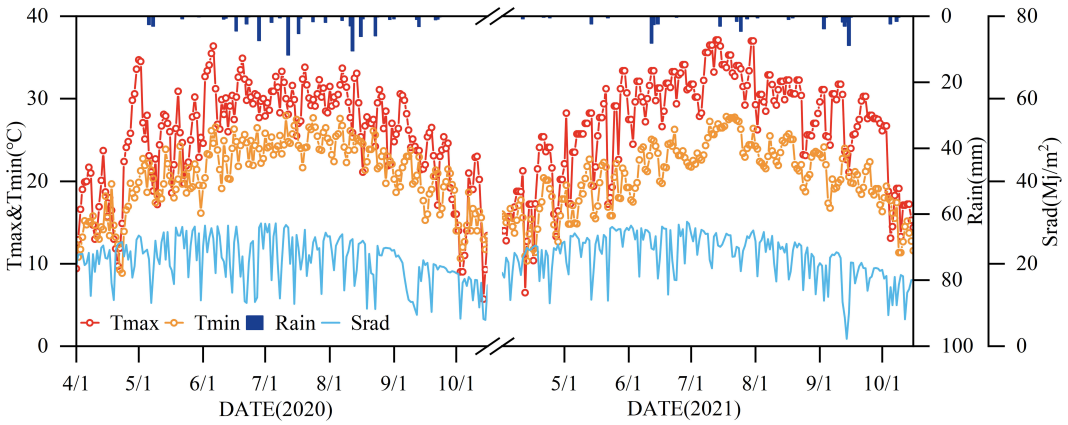

FIGURE 1
Precipitation (Rain), maximum and minimum temperatures (Tmax and Tmin), and solar radiation (Srad) during the crop fertility period in 2020 and 2021.

Total nitrogen concentration in sunflowers was determined using the micro-Kjeldahl method. Every 15–20 d, five sunflower plants were randomly selected from the diagonal and central areas of each plot using a five-point method. The plant samples were ground, sieved, and digested with a H_2SO_4-H_2O_2 solution. Total nitrogen concentration was measured using a Kjeldahl apparatus (China Ocean Energy Future Technology Group, K9860, China).

During the seedling stage (June 26, 2020 and July 2, 2021, respectively), bud stage (July 20, 2020 and July 26, 2021, respectively), flowering stage (August 9, 2020 and August 12, 2021, respectively), and post-flowering stage (September 10, 2020 and September 18, 2021, respectively), root samples from well-grown sunflowers were collected from the soil cross-section at depths of 0–10 cm, 10–20 cm, 20–30 cm, 30–40 cm, 40–50 cm, 50–60 cm, 60–70 cm, 70–80 cm, and 80–100 cm. The collected root samples were washed, sun-dried, and scanned using the Epson Perfection V700 PHOTO scanner. The root parameters were determined using WinRHIZO software.

From each plot, ten sunflowers were consistently selected for measuring mature sunflower yield, and this process was repeated three times.

2.4 APSIM simulation building

2.4.1 Introduction to the APSIM platform

The Agricultural Production Systems sIMulator (APSIM) is a versatile process-based modeling platform designed specifically for agricultural systems. It integrates multiple modules that cover various crop types, soil dynamics, and management strategies. APSIM can simulate crop growth, soil moisture, and nitrogen dynamics on a daily scale and is applicable to diverse management practices, farming systems, and environmental conditions. This model has been widely used in numerous studies to simulate agricultural production systems worldwide. The inputs to the model included daily meteorological data (such as solar radiation, maximum/minimum temperatures, and precipitation) and soil hydraulic parameters (such as bulk density, saturated water content, field capacity, and wilting point).

2.4.2 Application of APSIM modules

This study adopted the APSIM simulation, integrating the modules for fertilizers, soil moisture, soil nitrogen, and sunflowers. APSIM modules that control water and soil nitrogen are particularly crucial. The APSIM SoilWat module employs a cascade water balance model to estimate water and solute movement between soil layers, surface runoff and evaporation, and drainage from the system. This module balances the water content in each soil layer based on inputs and outputs. Soil water movement occurred through saturated, unsaturated, and oversaturated flows, each of which had specific model equations and parameters. The SoilN module manages the plant-available nitrogen supply, nitrate leaching, and nitrogen loss through denitrification. This module tracks the nutrient flow in the nitrogen cycle through mineralization, immobilization, nitrification, denitrification, and urea hydrolysis processes. Simulations involving CRF were conducted by adjusting the urea hydrolysis rate to approximate the CRF conditions. The APSIM model accommodates various fertilizer types, including urea and CRF, by introducing different release periods into the inorganic fertilizer module. The APSIM sunflower module simulated the daily root system growth from germination to grain-filling onset. The increase in root depth was calculated based on the daily growth rate and multiple factors. Daily root biomass growth was proportional to the shoot yield. Each growth stage had a specified root-to-shoot ratio that changed continuously from emergence to flowering. APSIM simulated the daily aging of root mass and length at a specific ratio, with aged roots becoming new organic matter incorporated into the soil nitrogen module.

2.4.3 Data sources and model calibration

This study calibrated the APSIM model using 2020 data and validated it with 2021 data, with the aim of minimizing

discrepancies between observed and measured values. APSIM version 7.10 was employed in this study.

In the APSIM model, the calibrated soil parameters are summarized as follows. The soil hydraulic parameters included saturated hydraulic conductivities (K_{s1}, K_{s2}, K_{s3}, and K_{s4}) with values of 53.1, 32.6, 26.5, and 32.2 mm/mm, respectively, for layers 0–20 cm, 20–40 cm, 40–60 cm and 60–100 cm, respectively. The saturated water contents (θ_{s1}, θ_{s2}, θ_{s3}, and θ_{s4}) of these layers were calibrated to 0.270, 0.281, 0.442, and 0.462 mm/mm, respectively. The field capacities (F_{c1}, F_{c2}, F_{c3}, and F_{c4}) were set to 0.243, 0.256, 0.421, and 0.452 mm/mm, respectively, and the wilting point water contents (θ_{wp1}, θ_{wp2}, θ_{wp3}, and θ_{wp4}) were calibrated to 0.09, 0.09, 0.10, and 0.11 mm/mm, respectively. Nitrogen turnover parameters included a soil nitrification potential of 40 μg NH_4^-/g soil, NH_4^- concentration at half potential of 90 ppm, denitrification rate coefficient of 0.0006 kg soil/mg C per day, and a power term (water factor for denitrification) set at 1.

The calibrated genetic coefficient values of the APSIM model for sunflowers are detailed as follows. The effective accumulated temperature from the end of the seedling stage to flower bud differentiation (tt_endjuv_to_init) was calibrated to 450°C/d. The temperature required for flower bud differentiation into flag leaves (tt_fi_to_flag) was set at 430°C/d. The effective accumulated temperature from flowering to the start of grain (tt_flower_to_start_grain) was 150°C/d, and from flowering to maturity (tt_flower_to_maturity) it is calibrated at 1100°C/d. The total leaf area coefficient (tpla_prod_coef) was set at 0.017, and the leaf emergence rate (rel_leaf_init_rate) at 0.5 leaf/d. The leaf senescence coefficient (spla_prod_coef) and the intercept (spla_intercept) were calibrated to 0.0035 and 0.01, respectively. The radiation use efficiency (RUE) is set at 1.15 g/MJ, and the daily increase in the harvest index (hi_incr) was 0.011.

2.5 Calculations analysis

(1) Principle and Improvement of the Jaccard Index

In bioinformatics and statistics, the Jaccard index can be widely applied to quantify similarity or overlap between two sample sets (Equation 1) (Real and Vargas, 1996). It is calculated as the ratio of the size of the intersection to the union of two sets, A and B:

$$J(A,B) = \left|\frac{A \cap B}{A \cup B}\right| \tag{1}$$

where A∩B is the number of elements in the intersection of sets A and B, and A∪B is the number of elements in their union.

To apply this index to analyze nitrate-nitrogen content and root length density, these metrics should first be categorized. The nitrate nitrogen content was divided into ten gradations within the 0–48 mg/kg range, with each gradation spanning 4.8 mg/kg. Similarly, the root length density was divided into ten gradations within the 0–2.8 cm/cm^3 range, with each gradation spanning 0.28 cm/cm^3. This categorization assigns each sample point to a specific gradation, thereby simplifying the matching analysis.

This study introduced a weighted mechanism to consider the correlation between adjacent gradations. Even if the samples were not in the same gradation, a certain degree of match was assigned if they were in adjacent gradations, based on their distance. The weight for a perfect match (same gradation) was 1; for adjacent gradations, it was 0.8; and it decreased by 0.2 for more distant gradations, until it reached 0. This weighting reflects the actual differences between the samples, thus enhancing the analysis. The improved formula for the weight calculation is:

The weight calculation formula can be represented as

$$W(g) = \max(0, 1 - \alpha \times |G - g|) \tag{2}$$

where $W(g)$ is the weight at grade g; G is the specified grade (e.g., grade of soil nitrate concentration or root length density); g represents the current grade under consideration, ranging from 1 to 10; and α is the weight interval, which is a fixed constant that controls the rate of change in weight with distance. In this study, α was set to 0.2.

The weighted intersection and union are calculated as follows:

$$N \cap R = \sum_{g=1}^{10} \min(W_N(g), W_R(g)) \tag{3}$$

$$N \cup R = \sum_{g=1}^{10} \max(W_N(g), W_R(g)) \tag{4}$$

where N∩R is the weighted intersection of soil nitrate nitrogen and root length density, and N∪R is the weighted union, with $W_N(g)$ and $W_R(g)$ being the weights for soil nitrate nitrogen and root length density at gradation g, respectively.

The Weighted Root Jaccard Index is calculated as:

$$RJ_{index} = \frac{\sum_{i=1}^{n} \frac{N \cap R}{N \cup R}}{n} \tag{5}$$

where RJ_{Index} is the Weighted Root Jaccard Index, and n is the number of days per growth stage.

This improved method involves the computation of weights, weighted intersection and union, and Weighted RJ_{Index}. This approach facilitated a more precise assessment of the match between soil nitrate-nitrogen content and root length density, particularly concerning subtle differences between the soil layers. This advancement provided a new tool for agricultural and ecological research, improving our understanding of the interactions between crop root systems and soil nutrients.

(2) NUE is a key agricultural indicator that measures the efficiency of crop nitrogen fertilizer utilization. It is calculated as the ratio of the crop yield to the amount of nitrogen absorbed by the crop.

$$NUE = \frac{Y}{SNU} \tag{6}$$

where Y (kg/ha) is the yield of each treatment, and SNU (kg/ha) is the sunflower nitrogen uptake.

2.6 Model evaluation statistics

In this study, the performance of the model in simulating soil NO_3-N concentration (SNC), sunflower root length density (RLD), crop nitrogen uptake, and yield was assessed using several statistical methods. These included the Coefficient of Determination (R^2), where a higher value indicated a better fit of the model to the data; Root Mean Square Error (*RMSE*), where lower values indicated a better fit; and Mean Absolute Error (*MAE*), where a lower value indicated more accurate model predictions.

$$R^2 = 1 - \frac{\sum_{i=1}^{n}(M_i - S_i)^2}{\sum_{i=1}^{n}(M_i - M)^2} \quad (7)$$

$$RMSE = \sqrt{\frac{\sum_{i=1}^{n}(M_i - S_i)^2}{n}} \quad (8)$$

$$MAE = \frac{1}{n}\sum_{i=1}^{n}|M_i - S_i| \quad (9)$$

Where, M_i represents the observed value, S_i represents the simulated value, M is the average of the observed value, and n is the sample size.

2.7 Statistical analysis

In this study, data processing was conducted using Microsoft Excel 2019, and graphical representations were generated using Origin 2021 software, Python programming was used to calculate the correlation between soil nitrate nitrogen and sunflower root length density.

3 Results

3.1 Model calibration and validation

This APSIM model was employed to simulate soil NO_3-N concentration (SNC), sunflower root length density (RLD), crop nitrogen uptake, and yield throughout the entire growth cycle. The model was calibrated using experimental data from 2020 and validated using data from 2021. Performance evaluation included key indicators such as the coefficient of determination (R^2) (Equation 7), root mean square error (*RMSE*) (Equation 8), and mean absolute error (*MAE*) (Equation 9) (Figures 2, 3 and Table 1).

During 2020–2021, the *RMSE* values were 0.421–1.801 mg/kg for SNC. 0.062–0.093 cm/cm^3 for sunflower RLD, 5.07–8.88 kg/ha for sunflower nitrogen uptake, and 168.37–178.52 kg/ha for yield. The average R^2 values were 0.895 (SNC), 0.894 (RLD), 0.764 (NU), and 0.893 (yield), with corresponding average *MAE* values of 0.989 mg/kg, 0.071 cm/cm^3, 6.37 kg/ha, and 151.45 kg/ha. These findings indicate the high precision and strong predictive capability of the model for simulating these variables from 2020 to 2021.

3.2 Effects of fertilizer application depth on SNC distribution

This study analyzed the 2020 and 2021 experimental data to investigate the relationship between fertilizer application depth and

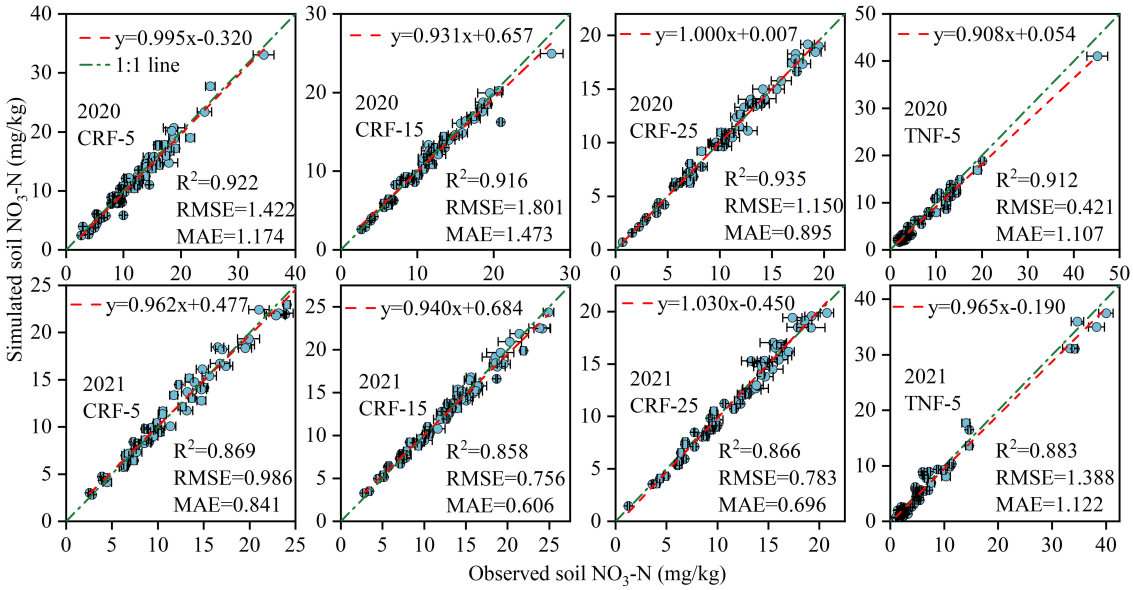

FIGURE 2
Statistical results for APSIM calibration (2020) and validation (2021) for soil NO_3-N concentrations (SNC), controlled-release fertilizer (CRF) at three depths of N-fertilizer application (5, 15, and 25 cm) and traditional nitrogen fertilizer (TNF) applied at a 5 cm depth. R^2, *RMSE*, and *MAE* are the determination coefficient, root mean square error, and mean absolute error, respectively.

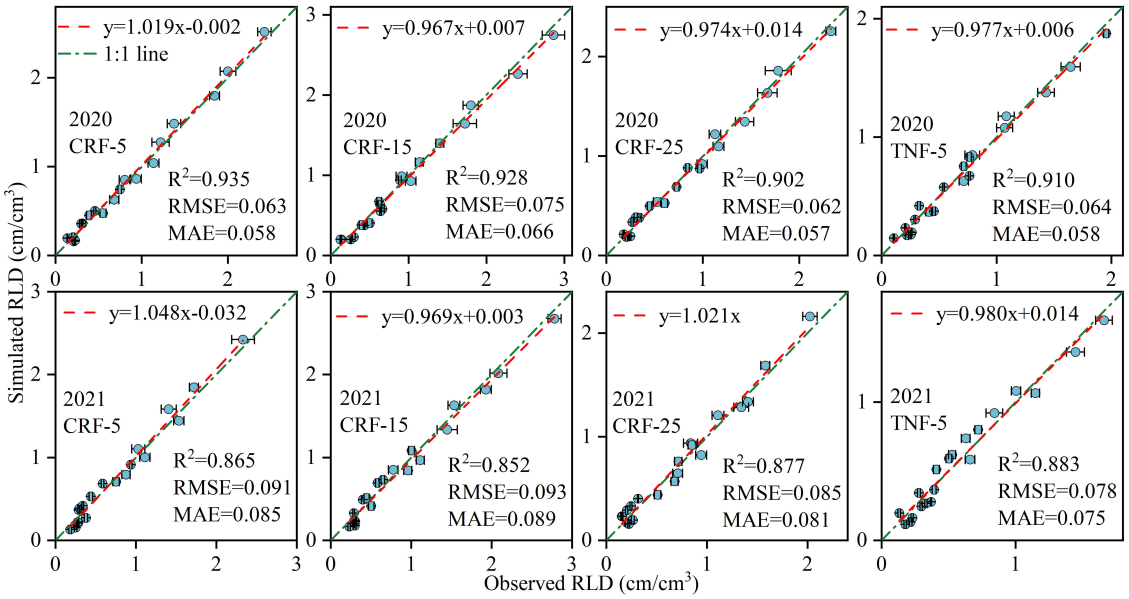

FIGURE 3
Statistical results for APSIM calibration (2020) and validation (2021) for root length density (RLD), controlled-release fertilizer (CRF) at three depths of N-fertilizer application (5, 15, and 25 cm) and traditional nitrogen fertilizer (TNF) applied at a 5 cm depth. R^2, *RMSE*, and *MAE* are the determination coefficient, root mean square error, and mean absolute error, respectively.

the distribution of SNC (Figure 4). The results indicated that at a depth of 5 cm, the SNC in the soil surface was significantly higher than that in deeper layers. In contrast, depths of 15 and 25 cm resulted in higher SNC in the deeper soil layers. Throughout the growth period, SNC under TNF treatment was lower than that under CRF treatment with the same amount of nitrogen. Specifically, during the 2020 and 2021 experimental periods, in the 0–10 cm soil layer during the sunflower seedling stage, the SNC of CRF-5 was 86.83% and 695.73% higher than that of the CRF-15 and CRF-25 treatments, respectively. At the budding and flowering stages, it was higher by 35.73% and 206.27%, respectively. In the 10–20 cm soil layer, at the seedling stage, the SNC of the CRF-15 treatment was 93.63% and 144.94% higher than that of the CRF-5 and CRF-25 treatments, respectively. At the budding and flowering stages, they were 11.08% and 33.28% higher, respectively. In the deep soil layer (20–100 cm), from the seedling stage to the end of the flowering stage, the SNC of the CRF-25 treatment was 19.91% and 13.44% higher than that of the CRF-5 and CRF-15 treatments, respectively. At the maturity stage, within the 0-40 cm soil layer, the SNC of the CRF-5 treatment increased by 5.00% and 18.81% compared with CRF-15 and CRF-25, respectively. In the 40–60 cm soil layer, CRF-25 increased by 11.84% and 8.13% compared with CRF-5 and CRF-15, respectively.

Throughout the growth period, the SNC of the CRF-5 treatment in the 0–100 cm soil layer was 114.01% higher than that of the TNF-5 treatment at the same nitrogen application rate. These findings are important for understanding the effects of deep CRF application on SNC distribution and its potential effects on soil fertility and plant growth.

3.3 Effects of fertilizer application depth on sunflower RLD across growth stages

The 2020–2021 data demonstrated that within each treatment group, sunflower RLD initially increased and then decreased throughout the growth period. Overall, RLD decreased gradually with increasing soil depth across the entire soil profile (Figure 5).

TABLE 1 Statistical results for APSIM calibration (2020) and validation (2021) for nitrogen uptake and yield, controlled-release fertilizer (CRF) at three depths of N-fertilizer application (5, 15, and 25 cm) and traditional nitrogen fertilizer (TNF) applied at a 5 cm depth.

Parameter	2020 for Calibration			2021 for Verification		
	R^2	*RMSE* (kg/ha)	*MAE* (kg/ha)	R^2	*RMSE* (kg/ha)	*MAE* (kg/ha)
Yield(kg/ha)	0.891	168.37	157.80	0.895	178.52	145.10
Nitrogen uptake(kg/ha)	0.794	5.07	4.11	0.733	8.88	8.63

R^2, *RMSE*, and *MAE* are the determination coefficient, root mean square error, and mean absolute error, respectively.

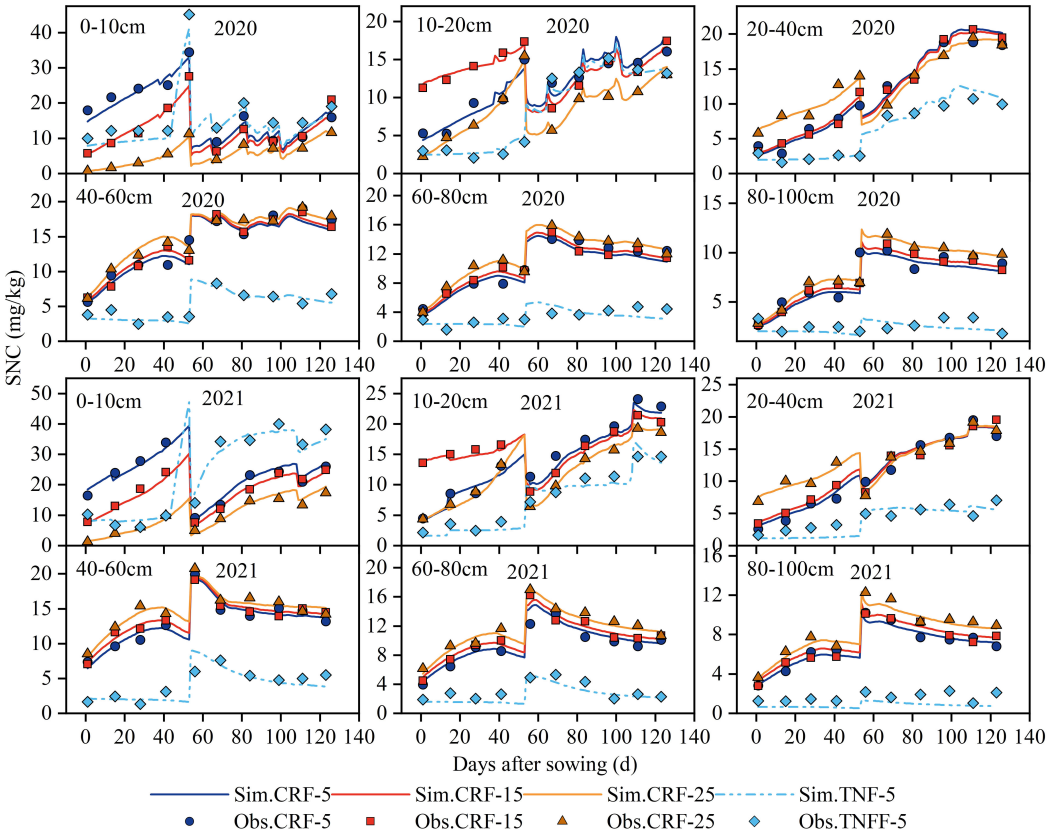

FIGURE 4
Soil NO_3-N concentrations (SNC) in 0–100 cm soil under controlled-release fertilizer (CRF) at three depths of N-fertilizer application (5, 15, and 25 cm) and traditional nitrogen fertilizer (TNF) applied at a 5 cm depth from 2020 to 2021.

Under the CRF-5 treatment, RLD was mainly concentrated in the surface layer, whereas under the CRF-15 and CRF-25 treatments, it increased at greater depths. Specifically, during the seedling stage, the RLD of the CRF-15 treatment in the 0–100 cm soil profile was 11.15% and 14.02% higher than that of the CRF-5 and CRF-25 treatments, respectively. At the budding, flowering, and maturity stages, these differences changed to 9.38% and 15.21%, 12.05% and 14.37%, and 17.63% and 19.67%, respectively, indicating that the RLD under CRF-15 treatment reached its maximum value at all growth stages. These findings suggest that fertilizer depth can influence the downward growth and distribution of the root system and that an appropriate depth can enhance sunflower RLD at different growth stages.

During the seedling, budding, flowering, and maturity stages of sunflower growth, the RLD of the CRF-5 treatment was 26.01%, 22.17%, 27.23%, and 19.32% higher than that of the TNF-5 treatment with the same amount of nitrogen, respectively. This suggests that CRF may enhance the growth of the crop root system by adjusting SNC. The bar charts in each figure illustrate that, under CRF treatments, as the depth of fertilizer application increased, the proportion of RLD in the 0–20 cm soil layer gradually decreased, whereas RLD in the 20–100 cm soil layer showed an increasing trend. These findings highlight the potential of different CRF fertilizer placement positions to optimize crop root distribution and promote downward root growth.

3.4 Evaluating the effects of fertilizer application depth using the root system Jaccard index

Using the root system Jaccard index (Equations 2–5) to quantify the match between crop RLD and SNC revealed the effect of CRF treatment depth on their compatibility (Figure 6). During the seedling stages of 2020 and 2021, the average Jaccard index of the root system in the 0–20 cm soil layer for the CRF-25 treatment was 48.48% and 34.44% higher than that for the CRF-5 and CRF-15 treatments, respectively, indicating better compatibility between RLD and SNC in the soil surface layer. However, during the budding, flowering, and maturity stages, the CRF-15 treatment had the highest average Jaccard index of root system. Specifically, during the budding and flowering stages, the CRF-15 treatment was 81.28% and 7.27% higher than that of the CRF-5 and CRF-25 treatments, respectively, whereas at the maturity stage, it increased by 11.18% and 17.42%, respectively. In the 20–60 cm soil layer, the Jaccard index ranking of the average root system during the seedling stage was CRF-5>CRF-25>CRF-15. During the budding and flowering stages, it was CRF-15>CRF-5>CRF-25, with the CRF-15 treatment being 15.76% and 10.37% higher than that of the CRF-5 and CRF-25 treatments, respectively. By the maturity stage, it changed to CRF-25>CRF-15>CRF-5, with the CRF-25 treatment being 38.58% and 15.83% higher than the CRF-5 and CRF-15

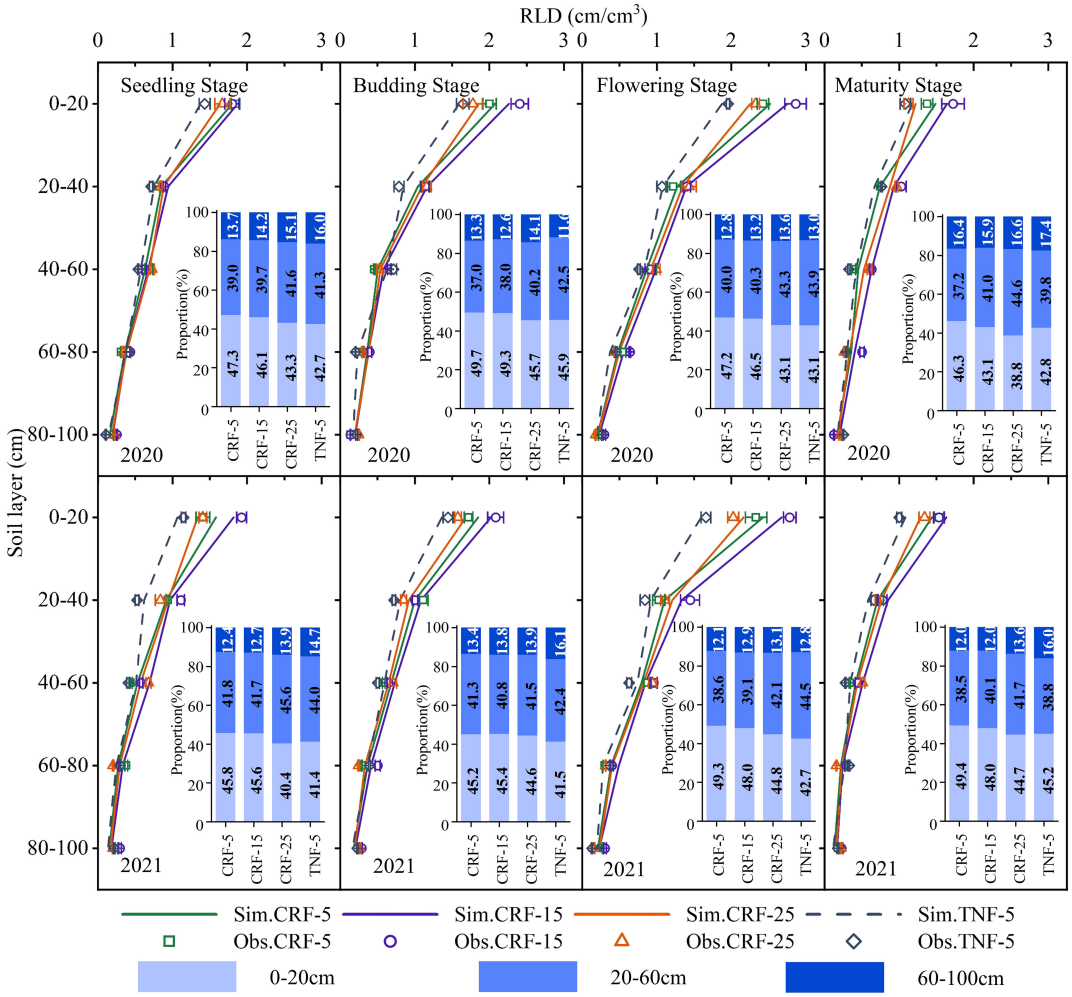

FIGURE 5
Effects of controlled-release fertilizer (CRF) at three depths of N-fertilizer application (5, 15, and 25 cm) and traditional nitrogen fertilizer (TNF) applied at a depth of 5 cm on the vertical distribution and distribution proportion of different soil layers (bar charts embedded in each figure) of root length density (RLD) of sunflower at seedling, budding, flowering, and maturity growth stages from 2020 to 2021.

treatments, respectively. In the deeper 60–100 cm soil layer, the Jaccard index ranking of the root system during the seedling and budding plus flowering stages was CRF-5>CRF-15>CRF-25. At the maturity stage, there was essentially no difference in the average Jaccard index of the root system among the different fertilizer depths.

Throughout the 0–100 cm soil profile, the average Jaccard index of the root system was consistently better for the CRF-15 treatment than for CRF-25 and CRF-5, increasing by 6.60% and 7.34%, respectively, during the seedling, budding plus flowering, and maturity stages. This suggests that CRF application at a depth of 15 cm can significantly improve the match between RLD and SNC throughout the growth period. Additionally, the root system Jaccard index for the CRF-5 treatment was 20.45% higher than that for the TNF-5 treatment with the same nitrogen application rate, indicating that CRF treatments can better optimize the match between RLD and SNC than TNF treatments.

3.5 Effects of fertilizer application depth on sunflower yield, nitrogen uptake, and NUE

This study investigated the effects of different CRF fertilizer application depths (5, 15, and 25 cm) on sunflower yield, nitrogen uptake (NU), and NUE in field experiments (Table 2). Synthesizing the data from 2020 and 2021 revealed a significant impact of fertilizer application depth on these indicators. In terms of yield, the CRF-15 treatment outperformed the other treatments in both years, with yields of 8.62% and 10.25% higher than the CRF-5 and CRF-25, respectively, indicating that medium-depth fertilization promoted crop growth and yield. Compared with TNF-5, the CRF-5 increased the yield by 30.62% under the same nitrogen application rate. CRF-15 exhibited the highest NU capacity, which was 4.82% and 5.97% higher than that of CRF-5 and CRF-25, respectively, highlighting the role of medium-depth fertilization in promoting effective NU. Regarding NUE (Equation 6), CRF-15 also exhibited higher efficiency, with

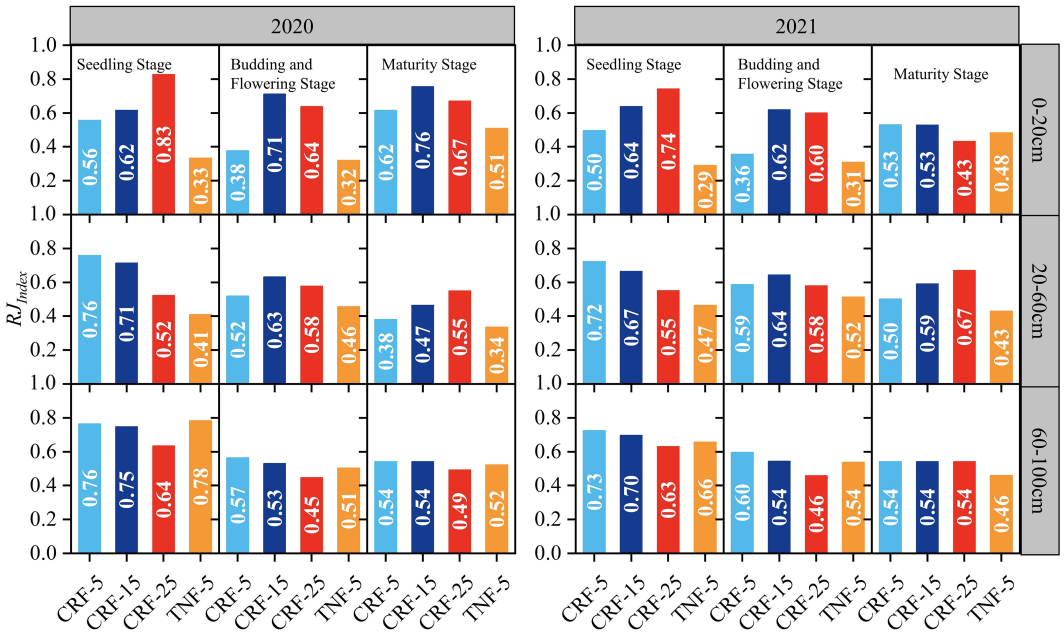

FIGURE 6
Root Jaccard Index of soil NO_3-N concentrations (SNC) and root length density (RLD) in the 0–100cm soil profile during the growing season under controlled-release fertilizer (CRF) at three depths of N-fertilizer applications (5, 15, and 25 cm) and traditional nitrogen fertilizer (TNF) applied at a 5 cm depth, from 2020 to 2021.

NUE 3.63% and 4.04% higher than those of CRF-5 and CRF-25, respectively. This suggests that at a depth of 15 cm, the NUE was optimized, enhancing the nitrogen absorption and utilization efficiency of the crop. Compared to TNF-5, under the same nitrogen application rate, the NU and NUE under CRF-5 increased by 14.95% and 13.45%, respectively, indicating that CRF treatment significantly improved yield, NU, and NUE compared to TNF.

Overall, these findings suggested that CRF application at a depth of 15 cm significantly enhances sunflower yield, NU capability, and NUE. This depth likely benefits from being closer to the main root zone of the crop, facilitating effective nitrogen absorption and utilization by the root system.

4 Discussion

4.1 Comprehensive analysis of influencing factors

4.1.1 Impact of fertilization depth on SNC distribution

This study indicated a significant impact of CRF application depth on SNC distribution, which is crucial for enhancing NUE and reducing environmental pollution (Xia et al., 2022). Shallow CRF application (5 cm) resulted in notably higher NO_3-N concentrations in the surface soil than in the deeper layers,

TABLE 2 Biennial comparative analysis of yield, nitrogen uptake (NU), and nitrogen use efficiency (NUE) under controlled-release fertilizer (CRF) at three depths of N-fertilizer application (5, 15, and 25 cm) and traditional nitrogen fertilizer (TNF) applied at a 5 cm depth from 2020 to 2021.

Years	Treatment	Sim.yield	Obs.yield	Sim.NU	Obs.NU	NUE
		kg/ha	kg/ha	kg/ha	kg/ha	kg/kg
2020	CRF-5	3886.00	4092.81 ± 56.09ab	236.7	238.70 ± 4.54ab	16.42
	CRF-15	4239.30	4385.20 ± 259.39a	246.4	249.40 ± 9.27a	17.20
	CRF-25	3789.70	3723.10 ± 92.63b	223.8	221.60 ± 7.87b	16.93
	TNF-5	3231.00	3019.11 ± 78.53c	215.5	224.72 ± 2.47b	14.99
2021	CRF-5	4246.30	4115.60 ± 98.77ab	241.7	248.60 ± 10.07a	17.57
	CRF-15	4471.90	4415.00 ± 118.55a	252.1	260.10 ± 0.45a	17.73
	CRF-25	4178.10	3859.20 ± 227.56b	247.6	240.20 ± 3.78a	16.87
	TNF-5	3012.50	2938.60 ± 98.48c	201.3	213.50 ± 12.21b	14.97

Lowercase letters (e.g., a, b, c, d) are used to indicate significant differences between groups. The significance level is determined based on statistical tests and is set at $p < 0.05$.

whereas deeper application (15 and 25 cm) increased NO_3-N concentration in the lower soil layers (Figure 4). This is consistent with previous findings (Wu et al., 2022a; Chen et al., 2022c). The impact of CRF application depth on SNC distribution was multifaceted. Shallow fertilization leads to surface soil NO_3-N accumulation owing to higher evaporation rates and limited water penetration, whereas deep fertilization promotes the downward NO_3-N percolation with soil moisture, reaching deeper layers (Kanwar et al., 1985). Moreover, fertilization depth may influence root system efficiency in NO_3-N absorption. The shallow fertilization can be more readily absorbed, affecting NO_3-N distribution, whereas deep fertilization may stimulate downward root growth for NO_3-N absorption from the deeper soil layers (Liu et al., 2018).

In summary, the effect of fertilization depth on SNC can be influenced by various factors, such as moisture dynamics, microbial activity, and root absorption. Understanding these mechanisms is crucial for guiding fertilization strategies in modern agriculture with the aim of enhancing nitrogen fertilizer efficiency and mitigating environmental pollution.

4.1.2 Correlation between RLD and SNC

RLD is a crucial indicator of root distribution in the soil, directly affecting the ability of a crop to absorb NO_3-N (Dusserre et al., 2009). This study demonstrated a strong correlation between RLD and SNC, highlighting the close link between soil nitrogen availability and crop root system structure. Across different fertilizer depth conditions, changes in root length density reflect the adaptation of the root system to nitrogen availability (Liu et al., 2018; Chen et al., 2022a). Shallow fertilization (5 cm) resulted in a higher RLD in the surface soil, indicating root growth in areas with higher SNC (Jia et al., 2020). In contrast, deep fertilization (15 and 25 cm) led to relatively higher RLD in deeper soil layers, suggesting downward root growth to access nitrogen in deeper layers (Figure 5) (van der Bom et al., 2020).

Root development and distribution are vital mechanisms for crops to adapt to the soil environment, particularly regarding soil nutrient distribution (Giehl and von Wiren, 2014; Zhao et al., 2020; Kang et al., 2022). The RLD distribution indicated that crop roots could adjust their growth based on the NO_3-N distribution, thereby optimizing nutrient absorption (Chen et al., 2020). To effectively absorb the nitrogen, roots should maintain an appropriate growth density in high-N areas (Fageria and Moreira, 2011). Therefore, adjusting fertilizer depth to optimize root growth and the distribution is a potential strategy for influencing soil nitrogen distribution. For instance, medium-depth CRF fertilization (15 cm) may better match the fertilizer with the main root system distribution area, improving nitrate-nitrogen absorption efficiency (Figure 6).

In summary, the correlation between root length density and SNC demonstrated how crop roots responded and adapted to soil nitrogen distribution. This understanding is vital for developing effective fertilization strategies, particularly for enhancing NUE and crop growth. Adjusting fertilizer depth can optimize SNC distribution and influence root structure and function, thereby improving nitrogen absorption and utilization efficiency (Morris et al., 2017).

4.2 Impact of fertilization depth on crop yield, nitrogen absorption, and strategies to improve NUE

In this study, different CRF fertilization depths (5, 15, and 25 cm) exhibited significant effects on the sunflower yield, NU, and NUE (Table 2). These effects could result from two main factors. First, fertilization depth directly affected NO_3-N distribution in the soil. Second, it indirectly affected root system distribution and functionality. NO_3-N distribution is critical for crop growth and yield, as higher concentrations in areas with denser root systems lead to increased absorption efficiency, which is conducive to higher yields (Barber and Mackay, 1986). Therefore, alignment between fertilization depth and root system distribution is crucial for maximizing yield.

In a spring maize experiment (Wu et al., 2021), trials were conducted at fertilizer depths of 5, 15, 25, and 35 cm. The results indicated that at 15 cm and 25 cm depths, maize yield increased by 5.68% and 13.83%, respectively, compared to the 5 cm depth, with NUE improving by 17.79% and 38.37%, respectively. The highest yield and NUE were observed at a depth of 25 cm. However, the 15 cm depth treatment yielded 3.90% and 4.32% higher NUE than the 5 cm and 25 cm treatments, respectively, with average NUE increases of 0.67% and 1.56%, respectively. The highest yield and NUE were obtained at the depth of 15 cm (Table 2). These variations in results may be attributed to meteorological conditions such as precipitation, soil texture, and initial nutrient concentration in the soil. Overall, the study suggested that appropriately increasing CRF application depth can enhance the crop yield and NUE in agricultural production. Medium-depth fertilization may be preferred because it avoids the excessive SNC in the surface layer and reduces the NO_3-N distribution in deeper soil layers, ensuring more even nitrogen distribution across soil layers where crop roots are concentrated. This depth also minimizes N volatilization and leaching losses (Min et al., 2021; Wu et al., 2021), enhancing the availability of NO_3-N for crop absorption and use. In medium-depth soils, N had a longer contact time with the root systems, improving NUE. Furthermore, the soil moisture and temperature conditions at this depth may promote root growth and enhance microbial activity, which facilitates N transformation through mineralization, making it more readily absorbable by crops (Niu et al., 2021). Therefore, this study demonstrated that the medium-depth application of CRF (such as at 15 cm) performed best, likely due to the creation of favorable conditions for crop nitrogen absorption, resulting in improved yield and NUE (Chen et al., 2022b). These findings are significant for guiding agricultural practices, particularly the application of precision fertilization techniques, to enhance NUE and crop productivity.

4.3 Future research directions and practical applications

The findings of this study hold practical value in agriculture. Optimizing CRF application depth can improve NUE, reduce costs (Sainju et al., 2006), and increase yields (Liu et al., 2022; Wu et al., 2022b), thus benefiting small-scale farmers with limited resources. This optimization also mitigates the environmental impact of nitrogen fertilizers, which could be crucial for addressing climate change and protecting ecosystems (Wu et al., 2021). The application of the weighted Jaccard index proposed a refined method for analyzing soil-root system interactions. This index considered not only the direct match between the SNC and RLD but also the match between adjacent gradations. While showing advantages, the practical application of the weighted Jaccard index faced challenges such as selecting the appropriate gradation and weight distribution, which significantly affected the analysis results. Future research should focus on effectively determining these parameters effectively to ensure the accuracy and reliability of the analysis. Additionally, further exploration is needed regarding the performance of the index in handling extreme values. Future studies could also investigate its application in broader agricultural and ecological research, such as assessing the responses of different crop varieties to soil nutrients or evaluating the impact of climate change on soil-root system interactions (Cangioli et al., 2022; Lamichhane et al., 2024).

Future research should be conducted under a broader range of geographical and climatic conditions to verify the general applicability of the findings of this study, considering the influence of different soil types and environmental conditions. It is also crucial to investigate how different crop varieties respond to fertilization depth, and how this interacts with crop genetic and physiological traits. Additionally, long-term experimental studies are needed to understand the lasting impact of fertilization depth on soil health and ecosystem services, such as carbon storage and biodiversity.

5 Conclusion

The APSIM model was used to analyze the effects of CRF application depth on SNC, sunflower RLD, nitrogen uptake, and yield. The results showed that CRF depth significantly influenced SNC distribution, affecting root growth and nitrogen absorption. Shallow fertilization increased the NO_3-N concentration in the soil surface layer, whereas deep fertilization moved NO_3-N to deeper soil layers. Medium-depth fertilization at 15 cm indicated the best performance in enhancing sunflower yield and nitrogen absorption, highlighting the importance of optimizing CRF application depth to improve NUE and promote crop growth. The application of an improved Jaccard index provided a new method for quantifying soil-root system interactions and enhancing understanding. However, the applicability of this study was limited to specific environmental and crop conditions. Future studies should validate these findings across a broader range of environmental and crop varieties. Further exploration of the long-term impacts of adjusting the fertilization depth on soil health and ecosystem services is necessary.

Data availability statement

The original contributions presented in the study are included in the article/supplementary material. Further inquiries can be directed to the corresponding author.

Author contributions

WR: Writing – review & editing, Data curation, Formal analysis, Methodology, Visualization, Writing – original draft. XL: Funding acquisition, Project administration, Resources, Writing – review & editing. TL: Conceptualization, Funding acquisition, Project administration, Writing – review & editing. NC: Methodology, Validation, Writing – review & editing. MX: Data curation, Supervision, Writing – original draft. BL: Software, Validation, Writing – original draft. QQ: Software, Validation, Writing – original draft. GL: Investigation, Validation, Writing – review & editing.

Funding

The author(s) declare financial support was received for the research, authorship, and/or publication of this article. This research was jointly supported by the National Key Research and Development Program of China (2021YFC3201202), Fundamental Research Funds for the Inner Mongolia Universities-Science Foundation for Distinguished Young Scholars of Inner Mongolia Agricultural University (BR220302), Inner Mongolia Science and Technology Program (2022YFHH0039), and National Natural Science Foundation of China (52079064).

Acknowledgments

We are grateful to MX, BL and QQ for their help with the experiments. We would also like to thank all reviewers for their careful, constructive, and insightful comments regarding this work.

Conflict of interest

The authors declare that the research was conducted in the absence of any commercial or financial relationships that could be construed as a potential conflict of interest.

Publisher's note

References

Azeem, B., KuShaari, K., Man, Z. B., Basit, A., and Thanh, T. H. (2014). Review on materials & methods to produce controlled release coated urea fertilizer. *J. Control Release* 181, 11–21. doi: 10.1016/j.jconrel.2014.02.020

Bag, S., Kumar, S. K., and Tiwari, M. K. (2019). An efficient recommendation generation using relevant Jaccard similarity. *Inf. Sci.* 483, 53–64. doi: 10.1016/j.ins.2019.01.023

Barber, S. A., and Mackay, A. D. (1986). Root growth and phosphorus and potassium uptake by two corn genotypes in the field. *Fertilizer Res.* 10, 217–230. doi: 10.1007/bf01049351

Cangioli, L., Mancini, M., Napoli, M., Fagorzi, C., Orlandini, S., Vaccaro, F., et al. (2022). Differential response of wheat rhizosphere bacterial community to plant variety and fertilization. *Int. J. Mol. Sci.* 23, 3616. doi: 10.3390/ijms23073616

Chen, G., Cai, T., Wang, J., Wang, Y., Ren, L., Wu, P., et al. (2022a). Suitable fertilizer application depth enhances the efficient utilization of key resources and improves crop productivity in rainfed farmland on the loess plateau, China. *Front. Plant Sci.* 13. doi: 10.3389/fpls.2022.900352

Chen, M., and Graedel, T. E. (2016). A half-century of global phosphorus flows, stocks, production, consumption, recycling, and environmental impacts. *Global Environ. Change* 36, 139–152. doi: 10.1016/j.gloenvcha.2015.12.005

Chen, Y., Hu, S., Guo, Z., Cui, T., Zhang, L., Lu, C., et al. (2021b). Effect of balanced nutrient fertilizer: A case study in Pinggu District, Beijing, China. *Sci. Total Environ.* 754, 142069. doi: 10.1016/j.scitotenv.2020.142069

Chen, L., Li, K. K., Shi, W. J., Wang, X. L., Wang, E. T., Liu, J. F., et al. (2021a). Negative impacts of excessive nitrogen fertilization on the abundance and diversity of diazotrophs in black soil under maize monocropping. *Geoderma* 393, 114999. doi: 10.1016/j.geoderma.2021.114999

Chen, J., Liu, L., Wang, Z., Zhang, Y., Sun, H., Song, S., et al. (2020). Nitrogen fertilization increases root growth and coordinates the root-shoot relationship in cotton. *Front. Plant Sci.* 11. doi: 10.3389/fpls.2020.00880

Chen, X., Liu, P., Zhao, B., Zhang, J., Ren, B., Li, Z., et al. (2022c). Root physiological adaptations that enhance the grain yield and nutrient use efficiency of maize (Zea mays L) and their dependency on phosphorus placement depth. *Field Crops Res.* 276, 108378. doi: 10.1016/j.fcr.2021.108378

Chen, G., Ren, L., Wang, J., Liu, F., Liu, G., Li, H., et al. (2022b). Optimizing fertilization depth can promote sustainable development of dryland agriculture in the Loess Plateau region of China by improving crop production and reducing gas emissions. *Plant Soil* 499, 73–89. doi: 10.1007/s11104-022-05795-6

Chen, X., Ren, H., Zhang, J., Zhao, B., Ren, B., Wan, Y., et al. (2024). Deep phosphorus fertilizer placement increases maize productivity by improving root-shoot coordination and photosynthetic performance. *Soil Tillage Res.* 235, 105915. doi: 10.1016/j.still.2023.105915

Ciampitti, I. A., Briat, J. F., Gastal, F., and Lemaire, G. (2022). Redefining crop breeding strategy for effective use of nitrogen in cropping systems. *Commun. Biol.* 5, 823. doi: 10.1038/s42003-022-03782-2

Connor, D. J., and Hall, A. J. (1997). "Sunflower physiology," in *Sunflower technology and production*, 35, 113–182. doi: 10.2134/agronmonogr35.c4

Duan, J., Shao, Y., He, L., Li, X., Hou, G., Li, S., et al. (2019). Optimizing nitrogen management to achieve high yield, high nitrogen efficiency and low nitrogen emission in winter wheat. *Sci. Total Environ.* 697, 134088. doi: 10.1016/j.scitotenv.2019.134088

Dusserre, J., Audebert, A., Radanielson, A., and Chopart, J. L. (2009). Towards a simple generic model for upland rice root length density estimation from root intersections on soil profile. *Plant Soil* 325, 277. doi: 10.1007/s11104-009-9978-0

Fageria, N., and Moreira, A. (2011). The role of mineral nutrition on root growth of crop plants. *Adv. Agron.* 110, 251–331. doi: 10.1016/B978-0-12-385531-2.00004-9

Gebre, M. G., and Earl, H. J. (2021). Soil water deficit and fertilizer placement effects on root biomass distribution, soil water extraction, water use, yield, and yield components of soybean [Glycine max (L.) merr.] grown in 1-m rooting columns. *Front. Plant Sci.* 12. doi: 10.3389/fpls.2021.581127

Geng, Y., Wang, J., Sun, Z., Ji, C., Huang, M., Zhang, Y., et al. (2021). Soil N-oxide emissions decrease from intensive greenhouse vegetable fields by substituting synthetic N fertilizer with organic and bio-organic fertilizers. *Geoderma* 383, 114730. doi: 10.1016/j.geoderma.2020.114730

Giehl, R. F., and von Wiren, N. (2014). Root nutrient foraging. *Plant Physiol.* 166, 509–517. doi: 10.1104/pp.114.245225

Guo, Y., Chen, Y., Searchinger, T. D., Zhou, M., Pan, D., Yang, J., et al. (2020). Air quality, nitrogen use efficiency and food security in China are improved by cost-effective agricultural nitrogen management. *Nat. Food* 1, 648–658. doi: 10.1038/s43016-020-00162-z

Haydar, M. S., Ghosh, D., and Roy, S. (2024). Slow and controlled release nanofertilizers as an efficient tool for sustainable agriculture: Recent understanding and concerns. *Plant Nano Biol.* 7, 100058. doi: 10.1016/j.plana.2024.100058

Heuer, S., Gaxiola, R., Schilling, R., Herrera-Estrella, L., Lopez-Arredondo, D., Wissuwa, M., et al. (2017). Improving phosphorus use efficiency: a complex trait with emerging opportunities. *Plant J.* 90, 868–885. doi: 10.1111/tpj.13423

Hui, X., Wang, X., Luo, L., Wang, S., Guo, Z., Shi, M., et al. (2022). Wheat grain zinc concentration as affected by soil nitrogen and phosphorus availability and root mycorrhizal colonization. *Eur. J. Agron.* 134, 126469. doi: 10.1016/j.eja.2022.126469

Jia, X., Wang, Y., Zhang, Q., Lin, S., Zhang, Y., Du, M., et al. (2023). Reasonable deep application of sheep manure fertilizer to alleviate soil acidification to improve tea yield and quality. *Front. Plant Sci.* 14. doi: 10.3389/fpls.2023.1179960

Jia, Q., Yang, L., An, H., Dong, S., Chang, S., Zhang, C., et al. (2020). Nitrogen fertilization and planting models regulate maize productivity, nitrate and root distributions in semi-arid regions. *Soil Tillage Res.* 200, 104636. doi: 10.1016/j.still.2020.104636

Jin, K., White, P. J., Whalley, W. R., Shen, J., and Shi, L. (2017). Shaping an optimal soil by root-soil interaction. *Trends Plant Sci.* 22, 823–829. doi: 10.1016/j.tplants.2017.07.008

Kang, J., Peng, Y., and Xu, W. (2022). Crop root responses to drought stress: molecular mechanisms, nutrient regulations, and interactions with microorganisms in the rhizosphere. *Int. J. Mol. Sci.* 23, 9310. doi: 10.3390/ijms23169310

Kant, S., Bi, Y. M., and Rothstein, S. J. (2011). Understanding plant response to nitrogen limitation for the improvement of crop nitrogen use efficiency. *J. Exp. Bot.* 62, 1499–1509. doi: 10.1093/jxb/erq297

Kanwar, R. S., Baker, J. L., and Laflen, J. M. (1985). Nitrate movement through the soil profile in relation to tillage system and fertilizer application method. *Trans. ASAE* 28, 1802–1807. doi: 10.13031/2013.32522

Kiniry, J. R., Blanchet, R., Williams, J. R., Texier, V., Jones, C. A., and Cabelguenne, M. (1992). Sunflower simulation using the EPIC and ALMANAC models. *Field Crops Res.* 30, 403–423. doi: 10.1016/0378-4290(92)90008-w

Kong, D., Jin, Y., Chen, J., Yu, K., Zheng, Y., Wu, S., et al. (2021). Nitrogen use efficiency exhibits a trade-off relationship with soil N2O and NO emissions from wheat-rice rotations receiving manure substitution. *Geoderma* 403, 115374. doi: 10.1016/j.geoderma.2021.115374

Lamichhane, J. R., Barbetti, M. J., Chilvers, M. I., Pandey, A. K., and Steinberg, C. (2024). Exploiting root exudates to manage soil-borne disease complexes in a changing climate. *Trends Microbiol.* 32, 27–37. doi: 10.1016/j.tim.2023.07.011

Li, J., Xu, X., Lin, G., Wang, Y., Liu, Y., Zhang, M., et al. (2018). Micro-irrigation improves grain yield and resource use efficiency by co-locating the roots and N-fertilizer distribution of winter wheat in the North China Plain. *Sci. Total Environ.* 643, 367–377. doi: 10.1016/j.scitotenv.2018.06.157

Li, G., Zhao, B., Dong, S., Zhang, J., Liu, P., and Lu, W. (2020). Controlled-release urea combining with optimal irrigation improved grain yield, nitrogen uptake, and growth of maize. *Agric. Water Manage.* 227, 105834. doi: 10.1016/j.agwat.2019.105834

Liu, W., Ma, G., Wang, C., Wang, J., Lu, H., Li, S., et al. (2018). Irrigation and nitrogen regimes promote the use of soil water and nitrate nitrogen from deep soil layers by regulating root growth in wheat. *Front. Plant Sci.* 9. doi: 10.3389/fpls.2018.00032

Liu, P., Yan, H., Xu, S., Lin, X., Wang, W., and Wang, D. (2022). Moderately deep banding of phosphorus enhanced winter wheat yield by improving phosphorus availability, root spatial distribution, and growth. *Soil Tillage Res.*, 220, 105388. doi: 10.1016/j.still.2022.105388

Lopez, G., Ahmadi, S. H., Amelung, W., Athmann, M., Ewert, F., Gaiser, T., et al. (2022). Nutrient deficiency effects on root architecture and root-to-shoot ratio in arable crops. *Front. Plant Sci.* 13. doi: 10.3389/fpls.2022.1067498

Luo, L., Zhang, X., Zhang, M., Wei, P., Chai, R., Wang, Y., et al. (2023). Improving wheat yield and phosphorus use efficiency through the optimization of phosphorus fertilizer types based on soil P pool characteristics in calcareous and non-calcareous soil. *Agronomy* 13, 928. doi: 10.3390/agronomy13030928

Lynch, J. P. (2013). Steep, cheap and deep: an ideotype to optimize water and N acquisition by maize root systems. *Ann. Bot.* 112, 347–357. doi: 10.1093/aob/mcs293

Ma, G., Liu, W., Li, S., Zhang, P., Wang, C., Lu, H., et al. (2019). Determining the optimal N input to improve grain yield and quality in winter wheat with reduced apparent N loss in the North China plain. *Front. Plant Sci.* 10. doi: 10.3389/fpls.2019.00181

Ma, T., Zeng, W., Lei, G., Wu, J., and Huang, J. (2021). Predicting the rooting depth, dynamic root distribution and the yield of sunflower under different soil salinity and nitrogen applications. *Ind. Crops Products* 170, 113749. doi: 10.1016/j.indcrop.2021.113749

Min, J., Sun, H., Wang, Y., Pan, Y., Kronzucker, H. J., Zhao, D., et al. (2021). Mechanical side-deep fertilization mitigates ammonia volatilization and nitrogen runoff and increases profitability in rice production independent of fertilizer type and split ratio. *J. Cleaner Production* 316, 128370. doi: 10.1016/j.jclepro.2021.128370

Momesso, L., Crusciol, C. A. C., Cantarella, H., Tanaka, K. S., Kowalchuk, G. A., and Kuramae, E. E. (2022). Optimizing cover crop and fertilizer timing for high maize yield and nitrogen cycle control. *Geoderma* 405, 115423. doi: 10.1016/j.geoderma.2021.115423

Morris, E. C., Griffiths, M., Golebiowska, A., Mairhofer, S., Burr-Hersey, J., Goh, T., et al. (2017). Shaping 3D root system architecture. *Curr. Biol.* 27, R919–R930. doi: 10.1016/j.cub.2017.06.043

Mou, P., Jones, R. H., Tan, Z., Bao, Z., and Chen, H. (2012). Morphological and physiological plasticity of plant roots when nutrients are both spatially and temporally heterogeneous. *Plant Soil* 364, 373–384. doi: 10.1007/s11104-012-1336-y

Nie, J., Zhou, J., Zhao, J., Wang, X., Liu, K., Wang, P., et al. (2022). Soybean crops penalize subsequent wheat yield during drought in the North China plain. *Front. Plant Sci.* 13. doi: 10.3389/fpls.2022.947132

Niu, W., Chen, H., and Wu, J. (2021). Soil Moisture and Soluble Salt Content Dominate Changes in Foliar delta(13)C and delta(15)N of Desert Communities in the Qaidam Basin, Qinghai-Tibetan Plateau. *Front. Plant Sci.* 12. doi: 10.3389/fpls.2021.675817

Postma, J. A., Schurr, U., and Fiorani, F. (2014). Dynamic root growth and architecture responses to limiting nutrient availability: linking physiological models and experimentation. *Biotechnol. Adv.* 32, 53–65. doi: 10.1016/j.bioteChadv.2013.08.019

Radočaj, D., Jurišić, M., and Gašparović, M. (2022). The role of remote sensing data and methods in a modern approach to fertilization in precision agriculture. *Remote Sens.* 14, 778. doi: 10.3390/rs14030778

Real, R., and Vargas, J. M. (1996). The probabilistic basis of jaccard's index of similarity. *Systematic Biol.* 45, 380–385. doi: 10.1093/sysbio/45.3.380

Ren, B., Guo, Y., Liu, P., Zhao, B., and Zhang, J. (2021). Effects of urea-ammonium nitrate solution on yield, N(2)O emission, and nitrogen efficiency of summer maize under integration of water and fertilizer. *Front. Plant Sci.* 12. doi: 10.3389/fpls.2021.700331

Ren, K., Xu, M., Li, R., Zheng, L., Liu, S., Reis, S., et al. (2022). Optimizing nitrogen fertilizer use for more grain and less pollution. *J. Cleaner Production* 360, 132180. doi: 10.1016/j.jclepro.2022.132180

Sainju, U. M., Whitehead, W. F., Singh, B. P., and Wang, S. (2006). Tillage, cover crops, and nitrogen fertilization effects on soil nitrogen and cotton and sorghum yields. *Eur. J. Agron.* 25, 372–382. doi: 10.1016/j.eja.2006.07.005

Sim, D. H. H., Tan, I. A. W., Lim, L. L. P., and Hameed, B. H. (2021). Encapsulated biochar-based sustained release fertilizer for precision agriculture: A review. *J. Cleaner Production* 303, 127018. doi: 10.1016/j.jclepro.2021.127018

Slafer, G. A., and Savin, R. (2018). Can N management affect the magnitude of yield loss due to heat waves in wheat and maize? *Curr. Opin. Plant Biol.* 45, 276–283. doi: 10.1016/j.pbi.2018.07.009

Su, W., Liu, B., Liu, X., Li, X., Ren, T., Cong, R., et al. (2015). Effect of depth of fertilizer banded-placement on growth, nutrient uptake and yield of oilseed rape (Brassica napus L.). *Eur. J. Agron.* 62, 38–45. doi: 10.1016/j.eja.2014.09.002

Tabuchi, M., Abiko, T., and Yamaya, T. (2007). Assimilation of ammonium ions and reutilization of nitrogen in rice (Oryza sativa L.). *J. Exp. Bot.* 58, 2319–2327. doi: 10.1093/jxb/erm016

Thorup-Kristensen, K., Halberg, N., Nicolaisen, M., Olesen, J. E., Crews, T. E., Hinsinger, P., et al. (2020). Digging deeper for agricultural resources, the value of deep rooting. *Trends Plant Sci.* 25, 406–417. doi: 10.1016/j.tplants.2019.12.007

van der Bom, F. J. T., Williams, A., and Bell, M. J. (2020). Root architecture for improved resource capture: trade-offs in complex environments. *J. Exp. Bot.* 71, 5752–5763. doi: 10.1093/jxb/eraa324

Vejan, P., Khadiran, T., Abdullah, R., and Ahmad, N. (2021). Controlled release fertilizer: A review on developments, applications and potential in agriculture. *J. Control Release* 339, 321–334. doi: 10.1016/j.jconrel.2021.10.003

Velasco-Muñoz, J. F., Mendoza, J. M. F., Aznar-Sánchez, J. A., and Gallego-Schmid, A. (2021). Circular economy implementation in the agricultural sector: Definition, strategies and indicators. *Resources Conserv. Recycling* 170, 105618. doi: 10.1016/j.resconrec.2021.105618

Wang, Y., Guo, Q., Xu, Y., Zhang, P., Cai, T., and Jia, Z. (2022b). Optimizing urea deep placement to rainfall can maximize crop water-nitrogen productivity and decrease nitrate leaching in winter wheat. *Agric. Water Manage.* 274, 107971. doi: 10.1016/j.agwat.2022.107971

Wang, Y., Guo, Q., Xu, Y., Zhang, P., Cai, T., and Jia, Z. (2023b). Sustainable nitrogen placement depth under different rainfall levels can enhance crop productivity and maintain the nitrogen balance in winter wheat fields. *Soil Tillage Res.* 233, 105817. doi: 10.1016/j.still.2023.105817

Wang, J., Hussain, S., Sun, X., Zhang, P., Javed, T., Dessoky, E. S., et al. (2022a). Effects of nitrogen application rate under straw incorporation on photosynthesis, productivity and nitrogen use efficiency in winter wheat. *Front. Plant Sci.* 13. doi: 10.3389/fpls.2022.862088

Wang, X., Wang, M., Chen, L., Shutes, B., Yan, B., Zhang, F., et al. (2023a). Nitrogen migration and transformation in a saline-alkali paddy ecosystem with application of different nitrogen fertilizers. *Environ. Sci. pollut. Res. Int.* 30, 51665–51678. doi: 10.1007/s11356-023-25984-9

Wasson, A. P., Richards, R. A., Chatrath, R., Misra, S. C., Prasad, S. V., Rebetzke, G. J., et al. (2012). Traits and selection strategies to improve root systems and water uptake in water-limited wheat crops. *J. Exp. Bot.* 63, 3485–3498. doi: 10.1093/jxb/ers111

Wu, X., Li, J., Xue, X., Wang, R., Liu, W., Yang, B., et al. (2023). Matching fertilization with available soil water storage to tackle the trade-offs between high yield and low N2O emissions in a semi-arid area: Mechanisms and solutions. *Agric. Water Manage.* 288, 108488. doi: 10.1016/j.agwat.2023.108488

Wu, P., Liu, F., Chen, G., Wang, J., Huang, F., Cai, T., et al. (2022a). Can deep fertilizer application enhance maize productivity by delaying leaf senescence and decreasing nitrate residue levels? *Field Crops Res.* 277, 108417. doi: 10.1016/j.fcr.2021.108417

Wu, P., Liu, F., Li, H., Cai, T., Zhang, P., and Jia, Z. (2021). Suitable fertilizer application depth can increase nitrogen use efficiency and maize yield by reducing gaseous nitrogen losses. *Sci. Total Environ.* 781, 146787. doi: 10.1016/j.scitotenv.2021.146787

Wu, P., Liu, F., Wang, J., Liu, Y., Gao, Y., Zhang, X., et al. (2022b). Suitable fertilization depth can improve the water productivity and maize yield by regulating development of the root system. *Agric. Water Manage.* 271, 107784. doi: 10.1016/j.agwat.2022.107784

Xia, H., Riaz, M., Zhang, M., Liu, B., Li, Y., El-Desouki, Z., et al. (2022). Biochar-N fertilizer interaction increases N utilization efficiency by modifying soil C/N component under N fertilizer deep placement modes. *Chemosphere* 286, 131594. doi: 10.1016/j.chemosphere.2021.131594

Xie, W. X., Wang, G. H., Zhang, Q. C., and Guo, H. C. (2007). Effects of nitrogen fertilization strategies on nitrogen use efficiency in physiology, recovery, and agronomy and redistribution of dry matter accumulation and nitrogen accumulation in two typical rice cultivars in Zhejiang, China. *J. Zhejiang Univ Sci. B* 8, 208–216. doi: 10.1631/jzus.2007.B0208

Zhang, Y., Ren, W., Zhu, K., Fu, J., Wang, W., Wang, Z., et al. (2024). Substituting readily available nitrogen fertilizer with controlled-release nitrogen fertilizer improves crop yield and nitrogen uptake while mitigating environmental risks: A global meta-analysis. *Field Crops Res.* 306, 109221. doi: 10.1016/j.fcr.2023.109221

Zhang, A., Wang, X.-X., Zhang, D., Dong, Z., Ji, H., and Li, H. (2023). Localized nutrient supply promotes maize growth and nutrient acquisition by shaping root morphology and physiology and mycorrhizal symbiosis. *Soil Tillage Res.* 225, 105550. doi: 10.1016/j.still.2022.105550

Zhao, C., Zhang, H., Song, C., Zhu, J. K., and Shabala, S. (2020). Mechanisms of plant responses and adaptation to soil salinity. *Innovation (Camb)* 1, 100017. doi: 10.1016/j.xinn.2020.100017

frontiers | Frontiers in Plant Science

TYPE Original Research
PUBLISHED 30 August 2024
DOI 10.3389/fpls.2024.1429548

OPEN ACCESS

EDITED BY
Xiaoli Hui,
Northwest A&F University, China

REVIEWED BY
Junsheng Lu,
Lanzhou University, China
Kailou Liu,
Jiangxi Institute of Red Soil, China

*CORRESPONDENCE
Hengjia Zhang
596088683@qq.com

†These authors have contributed equally to this work and share first authorship

RECEIVED 08 May 2024
ACCEPTED 13 August 2024
PUBLISHED 30 August 2024

CITATION
Chen X, Zhang H, Yu S, Zhou C, Teng A, Lei L, Ba Y and Li F (2024) Optimizing irrigation and nitrogen application strategies to improve sunflower yield and resource use efficiency in a cold and arid oasis region of Northwest China. *Front. Plant Sci.* 15:1429548. doi: 10.3389/fpls.2024.1429548

Optimizing irrigation and nitrogen application strategies to improve sunflower yield and resource use efficiency in a cold and arid oasis region of Northwest China

Xietian Chen[1,2†], Hengjia Zhang[1,2*†], Shouchao Yu[2], Chenli Zhou[2], Anguo Teng[3], Lian Lei[3], Yuchun Ba[3] and Fuqiang Li[1]

[1]College of Water Conservancy and Hydropower Engineering, Gansu Agricultural University, Lanzhou, China, [2]College of Agriculture and Biology, Liaocheng University, Liaocheng, China, [3]Yimin Irrigation Experimental Station, Hongshui River Management Office, Zhangye, China

In arid regions, water scarcity, land degradation and groundwater pollution caused by excessive fertilization are the main constraints to sustainable agricultural production. Optimizing irrigation and fertilizer management regime is an effective means of improving crop water and fertilizer productivity as well as reducing negative impacts on the ecosystem. In order to investigate the effects of different irrigation and nitrogen (N) fertilizer rates on sunflower growth, yield, and water and N use efficiency, and to determine the optimal water and N management strategy, a two-year (2021 and 2022) field experiment with under-mulched drip irrigation was conducted in the Hexi Oasis area of Northwest China. The experiment design comprised three irrigation levels (W1, 55%–65% F_C, where F_C represents field water capacity; W2, 65%–75% F_C; W3, 75% –85% F_C) and three N application levels (N1, 120 kg ha^{-1}; N2, 180 kg ha^{-1}; N3, 240 kg ha^{-1}), resulting in a total of nine treatments. The findings indicated that increasing irrigation and N application rates led to improvements in leaf area index (15.39%–66.14%), dry matter accumulation (11.43%–53.15%), water consumption (ET, 1.63%–42.90%) and sunflower yield (6.85%–36.42%), in comparison to the moderate water deficit and low N application (W1N1) treatment. However, excess water and N inputs did not produce greater yield gains and significantly decreased both water use efficiency (WUE) and nitrogen partial factor productivity (NPFP). Additionally, a multiple regression model was developed with ET and N application as explanatory variables and yield, WUE and NPFP as response variables. The results based on the regression model combined with spatial analysis showed that an ET range of 334.3–348.7 mm and N application rate of 160.9–175.3 kg ha^{-1} achieved an optimal balance between the multiple production objectives: yield, WUE and NPFP. Among the

Abbreviations: N, Nitrogen; S, Seedling; B, Budding; F, Flowering; M, Maturity; F_C, Field water capacity; LAI, Leaf area index; DM, Dry matter; DMA, Dry matter accumulation; ET, Water consumption; WUE, Water use efficiency; IWUE, Irrigation water use efficiency; NPFP, Nitrogen partial factor productivity.

different irrigation and N management strategies we evaluated, we found that W2N2 (65%–75% F_C and 180 kg N ha^{-1}) was the most fruitful considering yield, resource use efficiency, etc. This result can serve as a theoretical reference for developing appropriate irrigation and N fertilization regimes for sunflower cultivation in the oasis agricultural area of northwest China.

KEYWORDS

dry matter accumulation, multi-objective optimization, sunflower yield, water and nitrogen use efficiency, drip fertigation

1 Introduction

The Hexi Oasis agricultural area is recognized as a critical commercial grain base and a hub for cash crop production in Northwest China, earning its reputation as the "Northwest Granary" (Wu et al., 2021). The agricultural output in this region is paramount to ensuring food security and sustained economic progress in Northwest China (Chen et al., 2022). However, the arid climate, water scarcity and ecological fragility have seriously constrained the sustainable development of agriculture in this region (Li et al., 2015; Wang et al., 2023a). Over the past three decades, the continuous expansion of the oasis area in Hexi has resulted in a serious imbalance between water and land resources, further intensifying the agricultural water crisis (Sun et al., 2021). In addition, the pursuit of high crop yields has led to widespread excessive irrigation and fertilization practices in the Hexi Oasis region (Pan et al., 2024). This traditional "high yield – high water – high fertilizer" production model not only contributes to inefficient water and fertilizer use but also raises concerns about environmental consequences (Campbell et al., 2011; Lu et al., 2021a; Wang et al., 2023b; Zhang et al., 2016). These consequences include nitrogen leaching losses, groundwater pollution and soil quality degradation. Therefore, to achieve sustainable agricultural production and establish a positive feedback loop for the ecological environment in the Hexi Oasis area, a two-pronged approach is essential: the rational allocation of regional land and water resources, and optimization of irrigation and fertilization management strategies.

As one of the four most important oilseed crops in the world, sunflower (*Helianthus annuus L.*) is widely planted in different countries and regions due to its excellent adaptability to various environments and climates (Sinha et al., 2017; Stone et al., 2002). In 2020 alone, China planted 900,000 ha of sunflowers—representing approximately 3% of the world's total—and harvested a yield of 2.38 million tons, rendering it the fifth-largest producer globally (Zhang et al., 2023). In China, most sunflower cultivation occurs in the arid and semi-arid northern regions, with the Hexi Oasis irrigated area standing out as a major sunflower production center. In recent years, however, traditional irrigation practices (e.g. furrow and flood irrigation) have still been used for sunflower production in this area, resulting in serious waste and inefficient use of water resources (Wang et al., 2021a). Thankfully, research has indicated that drip fertigation technology can well coordinate the supply relationship between water and nutrients, thereby promoting the efficient use of water and fertilizer (Yan et al., 2019). This technology delivers water and fertilizer solution to the crop root system in a uniform, continuous and accurate manner through a pipeline system, thus avoiding nutrient loss and reducing the risk of soil environmental pollution (Li et al., 2022a; Ma et al., 2022). While drip fertigation is slowly being integrated into sunflower cultivation, developing sustainable and scientifically-backed drip irrigation and fertilizer management regimes remains a major challenge for agricultural production in the Hexi Oasis region.

As a fundamental building block of nucleic acids and proteins, nitrogen (N) is critical for maintaining plant life activities and crop yield formation (Long et al., 2021; Sinclair and Rufty, 2012). In irrigated agriculture, optimizing both water and N management is crucial for achieving high crop yields while promoting resource use efficiency and environmental sustainability (Ballester et al., 2021; Liu et al., 2019). Studies have demonstrated significant interactive and complementary effects between water and N (Sheshbahreh et al., 2019). While water can enhance N use efficiency, N, accordingly, affects plant growth and development, thereby affecting water uptake by crops (Gao et al., 2023; Wang et al., 2014a). However, the effects of water and N supply on crop growth and yield can be complex, resulting in either synergistic or antagonistic interactions depending on the specific input levels of both (Feng et al., 2023; Wang et al., 2016). For instance, Wang et al. (2021a) observed that under water stress combined with high N fertilization, excess N accumulated in the soil. This accumulation led to increased soil solution concentrations, hindering both water and nutrient uptake by sunflowers; whereas, excessive irrigation can lead to N leaching into deeper soil layers, depleting N levels in the root zone and potentially contaminating the groundwater resources. Kiani et al. (2016) highlighted that under severe water deficit conditions, simply increasing N fertilizer application is not an effective strategy for sunflowers. The optimum N application depends on various factors such as the source of N fertilizer and irrigation levels. Therefore, to develop effective water and N management strategies for sustainable and efficient crop

production, it is essential to conduct field experiments that investigate how sunflower growth and yield to different irrigation and N application rates under specific climatic conditions.

Multiple regression modeling has become a commonly applied method for determining the optimal irrigation and fertilization practices in recent years (Hao et al., 2022; He et al., 2023). For instance, Li et al. (2022b) devised a quadratic equation to represent the relationship between economic efficiency, irrigation amount, and N application rate. Utilizing this equation, they determined the optimal irrigation amount to be 360 mm with a corresponding N fertilizer rate of 225 kg ha^{-1} for sunflower production in the Hetao irrigation area of Inner Mongolia, China. Similarly, Zhang et al. (2023) employed a regression equation with sunflower yield as the dependent variable to determine the optimal irrigation and N application rates for sunflower production in the arid region of northern China. Their findings indicated that an irrigation amount of 159.2–177.1 mm and an N application rate of 166.0–218.3 kg ha^{-1} were most suitable. However, relying solely on a single indicator such as crop yield for evaluating irrigation and fertilization practices may not be sufficient to optimize other crucial production factors, such as water and N use efficiency (Xing et al., 2015). A more comprehensive approach involves considering multiple objectives simultaneously. To address this, previous studies have proposed constructing multiple binary quadratic models, each representing a specific objective. By projecting the resulting response surfaces utilizing spatial analysis, researchers can identify areas of overlap where acceptable ranges for each indicator intersect. This overlapping region represents the optima range for both water and N application (Thompson et al., 2000). This method has been successfully applied to establish multi-objective water and N management strategies for various crops, including tomato (Xing et al., 2015), maize (Feng et al., 2023), winter wheat (Gao et al., 2023) and cotton (Wang et al., 2018). Notwithstanding the success of this approach, there is limited research on optimizing water and N management strategies for sunflower production in oasis irrigated areas.

This research operates under the hypothesis that the current water and N application strategies employed for sunflower cultivation in the Hexi Oasis region of Northwest China are not conducive to maximizing production returns. Therefore, this study aims to propose a high-yielding, efficient and environmentally sound water and N management strategy based on a multi-objective regression model coupled with spatial analysis derived from a field trial. The specific objectives of this study are: (1) to investigate the interactive effects of different irrigation and N application rates on leaf area index (LAI), aboveground biomass, water consumption (ET), yield, and water and N use efficiency of sunflower; (2) to develop a multiple regression model utilizing ET and N application as independent variables and yield, water and N use efficiency as dependent variables; and (3) to determine the optimal water and N management strategies for sunflower in arid areas based on the regression equations and spatial analysis. This study aims to offer theoretical guidance for the efficient management of water and fertilizer in sunflower production in oasis irrigated areas in Northwest China.

2 Materials and methods

2.1 Experimental site and climatic conditions

A 2-year (2021 and 2022) field trial was performed at the Yimin Irrigation Experimental Station (100°47′ E, 38°35′ N, 1976.9 m a.s.l.) in Minle County, Gansu Province, Northwest China (Figure 1). The test region is characterized by an arid continental climate, with significant temperature differences between day and night. The region receives sufficient light and heat resources, offering naturally advantageous conditions for agricultural production. However, with average annual rainfall decline below 200 mm and average annual evaporation exceeding 2000 mm, irrigation becomes critical to sustain regular crop production. The study site experiences an average annual temperature of 6.2°C, approximately 3000 h of annual sunshine, and a frost-free period of approximately 140 days. Groundwater, at a depth exceeding 20 m, constitutes a primary source for local irrigation (Wang et al., 2023a). In 2021 and 2022, total rainfall during the sunflower growing season reached 164.4 mm and 136.3 mm, with average air temperatures of 17.30°C and 18.16°C, respectively (Figure 2). Additionally, the physical and chemical properties of the 0–60 cm soil profile at the test site were analyzed before sowing, as presented in Table 1.

2.2 Experimental design and field management

The experiment was conducted in a completely randomized block design with two factors and three replications. Three irrigation levels were employed: moderate water deficit (W1, 55%–65% F_C, F_C is the field water capacity), mild water deficit (W2, 65%–75% F_C) and full irrigation (W3, 75%–85% F_C). The N application rates consisted of three levels: low N fertilization (N1, 120 kg ha^{-1}), medium N fertilization (N2, 180 kg ha^{-1}) and high N fertilization (N3, 240 kg ha^{-1}, which was the local conventional N application rate). The experiment comprised nine treatments across 27 plots, with each plot measuring 27.2 m^2 (3.4 m×8 m). Adjacent plots were separated by 100 cm wide protected zones and were also fitted with 60 cm deep plastic membranes to prevent horizontal movement of water and N. Each irrigation event was initiated based on soil water content measurements at the planned wetted layer depth (40 cm during the seedling stage and 60 cm at other stage, contingent upon root distribution depth). When the soil water content neared or fell below the designated lower limit, irrigation promptly restored it to the designated upper limit. The calculation method for each irrigation amount is detailed in Wang et al. (2023a). Urea (N, 46%), superphosphate (P_2O_5, 12%) and potassium sulphate (K_2O, 51%) were selected as the sources of N, P and K. Prior to sowing, 150 kg P_2O_5 ha^{-1} and 180 kg K_2O ha^{-1} of phosphorus and potassium fertilizer and 40% N fertilizer were applied as base fertilizer for each treatment, respectively. The remaining N fertilizer was delivered through drip fertigation

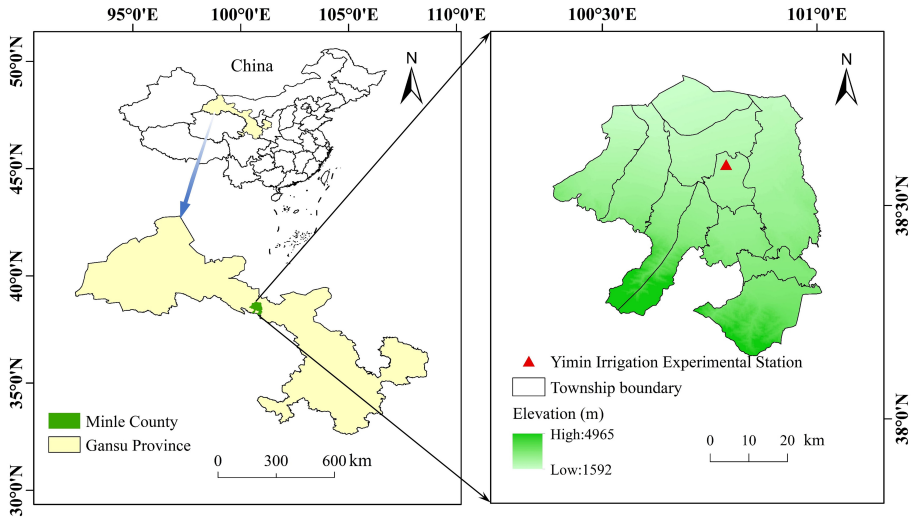

FIGURE 1
Location of the experimental site.

during the early stages of budding (30%) and flowering (30%). The specific irrigation and N application schemes are shown in Table 2.

The sunflower cultivar "JK601" (a widely grown variety in the region) was planted on 1st May 2021 and 5th May 2022, respectively. The harvest dates were 18th September 2021 and 20th September 2022, respectively. Seeds were planted by hand at a depth of 5 cm using a hole seeder. Irrigation was offered through drip tapes beneath plastic film (80 cm wide, 0.01 mm thick). Two rows of sunflowers were planted on each film, with a narrow row spacing of 50 cm, a wide row spacing of 80 cm and a plant spacing of 45 cm. A single irrigation tape (16 mm diameter) was centered under each film. Drippers were positioned every 30 cm along the tape, offering a flow rate of 3.0 L hour^{-1}. Figure 3 illustrates the sunflower planting pattern and the layout of drip irrigation under plastic film.

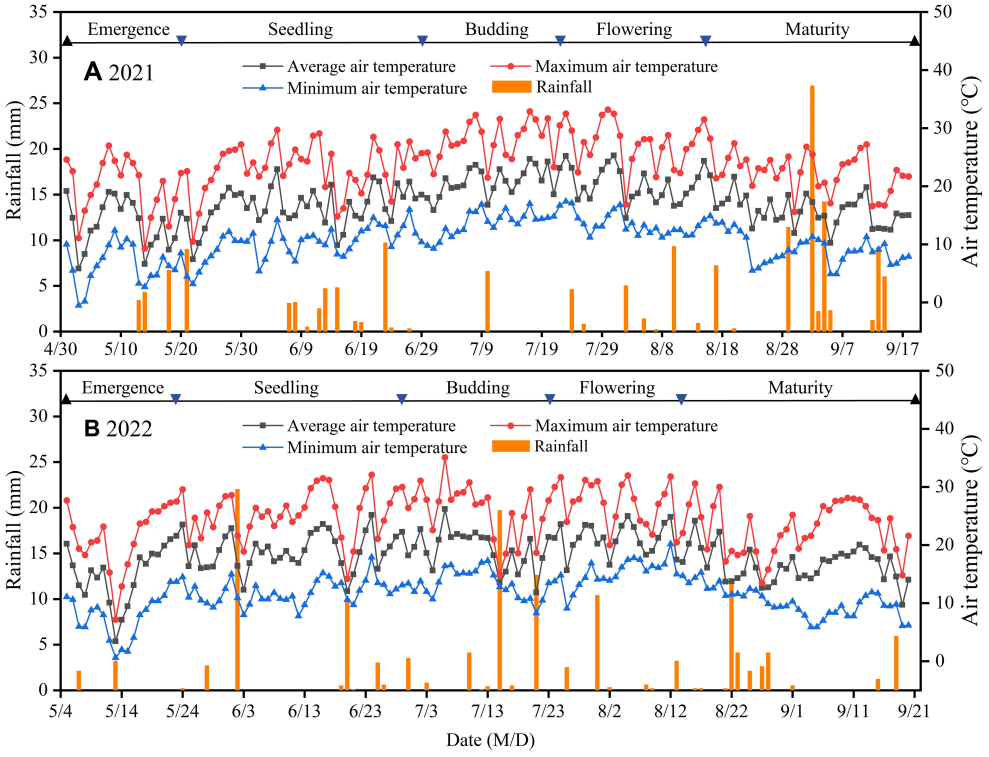

FIGURE 2
Daily air temperature and rainfall at the experimental site during the sunflower growing season in 2021 **(A)** and 2022 **(B)**.

10.3389/fpls.2024.1429548

TABLE 1 Soil physical and chemical properties (0–60 cm) at the experimental site.

Soil layer (cm)	Particle composition (%)			Soil texture	Organic matter (g kg^{-1})	Nitrate nitrogen (mg kg^{-1})	Ammonium nitrogen (mg kg^{-1})	Available phosphorus (mg kg^{-1})	Available potassium (mg kg^{-1})	Field capacity (%)	Bulk density (g cm^{-3})	pH
	< 0.002 mm	0.002 –0.02 mm	0.02–2 mm									
0–20	11.27	55.45	33.28	Silty loam	10.08	24.74	38.82	27.51	133.79	24.53	1.42	7.9
20–40	13.78	50.47	35.75	Silty loam	9.22	25.17	37.31	20.19	77.59	23.47	1.48	7.7
40–60	12.77	40.68	46.55	loam	8.68	14.27	35.56	16.00	58.48	23.89	1.49	8.0

2.3 Measurements, calculations and methodologies

2.3.1 Determination of leaf area index

Five sunflower plants were randomly sampled from each plot at the seedling (S), budding (B), flowering (F), and maturity (M) stages, and the maximum length and width of all leaves were determined using a steel ruler. Leaf area index (LAI) was calculated according to the following formula (Guo et al., 2019):

$$LAI = \frac{0.6564 \times NP \times \sum_{i=1}^{n} LL \times LB}{A} \quad (1)$$

where 0.6564 was the conversion factor of sunflower leaf area (Ma et al., 2020); NP was the total number of plants in a single plot; LL was the maximum leaf length of fully extended leaves of sunflower (cm); LB was the maximum leaf width (cm); n was the number of leaves in a single plant; A was the area of a single plot (cm^2).

2.3.2 Dry matter accumulation and seed yield

After sunflower reached the S stage, we randomly selected three plants from each plot every 20 days to determine the aboveground dry matter accumulation (DMA). The fresh sunflowers were separated into different organs (stems, leaves and flower discs). Each plant component was initially heated in an oven at 105 °C for 30 minutes, then dried to constant weight at 75°C. To calculate the DMA per hectare, we factored in the average weight of each plant, the sowing density and the seedling emergence rate (Wang et al., 2021b). After seed maturity, ten flower heads were selected from each plot for threshing and natural drying. Subsequently, the 100-seed weight and seed weight per head were determined and converted to yield per hectare.

2.3.3 Water consumption

Sunflower growing season water consumption (ET) was calculated as follows (Lu et al., 2021b):

$$ET = P + U + I + \Delta W - D - R \quad (2)$$

where P is rainfall (mm); U is groundwater recharge (mm); I is irrigation (mm); R and D are surface runoff and deep drainage (mm), respectively; and ΔW is the change in soil water storage between planting and harvest (mm). In this experiment, the soil water content was always below F_C and the groundwater depth was greater than 20 m. Therefore, the values of U, D, and R were set to zero.

2.3.4 Productivity indicators

Water use efficiency (WUE) and irrigation water use efficiency (IWUE) were calculated as follows (Pan et al., 2024):

$$WUE = \frac{GY}{10 \times ET} \quad (3)$$

TABLE 2 Irrigation and nitrogen application schemes for the experiment.

Treatment	Water deficit level (% of field water capacity)	The amount and stage of nitrogen application (kg ha^{-1})			
		Sowing (40%)	Budding (30%)	Flowering (30%)	Total amount
W1N1	55%–65%	48	36	36	120
W1N2	55%–65%	72	54	54	180
W1N3	55%–65%	96	72	72	240
W2N1	65%–75%	48	36	36	120
W2N2	65%–75%	72	54	54	180
W2N3	65%–75%	96	72	72	240
W3N1	75%–85%	48	36	36	120
W3N2	75%–85%	72	54	54	180
W3N3	75%–85%	96	72	72	240

W1, moderate water deficit (55%–65% of field water capacity, F_C); W2, mild water deficit (65%–75% F_C); W3, full irrigation (75%–85% F_C). N1, low nitrogen rate (120 kg ha^{-1}); N2, medium nitrogen rate (180 kg ha^{-1}); N3, high nitrogen rate (240 kg ha^{-1}).

$$IWUE = \frac{GY}{10 \times I} \tag{4}$$

where GY represents the grain yield (kg ha^{-1}), ET denotes the water consumption (mm), and I depicts the irrigation amount (mm).

Nitrogen partial factor productivity (NPFP) was calculated by the following formula (Gao et al., 2023):

$$NPFP = \frac{GY}{N_T} \tag{5}$$

where $N_T$represents the total nitrogen applied (kg ha^{-1}).

2.3.5 Logistic model

A logistic model was employed to explore the response of DMA to different irrigation and N application rates utilizing days after seedling emergence as the independent variable. The logistic equation is expressed as follows (Ding et al., 2019):

$$y = \frac{k}{1 + ae^{-bt}} \tag{6}$$

where y is the dry matter accumulation of sunflower (kg ha^{-1}), k is the maximum dry matter accumulation (kg ha^{-1}), t is the number of days after emergence (d), and a and b are parameters to be determined.

Taking the first derivative of the logistic equation gives the cumulative rate equation:

$$y = \frac{abke^{-bt}}{(1 + ae^{-bt})^2} \tag{7}$$

Based on Equations 6 and 7 the values of the relevant characteristic parameters can be calculated as follows:

$$V_{max} = \frac{kb}{4} \tag{8}$$

$$t_{max} = \frac{ln\, a}{b} \tag{9}$$

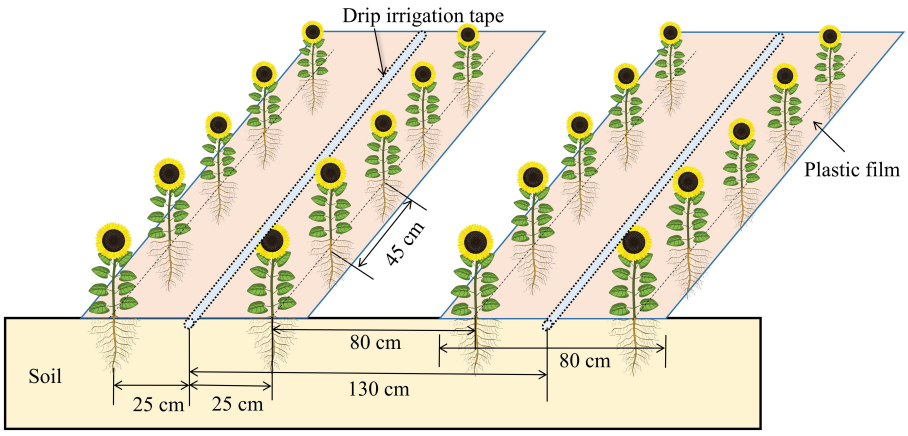

FIGURE 3
The sunflower planting pattern and the layout of drip irrigation under plastic film.

$$t_1 = \frac{1}{b} ln \left(\frac{a}{2 + \sqrt{3}} \right) \quad (10)$$

$$t_2 = \frac{1}{b} ln \left(\frac{a}{2 - \sqrt{3}} \right) \quad (11)$$

$$\Delta t = t_2 - t_1 \quad (12)$$

where V_{max} (kg ha^{-1} d^{-1}) and t_{max} (d) are the maximum accumulation rate of dry matter and its occurrence time; t_1 (d) and t_2 (d) are the start and end time of the rapid growth period, respectively; Δt (d) is the duration of rapid growth.

2.3.6 Water and nitrogen regression model based on multiple objectives

In this study, the effect of different water and N treatments on multiple target variables were evaluated by establishing a binary quadratic regression equation. The regression equation is expressed as follows (Pan et al., 2024):

$$y = y_0 + ax_1 + bx_2 + cx_1x_2 + dx_1^2 + ex_2^2 \quad (13)$$

where y represents the response variable; x_1 and x_2 denote water consumption and nitrogen application rate, respectively; y_0 depicts a constant term; and a, b, c, d and e indicate coefficients to be determined.

2.3.7 Data analysis

The data presented in the figures and tables represent the mean of three replicates. Excel 2019 was used for fundamental data organization and calculations. Analysis of variance (ANOVA) and regression equation modeling for each year's data were performed using SPSS 22.0 (SPSS Inc., Chicago, USA) software. Irrigation (W) and nitrogen application (N) and their interaction (W×N) were considered as fixed factors and replication was considered as a random factor. Duncan's multiple range test was employed for multiple comparisons of means between treatments at a significance level of $P < 0.05$. Origin 2021 (OriginLab Inc., USA) was used to generate the figures.

3 Results

3.1 Leaf area index

As shown in Figure 4, LAI under all treatments exhibited an initial increase followed by a decrease with the progression of growth stages, attaining a peak at the F period. Irrigation and N application treatments had a highly significant ($P < 0.01$) effect on LAI at each growth stage in both 2021 and 2022. Specifically, LAI was highest in W3N3 and lowest in W1N1 during the entire growing period. In comparison to W3N3, the LAI of W1N1 displayed reductions of 36.90%, 36.46%, 46.65% and 48.29% in 2021 and 40.35%, 31.00%, 40.81% and 33.85% in 2022 for S, B, F and M stages, respectively. Under consistent water deficit conditions, the LAI of N2 and N3 exhibited no significant ($P > 0.05$) difference, whereas the LAI of N1 was significantly lower than that of N2 and N3. In the concluding M stage, the LAI of N1 reduced by 15.9% and 17.3% in 2021 and by 11.9% and 11.6% in 2022, relative to N2 and N3, respectively. Under conditions of constant N application, LAI declined with increasing water deficit across each growth stage. The LAI of W1 was significantly lower than that of W2 and W3, but the difference in LAI between W2 and W3 was not significant. Relative to W3, the LAI of W1 at the S, B, F and M stages exhibited reductions of 24.86%, 21.41%, 33.85% and 38.83% in 2021, and 32.52%, 24.23%, 31.19% and 26.93% in 2022, respectively. In general, increasing irrigation and N application led to an increase in LAI, but past a specific limit, the effect ceased to be significant.

3.2 Dry matter accumulation characteristics

The aboveground dry matter (DM) of sunflower under different irrigation and N application treatments steadily accumulated as growth stages progressed, exhibiting a pattern of gradual increase in the early and late stages, with a rapid increase during the middle stage (Figure 5). Additionally, significant differences in DM were observed across different irrigation and N application treatments. At consistent irrigation levels, DM increased with increasing N application. In 2021 and 2022, the DM in N1 was lower by 14.87% and 13.83% relative to N2 and by 11.85% and 13.54% relative to N3 in the F stage, respectively. Under the same N application conditions, DM declined with increasing water deficit. In both growing seasons, DM was significantly lower in W1 than in W2 and W3. At the end of the F stage, DM in W1 experienced reductions of 25.47% and 23.18% compared to W3 and 21.28% and 19.91% compared to W2 in both years, respectively. In general, W3N3 yielded the highest DM among all treatments, demonstrating an increase of 54.10% in 2021 and 52.20% in 2022 relative to the lowest W1N1.

The DMA rate and its associated characteristic parameters fitted by the logistic model were shown in Figure 5 and Table 3, respectively. The results indicated that the determination coefficients (R^2) of the regression models consistently exceeded 0.99, suggesting that the logistic equation effectively modeled the process of DMA in sunflower with the days after seedling emergence. The duration of rapid growth in sunflower DMA across all treatments spanned from 33.77 d to 38.17 d. This duration contracted with decreasing irrigation and N application in 2021, while this pattern was not replicated in 2022. Moreover, the start of the rapid growth period in sunflower DMA occurred earlier with increasing irrigation and N application. In both seasons, the initiation of the rapid growth phase in N3 and N2 was observed on average 2.57 d and 1.23 d earlier than in N1, respectively. Similarly, the beginning of the rapid growth phase in W3 and W2 was on average 4.84 d and 1.90 d earlier than in W1, respectively. With increasing irrigation and N application, the maximum DMA rate in sunflower increased and its appearance was advanced. In 2021 and 2022, the maximum DMA rate exhibited increases of 12.97% and 16.44% in N3 and 11.32% and 15.71% in N2, respectively, compared to N1.

10.3389/fpls.2024.1429548

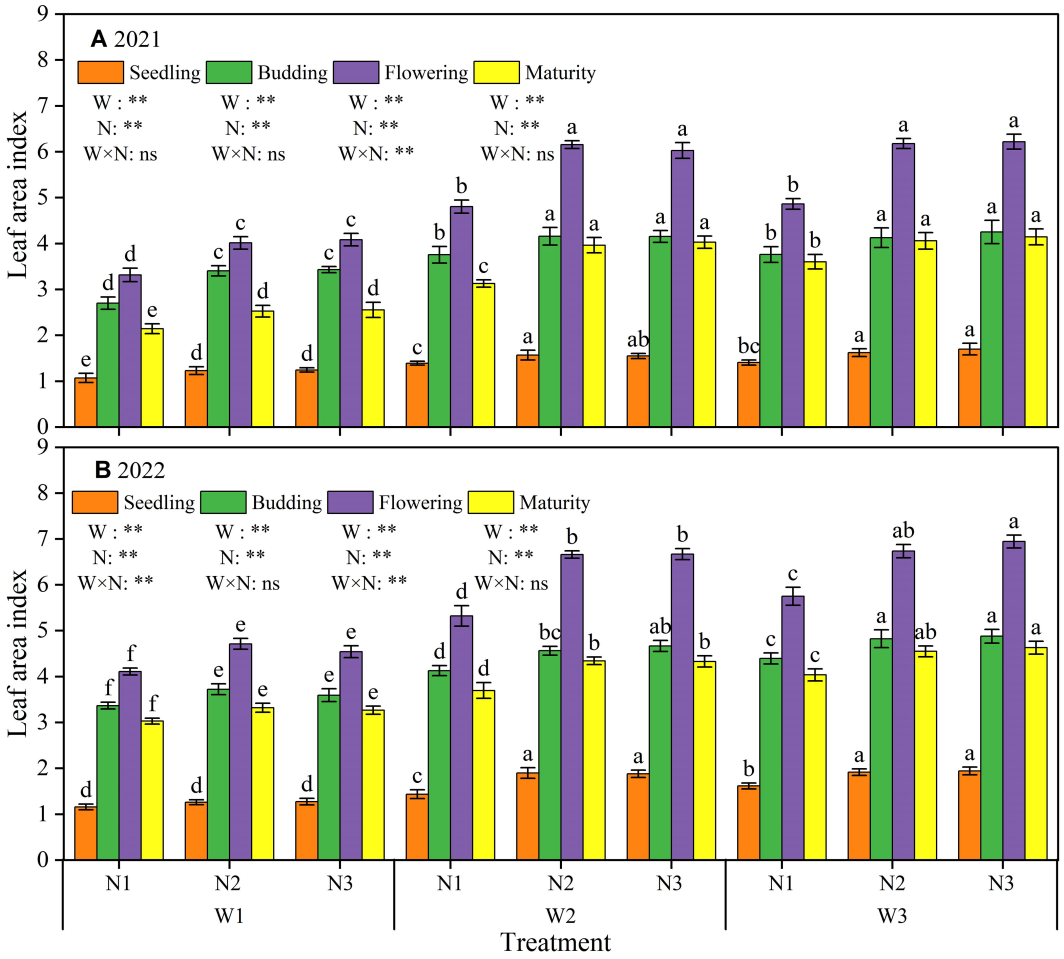

FIGURE 4
Effect of different irrigation and nitrogen application treatments on leaf area index in 2021 **(A)** and 2022 **(B)**. W1, moderate water deficit (55%–65% of field water capacity, F_C); W2, mild water deficit (65%–75% F_C); W3, full irrigation (75%–85% F_C). N1, low nitrogen rate (120 kg ha^{-1}); N2, medium nitrogen rate (180 kg ha^{-1}); N3, high nitrogen rate (240 kg ha^{-1}). Different lowercase letters above the error bar indicate significant differences between treatments in the same period at the $P < 0.05$ level. ** indicates a highly significant effect ($P < 0.01$); and ns indicates a non-significant effect ($P > 0.05$).

3.3 Yield and 100-seed weight

Different irrigation and N application treatments had highly significant ($P < 0.01$) effects on sunflower yield in both years (Figure 6). The interaction of water and N (W×N) had a highly significant effect on yield in 2022, while this effect was not significant ($P > 0.05$) in 2021. Yields across all treatments spanned from 4088.8 kg ha^{-1} to 5316.6 kg ha^{-1} in 2021 and from 3674.1 kg ha^{-1} to 5247.7 kg ha^{-1} in 2022. Specifically, yields from W3N3, W3N2, W2N2 and W2N3 treatments did not differ significantly in either year, yet these were significantly ($P < 0.05$) higher than other treatments. Under constant irrigation level, N2 obtained the highest yield of 5013.5 kg ha^{-1} in 2021 and 4826.4 kg ha^{-1} in 2022. While N3 demonstrated a slight yield reduction, this difference was insignificant compared to N2, suggesting that excess N fertilizer may not enhance yield and could potentially have a negative effect; whereas, N1 yielded significantly less, with reductions of 9.34% and 12.59% compared to N2 in both respective seasons. Besides, yields declined with increasing water deficit at constant N application. No significant yield differences were observed between W3 and W2. However, W3 yielded significantly more than W1, with increases of 19.92% in 2021 and 27.22% in 2022.

Irrigation and N application had a highly significant ($P < 0.01$) effect on 100-seed weight in both seasons. However, their interaction (W×N) had no significant ($P > 0.05$) effect on 100-seed weight (Figure 6). Specifically, 100-seed weight decreased with increasing water deficit. The lowest 100-seed weight was observed in W1, exhibiting reductions of 12.88% in 2021 and 9.24% in 2022 compared to W3. While W2 demonstrated a slight decrease in 100-seed weight compared to W3, this difference was not significant. No significant differences in 100-seed weight were observed between N2 and N3 under the same irrigation conditions. However, N1 demonstrated a significant reduction in 100-seed weight compared to N3, with decreases of 4.80% and 5.11% in the two years, respectively.

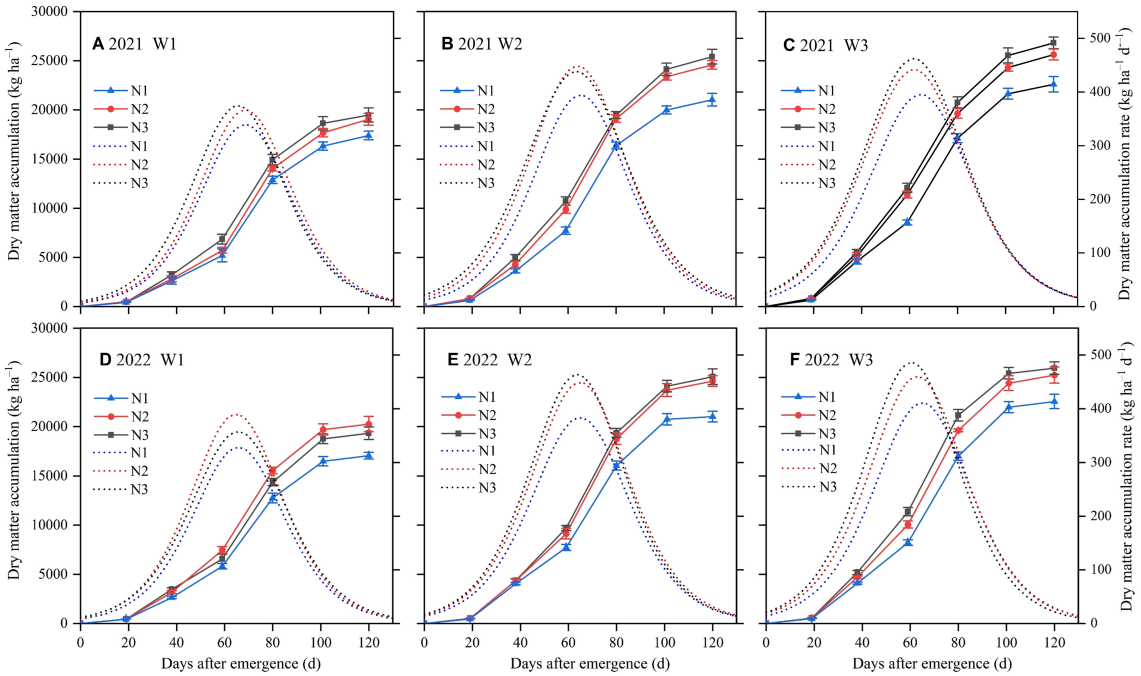

FIGURE 5
Effects of different irrigation and nitrogen treatments on dry matter accumulation and dry matter accumulation rate in 2021 **(A–C)** and 2022 **(D–F)**. W1, moderate water deficit (55%–65% of field water capacity, F_C); W2, mild water deficit (65%–75% F_C); W3, full irrigation (75%–85% F_C). N1, low nitrogen rate (120 kg ha^{-1}); N2, medium nitrogen rate (180 kg ha^{-1}); N3, high nitrogen rate (240 kg ha^{-1}). The solid and dashed lines represent dry matter accumulation and dry matter accumulation rate, respectively.

3.4 Water consumption and water and nitrogen use efficiency

Irrigation had a highly significant ($P < 0.01$) effect on ET in both 2021 and 2022. N application significantly ($P < 0.05$) affected ET in 2022, but not in 2021 ($P > 0.05$). W×N did not significantly affect ET in either year (Table 4). The total ET across the entire growing season for the different treatments ranged from 271.65 mm to 404.53 mm in 2021 and from 274.18 mm to 375.29 mm in 2022. The highest ET was observed in W3N3 and the lowest in W1N1. Specifically, ET exhibited a significant decrease with increasing water deficit. In 2021, the ET in W1 measured 275.34 mm, reflecting a reduction of 20.04% and 30.89% compared to W2 and W3, respectively. Similarly, in 2022, the ET in W1 measured 280.26 mm, indicating a reduction of 12.64% and 22.22% compared to W2 and W3, respectively.

As shown in Table 4, WUE was significantly ($P < 0.05$) affected by irrigation and N application in both years. IWUE was significantly affected by both factors in 2022, while in 2021, N application had no significant ($P > 0.05$) effect on IWUE. In addition, W×N did not significantly affect either WUE or IWUE in both years. In 2021, both WUE and IWUE showed an increasing trend with increasing water deficit. Compared to W1, WUE and IWUE in W3 were lower by 17.09% and 28.17%, respectively. In 2022, W2 attained the highest WUE, surpassing W1 and W3 by 9.22% and 10.39%, respectively; whereas, W1 reached the highest IWUE, surpassing W2 and W3 by 17.71% and 59.50%, respectively. Besides, under the same level of water deficit, N2 consistently exhibited the highest WUE and IWUE in both seasons, with an increase of 8.64% and 10.43% respectively, compared to N1, which had the lowest WUE and IWUE.

Different irrigation and N application rates, along with their interactions (W×N), significantly ($P < 0.05$) influenced NPFP in both 2021 and 2022 (Table 4). In general, NPFP demonstrated an increasing trend with higher irrigation amounts but decreased with higher N application rates. Compared to W1, NPFP in W2 and W3 increased by 16.92% and 19.88% in 2021 and by 22.20% and 26.96% in 2022, respectively. In contrast, compared to N1, NPFP in N2 and N3 decreased by 26.47% and 47.06% in 2021 and by 23.73% and 43.62% in 2022, respectively.

3.5 Multi-objective optimization of irrigation and nitrogen application strategies

3.5.1 Water and nitrogen regression models based on multiple objectives

This study evaluated the effects of varying water and N application rates on sunflower production under film-drip irrigation. The objective was to identify optimal combinations for water conservation, fertilizer efficiency, high yield, and reduced environmental effect. Yield, WUE, and NPFP were selected as key indicators. The binary quadratic regression equations for the three target variables with ET and N application were developed according to the principle of least squares (Table 5; Figure 7). The

10.3389/fpls.2024.1429548

TABLE 3 Logistic model parameters and characteristic values of sunflower dry matter accumulation under different irrigation and nitrogen application treatments.

Year	Treatment	Regression equation	R^2	t_1(d)	t_2 (d)	t_{max} (d)	Δt (d)	V_{max} (kg ha^{-1} d^{-1})
2021	W1N1	$y=17398.01/(1+204.06e^{-0.078x})$	0.996	51.30	85.07	68.18	33.77	339.26
	W1N2	$y=19048.33/(1+190.89e^{-0.077x})$	0.997	51.10	85.31	68.20	34.21	366.68
	W1N3	$y=19478.71/(1+151.80e^{-0.077x})$	0.997	48.12	82.33	65.23	34.21	374.97
	W2N1	$y=21040.56/(1+132.60e^{-0.075x})$	0.998	47.60	82.72	65.16	35.12	394.51
	W2N2	$y=24582.67/(1+106.24e^{-0.073x})$	0.999	45.87	81.95	63.91	36.08	448.63
	W2N3	$y=25419.8/(1+79.21e^{-0.069x})$	0.998	44.28	82.45	63.36	38.17	438.49
	W3N1	$y=22607.74/(1+91.64e^{-0.070x})$	0.995	45.73	83.36	64.54	37.63	395.64
	W3N2	$y=25622.8/(1+71.90e^{-0.069x})$	0.998	42.71	80.88	61.80	38.17	441.99
	W3N3	$y=26809.49/(1+70.540e^{-0.069x})$	0.998	42.60	80.77	61.68	38.17	462.46
2022	W1N1	$y=17049.45/(1+157.56e^{-0.077x})$	0.996	48.61	82.82	65.71	34.21	328.20
	W1N2	$y=20259.61/(1+146.96e^{-0.077x})$	0.997	47.70	81.91	64.81	34.21	390.00
	W1N3	$y=19329.24/(1+128.91e^{-0.074x})$	0.993	47.87	83.46	65.66	35.59	357.59
	W2N1	$y=21019.91/(1+113.64e^{-0.073x})$	0.992	46.79	82.88	64.84	36.08	383.61
	W2N2	$y=24625.74/(1+113.07e^{-0.073x})$	0.996	46.73	82.81	64.77	36.08	449.42
	W2N3	$y=25073.63/(1+110.70e^{-0.074x})$	0.996	45.81	81.40	63.61	35.59	463.86
	W3N1	$y=22549.49/(1+114.82e^{-0.073x})$	0.994	46.94	83.02	64.98	36.08	411.53
	W3N2	$y=25230.61/(1+98.41e^{-0.073x})$	0.996	44.82	80.91	62.87	36.08	460.46
	W3N3	$y=25948.89/(1+93.08e^{-0.075x})$	0.996	42.89	78.01	60.45	35.12	486.54

W1, moderate water deficit (55%–65% of field water capacity, F_C); W2, mild water deficit (65%–75% F_C); W3, full irrigation (75%–85% F_C). N1, low nitrogen rate (120 kg ha^{-1}); N2, medium nitrogen rate (180 kg ha^{-1}); N3, high nitrogen rate (240 kg ha^{-1}). R^2, determination coefficient; t_1, the start time of the rapid growth period; t_2, the termination time of the rapid growth period; t_{max}, the occurrence time of the maximum cumulative rate; Δt, the duration of rapid growth; V_{max}, the maximum accumulation rate.

resulting equations, equations, all significant with R^2 values exceeding 0.96 in both 2021 and 2022, effectively indicated the interactive effects of water and N application on each indicator. These equations were then utilized to determine the ET and N application rates that maximized each indicator (Table 5). In 2021, maximum yield was achieved at 371.99 mm ET and 191.02 kg ha^{-1} N application. WUE peaked at 290.63 mm ET and 183.67 kg ha^{-1} N application, while NPFP reached its maximum at 382.84 mm ET

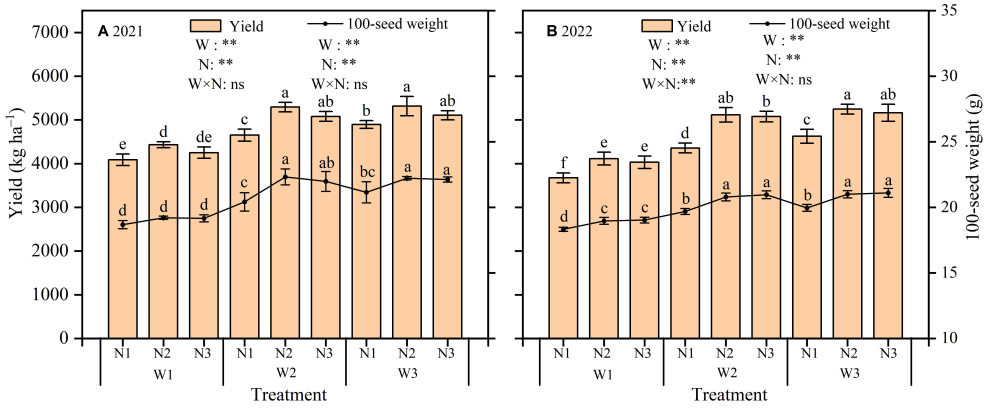

FIGURE 6
Effect of different irrigation and nitrogen treatments on sunflower yield and 100-seed weight in 2021 **(A)** and 2022 **(B)**. W1, moderate water deficit (55%–65% of field water capacity, F_C); W2, mild water deficit (65%–75% F_C); W3, full irrigation (75%–85% F_C). N1, low nitrogen rate (120 kg ha^{-1}); N2, medium nitrogen rate (180 kg ha^{-1}); N3, high nitrogen rate (240 kg ha^{-1}). Different lowercase letters above the error bar indicate significant differences between treatments in the same period at the $P < 0.05$ level. ** indicates a highly significant effect ($P < 0.01$); and ns indicates a non-significant effect ($P > 0.05$).

10.3389/fpls.2024.1429548

TABLE 4 Effects of different irrigation and nitrogen application rates on water consumption and water and nitrogen use efficiency in 2021 and 2022.

Year	Treatment	ET (mm)	WUE (kg m^{-3})	IWUE (kg m^{-3})	NPFP (kg kg^{-1})
2021	W1N1	271.65 ± 18.91a	1.51 ± 0.04b	2.49 ± 0.26b	34.07 ± 1.10c
	W1N2	274.11 ± 16.40a	1.62 ± 0.05a	2.69 ± 0.13a	24.62 ± 0.39e
	W1N3	280.25 ± 10.12a	1.51 ± 0.06b	2.54 ± 0.18ab	17.72 ± 0.53g
	W2N1	324.60 ± 5.84b	1.43 ± 0.07c	2.19 ± 0.20d	38.78 ± 1.15b
	W2N2	330.81 ± 8.96b	1.60 ± 0.08a	2.46 ± 0.16b	29.40 ± 0.60d
	W2N3	336.15 ± 12.04b	1.51 ± 0.08b	2.34 ± 0.15c	21.17 ± 0.47f
	W3N1	392.14 ± 13.72c	1.25 ± 0.06e	1.79 ± 0.11e	40.79 ± 0.59a
	W3N2	398.61 ± 11.96c	1.33 ± 0.05d	1.94 ± 0.16e	29.53 ± 1.24d
	W3N3	404.53 ± 18.09c	1.26 ± 0.03e	1.84 ± 0.05e	21.28 ± 0.44f
Significance level	W	**	**	**	**
	N	ns	*	ns	**
	W×N	ns	ns	ns	*
2022	W1N1	274.18 ± 14.98d	1.34 ± 0.05c	2.96 ± 0.12a	30.62 ± 0.52c
	W1N2	280.62 ± 8.84d	1.47 ± 0.05b	3.15 ± 0.10a	22.86 ± 0.71e
	W1N3	285.97 ± 5.71d	1.41 ± 0.04bc	2.99 ± 0.15a	16.80 ± 0.30g
	W2N1	308.93 ± 11.13c	1.41 ± 0.03bc	2.41 ± 0.11c	36.30 ± 0.56b
	W2N2	315.29 ± 8.96c	1.62 ± 0.01a	2.70 ± 0.08b	28.42 ± 0.91d
	W2N3	322.85 ± 12.55c	1.57 ± 0.07a	2.63 ± 0.13b	21.15 ± 0.16f
	W3N1	347.07 ± 9.35b	1.33 ± 0.05c	1.85 ± 0.07d	38.55 ± 1.15a
	W3N2	358.63 ± 16.55ab	1.47 ± 0.06b	1.99± 0.05d	29.15 ± 0.33d
	W3N3	375.29 ± 13.01a	1.38 ± 0.02c	1.87 ± 0.10d	21.51 ± 0.89f
Significance level	W	**	**	**	**
	N	*	**	**	**
	W×N	ns	ns	ns	**

Data are presented as mean of three replicates ± standard deviation (n = 3). W1, moderate water deficit (55%–65% of field water capacity, F_C); W2, mild water deficit (65%–75% F_C); W3, full irrigation (75%–85% F_C). N1, low nitrogen rate (120 kg ha^{-1}); N2, medium nitrogen rate (180 N ha^{-1}); N3, high nitrogen rate (240 kg ha^{-1}). Different lowercase letters within a column indicate significant differences at the $P < 0.05$ level. * means a significant differences at the $P<0.05$ significance level, ** means a highly significant differences ($P < 0.01$); and ns means no significant differences ($P > 0.05$).

and 120.00 kg ha^{-1} N application. In 2022, the highest yield occurred at 348.46 mm ET and 210.61 kg ha^{-1} N application. Maximum WUE was observed at 321.64 mm ET and 198.37 kg ha^{-1} N application, while NPFP was maximized at 348.46 mm ET and 120.00 kg ha^{-1} N application.

3.5.2 Determination of optimal water and N intervals based on spatial analysis

The optimal water and N application strategy aims to maximize both water and N productivity while maintaining yield. However, achieving optimal sunflower yield, WUE and NPFP simultaneously proves challenging in practical agricultural settings. In the current study, the response surface analysis indicated a large interaction area between yield and WUE projections when both reached 95% of their maximum value (Figure 7); whereas, the projection of NPFP at 95% of its maximum demonstrated no interaction with the combined projection of yield and WUE at their respective 95% maxima. Therefore, in order to determine the optimal ET and N application rates that balance yield, WUE and NPFP, this study defined acceptable ranges as 95% of the maximum yield and WUE, and 75% of the maximum NPFP. The comprehensive analysis results were obtained by plane projection of these acceptable ranges (Figure 8). As illustrated, the ET intervals ensuring 95% of maximum sunflower yield and WUE, while maintaining NPFP at 75% of its maximum, were 334.3–348.7 mm in 2021 and 319.9–349.3 mm in 2022. Simultaneously, N application rates fell in the ranges of 160.9–175.3 kg ha^{-1} in 2021 and 158.1–185.1 kg ha^{-1} in 2022. Combining those two years' findings suggests optimal ET and N application intervals for high yields and efficient utilization of water and N in sunflower in Hexi Oasis were 334.3–348.7 mm and 160.9–175.3 kg ha^{-1}, respectively.

10.3389/fpls.2024.1429548

TABLE 5 Regression equations of sunflower yield, Water use efficiency (WUE) and nitrogen partial factor productivity (NPFP) with water consumption (ET) and nitrogen application rate in 2021 and 2022.

Year	Response variable	Regression equation (*y*)	R^2	N and ET values at the maximum of the response variable		
				Max	N (kg ha^{-1})	ET (mm)
2021	Yield (kg ha^{-1})	$y=-1.072\times10^4 + 70.917x_1+30.557x_2+0.018x_1x_2-0.100{x_1}^2-0.097{x_2}^2$	0.966	5422.27	191.02	371.99
	WUE (kg m^{-3})	$y=-1.082 + 0.013x_1+0.010x_2+4.953\times10^{-6}x_1x_2-2.321\times10^{-5}{x_1}^2-2.974\times10^{-5}{x_2}^2$	0.982	1.63	183.67	290.63
	PFPN (kg kg^{-1})	$y=-17.083 + 0.433x_1-0.220x_2-1.3\times10^{-6}x_1x_2-5.47\times10^{-4}{x_1}^2 + 3.10\times10^{-4}{x_2}^2$	0.999	40.70	120.00	382.84
2022	Yield (kg ha^{-1})	$y=-2.661\times10^4 + 177.137x_1+10.162x_2+0.088x_1x_2-0.280{x_1}^2-0.097{x_2}^2$	0.992	5390.37	210.61	348.46
	WUE (kg m^{-3})	$y=-6.741 + 0.049x_1+0.004x_2+2.636\times10^{-5}x_1x_2-8.484\times10^{-5}{x_1}^2-3.129\times10^{-5}{x_2}^2$	0.983	1.62	198.37	321.64
	PFPN (kg kg^{-1})	$y=-113.438 + 1.009x_1-0.228x_2-2.735\times10^{-5}x_1x_2-1.457\times10^{-3}{x_1}^2 + 2.35\times10^{-4}{x_2}^2$	0.999	38.48	120.00	348.46

4 Discussion

4.1 Effect of different irrigation and nitrogen application on leaf area index and dry matter accumulation

LAI is a critical indicator for measuring the growth and development in crop populations. A higher LAI can give full play to the advantages of plant population, improve the photosynthetic capacity of the canopy, and promote the accumulation of photosynthetic products (Hikosaka, 2004). Previous studies have shown that crop LAI is susceptible to irrigation and fertilizer management practices (Zain et al., 2021). In this study, LAI in sunflower showed a significant increase followed by a slight increase at each growth stage with increasing irrigation and N application. Specifically, LAI was significantly lower ($P < 0.05$) in W1 compared to W2 and W3, with no significant difference ($P > 0.05$) between W2 and W3. Similarly, LAI was significantly lower in N1 compared to N2 and N3, with no significant difference between N2 and N3. These findings indicate that increasing water and N inputs in a

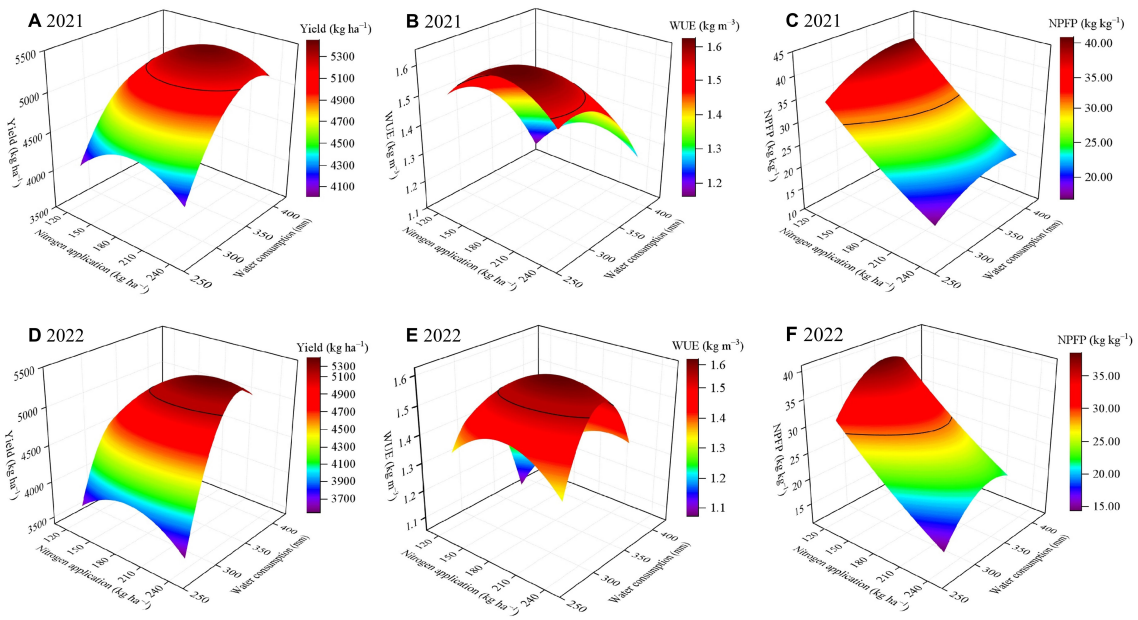

FIGURE 7
Relationships of sunflower yield, water use efficiency (WUE) and nitrogen partial factor productivity (NPFP) with water consumption (ET) and nitrogen application in 2021 **(A–C)** and 2022 **(D–F)**. The solid black lines in the figure represent 95% of the maximum yield and WUE and 75% of the maximum NPFP.

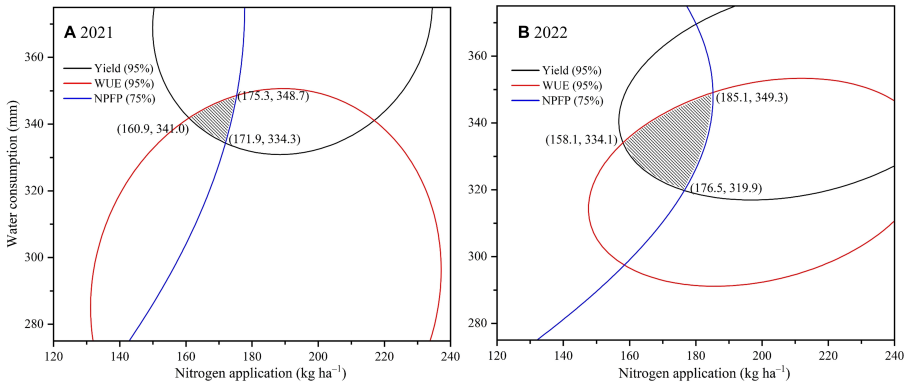

FIGURE 8
Comprehensive analysis based on yield and water use efficiency (WUE) and nitrogen partial factor productivity (NPFP) in 2021 **(A)** and 2022 **(B)**. The shaded areas indicate acceptable ranges where yield and WUE are greater than 95% of the maximum and NPFP is greater than 75% of the maximum.

reasonable range can significantly increase LAI. However, excessive applications of water and N do not lead to further significant increases in LAI. A similar finding was also reported by Yang et al. (2019), who observed a strong positive correlation between LAI and irrigation amount in sunflowers. Moreover, with increasing N fertilizer application, LAI in sunflower showed an increasing trend in the early and middle growth stages; whereas in the late growth stage, LAI showed an increasing and then decreasing trend.

As an important indicator of crop growth, DMA is closely related to yield formation (Wang et al., 2014b). Water and fertilizer management practices are used to regulate the final yield by influencing the crop DMA process (Guo et al., 2022). This study observed a positive correlation between irrigation levels and both DM and maximum DMA rates, aligning with observations made by Yang et al. (2019). This aligns with existing research indicating that increased water supply enhances both LAI and DMA (Gheysari et al., 2017), whereas water deficit can inhibit nutrient uptake and utilization by the root system, finally affecting both vegetative and reproductive growth (Fan et al., 2020). Furthermore, the results showed that under the same irrigation conditions, both DM and maximum DMA rates were significantly lower in N1 compared to N2 and N3. However, no significant differences were found between N2 and N3 for these parameters. This suggests that beyond a certain threshold, additional N application on may not significantly affect DMA. This finding is supported by Wu et al. (2023), who showed that N application increased DMA of each organ in sunflower, but excessive N application did not contribute to higher DMA compared to optimized N application. Similarly, Moraes et al. (2017) reported that N application significantly affected sunflower growth and development, but blindly increasing N fertilizer did not promote DMA.

4.2 Effect of different irrigation and nitrogen application on yield and water and nitrogen use efficiency

In agricultural production practices, water and N fertilizer management are essential measures to sustain plant growth and maintain stable yields (Chen et al., 2018). Many studies have demonstrated that in water-scarce regions, it is more beneficial to formulate a suitable irrigation and N application scheme based on the water and N requirements for crop growth rather than excessive supply (Li et al., 2022c; Si et al., 2020). In this study, the W3N2 treatment obtained the highest yield in both growing seasons. However, the difference was not significant ($P>0.05$) when compared to the yields of W3N3, W2N3, and W2N2. This suggests that a moderate reduction in water and N inputs, relative to full irrigation and high N fertilizer (W3N3), did not negatively affect sunflower yield formation. Consistent findings were obtained in several previous studies, which indicates that an appropriate supply of water and fertilizer can optimize resource access. Accordingly, this enhances photosynthetic capacity and carboxylation efficiency in plant leaves, finally leading to increased crop yield (Teixeira et al., 2014; Wang et al., 2015). Moreover, this study indicated a significant ($P<0.05$) reduction in sunflower yield under moderate water deficit and N treatments (W1N1, W1N2 and W1N3). This decline is attributed to the osmotic stress experienced by the plants due to the combined effects of water deficit and N application. This stress compromises the ability of the root system to absorb water and nutrients, finally resulting in yield reduction (Sheshbahreh et al., 2019).

Several previous studies have shown that appropriate irrigation and N application ratios can promote both water and nutrient availability, leading to significant improvements in water and N use efficiency (Dai et al., 2019; Xu et al., 2018). The results showed that under constant N application, reducing irrigation led to increased WUE and IWUE but decreased NPFP. This suggests that while appropriate water deficit improved water productivity, it limited the full utilization of fertilizer. In addition, under the same irrigation conditions, the medium nitrogen (N2) treatments resulted in the highest WUE and IWUE, with NPFP also reaching a high level. Similar results were obtained by Li et al. (2022b), who suggested that an optimal water and N management strategy should aim to align water and nutrient supply with crop uptake to better promote crop yield increases and efficient resource utilization.

4.3 Optimal water and nitrogen management strategies based on multi-objective optimization

Water scarcity and over-fertilization pose significant challenges to oasis farming in Northwest China. Accordingly, it is evident that enhancing water and fertilizer inputs to enhance crop yields is unsustainable. Therefore, irrigation and fertilizer management strategies that simultaneously optimize yield, water and fertilizer use efficiency are critical for ensuring sustainable agricultural production in the region. It is challenging to define optimal water and N application strategies through qualitative analysis alone, considering the inconsistent interaction effects of different water and N application rates on multiple production objectives. Numerous studies have employed multiple regression to establish the relationship between water and N inputs, yield, water and N use efficiency, utilizing spatial analysis to determine the optimal water and N application intervals (Gao et al., 2023; Wang et al., 2018). In this study, considering that the differences in rainfall between years would result in different water inputs to the cropland, we chose to build a binary quadratic regression model with ET and N application as explanatory variables and yield, WUE and NPFP as response variables. Subsequently, we defined acceptable conditions as 95% of the maximum values for yield and WUE, and 75% for NPFP. utilizing these thresholds, we solved for the water and N intervals that could simultaneously satisfy all three conditions. The results showed that multi-objective optimization and sustainable sunflower production in arid regions could be achieved with an ET range of 334.3 mm to 348.7 mm and a N application rate of 160.9 kg ha^{-1} to 175.3 kg ha^{-1}. It is important to acknowledge the limitations of this study. Our analysis did not incorporate production objectives such as economic benefits and seed quality when determining optimal irrigation and N management strategies, potentially affecting the results. Future research should consider incorporating these additional production objectives into regression models to develop more accurate and comprehensive irrigation and N application management strategies.

5 Conclusions

This study indicated that different irrigation and N application rates had significant effects on sunflower LAI, DMA, ET, 100-seed weight, yield and water and N use efficiency. Increasing irrigation and N application enhanced LAI, DMA, ET 100-seed weight and yield. However, LAI, DMA, 100-seed weight and yield did not increase significantly when water and N inputs exceeded certain thresholds. Additionally, reducing irrigation significantly improved WUE and IWUE, while reducing N application significantly increased NPFP. Among all treatment combinations, full irrigation and high N treatment (W3N3) not only did not give the best yield benefit, but also resulted in inefficient use of water and nitrogen. Therefore, moderate reductions in irrigation and N application were more favorable for improving water and N productivity of sunflower in the arid environments. Optimization utilizing binary quadratic regression equations and spatial analysis indicated that a balance between water conservation, high yield, resource use efficiency and environmental sustainability could be achieved when ET was 334.3–348.7 mm and N application was 160.9–175.3 kg ha^{-1}. Among the tested treatments, a mild water deficit combined with medium N rate (W2N2, 65%–75% F_C and 180 kg N ha^{-1}) closely aligned with this optimal range. Therefore, the W2N2 treatment can be recommended as the optimal irrigation and N management strategy for sustainable sunflower production in the cold and arid Hexi Oasis region of northwestern China.

Data availability statement

The datasets presented in this study can be found in online repositories. The names of the repository/repositories and accession number(s) can be found in the article/supplementary material.

Author contributions

XC: Writing – review & editing, Writing – original draft, Methodology, Formal analysis, Data curation. HZ: Writing – review & editing, Supervision, Funding acquisition, Formal analysis. SY: Writing – review & editing, Formal analysis. CZ: Writing – review & editing, Data curation. AT: Writing – review & editing, Investigation. LL: Writing – review & editing, Data curation. YB: Writing – review & editing, Data curation. FL: Writing – review & editing, Data curation.

Funding

The author(s) declare financial support was received for the research, authorship, and/or publication of this article. This work was supported by the Open Project of Liaocheng University Landscape Architecture Discipline (No. 31946221236), the Scientific Research Foundation for High-level Talented Scholars (No. 318042401) of Liaocheng University, the National Natural Science Foundation of China (No. 52269008, 51669001), the Industrial Support Plan Project of Gansu Provincial Department of Education (No. 2022CYZC-51), and the Key Research and Planning Projects of Gansu Province (No. 18YF1NA073).

Acknowledgments

We thank the Open Project of Liaocheng University Landscape Architecture Discipline (No. 31946221236), the Scientific Research Foundation for High-level Talented Scholars (No. 318042401) of Liaocheng University, the National Natural Science Foundation of China (No. 52269008, 51669001), the Industrial Support Plan Project of Gansu Provincial Department of Education (No. 2022CYZC-51), and the Key Research and Planning Projects of Gansu Province (No. 18YF1NA073) for funding and laboratory

facilities. We also thank the reviewers for their helpful comments and suggestions.

Conflict of interest

The authors declare that the research was conducted in the absence of any commercial or financial relationships that could be construed as a potential conflict of interest.

Publisher's note

References

Ballester, C., Hornbuckle, J., Brinkhoff, J., and Quayle, W. C. (2021). Effects of three frequencies of irrigation and nitrogen rates on lint yield, nitrogen use efficiency and fibre quality of cotton under furrow irrigation. *Agric. Water Manage.* 248, 10. doi: 10.1016/j.agwat.2021.106783

Campbell, C. A., Lafond, G. P., VandenBygaart, A. J., Zentner, R. P., Lemke, R., May, W. E., et al. (2011). Effect of crop rotation, fertilizer and tillage management on spring wheat grain yield and N and P content in a thin Black Chernozem: A long-term study. *Can. J. Plant Sci.* 91, 467–483. doi: 10.4141/cjps10032

Chen, S. C., Liu, W. F., and Du, T. S. (2022). Achieving high-yield and high-efficient management strategy based on optimized irrigation and nitrogen fertilization management and planting structure. *Trans. Chin. Soc Agric. Eng.* 16, 144–152. doi: 10.11975/j.issn.1002-6819.2022.16.016

Chen, J., Wang, P., Ma, Z. M., Lyu, X. D., Liu, T. T., and Siddique, K. H. M. (2018). Optimum water and nitrogen supply regulates root distribution and produces high grain yields in spring wheat (*Tritium aestivum* L.) under permanent raised bed tillage in arid northwest China. *Soil Tillage Res.* 181, 117–126. doi: 10.1016/j.sti11.2018.04.012

Dai, Z. G., Fei, L. J., Huang, D. L., Zeng, J., Chen, L., and Cai, Y. H. (2019). Coupling effects of irrigation and nitrogen levels on yield, water and nitrogen use efficiency of surge-root irrigated jujube in a semiarid region. *Agric. Water Manage.* 213, 146–154. doi: 10.1016/j.agwat.2018.09.035

Ding, D. Y., Feng, H., Zhao, Y., Hill, R. L., Yan, H. M., Chen, H. X., et al. (2019). Effects of continuous plastic mulching on crop growth in a winter wheat-summer maize rotation system on the Loess Plateau of China. *Agric. For. Meteorol.* 271, 385–397. doi: 10.1016/j.agrformet.2019.03.013

Fan, J. C., Lu, X. J., Gu, S. H., and Guo, X. Y. (2020). Improving nutrient and water use efficiencies using water-drip irrigation and fertilization technology in Northeast China. *Agric. Water Manage.* 241, 7. doi: 10.1016/j.agwat.2020.106352

Feng, Y. Y., Shi, H. B., Jia, Y. H., Li, R. P., Miao, Q. F., and Jia, Q. (2023). Multi-objective optimization water-nitrogen coupling zones of maize under mulched drip irrigation: A case study of West Liaohe Plain, China. *Agronomy-Basel* 13, 14. doi: 10.3390/agronomy13020486

Gao, R. P., Pan, Z. H., Zhang, J., Chen, X., Qi, Y. L., Zhang, Z. Y., et al. (2023). Optimal cooperative application solutions of irrigation and nitrogen fertilization for high crop yield and friendly environment in the semi-arid region of North China. *Agric. Water Manage.* 283, 13. doi: 10.1016/j.agwat.2023.108326

Gheysari, M., Sadeghi, S. H., Loescher, H. W., Amiri, S., Zareian, M. J., Majidi, M. M., et al. (2017). Comparison of deficit irrigation management strategies on root, plant growth and biomass productivity of silage maize. *Agric. Water Manage* 182, 126–138. doi: 10.1016/j.agwat.2016.12.014

Guo, J. J., Fan, J. L., Xiang, Y. Z., Zhang, F. C., Yan, S. C., Zhang, X. Y., et al. (2022). Coupling effects of irrigation amount and nitrogen fertilizer type on grain yield, water productivity and nitrogen use efficiency of drip-irrigated maize. *Agric. Water Manage.* 261, 13. doi: 10.1016/j.agwat.2021.107389

Guo, Y., Yin, W., Hu, F. L., Fan, Z. L., Fan, H., Zhao, C., et al. (2019). Reduced irrigation and nitrogen coupled with no-tillage and plastic mulching increase wheat yield in maize-wheat rotation in an arid region. *Field Crop Res.* 243, 9. doi: 10.1016/j.fcr.2019.107615

Hao, K., Fei, L. J., Liu, L. H., Jie, F. L., Peng, Y. L., Liu, X. G., et al. (2022). Comprehensive evaluation on the yield, quality, and water-nitrogen use efficiency of mountain apple under surge-root irrigation in the loess plateau based on the improved TOPSIS method. *Front. Plant Sci.* 13. doi: 10.3389/fpls.2022.853546

He, Z. J., Hu, Q. Y., Zhang, Y., Cao, H. X., and Nan, X. P. (2023). Effects of irrigation and nitrogen management strategies on soil nitrogen and apple yields in loess plateau of China. *Agric. Water Manage.* 280, 16. doi: 10.1016/j.agwat.2023.108220

Hikosaka, K. (2004). Interspecific difference in the photosynthesis-nitrogen relationship: patterns, physiological causes, and ecological importance. *J. Plant Res.* 117, 481–494. doi: 10.1007/s10265-004-0174-2

Kiani, M., Gheysari, M., Mostafazadeh-Fard, B., Majidi, M. M., Karchani, K., and Hoogenboom, G. (2016). Effect of the interaction of water and nitrogen on sunflower under drip irrigation in an arid region. *Agric. Water Manage.* 171, 162–172. doi: 10.1016/j.agwat.2016.04.008

Li, C., Feng, H., Luo, X. Q., Li, Y., Wang, N. J., Wu, W. J., et al. (2022c). Limited irrigation and fertilization in sand-layered soil increases nitrogen use efficiency and economic benefits under film mulched ridge-furrow irrigation in arid areas. *Agric. Water Manage.* 262, 11. doi: 10.1016/j.agwat.2021.107406

Li, Y., Huang, G. H., Chen, Z. J., Xiong, Y. W., Huang, Q. Z., Xu, X., et al. (2022a). Effects of irrigation and fertilization on grain yield, water and nitrogen dynamics and their use efficiency of spring wheat farmland in an arid agricultural watershed of Northwest China. *Agric. Water Manage.* 260, 14. doi: 10.1016/j.agwat.2021.107277

Li, S. E., Kang, S. Z., Zhang, L., Du, T. S., Tong, L., Ding, R. S., et al. (2015). Ecosystem water use efficiency for a sparse vineyard in arid northwest China. *Agric. Water Manage.* 148, 24–33. doi: 10.1016/j.agwat.2014.08.011

Li, X. Y., Xin, M. X., Shi, H. B., Yan, J. W., Zhao, C. Y., and Hao, Y. F. (2022b). Coupling effect and system optimization of controlled-release fertilizer and water in arid salinized areas. *Trans. Chin. Soc Agric. Mach.* 53, 397–406. doi: 10.6041/j.issn.1000-1298.2022.08.043

Liu, X., Li, M., Guo, P., and Zhang, Z. X. (2019). Optimization of water and fertilizer coupling system based on rice grain quality. *Agric. Water Manage.* 221, 34–46. doi: 10.1016/j.agwat.2019.04.009

Long, G. Q., Li, L. H., Wang, D., Zhao, P., Tang, L., Zhou, Y. L., et al. (2021). Nitrogen levels regulate intercropping-related mitigation of potential nitrate leaching. *Agric. Ecosys. Environ.* 319, 107540. doi: 10.1016/j.agee.2021.107540

Lu, J. S., Hu, T. T., Zhang, B. C., Wang, L., Yang, S. H., Fan, J. L., et al. (2021a). Nitrogen fertilizer management effects on soil nitrate leaching, grain yield and economic benefit of summer maize in Northwest China. *Agric. Water Manage.* 247, 10. doi: 10.1016/j.agwat.2021.106739

Lu, J. S., Xiang, Y. Z., Fan, J. L., Zhang, F. C., and Hu, T. T. (2021b). Sustainable high grain yield, nitrogen use efficiency and water productivity can be achieved in wheat-maize rotation system by changing irrigation and fertilization strategy. *Agric. Water Manage.* 258, 10. doi: 10.1016/j.agwat.2021.107177

Ma, S. T., Wang, T. C., and Ma, S. C. (2022). Effects of drip irrigation on root activity pattern, root-sourced signal characteristics and yield stability of winter wheat. *Agric. Water Manage.* 271, 10. doi: 10.1016/j.agwat.2022.107783

Ma, T., Zeng, W. Z., Wu, J. W., Ding, J. H., Yu, S. E., and Huang, J. S. (2020). Sunflower canopy development, radiation absorption and use efficiency at different nitrogen application rates in saline fields. *Trans. Chin. Soc Agric. Mach.* 51, 292–303. doi: 10.6041/j.issn.10001298.2020.12.032

Moraes, L. A. C., Moreira, A., Souza, L. G. M., and Cerezini, P. (2017). Nitrogen sources and rates effect on yield, nutritional status, and yield components of sunflower. *Commun. Soil Sci. Plant Anal.* 48, 1627–1635. doi: 10.1080/00103624.2017.1373792

Pan, X. F., Zhang, H. J., Yu, S. C., Deng, H. L., Chen, X. T., Zhou, C. L., et al. (2024). Strategies for the management of water and nitrogen interaction in seed maize production; A case study from China Hexi Corridor Oasis Agricultural Area. *Agric. Water Manage.* 292, 19. doi: 10.1016/j.agwat.2024.108685

Sheshbahreh, M. J., Dehnavi, M. M., Salehi, A., and Bahreininejad, B. (2019). Effect of irrigation regimes and nitrogen sources on biomass production, water and nitrogen use efficiency and nutrients uptake in coneflower (*EChinacea purpurea L.*). *Agric. Water Manage.* 213, 358–367. doi: 10.1016/j.agwat.2018.10.011

Si, Z. Y., Zain, M., Mehmood, F., Wang, G. S., Gao, Y., and Duan, A. W. (2020). Effects of nitrogen application rate and irrigation regime on growth, yield, and water-nitrogen use efficiency of drip-irrigated winter wheat in the North China Plain. *Agric. Water Manage.* 231, 8. doi: 10.1016/j.agwat.2020.106002

Sinclair, T. R., and Rufty, T. W. (2012). Nitrogen and water resources commonly limit crop yield increases, not necessarily plant genetics. *Glob. Food Secur* 1, 94–98. doi: 10.1016/j.gfs.2012.07.001

Sinha, I., Buttar, G. S., and Brar, A. S. (2017). Drip irrigation and fertigation improve economics, water and energy productivity of spring sunflower *(Helianthus annuus L.)* in Indian Punjab. *Agric. Water Manage.* 185, 58–64. doi: 10.1016/j.agwat.2017.02.008

Stone, L. R., Goodrum, D. E., Schlegel, A. J., Jaafar, M. N., and Khan, A. H. (2002). Water depletion depth of grain sorghum and sunflower in the central high plains. *Agron. J.* 94, 4, 936–943. doi: 10.2134/agronj2002.9360

Sun, Q. K., Zhou, L., Tang, X. F., Sun, D. Q., and Dang, X. W. (2021). Spatial influence and prediction of oasis urban expansion on cultivated land in arid areas: A case study of the Hexi Corridor. *J. Nat. Resour* 36, 1008–1020. doi: 10.31497/zrzyxb.20210415

Teixeira, A. I., George, M., Herreman, T., Brown, H., Fletcher, A., Chakwizira, E., et al. (2014). The impact of water and nitrogen limitation on maize biomass and resource-use efficiencies for radiation, water and nitrogen. *Field Crop Res.* 168, 109–118. doi: 10.1016/j.fcr.2014.08.002

Thompson, T. L., Doerge, T. A., and Godin, R. E. (2000). Nitrogen and water interactions in subsurface drip-irrigated cauliflower II. Agronomic, economic, and environmental outcomes. *Soil Sci. Soc Am. J.* 64, 412–418. doi: 10.2136/sssaj2000.641412x

Wang, H. D., Cheng, M. H., Zhang, S. H., Fan, J. L., Feng, H., Zhang, F. C., et al. (2021b). Optimization of irrigation amount and fertilization rate of drip-fertigated potato based on Analytic Hierarchy Process and Fuzzy Comprehensive Evaluation methods. *Agric. Water Manage.* 256, 18. doi: 10.1016/j.agwat.2021.107130

Wang, Z. G., Gao, J. L., and Ma, B. L. (2014b). Concurrent improvement in maize yield and nitrogen use efficiency with integrated agronomic management strategies. *Agron. J.* 106, 1243–1250. doi: 10.2134/agronj13.0487

Wang, C. Y., Liu, W. X., Li, Q. X., Ma, D. Y., Lu, H. F., Feng, W., et al. (2014a). Effects of different irrigation and nitrogen regimes on root growth and its correlation with above-ground plant parts in high-yielding wheat under field conditions. *Field Crop Res.* 165, 138–149. doi: 10.1016/j.fcr.2014.04.011

Wang, X., Shi, Y., Guo, Z. J., Zhang, Y. L., and Yu, Z. W. (2015). Water use and soil nitrate nitrogen changes under supplemental irrigation with nitrogen application rate in wheat field. *Field Crop Res.* 183, 117–125. doi: 10.1016/j.fcr.2015.07.021

Wang, T. Y., Wang, Z. H., Wu, Q., Zhang, J. Z., Quan, L. S., Fan, B. H., et al. (2021a). Coupling effects of water and nitrogen on photosynthetic characteristics, nitrogen uptake, and yield of sunflower under drip irrigation in an oasis. *Int. J. Agric. Biol. Eng.* 14, 130–141. doi: 10.25165/j.ijabe.20211405.6399

Wang, H. D., Wu, L. F., Cheng, M. H., Fan, J. L., Zhang, F. C., Zou, Y. F., et al. (2018). Coupling effects of water and fertilizer on yield, water and fertilizer use efficiency of drip-fertigated cotton in northern Xinjiang, China. *Field Crop Res.* 219, 169–179. doi: 10.1016/j.fcr.2018.02.002

Wang, Z. Y., Yu, S. C., Zhang, H. J., Lei, L., Liang, C., Chen, L. L., et al. (2023a). Deficit mulched drip irrigation improves yield, quality, and water use efficiency of watermelon in a desert oasis region. *Agric. Water Manage.* 277, 2. doi: 10.1016/j.agwat.2022.108132

Wang, Z. Q., Zhang, W. Y., Beebout, S. S., Zhang, H., Liu, L. J., Yang, J. C., et al. (2016). Grain yield, water and nitrogen use efficiencies of rice as influenced by irrigation regimes and their interaction with nitrogen rates. *Field Crop Res.* 193, 54–69. doi: 10.1016/j.fcr.2016.03.006

Wang, N., Zhang, T. H., Cong, A. Q., and Lian, J. (2023b). Integrated application of fertilization and reduced irrigation improved maize (*Zea mays L.*) yield, crop water productivity and nitrogen use efficiency in a semi-arid region. *Agric. Water Manage.* 289, 14. doi: 10.1016/j.agwat.2023.108566

Wu, S., Duan, Y., Zhang, T. T., An, H., Zhang, J., Liang, J. M., et al. (2023). Relationships between dry Matter accumulation, transport and yield of confectionary sunflower and response to water and nitrogen interactions. *Crops 06*, 243–251. doi: 10.16035/j.issn.1001-7283.2023.06.033

Wu, Y., Liu, X. J., Lin, F., and Kuai, J. L. (2021). Nitrogen application effect and soil carbon and nitrogen characteristics of rotation alfalfa in vegetable field in Hexi irrigated area, Gansu Province, Northwest China. *Chin. J. Appl. Ecol.* 32, 4011–4020. doi: 10.13287/j.1001-9332.202111.029

Xing, Y. Y., Zhang, F. C., Wu, L. F., Fan, J. L., Zhang, Y., and Li, J. (2015). Determination of optimal amount of irrigation and fertilizer under, drip fertigated system based on tomato yield, quality, water and, fertilizer use efficiency. *Trans. Chin. Soc Agric. Eng.* 31, 110–121. doi: 10.3969/j.issn.1002-6819.2015.z1.014

Xu, G. W., Lu, D. K., Wang, H. Z., and Li, Y. J. (2018). Morphological and physiological traits of rice roots and their relationships to yield and nitrogen utilization as influenced by irrigation regime and nitrogen rate. *Agric. Water Manage.* 203, 385–394. doi: 10.1016/j.agwat.2018.02.033

Yan, S. C., Wu, Y., Fan, J. L., Zhang, F. C., Qiang, S. C., Zheng, J., et al. (2019). Effects of water and fertilizer management on grain filling characteristics, grain weight and productivity of drip-fertigated winter wheat. *Agric. Water Manage* 213, 983–995. doi: 10.1016/j.agwat.2018.12.019

Yang, L., Wei, Z. M., Xu, D. W., Su, T. T., and Zhang, J. D. (2019). Growth and water-nitrogen use efficiency of sunflower under mulched drip fertigation with different water-nitrogen ratios. *J. Irrig. Drain* 38, 50–55. doi: 10.13522/j.cnki.ggps.20180183

Zain, M., Si, Z. Y., Li, S., Gao, Y., Mehmood, F., Rahman, S. U., et al. (2021). The coupled effects of irrigation scheduling and nitrogen fertilization mode on growth, yield and water use efficiency in drip-irrigated winter wheat. *Sustainability* 13, 17. doi: 10.3390/su13052742

Zhang, T. T., Duan, Y., Zhang, J., An, H., Liang, J. M., Fan, X., et al. (2023). Study on water Demand and coupling Effect of water and nitrogen on Sunflower in the North of Yinshan mountain. *J. Irrig. Drain.* 42, 23–31. doi: 10.13522/j.cnki.ggps.2022624

Zhang, Y. L., Li, C. H., Wang, Y. W., Hu, Y. M., Christie, P., Zhang, J. L., et al. (2016). Maize yield and soil fertility with combined use of compost and inorganic fertilizers on a calcareous soil on the North China Plain. *Soil Tillage Res.* 155, 85–94. doi: 10.1016/j.still.2015.08.006

frontiers | Frontiers in Plant Science

TYPE Original Research
PUBLISHED 11 September 2024
DOI 10.3389/fpls.2024.1432875

OPEN ACCESS

EDITED BY
Laichao Luo,
Anhui Agricultural University, China

REVIEWED BY
Ahmed M. El-Sawah,
Mansoura University, Egypt
Pankaj Singh,
Dr. Rammanohar Lohia Avadh University, India

*CORRESPONDENCE
Zhigang Zhao
zhaozg_77@163.com
Xian Sun
sunx27@mail.sysu.edu.cn

†These authors have contributed equally to this work

RECEIVED 14 May 2024
ACCEPTED 16 August 2024
PUBLISHED 11 September 2024

CITATION
He N, Huang F, Luo D, Liu Z, Han M, Zhao Z and Sun X (2024) Oilseed flax cultivation: optimizing phosphorus use for enhanced growth and soil health.
Front. Plant Sci. 15:1432875.
doi: 10.3389/fpls.2024.1432875

Oilseed flax cultivation: optimizing phosphorus use for enhanced growth and soil health

Ning He[1†], Fang Huang[1†], Dingyu Luo[2], Zhiwei Liu[3], Mingming Han[4], Zhigang Zhao[1*] and Xian Sun[2*]

[1]Yichun Key Laboratory of Functional Agriculture and Ecological Environment, Yichun University, Yichun, China, [2]School of Marine Sciences, Zhuhai Key Laboratory of Marine Bioresources and Environment, Guangdong Provincial Key Laboratory of Marine Resources and Coastal Engineering, Pearl River Estuary Marine Ecosystem Research Station, Ministry of Education, Research Center of Ocean Climate, Sun Yat-Sen University, Southern Marine Science and Engineering Guangdong Laboratory (Zhuhai), Zhuhai, China, [3]School of Ecology, Sun Yat-sen University, Guangzhou, China, [4]Biology Program, School of Distance Education, Universiti Sains Malaysia, Gelugor, Penang, Malaysia

Introduction: Oilseed flax (*Linum usitatissimum* L.) yields are phosphate (P) fertilizer-limited, especially in the temperate semiarid dryland regions of North China. However, there are limited studies on the effects of P-fertilizer inputs on plant growth and soil microorganisms in flax planting systems.

Methods: To address this gap, a field experiment was conducted with four treatments: no P addition and application of 40, 80, and 120 kg P ha^{-1}, respectively. The aim was to investigate the influence of various P fertilizer inputs on yield, plant dry matter, P use efficiency, as well as the population of soil arbuscular mycorrhizal fungi (AMF) and bacteria in dryland oilseed flax.

Results: Our results show that the P addition increased the dry matter, and the yield of oilseed increased by ~200% at 120 kg P ha^{-1} addition with inhibition on the growth of AMF hyphae. The moderate P supply (80 kg ha^{-1}) was adequate for promoting P translocation, P use efficiency, and P recovery efficiency. Soil pH, available P, and available K significantly ($p< 0.05$) promoted the abundance of the dominant taxa (*Acidobacteria_GP6, Sphingobacteria* and *Bacteroidetes*). In addition, it is imperative to comprehend the mechanism of interaction between phosphorus-fertilizer inputs and microbiota in oilseed flax soil.

Discussion: This necessitates further research to quantify and optimize the moderate phosphorus supply, regulate soil microbes to ensure high phosphorus utilization, and ultimately establish a sustainable system for oilseed flax cultivation in the local area.

KEYWORDS

oilseed flax, phosphorus fertilization, nutrient dynamics, soil bacterial community, soil health

1 Introduction

Phosphorus (P) is one of the most limiting nutrients for crops, affecting 30-40% of arable land globally and increasing the demand for P fertilizer (Lang et al., 2018; Yu et al., 2021). The global P fertilizer use has increased from 4.6 million tons in 1961 to approximately 21 million tons in 2015, contributing to the green revolution and food security (Bindraban et al., 2020). However, massive use of P fertilizer has led to water body eutrophication and high P accumulation in soil (Sharpley and Tunney, 2000; Song et al., 2023). The use of a balanced P fertilizer can improve P fertilizer efficiency, as well as soil fertility, which was regarded as an efficient and environmentally friendly method in agricultural production (Guo et al., 2016; Mauchline and Malone, 2017). The economic impact of using phosphate fertilizer in agriculture is substantial, as it significantly affects crop growth, development, and resilience to environmental stresses (Donipati et al., 2023). Phosphorus, a key component of these fertilizers, is essential for energy transfer, photosynthesis, and nutrient movement, leading to higher yields and improved crop quality, ultimately contributing to increased profitability (Zou et al., 2022). Despite cost concerns, particularly for small farmers, the benefits of using phosphate fertilizers often outweigh the expenses (Lambers, 2022). Enhanced yields result in higher marketable produce, boosting farm income. Moreover, phosphate fertilizers enhance crop resilience to drought, pests, and diseases, reducing the risk of crop failure and ensuring stable production (Nelson et al., 2023).

It is essential to prioritize environmental management when it comes to fertilizer use. Excessive application can lead to soil degradation and water pollution, particularly through eutrophication. Thus, it is crucial to emphasize precision agriculture and integrated nutrient management. These strategies are necessary to optimize the use of phosphate fertilizers, ensuring that economic benefits are balanced with environmental sustainability. While phosphate fertilizers may have initial costs, they can yield significant economic returns by enhancing crop quality and improving yields, as long as their application is carefully managed to mitigate environmental harm (Zou et al., 2022). Therefore, effective management of phosphorus in agricultural ecosystems is indispensable for addressing challenges related to food security and environmental degradation.

In soil, P-solubilizing fungi and bacteria constitute approximately 0.1-0.5% and 1-50% of the total population, respectively (Chen et al., 2006; Smith and Read, 2008). The efficiency of crops to absorb P from the soil can be directly and/or indirectly influenced by soil microbes (Richardson and Simpson, 2011; Mbuthia et al., 2015). The microbial abundance, diversity, and composition had various responses to P fertilizer application (Spohn et al., 2015; Tripathi et al., 2018). P-solubilizing microorganisms, including bacteria and fungi, employ various mechanisms to solubilize phosphorus. One of the primary mechanisms is the production of organic acids, such as citric acid, lactic acid, and gluconic acid. These acids lower the soil pH and help dissolve phosphate minerals, releasing soluble phosphorus into the soil solution (Demay et al., 2023). Additionally, these microorganisms produce enzymes like phosphatases that break down organic phosphorus compounds in the soil, converting them into inorganic forms that plants can use (Tan et al., 2013). Another mechanism involves proton extrusion, where some microorganisms extrude protons (H^+ ions) that aid in dissolving phosphate compounds (Wang et al., 2018). Furthermore, the production of chelating compounds by these microorganisms binds to cations (e.g., calcium, iron, aluminum) associated with phosphorus, freeing the phosphate ions and making them available to plants (Pan and Cai, 2023). P-solubilizing microorganisms are crucial for plant nutrition as they increase the availability of phosphorus in the soil, which is essential for plant growth and development (Sharma et al., 2013). This increased phosphorus availability stimulates root growth and development, enhancing the plant's ability to uptake water and nutrients (Aberathna et al., 2023). As a result, plants benefit from improved health, increased biomass, and higher crop yields. Moreover, utilizing P-solubilizing microorganisms reduces the need for chemical fertilizers, promoting sustainable agricultural practices and minimizing environmental pollution. By integrating these microorganisms into soil management practices, farmers can achieve more sustainable and productive agricultural systems.

Recent studies have reported that the diversity of the arbuscular mycorrhizal fungi (AMF) community in soils would be reduced by application of P fertilizers (Chen et al., 2014; Lin et al., 2012; Camenzind et al., 2014). Similarly, P fertilization is reported to reduce AMF richness and diversity in plant roots (Liu et al., 2012; Gosling et al., 2013; Liu et al., 2016a). AMF play a vital role in sustainable agriculture by enhancing plant growth and resilience through their involvement in the phosphorus cycle (El-Sawah et al., 2023). AMF form symbiotic relationships with plant roots, facilitating the uptake of phosphorus and other essential nutrients from the soil, which are otherwise inaccessible to plants (Sheteiwy et al., 2023). This symbiosis not only improves nutrient acquisition but also enhances the plant's tolerance to various abiotic stresses, such as drought and salinity (Nader et al., 2024). By improving soil structure and health, AMF contribute to sustainable agricultural practices, reducing the need for chemical fertilizers and promoting ecological balance (El-Sawah et al., 2023; Nader et al., 2024; Sheteiwy et al., 2023). Their ability to enhance soil key enzyme activities and improve plant growth under stress conditions underscores their importance in achieving sustainable crop production and maintaining soil health.

It is essential to adjust fertilizer schedules to effectively manage the impact of soil microorganisms and optimize agricultural practices (Mander et al., 2012). The availability of phosphorus significantly influences the abundance and diversity of phosphate-solubilizing bacteria, which play a crucial role in mobilizing P into plant-available forms (Li et al., 2023). Long-term P fertilization leads to alterations in soil microbial communities, with high-P soils promoting different bacterial compositions compared to low-P soils (Cheng et al., 2020). Continuous use of P fertilizers can result in an overabundance of certain microbial communities, potentially disrupting soil health (Dincă et al., 2022). Integrating organic matter with inorganic fertilizers can enhance beneficial microbial activity and improve overall soil fertility (Demay et al., 2023). Organic amendments increase the population of bacteria capable

of solubilizing inorganic P and contribute to a balanced microbial ecosystem (Demay et al., 2023). Customized fertilization strategies, guided by regular soil testing, should take into account the existing soil P status and microbial community composition to optimize plant growth and maintain microbial balance (Peng et al., 2021). Reducing excessive P application minimizes environmental risks such as runoff and water pollution, promoting sustainable agricultural practices and environmental protection. By implementing these strategies, the impact of soil microorganisms can be effectively managed, leading to improved soil health and sustainable crop production. Therefore, to minimize the impact of soil microorganisms, it may be necessary to make adjustments to fertilizer schedules.

The selection of oilseed flax (*Linum usitatissimum* L.) for this research is based on its economic significance, ability to thrive in semi-arid regions, and its positive impact on soil health. Oilseed flax is a key source of linseed oil, valued for its nutritional advantages and its role in crop rotation (Fao, 2008). Adding phosphorus fertilizer has shown to be effective in increasing oilseed crop yield and enhancing grain quality (Liu et al., 2016b; Powers et al., 2016). However, there is limited knowledge about how varying levels of P-fertilizer affect the growth of oilseed flax and soil microorganisms within the flax planting system, and what the optimal phosphorus application rate is for promoting the growth of oilseed flax and improving soil health. To fill this gap, a field experiment was conducted involving four treatments: application of different P doses and a control group. The goals of this study were to determine: (1) the impact of P fertilizer application on the yield, dry matter, P use efficiency, accumulation, and translocation in oilseed flax, (2) the interaction between soil microbial community composition and structure with varying levels of phosphorus fertilizer inputs and environmental factors, and (3) the economically viable rate of phosphate fertilizer application, in order to contribute towards sustainable agriculture practices and increased productivity.

2 Materials and methods

2.1 Study site and fertilization treatment

The field experiment is performed at Zhangbei County, Zhangjiakou City, Hebei Province, China (114°57'10" E, 41°7'23" N, altitude 1,430 m). The area experiences a mean annual temperature of 3.2°C, 2300-3100 sunshine hours, 140 KJ cm^{-2} radiation dose, a frost-free period of 90-120 days, annual precipitation of 392.7 mm, and evaporation of 1722 mm. This region is characterized by a semi-arid climate. The soil texture is clay loam. The chemical properties of the topsoil (0~20 cm) before the experiment are shown in Supplementary Table S1.

The oilseed flax cultivar in this study was Baxuan 3, which was widely used in the local. A field experiment was set up on May 10, 2017, and harvested on September 24. The experiment included four treatments: a control without P fertilizer, and three different P fertilizer treatments with application of 40 (P40), 80 (P80), and 120 (P120) kg P hm^{-1}. The applied mineral fertilizers were urea (N 46%), superphosphate (P_2O_5 16%, Ca 15%), and potassium sulfate (K_2O 50%). Addition N (90 kg N ha^{-1}) and K (90 kg K ha^{-1}) fertilizer in all treatments. The experimental design had a completely randomized block design, and the size of each experimental plot was 6 × 10 m, with three replicates. The land management methods employed for the fields adhere to the traditional local model and encompass several specific practices. Soil preparation entails plowing the fields in early spring to a depth of approximately 20-25 cm to loosen the soil and integrate organic matter. For seed sowing, a seeder is used to plant the seeds at a depth of 2-3 cm, with a row spacing of 20 cm to ensure proper plant density and optimal growth conditions. Due to the semi-arid climate, supplementary irrigation is applied during crucial growth stages, particularly during seed germination and flowering, to maintain adequate soil moisture. Weed control is achieved through a combination of manual weeding and the judicious application of herbicides in accordance with local agricultural guidelines. Moreover, pest and disease management involve regular monitoring for pests and diseases, along with the targeted use of pesticides and fungicides as needed to minimize crop damage. Harvesting is performed manually when the majority of the seed capsules turn brown, indicating physiological maturity; the harvested plants are then dried and threshed to extract the seeds. These practices align with regional agricultural methods and optimize the conditions for oilseed flax cultivation in Zhangbei County.

2.2 Plant sampling and analysis

The dry weight of the above-ground (shoot) and belowground plant parts (root) and non-grain reproductive parts (including peels, axles, sepals, flower buds, and pedicels) were measured. Samples were collected at key growth stages of oilseed flax: 35 days (budding), 55 days (anthesis), 85 days (kernel formation), and 105 days (maturity). During each sampling, one 1-meter-long plant row was randomly selected from the center of the experimental plot. The root, stem, grains, and non-grain reproductive were separately collected. The various flax organ samples were isolated and dried at 105°C for 30 min in the thermotank, then dried at 70°C until the weight was constant. The dried samples were thoroughly ground and then filtered with a 1 mm sieve. H_2SO_4-H_2O_2 decoction and vanadium-molybdenum yellow colorimetry were used to determine the P content in various flax parts (Masoni et al., 2007; Mei et al., 2012). The phosphorus translocation rate (Cassman et al., 1998), contribution rate (Fageria and Baligar, 2003), agronomic utilization rate (Rathke et al., 2006), and recovery efficiency (Rathke et al., 2006) were calculated using the following formulas:

$$\text{Phosphorus translocation rate (\%)} = \frac{\text{PT}}{\text{P accumulation in organs at flowering stage}} \times 100 \quad (1)$$

$$\text{Phosphorus contribution rate (\%)} = \frac{\text{PT}}{\text{P accumulation in mature seeds}} \times 100 \quad (2)$$

$$\text{Phosphate fertilizer agronomic utilization rate} = \frac{(\text{crops in the P application area} - \text{crops in the control area})}{\text{P fertilizer consumption}} \quad (3)$$

$$\text{Apparent phosphate recovery efficiency (\%)} = \frac{(\text{P uptake in the above ground part of crops in the P application area} - \text{P uptake of the above ground crops in the control area})}{\text{P fertilizer consumption}} \times 100 \quad (4)$$

Phosphorus translocation (PT, kg ha^{-1}) was the accumulation of phosphorus in stems, leaves, and dry matter in the flowering and mature stages and the cumulative amount of phosphorus in dry matter (Masoni et al., 2007).

2.3 Soil sampling and preparation processing

Three rhizosphere soil samples were randomly selected from the center rows of the experimental area for each experiment replicate. A hydraulic probe was used to collect the soil core with a depth of 0-200 mm (Giddings Machine Company Inc.), and plastic liners were used to avoid sample contamination. After sampling, soil samples were stored at 4°C till transferred to the laboratory. Then, the mixed soil samples were frozen rapidly to -80° C to preserve their original microbial community and biochemical properties. Soil physicochemical properties were measured through air-dried subsamples.

2.4 Soil chemical analysis

A pH meter was used to measure pH value at 1:2.5 (w/v) soil/solution ratio (Thermo ORION STAR A211). A Leco CN-2000 dry combustion analysis meter was used to determine soil organic carbon (SOC) (LecoCorp, USA). Determination of nitrogen (N) in soils was performed with the Kjeldahl method, while the exchange capacity was determined by a new generation of ammonium acetate forced replacement assay. Detection of potassium (K) in soils was carried out using a flame photometer (FP-640, China). Available P (Olsen P) was extracted from soils using 0.5 M sodium bicarbonate ($NaHCO_3$) solution. Then, the extracts were subject to colorimetric determination (Olsen, 1954). At each sampling, the alkaline phosphatase (ALP) activities of 1 g wet-weight soil samples were determined (Tabatabai, 1982). P fractionation was performed using the Hedley method (Hedley et al., 1982; Li et al., 2008). 1.0 m HCl-P, 0.1 m NaOH-P, 0.5 m $NaHCO_3$-P (pH 8.5), concentrated HCl-P, Resin-P, and residual-P were digested with H_2SO_4-HNO_3. Organic and inorganic P (Pi and Po) were determined using the filtrate derived from 0.5m $NaHCO_3$-P (pH 8.5), 0.1m NaOH-P, and concentrated HCl-P fractionation.

2.5 AM fungal analysis

Spores of AM fungi in soil were counted using the method described by Daniels (1982). For each sample, spores were extracted from 20 g of soil through a series of sieves. The spores of AM fungi in soil samples were counted on a gridded disk under a binocular stereoscopic microscope at 200 x magnification. The length of the hyphal was determined by Jakobsen et al. (1992). Mycelia lengths were determined by grid line intersection, and AM fungal hyphae and non-AM fungal hyphae were distinguished by irregular septum, binary branching, irregular wall thickness, and/or connection with chlamydia pores (Rillig et al., 2002).

2.6 DNA extraction, PCR, and sequencing

Microbial DNA in soil was extracted during the oilseed seedling stage, budding stage, anthesis stage, kernel stage, and maturity stage. The microbial DNA was extracted from a 0.5 g soil sample using the Power Soil DNA Isolation Kit (MO BIO) according to the manufacturer's protocols (Lopes et al., 2011). The DNA extracts were purified using the Bacteria Genomic Prep Mini Spin Kit (Amersham Biosciences, NJ) and quantified by the Nanodrop-2000 (Thermo Scientific, USA). The DNA extracts were amplified by primers containing the Roche-454 A and B Titanium sequencing adapters, an eight-base barcode sequence in adaptor A, 515 F-5′-GTGCCAGCMGCCGCGGTAA-3 and V4R 5′-TACNVRR GTHTCTAATYC-3′ for the ribosomal region (Wang et al., 2015). The amplicons were quantified by fluorimetry with Pico Green dsDNA quantitation kit (Invitrogen, Life Technologies, Carlsbad, CA). Pyrosequencing libraries were obtained using the 454 Genome Sequencer FLX platform according to standard 454 protocols (Roche 454 Life Sciences, Branford, CT) at Biocant (Cantanhede, Portugal).

All sequences were processed by the UPARSE pipeline, with those at 97% similarity being clustered into operational taxonomic units (OTUs) (Edgar, 2013). Following that, a classification method was assigned to the OTUs by the RDP classifier shipped trained with a 16S rRNA training set (Wang et al., 2007). Samples were resampled to the lowest number of reads (1010) prior to statistical analysis to normalize the sequence read variability among the samples using the rarefy command of the vegan add-on package (Oksanen et al., 2017) in R (3.0.2).

2.8 Statistical analysis

ANOVA was performed with SPSS 19.0 after the homogeneity test of multivariate data. The main properties of control oilseed flax and P fertilization were determined by a single degree of freedom control experiment. The significant difference in the measured data was calculated by the T-test ($P = 0.05$). Spearman correlation analysis was used to determine the relationship between microbial gene copy number, plant (biomass, phosphorus concentration, and content) and soil phosphorus variables. A stepwise regression model was built to predict the relationship between soil properties and systemic bacteriology. Prior to permutational multivariate analysis of variance (PERMANOVA), the

Mantel test, and redundancy analysis (RDA), rare OTUs (present in less than 10% of the samples in the data set) were removed to reduce inaccurate estimates. Additionally, the changes in α-diversity (including the Simpson and Shannon diversity) of the microbial community due to different treatments were also determined. Heatmaps were used to display the abundance of species in the different samples using the "vegan" package in R (version 4.0.3, http://www.r-project.org/).

3 Results

3.1 Effects of phosphorus-fertilizer inputs on the phosphorus accumulation

P fertilizer inputs significantly increased the P accumulation, as compared with control (Figure 1). The P accumulation increased with P addition from 40 to 120 kg ha^{-1} in the different flax organs at five growth stages (seedling, budding, mid-anthesis, kernel-forming, and maturity stage) (Figure 1). P accumulation in the leaves reached its maximum at the mid-anthesis stage under the P120 treatment (Figure 1B). In contrast, P accumulation in the stems, non-grain reproductive tissues, and roots reached their maximal values at the maturity stage with P120 fertilization. But the P accumulation in leaves was similar between P80 and P120 (Figure 1B). In sum, the application of P fertilizer can lead to an increase of about 102% in the total phosphorus contents of the ground aboveground plant parts, including grains (Figure 1). The study revealed that the application of phosphorus fertilizer significantly increases phosphorus accumulation in oilseed flax. This enhancement is particularly notable during the mid-anthesis and maturity stages, leading to a substantial overall increase in phosphorus content in the aboveground parts of the plant.

3.2 Response of plant dry matter and Olsen-P to phosphorus-fertilizer inputs

P fertilization significantly increased the dry matter of flax, but no significant impact was observed on root/shoot (Table 1). Though P fertilizer application increased flax root biomass, no significant difference was found among different P fertilizer treatments (Table 1). Olsen-P increased with the increase in P fertilizer application (Table 1). Typical P deficiency symptoms were observed in the leaves, roots, no-grains, and stems under nil P treatments in control plots (Figure 1; Table 1). Olsen-P at P120 showed a higher-level value than P0, P40, and P80, with the maximum value at the anthesis stage (7.03 mg kg^{-1}). The maximum ALP appeared at the anthesis stage (Table 1). In contrast, the input of P fertilization showed a negligible impact on ALP activity. Compared to control groups, the P concentrations in Resin-P, $NaHCO_3$-Pi, $NaHCO_3$-Po, HCl-Pi, NaOH-Pi, and residual-P increased significantly at P120 (Supplementary Table S2). Phosphorus fertilization significantly increases flax dry matter and soil Olsen-P levels, especially at higher application rates. However, it has little impact on root/shoot ratios, root biomass differences among treatments, and ALP activity.

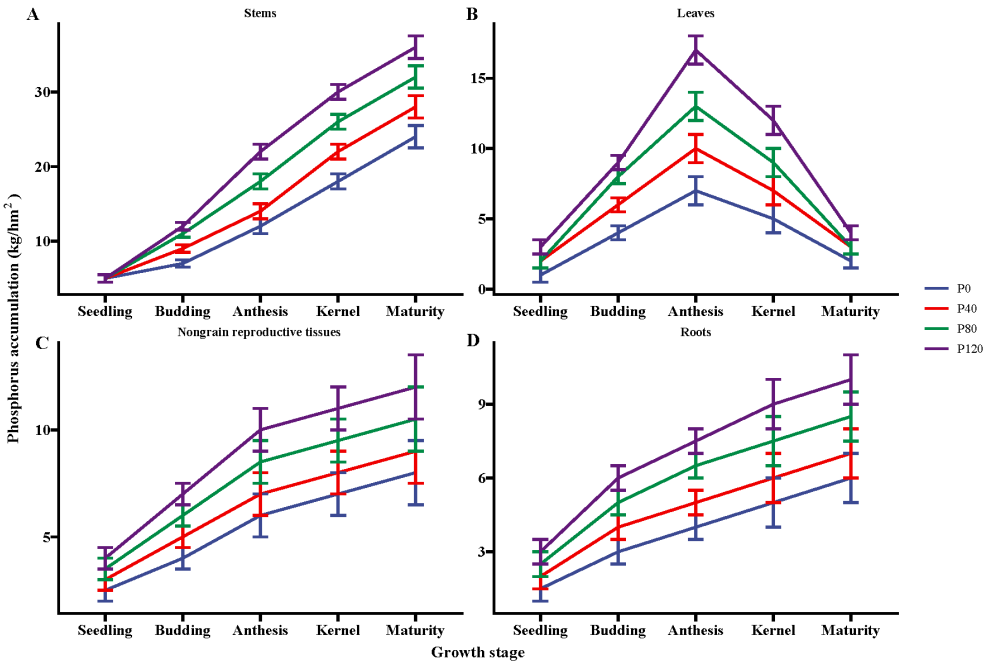

FIGURE 1
Phosphorus accumulation in the stems **(A)**, leaves **(B)**, nongrain reproductive tissues **(C)**, and roots **(D)** of flax during the growing season affected by different phosphorus management treatments. Bars represent standard error (SE) (n = 4).

10.3389/fpls.2024.1432875

TABLE 1 Effects of P-fertilizer inputs on biomass, root/shoot ratio, Olsen-P and alkaline phosphatase activities (ALP) in different sampling times.

Sampling time	P-fertilizer input	Dry weight (g)		Root/shoot ratio	Olsen P (mg kg^{-1})	ALP (nmol g^{-1} soil h^{-1})
		Shoot	Root			
Seedling	P0	6.13b	1.33b	0.22a	0.87c	7.39b
	P40	8.41a	1.71b	0.20a	2.11b	9.31a
	P80	9.96a	2.93a	0.26a	4.32b	10.23a
	P120	10.49a	2.44a	0.21a	8.32a	12.44a
Budding	P0	15.45b	2.43b	0.16a	0.97c	0.63b
	P40	16.41b	2.97a	0.18a	2.23b	9.94a
	P80	17.23a	2.87a	0.17a	4.73a	10.78a
	P120	18.47a	2.46b	0.13b	6.78a	12.48a
Anthesis	P0	21.77b	3.41b	0.16a	1.47d	9.96b
	P40	24.53a	4.69a	0.19a	2.51c	10.13b
	P80	25.69a	5.59a	0.21a	4.89b	11.23a
	P120	25.41a	5.43a	0.21a	7.03a	13.09a
kernel	P0	26.45b	5.73b	0.22a	0.96c	9.31b
	P40	28.99a	6.24a	0.22a	1.78b	9.97a
	P80	32.33a	6.88a	0.21a	4.33a	10.97a
	P120	33.46a	7.03a	0.21a	6.11a	12.95a
Maturity	P0	23.48c	6.47b	0.28a	0.74c	8.43b
	P40	27.71b	6.82a	0.30a	0.23c	8.04b
	P80	29.44a	6.93a	0.25a	3.44b	9.43b
	P120	29.75a	7.11a	0.24a	4.58a	11.23a
Summary of ANOVA						
P-fertilizer input	***	***	***	*	**	*
Time	***	*	**	**	*	*
P-fertilizer input * Time	***	**	**	NS	NS	NS

Significant differences among three phosphorus fertilization inputs and sampling times within each variable are indicated by different lowercase letters. Additionally, *, **, and *** separately represent P<0.05, 0.01, and 0.001, while NS represents not significant.

3.3 Response of yield, phosphorus translocation, use efficiency and apparent phosphorus recovery efficiency to phosphorus-fertilizer inputs

The translocation and translocation efficiency of phosphorus in leaves and dry matter presented the highest value at the P80 level (Table 2). Similarly, the contribution rate of phosphorus in leaves and dry matter increased with P addition (from 0 to 80 kg ha-1) and then decreased with the increase of P application (> 80 kg ha^{-1}). Compared with control groups, the yield of P40, P80, and P120 treatments increased by 229.0, 259.7, and 353.7 kg ha^{-1}, respectively (Table 2). When the phosphate fertilizer increased by 200% (from 40 to 120 kg ha^{-1}), the yield only increased by 1.73% to 7.04%, suggesting the increase in phosphate fertilizer far exceeded the increase in yield. Apparent P recovery (APR) efficiency and agronomic use efficiency of phosphate fertilizer were both increased in oilseed flax exposed to low P fertilization rates (< 80 P kg ha^{-1}), with the highest found at the P80 level (Table 2). The decrease that followed indicated that the yield-boosting impact of phosphate fertilizer lessens as the input of phosphorus fertilizer increases. The optimal application of phosphorus at 80 kg ha^{-1} maximizes phosphorus translocation, recovery efficiency, and agronomic use efficiency in oilseed flax. However, higher rates result in diminishing yield returns.

3.4 Effects of P-fertilizer input on the AM fungal diversity, spore density and hyphal length density

The spore density, evenness, Shannon-Wiener diversity index, Simpson diversity index, and AM fungal richness are different at

10.3389/fpls.2024.1432875

TABLE 2 Effect of phosphorus management treatments on the seed yield, phosphorus translocation, translocation efficiency, contribution rate, agronomic use efficiency, and apparent phosphorus recovery efficiency of oilseed flax.

Treatment	P translocation (kg ha^{-1} Dry weight)		P translocation efficiency (%)		Contribution rate (%)		Seed yield (kg ha^{-1})	Increase seed yield (%)	Agronomic use efficiency (kg kg^{-1})	Apparent P recovery efficiency (%)
	Leaves	Dry matter	Leaves	Dry matter	Leaves	Dry matter				
P0	41.32c	0.21c	37.28c	30.31c	45.31a	4.34c	1543.37b	—	—	—
P40	53.44b	12.45b	46.32b	32.43bc	20.14c	5.01b	1772.36a	20.35	5.13	16.61
P80	66.83a	20.63a	58.38a	46.79a	30.09b	6.44a	1803.11a	25.85	5.23	18.88
P120	59.14b	15.62b	47.31b	34.53b	19.17c	4.39c	1897.11a	32.41	4.76	15.77

The different letters in the same column indicate significant differences among treatments (P<0.05).

each sampling time (Table 3). No consistent model could be used to describe temporal changes in AM fungal diversity indexes. The number of OTUs and diversity indexes did not show any significant difference between P fertilization treatments (Table 3). No significant difference in hyphal length density (HLD) was found under different P fertilizer applications, and spore density decreased in the P120 relative to the low P application rate at budding and anthesis stages (Table 3). To sum up, sampling time was an essential factor influencing evenness, Shannon-Wiener diversity index, Simpson diversity index, and AM fungal richness. The impact of the P fertilization rate on these indicators was not significant, with the exception of seedling abundance as shown in Table 3. Sampling time had a significant influence on AM fungal diversity and spore density. Phosphorus fertilization rates had minimal impact on these metrics, except for a decrease in spore density at higher P levels during specific growth stages.

TABLE 3 AM fungal diversity, spore density and hyphal length density affected by P-fertilizer input and sampling time.

Sampling time	P-fertilizer input	Richness	Shannon-wiener	Simpson	Evenness	Hyphal length density (mg^{-1} soil)	Spore density (g^{-}1 soil)
Seedling	P0	8.75a	0.97a	0.21a	0.19a	0.94a	1.77a
	P40	6.75a	0.72b	0.18a	0.09b	0.87b	1.78a
	P80	7.83a	0.83b	0.19a	0.07b	0.82b	1.78a
	P120	8.44a	0.96a	0.22a	0.06b	0.80b	1.77a
Budding	P0	9.42a	0.72a	0.24a	0.17a	0.87a	1.43a
	P40	7.78a	0.33c	0.21a	0.08b	0.83b	1.31b
	P80	8.62a	0.41c	0.23a	0.06b	0.79b	1.27b
	P120	0.14b	0.63b	0.27a	0.05b	0.70c	1.19b
Anthesis	P0	8.47a	0.81a	0.23a	0.14a	0.81a	1.14a
	P40	6.37a	0.45c	0.19a	0.09b	0.83a	1.01a
	P80	6.72a	0.49c	0.21a	0.07b	0.74b	0.97b
	P120	8.71a	0.79a	0.24a	0.06b	0.63c	0.87b
kernel	P0	9.32a	0.94a	0.21a	0.13a	0.71a	1.02a
	P40	7.32a	0.57b	0.17a	0.10a	0.33b	0.71b
	P80	8.21a	0.61b	0.18a	0.08b	0.45b	0.70b
	P120	9.73a	0.87a	0.21a	0.05b	0.40b	0.68b
Maturity	P0	10.12a	1.03a	0.24a	0.17a	0.68a	0.97a
	P40	8.07a	0.71a	0.18a	0.12b	0.57a	0.74b
	P80	9.77a	0.83a	0.20a	0.11b	0.39b	0.61b
	P120	10.03a	0.97a	0.22a	0.10b	0.30b	0.58b

(Continued)

10.3389/fpls.2024.1432875

TABLE 3 Continued

Sampling time	P-fertilizer input	Richness	Shannon-wiener	Simpson	Evenness	Hyphal length density (mg^{-1} soil)	Spore density ($g^{-}1$ soil)
Summary of ANOVA							
P rates		NS	*	NS	NS	NS	*
Time		**	**	NS	**	*	*
P rates * Time		NS	NS	NS	NS	NS	NS

Significant differences among P-fertilizer inputs and sampling times within each variable are indicated by dissimilar lowercase letters according to the Duncan test. Additionally, *, **, and *** separately represent P<0.05, 0.01, and 0.001, while NS represents not significant.

3.5 Response of bacterial communities to phosphorus-fertilizer inputs

In this study, according to 16S rRNA gene sequence taxonomy assignments, 28,724 OTUs were obtained from 435,869 soil sequences. The top four phyla were *Acidobacteria* (126,173 sequences, 23.6% of relative abundance), *Proteobacteria* (88,916 sequences, 17.5% of relative abundance), *Bacteroidetes* (66,393 sequences, 15.4% of relative abundance) and *Actinobacteria* (52,910 sequences, 9.43% of relative abundance) (Figure 2). It was also consistent with the conclusion of Chu et al. (2010). It indicated that maintaining sufficient soil P can result in higher abundances of *Proteobacteria*. Archaea accounted for less than 5% of the total prokaryote abundance. Most of the archaea species (more than 95%) were classified as the family *Nitrososphaeraceae*.

Heatmap analysis was used to illustrate the distribution of the seven dominant classes under various P fertilizer inputs (Figure 3). P fertilizer input increased the relative abundance of *Bacteroidetes*, *Sphingobacteria*, and Acidobacteria_Gp16 in flax soils, while the abundance of *Proteobacteria* decreased. Furthermore, the abundance of *Bacteroidetes* increased with growth time, and these taxa were the most abundant in P-fertilized soils at the maturity stage. As shown in Table 4, P fertilization significantly impacted all classes in flax soils ($P< 0.05$). The combined effect of P fertilizer input and available P significantly impacted *Acidobacteria_GP6*, *Sphingobacteria*, and *Bacteroidetes* in flax soils ($P< 0.05$, Table 4). Phosphorus fertilization has a significant impact on the soil bacterial community in oilseed flax fields. It increases the abundance of certain bacterial classes while decreasing others, and this effect is influenced by both P fertilizer input and available phosphorus levels.

3.6 Effects of environmental variables on microbial community

The impact of environmental factors on microbial community structure was determined by analysis of variance

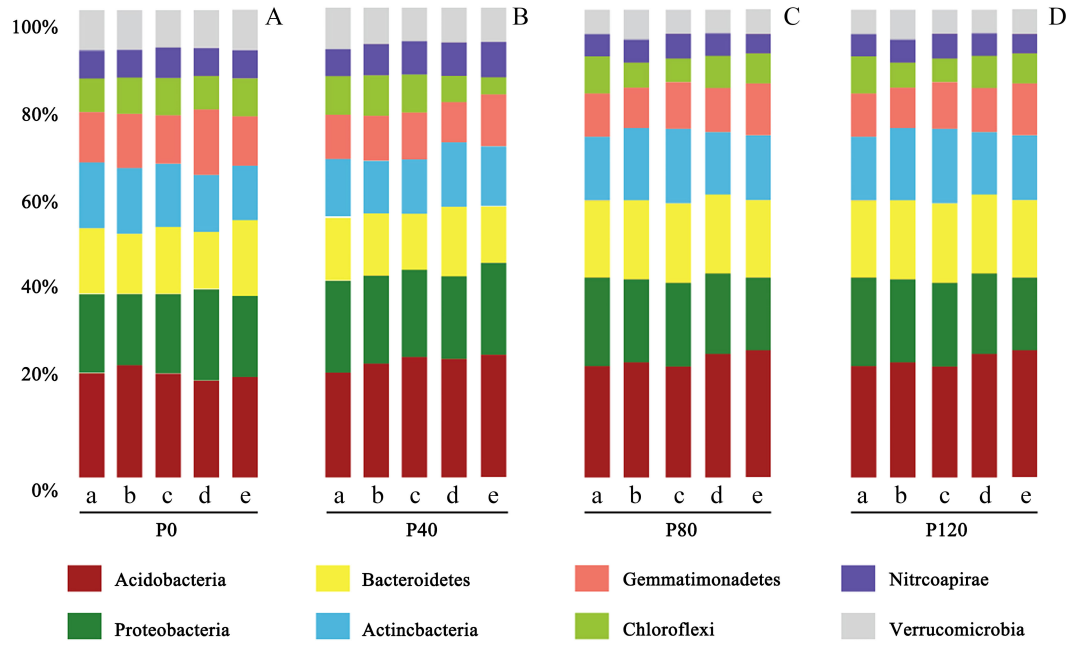

FIGURE 2
Taxonomic abundance of prokaryotic-16S rRNA OTUs at phylum level at the flax seedling **(a)**, budding **(b)**, anthesis **(c)**, kernel **(d)**, and maturity stage **(e)** influenced by different phosphorus management treatments (**A**: P0, **B**: P40, **C**: P80, **D**: P120). This demonstrates how different levels of phosphorus fertilizer impact the composition of soil bacterial communities. *Acidobacteria* consistently dominate, but increasing phosphorus levels tend to promote the abundance of Proteobacteria and Bacteroidetes.

10.3389/fpls.2024.1432875

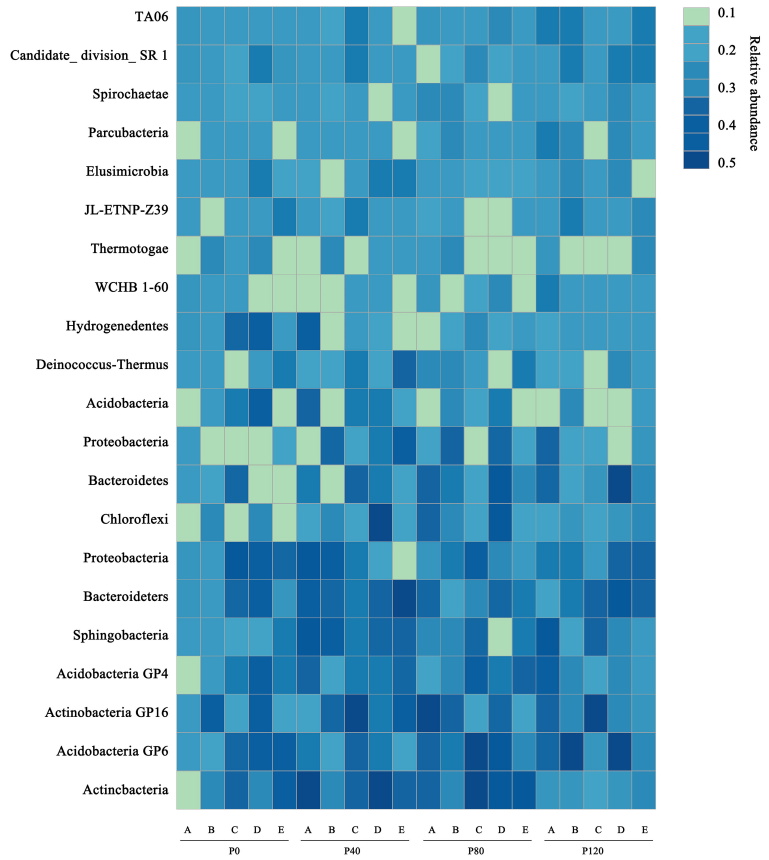

FIGURE 3
A heatmap showing the dominant classes for flax soils at maturity stage (E) under different phosphorus management treatments. The color scale is rank-based, with the darkest and lightest colors representing the highest and lowest relative abundance of each taxon among the four systems, respectively. The superscript numbers denote marginal ($p \approx 0.08$) and significant ($P < 0.05$).

(VPA) and redundancy analysis (RDA) (Figure 4). The first two plots of the RDA accounted for the total data variance of 18.26% and 13.17%, respectively. The results showed a significant correlation between environmental variables and abundant bacterial communities ($P = 0.002$, Monte Carlo test). The combined environmental parameters, P fertilization addition, soil properties, available phosphorus, and P recovery efficiency explained 42.86%, 17.23%, 13.72%, 3.02%, and 1.08% of bacterial community variation, respectively (Figure 4B).

The relationship between the dominated bacterial categories and soil properties was evaluated by stepwise regression (Table 5). Soil TN and pH accounted for 17.9% and 42.9% of the variations of *Actinobacteria_GP4*, respectively. Soil pH, TN, and TP accounted for 46.1%, 26.7 and 9.1% of the variations of *Acidobacteria_GP6*, respectively. Soil TN, TP, and Olsen-P accounted for 17.5%, 6.8%, and 19.3 of the variations of *Actinobacteria*, respectively. Soil TK, Olsen-P, and SOC accounted for the variations of *Actinobacteria_GP4*. Soil TK, Olsen-P, TN, and TP accounted for 6.9%, 19.9%, 24.6%, and 49.2% of the variations of *Sphingobacteria*, respectively. SOC and TN accounted for 6.7% and 8.8% of the

TABLE 4 Results from a two-way ANOVA testing the effects of fertilizer regimes (FR), available phosphorus (AP), and FR × AP on relative abundances of the 7 dominant classes in flax soils.

Factors	FR[a]	AP[b]	FR[a]*AP[b]
Actinobacteria	5.27**	18.07***	0.94ns
Acidobacteria GP4	4.77**	16.82***	0.78ns
Acidobacteria GP6	18.23**	16.77***	5.71***
Acidobacteria GP16	2.72*	17.88***	1.09ns
Sphingobacteria	22.43***	12.72***	2.58*
Bacteroideters	12.31***	11.44***	4.78**
Proteobacteria	5.11**	14.37***	1.26ns

ns: not significant.
*$P < 0.05$, **$P < 0.01$, ***$P < 0.001$.
[a]FR: No P fertilization (P0) and P fertilization during flax season.
[b]AP: different soil available phosphorus before planting flax.

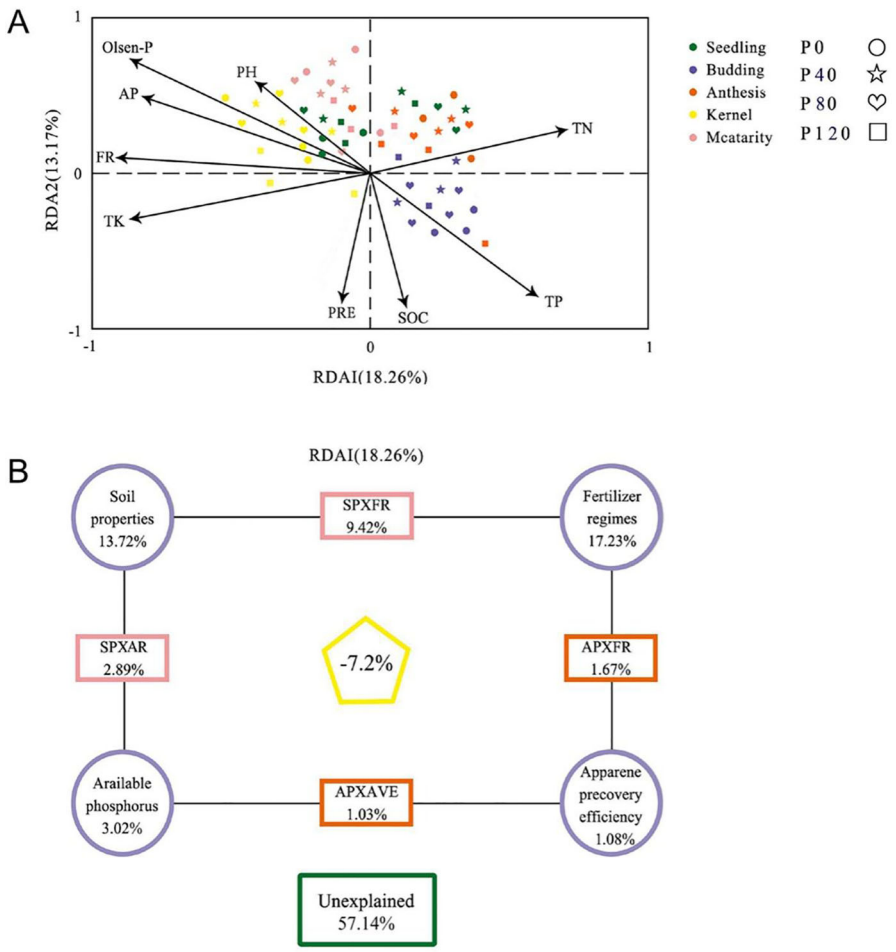

FIGURE 4
Redundant analysis (RDA) **(A)** and variance distribution analysis (VPA) **(B)** were performed on partial RDA of soil bacterial communities according to available phosphorus (AP) and fertilizer system (FR) from Zhangjiakou City. The RDA factors were selected based on the Variable Expansion Test (VIF). Soil properties include SOC (Soil organic C), TN (total N), TK (total K), apparent P recovery efficiency (AVE), Olsen-P, and pH with different phosphorus management treatments during the 2017 flax season.

variations of *Bacteroidetes*, respectively. Soil Olsen-P, Tk, and SOC accounted for 29.8%, 16.7%, and 10.8% of the variations of *Proteobacteria*, respectively (Table 5). Soil bacterial communities in oilseed flax fields are significantly influenced by environmental variables, especially soil properties and phosphorus management.

4 Discussion

The use of phosphorus fertilizer resulted in a substantial increase in phosphorus accumulation from the flowering to maturity stages, leading to a significant shift in phosphorus accumulation in a particular flax organ (Figure 1). The enhanced phosphorus accumulation and its redistribution among various plant organs as a result of phosphorus fertilization support the conclusion of the study that optimizing phosphorus application is crucial for improving dry matter accumulation, phosphorus remobilization, and ultimately grain yield in oilseed flax (Xie et al., 2014). The P content in leaves decreased sharply, which inferred that those leaves play an important role in increasing the P content in grains. In wheat, the phosphorus deposited in the seed comes from the vegetative organs and leaves (Peng and Li, 2005). Because the leaves and stems have significant phosphorus translocation efficiency during seed development (Papakosta, 1994; Dordas, 2009). The P translocation efficiency, contribution rate, recovery efficiency, and agronomic use efficiency increase with P addition (from 0 to 80 kg ha-1) but decrease with the increase of P application (> 80 kg ha^{-1}) (Table 2). Many studies have reported the relationship among yield, yield components, the rate of P fertilizer application, and P accumulation in field and pot experiments (Fageria, 2014; Vandamme et al., 2016). For improved phosphorus acquisition and accumulation in straw biomass, high phosphorus concentration may lead to reduced use efficiency and translocation efficiency for grain production (Wang et al., 2017a). The fiber content in the stem of oilseed flax was higher, suggesting that the stem and non-grain reproductive parts of oilseed flax had a higher demand for phosphorus (Grant et al., 2010), which was consistent with the results of this study. Therefore, a low straw P

TABLE 5 Stepwise regression analysis of the relationship between the relative abundance of 7 dominant classes and soil properties in flax soils.

Classes	Predictor variable	Partial R^2	Sign	F	*P*
Actinobacteria	TN	0.18	+	7.46	0.001
	TP	0.07	–	8.23	0.002
	Olsen-P	0.19	–	13.88	0.001
Acidobacteria GP4	pH	0.43	+	41.22	<0.001
	TN	0.18	+	50.46	<0.001
Acidobacteria GP6	pH	0.46	+	48.11	<0.001
	TN	0.27	+	56.67	<0.001
	TP	0.09	–	6.88	0.002
Acidobacteria GP16	TK	0.32	+	31.07	<0.001
	Olsen-P	0.19	–	8.03	0.005
	SOC	0.10	–	8.13	0.006
Sphingobacteria	TP	0.49	–	44.82	<0.001
	TN	0.25	–	18.23	<0.001
	TK	0.07	+	11.22	0.002
	Olsen-P	0.20	+	17.62	<0.001
Bacteroideters	TN	0.09	+	4.97	0.005
	SOC	0.07	+	10.23	0.002
Proteobacteria	SOC	0.11	–	13.42	0.002
	Olsen-P	0.30	+	21.10	<0.001
	TK	0.17	–	13.80	<0.001

It provides insights into how different soil properties influence the abundance of various bacterial classes in flax soils, which is valuable for understanding soil microbial ecology and managing soil health in agricultural systems. +, significance; -, no significance.

concentration, which may be beneficial for yield formation, can be used as a criterion for the estimation of high P use efficiency during the selection of genotypes for breeding programs (Figure 5).

The input of phosphate fertilizer had a more significant reduction in the diversity indexes of AM fungal (Table 3; Figure 4), which was consistent with previous research by Zhao et al. (2014). However, the number of OTUs and diversity indexes did not present any significant difference among P fertilization treatments (Table 3). These results were consistent with the response of AM fungi community at roots to P input in the exact field location (Wang et al., 2017b). Both shoots and roots will select a stable community of AMF if the same crop has been planted in the same field for a long time. The impact of soil on the diversity of AM fungi may be more significant than its impact on phosphorus availability (Williams et al., 2016; Lang et al., 2018). No significant difference in hyphal length density (HLD) was found under different phosphorus fertilizer applications. Additionally, the spore density of P120 was decreased, relative to the low phosphorus application at the budding and anthesis stages. (Table 3). The diversity and growth of AM fungi are significantly impacted by the application of phosphorus fertilizer and the timing of sampling. Optimal diversity and growth of AM fungi are observed at either very low or very high phosphorus levels, depending on the growth stage of maize plants. These findings underscore the importance of phosphorus management in sustaining a healthy AM fungal community, with potential implications for soil health and plant development. These results align with previous studies showing a decrease in spore density (Bhadalung et al., 2005), and HLD did not show any significant change and even decreased under high soil P levels (Lang et al., 2018). Because P enrichment generally suppressed mycorrhizal root colonization and reduced AM fungal hyphae growth (D'Avolio et al., 2014). High P availability in soil reduces C allocation to plant roots, thus directly weakening C-allocation to the AM fungal partner (Johnson et al., 2015). We assume that there should be a P threshold that can act on fungi diversity. More P fertilization gradient experiments need to be set in the future to verify our hypothesis.

It is well established that soil pH is the most vital factor in structuring bacterial communities (Rousk et al., 2010; Shen et al., 2013). We detected that the relative abundance of *Acidobacteria* was significantly affected by soil pH (Figure 4, Table 5); which agreed with the recent findings by Shen et al. (2013) and Wang et al. (2018). Moreover, it was also found that other soil properties like soil TN were positively correlated with the community composition of Acidobacteria_GP4 and Acidobacteria_GP6, which are consistent with the findings of Nacke et al. (2011) and Zhao et al. (2014). Soil properties, especially TP and Olsen-P, were the main factors that influenced the dominant bacterial classes in the soil. The relative abundance of *Acidobacteria* was significantly correlated with soil TN,

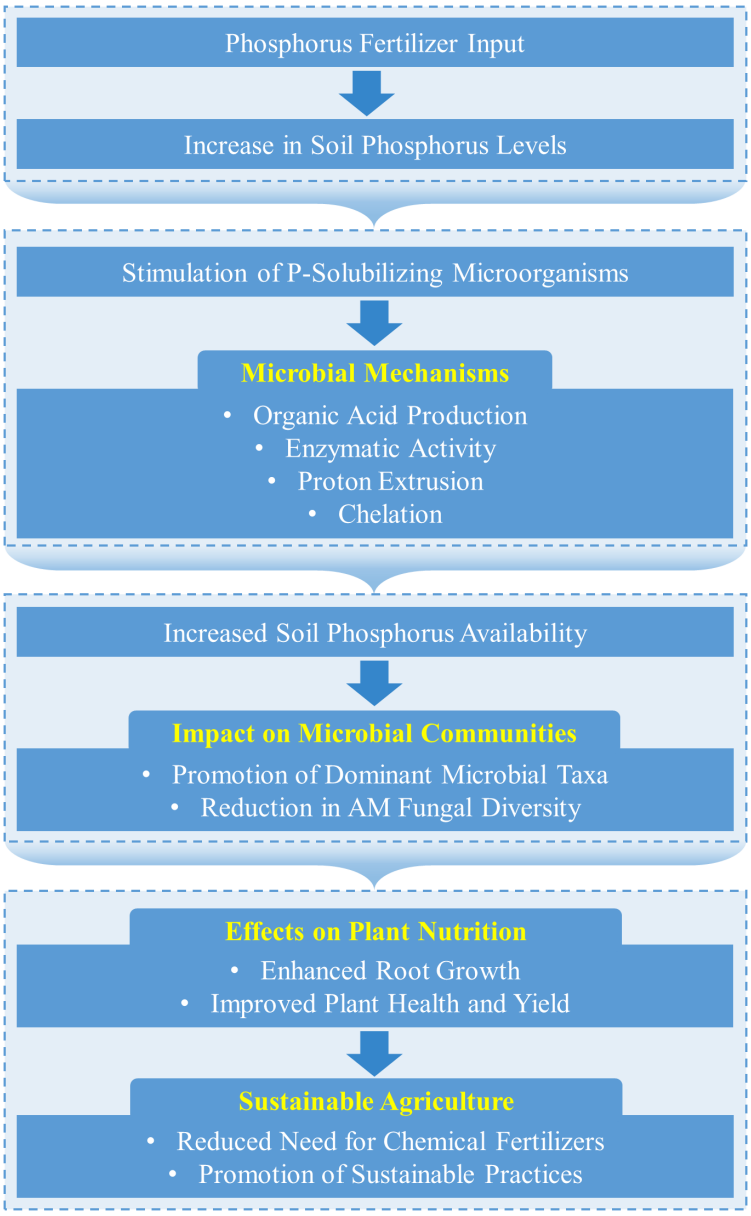

FIGURE 5
mechanism of interaction between phosphorus-fertilizer inputs and microbiota. Phosphorus fertilizer input initiates a series of beneficial changes in soil chemistry and microbial activity, leading to improved plant nutrition and sustainable agricultural practices. The stimulation of phosphorus-solubilizing microorganisms and their mechanisms play a crucial role in making soil phosphorus more available, which enhances plant growth and reduces the reliance on chemical fertilizers.

TP, and Olsen-P, suggesting that *Acidobacteria* thrives in soils when available P increases Wang et al. (2017). *Bacteroidetes* are highly correlated with TN and SOC in the soil, which is consistent with the previous study of Nacke et al. (2011). However, this study showed that there was no significant effect of P fertilization on the relative abundance of Acidobacteria or Proteobacteria despite the fact that Olsen-P was higher in treatments than in control (Table 1; Figure 2), which was a discrepancy with Fierer et al. (2005) and Campbell et al. (2010). Though soil microbial community variation is related to multiple indicators even under P fertilization, the supplement and limitation of P may be an essential factor for affecting the microbial community.

5 Conclusions

To sum up, the moderate-P supply (80 kg ha^{-1}) not only promoted the productivity of oilseed flax but also was good for increased P translocation and P use efficiency. High P-fertilizer input has no significant effects on fungal diversity, and it even backfired. However, phosphate fertilizer action is a primary driving factor of the structure of bacteria in the soil planted with flax. So far, phosphorus management in such soil types has not exerted any negative influence on microbial communities in the soil. The accumulated evidence highlights the importance of incorporating microbial communities to maximize the absorption efficiency of

phosphorus. Therefore, it is crucial to understand the interaction between flax and microbiota, use soil microbes most effectively through a fertilization regime, and finally create a sustainable system for flax cultivation in local areas. In the future, the interaction between P cycling and microbial function, as well as the specific mechanism of influence on plant growth by P fertilizer, should be fully explored to design and develop more efficient agricultural management schemes.

Data availability statement

The original contributions presented in the study are included in the article/Supplementary Material, further inquiries can be directed to the corresponding author/s.

Author contributions

NH: Project administration, Visualization, Writing – original draft. FH: Data curation, Methodology, Writing – original draft. DL: Data curation, Visualization, Writing – original draft. ZL: Data curation, Visualization, Writing – review & editing. MH: Conceptualization, Data curation, Investigation, Methodology, Visualization, Writing – original draft. ZZ: Writing – review & editing. XS: Conceptualization, Data curation, Investigation, Supervision, Writing – review & editing.

Funding

The author(s) declare that financial support was received for the research, authorship, and/or publication of this article. This work was supported by the Jiangxi Province Natural Science Foundation of China (No.20202BAB213021) and the Science and Technology Research Project of Jiangxi Education Department, China (GJJ2201734).

Acknowledgments

We would like to extend our special thanks to M.B.A. Qiupin Zhang, who provided excellent support and always encouraged us while we conducted this study.

Conflict of interest

The authors declare that the research was conducted in the absence of any commercial or financial relationships that could be construed as a potential conflict of interest.

Publisher's note

Supplementary material

The Supplementary Material for this article can be found online at: https://www.frontiersin.org/articles/10.3389/fpls.2024.1432875/full#supplementary-material

References

Aberathna, A., Satharasinghe, D., Jayasooriya, A., Jinadasa, R., Manopriya, S., Jayaweera, A., et al. (2023). *Managing Soil and Plant Nutrients: Role of Microbial Phosphate Solubilisation*.

Bhadalung, N. N., Suwanarit, A., Dell, B., Nopamornbodi, O., Thamchaipenet, A., and Rungchuang, J. (2005). Effects of long-term NP-fertilization on abundance and diversity of arbuscular mycorrhizal fungi under a maize cropping system. *Plant Soil* 270, 371–382. doi: 10.1007/s11104-004-1829-4

Bindraban, P. S., Dimkpa, C. O., and Pandey, R. (2020). Exploring phosphorus fertilizers and fertilization strategies for improved human and environmental health. *Biol. Fertil. Soils.* 56, 299–317. doi: 10.1007/s00374-019-01430-2

Camenzind, T., Hempel, S., Homeier, J., Horn, S., Velescu, A., Wilcke, W., et al. (2014). Nitrogen and phosphorus additions impact arbuscular mycorrhizal abundance and molecular diversity in a tropical montane forest. *Global Change Biol.* 20, 3646–3659. doi: 10.1111/gcb.12618

Campbell, B. J., Polson, S. W., Hanson, T. E., Mack, M. C., and Schuur, E. A. (2010). The effect of nutrient deposition on bacterial communities in Arctic tundra soil. *Environ. Microbiol.* 12, 1842–1854. doi: 10.1111/j.1462-2920.2010.02189.x

Cassman, K. G., Peng, S., Olk, D. C., Ladha, J. K., Reichardt, W., Dobermann, A., et al. (1998). Opportunities for increased nitrogen-use efficiency from improved resource management in irrigated rice systems. *Field Crops Res.* 56, 7–39. doi: 10.1016/S0378-4290(97)00140-8

Chen, Y. L., Zhang, X., Ye, J. S., Han, H. Y., Wan, S. Q., and Chen, B. D. (2014). Six-year fertilization modifies the biodiversity of arbuscular mycorrhizal fungi in a temperate steppe in Inner Mongolia. *Soil Biol. Biochem.* 69, 371–381. doi: 10.1016/j.soilbio.2013.11.020

Chen, Y. P., Rekha, P. D., Arun, A. B., Shen, F. T., Lai, W. A., and Young, C. C. (2006). Phosphate solubilizing bacteria from subtropical soil and their tricalcium phosphate solubilizing abilities. *Appl. Soil Ecol.* 34, 33–41. doi: 10.1016/j.apsoil.2005.12.002

Cheng, H., Yuan, M., Duan, Q., Sun, R., Shen, Y., Yu, Q., et al. (2020). Influence of phosphorus fertilization patterns on the bacterial community in upland farmland. *Ind. Crops Products.* 155, 112761. doi: 10.1016/j.indcrop.2020.112761

Chu, H., Fierer, N., Lauber, C. L., Caporaso, J. G., Knight, R., and Grogan, P. (2010). Soil bacterial diversity in the Arctic is not fundamentally different from that found in other biomes. *Environ. Microbiol.* 12 (11), 2998–3006.

D'Avolio, A., Pensi, D., Baietto, L., and Di Perri, G. (2014). Therapeutic drug monitoring of intracellular anti-infective agents. *J. Pharm. Biomed. Anal.* 101, 183–193.

Daniels, B. A. (1982). Methods for the recovery and quantitative estimation of propagules from soil. *Methods Principles. Mycorrhizal. Res.*, 29–35.

Demay, J., Ringeval, B., Pellerin, S., and Nesme, T. (2023). Half of global agricultural soil phosphorus fertility derived from anthropogenic sources. *Nat. Geosci.* 16, 69–74. doi: 10.1038/s41561-022-01092-0

Dincă, L. C., Grenni, P., Onet, C., and Onet, A. (2022). Fertilization and soil microbial community: a review. *Appl. Sci.* 12, 1198. doi: 10.3390/app12031198

Donipati, J., Moses, S., and Rao, T. (2023). Development of a manually operated fertilizer applicator with precision metering mechanism for enhanced crop growth and sustainable agriculture. *Pharma. Innovation* SP-12, 1929–1935. doi: 10.22271/tpi

Dordas, C. (2009). Dry matter, nitrogen and phosphorus accumulation, partitioning and remobilization as affected by N and P fertilization and source-sink relations. *Eur. J. Agron.* 30, 129–139. doi: 10.1016/j.eja.2008.09.001

Edgar, R. C. (2013). UPARSE: highly accurate OTU sequences from microbial amplicon reads. *Nat. Methods* 10, 996. doi: 10.1038/nmeth.2604

El-Sawah, A. M., Abdel-Fattah, G. G., Holford, P., Korany, S. M., Alsherif, E. A., AbdElgawad, H., et al. (2023). Funneliformis constrictum modulates polyamine metabolism to enhance tolerance of Zea mays L. @ to salinity. *Microbiol. Res.* 266, 127254. doi: 10.1016/j.micres.2022.127254

Fageria, N. K. (2014). Yield and yield components and phosphorus use efficiency of lowland rice genotypes. *J. Plant Nutr.* 37, 979–989. doi: 10.1080/01904167.2014.888735

Fageria, N. K., and Baligar, V. C. (2003). Methodology for evaluation of lowland rice genotypes for nitrogen use efficiency. *J. Plant Nutr.* 26, 1315–1333. doi: 10.1081/PLN-120020373

Fao, F. A. O. S. T. A. T. (2008). *Food and agriculture organisation of the United Nations* (Rome, Italy: Food and Agriculture Organization of the United Nations), Retrieved on, 15.

Fierer, N., Jackson, J. A., Vilgalys, R., and Jackson, R. B. (2005). Assessment of soil microbial community structure by use of taxon-specific quantitative PCR assays. *App. Environ. Microbiol.* 71 (7), 4117–4120.

Gosling, P., Mead, A., Proctor, M., Hammond, J. P., and Bending, G. D. (2013). Contrasting arbuscular mycorrhizal communities colonizing different host plants show a similar response to a soil phosphorus concentration gradient. *New Phytol.* 198, 546–556. doi: 10.1111/nph.12169

Grant, C. A., Monreal, M. A., Irvine, R. B., Mohr, R. M., McLaren, D. L., and Khakbazan, M. (2010). Preceding crop and phosphorus fertilization affect cadmium and zinc concentration of flaxseed under conventional and reduced tillage. *Plant Soil* 333, 337–350. doi: 10.1007/s11104-010-0349-7

Guo, L., Zheng, S., Cao, C., and Li, C. (2016). Tillage practices and straw-returning methods affect topsoil bacterial community and organic C under a rice-wheat cropping system in central China. *Sci. Rep.* 6, 33155. doi: 10.1038/srep33155

Hedley, M. J., Stewart, J. W. B., and Chauhan, B. (1982). Changes in inorganic and organic soil phosphorus fractions induced by cultivation practices and by laboratory incubations 1. *Soil Sci. Soc. America J.* 46, 970–976. doi: 10.2136/sssaj1982.03615995004600050017x

Jakobsen, I., Abbott, L. K., and Robson, A. D. (1992). External hyphae of vesicular—arbuscular mycorrhizal fungi associated with Trifolium subterraneum L. 2. Hyphal transport of 32P over defined distances. *New Phytol.* 120, 509–516. doi: 10.1111/j.1469-8137.1992.tb01800.x

Johnson, N. C., Wilson, G. W., Wilson, J. A., Miller, R. M., and Bowker, M. A. (2015). Mycorrhizal phenotypes and the L aw of the M inimum. *New Phytol.* 205, 1473–1484. doi: 10.1111/nph.13172

Lambers, H. (2022). Phosphorus acquisition and utilization in plants. *Annu. Rev. Plant Biol.* 73, 17–42. doi: 10.1146/annurev-arplant-102720-125738

Lang, M., Christie, P., Zhang, J., and Li, X. (2018). Long-term phosphorus application to a maize monoculture influences the soil microbial community and its feedback effects on maize seedling biomass. *Appl. Soil Ecol.* 128, 12–22. doi: 10.1016/j.apsoil.2018.01.005

Li, H. P., Han, Q. Q., Liu, Q. M., Gan, Y. N., Rensing, C., Rivera, W. L., et al. (2023). Roles of phosphate-solubilizing bacteria in mediating soil legacy phosphorus availability. *Microbiol. Res.* 272, 127375. doi: 10.1016/j.micres.2023.127375

Li, H., Shen, J., Zhang, F., Clairotte, M., Drevon, J. J., Le Cadre, E., et al. (2008). Dynamics of phosphorus fractions in the rhizosphere of common bean (Phaseolus vulgaris L.) and durum wheat (*Triticum turgidum durum* L.) grown in monocropping and intercropping systems. *Plant Soil* 312, 139–150. doi: 10.1007/s11104-007-9512-1

Lin, X., Feng, Y., Zhang, H., Chen, R., Wang, J., Zhang, J., et al. (2012). Long-term balanced fertilization decreases arbuscular mycorrhizal fungal diversity in an arable soil in North China revealed by 454 pyrosequencing. *Environ. Sci. Technol.* 46, 5764–5771. doi: 10.1021/es3001695

Liu, X., Sheng, H., Jiang, S., Yuan, Z., Zhang, C., and Elser, J. J. (2016a). Intensification of phosphorus cycling in China since the 1600s. *Proc. Natl. Acad. Sci.* 113, 2609–2614. doi: 10.1073/pnas.1519554113

Liu, Y., Shi, G., Mao, L., Cheng, G., Jiang, S., Ma, X., et al. (2012). Direct and indirect influences of 8 yr of nitrogen and phosphorus fertilization on Glomeromycota in an alpine meadow ecosystem. *New Phytol.* 194, 523–535. doi: 10.1111/j.1469-8137.2012.04050.x

Liu, W., Zhang, Y., Jiang, S., Deng, Y., Christie, P., Murray, P. J., et al. (2016b). Arbuscular mycorrhizal fungi in soil and roots respond differently to phosphorus inputs in an intensively managed calcareous agricultural soil. *Sci. Rep.* 6, 1–11. doi: 10.1038/srep24902

Lopes, A. R., Faria, C., Prieto-Fernández, Á., Trasar-Cepeda, C., Manaia, C. M., and Nunes, O. C. (2011). Comparative study of the microbial diversity of bulk paddy soil of two rice fields subjected to organic and conventional farming. *Soil Biol. Biochem.* 43, 115–125. doi: 10.1016/j.soilbio.2010.09.021

Mander, C., Wakelin, S., Young, S., Condron, L., and O'Callaghan, M. (2012). Incidence and diversity of phosphate-solubilising bacteria are linked to phosphorus status in grassland soils. *Soil Biol. Biochem.* 44, 93–101. doi: 10.1016/j.soilbio.2011.09.009

Masoni, A., Ercoli, L., Mariotti, M., and Arduini, I. (2007). Post-anthesis accumulation and remobilization of dry matter, nitrogen and phosphorus in durum wheat as affected by soil type. *Eur. J. Agron.* 26, 179–186. doi: 10.1016/j.eja.2006.09.006

Mauchline, T. H., and Malone, J. G. (2017). Life in earth-the root microbiome to the rescue? *Curr. Opin. Microbiol.* 37, 23–28. doi: 10.1016/j.mib.2017.03.005

Mbuthia, L. W., Acosta-Martínez, V., DeBruyn, J., Schaeffer, S., Tyler, D., Odoi, E., et al. (2015). Long term tillage, cover crop, and fertilization effects on microbial community structure, activity: Implications for soil quality. *Soil Biol. Biochem.* 89, 24–34. doi: 10.1016/j.soilbio.2015.06.016

Mei, P. P., Gui, L. G., Wang, P., Huang, J. C., Long, H. Y., Christie, P., et al. (2012). Maize/faba bean intercropping with rhizobia inoculation enhances productivity and recovery of fertilizer P in a reclaimed desert soil. *Field Crops Res.* 130, 19–27. doi: 10.1016/j.fcr.2012.02.007

Nacke, H., Thürmer, A., Wollherr, A., Will, C., Hodac, L., Herold, N., et al. (2011). Pyrosequencing-based assessment of bacterial community structure along different management types in German forest and grassland soils. *PloS One* 6, e17000. doi: 10.1371/journal.pone.0017000

Nader, A. A., Hauka, F. I. A., Afify, A. H., and El-Sawah, A. M. (2024). Drought-Tolerant Bacteria and Arbuscular Mycorrhizal Fungi Mitigate the Detrimental Effects of Drought Stress Induced by Withholding Irrigation at Critical Growth Stages of Soybean (*Glycine max*, L.). *Microorganisms*. doi: 10.3390/microorganisms12061123

Nelson, N. O., Roozeboom, K. L., Yeager, E. A., Williams, J. R., Zerger, S. E., Kluitenberg, G. J., et al. (2023). Agronomic and economic implications of cover crop and phosphorus fertilizer management practices for water quality improvement. *J Environ Qual.* (2023) 52(1):113–125. doi: 10.1002/jeq2.20427

Oksanen, J., Blanchet, F. G., Kindt, R., Legendre, P., Minchin, P., O'Hara, B., et al. (2017). *Vegan: Community Ecology Package. Version 2.3-3*. Available online at: https://cran.r-project.org/web/packages/vegan/.

Olsen, S. R. (1954). *Estimation of available phosphorus in soils by extraction with sodium bicarbonate (No. 939)* (Washington, DS, USA: US Dept. of Agriculture).

Pan, L., and Cai, B. (2023). Phosphate-solubilizing bacteria: advances in their physiology, molecular mechanisms and microbial community effects. *Microorganisms*. doi: 10.3390/microorganisms11122904

Papakosta, D. K. (1994). Phosphorus accumulation and translocation in wheat as affected by cultivar and nitrogen fertilization. *J. Agron. Crop Sci.* 173 (34), 260–270.

Peng, Y., Duan, Y. S., Huo, W. G., Xu, M. G., Yang, X. Y., Wang, X. H., et al. (2021). Soil microbial biomass phosphorus can serve as an index to reflect soil phosphorus fertility. *Biol. Fertil. Soils.* 57, 657–669. doi: 10.1007/s00374-021-01559-z

Peng, Z., and Li, C. (2005). Transport and partitioning of phosphorus in wheat as affected by P withdrawal during flag-leaf expansion. *Plant Soil* 268, 1–11. doi: 10.1007/s11104-004-0297-1

Powers, S. M., Bruulsema, T. W., Burt, T. P., Chan, N. I., Elser, J. J., Haygarth, P. M., et al. (2016). Long-term accumulation and transport of anthropogenic phosphorus in three river basins. *Nat. Geosci.* 9, 353. doi: 10.1038/ngeo2693

Rathke, G. W., Behrens, T., and Diepenbrock, W. (2006). Integrated nitrogen management strategies to improve seed yield, oil content and nitrogen efficiency of winter oilseed rape (Brassica napus L.): a review. *Agricult. Ecosyst. Environ.* 117, 80–108. doi: 10.1016/j.agee.2006.04.006

Richardson, A. E., and Simpson, R. J. (2011). Soil microorganisms mediating phosphorus availability update on microbial phosphorus. *Plant Physiol.* 156, 989–996. doi: 10.1104/pp.111.175448

Rillig, M. C., Wright, S. F., Shaw, M. R., and Field, C. B. (2002). Artificial climate warming positively affects arbuscular mycorrhizae but decreases soil aggregate water stability in an annual grassland. *Oikos* 97, 52–58. doi: 10.1034/j.1600-0706.2002.970105.x

Rousk, J., Bååth, E., Brookes, P. C., Lauber, C. L., Lozupone, C., Caporaso, J. G., et al. (2010). Soil bacterial and fungal communities across a pH gradient in an arable soil. *The ISME J* 4 (10), 1340–1351. doi: 10.1038/s41586-022-05220-z

Sharma, S. B., Sayyed, R. Z., Trivedi, M. H., and Gobi, T. A. (2013). Phosphate solubilizing microbes: sustainable approach for managing phosphorus deficiency in agricultural soils. *Springerplus* 2, 587. doi: 10.1186/2193-1801-2-587

Sharpley, A., and Tunney, H. (2000). Phosphorus research strategies to meet agricultural and environmental challenges of the 21st century. *J. Environ. Qual.* 29, 176–181. doi: 10.2134/jeq2000.00472425002900010022x

Shen, C., Xiong, J., Zhang, H., Feng, Y., Lin, X., Li, X., et al. (2013). Soil pH drives the spatial distribution of bacterial communities along elevation on Changbai Mountain. *Soil Biol. Biochem.* 57, 204–211. doi: 10.1016/j.soilbio.2012.07.013

Sheteiwy, M. S., El-Sawah, A. M., Kobae, Y., Basit, F., Holford, P., Yang, H., et al. (2023). The effects of microbial fertilizers application on growth, yield and some biochemical changes in the leaves and seeds of guar (*Cyamopsis tetragonoloba* L.). *Food Res. Int.* 172, 113122. doi: 10.1016/j.foodres.2023.113122

Smith, S. E., and Read, D. J. (2008). "Arbuscular mycorrhizas," in *Mycorrhizal Symbiosis*. Eds. S. E. Smith and D. J. Read (Academic Press, London), 11–145.

Song, Y., Yao, S., Li, X. N., Wang, T., Jiang, X., Bolan, N., et al. (2023). Soil metabolomics: Deciphering underground metabolic webs in terrestrial ecosystems. *Eco-Environment. Health* 3, 227–237. doi: 10.1016/j.eehl.2024.03.001

Spohn, M., Treichel, N. S., Cormann, M., Schloter, M., and Fischer, D. (2015). Distribution of phosphatase activity and various bacterial phyla in the rhizosphere of

Hordeum vulgare L. depending on P availability. *Soil Biol. Biochem.* 89, 44–51. doi: 10.1016/j.soilbio.2015.06.018

Tabatabai, M. A. (1982). "Soil enzymes," in *Methods of Soil Analysis*. Eds. A. Miller and R. D. Keeney (American Society for Agronomy, Madison), 903–947.

Tan, H., Barret, M., Mooij, M. J., Rice, O., Morrissey, J. P., Dobson, A., et al. (2013). Long-term phosphorus fertilisation increased the diversity of the total bacterial community and the phoD phosphorus mineraliser group in pasture soils. *Biol. Fertil. Soils.* 49, 661–672. doi: 10.1007/s00374-012-0755-5

Tripathi, B. M., Stegen, J. C., Kim, M., Dong, K., Adams, J. M., and Lee, Y. K. (2018). Soil pH mediates the balance between stochastic and deterministic assembly of bacteria. *ISME. J.* 12, 1072. doi: 10.1038/s41396-018-0082-4

Vandamme, E., Rose, T., Saito, K., Jeong, K., and Wissuwa, M. (2016). Integration of P acquisition efficiency, P utilization efficiency and low grain P concentrations into P-efficient rice genotypes for specific target environments. *Nutrient. Cycling. Agroecosyst.* 104, 413–427. doi: 10.1007/s10705-015-9716-3

Wang, K., Cui, K., Liu, G., Luo, X., Huang, J., Nie, L., et al. (2017b). Low straw phosphorus concentration is beneficial for high phosphorus use efficiency for grain production in rice recombinant inbred lines. *Field Crops Res.* 203, 65–73. doi: 10.1016/j.fcr.2016.12.017

Wang, Q., Garrity, G. M., Tiedje, J. M., and Cole, J. R. (2007). Naive Bayesian classifier for rapid assignment of rRNA sequences into the new bacterial taxonomy. *Appl. Environ. Microbiol.* 73, 5261–5267. doi: 10.1128/AEM.00062-07

Wang, C., White, P. J., and Li, C. J. (2017a). Colonization and community structure of arbuscular mycorrhizal fungi in maize roots at different depths in the soil profile respond differently to phosphorus inputs on a long-term experimental site. *Mycorrhiza* 27, 369–381. doi: 10.1007/s00572-016-0757-5

Wang, Y., Zhao, X., Guo, Z., Jia, Z., Wang, S., and Ding, K. (2018). Response of soil microbes to a reduction in phosphorus fertilizer in rice-wheat rotation paddy soils with varying soil P levels. *Soil Tillage. Res.* 181, 127–135. doi: 10.1016/j.still.2018.04.005

Wang, Y., Zhao, X., Wang, L., Wang, Y., Li, W., Wang, S. Q., et al. (2015). The regime and P availability of omitting P fertilizer application for rice in rice/wheat rotation in the Taihu Lake Region of southern China. *J. Soils. Sediments.* 15, 844–853. doi: 10.1007/s11368-014-1047-5

Williams, A., Kane, D. A., Ewing, P. M., Atwood, L. W., Jilling, A., Li, M., et al. (2016). Soil functional zone management: a vehicle for enhancing production and soil ecosystem services in row-crop agroecosystems. *Front. Plant Sci.* 7, 65

Xie, Y., Niu, J., Gan, Y., Gao, Y., and Li, A. (2014). Optimizing phosphorus fertilization promotes dry matter accumulation and P remobilization in oilseed flax. *Crop Sci.* 54, 1729–1736. doi: 10.2135/cropsci2013.10.0672

Yu, X., Keitel, C., and Dijkstra, F. A. (2021). Global analysis of phosphorus fertilizer use efficiency in cereal crops. *Global Food Secur.* 29, 100545. doi: 10.1016/j.gfs.2021.100545

Zhao, J., Zhang, R., Xue, C., Xun, W., Sun, L., Xu, Y., et al. (2014). Pyrosequencing reveals contrasting soil bacterial diversity and community structure of two main winter wheat cropping systems in China. *Microbial. Ecol.* 67, 443–453. doi: 10.1007/s00248-013-0322-0

Zou, T., Zhang, X., and Davidson, E. A. (2022). Global trends of cropland phosphorus use and sustainability challenges. *Nature* 611, 81–87. doi: 10.1038/s41586-022-05220-z

frontiers | Frontiers in Plant Science

TYPE Original Research
PUBLISHED 12 September 2024
DOI 10.3389/fpls.2024.1447469

OPEN ACCESS

EDITED BY
Xiaoli Hui,
Northwest A&F University, China

REVIEWED BY
Changjiang Li,
Hainan University, China
Qingfang Han,
Northwest A&F University, China

*CORRESPONDENCE
Hengjia Zhang
zhanghengjia@lcu.edu.cn

RECEIVED 11 June 2024
ACCEPTED 21 August 2024
PUBLISHED 12 September 2024

CITATION
Pan X, Zhang H, Deng H, Yu S, Zhou C and Li F (2024) Selecting reasonable soil moisture-maintaining measures to improve the soil physicochemical properties and achieve high yield and quality of purple garlic in the China Hexi Corridor oasis agricultural area. *Front. Plant Sci.* 15:1447469. doi: 10.3389/fpls.2024.1447469

Selecting reasonable soil moisture-maintaining measures to improve the soil physicochemical properties and achieve high yield and quality of purple garlic in the China Hexi Corridor oasis agricultural area

Xiaofan Pan[1], Hengjia Zhang[1,2*], Haoliang Deng[3], Shouchao Yu[2], Chenli Zhou[2] and Fuqiang Li[1]

[1]State Key Laboratory of Aridland Crop Science, College of Water Conservancy and Hydropower Engineering, Gansu Agricultural University, Lanzhou, China, [2]College of Agriculture and Biology, Liaocheng University, Liaocheng, China, [3]College of Civil Engineering, Hexi University, Zhangye, China

Agricultural plastic film, as an important agricultural production material in the China Hexi Corridor oasis agricultural area, is widely used in the intensive production process of purple garlic, which plays an important role in increasing yield, improving quality, ensuring supply, etc. However, the difference in decomposition characteristics between ordinary plastic film and degradable plastic film may affect soil moisture and temperature, thereby affecting soil biochemical properties. Therefore, we conducted a study to solve this problem. Specifically, in the Minle area of the Hexi Corridor, we selected 10 moisture-maintaining measures of ordinary transparent plastic film, transparent oxo-biodegradable plastic film (50-, 80-, and 110-day induction period), ordinary black plastic film, black oxo-biodegradable plastic film (50-, 80-, and 110-day induction period), wheat straw, and aubergine-super absorbent polymers and used the traditional open field without super absorbent polymers as a control. To analyze the effects of different moisture-maintaining measures on soil quality, garlic yield and quality, and water-fertilizer productivity in purple garlic farmland, and conduct a comprehensive evaluation of moisture-maintaining measures using principal component analysis. The results showed that all the moisture-maintaining measures could increase garlic yield, improve bulb quality and water–fertilizer productivity, improve the soil hydrothermal conditions, maintain soil fertility, increase the microbial quantity, and improve enzyme activity. Overall, transparent plastic film mulching was superior to black plastic film mulching, straw mulching, and A-SAP, with 110-day transparent oxo-biodegradable plastic film mulching being the most effective, and was not significantly different from the ordinary transparent plastic film. Compared with other moisture-maintaining measures, the yield, water productivity, irrigation water productivity, and nitrogen fertilizer partial factor productivity of purple garlic were significantly increased by 13.33% to 119.77%, 13.81% to 126.77%, 13.41% to 119.95%, and 13.33% to 119.76%, respectively. Meanwhile, the contents of allicin, soluble sugar, soluble protein, crude fiber, and amino acid content were

increased by 1.44% to 14.66%, 4.64% to 36.46%, 0.38% to 28.27%, 1.89% to 26.29%, and 0.38% to 3.74%, and, due to the prolongation of oxo-biodegradable plastic film induction period, the soil microbial community changes from "fungi type" to "bacterium type," reducing the occurrence of soil diseases and improving soil quality. On the basis of the Technique for Order Preference by Similarity to an Ideal Solution (TOPSIS) method, the soil quality was evaluated, and the yield, quality, and water productivity of garlic were comprehensively evaluated under each moisture-maintaining measure using principal component analysis. It was determined that the best soil quality and better bulb quality as well as higher garlic yield and water productivity were obtained when using the 110-day induction period transparent oxo-biodegradable plastic film. It can be used as a more reasonable moisture-maintaining measure and technical reference for the purple garlic industry in the China Hexi Corridor oasis agricultural area, which can ensure the improvement of quality and stabilization of yield and also solve the risk of environmental pollution caused by plastic film mulching at the source.

KEYWORDS

soil physicochemical properties, purple garlic, yield, quality, oxo-biodegradable plastic film, Hexi Corridor oasis

1 Introduction

Dryland accounts for about 52.5% of the total arable land in China. The sustainable and stable development of dryland agriculture is related to national food security, effective supply of agricultural products, and sustained income increase for farmers in dryland areas (Lv and Ji, 2013). However, dryland agriculture is the most sensitive to climate change, and its development is deeply affected and constrained by temperature and precipitation (Oo et al., 2020). The plastic film–mulching technology was introduced to China in 1978 because of its important functions such as increasing temperature (Zhang et al., 2019), maintaining moisture (Yang et al., 2018), inhibiting inter-plant evaporation (Li et al., 2021a), weeding (Wang et al., 2020), preventing soil erosion (Lin et al., 2010), improving soil pH (Wang et al., 2017b), reducing soil nitrogen loss (Zhu et al., 2022), increasing microbial diversity and richness (Dong et al., 2017), improving crop resource utilization efficiency (Quan et al., 2022), and increasing crop yields (Fu et al., 2021). It is widely used in dryland agricultural areas and has also become one of the most important material production means in dryland agricultural production. China is the world's largest consumer of agricultural plastic film, accounting for 75% of the global total (Petrescu-Mag et al., 2020), and the use of plastic film has reached 1.357 million t in 2020, with a total coverage area of 17.387 million hm^2, accounting for about 12.89% of the total sown area of crops (China Rural Statistical Yearbook, 2021) and covering more than 40 types of crops, including grains, melons, fruits, vegetables, flowers, and grasses (Zhao et al., 2023), and it will remain at a high level for a long time. By 2025, projections estimate that China's consumption of plastic film will soar to 2.28 million tons, covering an area spanning 23.4 million hm^2 (Qi et al., 2020). Nonetheless, the prevalent agricultural plastic film materials, primarily crafted from polyolefin, possess a robust chemical structure, rendering them exceptionally resistant to degradation. With the continuous use of plastic film, the residual plastic film will form a large number of plastic fragments or microplastics retained in the soil after ultraviolet light irradiation and natural weathering, which leads to a series of problems, such as soil compaction (Liu et al., 2014), water and nutrient transportation obstacles (Gao et al., 2023), microbial activity reduction (Muñoz et al., 2017), agricultural operation obstruction (Gao et al., 2022), crop emergence rate reduction (Wang et al., 2023), nutrient absorption and root growth and development restriction (Chen et al., 2022), and even a reduction in yields (Li et al., 2022e), which are no longer in line with the current development direction of green and sustainable agriculture.

Studies have shown that the high air tightness of plastic film inhibits gas exchange at the soil–gas interface and leads to poor soil aeration, creating an environment where the partial pressure of soil gas carbon dioxide is too high and oxygen is lacking, which inhibits root respiration and leads to root growth restriction, yellow leaves, senescence, and even death of the plant (Zhou et al., 2024). For example, in Northwest China, poor soil aeration under drip irrigation stimulated the growth of maize roots, resulting in a shallow distribution of root growth, limiting root uptake of soil water and fertilizer, and increasing the risk of premature crop aging (Zhou et al., 2020). Plastic film mulching in the late growth stage of wheat causes membrane lipid oxidation in flag leaf cells, disrupting the balance of reactive oxygen species metabolism and the photosynthetic structure of leaves, which is not conducive to the

accumulation and transportation of photosynthetic products (Zhang et al., 2023b). These phenomena are due to the generally thick plastic film thickness, resulting in poor air permeability, which is why China mandated the use of 0.01-mm ultra-thin polyethylene plastic film in 2020. Although weeds are more likely to break through the plastic film in the middle and late stages of crop growth, thus improving the air permeability, there is still a phenomenon of crop root rot (Guo et al., 2023a).

Therefore, researchers have focused on other environmentally friendly materials to replace plastic film, through the rational use of environmentally friendly materials not only to play a role in water conservation and moisture-maintaining but also to avoid the problem of environmental pollution, in which oxo-biodegradable plastic film, wheat straw, and other biological resources and mineral resources such as aubergine-super absorbent polymers (A-SAP) all retaining water and stabilizing the temperature and fertilization of the soil have been popularized and applied in agricultural production in some areas. Although, in many crop productions, it has been demonstrated that covering oxo-biodegradable plastic film and wheat straw or applying A-SAP reduces inter-plant evaporation, increases soil water storage, improves soil temperatures, improves the quality of arable land, and promotes crop growth, thereby increasing precipitation use efficiency and crop yield. Among them, oxo-biodegradable plastic film is favored by agricultural producers because it has the same heat and moisture-maintaining effect and the same mechanical properties as ordinary plastic film, and it can be completely degraded and will not pollute the soil. China, as the largest agricultural country in the world in terms of production and use of plastic agricultural film, is concerned about whether oxo-biodegradable plastic film can replace ordinary plastic film.

With high nutritional value and economic value, purple garlic has been cultivated in a large area in the China Hexi Corridor oasis agricultural area for a hundred years, forming a large-scale, scientific, and industrialized development, and has become a pillar industry for farmers to increase income and rural economic development. Among them, ground mulching, as an important cultivation measure, plays an important role in increasing soil physicochemical properties and improving the yield and quality of garlic and has been widely used in garlic cultivation. Ground-mulching materials mainly include plastic film, straw, and decomposed sheep manure (Li et al., 2021b). Yu and Yang (1988) have confirmed that the use of polyethylene plastic film for ground mulching can significantly increase the yield of garlic. However, due to the late growth of garlic, the long-term high-temperature and high-humidity environment under the plastic film is not conducive to bulb growth and quality accumulation and even large areas of "aerial garlic," resulting in yield reduction. Li (2023) showed that the use of decomposed sheep manure to mulch garlic farmland could obtain the same yield as that of plastic film mulching and showed good ecological benefits. Hu et al. (2023) showed that the use of biodegradable plastic film mulching to obtain high yield could also improve the soil structure of garlic farmland, increase the soil active organic carbon components and the organic carbon content of >0.25-mm water-stable aggregates, and contribute to the improvement of soil quality. Li et al. (2021b), by comparing the effects of white plastic film, black plastic film, straw mulching on the quality of farmland soil, and the yield and quality of garlic, found that the mulching measures could all improve the soil enzyme activity, increase the yield of garlic, and improve the quality of bulbs, among which the comprehensive effect of white plastic film mulching was superior than that of other mulching measures. Therefore, moisture-maintaining measures should be rationally selected to ensure garlic production and quality safety while improving soil quality and to realize the sustainable development of agroecosystem. Because different soil moisture-maintaining measures have great differences on soil moisture, temperature, nutrients, microbial quantity, enzyme activity, and other physicochemical properties, different moisture-maintaining measures make significant changes in the soil micro-region environment and affect garlic growth and dry matter accumulation, especially in the cold and drought conditions. What changes do different soil moisture-maintaining measures have on soil physicochemical properties and nutrient status of garlic? Which moisture-maintaining measures are more suitable for garlic production in the cool irrigation area? There is still a lack of in-depth research to truly achieve water conservation and moisture maintaining, soil improvement, and stable yield and quality improvement. Focusing on the above problems, under different moisture-maintaining measures, this paper researched the soil water and heat condition of garlic in different growth stages and the soil micro-region environmental changes after each harvest; analyzed the interrelationships among soil moisture, temperature, nutrients, and microbial and enzyme activities through comparative experiments; and evaluated the soil quality on the basis of the TOPSIS method. Combined with the principal component analysis, the effects of moisture-maintaining measures on garlic yield, quality, and water–fertilizer productivity were comprehensively evaluated, and the best moisture-maintaining measures for garlic in the cool irrigation area were defined, which provided theoretical basis and application reference for the sustainable development of garlic industry in the China Hexi Corridor oasis agricultural area.

2 Materials and methods

2.1 Experimental site profile

The experimental site is located in Yimin irrigation experimental station, Minle county, the middle part of the Hexi Corridor, Gansu province (100°43′E, 38°39′N) (Figure 1). The experimental area belongs to the edge area of the Qinghai-Tibetan Plateau, in the water conservation area at the Northern of the Qilian Mountains. It has an altitude of 1,970 m, an annual average temperature of 7.6°C, an effective cumulative temperature of ≥10°C of 2,985°C, an annual average of 2,932 h of sunshine, a frost-free stage of about 109~174 days, an average annual precipitation of about 200 mm, and an evaporation of 1,638 mm, which belongs to the typical continental desert-steppe climate. The field water capacity (θ_f) is 24.0%, and the

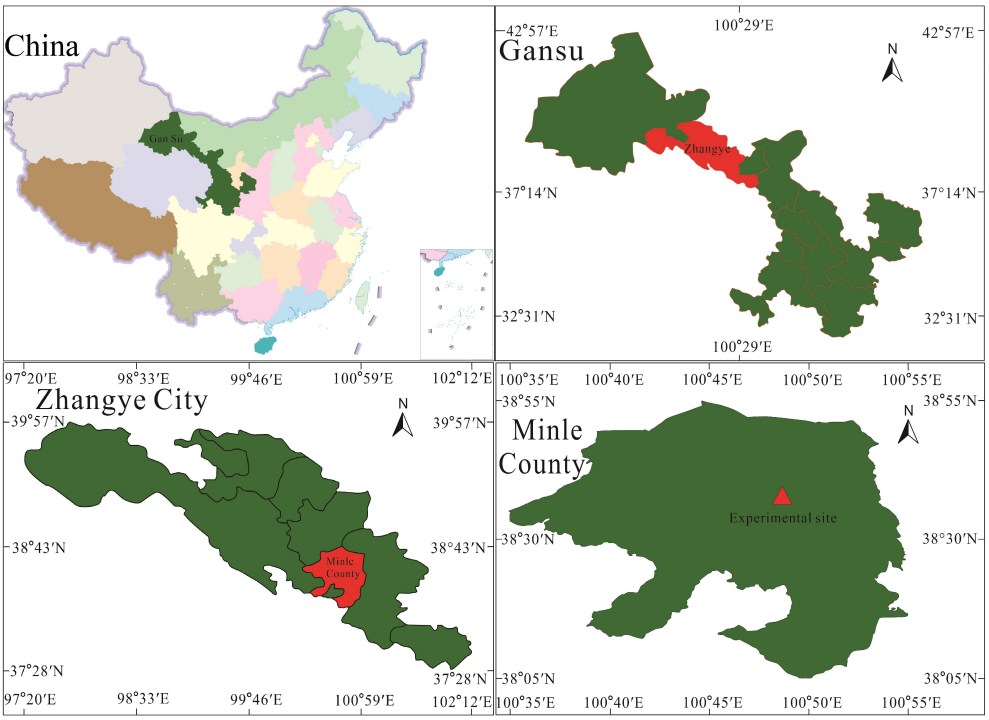

FIGURE 1
Location of the experimental site.

region has a deeper buried water table and less salinization impact and is characterized by less and unevenly distributed rainfall and shortage of river source, leading to outstanding supply–demand contradictions and frequent drought. The effective precipitation during the growth stage of purple garlic in 2020 was 67.88 mm and in 2021 was 111.91 mm. The basic physicochemical properties of the soil in the experimental site before planting are shown in Table 1, and the precipitation and average temperature during the experiment are shown in Figure 2.

2.2 Experimental materials and design

2.2.1 Experimental materials

Garlic: The variety was "Minle purple Garlic," which is a high-quality garlic variety with the clove large and fat, juicy and flavorful, mellow and pungency, and storable and is supplied by Minle County Garlic Distribution Company Limited, with a planting density of 4.4×10^5 plants hm^{-2}.

A-SAPs: It is selected agroforestry long-term SAP (validity stage of 3 years), provided by Gansu Hairida Ecological Environment Technology Co., Ltd. It is made of attapulgite and polyacrylamide through special physical and chemical processes, which has large water-absorbing multiplier and good soil improvement effect. By improving the properties of the crop soil such as soil compaction and other problems, it can better improve the efficiency of the use of water and fertilizers in agricultural production, reduce the loss of soil nutrients, and increase the economic benefits of agricultural production. A-SAP mixed with seed fertilizer to apply into the soil before planting, with an application rate of 45 kg hm^{-2}, and the application depth of 10 cm.

Polyethylene plastic film: Provided by Lanzhou Jintudi Plastic Products Co., Ltd., with polyethylene as the main raw material, it has good functions of heat preservation, moisture preservation, and insect and disease prevention, which can promote crop growth, improve yield and quality, and facilitate the recycling of crops after harvest. The plastic film width is 120 cm, the thickness is 0.02 mm, the mulching ratio is 100%, and the mulching amount is 150 kg hm^{-2}.

Oxo-biodegradable plastic film: Provided by Shandong Tianzhuang Environmental Protection Technology Co., Ltd., with ordinary polyethylene base material co-blend and oxo-biodegradable additives as the main raw materials, it has good tensile, light transmission, and other use performance and also can be controlled degradation according to the growth needs of different crops. The oxidative degradation of large–molecular weight polyethylene into small–molecular weight oligomers through the action of light, heat, and microorganisms in nature, and further degradation by microorganisms in the soil into carbon dioxide, water, and humus finally returns to the ecosystem. The plastic film width is 120 cm, the thickness is 0.008 mm, the mulching ratio is 100%, and the mulching amount is 86.0 kg hm^{-2}.

Wheat straw: The milled wheat straw was cut into sections of 3–5 cm in length, mulching ratio with 100%, and mulching amount with 6,000 kg hm^{-2}.

Drip irrigation pipe: Provided by Dayu Irrigation Group Co., Ltd., with an inlaid patch type, bearing pressure of 0.1 Mpa, diameter of 16 mm, wall thickness of 0.3 mm, drippers spacing of 150 mm, and rated flow rate of 2.0 L h^{-1}.

10.3389/fpls.2024.1447469

TABLE 1 Basic physicochemical properties of 0-40 cm soil layer in the experimental site.

Soil type	Soil depth (cm)	OM (g kg^{-1})	TN (g kg^{-1})	TP (g kg^{-1})	TK (g kg^{-1})	NN (mg kg^{-1})	AN (mg kg^{-1})	AP (mg kg^{-1})	AK (mg kg^{-1})	pH	BD (g cm^{-3})
Light loam	0–20	14.5	1.23	1.11	23.5	190.50	24.60	113.7	751	8.16	1.43
	20–40	13.8	1.14	0.94	22.5	89.15	23.20	56.2	669	8.36	1.48

OM, soil organic matter content; TN, soil total nitrogen content; TP, soil total phosphorus content; TK, soil total potassium content; NN, soil nitrate nitrogen content; AN, soil ammonium nitrogen content; AP, soil available phosphorus content; AK, soil available potassium content; BD, soil bulk density.

2.2.2 Experimental design

The experiment was conducted from March to August in 2020 and 2021 with open-field no mulching and no A-SAP as control (CK), ordinary transparent plastic film mulching (WN), 50-day transparent oxo-biodegradable plastic film mulching (WS), 80-day transparent oxo-biodegradable plastic film mulching (WM), 110-day transparent oxo-biodegradable plastic film mulching (WL), 50-day black oxo-biodegradable plastic film mulching (BS), 80-day black oxo-biodegradable plastic film mulching (BM), 110-day black oxo-biodegradable plastic film mulching (BL), straw mulching (SM), and applying A-SAP (WR), a total of 11 treatments (Figure 3). Randomized block design was adopted in the experiment, each treatment was repeated three times, with a total of 33 plots, and the plot area was 5.0 $m \times 10\ m = 50\ m^2$. Surface-water (electrical conductivity, 5.1 μS cm^{-1}; total salt content, 376 mg L^{-1}; pH, 7.9) was used as the irrigation source. Each plot was installed with an independent ball valves, filters, and water meter to control the amount of irrigation; pressure differential fertilization tanks were used for fertilization. Filters were 120-mesh, and accuracy of water meters was 0.0001 m^3 (Figure 4). Urea (N ≥ 46%; 610 *kg* hm^{-2}), diammonium phosphate (P_2O_5 ≥ 42%; 536 *kg* hm^{-2}), and potassium sulfate (K_2O ≥ 52%; 300 *kg* hm^{-2}) were used for seed fertilizer. All treatments were irrigated eight times throughout the growth period, and the dates and times of irrigation and fertilized are shown in Figure 5. Garlic was cropped for 2 years in a row, and the experimental plots were stable. The 2020 experimental was sown on 1 April and harvested

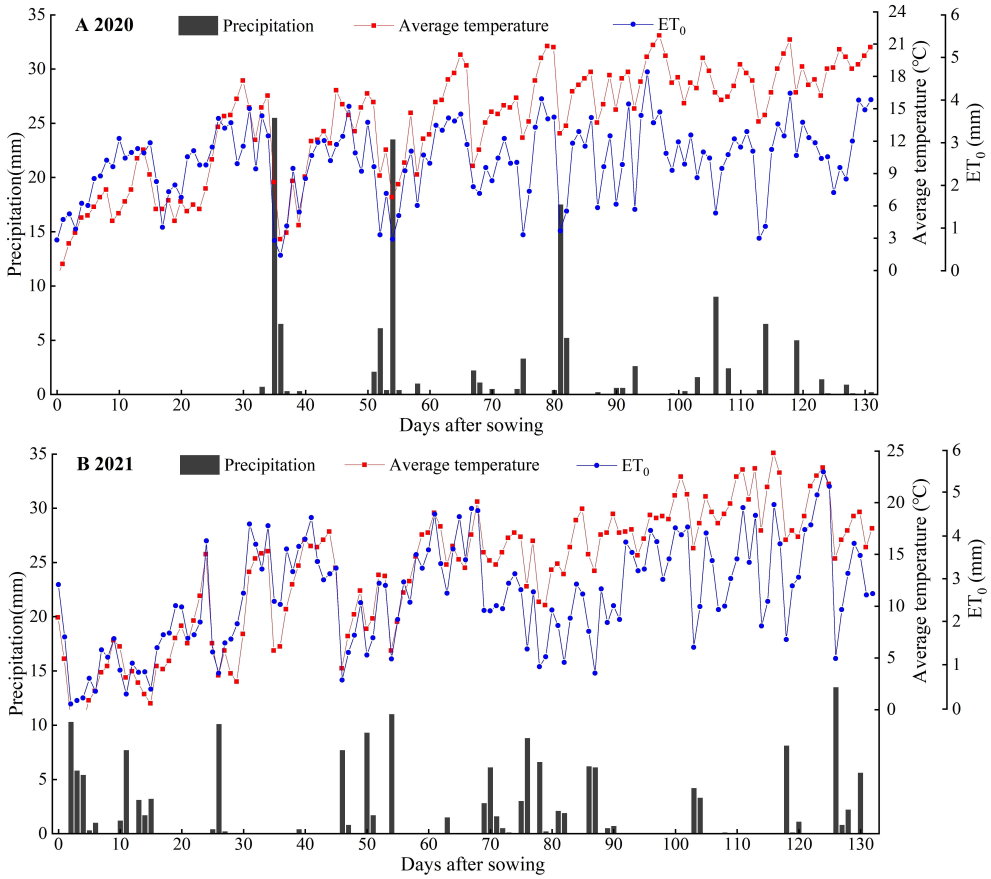

FIGURE 2
Daily variation of average temperature, reference crop evapotranspiration (ET_0) and precipitation throughout the purple garlic growing seasons of 2020 **(A)** and 2021 **(B)**.

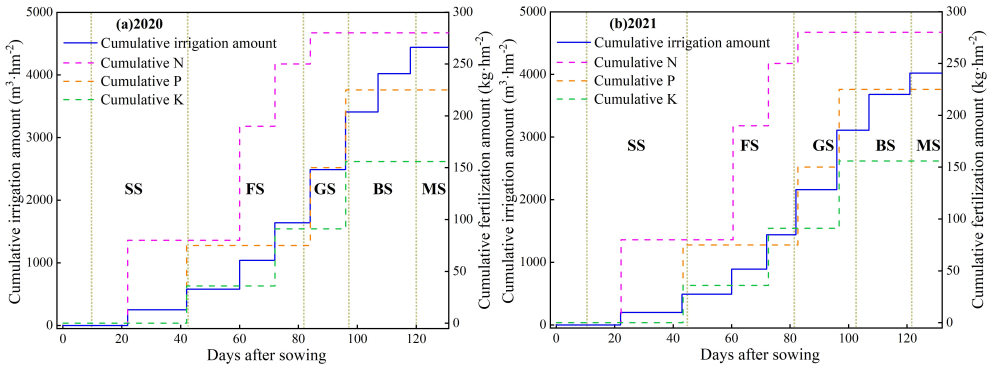

FIGURE 3
Design of different irrigation and fertilization systems of purple garlic in 2020 and 2021. SS, seedling stage; FS, flower bud differentiation stage; GS, garlic stem elongation stage; BS, bulb enlargement stage; MS, mature stage.

on 10 August. The 2021 experimental was sown on 29 March and harvested on 8 August.

2.3 Measurement items and methods

2.3.1 Soil water storage

Soil samples of 0–20, 20–40, 40–60, 60–80, and 80–100 cm were taken during the garlic seedling stage, scaly bud and flower bud differentiation stage, garlic bolt elongation stage, bulb swelling stage, and mature stage, respectively, and the soil water content was determined by traditional drying and weighing method, and, then, the soil water storage was calculated.

The formula for calculating soil water storage is: $M = h \times \rho \times \omega \times 10$, where M is the soil water storage (mm), h is the soil layer depth (cm), ρ is the soil bulk density (g cm^{-3}), and ω is the soil water content (%).

2.3.2 Soil temperature

Soil temperatures of 5-, 10-, 15-, 20-, and 25-cm soil layers were measured by right-angle mercury geothermometer (−30°C~50°C, accuracy of 1°C) at the garlic seedling stage, scaly bud and flower bud differentiation stage, garlic bolt elongation stage, bulb swelling stage, and mature stage, respectively. In order to ensure the representativeness of the data, one set was arranged in the front, middle, and rear positions of each plot, and the observations were made every 2 h from 8:00 am to 20:00 pm every day. Each growth stage was observed continuously for 5 days, and the average value was taken.

2.3.3 Soil nutrients

Soil samples of 0- to 20-cm and 20- to 40-cm soil layers were taken after garlic harvesting according to the five-point method, and the contents of soil organic matter, total nitrogen, total phosphorus, total potassium, nitrate nitrogen, ammonium nitrogen, available phosphorus, and slow-release potassium were determined after air drying. Soil organic matter was determined by external heating with potassium dichromate-concentrated sulfuric acid, total nitrogen by semimicro-Kjeldahl determination, total phosphorus by molybdenum antimony colorimetric method, total potassium by flame photometric method, nitrate nitrogen by ultraviolet spectrophotometry method, ammonium nitrogen by indophenol blue colorimetric method, available phosphorus by molybdenum antimony colorimetric method, and slow-release potassium by ammonium acetate extraction-flame photometric method (Lu, 2000).

2.3.4 Soil microbial measurement

Soil samples of 0- to 20-cm and 20- to 40-cm soil layers were taken after garlic harvesting according to the five-point method, and soil microbial quantity was determined immediately. Bacterium were determined by beef extract peptone agar medium method, fungi by Martin-Bengal red agar medium method, and actinomycetes by modified Gau No. 1 agar medium method (Wang et al., 2017a). Soil microbial biomass carbon and soil microbial biomass nitrogen were determined by chloroform fumigation–K_2SO_4 extraction method (Wu et al., 2006).

2.3.5 Soil enzyme activity measurement

Soil samples of 0- to 20-cm and 20- to 40-cm soil layers were taken after garlic harvesting according to the five-point method, and the soil enzyme activity was determined after air-drying. Urease activity was determined by the sodium phenol-sodium hypochlorite colorimetric method, sucrase activity by the 3,5-dinitrosalicylic acid method, catalase activity by the $KMnO_4$ titrimetric method, and alkaline phosphatase activity by the disodium benzene phosphate colorimetric method (Guan, 1986).

2.3.6 Yield and quality measurement

After the garlic was mature, it was individually harvested by plot and then transported to a sunshade for drying, and left to dry for 2–3 days to remove the pseudostems, retain the bulbs and calculate the yield, and plot yields were converted to kg hm^{-2}. At the same time,

10.3389/fpls.2024.1447469

10 garlic plants were randomly taken from each plot for quality determination of allicin, soluble sugar, soluble protein, vitamin C, crude fiber, ash content, and amino acid. Allicin was determined by Ultra Performance Liquid Chromatography (UPLC) method (Wang et al., 2024), soluble sugar by anthrone colorimetric method (Wang et al., 2024), soluble protein by Kaomas Brilliant Blue G-250 method (Wang et al., 2024), vitamin C by red phenanthroline colorimetric method (Wang et al., 2024), crude fiber by filter-bag method (Zhou et al., 2023), and ash content by reference to GB-5009.4-2016 (Guo et al., 2023b), and amino acid was performed in accordance with the operating procedures of the kit manual (Zhou et al., 2023).

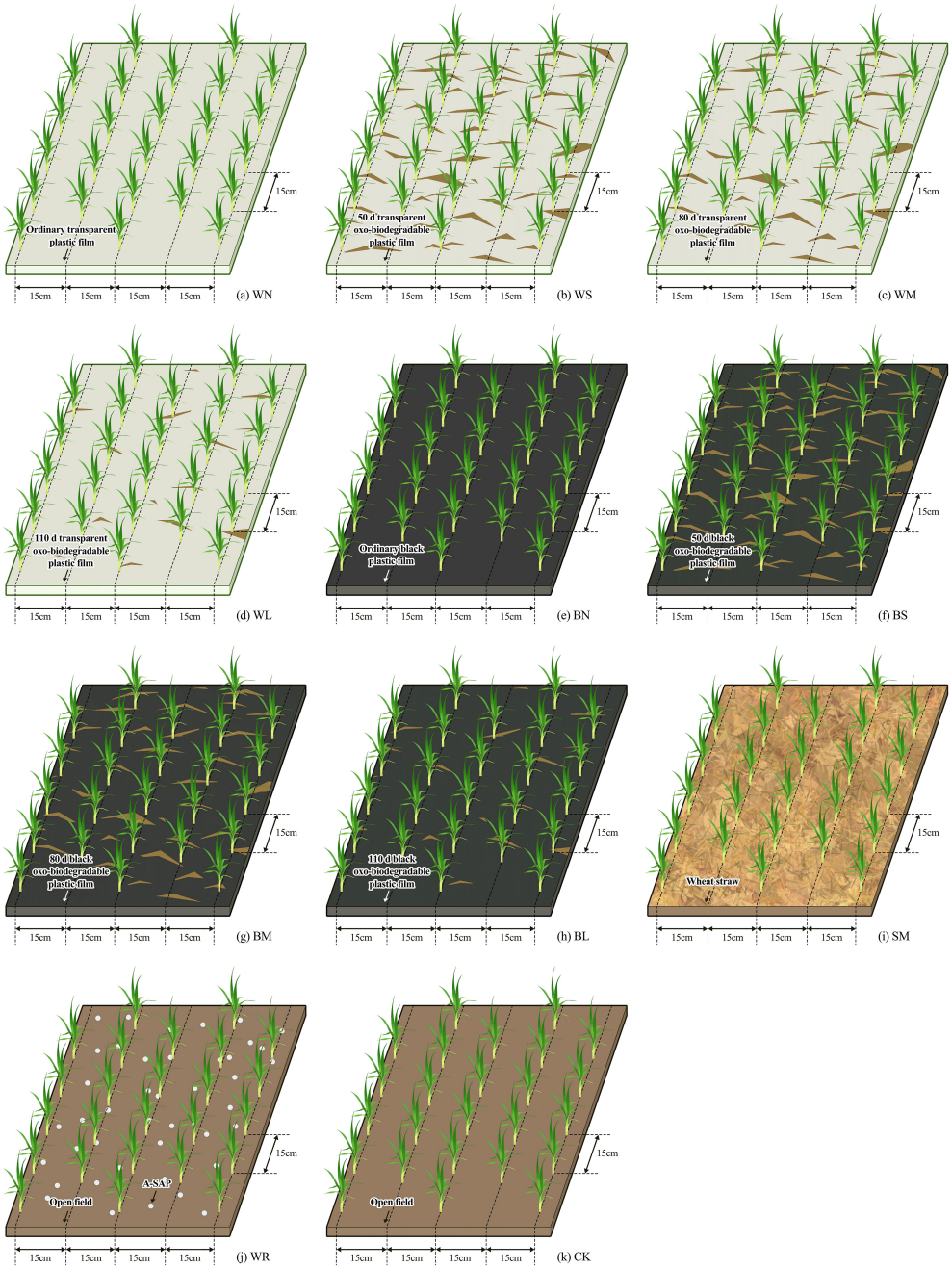

FIGURE 4
Schematic diagram of the planting mode. WN, ordinary transparent plastic film mulching; WS, 50-day transparent oxo-biodegradable plastic film mulching; WM, 80-day transparent oxo-biodegradable plastic film mulching; WL, 110-day transparent oxo-biodegradable plastic film mulching; BN, ordinary black plastic film mulching; BS, 50-day black oxo-biodegradable plastic film mulching; BM, 80-day black oxo-biodegradable plastic film mulching; BL, 110-day black oxo-biodegradable plastic film mulching; SM, straw mulching; WR, applying A-SAP; CK, no mulching and no A-SAP. The open filed is the farmland has no mulch and no A-SAP and remained in its original state.

2.3.7 Water productivity and irrigation water productivity

Water productivity is calculated as $WP = Y \cdot ET^{-1} \cdot 10^{-1}$, where WP is water productivity (kg m^{-3}), Y is garlic yield (kg hm^{-2}), ET is the garlic water consumption during the whole growth stage, and ET (mm) = P + I + B − A, where P is the rainfall during the growth stage, I is the irrigation amount during the growth stage, and B and A are the 0- to 100-cm soil water storage before planting and after harvesting, respectively.

Irrigation water productivity is calculated as $IP = Y \cdot I^{-1} \cdot 10^{-1}$, where IP is irrigation water productivity (kg m^{-3}), Y is garlic yield (kg hm^{-2}), and I is the irrigation amount during the growth stage (mm).

2.3.8 Nitrogen, phosphorus, and potassium fertilizer partial factor productivity

Nitrogen fertilizer partial factor productivity (NP, kg kg^{-1}) = garlic yield/nitrogen application amount.

Phosphorus fertilizer partial factor productivity (PP, kg kg^{-1}) = garlic yield/phosphorus application amount.

Potassium fertilizer partial factor productivity (KP, kg kg^{-1}) = garlic yield/potassium application amount.

2.4 Data statistics and analysis

Microsoft Excel 2019 (Microsoft Corp., Raymond, Washington, DC, USA) software was used to for initial data checking and calculations. SPSS Statistics 24.0 (IBM, Inc., New York, NY, USA) was used to analyze the variability in data for each treatment, and Origin Pro 8.0 (Origin Lab, Corp., Hampton, MA, USA) software was used for plotting. Yaaph v12.5.7528.33196 (Meta Decision Software Technology Co., Ltd., Corp., Shanxi, China) software was used to draw the comprehensive analytical hierarchical model of the weight analysis of each index; Matlab (Version R2023b, MathWorks, Corp., Natick, MA, USA) was used to calculate the weights of soil moisture conservation measures based on game theory and the comprehensive score of TOPSIS.

3 Results and analysis

3.1 Effects of different moisture-maintaining measures on the soil environment

3.1.1 Effects of different moisture-maintaining measures on the soil water storage during garlic growth stage

Soil water storage is not only closely related to irrigation amount and precipitation but also affected by the water consumption of garlic growth and continuation. The experimental years showed the same trend of change, both increasing with irrigation or precipitation replenishment and showing a decreasing trend with garlic growth and continuation (Figure 6). In a comprehensive analysis of 2-year experiment result, all soil moisture-maintaining measures showed inhibiting evaporation effects, effectively increasing soil water storage by 0.77% to 48.59% compared with that of CK. However, the soil moisture-maintaining effects of each measure varied at different growth stages of garlic. There was no significant difference between soil water storage in plastic film mulching at seedling stage and scaly bud and flower bud differentiation stage, which increased significantly by 14.92% to 31.57% and 12.98% to 46.86%, respectively, compared with that of CK. During the bulb swelling stage, which was in the high temperature with intense evaporation, the WS and BS had already entered the dehiscence period, resulting in a significant reduction of 21.13% and 18.63% in soil water storage compared with that of WN but still a significant increase of 16.69% and 14.15% compared with that of CK. At this time, SM showed better moisture-maintaining effect than WR, with a significant increase of 17.03% in soil water storage compared with that of CK. At mature stage, the WS and BS had entered the macrofracture period; the WM and BM entered the

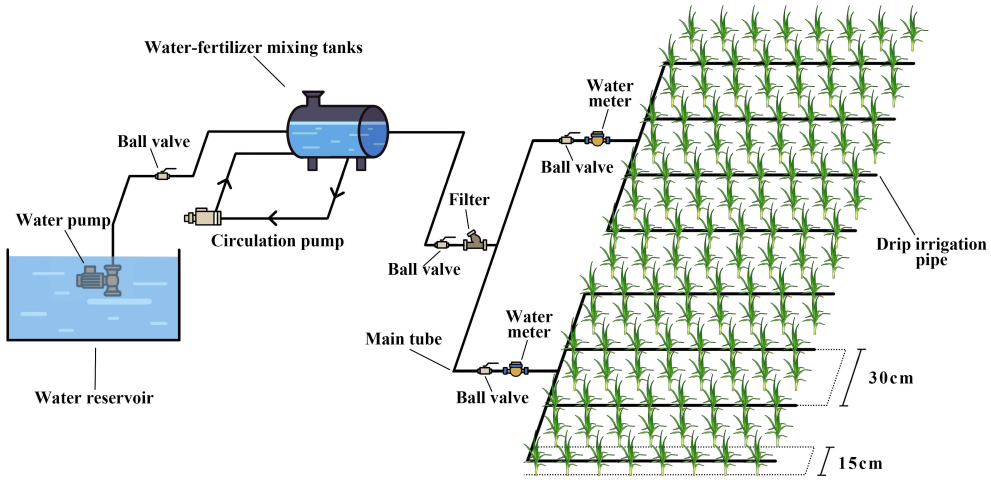

FIGURE 5
The head unit fitting drawing in the experiment.

dehiscence period; and the soil water storage was significantly reduced by 28.09%, 25.02%, 20.69%, and 20.44% compared with that of WN, whereas the WM and BM were still significantly higher by 17.85% and 14.85% compared with that of the CK. During this stage, the WN and BN had the best moisture-maintaining effect and the highest soil water storage, followed by the WL and BL, whereas the SM and WR did not show a significant moisture increase effect. It can be seen that the use of moisture-maintaining measures was all effective in maintaining moisture, with plastic film mulching being the most effective in maintaining moisture, followed by SM, and the WR increases the least. In the oxo-biodegradable plastic film–mulching treatments, the moisture-maintaining effect was gradually weakened as the oxo-biodegradable plastic film entered the induction period, dehiscence and macrofracture period.

3.1.2 Effects of different moisture-maintaining measures on the soil temperature during garlic growth stage

The effects of moisture-maintaining measures on soil temperature showed the same trend in the two experimental years, both increasing with the increase of atmospheric temperature and continuous decreasing with the increase of pyrolysis degree under the condition of oxo-biodegradable plastic film mulching (Figure 7). During the garlic sowing and seedling stages, all the mulching measures significantly increased the average soil temperature in the 0- to 25-cm soil layer compared with CK, with increases of 14.70% to 69.44% and 10.28% to 44.15%, respectively. In addition, there was no significant difference among all the plastic film–mulching treatments during the sowing stage, but it was significantly higher than that of the SM. During the scaly bud and flower bud differentiation stage, the heat-maintaining effect of plastic film–mulching treatments was significant, which was significantly increased by 18.07% to 33.11% compared with that of CK. During the garlic bolt elongation stage, WS and BS entered the mid-induction period, which was significantly decreased compared with other plastic film–mulching treatments. During the bulb swelling stage, WM and BM entered the initial-induction period, which were still significantly increased by 14.77% to 22.42% and 13.52% to 19.52% compared with that of CK. However, the WS and BS had entered the dehiscence period, which was significantly lower than that of other plastic film–mulching treatments. During the mature stage, WS and BS had entered the macrofracture period, WM and BM entered the dehiscence period, showing no warming effect, whereas WL and BL were at the early stage of induction, which was significantly higher than that of CK, by 29.09% to 29.80% and 19.73% to 23.45%. SM did not show warming effect from scaly bud and flower bud differentiation stage to mature stage, whereas WR and CK had no significant difference in soil temperature during the whole growth stage. It can be seen that the plastic film has the best warming effect, WN is better than BN, followed by SM, whereas WR had no significant effect on soil temperature.

3.1.3 Effects of different moisture-maintaining measures on the soil nutrients during garlic growth stage

Soil nutrient content varied as a function of moisture-maintaining measures, with similar trends in the effects of moisture-maintaining measures on soil nutrient content in the two experimental years (Table 2). Compared with CK, in 0- to 20-cm soil layer, organic matter, total nitrogen, total phosphorus, total potassium, nitrate nitrogen, ammonium nitrogen, available phosphorus, and slow-release potassium contents were significantly increased by using soil moisture-maintaining measures, by up to 10.83% to 59.17%, 11.26% to 80.13% and 22.56% to 77.44%, 18.18% to 33.81%, 22.99% to 72.12%, 58.05% to 192.92% and 50.63% to 233.44%, and 12.21% to 28.14%, respectively. In the 20- to 40-cm soil layer, organic matter, total nitrogen, total phosphorus, total potassium, nitrate nitrogen, and slow-release potassium contents were increased by using soil moisture-maintaining measures, by up to 10.66% to 34.43%, 6.08% to 30.41%, 7.86% to 45.71%, 22.09% to 55.21%, 19.75% to 105.49%, and 16.01% to 22.71%, respectively. Between the same colored biodegradable plastic films, organic matter, total phosphorus, nitrate nitrogen, and slow-release potassium accumulation gradually increased, whereas total

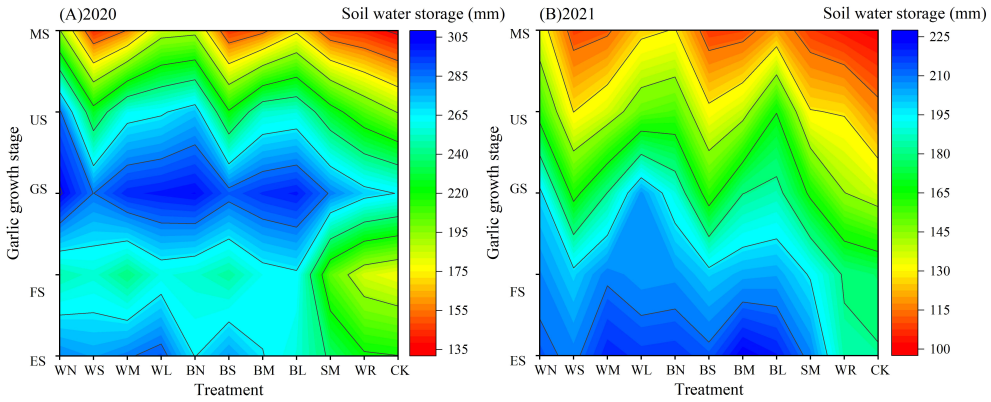

FIGURE 6
Dynamic changes of soil water storage in different growth stages of garlic under different soil moisture-maintaining measures.

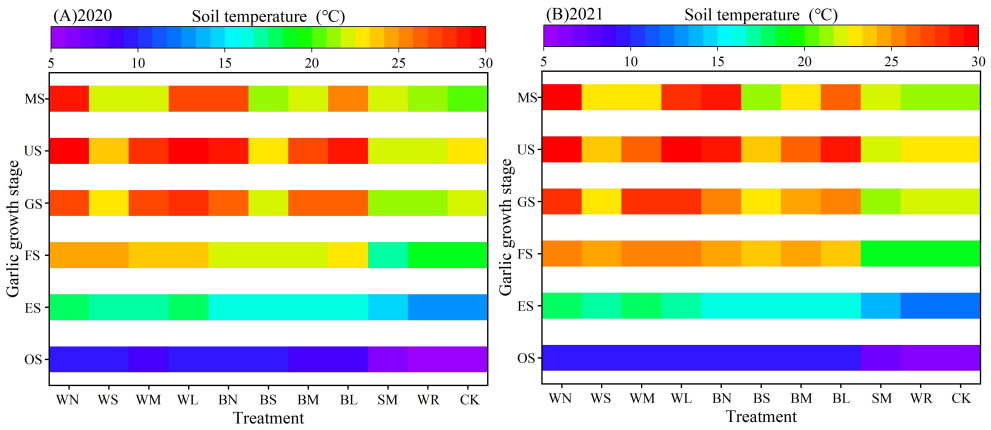

FIGURE 7
Dynamic changes of soil temperature in different growth stages of garlic under different soil moisture-maintaining measures.

nitrogen and ammonium nitrogen accumulation gradually decreased with the prolongation of the induction period.

3.1.4 Effects of different moisture-maintaining measures on the soil microbe during garlic growth stage

The effects of different moisture-maintaining measures, experimental year, and soil depth on the quantity of soil fungi, bacterium, actinobacteria, and microbial biomass carbon and nitrogen varied (Figure 8, Table 3), and, under soil moisture-maintaining measures, microbial quantity and microbial biomass carbon and nitrogen were significantly higher than that of CK. By comparing the average values of the two experimental years, it was found that all treatments could significantly increase the fungi and bacteria quantity in the 0- to 20-cm soil layer compared with that of CK, with increases of up to 159.90% to 577.63% and 233.65% to 667.88%, respectively. WN and SM inhibited soil actinobacteria reproduction, and all other moisture-maintaining measures promoted soil actinobacteria reproduction with a significant increase in quantity. Meanwhile, each treatment increased soil microbial biomass carbon and soil microbial biomass nitrogen by 15.38% to 212.80% and 0.77% to 189.00%, respectively, compared with that of CK, with the SM showing the largest increase in soil microbial biomass carbon and nitrogen. Each treatment also significantly increased the quantity of fungi, bacterium, and actinobacteria in the 20- to 40-cm soil layer compared with that of CK, with increases of up to 354.18% to 761.93%, 85.91% to 337.02%, and 81.71% to 291.12%, respectively, and the fungi quantity in BS increased by the largest. BL had the largest increase in bacterium quantity, and WL had the largest increase in actinobacteria quantity. All treatments could increase soil microbial biomass carbon and microbial biomass nitrogen, ranging from 38.12% to 205.76% and 6.89% to 64.81%, respectively, in which the increase of microbial biomass carbon was the largest in the SM, the increase of microbial biomass nitrogen was the largest in the WR.

3.1.5 Effects of different moisture-maintaining measures on the soil enzyme activity during garlic growth stage

The effects of different moisture-maintaining measures, experimental year, and soil depth on the soil enzyme activities of urease, sucrase, catalase, alkaline phosphatase, and cellulase varied (Figure 9, Table 4). By comparing the average values of the two experimental years, it was found that all treatments could increase the activities of urease, sucrase, and alkaline phosphatase in the 0- to 20-cm soil layer by 5.49% to 147.07%, 6.17% to 146.91%, and 21.66% to 131.24%, respectively, compared with that of CK, among which the SM had the largest increase. There was no significant difference in soil catalase activity between BS treatment and CK treatment, and all other moisture-maintaining measures significantly increased by 19.06% to 94.21% compared with that of CK. Soil cellulase activity under SM was significantly reduced by 22.99% compared with that of CK, and other soil moisture-maintaining measures were increased by 2.01% to 48.12%, among which WN had the largest increase. Similarly, each treatment could increase the activities of soil urease, sucrase, and catalase in 20- to 40-cm soil layer, which increased by 18.24% to 368.55%, 9.96% to 104.98%, and 15.80% to 155.39%, respectively. There was no significant difference in alkaline phosphatase activity between BS treatment and CK treatment, and all other moisture-maintaining measures were significantly increased by 11.36% to 142.05%, among which SM had the largest increase. The soil cellulase activity under SM was significantly reduced by 27.80% compared with that of CK, and other soil moisture-maintaining measures were increased by 2.97% to 69.23% compared with that of CK, among which WN had the largest increase.

TABLE 2 Effect of different moisture-maintaining measures on soil nutrients in the 0-40 cm soil layer of purple garlic farmland.

Year	Soil depth (cm)	Treatment	Organic matter (g kg^{-1})	Total nitrogen (g kg^{-1})	Total phosphorus (g kg^{-1})	Total potassium (g kg^{-1})	Nitrate Nitrogen (mg kg^{-1})	Ammonium nitrogen (mg kg^{-1})	Available Phosphorus (mg kg^{-1})	Slowly available potassium (mg kg^{-1})
2020	0–20	WN	17.9 ± 0.30bc	0.86 ± 0.03c	1.05 ± 0.02c	21.5 ± 0.29e	27.76 ± 0.77b	4.80 ± 0.17g	40.4 ± 0.89b	700 ± 11.81a
		WS	14.7 ± 0.48f	0.81 ± 0.02cd	0.91 ± 0.02e	23.3 ± 0.42bc	22.13 ± 0.66d	7.45 ± 0.16d	37.8 ± 1.21b	676 ± 14.94a
		WM	15.6 ± 0.43ef	0.83 ± 0.02c	0.97 ± 0.02de	22.1 ± 0.36de	24.07 ± 0.67cd	5.93 ± 0.18e	39.0 ± 0.94b	683 ± 16.64a
		WL	17.1 ± 0.56cd	0.86 ± 0.01c	1.03 ± 0.03cd	21.9 ± 0.36e	26.44 ± 0.75bc	5.24 ± 0.15fg	39.5 ± 1.19b	689 ± 17.76a
		BN	19.5 ± 0.50a	0.97 ± 0.01b	1.15 ± 0.02a	22.9 ± 0.16cd	41.15 ± 1.09a	9.03 ± 0.35c	49.7 ± 1.46a	663 ± 18.99ab
		BS	16.4 ± 0.26de	1.06 ± 0.01a	1.01 ± 0.02cd	24.7 ± 0.10a	38.65 ± 1.16a	12.50 ± 0.24a	48.2 ± 0.93a	644 ± 22.62ab
		BM	18.0 ± 0.47bc	1.01 ± 0.02ab	1.08 ± 0.03bc	24.1 ± 0.35ab	38.93 ± 1.34a	10.78 ± 0.25b	48.5 ± 1.06a	651 ± 13.60ab
		BL	18.7 ± 0.66ab	0.98 ± 0.03b	1.13 ± 0.04ab	23.5 ± 0.47bc	40.28 ± 1.20a	9.66 ± 0.31c	49.3 ± 0.73a	660 ± 19.63ab
		SM	12.4 ± 0.27g	0.82 ± 0.03c	0.77 ± 0.01f	22.3 ± 0.25de	21.65 ± 0.19d	7.70 ± 0.21d	31.8 ± 1.09c	689 ± 21.76a
		WR	12.1 ± 0.39g	0.80 ± 0.02cd	0.68 ± 0.02g	21.5 ± 0.18e	14.70 ± 0.49e	5.65 ± 0.19ef	12.9 ± 0.29d	607 ± 26.79bc
		CK	11.8 ± 0.29g	0.76 ± 0.01d	0.63 ± 0.02g	19.8 ± 0.32f	11.39 ± 0.29f	3.27 ± 0.10h	10.6 ± 0.19d	552 ± 27.06c
	20–40	WN	16.7 ± 0.58a	0.73 ± 0.02de	0.91 ± 0.02cd	19.5 ± 0.43d	40.55 ± 1.38a	4.45 ± 0.14g	24.9 ± 0.61de	710 ± 13.18b
		WS	15.3 ± 0.17ab	0.58 ± 0.02f	0.86 ± 0.02de	21.9 ± 0.38ab	25.46 ± 0.80e	7.35 ± 0.21d	23.3 ± 0.46e	713 ± 21.21b
		WM	15.5 ± 0.51ab	0.62 ± 0.02f	0.88 ± 0.03de	21.3 ± 0.50bc	29.10 ± 0.75cd	6.16 ± 0.23ef	23.6 ± 0.36e	721 ± 19.17ab
		WL	16.1 ± 0.38ab	0.69 ± 0.02e	0.95 ± 0.03c	20.2 ± 0.53cd	37.42 ± 1.24b	5.73 ± 0.21f	24.1 ± 0.24e	730 ± 21.93ab
		BN	15.4 ± 0.41ab	0.78 ± 0.02cd	0.85 ± 0.2de	23.2 ± 0.62a	40.88 ± 1.04a	6.18 ± 0.23ef	27.0 ± 0.96	697 ± 11.44b
		BS	13.8 ± 0.45cd	0.91 ± 0.03a	0.71 ± 0.02f	22.7 ± 0.31ab	37.13 ± 0.79b	8.55 ± 0.27c	26.6 ± 0.39d	735 ± 13.71ab
		BM	14.9 ± 0.43bc	0.88 ± 0.01ab	0.74 ± 0.01f	22.9 ± 0.66ab	38.40 ± 0.34ab	7.16 ± 0.15d	25.4 ± 0.45de	748 ± 14.26ab
		BL	15.0 ± 0.36bc	0.81 ± 0.02c	0.82 ± 0.02e	23.4 ± 0.68a	40.25 ± 1.16a	6.64 ± 0.21de	25.1 ± 0.42de	749 ± 16.24ab
		SM	15.3 ± 0.45ab	0.94 ± 0.02a	1.12 ± 0.02b	22.5 ± 0.66ab	30.80 ± 0.74c	11.50 ± 0.39a	40.8 ± 0.90b	705 ± 17.34b
		WR	16.2 ± 0.48ab	0.94 ± 0.03a	1.20 ± 0.01a	22.5 ± 0.65ab	26.50 ± 0.66de	9.90 ± 0.29b	70.2 ± 1.37a	777 ± 24.80a
		CK	13.5 ± 0.35d	0.82 ± 0.02bc	0.89 ± 0.03cd	19.3 ± 0.46d	20.37 ± 0.68f	6.11 ± 0.22ef	36.5 ± 1.23c	614 ± 15.04c
2021	0–20	WN	18.9 ± 0.32a	1.41 ± 0.03bc	1.23 ± 0.05a	20.1 ± 0.56c	91.33 ± 2.37b	4.13 ± 0.11bcd	56.8 ± 2.13a	780 ± 16.11a
		WS	15.3 ± 0.40cd	1.08 ± 0.04e	1.12 ± 0.02bc	22.8 ± 0.51a	77.75 ± 1.26d	4.60 ± 0.14a	47.1 ± 1.23c	747 ± 20.84ab
		WM	16.5 ± 0.54bc	1.13 ± 0.04de	1.19 ± 0.03ab	22.1 ± 0.36ab	84.91 ± 3.06c	4.39 ± 0.05ab	52.0 ± 1.80b	759 ± 22.76a
		WL	18.2 ± 0.53a	1.37 ± 0.02c	1.25 ± 0.03a	20.9 ± 0.63bc	89.26 ± 2.02bc	4.27 ± 0.06bc	54.3 ± 2.08ab	776 ± 21.65a
		BN	18.7 ± 0.33a	1.31 ± 0.02c	1.21 ± 0.04a	20.2 ± 0.64c	49.16 ± 0.32g	3.74 ± 0.09e	57.0 ± 0.61a	675 ± 19.30c

(Continued)

10.3389/fpls.2024.1447469

TABLE 2 Continued

Year	Soil depth (cm)	Treatment	Organic matter (g kg^{-1})	Total nitrogen (g kg^{-1})	Total phosphorus (g kg^{-1})	Total potassium (g kg^{-1})	Nitrate Nitrogen (mg kg^{-1})	Ammonium nitrogen (mg kg^{-1})	Available Phosphorus (mg kg^{-1})	Slowly available potassium (mg kg^{-1})
		BS	15.3 ± 0.26cd	1.66 ± 0.06a	1.08 ± 0.02bc	22.4 ± 0.64ab	46.45 ± 0.75g	4.05 ± 0.10cd	52.7 ± 1.54ab	654 ± 17.34cd
		BM	16.9 ± 0.10b	1.51 ± 0.02b	1.11 ± 0.03bc	21.0 ± 0.57bc	47.82 ± 1.61g	3.94 ± 0.07de	53.3 ± 1.23ab	661 ± 19.80cd
		BL	19.1 ± 0.41a	1.20 ± 0.04d	1.19 ± 0.03ab	20.7 ± 0.35bc	48.03 ± 1.64g	3.91 ± 0.14de	55.8 ± 1.10ab	670 ± 23.12c
		SM	15.3 ± 0.55cd	0.86 ± 0.02f	0.99 ± 0.03c	23.5 ± 0.34a	64.10 ± 0.85e	4.15 ± 0.07bcd	43.2 ± 0.82c	654 ± 19.43cd
		WR	14.5 ± 0.23d	0.89 ± 0.03f	0.95 ± 0.01c	20.7 ± 0.76bc	101.95 ± 1.45a	4.05 ± 0.11cd	35.3 ± 0.91d	689 ± 16.20bc
		CK	12.2 ± 0.40e	0.75 ± 0.02g	0.70 ± 0.02d	15.4 ± 0.38d	57.80 ± 1.05f	2.38 ± 0.08f	21.4 ± 0.70e	603 ± 20.16d
	20–40	WN	16.1 ± 0.36ab	1.20 ± 0.02a	1.06 ± 0.03ab	20.3 ± 0.25e	60.57 ± 1.36ab	3.25 ± 0.04c	25.6 ± 0.49a	752 ± 25.27a
		WS	13.7 ± 0.41de	1.03 ± 0.03b	0.87 ± 0.02e	22.0 ± 0.16c	45.10 ± 1.27d	3.80 ± 0.10b	23.1 ± 0.67b	740 ± 14.67a
		WM	15.1 ± 0.36bc	1.04 ± 0.02b	0.95 ± 0.03cd	20.7 ± 0.39de	56.73 ± 1.91b	3.29 ± 0.04c	24.8 ± 0.67a	747 ± 23.30a
		WL	15.9 ± 0.45ab	1.18 ± 0.03a	1.09 ± 0.02a	19.6 ± 0.41e	58.29 ± 1.54b	3.13 ± 0.06cd	25.0 ± 0.55a	758 ± 23.31a
		BN	15.6 ± 0.44ab	0.79 ± 0.02de	1.00 ± 0.03bc	27.4 ± 0.57a	62.85 ± 1.26a	2.96 ± 0.07d	25.4 ± 0.72a	737 ± 14.60a
		BS	13.2 ± 0.22ef	0.83 ± 0.02d	0.80 ± 0.02f	22.5 ± 0.22c	51.10 ± 1.03c	3.60 ± 0.04b	26.3 ± 0.57a	724 ± 26.51a
		BM	15.1 ± 0.16bc	0.77 ± 0.01de	0.85 ± 0.01ef	25.3 ± 0.19b	58.43 ± 1.54b	3.08 ± 0.09cd	25.7 ± 0.47a	730 ± 27.21a
		BL	16.4 ± 0.34a	0.76 ± 0.02e	0.94 ± 0.02d	26.8 ± 0.48a	60.76 ± 0.73ab	2.74 ± 0.03e	25.0 ± 0.44a	733 ± 17.22a
		SM	14.3 ± 0.17cd	0.83 ± 0.02d	0.86 ± 0.01ef	21.5 ± 0.55cd	59.65 ± 0.99ab	4.10 ± 0.12a	21.2 ± 0.52cd	715 ± 24.63a
		WR	12.6 ± 0.33f	0.89 ± 0.02c	0.84 ± 0.03ef	19.5 ± 0.53e	33.95 ± 0.49e	3.80 ± 0.05b	22.6 ± 0.12bc	725 ± 11.59a
		CK	10.9 ± 0.21g	0.66 ± 0.01f	0.51 ± 0.01g	13.3 ± 0.18f	30.11 ± 0.90f	2.05 ± 0.06f	19.7 ± 0.17d	610 ± 19.95b
2 years average	0–20	WN	18.4 ± 0.27ab	1.14 ± 0.02c	1.14 ± 0.03abc	20.8 ± 0.36e	59.55 ± 1.54a	4.47 ± 0.12g	48.6 ± 1.41bc	740 ± 13.82a
		WS	15.0 ± 0.31c	0.95 ± 0.02d	1.02 ± 0.02e	23.1 ± 0.46ab	49.94 ± 0.96c	6.03 ± 0.15de	42.5 ± 1.20d	712 ± 17.25abc
		WM	16.1 ± 0.48c	0.98 ± 0.03d	1.08 ± 0.02cde	22.1 ± 0.34bcd	54.49 ± 1.61b	5.16 ± 0.11f	45.5 ± 1.35cd	721 ± 19.08ab
		WL	17.7 ± 0.54b	1.12 ± 0.01c	1.14 ± 0.03abc	21.4 ± 0.45cde	57.85 ± 1.36a	4.76 ± 0.11fg	46.9 ± 1.41c	733 ± 19.15a
		BN	19.1 ± 0.41a	1.14 ± 0.01c	1.18 ± 0.03a	21.6 ± 0.40cde	45.16 ± 0.62d	6.39 ± 0.22cd	53.4 ± 0.98a	669 ± 19.15bcd
		BS	15.9 ± 0.26c	1.36 ± 0.04a	1.05 ± 0.02de	23.6 ± 0.31a	42.55 ± 0.60d	8.28 ± 0.16a	50.5 ± 1.22ab	649 ± 18.10d
		BM	17.5 ± 0.30b	1.26 ± 0.02b	1.10 ± 0.02bcd	22.6 ± 0.46abc	43.38 ± 1.20d	7.32 ± 0.16b	50.9 ± 1.03ab	656 ± 13.52cd
		BL	18.9 ± 0.50a	1.09 ± 0.03c	1.16 ± 0.03ab	22.1 ± 0.39bcd	44.16 ± 1.13d	6.79 ± 0.20c	52.6 ± 0.85a	665 ± 21.36bcd
		SM	13.9 ± 0.26d	0.84 ± 0.02e	0.88 ± 0.02f	22.9 ± 0.24ab	42.88 ± 0.52d	5.93 ± 0.13e	37.5 ± 0.93e	672 ± 20.26bcd
		WR	13.3 ± 0.31d	0.85 ± 0.02e	0.82 ± 0.01f	21.1 ± 0.43de	58.30 ± 0.95a	4.85 ± 0.15fg	24.1 ± 0.59f	648 ± 13.88d

(Continued)

10.3389/fpls.2024.1447469

TABLE 2 Continued

Year	Soil depth (cm)	Treatment	Organic matter (g kg^{-1})	Total nitrogen (g kg^{-1})	Total phosphorus (g kg^{-1})	Total potassium (g kg^{-1})	Nitrate Nitrogen (mg kg^{-1})	Ammonium nitrogen (mg kg^{-1})	Available Phosphorus (mg kg^{-1})	Slowly available potassium (mg kg^{-1})
		CK	12.0 ± 0.35e	0.76 ± 0.01f	0.67 ± 0.01g	17.6 ± 0.35f	34.60 ± 0.56e	2.83 ± 0.10h	16.0 ± 0.42g	578 ± 23.54e
	20–40	WN	16.4 ± 0.46a	0.97 ± 0.01a	0.99 ± 0.02a	19.9 ± 0.34d	50.56 ± 1.37ab	3.85 ± 0.09h	25.3 ± 0.55def	731 ± 18.29a
		WS	14.5 ± 0.29de	0.81 ± 0.03ef	0.87 ± 0.02b	22.0 ± 0.26bc	35.28 ± 0.66e	5.58 ± 0.16d	23.2 ± 0.50g	727 ± 16.87a
		WM	15.3 ± 0.43abc	0.83 ± 0.02def	0.92 ± 0.03b	21.0 ± 0.44cd	42.92 ± 1.27d	4.73 ± 0.13ef	24.2 ± 0.47fg	734 ± 19.26a
		WL	16.0 ± 0.41ab	0.94 ± 0.02ab	1.02 ± 0.02a	19.9 ± 0.46d	47.86 ± 1.38bc	4.43 ± 0.13fg	24.6 ± 0.40efg	744 ± 21.91a
		BN	15.5 ± 0.38abc	0.79 ± 0.02fg	0.93 ± 0.02b	25.3 ± 0.59a	51.87 ± 1.14a	4.57 ± 0.14f	26.2 ± 0.66de	717 ± 13.01a
		BS	13.5 ± 0.28e	0.87 ± 0.02cde	0.76 ± 0.02cd	22.6 ± 0.23b	44.12 ± 0.90d	6.08 ± 0.14c	26.5 ± 0.38d	730 ± 17.77a
		BM	15.0 ± 0.27bcd	0.83 ± 0.01ef	0.80 ± 0.01c	24.1 ± 0.42a	48.42 ± 0.92b	5.12 ± 0.12e	25.6 ± 0.45def	739 ± 18.58a
		BL	15.7 ± 0.34abc	0.79 ± 0.02fg	0.88 ± 0.02b	25.1 ± 0.57a	50.51 ± 0.82ab	4.69 ± 0.12ef	25.1 ± 0.39def	741 ± 16.46a
		SM	14.8 ± 0.29cd	0.89 ± 0.02bcd	0.99 ± 0.02a	22.0 ± 0.40bc	45.23 ± 0.51cd	7.80 ± 0.26a	31.0 ± 0.70b	710 ± 20.30a
		WR	14.4 ± 0.40de	0.92 ± 0.03abc	1.02 ± 0.02a	21.0 ± 0.58cd	30.23 ± 0.49f	6.85 ± 0.17b	46.4 ± 0.67a	751 ± 18.19a
		CK	12.2 ± 0.24f	0.74 ± 0.01g	0.70 ± 0.02d	16.3 ± 0.26e	25.24 ± 0.78g	4.08 ± 0.13gh	28.1 ± 0.70c	612 ± 12.06b
ANOVA										
Year (Y)			ns	***	***	***	***	***	***	***
Treatment (T)			***	***	***	***	***	***	***	***
Soil depth (S)			***	***	***	ns	***	***	***	***
Y × T			**	***	***	***	***	***	***	ns
Y × S			***	***	***	***	***	***	***	**
T × S			***	***	***	***	***	***	***	**
Y × T × S			***	***	***	***	***	***	***	ns

Different lowercase letters in the same column indicate significant differences among different treatments ($P < 0.05$). The ** and *** indicate significant differences among different treatments at the levels of $P < 0.01$ and $P < 0.001$, respectively. The ns means not significant at the level of $P \geq 0.05$.

10.3389/fpls.2024.1447469

10.3389/fpls.2024.1447469

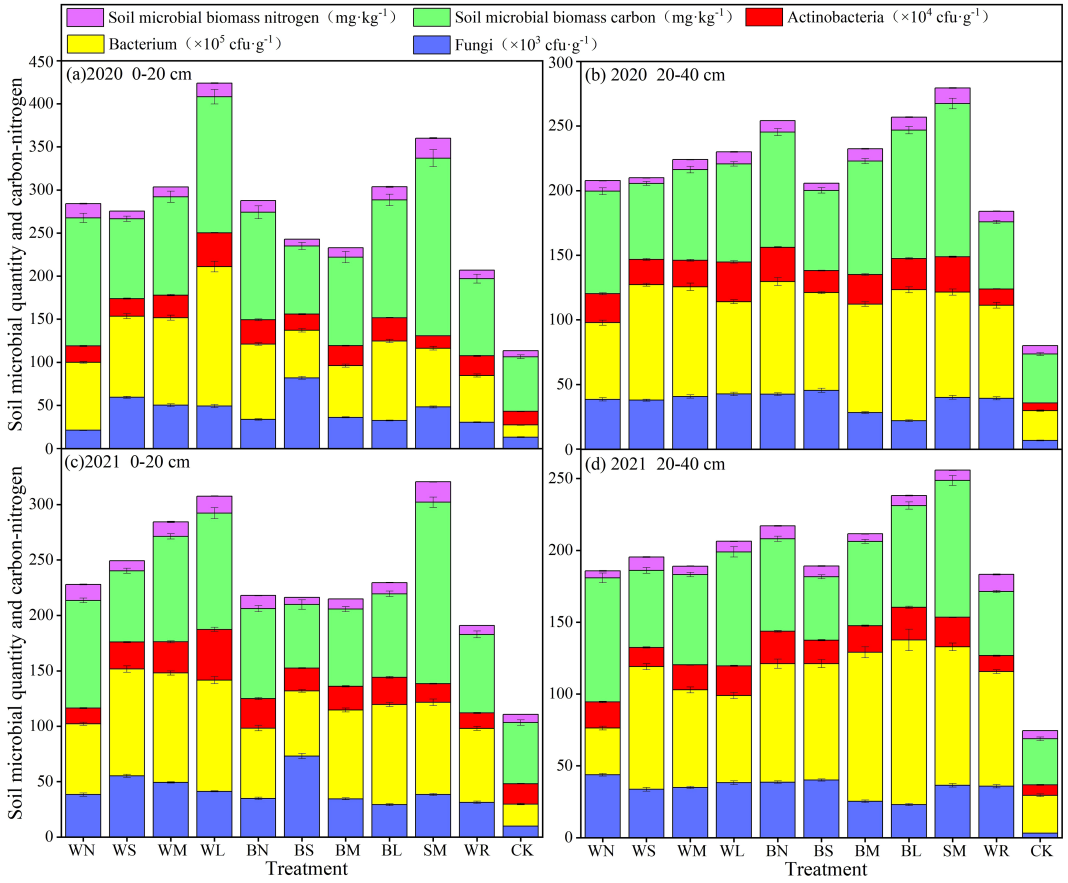

FIGURE 8
Effect of different moisture-maintaining measures on soil microbial in the 0-40 cm soil layer of purple garlic. Bars indicate standard deviations.

3.2 Effects of different moisture-maintaining measures on the soil quality

3.2.1 Soil quality comprehensive evaluation hierarchical model

A hierarchical model for the comprehensive evaluation of soil quality was established using Yaaph software. The target layer of soil quality (C) was divided into four guideline layers: soil hydrothermal (C_1), soil nutrients (C_2), soil microbial (C_3), and soil enzyme activity (C_4); soil hydrothermal index included two index layers: water storage (C_{11}) and temperature (C_{12}); soil nutrient index included eight index layers: organic matter (C_{21}), total nitrogen (C_{22}), total phosphorus (C_{23}), total potassium (C_{24}), nitrate nitrogen (C_{25}), ammonium nitrogen (C_{26}), available

TABLE 3 ANOVA results of different moisture-maintaining measures, experimental year, and soil depth on soil microorganism.

Factors	Fungi	Bacterium	Actinomyceteria	Soil microbial biomass carbon	Soil microbial biomass nitrogen
Year (Y)	***	*	***	***	***
Treatment (T)	***	***	***	***	***
Soil depth (S)	***	ns	***	***	***
Y × T	***	***	***	***	***
Y × S	ns	**	***	***	***
T × S	***	***	***	***	***
Y × T × S	***	***	***	***	***

Different lowercase letters in the same column indicate significant differences among different treatments ($P < 0.05$). The *, **, and *** indicate significant differences among different treatments at the levels of $P < 0.05$, $P < 0.01$, and $P < 0.001$, respectively. The ns means not significant at the level of $P \geq 0.05$.

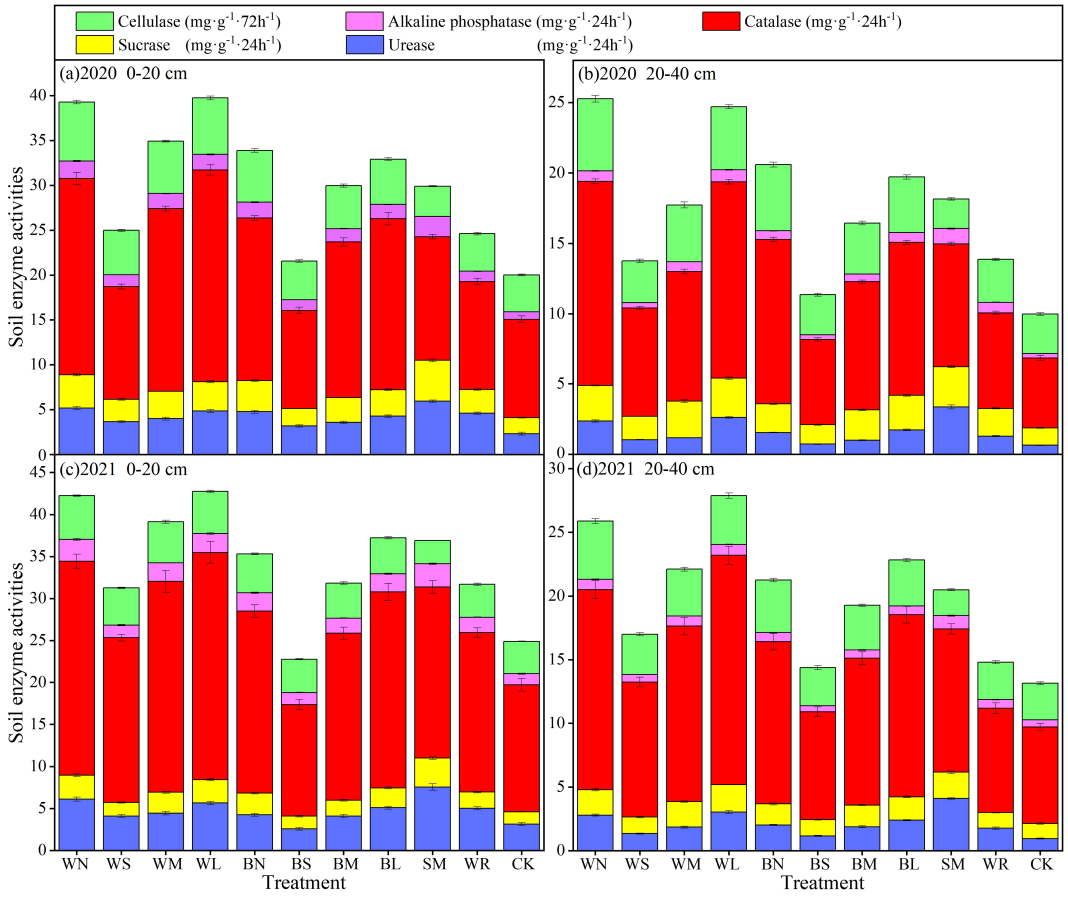

FIGURE 9
Effect of different moisture-maintaining measures on soil enzyme activities in 0-40 cm soil layer of purple garlic. Bars indicate standard deviations.

phosphorus (C_{27}), and slow-release potassium (C_{28}); soil microbial index include five index layers: fungi (C_{31}), bacterium (C_{32}), actinobacteria (C_{33}), microbial biomass carbon (C_{34}), and microbial biomass nitrogen (C_{35}); soil enzyme activity index include five index layers: sucrase (C_{41}), urease (C_{42}), catalase (C_{43}), alkaline phosphatase (C_{44}), and cellulase (C_{45}).

3.2.2 Index weighting

3.2.2.1 AHP method

On the basis of the analytic hierarchy process (AHP) method to determine the weight hierarchical model and then the proportion of the scale method of 1 to 10 to establish the judgment matrix, and the consistency of the matrix is tested. The judgment matrix of comprehensive soil hydrothermal, soil nutrient, soil microbial, soil enzyme activity is as follows:

$$C = \begin{bmatrix} 1.0000 & 2.0000 & 3.5000 & 2.5000 \\ 0.5000 & 1.0000 & 2.4000 & 3.8000 \\ 0.2857 & 0.4167 & 1.0000 & 0.5000 \\ 0.4000 & 0.2632 & 2.0000 & 1.0000 \end{bmatrix}$$

$$C_1 = \begin{bmatrix} 1.0000 & 1.2000 \\ 0.8333 & 1.0000 \end{bmatrix}$$

$$C_2 = \begin{bmatrix} 1.0000 & 2.0000 & 3.0000 & 3.50000 & 1.4000 & 4.5000 & 3.8000 & 4.1000 \\ 0.5000 & 1.0000 & 0.5000 & 2.8000 & 1.2000 & 3.0000 & 2.5000 & 2.7000 \\ 0.3333 & 2.0000 & 1.0000 & 4.0000 & 1.3000 & 4.0000 & 1.8000 & 2.1000 \\ 0.2857 & 0.3571 & 0.2500 & 1.0000 & 0.3333 & 2.0000 & 0.2500 & 0.2500 \\ 0.7143 & 0.8333 & 0.7692 & 3.0000 & 1.0000 & 2.5000 & 1.4000 & 1.5000 \\ 0.2222 & 0.3333 & 0.2500 & 0.5000 & 0.4000 & 1.0000 & 0.5000 & 0.3333 \\ 0.2632 & 0.4000 & 0.5556 & 4.0000 & 0.7143 & 2.0000 & 1.0000 & 0.5000 \\ 0.2439 & 0.3704 & 0.4762 & 4.0000 & 0.6667 & 3.0000 & 2.0000 & 1.0000 \end{bmatrix}$$

$$C_3 = \begin{bmatrix} 1.0000 & 0.3333 & 0.2500 & 0.5000 & 1.2000 \\ 3.0000 & 1.0000 & 0.2500 & 2.5000 & 2.2000 \\ 4.0000 & 4.0000 & 1.0000 & 3.0000 & 3.5000 \\ 2.0000 & 0.4000 & 0.3333 & 1.0000 & 1.5000 \\ 0.8333 & 0.4545 & 0.2857 & 0.6667 & 1.0000 \end{bmatrix}$$

TABLE 4 ANOVA results of different moisture-maintaining measures, experimental year, and soil depth on soil enzyme activities.

Factors	Urease	Sucrase	Catalase	Alkaline phosphatase	Cellulase
Year (Y)	***	***	***	***	***
Treatment (T)	***	***	***	***	***
Soil depth (S)	***	***	***	***	***
Y × T	***	***	**	ns	***
Y × S	ns	***	***	***	***
T × S	***	***	***	***	***
Y × T × S	***	*	**	***	ns

Different lowercase letters in the same column indicate significant differences among different treatments ($P < 0.05$). The *, **, and *** indicate significant differences among different treatments at the levels of $P < 0.05$, $P < 0.01$, and $P < 0.001$, respectively. The ns means not significant at the level of $P \geq 0.05$.

$$C_4 = \begin{bmatrix} 1.0000 & 1.5000 & 0.2500 & 0.5000 & 0.2500 \\ 0.6667 & 1.0000 & 0.2000 & 0.5000 & 0.2000 \\ 4.0000 & 5.0000 & 1.0000 & 2.5000 & 1.2000 \\ 2.0000 & 2.0000 & 0.4000 & 1.0000 & 0.2500 \\ 4.0000 & 5.0000 & 0.8333 & 4.0000 & 1.0000 \end{bmatrix}$$

The consistency test coefficients C_R of comprehensive soil hydrothermal, soil nutrient, soil microbial, and soil enzyme activity were all less than 0.10, indicating that the consistency test results are good and that the established judgment matrix is reliable and reasonable (Table 5, where λ_{max} is the maximum eigenvalue). The results showed that the weights of the soil quality indices, in descending order, were water storage, temperature, organic matter, total phosphorus, cellulase, catalase, actinobacteria, total nitrogen, nitrate nitrogen, slow-release potassium, available phosphorus, bacterium, alkaline phosphatase, total potassium, microbial biomass carbon, ammonium nitrogen, sucrase, microbial biomass nitrogen, urease, and fungi.

3.2.2.2 Entropy weight method

The entropy weight method was used to assign weights to a single index of soil quality, and the weights of soil quality index were calculated (Table 6). As can be seen from Table 6, the weights of the index determined by the entropy weight method are, in descending order, temperature, microbial biomass nitrogen, catalase, sucrase, urease, microbial biomass carbon, alkaline phosphatase, actinobacteria, water storage, ammonium nitrogen, cellulase, total nitrogen, organic matter, fungi, total potassium, nitrate nitrogen, bacterium, total phosphorus, slow-release potassium, and available phosphorus.

3.2.2.3 Game theory combinatorial empowerment

In order to improve the reliability and scientificity of the weight assignment values and to avoid the influence of subjective factors on the evaluation, a basic weight set was constructed on the basis of the two assignment values obtained by the AHP method and the entropy weight method $w = \sum_{k=1}^{l} \alpha_k \times w_k^T (\alpha_k > 0)$ where a_k is AHP method; w_k is entropy weight method.

On the basis of the weight set model of game theory, the game model is derived $Min \| \sum_{j=1}^{i} a_j \times u_j^T - u_i^T \| \ i = 1, 2$. The combination coefficients after normalization of the above equation can be obtained using Matlab: $a_1 = 0.9213$, $a2 = 0.0787$, This yields a vector of combined weights as $w^* = \sum_{k=1}^{2} a_k^* \times u_k^T$, the final results are presented in Table 7. As can be seen from the table, the weights of the indices, in descending order, are water storage, temperature, organic matter, catalase, cellulase, total phosphorus, actinobacteria, total nitrogen, nitrate nitrogen, slow-release potassium, available phosphorus, bacterium, alkaline phosphatase, microbial biomass carbon, sucrase, total potassium, ammonium nitrogen, microbial biomass nitrogen, and urease, fungi.

3.2.3 Comprehensive evaluation based on the TOPSIS method

On the basis of the combination assignment TOPSIS method for comprehensive evaluation, the decision matrix was normalized, the weighting matrix was established, and the ideal solution and fit C_i of the evaluation index were calculated, and the results were shown in Table 8. As can be seen from Table 8, soil quality in WL of soil moisture-maintaining measures had the largest degree of fit of the comprehensive indices (0.7798), which was optimal for comprehensive evaluation, followed by the BN and WN, whereas the WR had the lowest degree of fit, indicating that the comprehensive performance was the worst.

3.3 Effects of different moisture-maintaining measures on garlic quality

Soil moisture-maintaining measures could improve garlic bulb quality, but the increase rate was slightly different among different measures (Table 9). Compared with CK, each water maintaining measure could increase the content of bulb allicin, soluble sugar, soluble protein, vitamin C, and crude fiber by 1.96% to 17.82%, 4.24% to 46.27%, 12.10% to 44.21%, 6.92% to 60.75%, and 2.97% to 31.68%, respectively, among which WL significantly increased the content of allicin, soluble protein, and crude fiber; WN significantly increased the content of soluble sugar; BL significantly increased the content of vitamin C. Although the use of moistur-maintaining measures increased the ash content and amino acid content of garlic, the increases were small and did not show significant differences with CK. Overall, the quality of garlic under

10.3389/fpls.2024.1447469

TABLE 5 Results of AHP hierarchical analysis for calculating weights.

Hierarchy	Index	Local weight	Final weight	Consistency test parameter
Target layer	Soil hydrothermal	0.4303	0.4303	$C_R = 0.0669 < 0.1$ λmax = 4.1786
	Soil nutrient	0.3203	0.3203	
	Soil microbial	0.1036	0.1036	
	Soil enzyme activity	0.1458	0.1458	
Target layer 1	Soil water storage	0.5455	0.2347	$C_R = 0.0000 < 0.1$ λmax = 2.0000
	Soil temperature	0.4545	0.1956	
Target layer 2	Organic matter	0.2772	0.0888	$C_R = 0.0499 < 0.1$ λmax = 8.4930
	Total nitrogen	0.1493	0.0478	
	Total phosphorus	0.1701	0.0545	
	Total potassium	0.0462	0.0148	
	Nitrate nitrogen	0.1290	0.0413	
	Ammonium nitrogen	0.0407	0.0130	
	Available phosphorus	0.0850	0.0272	
	Slow-release potassium	0.1024	0.0328	
Target layer 3	Fungi	0.0878	0.0091	$C_R = 0.0445 < 0.1$ λmax = 5.1994
	Bacterium	0.2191	0.0227	
	Actinobacteria	0.4659	0.0483	
	Microbial biomass carbon	0.1333	0.0138	
	Microbial biomass nitrogen	0.0940	0.0097	
Target layer 4	Sucrase	0.0846	0.0123	$C_R = 0.0133 < 0.1$ λmax = 5.0596
	Urease	0.0655	0.0095	
	Catalase	0.3529	0.0515	
	Alkaline phosphatase	0.1312	0.0191	
	Cellulase	0.3658	0.0533	

transparent plastic film mulching was higher than that of black plastic film mulching, and, between oxo-biodegradable plastic film of the same color, the quality content of garlic increased with the prolongation of the induction period.

3.4 Effects of different moisture-maintaining measures on garlic yield

The use of moisture-maintaining measures to increase garlic yield also increased water–fertilizer productivity, and the increases varied between measures (Table 10). The WR had the lowest yield, which increased only 489.14 to 1,082.55 kg hm^{-2} compared with that of CK, and there was no significant difference; whereas the other treatments showed significant advantages in increasing yield, which could be 32.70% to 158.96%, with the highest yield of WN and WL, which could be 181,93.09 to 18,661.33 kg hm^{-2} and 18,064.73 to 18,796.05 kg hm^{-2}, respectively, which were significantly increased by 128.27% to 158.96% and 129.92% to 157.13%, respectively, compared with that of CK. The use of moisture-maintaining measures could increase the water productivity of garlic, in which the WN had the highest water productivity of 3.10 to 3.14 kg m^{-3}, followed by the WL and BN, which significantly increased by 145.31% to 164.96%, 141.41% to 157.26%, and 114.06% to 123.93% compared with that of CK, respectively. The water productivity of WR was the least, which was only 6.25% to 13.68% higher than that of CK, and there was no significant difference. Irrigation water productivity and nitrogen, potassium, and phosphate fertilizer partial factor productivity performance trends were consistent with yield change; WN and WL were the highest; WR was the lowest; and there was no significant difference from CK.

3.5 Principal component analysis

Interactions between factors affect the growth of purple garlic, which makes many index information interweave and overlap.

10.3389/fpls.2024.1447469

Principal component analysis (PCA) is a statistical analysis method that transforms multiple indices into fewer comprehensive indices to reveal the internal structure among multiple variables with less information loss (Hu et al., 2019). The application of PCA can be used to sift out a number of comprehensive indices that are not related to each other in a complex quality indices and growth indices and can reflect most of the information provided by the original full set of indices (Zhang et al., 2023a). In this study, a total of 13 data on yield, water productivity, and bulb quality indices of purple garlic were selected for PCA, and six principal components were finally generated. As can be seen from Table 11, the six principal components generated eigenvalues of 10.94, 1.33, 0.48, 0.15, 0.06, and 0.02, respectively, and their contribution rates to the total variance was 84.18%, 10.25%, 3.66%, 1.15%, 0.45%, and 0.17%, respectively. According to the principle that the cumulative contribution rate of the number of extracted principal components is ≥85%, the cumulative contribution rate of the six principal components has reached 99.86%, indicating that yield, water productivity, nitrogen fertilizer partial factor productivity, allicin, amino acids, and soluble sugar can measure all the information of these 13 indices, and, therefore, only these six indices were selected to establish the comprehensive evaluation equation.

3.6 Evaluation of various moisture-maintaining measures based on PCA

Because the 13 indices in this test had different scales, in order to eliminate the influence of scales and orders of magnitude on the evaluation results, it is necessary to standardize the original data to ensure the objectivity and scientificity of the PCA results. The standardized indices were represented by X_1~X_{14} respectively, and the comprehensive evaluation equation for each principal component is as follows:

$$Y_1 = 0.2893X_1 + 0.2893X_2 + 0.2893X_3 + 0.2524X_4 + 0.2835X_5 + 0.2778X_6 + 0.2246X_7 + 0.2621X_8 + 0.2984X_9 + 0.2615X_{10} + 0.2896X_{11} + 0.2893X_{12} + 0.2893X_{13}$$

$$Y_2 = -0.2443X_1 - 0.2495X_2 - 0.2443X_3 + 0.4306X_4 + 0.1707X_5 + 0.1672X_6 + 0.5407X_7 + 0.3145X_8 + 0.0788X_9 - 0.0260X_{10} - 0.2417X_{11} - 0.2435X_{12} - 0.2435X_{13}$$

$$Y_3 = -0.0826X_1 - 0.0290X_2 - 0.0826X_3 + 0.2812X_4 - 0.3145X_5 + 0.4363X_6 - 0.2015X_7 - 0.3971X_8 + 0.0319X_9 + 0.6305X_{10} - 0.0812X_{11} - 0.0841X_{12} - 0.0826X_{13}$$

$$Y_4 = 0.1110X_1 + 0.0568X_2 + 0.1110X_3 + 0.2995X_4 - 0.3770X_5 + 0.2427X_6 + 0.3202X_7 - 0.4389X_8 - 0.0594X_9 - 0.5861X_{10} + 0.1110X_{11} + 0.1110X_{12} + 0.1110X_{13}$$

TABLE 6 Weights of single index of soil quality determined by entropy weight method.

Indices	C_{11}	C_{12}	C_{21}	C_{22}	C_{23}	C_{24}	C_{25}	C_{26}	C_{27}	C_{28}	C_{31}	C_{32}	C_{33}	C_{34}	C_{35}	C_{41}	C_{42}	C_{43}	C_{44}	C_{45}
Weights	0.0503	0.0801	0.0419	0.0446	0.0309	0.0319	0.0318	0.0483	0.0282	0.0285	0.0353	0.0314	0.0559	0.0648	0.0787	0.0725	0.0661	0.0747	0.0586	0.0457

TABLE 7 Soil quality single index weights determined on the basis of game theory combinatorial empowerment.

Indices	C_{11}	C_{12}	C_{21}	C_{22}	C_{23}	C_{24}	C_{25}	C_{26}	C_{27}	C_{28}	C_{31}	C_{32}	C_{33}	C_{34}	C_{35}	C_{41}	C_{42}	C_{43}	C_{44}	C_{45}
Weights	0.2202	0.1865	0.0851	0.0475	0.0526	0.0161	0.0406	0.0158	0.0273	0.0325	0.0112	0.0234	0.0489	0.0178	0.0151	0.0170	0.0139	0.0533	0.0222	0.0527

TABLE 8 Comprehensive indices of soil quality based on the TOPSIS method and ranking.

Treatment	C_{11}	C_{12}	C_{21}	C_{22}	C_{23}	C_{24}	C_{25}	C_{26}	C_{27}	C_{28}	C_{31}	C_{32}	C_{33}	C_{34}	C_{35}	C_{41}	C_{42}	C_{43}	C_{44}	C_{45}	D^+	D^-	C	Sequence
WN	0.3312	0.3439	0.3368	0.3329	0.3326	0.2815	0.3600	0.2246	0.3136	0.3168	0.2736	0.2235	0.2545	0.3464	0.3270	0.3758	0.3599	0.3884	0.3696	0.3874	0.0683	0.1233	0.6434	3
WS	0.2951	0.2982	0.2855	0.2774	0.2942	0.3112	0.2786	0.3133	0.2788	0.3097	0.3592	0.3485	0.2677	0.2267	0.2337	0.2413	0.2286	0.2507	0.2244	0.2834	0.1003	0.0808	0.4462	8
WM	0.3110	0.3179	0.3034	0.2869	0.3122	0.2980	0.3185	0.2670	0.2960	0.3134	0.3382	0.3365	0.3189	0.2881	0.2811	0.2642	0.3230	0.3434	0.3205	0.3384	0.0699	0.1055	0.6015	5
WL	0.3267	0.3374	0.3256	0.3249	0.3380	0.2856	0.3456	0.2481	0.3034	0.3180	0.3309	0.3757	0.4713	0.3518	0.3545	0.3614	0.3496	0.4056	0.3387	0.3618	0.0401	0.1421	0.7798	1
BN	0.3234	0.3262	0.3348	0.3051	0.3294	0.3240	0.3172	0.2959	0.3378	0.2985	0.2890	0.3056	0.3584	0.3025	0.3204	0.2904	0.3214	0.3231	0.3198	0.3460	0.0616	0.1139	0.6491	2
BS	0.2950	0.2846	0.2840	0.3535	0.2817	0.3191	0.2834	0.3875	0.3266	0.2969	0.4645	0.2580	0.2510	0.2042	0.2050	0.1785	0.1913	0.1897	0.2083	0.2565	0.1156	0.0810	0.4120	9
BM	0.3090	0.3055	0.3140	0.3305	0.2958	0.3226	0.3001	0.3360	0.3247	0.3005	0.2400	0.3124	0.2962	0.2685	0.2596	0.2391	0.2694	0.2910	0.2672	0.2889	0.0859	0.0909	0.5142	7
BL	0.3173	0.3190	0.3348	0.2972	0.3193	0.3264	0.3095	0.3099	0.3296	0.3028	0.2062	0.3798	0.3398	0.3216	0.3143	0.3055	0.3075	0.3346	0.3107	0.3042	0.0671	0.1105	0.6222	4
SM	0.2822	0.2583	0.2772	0.2734	0.2927	0.3105	0.2881	0.3707	0.2909	0.2976	0.3147	0.3139	0.2728	0.4912	0.4514	0.4639	0.4310	0.2693	0.4285	0.1887	0.0908	0.1084	0.5441	6
WR	0.2618	0.2524	0.2681	0.2790	0.2872	0.2911	0.2895	0.3160	0.2994	0.3013	0.2642	0.2599	0.2095	0.2163	0.2832	0.3000	0.2595	0.2376	0.2609	0.2563	0.1166	0.0630	0.3509	10
CK	0.2527	0.2551	0.2342	0.2370	0.2136	0.2344	0.1956	0.1865	0.1873	0.2562	0.0633	0.0796	0.1637	0.1584	0.1973	0.1680	0.1774	0.1947	0.1746	0.2478	0.1628	0.0137	0.0775	11
S^+	0.3312	0.3439	0.3368	0.3535	0.3380	0.3264	0.3600	0.3875	0.3378	0.3180	0.4645	0.3798	0.4713	0.4912	0.4514	0.4639	0.4310	0.4056	0.4285	0.3874	—	—	—	—
S^-	0.2527	0.2524	0.2342	0.2370	0.2136	0.2344	0.1956	0.1865	0.1873	0.2562	0.0633	0.0796	0.1637	0.1584	0.1973	0.1680	0.1774	0.1897	0.1746	0.1887	—	—	—	—

S^+ is the ideal solution, S^- is the inverse ideal solution; D^+ is the distance of each treatment from the ideal solution; D^- is the distance of each treatment from the inverse ideal solution.

10.3389/fpls.2024.1447469

10.3389/fpls.2024.1447469

TABLE 9 Effect of different moisture-maintaining measures on the quality of purple garlic.

Year	Treatment	Allicin (mg g^{-1})	Soluble sugar (%)	Soluble protein (mg g^{-1})	Vitamin C (mg kg^{-1})	Crude fiber (%)	Ash content (%)	Amino acid (mg g^{-1})
2020	WN	7.05 ± 0.18abc	22.03 ± 0.70a	23.38 ± 0.77b	371.28 ± 13.95bc	1.32 ± 0.03ab	0.965 ± 0.03a	48.42 ± 0.93a
	WS	6.48 ± 0.07def	17.06 ± 0.43d	21.34 ± 0.53cd	310.08 ± 9.37ef	1.18 ± 0.01ef	0.921 ± 0.02a	47.41 ± 0.67a
	WM	6.81 ± 0.08cd	19.11 ± 0.70c	24.58 ± 0.46ab	406.47 ± 10.48ab	1.26 ± 0.03cd	0.937 ± 0.03a	48.63 ± 1.34a
	WL	7.34 ± 0.09a	21.94 ± 0.37a	26.52 ± 0.65a	425.34 ± 17.02a	1.36 ± 0.02a	0.945 ± 0.02a	48.82 ± 1.20a
	BN	6.97 ± 0.16bc	19.56 ± 0.53bc	23.16 ± 0.82bc	379.44 ± 12.95bc	1.30 ± 0.01bc	0.950 ± 0.02a	48.31 ± 0.92a
	BS	6.36 ± 0.07ef	16.00 ± 0.41de	20.71 ± 0.30d	291.72 ± 11.57fg	1.14 ± 0.01fg	0.924 ± 0.03a	47.21 ± 1.57a
	BM	6.72 ± 0.04cd	17.44 ± 0.53d	24.57 ± 0.49ab	388.11 ± 7.83b	1.24 ± 0.01d	0.933 ± 0.02a	48.57 ± 0.65a
	BL	7.22 ± 0.20ab	20.82 ± 0.55ab	26.45 ± 0.53a	438.60 ± 7.14a	1.35 ± 0.02ab	0.941 ± 0.02a	48.75 ± 1.67a
	SM	7.18 ± 0.05ab	19.52 ± 0.48bc	25.87 ± 0.70a	347.31 ± 12.64cd	1.21 ± 0.02de	0.928 ± 0.01a	47.88 ± 1.66a
	WR	6.60 ± 0.03de	16.17 ± 0.39de	22.81 ± 0.77bc	328.95 ± 7.52de	1.09 ± 0.02gh	0.919 ± 0.03a	47.05 ± 1.64a
	CK	6.23 ± 0.07f	15.09 ± 0.47e	18.39 ± 0.47e	272.85 ± 10.07g	1.05 ± 0.01h	0.916 ± 0.02a	46.67 ± 1.62a
2021	WN	6.85 ± 0.35ab	21.75 ± 0.65a	23.03 ± 0.80b	354.45 ± 16.01cd	1.27 ± 0.03abc	0.963 ± 0.03a	48.33 ± 1.87a
	WS	6.31 ± 0.31ab	16.75 ± 0.41c	20.95 ± 0.76cd	295.29 ± 9.85fg	1.11 ± 0.02ef	0.916 ± 0.02a	47.35 ± 1.37a
	WM	6.68 ± 0.21ab	18.74 ± 0.42b	24.47 ± 0.71ab	399.84 ± 12.52ab	1.21 ± 0.02cd	0.932 ± 0.01a	48.58 ± 0.63a
	WL	7.09 ± 0.33a	21.04 ± 0.65a	26.30 ± 0.61a	412.59 ± 11.31ab	1.33 ± 0.02a	0.940 ± 0.01a	48.76 ± 0.61a
	BN	6.77 ± 0.32ab	19.38 ± 0.35b	22.89 ± 0.74bc	357.51 ± 5.44cd	1.25 ± 0.02bc	0.946 ± 0.03a	48.21 ± 1.34a
	BS	6.23 ± 0.28ab	15.50 ± 0.53cd	20.47 ± 0.72d	287.13 ± 10.94fg	1.07 ± 0.03fg	0.920 ± 0.03a	47.15 ± 1.48a
	BM	6.56 ± 0.29ab	16.92 ± 0.51c	24.24 ± 0.41ab	385.05 ± 10.91bc	1.17 ± 0.02de	0.929 ± 0.01a	48.54 ± 0.47a
	BL	7.01 ± 0.38ab	20.25 ± 0.66ab	26.17 ± 0.32a	421.77 ± 13.67a	1.29 ± 0.02ab	0.936 ± 0.02a	48.70 ± 1.56a
	SM	6.93 ± 0.20ab	19.41 ± 0.44b	25.82 ± 0.74a	330.48 ± 10.11de	1.14 ± 0.02e	0.925 ± 0.04a	47.76 ± 1.42a
	WR	6.44 ± 0.05ab	15.80 ± 0.48cd	22.60 ± 0.68bc	307.02 ± 5.29ef	1.04 ± 0.01g	0.915 ± 0.03a	47.01 ± 0.81a
	CK	6.11 ± 0.28b	14.87 ± 0.50d	18.26 ± 0.53e	267.24 ± 9.04g	1.01 ± 0.03g	0.907 ± 0.02a	46.69 ± 0.69a
2 years average	WN	6.95 ± 0.09abc	21.89 ± 0.67a	23.21 ± 0.79c	362.87 ± 14.24cd	1.30 ± 0.03abc	0.964 ± 0.03a	48.37 ± 1.39
	WS	6.40 ± 0.12fgh	16.91 ± 0.42d	21.15 ± 0.38de	302.69 ± 9.61f	1.15 ± 0.01ef	0.919 ± 0.02a	47.38 ± 1.00
	WM	6.74 ± 0.07cde	18.93 ± 0.56c	24.53 ± 0.58bc	403.16 ± 11.49ab	1.24 ± 0.02cd	0.935 ± 0.02a	48.60 ± 0.99
	WL	7.22 ± 0.13a	21.49 ± 0.41a	26.41 ± 0.62a	418.97 ± 14.13a	1.35 ± 0.02a	0.943 ± 0.02a	48.79 ± 0.90
	BN	6.87 ± 0.08bcd	19.47 ± 0.44bc	23.03 ± 0.78c	368.48 ± 8.90cd	1.28 ± 0.01bc	0.948 ± 0.02a	48.26 ± 1.13
	BS	6.29 ± 0.11gh	15.75 ± 0.28de	20.59 ± 0.45e	289.43 ± 11.14fg	1.11 ± 0.02fg	0.922 ± 0.03a	47.18 ± 1.22
	BM	6.64 ± 0.12def	17.18 ± 0.48d	24.41 ± 0.45bc	386.58 ± 8.53bc	1.21 ± 0.02de	0.931 ± 0.02a	48.56 ± 0.56
	BL	7.11 ± 0.09ab	20.54 ± 0.42ab	26.31 ± 0.41a	430.19 ± 7.77a	1.32 ± 0.02ab	0.939 ± 0.02a	48.72 ± 1.52
	SM	7.05 ± 0.07ab	19.46 ± 0.46bc	25.85 ± 0.58ab	338.90 ± 6.52de	1.18 ± 0.01e	0.927 ± 0.02a	47.82 ± 1.42
	WR	6.52 ± 0.01efg	15.99 ± 0.35de	22.71 ± 0.61cd	317.99 ± 5.61ef	1.07 ± 0.02gh	0.917 ± 0.02a	47.03 ± 1.22
	CK	6.17 ± 0.11h	14.98 ± 0.46e	18.33 ± 0.46f	270.05 ± 8.04g	1.03 ± 0.02h	0.912 ± 0.02a	46.68 ± 1.13
ANOVA								
Year (Y)		ns	ns	ns	**	***	ns	ns
Treatment (T)		***	***	***	***	***	ns	ns
Y × T		ns	ns	ns	ns	ns	ns	ns

Different lowercase letters in the same column indicate significant differences among different treatments ($P < 0.05$). The ** and *** indicate significant differences among different treatments at the levels of $P < 0.01$ and $P < 0.001$, respectively. The ns means not significant at the level of $P \geq 0.05$.

TABLE 10 Effect of different moisture-maintaining measures on yield and water productivity of purple garlic.

Year	Treatment	Yield (kg hm^{-2})	Water productivity (kg m^{-3})	Irrigation water productivity (kg m^{-3})	N fertilizer partial factor productivity (kg kg^{-1})	P fertilizer partial factor productivity (kg kg^{-1})	K fertilizer partial factor productivity (kg kg^{-1})
2020	WN	18,661.33 ± 751.45a	3.14 ± 0.14a	4.20 ± 0.17a	83.31 ± 3.35a	119.62 ± 4.82a	82.94 ± 3.34a
	WS	14,071.49 ± 708.61d	2.21 ± 0.10d	3.17 ± 0.16d	62.82 ± 3.16d	90.20 ± 4.54d	62.54 ± 3.15d
	WM	17,063.28 ± 833.20ab	2.77 ± 0.14b	3.84 ± 0.19ab	76.18 ± 3.72ab	109.38 ± 5.34ab	75.84 ± 3.70ab
	WL	18,796.05 ± 801.97a	3.09 ± 0.15a	4.23 ± 0.18a	83.91 ± 3.58a	120.49 ± 5.14a	83.54 ± 3.57a
	BN	16327.94 ± 476.01bc	2.74 ± 0.05b	3.68 ± 0.11bc	72.89 ± 2.12bc	104.67 ± 3.05bc	72.57 ± 2.12bc
	BS	13,761.57 ± 289.72d	2.18 ± 0.03d	3.10 ± 0.07d	61.44 ± 1.29d	88.22 ± 1.86d	61.16 ± 1.29d
	BM	14,479.16 ± 730.34cd	2.36 ± 0.10cd	3.26 ± 0.17cd	64.64 ± 3.26cd	92.82 ± 4.68cd	64.35 ± 3.25cd
	BL	15,953.72 ± 749.07bc	2.61 ± 0.11bc	3.59 ± 0.17bc	71.22 ± 3.34bc	102.27 ± 4.80bc	70.91 ± 3.33bc
	SM	10,848.65 ± 299.52e	1.72 ± 0.03e	2.44 ± 0.07e	48.43 ± 1.34e	69.54 ± 1.92e	48.22 ± 1.33e
	WR	8,664.23 ± 290.27f	1.36 ± 0.05f	1.95 ± 0.07f	38.68 ± 1.30f	55.54 ± 1.86f	38.51 ± 1.29f
	CK	8,175.09 ± 215.77f	1.28 ± 0.03f	1.84 ± 0.05f	36.50 ± 0.96f	52.40 ± 1.38f	36.33 ± 0.96f
2021	WN	18,193.09 ± 977.36a	3.10 ± 0.16a	4.52 ± 0.24a	81.22 ± 4.36a	116.62 ± 6.27a	80.86 ± 4.34a
	WS	13,415.83 ± 626.27c	2.22 ± 0.09d	3.33 ± 0.16c	59.89 ± 2.80c	86.00 ± 4.01c	59.63 ± 2.78c
	WM	15,460.94 ± 264.12b	2.50 ± 0.02bc	3.84 ± 0.07b	69.02 ± 1.18b	99.11 ± 1.69b	68.72 ± 1.17b
	WL	18,064.73 ± 176.28a	3.01 ± 0.02a	4.48 ± 0.04a	80.65 ± 0.79a	115.80 ± 1.13a	80.29 ± 0.78a
	BN	15,767.05 ± 642.92b	2.62 ± 0.09b	3.91 ± 0.16b	70.39 ± 2.87b	101.07 ± 4.12b	70.08 ± 2.86b
	BS	12904.17 ± 591.07cd	2.17 ± 0.10d	3.20 ± 0.15cd	57.61 ± 2.64cd	82.72 ± 3.79cd	57.35 ± 2.63cd
	BM	13,832.67 ± 511.83c	2.30 ± 0.09cd	3.43 ± 0.13c	61.75 ± 2.28c	88.67 ± 3.28c	61.48 ± 2.27c
	BL	15,610.42 ± 620.59b	2.56 ± 0.10bc	3.88 ± 0.15b	69.69 ± 2.77b	100.07 ± 3.98b	69.38 ± 2.76b
	SM	11,351.38 ± 514.60d	1.88 ± 0.09e	2.82 ± 0.13d	50.68 ± 2.30d	72.77 ± 3.30d	50.45 ± 2.29d
	WR	8,107.96 ± 144.75e	1.33 ± 0.03f	2.01 ± 0.04e	36.20 ± 0.65e	51.97 ± 0.93e	36.04 ± 0.64e
	CK	7,025.41 ± 253.48e	1.17 ± 0.05f	1.74 ± 0.06e	31.36 ± 1.13e	45.03 ± 1.62e	31.22 ± 1.13e
2 years average	WN	18,427.21 ± 853.86a	3.12 ± 0.15a	4.36 ± 0.20a	82.27 ± 3.81a	118.12 ± 5.47a	81.90 ± 3.80a
	WS	13,743.66 ± 609.62c	2.22 ± 0.09c	3.25 ± 0.14c	61.36 ± 2.72c	88.10 ± 3.91c	61.09 ± 2.71c
	WM	16,262.11 ± 545.78b	2.64 ± 0.08b	3.84 ± 0.13b	72.60 ± 2.44b	104.25 ± 3.50b	72.28 ± 2.43b
	WL	18,430.39 ± 476.88a	3.05 ± 0.07a	4.36 ± 0.11a	82.28 ± 2.13a	118.15 ± 3.06a	81.92 ± 2.12a

(Continued)

10.3389/fpls.2024.1447469

TABLE 10 Continued

Year	Treatment	Yield (kg hm^{-2})	Water productivity (kg m^{-3})	Irrigation water productivity (kg m^{-3})	N fertilizer partial factor productivity (kg kg^{-1})	P fertilizer partial factor productivity (kg kg^{-1})	K fertilizer partial factor productivity (kg kg^{-1})
	BN	16,047.50 ± 554.80b	2.68 ± 0.08b	3.80 ± 0.13b	71.64 ± 2.48b	102.87 ± 3.55b	71.33 ± 2.47b
	BS	13,332.87 ± 412.54c	2.18 ± 0.09c	3.15 ± 0.10c	59.53 ± 1.84c	85.47 ± 2.64c	59.26 ± 1.83c
	BM	14,155.92 ± 600.05c	2.33 ± 0.10c	3.35 ± 0.14c	63.20 ± 2.68c	90.75 ± 3.85c	62.92 ± 2.67c
	BL	15,782.07 ± 647.09b	2.59 ± 0.10b	3.74 ± 0.15b	70.46 ± 2.89b	101.17 ± 4.15b	70.15 ± 2.88b
	SM	11,100.02 ± 406.96d	1.80 ± 0.06d	2.63 ± 0.10d	49.56 ± 1.82d	71.16 ± 2.62d	49.34 ± 1.81d
	WR	8,386.10 ± 195.66e	1.35 ± 0.03e	1.98 ± 0.05e	37.44 ± 0.87e	53.76 ± 1.25e	37.28 ± 0.87e
	CK	7,600.25 ± 213.77e	1.23 ± 0.04e	1.79 ± 0.05e	33.93 ± 0.95e	48.72 ± 1.37e	33.78 ± 0.95e
ANOVA							
Year (Y)		*	ns	**	*	*	*
Treatment (T)		***	***	***	***	***	***
Y × T		ns	ns	ns	ns	ns	ns

Different lowercase letters in the same column indicate significant differences among different treatments ($P < 0.05$). The *, **, and *** indicate significant differences among different treatments at the levels of $P < 0.05$, $P < 0.01$, and $P < 0.001$, respectively. The ns means not significant at the level of $P \geq 0.05$.

10.3389/fpls.2024.1447469

TABLE 11 Principal component analysis of indices affecting the growth of purple garlic.

Serial number	Index	Principal component 1	Principal component 2	Principal component 3	Principal component 4	Principal component 5	Principal component 6
1	Yield	0.2893	−0.2443	−0.0826	0.1110	0.0453	0.0138
2	Water productivity	0.2893	−0.2495	−0.0290	0.0568	0.0576	0.0138
3	N fertilizer partial factor productivity	0.2893	−0.2443	−0.0826	0.1110	0.0494	0.0138
4	Allicin	0.2524	0.4306	0.2812	0.2995	−0.1194	0.2553
5	Amino acid	0.2835	0.1707	−0.3145	−0.3770	0.0494	−0.5935
6	Soluble sugar	0.2778	0.1672	0.4363	0.2427	−0.4240	−0.5659
7	Soluble protein	0.2246	0.5407	−0.2015	0.3202	0.6134	0.0207
8	Vitamin C	0.2621	0.3145	−0.3971	−0.4389	−0.3376	0.2070
9	Crude fiber	0.2984	0.0788	0.0319	−0.0594	−0.3623	0.4761
10	Ash content	0.2615	−0.0260	0.6305	−0.5861	0.4076	0.1035
11	Irrigation water productivity	0.2896	−0.2417	−0.0812	0.1110	0.0535	0.0276
12	P fertilizer partial factor productivity	0.2893	−0.2435	−0.0841	0.1110	0.0453	0.0138
13	K fertilizer partial factor productivity	0.2893	−0.2435	−0.0826	0.1110	0.0453	0.0138
Eigenvalue		10.94	1.33	0.48	0.15	0.06	0.02
Contribution rate		84.18	10.25	3.66	1.15	0.45	0.17
Accumulate contribution rate		84.18	94.43	98.09	99.24	99.70	99.86

$$Y_5 = 0.0453X_1 + 0.0576X_2 + 0.0494X_3 - 0.1194X_4 + 0.0494X_5 - 0.4240X_6 + 0.6134X_7 - 0.3376X_8 - 0.3623X_9 + 0.4076X_{10} + 0.0535X_{11} + 0.0453X_{12} + 0.0453X_{13}$$

$$Y_6 = 0.0138X_1 + 0.0138X_2 + 0.0138X_3 + 0.2553X_4 - 0.5935X_5 - 0.5659X_6 + 0.0207X_7 + 0.2070X_8 + 0.4761X_9 + 0.1035X_{10} + 0.0276X_{11} + 0.0138X_{12} + 0.0138X_{13}$$

Ranking by the D value of the comprehensive evaluation of the affiliation function was WL>WN>BL>BN>WM>BM>SM>WS>BS>WR>CK (Table 12), indicating that each moisture-maintaining measure could significantly increase garlic yield, bulb quality, and water–fertilizer productivity compared to the traditional planting system, in which the use of 110-day transparent oxo-biodegradable plastic film mulching was the most effective.

3.7 Correlation analysis between soil quality indices and growth indices of purple garlic

As can be seen from Figure 10, there were significant positive correlations between soil water storage, soil temperature, organic matter, actinobacteria, catalase, cellulase, yield, quality indices, and water–fertilizer productivity, and there was also a significant positive correlation between soil water storage and soil temperature but no significant correlation with other indicators, which indicated that, with the improvement of the soil hydrothermal environment conditions, the content of soil organic matter and the number of actinobacteria increased and that the activities of catalase and cellulase were increased, which led to a significant increase in the quality, yield, and water–fertilizer productivity of garlic. Soil microbial biomass carbon and nitrogen were significantly positively correlated not only with the activities of urease, sucrase, and alkaline phosphatase but also with allicin, soluble sugar, and soluble protein. All these results indicated that microbial biomass had an important influence on the activities of soil urease, sucrase, and alkaline phosphatase and significantly contributed to the accumulation of allicin, soluble sugar, and soluble protein. Allicin, soluble sugar, vitamin C, crude fiber, ash content, and amino acid were significantly positively correlated with each other, whereas soluble protein was significantly positively correlated with vitamin C, crude fiber, and amino acid, suggesting that garlic quality indices can be both mutually reinforcing and independent of each other, and integrally affect quality. There was a significant positive correlation between garlic yield and water–fertilizer productivity, that is, an increase in yield was accompanied by a corresponding increase in water–fertilizer productivity.

10.3389/fpls.2024.1447469

TABLE 12 Comprehensive evaluation of the effects of different treatments on garlic yield, water–fertilizer productivity, and bulb quality indices.

Treatment	F1	F2	F3	F4	F5	F6	U1	U2	U3	U4	U5	U6	D	Sequence
WN	3.7008	−1.1608	1.2700	−0.1721	0.0705	−0.2023	0.9405	0.1329	1.0000	0.3401	0.7162	0.0209	0.8504	2
WS	−1.5272	−1.3152	−0.2538	0.4570	−0.0252	0.0187	0.4336	0.0909	0.3228	0.9412	0.5924	0.5664	0.4012	8
WM	1.8169	−0.1360	−0.9712	−0.0735	−0.0639	−0.2107	0.7578	0.4121	0.0040	0.4343	0.5423	0.0000	0.6887	5
WL	4.3145	0.3428	−0.2646	0.5185	−0.2364	0.0853	1.0000	0.5425	0.3180	1.0000	0.3192	0.7306	0.9245	1
BN	1.9516	−0.4874	0.6371	−0.4919	0.0372	0.1944	0.7709	0.3163	0.7188	0.0345	0.6730	1.0000	0.7138	4
BS	−2.2251	−1.6488	−0.2929	0.3378	0.2598	0.1236	0.3659	0.0000	0.3055	0.8273	0.9611	0.8253	0.3349	9
BM	0.3748	0.2891	−0.9802	−0.5280	0.2899	−0.0921	0.6180	0.5278	0.0000	0.0000	1.0000	0.2928	0.5801	6
BL	2.7987	1.2123	−0.2607	−0.1682	−0.2415	0.1217	0.8530	0.7793	0.3198	0.3438	0.3127	0.8204	0.8175	3
SM	−0.9858	2.0226	0.6705	0.4948	0.1957	−0.1412	0.4861	1.0000	0.7336	0.9774	0.8781	0.1715	0.5548	7
WR	−4.2203	1.1851	0.2069	−0.1378	0.1971	0.1679	0.1724	0.7719	0.5276	0.3728	0.8799	0.9346	0.2537	10
CK	−5.9988	−0.3037	0.2389	−0.2365	−0.4832	−0.0653	0.0000	0.3664	0.5418	0.2785	0.0000	0.3590	0.0613	11

3.8 Path analysis of soil physical and chemical properties on yield and quality of purple garlic

As can be seen in Figure 11, soil water storage, soil temperature, soil nutrients, soil microorganisms, and soil enzyme activities have direct or indirect effects with the yield of purple garlic. The degree of influence of soil factors on the yield of purple garlic was in the order of soil microbial biomass carbon > soil temperature > cellulase > total phosphorus > total potassium > catalase > nitrate nitrogen > actinobacteria > soil water storage. Soil microbial biomass carbon and soil temperature were important factors promoting the increase in

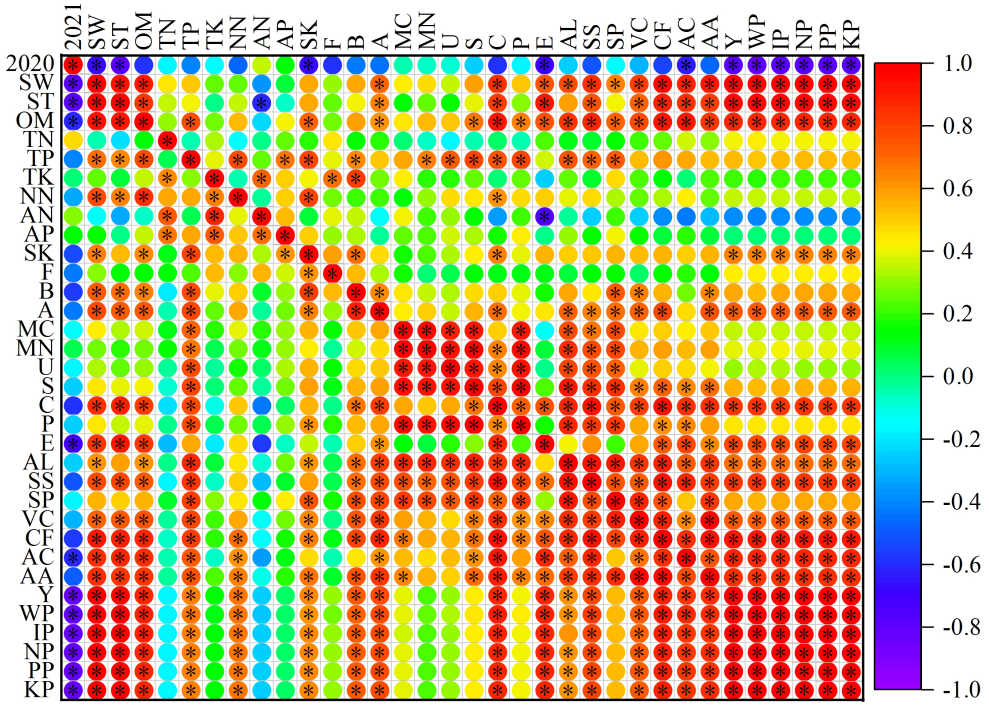

FIGURE 10
Pearson's correlation analyses between yield and water productivity and nitrogen use efficiency under drip irrigation under plastic film mulching in growth periods of purple garlic in 2020 and 2021. Correlations between two indices were significant at *p < 0.01. SW, soil water storage; ST, soil temperature; OM, organic matter; TN, total nitrogen; TP, total phosphorus; TK, total potassium; NN, nitrate nitrogen; AN, ammonium nitrogen; AP, available phosphorus; SK, slow-release potassium; F, fungi; B, bacterium; A, actinobacteria; MC, soil microbial biomass carbon; MN, soil microbial biomass nitrogen; U, urease; S, sucrase; C, catalase; P, alkaline phosphatase; E, cellulase; AL, allicin; SS, soluble sugar; SP, soluble protein; VC, vitamin C; CF, crude fiber; AC, ash content; AA, amino acid; Y, yield; WP, water productivity; IP, irrigation water productivity; NP, nitrogen fertilizer partial factor productivity; PP, potassium fertilizer partial factor productivity; KP, phosphate fertilizer partial factor productivity.

yield of purple garlic, whereas soil microbial biomass nitrogen, organic matter, and slow-release potassium were the factors inhibiting the increase in yield of purple garlic. As can be seen in Figure 12, soil water storage, soil temperature, soil nutrients, soil microorganisms, and soil enzyme activities also have direct or indirect effects with the quality of purple garlic. Among them, the degree of influence of soil factors on allicin of purple garlic was in the order of ammonium nitrogen > catalase > sucrase > slow-release potassium. The degree of effect on soluble protein of purple garlic was in the following order: catalase > bacterial > alkaline phosphatase, whereas sucrase and cellulase were the factors that inhibited the increase of soluble protein of purple garlic. The degree of influence on soluble sugars of purple garlic was in the order of ammonium nitrogen > sucrase > organic matter > catalase > cellulase, whereas soil water storage, total phosphorus, total potassium, soil microbial biomass carbon, and alkaline phosphatase were the factors inhibiting the increase of soluble sugars of purple garlic. The degree of influence on vitamin C of purple garlic was in the order of actinobacteria > available phosphorus > organic matter > total nitrogen > catalase, whereas sucrase was the factor inhibiting the increase of vitamin C of purple garlic.

4 Discussion

4.1 Effect of soil moisture-maintaining measures on soil water storage characteristics

The soil moisture intense evaporation during the growing period of purple garlic in the China Hexi Corridor oasis agricultural area and the precipitation are very limited, with large inter-annual and intra-annual differences in precipitation, especially during the sowing stage; there is virtually no precipitation, and channel irrigation water has not been supplied; at this time, the soil water storage will be a very important source of water supply for garlic. Therefore, taking appropriate moisture-maintaining measures can effectively reduce the ineffective evaporation of water, store soil water, reduce the unproductive water consumption of farmland, optimize the soil water environment of farmland, and enhance the water use of crops. Numerous studies had confirmed that plastic film, straw mulching, and A-SAP application can effectively improve soil water conditions, which can inhibit soil water evaporation and increase water storage during the whole growth stage of crops (Tang et al., 2016; Tian et al., 2020). Surface mulching avoids evapotranspiration of most of the soil water storage during the garlic growing season, reduces ineffective water evaporation, forces the lateral migration of water, and therefore has a significant mitigating effect on soil-crop drought stress (Lin et al., 2014; Zhou et al., 2009). This study showed that, compared with the open-field planting system, both transparent plastic film and black plastic film could significantly increase the soil water storage in the 0- to 100-cm soil layer by up to 16.00% to 48.59% and 14.84% to 44.35%, respectively, and the water storage capacity of the transparent plastic film mulching was better than that of the black plastic film mulching as a whole. Oxo-biodegradable plastic film had significant moisture-maintaining effect in garlic seedling stage and scaly bud and flower bud differentiation stage, but the water storage effect gradually weakened with the expanding degree of cleavage. Therefore, WL and BL had a better moisture-maintaining effect. Compared with open-field planting, garlic harvesting can significantly increase soil water storage by 25.38% to 42.45% and 19.50% to 30.66%, whereas WM, BM, WS, and BS did not show lasting moisture-maintaining effect due to earlier induction period, and similar conclusion was also shown in the results of Wu et al. (2022). There have been many studies on the moisture-maintaining effect of straw and plastic film mulching. Li et al. (2013) showed that straw mulching improved the intensity of precipitation infiltration, so the soil moisture increased effect of straw mulching was better than that of ordinary transparent plastic film mulching and oxo-biodegradable plastic film mulching, whereas Chen et al. (2012) showed that the moisture increased effect of ordinary transparent plastic film was better than that of oxo-biodegradable plastic film and straw mulching. The results of this experiment showed that straw mulching showed moisture-maintaining advantages throughout the growth stage of garlic, and the soil water storage was increased by 7.35% to 17.20% compared with that of open-field planting as a whole, the inter-annual increase varied greatly, and the water storage capacity was lower than that of ordinary transparent plastic film and oxo-biodegradable plastic film. The results of this study better confirmed the findings of Chen et al. (2012) but were different from those conclusions of Li et al. (2013), which may be related to factors such as differences in precipitation in the experimental area and different water consumption of planted crops. A-SAP is as a new type of polymer water-absorbing material; Yang et al. (2015) concluded that the application of A-SAP can effectively improve soil water absorption and water-holding capacity, which can significantly improve the soil water status of the 0- to 60-cm soil layer, and the soil water storage continues to rise with the increase of the application of A-SAP. However, in other related studies, it was shown that excessive application of A-SAP caused excessive cohesion of soil particles and clogging of soil pores by swollen A-SAP sols, which was instead unfavorable for soil water infiltration and storage (Liu et al., 2022a). In this study, the application of 45 kg hm^{-2} A-SAP increased the soil water storage capacity of 0- to 100-cm soil layer in each growth stage of garlic by 0.77% to 9.47% compared with that of open field, but the increase was small and not significantly different from that of open field. However, the gradient of application rate was not set in this experiment, and further experiments are needed to verify whether the soil water storage capacity continued to increase with the increase of application rate.

4.2 Effect of soil moisture-maintaining measures on soil temperature

Although purple garlic is a shade-loving crop, unreasonable mulching measures caused the soil accumulated temperature to be too high, which exceeds the appropriate growth temperature, leading to yellowing of the stems and leaves of garlic and growth retardation. Therefore, optimal moisture-maintaining measures not only can provide adequate water but also can improve soil temperature and

maintain a favorable hydrothermal environment. Different mulching measures have different effects on the regulation of soil temperature. Plastic film mulching can block the heat exchange between the soil and the external environment, and, at the same time, the inner membrane attached to the aquifer to weaken the short-wave radiation of the sun during the daytime and the long-wave radiation of the soil at night, the warming during the daytime, and the cooling at night are slowed down, so that the average temperature of the soil increased significantly (Ochege et al., 2022). Wang et al. (2021) showed that, in the early stage of crop growth, the film surface of oxo-biodegradable plastic film remained intact, and the difference between the thermal insulation effect and that of ordinary transparent plastic film was not significant, but, as the film surface of oxo-biodegradable plastic film degraded and ruptured, the soil temperature under the film began to decrease, and, in the late stage of crop growth, the average daily soil temperature of oxo-biodegradable plastic film was significantly lower than that of ordinary transparent plastic film. The results of this study showed that, compared with the open-field planting mode, plastic film mulching can significantly increase the soil temperature during the growth period of garlic. There was no significant difference in soil temperature between the plastic film of the same color because the surface of the oxo-biodegradable plastic film remained intact during the sowing period, seedling period, and scaly bud and flower bud differentiation stage of garlic. However, as the oxo-biodegradable plastic film entered the induction, cracking and macro-cracking periods, the soil temperature was significantly lower than that of ordinary plastic film, whereas the oxo-biodegradable plastic film with later induction did not show significant changes, which better verified the viewpoints of Wang et al. (2021). However, this study further found that, as garlic entered the mature stage, the effect of plastic film warming again prominent; especially, the ordinary plastic film mulching was the most significant, whereas the soil temperature of oxo-biodegradable plastic film significantly decreased compared with ordinary plastic film, which was slightly different from the results of the study by Liu et al. (2021), which is due to the different types of planted crops; the aboveground stalks of garlic gradually dried up during the mature stage; and the soil temperature increased significantly due to the direct light shining on the surface. Straw mulching has a weaker barrier to air heat compared to plastic film, and, at the same time, it can reduce the direct sunlight on the ground to a certain extent, thus weakening the influence of external environment on soil temperature (Liu et al., 2022b). The results of this study found that the straw mulching soil temperature was still significantly increased by 14.70% to 19.80% and 10.82% to 16.29% in

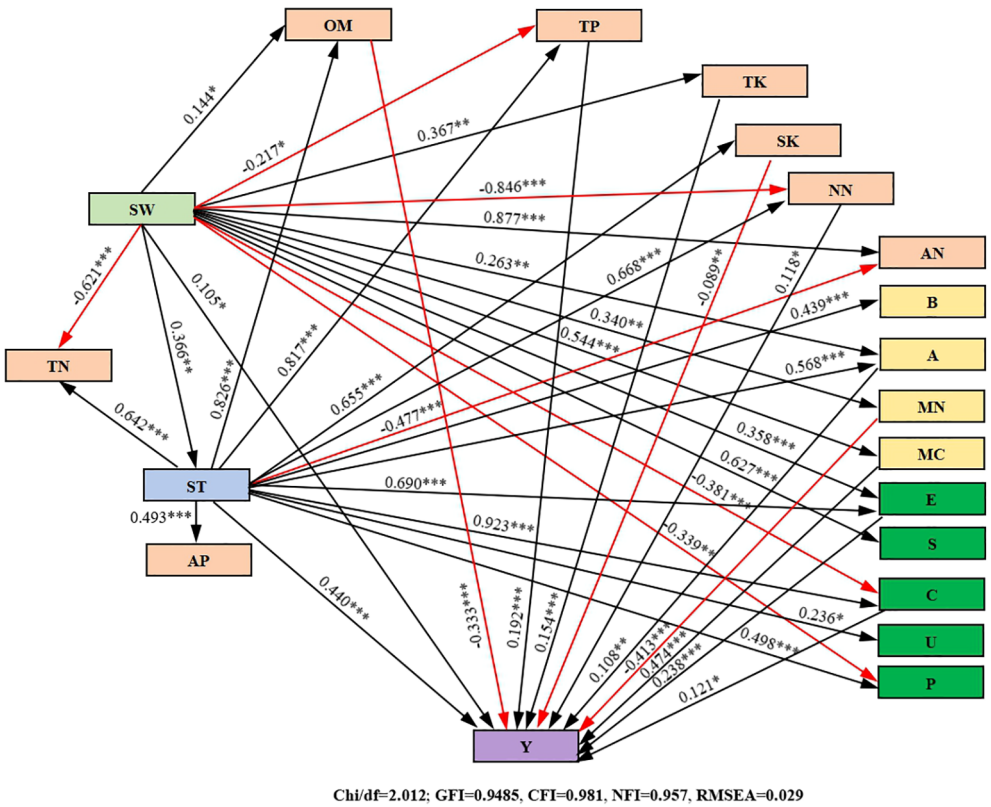

FIGURE 11
Path analysis of soil physical and chemical properties on yield of purple garlic. The data on the arrows are standardized path coefficients (λ). The black arrows indicate positive impacts. The red arrows indicate negative impacts. SW, soil water storage; ST, soil temperature; OM, organic matter; TN, total nitrogen; TP, total phosphorus; TK, total potassium; NN, nitrate nitrogen; AN, ammonium nitrogen; AP, available phosphorus; SK, slow-release potassium; B, bacterium; A, actinobacteria; MC, soil microbial biomass carbon; MN, soil microbial biomass nitrogen; U, urease; S, sucrase; C, catalase; P, alkaline phosphatase; E, cellulase; Y, yield. The *, **, and *** indicate significant correlation of different indicators at the levels of $P < 0.05$, $P < 0.01$, and $P < 0.001$, respectively.

the sowing and seedling stages of garlic than that of open field, whereas there was no significant difference in the middle and late stages of growth, and the results of this experiment better confirmed the above conclusion. There are different conclusions about the effect of A-SAP on soil temperature. Zhang et al. (2012) showed that the application of A-SAP kept more water in the soil layer, and the average daily soil temperature was reduced due to the high heat capacity of water, which impeded the conduction of solar radiation to the deeper soil layers; whereas Yang et al. (2020) showed that the application of A-SAP increased the average daily soil temperature. In this study, although the application of A-SAP reduced the soil temperature, there was no significant difference with the open field, which better supported the conclusion of Zhang et al. (2012). The reason for the difference with the research results of Yang et al. (2020) may be related to the process of A-SAP absorption and release.

4.3 Effect of soil moisture-maintaining measures on soil nutrient

The use of reasonable moisture-maintaining measures not only can improve the soil erosion resistance and scour resistance but also can effectively reduce soil erosion and nutrient leaching, so as to achieve the role of nutrient retention. Fu et al. (2021) found that plastic film mulching improved soil hydrothermal conditions, accelerated soil organic carbon mineralization, and increased organic carbon input of crop roots, which resulted in a significant increase in soil organic matter and fast-release nutrient content; whereas Rahmani et al. (2021) found that mulching treatments had a significant effect on soil total potassium content but not on soil organic matter, total nitrogen, and fast-release phosphorus content. Yang et al. (2022a) found that plastic film mulching could promote the growth and development of the crop roots and promote crops to absorb more nutrients, which in turn, caused a significant reduction in the soil fast-release nutrient content. The results of this experiment showed that plastic film mulching can significantly increase the soil nutrient content in the 0- to 20-cm soil layer compared with that in the open field, only the available phosphorus content in the 20- to 40-cm soil layer showed a decreasing change, and the other nutrient parameters also showed a tendency to increase. With the prolongation of oxo-biodegradable plastic film induction period, the content of soil organic matter, total phosphorus, nitrate nitrogen, and slow-release potassium showed an increasing change, whereas the content of total potassium and ammonium nitrogen showed a decreasing change, which was similar to the relevant research results of Fu et al. (2021) and also confirmed the conclusions of Duan et al. (2022), but there was a difference from the results of the studies by Rahmani et al. (2021) and Yang et al. (2022a), which may be related to the climatic environment of the experimental area; the characteristics of soil hydrothermal environment improved by plastic film mulching and the growth state of crops. The improvement of soil nutrient content by straw mulching has been confirmed in many studies (Dung et al., 2023; Lv et al., 2023), and this study is no exception, which also showed that soil nutrient content could be significantly increased by straw mulching, which was mainly due to the fact that after straw mulching; straw near the soil surface layer was gradually decomposed into organic matter in hydrothermal environment,

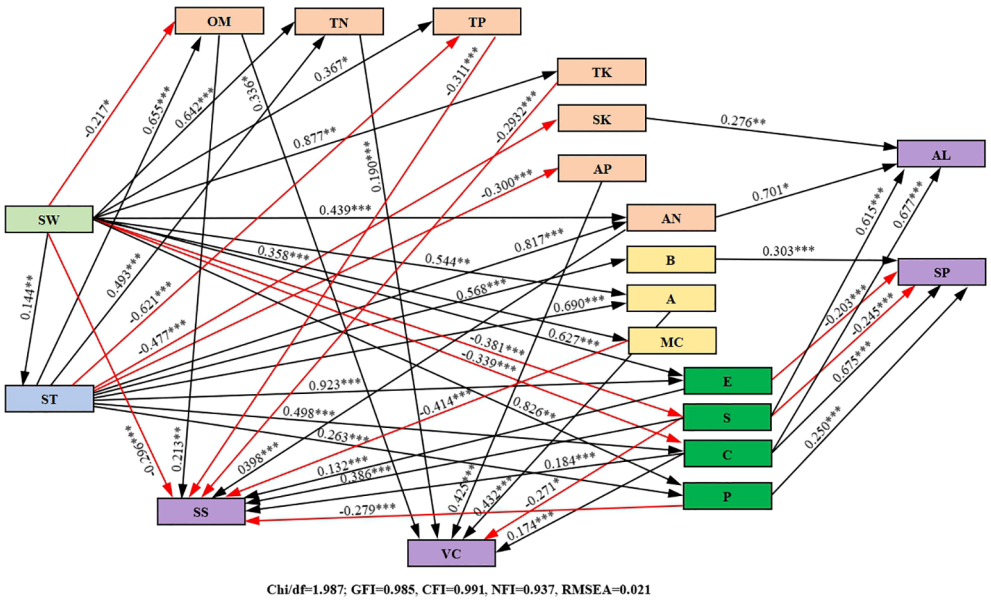

FIGURE 12
Path analysis of soil physical and chemical properties on quality of purple garlic. The data on the arrows are standardized path coefficients (λ). The black arrows indicate positive impacts. The red arrows indicate negative impacts. SW, soil water storage; ST, soil temperature; OM, organic matter; TN, total nitrogen; TP, total phosphorus; TK, total potassium; AN, ammonium nitrogen; AP, available phosphorus; SK, slow-release potassium; B, bacterium; A, actinobacteria; MC, soil microbial biomass carbon; S, sucrase; C, catalase; P, alkaline phosphatase; E, cellulase; AL, allicin; SS, soluble sugar; SP, soluble protein; VC, vitamin C. The *, **, and *** indicate significant correlation of different indicators at the levels of $P < 0.05$, $P < 0.01$, and $P < 0.001$, respectively.

which made the soil organic matter content rise; and, at the same time, heat was generated, which slowed down the soil nutrient loss and better maintain land productivity. Application of A-SAP can also improve soil nutrient status and enhance soil fertilizer retaining performance (He et al., 2023; Li et al., 2022c). The results of this study showed that the application of A-SAP also increased soil organic matter and soil nutrient content, and the increase in nutrient content in the 20- to 40-cm soil layer was greater than that in the 0- to 20-cm soil layer, which was in agreement with the research results of Cao et al. (2017), but Jamal et al. (2022) concluded that the application of A-SAP accelerated the transfer rate of nutrients from the soil to the plant, and, at the same time, due to the effect of fertilizer absorption and retention, which reduced the soil nutrient content, the reason for the difference in conclusions may be related to factors such as different tillage practices, A-SAP application rates, and the application depth.

4.4 Effect of soil moisture-maintaining measures on soil microorganisms

Soil microorganisms are involved in soil ecological functions, environmental functions, and immune functions to coordinate the regulation of soil health, which is the core and key to maintaining soil quality (Daunoras et al., 2024). Soil microorganisms with the largest populations of soil bacterium, actinobacteria, and fungi are extremely sensitive to environmental changes, and changes in soil physicochemical properties can significantly affect the population composition (Guo et al., 2018). Therefore, the selection of reasonable moisture-maintaining measures can promote reproductive growth by improving the microbial living environment such as soil hydrothermal and aeration. Many studies have shown that either plastic film mulching or straw mulching can increase the relative abundance and activity of soil flora and improve the diversity and structure of soil microbial communities (Li et al., 2022d; Liu et al., 2023), but the conclusions varied due to the different climatic conditions, soil types, crop species, fertilizer application, etc., in the experimental areas; e.g., Zhang et al. (2024) showed that plastic film mulching or straw mulching increased the number of bacterium, fungi, and actinobacteria in soil, and the effect of straw mulching was better than that of plastic film mulching; whereas Li et al. (2022a) showed that plastic film mulching could significantly increase the total number of soil microorganisms, but the number of fungi decreased, and the oxo-biodegradable plastic film has the same effect as that of ordinary plastic film. In this study, it was found that plastic film mulching or straw mulching could significantly increase the number of soil fungi, bacterium, and actinobacteria in the 0- to 40-cm soil layer of garlic farmland, which better confirmed the study conclusion of the former. This study further found that, with the prolongation of the induction period of oxo-biodegradable plastic film, the number of soil fungi decreased and the number of bacterium and actinobacteria increased, so the prolongation of the induction period of oxo-biodegradable plastic film can effectively maintain the balance of soil microbial populations, make the soil microbial community changed from the "fungi type" to the "bacterium type," and reduce the occurrence of soil diseases, thus improving the soil quality. Meanwhile, it was found in this study that the application of A-SAP could significantly increase the number of soil fungi, bacterium, and actinobacteria, and this conclusion was also confirmed in the study of Bana et al. (2023), which may be due to the fact that the application of A-SAP significantly improves the soil physical properties, enhances the root vitality, and stimulates the root to secrete a large amount of inorganic and organic substances, thus creating a superior environmental condition for the activity and development of microorganisms. Under the conditions of this experiment, all the moisture-maintaining measures could increase soil microbial biomass carbon and nitrogen, but there is a significant difference in the increase rate among different treatments. Generally, straw mulching had the greatest increase, followed by ordinary transparent plastic film mulching; with the prolongation of the induction period of oxo-biodegradable plastic film, soil microbial biomass carbon and nitrogen showed an increasing change; and the result was similar to Fu et al. (2019). Whereas Song et al. (2023) concluded that plastic film mulching decreased the soil biomass carbon and nitrogen content, Li et al. (2022b) showed that the application of oxo-biodegradable plastic film had no significant effect on soil biomass carbon and nitrogen content. The difference in results may be caused by the different environment of the experimental area, farmland management measures, and crop root exudates.

4.5 Effect of soil moisture-maintaining measures on soil enzyme activity

Soil enzyme is often used as an important index for evaluating soil quality and soil microbial function (Ma et al., 2017). Different types of soil enzymes have different molecular compositions and structures and respond differently to a variety of factors such as external climatic conditions, soil environment, and farmland management measures. It has been confirmed that the rational use of moisture-maintaining measures can improve soil structure and provide a favorable environment for the synthesis and accumulation of soil enzymes, which, in turn, promote the improvement of enzyme activity (Chen et al., 2018). For example, ordinary plastic film, oxo-biodegradable plastic film, and straw mulching and application of A-SAP can all improve soil urease, sucrase, alkaline phosphatase, and catalase enzyme activities (Chen et al., 2021; Duanyuan et al., 2023; Yang et al., 2022b), which is basically consistent with the results of this experiment. In addition, this experiment found that the enzyme activities of urease, sucrase, and alkaline phosphatase under straw mulching have obvious effects, which may be due to the fact that straw mulching makes the shallow soil hydrothermal environment to be improved, accelerates the decomposition of straw, and then increases the soil organic matter content, which makes the original carbon and nitrogen ratio in the soil to be changed and enhances the enzymatic reaction, and stimulated the soil organisms to secrete more urease, sucrase, and alkaline phosphatase; at the same time, the surface water of soil under straw mulching increases, which increased the reductivity of catalase, and led to the decrease of

catalase activity. In this study, both ordinary plastic film and oxo-biodegradable plastic film as well as application of A-SAP could increase soil cellulase activity, in which ordinary plastic film had the best effect, followed by oxo-biodegradable plastic film, which showed no significant difference in A-SAP, whereas straw mulching showed a significant inhibitory effect, with a significant reduction of 22.99% to 27.80% compared with that of CK, contrary to the results of Du et al. (2022). The reason for this may be related to the climatic environment, mulch thickness, and type of crops grown in the experimental area. It was further found that, with the prolongation of the induction period of oxo-biodegradable plastic film, the soil enzyme activity showed an incremental change, and the increase of transparent plastic film was slightly higher than that of black plastic film, so the appropriate prolongation of the induction period of transparent oxo-biodegradable plastic film can effectively improve soil enzyme activity, thus improving soil quality.

4.6 Effect of soil moisture-maintaining measures on yield, quality, and water–fertilizer productivity of purple garlic

The yield and quality of garlic bulbs are generally determined by varieties, climate, cultivation, management measures, etc. Reasonable moisture-maintaining measures can effectively ameliorate soil and improve soil fertility, thereby increasing crop productivity, while improving the living environment of soil microorganisms and promoting the root absorption of water and nutrients, which enables garlic to accumulate more dry matter in different development stages, thus improving bulb yield, quality, and water–fertilizer productivity (Shan et al., 2022). Li et al. (2021b) found that mulching farmland with plastic film, straw, and rice hulls can increase soil water content and enzyme activity, promote garlic plant height and bulb growth, and improve garlic yield and quality, and plastic film mulching can also improve soil temperature, so that the transparent plastic film mulching has the best effect, followed by black plastic film mulching. Xu (2015) found that plastic film mulching had a significant effect on increasing soil temperature and moisture-maintaining, and garlic plant grew vigorously, which was conducive to the accumulation and transformation of nutrients, and improved bulb quality while promoting the dry matter accumulation of the whole plant, which, in turn, increases bulb yield, whereas the garlic yield of straw mulching was significantly lower than that of plastic film mulching, and there was no significant difference in bulb quality between plastic film mulching and open field. This study further corroborates this theory. Compared with open-field planting, different moisture-maintaining measures improved garlic bulb yield and quality, of which the highest yield and best quality was achieved with 110-day transparent oxo-biodegradable plastic film, which was mainly attributed to the fact that the WL not only improved the water and fertilizer conditions but also inhibited weed growth and reduced nutrient competition in crop growth, therefore improving garlic yield and quality, whereas the yield of A-SAP increased little, which was not a strong advantage for agricultural production. Therefore, under the same irrigation and fertilization conditions, the rational selection of oxo-biodegradable plastic film type has a good water and fertilizer regulating effect, which can significantly improve the water productivity and crop yield. Therefore, in the China Hexi Corridor oasis agricultural area, where there is a serious resource-based water shortage, the application of 110-day transparent oxo-biodegradable plastic film mulching technology in garlic production can alleviate the contradiction between the crop water demand and water supply, achieve higher water–fertilizer productivity, and can increase the yield and improve the quality, which can be a feasible measure to maintain the substitution of the ordinary transparent plastic film in garlic production in the China Hexi Corridor oasis agricultural area.

5 Conclusion

The different moisture-maintaining measures effectively improved the soil hydrothermal environment, activated soil nutrients, changed and optimized the soil microbial growth environment, increased the number of microorganisms, and enhanced soil enzyme activities in garlic farmland in the China Hexi Corridor oasis agricultural area. The results of correlation analysis showed that soil hydrothermal, nutrients, microorganisms, and enzymes were associated with garlic yield and quality. Therefore, soil moisture-maintaining measures can improve garlic farmland soil hydrothermal environment to promote rapid microbial reproduction, increase enzyme activity, and promote nutrient decomposition, which, in turn, improves garlic yield and quality, among which 110-day transparent oxo-biodegradable plastic film mulching has the best effect on optimizing soil micro-region environment and improving garlic yield and quality, which can achieve arable land production capacity enhancement and agro-ecosystem sustainable development. However, it was still found in the test process that the current market oxo-biodegradable plastic film does not match well with the plastic film mulching needs of purple garlic, which limited the further improvement of the yield and quality of purple garlic. Therefore, the formulation of biodegradable plastic film based on ordinary polyethylene substrate blends and oxo-biodegradable additives as the main raw materials need to be further improved, especially in the regulation of degradation performance, and it is urgent to design the molecular chain structure of the material and postpone the degradation induction period to match the needs of purple garlic plastic film warming and moisture-maintaining and to achieve rapid degradation when the purple garlic enters into the mature stage. It is expected to replace the ordinary polyethylene plastic film in the production system of purple garlic in Hexi Oasis.

Data availability statement

The original contributions presented in the study are included in the article/supplementary material. Further inquiries can be directed to the corresponding author.

Author contributions

XP: Data curation, Formal analysis, Writing – original draft, Writing – review & editing. HZ: Funding acquisition, Supervision, Writing – review & editing. HD: Formal analysis, Funding acquisition, Writing – review & editing. SY: Data curation, Writing – review & editing. CZ: Data curation, Writing – review & editing. FL: Formal analysis, Writing – review & editing.

Funding

The author(s) declare financial support was received for the research, authorship, and/or publication of this article. This work was supported by the Research Program Sponsored by State Key Laboratory of Aridland Crop Science (No. GSCS-2021-11), the National Natural Science Foundation of China (Nos. 52269008 and 51669001), the Industrial Support Plan Project of Gansu Provincial Department of Education (No. 2022CYZC-51), and the Key Research and Planning Projects of Gansu Province (No. 18YF1NA073).

Acknowledgments

We thank everyone who helped during the manuscript writing. We also thank the reviewers for their useful comments and suggestions.

Conflict of interest

The authors declare that the research was conducted in the absence of any commercial or financial relationships that could be construed as a potential conflict of interest.

Publisher's note

References

Bana, R. S., Grover, M., Singh, D., Bamboriya, S. D., Godara, S., Kumar, M., et al. (2023). Enhanced pearl millet yield stability, water use efficiency and soil microbial activity using superabsorbent polymers and crop residue recycling across diverse ecologies. *Eur. J. Agron.* 148, 126876. doi: 10.1016/j.eja.2023.126876

Cao, Y. B., Wang, B. T., Guo, H. Y., Xiao, H. J., and Wei, T. T. (2017). The effect of super absorbent polymers on soil and water conservation on the terraces of the loess plateau. *Y. Ecol. Eng.* 102, 270–279. doi: 10.1016/j.ecoleng.2017.02.043

Chen, K. Y., Ali, S., Chen, Y. Y., Manzoor,, Sohail, A., Jan, A., et al. (2018). Effect of ridge-covering mulching materials on hormonal changes, antioxidative enzyme activities and production of maize in semi-arid regions of China. *Agric. Water Manage.* 204, 281–291. doi: 10.1016/j.agwat.2018.03.023

Chen, N., Li, X. Y., Shi, H. B., Hu, Q., Zhang, Y. H., and Leng, X. (2021). Effect of biodegradable film mulching on crop yield, soil microbial and enzymatic activities, and optimal levels of irrigation and nitrogen fertilizer for the Zea mays crops in arid region. *Sci. Total Environ.* 776, 145970. doi: 10.1016/j.scitotenv.2021.145970

Chen, P. P., Gu, X. B., Li, Y. N., Qiao, L. R., Li, Y. P., Fang, H., et al. (2022). Effects of residual film on maize root distribution, yield and water use efficiency in Northwest China. *Agric. Water Manage.* 260, 107289. doi: 10.1016/j.agwat.2021.107289

Chen, X. L., Wu, P. T., Zhao., X. N., Ren., X. L., and Jia., Z. K. (2012). Rainfall harvesting and mulches combination for corn production in the subhumid areas prone to drought of China. *J. Agron. Crop Sci.* 198, 304–313. doi: 10.1111/j.1439-037X.2012.00508.x

China Rural Statistical Yearbook. (2021). Rural social and economic survey department of the national bureau of statistics. *China Stat. Press*. 47, 49

Daunoras, J., Kacergius, A., and Gudiukaite, R. (2024). Role of soil microbiota enzymes in soil health and activity changes depending on climate change and the type of soil ecosystem. *Biology.* 13, 85. doi: 10.3390/biology13020085

Dong, W. Y., Si, P. F., Liu, E. K., Yan, C. R., Zhang, Z., and Zhang, Y. Q. (2017). Influence of film mulching on soil microbial community in a rainfed region of northeastern China. *Sci. Rep.* 7, 8468. doi: 10.1038/s41598-017-08575-w

Du, C. L., Li, L. L., and Effah, Z. (2022). Effects of straw mulching and reduced tillage on crop production and environment:A Review. *Water.* 14, 2471. doi: 10.3390/w14162471

Duan, X. Y., Yan, Y. S., Han, X., Wang, Y., Li, R. H., Gao, F. F., et al. (2022). Effects of biodegradable liquid film on the soil and fruit quality of vitis franco-american L. Hutai-8 Berries. *Horticulturae.* 8, 418. doi: 10.3390/horticulturae8050418

Duanyuan, H. Z., Zhou, T., He, Z., Peng, Y. Y., Lei, J. J., Dong, J. Y., et al. (2023). Effects of straw mulching on soil properties and enzyme activities of camellia oleifera-cassia intercropping agroforestry systems. *Plants.* 12, 3046. doi: 10.3390/plants12173046

Dung, T. V., Dang, L. V., Ngoc, N. P., and Hung, N. N. (2023). Soil fertility and pomelo yield influenced by soil conservation practices. *Open Agric.* 8, 20220181. doi: 10.1515/opag-2022-0181

Fu, W., Fan, J., Hao, M. D., Hu, J. S., and Wang, H. (2021). Evaluating the effects of plastic film mulching patterns on cultivation of winter wheat in a dryland cropping system on the loess plateau, China. *Agric. Water Manage.* 2244, 106550. doi: 10.1016/j.agwat.2020.106550

Fu, X., Wang, J., Sainju, U. M., Zhao, F. Z., and Liu, W. Z. (2019). Soil microbial community and carbon and nitrogen fractions responses to mulching under winter wheat. *Appl. Soil Ecol.* 139, 64–68. doi: 10.1016/j.apsoil.2019.03.018

Gao, C., Shao, X. H., Yang, X., Li, X. N., and Wu, W. B. (2022). Effects of biochar and residual plastic film on soil properties and root of flue-cured tobacco. *J. Irrig. Drain Eng.* 148, 04022005. doi: 10.1061/(ASCE)IR.1943-4774.0001673

Gao, C., Yang, X., Li, X. N., and Shao, X. H. (2023). Effect of residual plastic film on infiltration of one-dimensional soil columns under drip irrigation. *Arch. Agron. Soil Sci.* 69, 3073–3086. doi: 10.1080/03650340.2023.2200998

Guan, S. Y. (1986). Soil enzymes and their research methods. *Beijing: China Agric. Press*.

Guo, H. Z., Yang, X. J., Dang, B., Liang, F., and Ma, P. (2023b). Quality characteristics of highland barley powder with different particle sizes. *Food Mach.* 39, 150–156. doi: 10.13652/j.spjx.10.1003.5788.2023.80028

Guo, B., Yang, Z. X., He, W. Q., and Liu, J. L. (2023a). Application effectiveness and problems of biodegradable mulch. *Chin. J. Agrometeorol.* 44, 977–994. doi: 10.3969/j.issn.1000-6362.2023.11.001

Guo, Y. P., Yang, Y., Li, J. G., Li, J., Liu, S. L., Zhu, S. L., et al. (2018). Analyses of the distribution and characterization of rhizosphere microorganisms of ziziphus jujuba L. in the Tarim Basin. *Fresenius Environ.Bull.* 27, 4689–4698.

He, Y. Z., Tian, Z. Y., Ma, R., Liang, Y., Zhu, X. C., and Qu, L. L. (2023). Effects of superabsorbent polymers (SAP) incorporated with organic and inorganic fertilizer on the water and nutrient retention of soil in rare earth mine tailing areas. *J. Soils Sediments.* 23, 3384–3395. doi: 10.1007/s11368-023-03538-3

Hu, N. J., Chen, Q., Zhang, Q., Zhang, H. Y., and Sun, H. W. (2023). Effects of biodegradable plastic film mulching on soil organic carbon pool and aggregates in the garlic field. *Chin. J. Soil Sci.* 54, 1326–1332. doi: 10.19336/j.cnki.trtb.2022082302

Hu, L. X., Zhang, X. H., and Zhou, Y. H. (2019). Farm size and fertilizer sustainable use: An empirical study in Jiangsu. *China J. Inte. Agric.* 18, 2898–2909. doi: 10.1016/S2095-3119.62732-2

Jamal, A., Hussain, S., Hussain, S., Matloob, A., Awan, T. H., Irshad, F., et al. (2022). Super absorbent polymer application under suboptimal environments: implications and challenges for marginal lands and abiotic stresses. *Turk. J. Agric. For.* 46, 6. doi: 10.55730/1300-011X.3034

Li, S. Q. (2023). The influence of different surface coverings on the growth and yield of garlic. *Spec. Econ. Anim. Plants.* 26, 28–30.

Li, R., Chai, S. X., Chai, Y. W., Li, Y. W., Lan, X. M., Ma, J. T., et al. (2021a). Mulching optimizes water consumption characteristics and improves crop water productivity on the semi-arid loess plateau of China. *Agric. Water Manage.* 254, 106965. doi: 10.1016/j.agwat.2021.106965

Li, R., Hou, X. Q., Jia, Z. K., Han, Q. F., Ren, X. L., and Yang, B. P. (2013). Effects on soil temperature, moisture, and maize yield of cultivation with ridge and furrow mulching in the rainfed area of the Loess Plateau, China. *Agric. Water Manage.* 116101–109. doi: 10.1016/j.agwat.2012.10.001

Li, R., Hou, X. Q., Li, P. F., and Wang, X. N. (2022c). Multifunctional superabsorbent polymer under residue incorporation increased maize productivity through improving sandy soil properties. *Adv. Polym. Technol.* 2022, 6554918. doi: 10.1155/2022/6554918

Li, M. X., Ji, D. C., Wang, Z. Y., Xu, Y. D., Jia, Z. J., Li, S. T., et al. (2022b). Effects of biodegradable plastic film mulching on soil microbial abundance, activity, and community structure. *J. Agro-Environ. Sci.* 41, 1758–1767. doi: 10.11654/jaes.2021-1413

Li, K., Luo, S. W., Wang, Z., Chen, B. W., Yang, J. X., Zhang, S. P., et al. (2022a). Effects of different plastic film mulching on the microbial characteristics of rhizosphere soil and yield of millet in arid area. *J. Shanxi Agric. Univ.(Natural Sci. Edition).* 42, 1–8. doi: 10.13842/j.cnki.issn1671-8151.202203025

Li, Z. R., Ma, J. J., Sun, X. J., Guo, X. H., Zheng, L. J., and Chen, J. P. (2022e). Plastic Pollution in Soil and Crops: Effects of film residuals on soil water content and tomato physiology. *Agronomy.* 12, 1222. doi: 10.3390/agronomy12051222

Li, Y. Z., Xie, H. X., Ren, Z. H., Ding, Y. P., Long, M., Zhang, G. X., et al. (2022d). Response of soil microbial community parameters to plastic film mulch: A meta-analysis. *Geoderma.* 418, 115851. doi: 10.1016/j.geoderma.2022.115851

Li, W. W., Zhou, S. Y., Liu, M., Jiang, F. L., Peng, Y. L., and Wu, Z. (2021b). Effects of different ground mulches on soil properties, yield and quality of autumn-sown Garlic. *Soils.* 53, 305–312. doi: 10.13758/j.cnki.tr.2021.02.013

Lin, L. R., Chen, J. Z., Wang, F., and Deng, S. H. (2014). Several conservation practices influencing the hydrologic processes and drought of the red soil sloping farmland. *Sci. Agric. Sin.* 47, 4858–4867. doi: 10.3864/j.issn.0578-1752.2014.24.009

Lin, C. W., Luo, C. Y., Pang, L., Huang, J. J., Fu, D. W., Tu, S. H., et al. (2010). Effects of different cultivation and mulching methods on soil erosion and nutrient losses from apurple soil of sloping land. *Acta Ecol. Sin.* 30, 6091–6101.

Liu, B. Y., Dai, Y. S., Cheng, X., He, X., Bei, Q. C., Wang, Y. F., et al. (2023). Straw mulch improves soil carbon and nitrogen cycle by mediating microbial community structure and function in the maize field. *Front. Microbiol.* 14. doi: 10.3389/fmicb.2023.1217966

Liu, E. K., He, W. Q., and Yan, C. R. (2014). [amp]]lsquo;White revolution' to 'white pollution'-agricultural plastic film mulch in China. *Environ. Res. Lett.* 9, 91001. doi: 10.1088/1748-9326/9/9/091001

Liu, C. Y., Ma, R., Luo, W. J., Han, L., and Wang, H. Z. (2022a). Effects of super absorbent polymer dosage on growth, photosynthetic characteristics and stress-resistance physiology of Populus euphratica seedlings. *J. Beijing For. Univ.* 44, 36–44. doi: 10.12171/j.1000–1522.20210300

Liu, R. H., Wang, Z. H., Ye, H. C., Li, W. H., Zong, R., and Tian, X. L. (2021). Effects of Different Plastic mulching film on soil hydrothermal status and water utilization by spring maize in Northwest China. *Front. Mater* 8. doi: 10.3389/fmats.2021.774833

Liu, S. D., Yi, S. J., and Ma, Y. C. (2022b). Effects of straw mulching on soil temperature and maize growth in Northeast China. *Orig. Sci. Pap.* 29, 1805–1810. doi: 10.17559/TV-20210330091001

Lu, R. K. (2000). Soil agrochemical analysis. *China Agric. Sci. Technol. Press*.

Lv, L. G., Gao, Z. B., Liao, K. H., Zhu, Q., and Zhu, J. J. (2023). Impact of conservation tillage on the distribution of soil nutrients with depth. *Soil Tillage Res.* 225, 105527. doi: 10.1016/j.still.2022.105527

Lv, X. Y., and Ji, X. Q. (2013). Rethinking food security in China. *Agric. Econ. Issues.* 09), 15–24. doi: 10.13246/j.cnki.iae.2013.09.010

Ma, Y. H., Fu, S. L., Zhang, X. P., Zhao, K., and Chen, H. Y. H. (2017). Intercropping improves soil nutrient availability, soil enzyme activity and tea quantity and quality. *Appl. Soil Ecol.* 119, 171–178. doi: 10.1016/j.apsoil.2017.06.028

Muñoz, K., Buchmann, C., Meyer, M., Schmidt-Heydtb, M., Steinmetza, Z., Diehl, D., et al. (2017). Physicochemical and microbial soil quality indicators as affected by the agricultural management system in strawberry cultivation using straw or black polyethylene mulching. *Appl. Soil Ecol.* 113, 36–44. doi: 10.1016/j.apsoil.2017.01.014

Ochege, F. U., Luo, G. P., Yuan, X. L., Li, C. F., and Justine, F. M. (2022). Simulated effects of plastic film-mulched soil on surface energy fluxes based on optimized TSEB model in a drip-irrigated cotton field. *Agric. Water Manage.* 262, 107394. doi: 10.1016/j.agwat.2021.107394

Oo, A. T., Huylenbroeck, G. V., and Speelman, S. (2020). Measuring the economic impact of climate change on crop production in the dry zone of Myanmar: a ricardian approach. *Climate.* 8, 9. doi: 10.3390/cli8010009

Petrescu-Mag, R. M., Petrescu, D. C., and Azadi, H. (2020). A social perspective on soil functions and quality improvement: Romanian farmers' perceptions. *Geoderma.* 380, 114573. doi: 10.1016/j.geoderma.2020.114573

Qi, R. M., Jones, D. L., Li, Z., Liu, Q., and Yan, C. G. (2020). Behavior of microplastics and plastic film residues in the soil environment: a critical review. *Sci. Total Environ.* 703, 134722. doi: 10.1016/j.scitotenv.2019.134722

Quan, H., Wu, L. H., Ding, D. Y., Yang, Z. T., Wang, N. J., Chen, G. J., et al. (2022). Interaction between soil water and fertilizer utilization on maize under plastic mulching in an arid irrigation region of China. *Agric. Water Manage.* 265, 107494. doi: 10.1016/j.agwat.2022.107494

Rahmani, W., Salleh, M. N., Hamzah, M. Z., Abdu, A., Ishak, M. F., Khadir, W. R. W. A., et al. (2021). Effect of different types of mulching on soi properties and tree growth of magnolia champaca planted at the montane rainforest in Cameron Highlands, Pahang, Malaysia. *Int. J. For. Res.* 2021, 5517238. doi: 10.1155/2021/5517238

Shan, X., Zhang, W., Dai, Z. L., Li, J. B., Mao, W. W., Yu, F. W., et al. (2022). Comparative analysis of the effects of plastic mulch films on soil nutrient, yields and soil microbiome in three vegetable fields. *Agronomy*. 12, 506. doi: 10.3390/agronomy12020506

Song, N. N., Wang, B., Liu, J., Wang, F. L., Wang, X. X., and Zong, H. Y. (2023). Is degradable plastic film alternative? Insights from crop productivity enhancement and soil environment improvement. *Eur. J. Agron.* 149, 126882. doi: 10.1016/j.eja.2023.126882

Tang, H. M., Xiao, X. P., Tang, W. G., Guo, L. J., and Wang, K. (2016). Effects of different mulching models on soil temperature, moisture, and yield of maize (Zea Mays L.) in hilly red soil upland in SouthernChina. *Rom. Agric. Res.* 33, 169–177.

Tian, X. M., Wang, K. Y., Fan, H., Wang, J. Q., and Wang, L. N. (2020). Effects of polymer materials on the transformation and utilization of soil nitrogen and yield of wheat under drip irrigation. *Soil Use Manage.* 37, 712–722. doi: 10.1111/sum.12651

Wang, A., Chang, Q. T., Zhao, Y., Sun, J. X., Jiang, Y., and Wu, W. (2020). Effects of different membranes on soil temperature and humidity, weed suppression and growth of taro. *J. Yangzhou Univ.* 41, 102–105 + 124. doi: 10.16872/j.cnki.1671-4652.2020.05.017

Wang, L., He, X. W., Hu, C., Wang, X. F., Liu, Q., Yan, C. R., et al. (2021). Effects of degradation properties of biodegradable plastic mulches on soil temperature humidity and cotton yield in Southern Xinjiang. *Agric. Res. Arid. Areas.* 39, 64–70 + 79. doi: 10.7606/j.issn.1000-7601.2021.04.08

Wang, G. L., Li, L. K., and Hao, M. D. (2017a). Effect of long-term fertilization and straw mulch on the contents of labile organic matter and carbon management index. *J. Plant Nutr. Fert.* 23, 20–26. doi: 10.11674/zwyf.16095

Wang, L., Li, X. G., Lv, J. T., Fu, T. T., Ma, Q. J., Song, W. Y., et al. (2017b). Continuous plastic-film mulching increases soil aggregation but decreases soil pH in semiarid areas of China. *Soil Tillage Res.* 167, 46–53. doi: 10.1016/j.still.2016.11.004

Wang, M. L., Wei, J. J., Zhou, S. Y., Wu, Q. T., Li, M. G., Zhou, R., et al. (2024). Effects of biostimulants on growth, yield and quality of 'majianghongsuan'. *China Veg.* 1), 81–89. doi: 10.19928/j.cnki.1000-6346.2023.3062

Wang, D., Xi, Y., Shi, X. Y., Gou, C. L., Zhong, Y. J., Song, C., et al. (2023). Effects of residual plastic film on crop yield and soil fertility in a dryland farming system. *J. Integr. Agric.* 22, 3783–3791. doi: 10.1016/j.jia.2023.04.026

Wu, J. S., Lin, Q. M., and Huang, Q. Y. (2006). Methods for measuring soil microbial biomass and their applications. 54–74.

Wu, K. Q., Xiao, R., Zhao, W. Q., Zhang, Y. L., Deng, H. L., Yu, H. Y., et al. (2022). Effect of degradable plastic film on soil hydrothermal characteristics and yield of seed maize in Hexi arid area. *J. Drain. Irrig. Mach. Eng.* 40, 952–958. doi: 10.3969/j.issn.1674-8530.21.0103

Xu, L. (2015). Effects of film mulching and straw mulching on growth yield and quality of garlic. *Shandong Agric. Univ.*

Yang, F., Cen, R., Feng, W. Y., Liu, J., Qu, Z. Y., and Miao, Q. F. (2020). Effects of super-absorbent polymer on soil remediation and crop growth in arid and semi-arid areas. *Sustainability.* 12, 7825. doi: 10.3390/su12187825

Yang, Y. H., Ding, J. L., Zhang, Y. H., Wu, J. C., Zhang, J. M., Pan, X. Y., et al. (2018). Effects of tillage and mulching measures on soil moisture and temperature, photosynthetic characteristics and yield of winter wheat. *Agric. Water Manage.* 201, 299–308. doi: 10.1016/j.agwat.2017.11.003

Yang, L. L., Han, Y. G., Yang, P. L., Wang, C. G., Yang, S. G., Kuang, S. Y., et al. (2015). Effects of superabsorbent polymers on infiltration and evaporation of soil moisture under point source drip irrigation. *Irrig. Drain.* 64, 275–282. doi: 10.1002/ird.1883

Yang, C., Huang, Y. Z., Long, B. B., and Gao, X. H. (2022a). Effects of biodegradable and polyethylene film mulches and their residues on soil bacterial communities. *Environ. Sci. pollut. Res.* 29, 89698–89711. doi: 10.1007/s11356-022-22014-y

Yang, Y. H., Zhang, S. S., Wu, J. C., Gao, C. M., Lu, D. F., and Tang, D. S. (2022b). Effect of long term application of super absorbent polymer on soil structure, soil enzyme activity, photosynthetic characteristics, water and nitrogen use of winter wheat. *Front. Plant Sci.* 13. doi: 10.3389/fpls.2022.998494

Yu, X., and Yang, G. H. (1988). Scientific basis for improving the cultivation effect of purple garlic. *Liaoning Agric. Sci.* 2, 31–35.

Zhang, Y., Cheng, H. B., Yang, J. J., Ma, J. T., Chai, S. X., Ji, W. N., et al. (2023b). Effect of mulching methods on drought resistance physiology and grain weight formation of dryland wheat in post-fiowering fiag leaf. *Agric. Res. Arid. Areas.* 41, 141–150. doi: 10.7606./j.issn.1000-7601.2023.04.15

Zhang, R., Geng, G. J., Bai, G. S., and Di, S. N. (2012). Effects of super absorbent polymer with different application methods on soil moisture, soil temperature andproduction of spring wheat. *J. Zhejiang Univ. (Agric.&Life Sic.)* 38, 211–219. doi: 10.3785/j.issn.1008-9209.2012.02.013

Zhang, Y. Y., Li, W. J., Kang, T., Li, H. D., Chen, J. S., Zhang, L., et al. (2024). The effect of straw coverage on the growth, yield, and soil microbial quantity of summer

flowering plants. *Jiangsu Agric. Sci.* 52, 104–104. doi: 10.15889/j.issn.1002-1302.2024.03.016

Zhang, J. H., Zhang, Y. X., Hou, S. S., Li, H. B., Zhang, R. F., Wang, H., et al. (2023a). Research progress on benefits and rational selection of cover crops. *Trans. Chin. Soc Agric. Eng.* 39, 23–34. doi: 10.11975/j.issn.1002-6819.202303144

Zhang, X. D., Zhao, J., Yang, L. C., Kamran, M., Xue, X. K., Dong, Z. Y., et al. (2019). Ridge-furrow mulching system regulates diurnal temperature amplitude and wetting-drying alternation behavior in soil to promote maize growth and water use in a semiarid region. *Field Crops Res.* 233, 121–130. doi: 10.1016/j.fcr.2019.01.009

Zhao, Y., Mao, X. M., Li, S. E., Huang, X., Che, J. G., and Ma, C. J. (2023). A Review of plastic film mulching on water, heat, nitrogen balance, and crop growth in farmland in China. *Agronomy.* 13, 2515. doi: 10.3390/agronomy13102515

Zhou, Y. P., Bastida, F., Zhou, B., Sun, Y. F., Gu, T., Li, S. Q., et al. (2020). Soil fertility and crop production are foster by micro-nano bubble irrigation with associated changes in soil bacterial community. *Soil Biol. Biochem.* 141, 107663. doi: 10.1016/j.soilbio.2019.107663

Zhou, M. L., Jin, S. L., and Song, Y. J. (2009). How two ridges and the furrow mulched with plastic film affect soil water, soil temperature and yield of maize on the semiarid Loess Plateau of China. *Field Crops Res.* 113, 41–47. doi: 10.1016/j.fcr.2009.04.005

Zhou, P., Yang, Y., Fu, W. T., Wang, N. Y., Peng, S. Q., and He, J. W. (2023). Quality analysis and evaluation of 25 main papper arieties in Guizhou. *J. Food Saf. Qual.* 14, 292–298. doi: 10.19812/j.cnki.jfsq11-5956/ts.2023.21.048

Zhou, L. F., Yang, Y. X., and Yang, R. (2024). Root and leaf senescence of maize subject to spatial differentiation of soil water and CO_2 in sandy fields with plastic film mulching. *Chin. J. Eco-Agric.* 32, 83–94. doi: 10.12357/cjea.20230289

Zhu, L. X., Xu, S. W., Chen, R. B., Li, L. L., and Liu, T. X. (2022). Nitrogen use efficiency was increased by manure combined with plastic film mulching. *Nutr. Cycl. Agroecosyst.* 122, 31–39. doi: 10.1007/s10705-021-10179-w

frontiers | Frontiers in Plant Science

TYPE Original Research
PUBLISHED 01 November 2024
DOI 10.3389/fpls.2024.1408515

OPEN ACCESS

EDITED BY
Laichao Luo,
Anhui Agricultural University, China

REVIEWED BY
Meraj Alam Ansari,
ICAR-Indian Institute of farming system research, India
Vesna Vasić,
Educons University, Serbia

*CORRESPONDENCE
Ajay Kumar Mishra
a.k.mishra@irri.org

RECEIVED 28 March 2024
ACCEPTED 23 September 2024
PUBLISHED 01 November 2024

CITATION
Mishra AK, Maurya PK and Sharma S (2024) Impact of different farming scenarios on key soil sustainability indicators driving soil carbon and system productivity of rice-based cropping systems.
Front. Plant Sci. 15:1408515.
doi: 10.3389/fpls.2024.1408515

Impact of different farming scenarios on key soil sustainability indicators driving soil carbon and system productivity of rice-based cropping systems

Ajay Kumar Mishra*, Piyush Kumar Maurya and Sheetal Sharma

Sustainable Impact through Rice-Based Systems, International Rice Research Institute South Asia Regional Centre, Varanasi, India

This research explores the relationships among soil characteristics, carbon dynamics, and soil biome in rice-based cropping systems across four farming scenarios: conventional farming, organic farming with conventional tillage, integrated nutrient management, and conservation agriculture with zero tillage. Conducted at the International Rice Research Institute, India (2020-2022), the study analyzed physical, chemical, and biological soil parameters. The findings reveal significant effects of farming scenarios on soil organic carbon (SOC), available nitrogen (N), phosphorus (P), and potassium (K), with no notable impact on bulk density, pH, electrical conductivity, or water-holding capacity. Organic farming enhanced microbial health, showing microbial biomass carbon (MBC) at 194.0 µg g^{-1}, microbial biomass nitrogen (MBN) at 134.2 µg g^{-1}, and dehydrogenase activity (DHA) at 36.80 µg TPF h^{-1} g^{-1}, reflecting a more active microbial community important for nutrient cycling. Conservation agriculture reduced soil compaction, promoting better root growth and water penetration, leading to higher crop yields (10.95 $\pm$ 0.49 t ha^{-1}). The study highlights the role of SOC in enhancing soil health, nutrient availability, and crop productivity, emphasizing sustainable agricultural practices.

KEYWORDS

carbon pools, cover crop, crop yield, environment, natural farming, reduce-tillage, soil health, sustainability

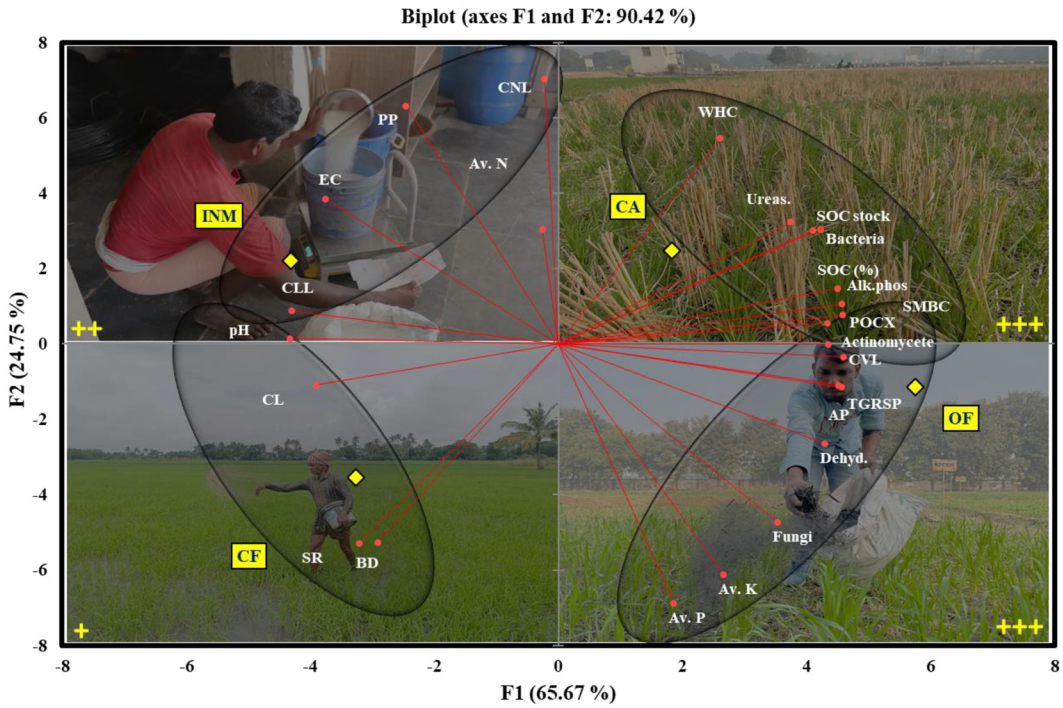

GRAPHICAL ABSTRACT
CF, Conventional farming; CA, Conservation agriculture; INM, Integrated nutrient management, OF, Organic farming along with various soil quality parameters.

Highlights

- The study compared four modified farming methods showing varied benefits over the conventional framing.
- Organic farming boosts soil microbial health as compared to conventional farming.
- Conservation agriculture reduces soil compaction, benefiting root growth and enhancing crop yields.
- Both organic farming and conservation agriculture improve soil organic carbon, aiding in carbon sequestration.
- Conservation agriculture achieves the highest crop yield, highlighting the efficacy of sustainable practices.

1 Introduction

Climate change and its impact on food production is a pressing global challenge (FAO, 2019). Continuous application of chemical-based fertilizers is another challenge, degrading the soil fertility and causing acidification. Several investigations have found alterations in soil microbial populations after fertilizer application (Wang et al., 2022; Sivojiene et al., 2021). Sivojiene et al. (2021) found that organic fertilizer increases microbial biomass and diversity, while Wang et al. (2022) studied how different fertilization methods affect bacterial communities. Ren et al. (2018, 2020) found that appropriate nitrogen and carbon from organic fertilizer boost soil microbial growth, while excess phosphorus from fertilization lowers microbial community variety (Liu et al., 2022). Applying fertilizers, particularly chemicals, can harm soil characteristics and indirectly affect the microbial community (Cheng et al., 2020). The continuous application of chemical fertilizers can promote soil acidification, which negatively impacts soil structure and fertility (Pahalvi et al., 2021).

Further, soil management practices are crucial, as they directly influence soil health, nutrient availability, and carbon sequestration potential (Six et al., 2002; Lal, 2004). Understanding the interrelationships among soil characteristics, carbon input, carbon pools, and the soil biome is essential for developing effective management strategies that enhance soil fertility, improve crop productivity, and mitigate greenhouse gas emissions (Smith et al., 2016; Hinz et al., 2020).

Mineral and organic fertilizers enhance soil fertility (SOC, nutrient profile) and crop yield, acting as crucial nutrient sources in agricultural soils (Wu et al., 2021; Wang et al., 2017; Kpan et al., 2023).

Global and regional data on SOC stocks are available (Mishra et al., 2009). There have been very limited practical data on the effect of land use patterns on soil carbon and nutrient level at different soil depths under the various land use practices, such as conventional farming, forest land to conventional farming, though numerous studies have explored the effects of different farming practices on soil properties and nutrient dynamics (Wang et al., 2019; Zhang et al., 2020). However, there remains a knowledge gap regarding the specific impacts of these

practices on Vertisols, on which rice-based cropping systems are frequently followed (Richards et al., 2015). Vertisols are characterized by high clay content and exhibit unique properties, such as high water-holding capacity and shrink-swell behavior, influencing their response to agricultural management practices (Yadav et al., 2017). Additionally, vertical soil profile has a significant role in the plant growth and root biomass and thus on the SOC. The climate crisis is undeterred by population growth, and urbanization plaguing agricultural sustainability through unmanaged agricultural practices is also threatening and alarming (Yadav et al., 2021). Kumar et al. (2022) have reported that crop productivity has decreased and soil health has deteriorated as a consequence of agriculture based on tillage; thus, zero tillage and residue management can improve soil health (Kumar et al., 2021; Singh et al., 2018).

Further, Yadav et al. (2021) reported that integrating cowpea live mulch in no-till and reduced tillage systems enhances crop and soil productivity in the eastern Himalayan region of India. These practices have also resulted in increased water productivity and saving technologies in sensitive regions like the Himalayan regions. Long-term application of organic amendments also positively impacts soil nitrogen and carbon in irrigated semi-arid cropping systems of India.

Globally, the agricultural system produces approx. 4.6 billion tons of agri-waste residues annually that can be used in the field again (Bentsen et al., 2014). Specifically, Indian agriculture contributes about 500 million tonnes of crop residues each year, with over a quarter of these being burned on farms. This practice of dumping or burning agricultural waste harms soil fertility and impacts environmental quality adversely. Additionally, the intense use of energy could lead to a 6% increase in CO2 emissions by the year 2050 (Gielen et al., 2019). So, developing residue utilization-based farming practices is also crucial under the alarming impact of climate change.

The growing risk of decline in soil health caused by anthropogenic activity is another challenging issue. The nexus between soil degradation, nutrient loss, and GHG emissions under various land use practices is critical to estimate and control. Additionally, in continents such as Asia and Africa, the agricultural sector is predominantly characterized by farmers who are both resource-poor and marginal, holding small parcels of land (Das et al., 2021). These farmers exhibit a constellation of challenges, including limited capital, constrained access to institutional credit, a low capacity for risk absorption, and a reliance on subsistence farming practices typically centered around a single annual crop. Consequently, their ability to generate significant marketable surpluses is challenged. Despite these impediments, there is a pressing imperative for these farmers to enhance agricultural productivity per unit of land, water, nutrients, and energy input (Babu et al., 2023).

Thus, the present study was conducted at the International Rice Research Institute, South Asia Regional Centre in Varanasi, Uttar Pradesh, India, to address these research gaps. The study aimed to investigate the influence of four farming scenarios, namely conventional farming, organic farming with conventional tillage, integrated nutrient management, and conservation agriculture with zero tillage, respectively, on soil characteristics, carbon input, carbon pools, and the soil biome in Vertisols under rice-based cropping systems.

Therefore, considering these aspects, comprehensive analyses were performed on the soil's physical, chemical, and biological parameters. Soil samples were collected before and after crop harvest, and a range of measurements, including soil organic carbon content, available nutrient content, microbial biomass and activity, enzyme activities, microbial population abundances, soil compaction, and distribution of different organic carbon fractions, were conducted. Moreover, understanding the intricate relationships among soil characteristics, carbon input, carbon pools, and the soil biome is crucial for devising evidence-based strategies that promote soil health, enhance nutrient cycling, and mitigate climate change impacts (Mishra et al., 2018; Lal, 2020).

2 Materials and methods

2.1 The experimental site

The experiment was conducted during the year 2020 to 2022 at the International Rice Research Institute South Asia Regional Centre (ISARC), Varanasi (25.30° N – 82.95° E, 83 m above mean sea level), Uttar Pradesh, India (Figure 1) with rice-based cropping systems under different farming scenarios. The mean minimum and maximum temperatures at the experimental site during experimental period was 15.5°C and 36°C, respectively. Annual rainfall recorded ranges between 900 and 1113 mm and more than 70% rainfall occurred during the monsoon season from July to September (Figure 2). The soil at the experimental site is sandy clay loam and it was classified as *Typic Natrustalf* (US Taxonomy).

The ISARC, Varanasi was selected as it is a site representative of rice-based cropping systems in similar agroecological zones. While the findings provide valuable insights, the results may be limited in their generalizability to other regions with different environmental and soil conditions. We advocate that future research should be conducted across diverse locations to validate these findings and extend their applicability to broader contexts.

2.2 Treatments, experimental design and crop management

The experiment was established in a randomized complete block design in which four farming scenarios constituted the treatments as follows: Conventional farming (Scenario 1) ploughing and use of chemical-based fertilizers and pesticides, Organic farming (using bio-pesticide, farm yard manure and compost) with conventional tillage (CT) for rice and wheat (Scenario 2), Integrated nutrient management (Organic and chemical based combined input, Scenario 3), and Conservation agriculture with zero tillage (ZT) for rice and wheat (Scenario 4). There were three replications of each treatment. While rice and wheat were grown under all the scenarios, in Scenarios 2 and 4, ZT mungbean was grown as a Zaid crop between wheat and rice.

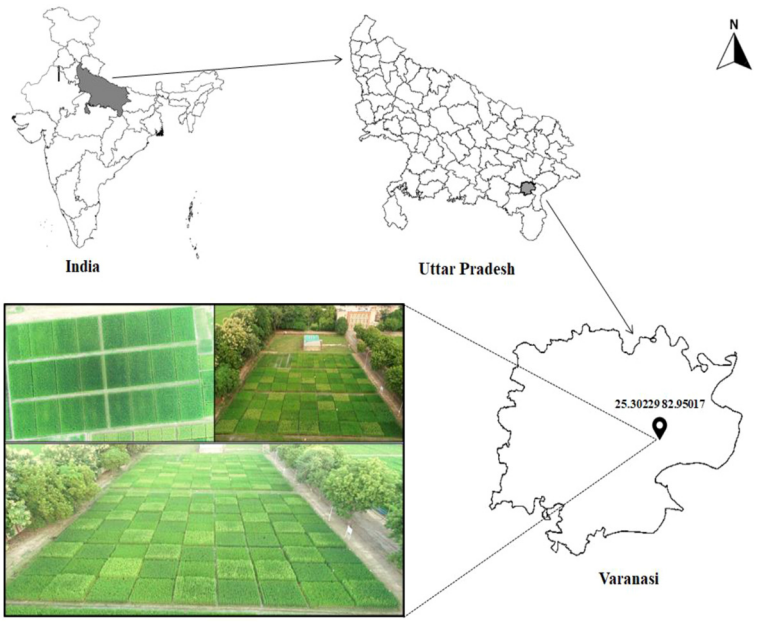

FIGURE 1
Location of study sites. Comparable to Conventional farming (CF), Organic farming (OF), Integrated nutrient management (INM) and Conservation agriculture (CA) farming systems.

The management practices, viz. tillage, sowing method, fertilizer application, water management, crop geometry and spacing (between the rice, wheat and mungbean system, as provided in Table 1. It is also same in all the scenarios, 22.5–22.5– 45 cm), and crop varieties used for growing rice, wheat, and maize under different farming scenarios are described in Tables 1, 2. Crop geometry in agronomy refers to the arrangement of the crop plants in each plots, including the shape of the space available for each plant, and the spacing between rows and plants. While in Scenario 1 wheat was sown by broadcasting the seeds and rice was manually transplanted, in Scenario 3 Happy Seeder machine was used for seeding both rice and wheat.

Fertilizer management practices for different crops under the four scenarios were: Scenario 1 – 120 kg Nitrogen (N), 60 kg Phosphorus (P) and 40 kg Pottassium (K) per ha for rice and wheat, Scenario 2 - bio-inputs (BGA, Azolla, Vermivash, Vermicompost, FYM) for both rice (BGA and Azolla only applicable for paddy) and wheat, and Scenario 3 using 75% of RDF along with 25% bio-inputs (bio-liquid formulations: details mentioned in Table 1) and Scenario 4 - Site-Specific Nutrient Management (SSNM) and 25% bio-inputs (bio-liquids formulations). The specific quantities for SSNM are detailed in Tables 1, 2. For SSNM, 75% RDF (90:45:30 NPK) with 25% from bio-inputs was used. RDF in Scenario 1 is the same as specified for other scenarios, except when combined with bio-inputs.

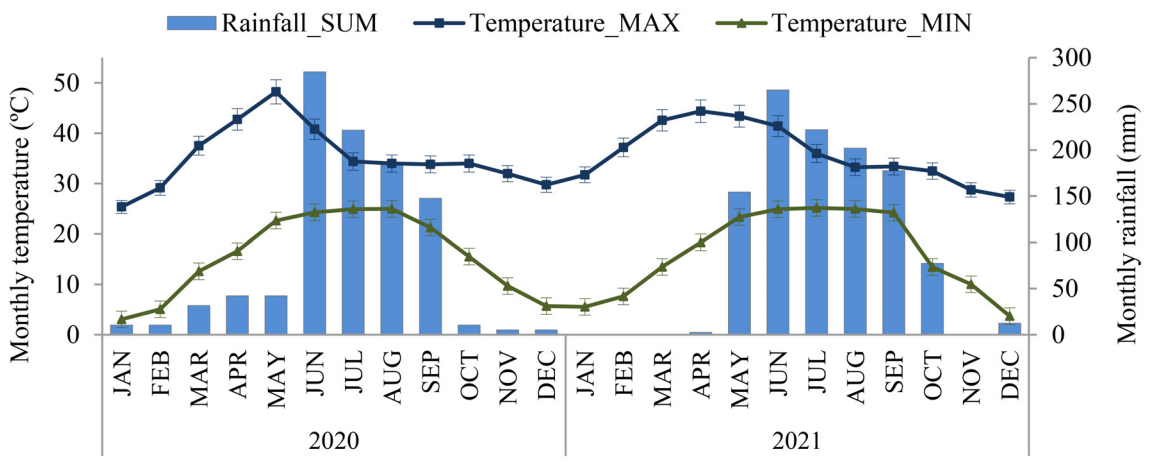

FIGURE 2
Monthly average maximum-minimum temperature and rainfall distribution for 2020 and 2021.

10.3389/fpls.2024.1408515

TABLE 1 Tillage, seed rate, cropping system, and agronomic management practices followed under the four farming scenarios.

Management practices	Scenario 1 (CF*)	Scenario 2 (OF*)	Scenario 3 (INM*)	Scenario 4 (CA*)
Field Preparation	Rice: CT Wheat: CT	Rice: CT Wheat: RT Mungbean: ZT	Rice: ZT Wheat: ZT	Rice: ZT Wheat: ZT Mungbean: ZT
Seed rate (kg ha^{-1})	Rice: 25 Wheat: 100 -	Rice: 25 Wheat: 100 Mungbean: 20	Rice: 25 Wheat: 100	Rice: 25 Wheat: 100 Mungbean: 20
Sowing method	Manual transplanting of rice and broadcasting of wheat	Manual transplanting in rice and seed drill sowing in wheat and mungbean	Seeding with a happy seeder machine	Manual transplanting in rice and seed drill sowing in wheat and mungbean
Crop geometry & spacing (cm)	Random	(22.5– 22.5– 45 cm)	(22.5– 22.5– 45 cm)	(22.5– 22.5– 45 cm)
Fertilizer (Nitrogen-Phosphorus and Potassium; NPK) in kg ha^{-1}	Rice: 120:60:40	Nutrients applied through bio-inputs** (Table 1A)	75% RDF (90:45:30 NPK) + 25% through bio-inputs** (in the form of bioliquids: This bio-liquid is a new formulation of ISARC and Grassroot Energies Pvt. Ltd, which contains 1% of nitrogen, 0.2% of P and 0.5% of K). Quantity: 200 L/ha, time of application: Basal (0-15), 30-40 DAS and 60-70 DAS)	Nutrients applied through SSNM + 25% of bio-inputs** (basal dose FYM @ 3 t/ha)
Water management *(no. of Irrigation)*	Rice: Soil was wet for up to 20 days after sowing Irrigation applied at hair-line cracks (30-35 irrigations). Wheat: 3-4	Rice: Soil was wet for up to 20 days after sowing Irrigation applied at hair-line cracks (25-30 irrigations) Wheat: 3-4 Mungbean: 1-2	Rice: After transplanting, Irrigation was done by alternate wet and dry methods (20-25 irrigation) Wheat: 3-4	Rice: After transplanting, Irrigation was done by alternate wet and dry methods (20-25 irrigation) Wheat: 3-4 Mungbean: 1-2
Crop Varieties	Rice: Arize 6444 Gold Wheat: PBW 187	Rice: Arize 6444 Gold Wheat: PBW 187 Mungbean: Virat	Rice: Arize 6444 Gold Wheat: PBW 187	Rice: Arize 6444 Gold Wheat: PBW 187 Mungbean: Virat

*CF, Conventional Farming; OF, Organic farming; INM, Integrated nutrient management; CA, Conservation agriculture practices; RDF, Recommended dose of fertilizer; CT, Conventional tillage; RT, Reduce tillage; ZT, Zero tillage practices.
**Bio-inputs OF- Azolla*, BGA*, Vermicompost, Vermiwash and Mycorrhiza.

Water management practices also varied, with Scenarios 1 and 2 using frequent irrigations for rice and wheat and Scenario 3 and 4 using alternate wet and dry (AWD) methods. The exact number of irrigations for each scenario is as follows: Scenario 1: 30 irrigations for rice, 3 for wheat; Scenario 2: 26 irrigations for rice, 3 for wheat, 1 for mungbean; Scenarios 3 and 4: 22 irrigations for rice, 3 for wheat, 1 for mungbean.

The crop varieties used in all scenarios were Arize 6444 Gold for rice, PBW 187 for wheat, and Virat for mungbean. These varieties

TABLE 1A Seed treatments and nutrients applied through bio-inputs.

Growth stage	DAS	Bio-inputs					
		Trichoderma (g/kg seed)	Azolla* (t/ha)	BGA: Blue-green algae* (kg/ha)	Vermicompost (t/ha)	Vermiwash (L/ha)	Mycorrhiza (kg/ha)
Seed treatment	–	10	–	–	–	–	–
Basal	0-15	–	1	15	3	200	10
Active tillering	30-40	–	–	–	3	200	–
Panicle initiation	60-70	–	–	–	3	200	–

DAS, Days after sowing, (*applicable only for rice crop).

10.3389/fpls.2024.1408515

TABLE 2 Crop establishment method, cropping pattern and residue management under the four farming scenarios.

Scenarios	Treatments	Crop Rotation	Tillage	Crop establishment method	Residue Management	Water management
Scenario 1	CF*	Rice-wheat-fallow	Rice: CT Wheat: CT	Rice: Puddled transplanted rice (PTR) with random geometry Wheat: Conventional till (CT) with broadcast seedling	All crop residue removed	Border irrigation
Scenario 2	OF*	Rice-wheat-mungbean	Rice: CT Wheat: RT Mungbean: ZT	Rice: Puddled transplanted rice (PTR) with random geometry Wheat: Reduce tillage (RT) - line seedling Mungbean: Zero tillage (ZT) with row geometry	Rice & Wheat: 30% anchored residue retained Mungbean: Fully incorporated	Border irrigation
Scenario 3	INM*	Rice-wheat-fallow	Rice: ZT Wheat: ZT	Rice: Puddled transplanted rice (PTR) with random geometry Wheat: Zero tillage (ZT) - drill seedling	All crop residue incorporated (30% of the above ground biomass- only straw)	Alternate wet drying (AWD)
Scenario 4	CA*	Rice-wheat-mungbean	Rice: ZT Wheat: ZT Mungbean: ZT	Rice: Puddled transplanted rice (PTR) with random geometry Wheat: Zero tillage (ZT) - drill seedling Mungbean: Zero tillage (ZT) - drill seedling	All crop residue incorporated (30%)	Alternate wet drying (AWD)

*CF, Conventional Farming; OF, Organic farming; INM, Integrated nutrient management; CA, Conservation agriculture practices; CT, Conventional tillage; RT, Reduce tillage; ZT, Zero tillage practices.

were selected based on their suitability and high yield potential in Eastern Uttar Pradesh, India.

2.3 Soil sampling and analysis

After two cropping system cycles (2020-2022), soil samples were collected from the surface layer (0-15 cm) randomly within each plot by using an auger. Three samples within a plot were thoroughly mixed to make composite samples. Composite samples were air-dried under shade. One portion of the sample was ground and the whole amount was filtered using 2.0 mm sieve as per the requirement of different parameter analysis.

TABLE 3 Initial soil properties of the experiment site before commencement of study.

Properties	Value	Method Used
Sand (%)	58	Particle size analysis
Slit (%)	20	
Clay (%)	22	
Textural class	Sandy clay loam	USDA triangle
Bulk density (g cm^{-3})	1.66 ± 0.03	Blake and Hartge, 1986
pH (1:2.5 soil: water)	7.94 ± 0.03	Jackson, 1967
EC (dS m^{-1})	0.151 ± 1.37	Jackson, 1967
Organic carbon (SOC%)	0.53 ± 0.03	Walkley and Black's method
Available N (kg ha^{-1})	143.1 ± 3.66	Subbiah and Asija, 1956
Available P (kg ha^{-1})	36.2 ± 3.60	Olsen et al., 1954
Available K (kg ha^{-1})	46.4 ± 2.05	

The initial soil properties (pH, EC, organic carbon, and available N, P, K) were estimated in air-dried samples using standard protocols (Table 3).

2.3.1 Soil organic carbon stock calculation

Soil organic carbon (SOC) content of the soils under different treatments was determined, following Walkley and Black's method. SOC stock was calculated using the following formula given below (Datta et al., 2015).

$$SOC\ stock\ in\ soil = C\ content \times BD \times Soil\ depth$$

Where 'SOC stock' is in g ha^{-1}, 'C content' is given in g-C kg^{-1}, 'BD' is the bulk density of soil in g cm^{-3} and 'soil depth' is in cm.

2.3.2 SOC fractions of different oxidizability

Based on the hypothesis that sulphuric acid dilution generates less heat of dilution, three labile fractions of oxidizable SOC were determined using Wakley and Black's methods. By lowering sulphuric acid normality, which is 24, 18, and 12 N H_2SO_4 equivalent, the amount of C thus calculated permitted apportionment of total organic Carbon into four separate pools, which is Pool 1 (OC oxidisable by 12 N H_2SO_4), Pool 2 (Difference in C oxidizable by 18~12 *N* H_2SO_4), Pool 3 (Difference in C oxidisable by 24~18 *N* H_2SO_4) and Pool 4 (Difference between C_{tot} and C oxidisable by 24 N H_2SO_4) (Samal et al., 2017).

$$\text{Active pool} = \Sigma\ (\text{OC oxidisable by 12 N } H_2SO_4) + (\text{Difference in C oxidizable by 18} \sim \text{12 N } H_2SO_4)$$

$$\text{Passive pool} = \Sigma\ (\text{Difference in C oxidisable by 24} \sim \text{18 } N\ H_2SO_4) + (\text{Difference between } C_{tot} \text{ and C oxidisable by 24 } N\ H_2SO_4)$$

2.3.3 Soil biological analyses

Fresh soil samples were sieved using a 2-mm sieve and sent to the laboratory to evaluate various soil biological characteristics (SMBC, dehydrogenase activity, alkaline phosphatase activity, soil respiration and microbial count). SMBC was calculated using the chloroform fumigation methods (Vance et al., 1987). Dehydrogenase and alkaline phosphatase activities were estimated as described by Dick et al. (1996).

We used the pour plate method for isolating and counting the viable microorganisms present in the soil, which is added with or before molten agar medium before solidification (Zuberer, 1994). The plate was incubated at 32°C inside an incubator and allowed to grow. Colonies were counted after 3 days. To prevent bacterial growth, a total fungal count was performed on rose bengal agar medium (RBA) treated with streptomycin (Martin, 1950). For five days, the plate was incubated at 30°C. Total actinomycetes were counted on actinomycetes isolation agar (AAI) plates that were treated with nalidixic acid to inhibit fungal growth (HiMedia Manual, 2009). AAI plates were incubated at 28°C for seven days.

2.4 Crop harvest and yield estimation

At crop maturity, rice, wheat and mungbean crops were harvested manually from 2×2 m^2 randomly selected three places from each plot for recoding the grain yield. System productivity was calculated on rice equivalent yield (RQY) basis for wheat and mungbean to express the overall impact of treatments. Grain yield was reported at 15% moisture. System productivity (t ha^{-1}) was computed using the following Equation.

$$\text{Rice equivalent yield non rice crop } (t\ ha-1) = \frac{\text{Non rice crop yield (t ha} - 1) \times \textit{MSP of non rice crop } (INR\ q-1)}{\text{MSP of rice (INR q} - 1)}$$

Where, MSP- minimum support price and INR-Indian Rupees.

2.5 Statistical analysis and evaluation

The Windows-based XLSTAT software program was used to calculate the mean of the data that was analyzed for each parameter and then processed for analysis of variance (ANOVA) to establish the statistical significance of the consequences of various scenarios. The data were subjected to variance analysis to identify relevant effects, and the means were compared using Tukey's HSD test as a *post hoc* mean separation test (P 0.05). Bivariate Pearson's correlation coefficients, regression equations, and PCA were computed for all soil variables, namely pH, EC, SOC, BD, DHA, APA, MBC, fungus, bacteria, actinomycetes, and soil respiration under different farming scenarios.

2.6 Ethics declaration

No human based study was performed in this work. Experiments were as per the IRRI mandate.

3 Results and discussion

3.1 Soil chemical properties in different scenarios

The present study investigated the effect of different scenarios on soil chemical properties. The results showed no significant differences in bulk density (BD), pH, EC, and water holding capacity (WHC) among the four farming scenarios. Growing rice and wheat under different farming scenarios exerted a significant impact on SOC, available N, available P and available K (Table 4). The SOC content ranged from 0.49% to 0.59% among the farming scenarios; the highest value was observed in Scenario 2. The SOC stock was the highest in Scenario 4 (13.75 Mg C ha^{-1}) and the lowest in Scenario 1 (12.65 Mg C ha^{-1}). The variations in SOC content and stock can be attributed to the management practices in each scenario, such as the type and amount of organic inputs, tillage practices, and cropping systems. The available N was the highest in Scenario 1 (144 kg ha^{-1}) and the lowest in Scenario 2 (140 kg ha^{-1}), while available K was highest in Scenario 2 (56 kg ha^{-1}) and lowest in Scenario 3 (38 kg ha^{-1}). The available P was highest in Scenario 1 (38.5 kg ha^{-1}) and lowest in Scenario 3 (12 kg ha^{-1}).

The differences in available nutrient content among the scenarios can be due to the differences in the soil organic matter content and the

TABLE 4 After two years of the experiment, the effect of soil characteristics in various scenarios of agricultural practices.

Scenarios*	BD (g cm^{-3})	pH (1:2.5)	EC (dS m^{-1})	WHC (%)	SOC (%)	SOC stock (Mg C ha^{-1})	Av. N (kg ha^{-1})	Av. K (kg ha^{-1})	Av. P (kg ha^{-1})
Scenario 1	1.73 ± 0.03^{a}	7.98 ± 0.03^{a}	0.123 ± 0.01^{a}	55.0 ± 1.96^{a}	0.49 ± 0.02^{a}	12.65 ± 0.44^{a}	144.0 ± 4.00^{a}	53.0 ± 2.5^{a}	38.5 ± 1.5^{a}
Scenario 2	1.65 ± 0.06^{a}	7.83 ± 0.07^{a}	0.113 ± 0.01^{a}	57.3 ± 1.41^{a}	0.59 ± 0.06^{a}	14.53 ± 0.06^{a}	140.0 ± 8.00^{a}	56.0 ± 4.0^{a}	38.0 ± 3.0^{a}
Scenario 3	1.67 ± 0.02^{a}	7.97 ± 0.06^{a}	0.143 ± 0.02^{a}	57.0 ± 1.73^{a}	0.51 ± 0.02^{a}	12.72 ± 0.04^{a}	142.3 ± 7.25^{a}	38.0 ± 1.0^{b}	12.0 ± 1.1^{c}
Scenario 4	1.66 ± 0.01^{a}	7.93 ± 0.06^{a}	0.123 ± 0.01^{a}	57.0 ± 2.65^{a}	0.55 ± 0.06^{a}	13.75 ± 0.50^{a}	150.7 ± 3.56^{a}	45.0 ± 7.0^{ab}	18.0 ± 2.0^{b}
Pr>F(Model)	0.059	0.834	0.132	0.271	0.039	0.920	0.853	0.001	0.0001
Significant	No	No	No	No	No	No	No	Yes	Yes

*Scenario1 - CF (Conventional Farming), Scenario2 - OF (Organic farming), Scenario3 - INM (Integrated nutrient management), Scenario 4 - CA (Conservation agriculture practices); EC, Electric Conductivity; BD, Bulk density; SOC, Soil organic carbon; Av. N, Available nitrogen; Av. K, Available potassium; Av. P, Available phosphorus.
Alphabetical symbols (a, b, c etc.) denoted the significance difference between the data.

nutrient management practices. The findings of this study are consistent with previous studies (Lal, 2004). Magnitude of SOC stocks at any place is decided by various governing parameters, such as, land use pattern, extent of land degradation, soil type, depth profile and total input of biomass C annually. Therefore, practices that increase SOC content, such as conservation tillage, cover cropping, and organic amendments can enhance soil quality and crop productivity. SOC is one of the most important sustainability parameter of soil health and agricultural sustainability that work at the ecosystem interface (Shelef et al., 2018; Mishra et al., 2022b). It also helps quantitatively in mitigating the net rate of greenhouse gas emissions.

The results suggest that management practices that enhance SOC content could improve soil fertility and nutrient availability. Further studies are needed to investigate the long-term effects of different management practices on soil properties and crop productivity.

3.2 Scenario-specific alterations in soil biological properties

3.2.1 Soil microbial properties

Significant differences in microbial biomass carbon (MBC), microbial biomass nitrogen (MBN), dehydrogenase activity (DHA), alkaline phosphatase activity (APA), and urease activity (UA) were observed among the four farming scenarios. values of MBC and MBN ranged from 107.9 to 194.0 and 74.4 to 134.2 μg g^{-1} in dry soil, with the lowest values in Scenario 1 and the highest in Scenario 2. In Scenario 2, SMBC and SMBN were 79.9% and 80.6%, respectively and these were statistically higher than in Scenario 1.

Soil dehydrogenase activity (DHA), alkaline phosphatase activity (APA), and urease activity (UA) in different farming practices are presented in Table 5. There were significant differences among farming scenarios for DHA and APA, but UA was similar in different scenarios. The DHA ranging from 21.06 to 36.80 μg TPF g^{-1} h^{-1} was found in the order: Scenario 3< Scenario 1< Scenario 4 ≤ Scenario 2. Compared to Scenario 1, DHA was 22.74% lower in Scenario 3 but 42.35% and 5.02% higher in Scenario 2 and Scenario 4, respectively, from Scenario 1.

The highest values of MBC and MBN were recorded in Scenario 2, which suggests a higher potential for C and N cycling in this scenario compared to the others. Similarly, Scenario 2 also showed the highest values for DHA and APA, the indicators of soil microbial activity and nutrient availability, respectively. These results suggest that Scenario 2 is likely to have a more active and diverse microbial community, which is known to play a critical role in SOM decomposition and nutrient cycling (Li et al., 2019). Microbiomes also play an important role in nutrient acquisition, protection from pathogens, boosting plant immunity, competition, tolerances to abiotic stresses, and phytohormone production. Scenario 1 and Scenario 3 had the lowest MBC, MBN, and DHA values, indicating relatively lower microbial biomass and activity. It may be attributed to soil contaminants or environmental stressors, negatively affecting soil microbial communities (Bastida et al., 2016). Scenario 4, on the other hand, showed intermediate values for all the parameters tested, indicating a moderate level of soil microbial activity and nutrient availability. The similar and high UA values observed in all the scenarios suggest that the soil has a high capacity for nitrogen mineralization, which is essential for plant growth and productivity (Kumar et al., 2019). However, it is worth noting that excessive UA can lead to N leaching and subsequent environmental degradation. Thus, high UA values suggest that precise and site-specific N management practices should be implemented to minimize the negative ecological impacts. Previous studies have reported a negative correlation between soil depth and enzyme activity, specifically with regards to sucrase and urease (Taylor et al., 2002; Xu et al., 2022). The presence of increased levels of oxygen and nutrients (provided by organic/bio inputs) within the topsoil fostered a heightened state of microbial activity, and consequently leading to a greater degree of biochemical reactions occurring within the soil. Studies have consistently demonstrated that the use of nature based, organic, bio-inputs amendments leads to a significant increase in the activity of enzymes such as urease in the soil (Lazcano et al., 2013; Liang et al., 2014). Their finding suggests that soil amendments have a positive impact on the biochemical properties of soil.

The results of this study provide valuable insights into the microbial community structure and soil nutrient dynamics in different scenarios. The high values of MBC, MBN, DHA, and APA observed in Scenario 2 suggest that organic farming has the potential for enhanced soil health and productivity. Further research is needed to determine the underlying factors responsible for the observed differences among the scenarios and to develop effective management strategies for improving soil quality and productivity.

TABLE 5 Effect of cropping system and different agriculture practices on soil microbial properties after two years of the experiment.

Scenarios	Microbial biomass carbon (μg g^{-1})	Microbial biomass nitrogen (μg g^{-1})	Dehydrogenase activity (μg TPF h^{-1} g^{-1})	Alkaline phosphatase activity (μg p- soil g^{-1} h^{-1})	Urease activity (mg urea g^{-1} soil h^{-1})
Scenario 1	107.8 ± 5.14^{b}	74.30 ± 3.50^{b}	25.85 ± 0.88^{ab}	7.96 ± 0.62^{b}	180.5 ± 2.58^{a}
Scenario 2	194.0 ± 23.3^{a}	134.2 ± 16.1^{a}	36.80 ± 0.37^{a}	13.4 ± 4.54^{a}	185.5 ± 1.50^{a}
Scenario 3	111.1 ± 7.10^{b}	76.90 ± 4.90^{b}	21.06 ± 0.40^{b}	7.87 ± 0.27^{b}	180.9 ± 5.51^{a}
Scenario 4	159.7 ± 13.8^{ab}	116.8 ± 10.1^{ab}	27.15 ± 5.29^{ab}	11.9 ± 0.63^{ab}	187.7 ± 1.43^{a}

Where; Scenario1- Conventional farming; Scenario2- Organic farming; Scenario3- Integrated nutrient management; Scenario4- Conservation agriculture practices.
Alphabetical symbols (a, b, c etc.) denoted the significance difference between the data.

10.3389/fpls.2024.1408515

3.2.2 Soil respiration and microbial population (fungi, bacteria and actinomycetes) count

The results listed in Table 6 show that the total bacterial counts ranged from 11.2 ± 1.3 to 24.3 ± 0.1 × 105 CFU g^{-1} soil, with the highest abundance in Scenario 2, followed by Scenario 4, Scenario 3, and Scenario 1. In contrast, fungi count ranged from 6.70 ± 0.6 to 13.0 ± 1.4 × 104 CFU g^{-1} soil, with the highest abundance observed in Scenario 2, followed by Scenario 4, Scenario 1, and Scenario 3. The actinomycetes count ranged from 6.80 ± 1.5 to 16.7 ± 1.4 × 105 CFU g^{-1} soil, with the highest abundance observed in Scenario 2, followed by Scenario 4, Scenario 3, and Scenario 1. These results suggest that farming scenarios can differently affect soil microbial communities and that some scenarios may be more favorable to certain microbial groups than others.

Compared to Scenario 1 the count of bacteria and actinomycetes were 117.9%, 143.9% higher in Scenario 2, 34.3%, 17.1% higher in Scenario 3 and 103%, 51.2% higher in Scenario 4, respectively. In fungi, Scenario 1, Scenario 2 and Scenario 4 showed 65%, 95% and 50% higher population, respectively than Scenario 3. The trend of microbial counts in the four farming scenarios was in the order as listed in Table 6A.

The soil respiration rates ranged from 52.3 ± 1.4 to 56.7 ± 1.5 µg g^{-1} d^{-1}, with no significant differences observed among the farming scenarios. It suggests that different scenarios did not significantly affect the metabolic activity of soil microorganisms. It is important to note that soil respiration is influenced by various factors, such as soil moisture, temperature, and substrate availability, which were not measured in this study. Therefore, further investigation is needed to fully understand the relationship between soil microbial communities and soil respiration in different scenarios.

The findings of the present study are consistent with previous research that has shown the influence of different management practices on soil microbial communities and their activities (Zhang et al., 2020). It is a well-known fact that organic farming is mostly dependent on the soil's natural microflora, organic biofertilizers and use of bio-pest control chemicals. When nature based biofertilizers (PGPRs) are applied as seed priming bio-agents or soil inoculants, they multiply and participate in nutrient cycling/availability and benefit the crop in many ways. The application of PGPRs, nitrogen fixers, phosphate solubilizers and AMF improves plants' performance by enhancing nutrient availability, phyto-hormone production and pest-pathogen control (Mohanram and Kumar, 2019; Poonam et al., 2017; Upadhyay et al., 2018). Further research is needed to fully understand these responses' mechanisms and develop effective management strategies for enhancing soil health and productivity.

3.3 Soil penetration and organic carbon fractions of different oxidizability

The measured soil penetration resistance values at different soil depths and scenarios are presented in Figure 3. The results indicate variations in soil compaction across the different scenarios and depths. At a soil depth of 5 cm, all scenarios exhibited relatively low penetration resistance values, ranging from 0.07 MPa to 0.14 MPa. This suggests minimal compaction at this shallow depth, which could be attributed to reduced external forces or a less compacted topsoil layer. As the depth increased to 10 cm, the soil penetration resistance values generally doubled across all scenarios. This suggests a gradual increase in soil compaction, potentially due to increased weight-bearing and compaction forces exerted on the underlying soil layers. At a depth of 15 cm, significantly higher soil penetration resistance values were observed compared to the shallower depths, ranging from 0.47 MPa to 1.45 MPa.

The data as plotted in Figure 3 suggest the presence of compacted soil layers, which can hinder plants' root growth and nutrient uptake. The soil penetration resistance values at depths of 20 cm, 25 cm, and 30 cm remained relatively constant across all scenarios, with values ranging from 1.80 MPa to 2.93 MPa. These consistently high resistance values indicate considerable soil compaction at these depths, which may limit root penetration and water movement through the soil profile. The variations in soil penetration resistance across the farming scenarios highlight the impact of different agricultural practices or land use patterns on soil compaction. Further investigations are necessary to identify the specific factors contributing to these differences.

Organic farming systems had a (46%) higher pool of very labile C (CVL) compared to conventional (p=0.05). Soils under rice–wheat-mungbean cropping systems (Scenario 2 & Scenario 4) exhibited larger very labile C pool than in soils under Scenario 1 & Scenario 3. The results showed that the distribution of SOC fractions varied significantly among the four scenarios. In Scenario 1, the easily oxidizable fraction (CVL) had the highest proportion (0.30), followed by moderately oxidizable (CL, 0.08), slowly oxidizable (CLL, 0.04), and non-oxidizable (CNL, 0.07) fractions. In Scenario 2, the proportion of CVL was the highest (0.44), followed by CNL (0.07), CL (0.05), and CLL (0.03). In Scenario 3,

TABLE 6 Respiration of soil and the count population of fungi, bacteria, and actinomycetes.

Scenarios	Total bacteria (CFU* × 10^5 g^{-1} soil)	Fungi (CFU × 10^4 g^{-1} soil)	Actinomycetes (CFU × 10^5 g^{-1} soil)	Soil respiration (µg g^{-1} d^{-1})
Scenario 1	11.2 ± 1.3^b	11.0 ± 3.5^a	6.80 ± 1.5^b	56.7 ± 1.5^a
Scenario 2	24.3 ± 0.1^a	13.0 ± 1.4^a	16.7 ± 1.4^a	52.3 ± 1.4^a
Scenario 3	15.0 ± 3.0^b	6.70 ± 0.6^a	8.00 ± 1.0^b	53.7 ± 1.0^a
Scenario 4	22.7 ± 8.4^a	10.0 ± 1.0^a	10.3 ± 1.5^a	52.3 ± 1.5^a

*CFU, Colony forming unit; Scenario 1- Conventional farming; Scenario 2- Organic farming; Scenario 3- Integrated nutrient management; Scenario 4- Conservation agriculture practices.

10.3389/fpls.2024.1408515

TABLE 6A Effect of different farming practices on soil microbial population and soil respiration in order.

Parameters	Order in four scenarios*	Significant
Bacteria	Scenario 2 ≥ Scenario 4 > Scenario 3 > Scenario 1	Yes; p>0.0001
Actinomycete	Scenario 2 > Scenario 4 > Scenario 3 > Scenario 1	Yes; p>0.0001
Fungi	Scenario 2 > Scenario 1 ≥ Scenario 4 > Scenario 3	No; p>0.078
Soil respiration	Scenario 3 > Scenario 2 ≥ Scenario 4 > Scenario 1	No; p>0.229

*Scenario 1- Conventional farming; Scenario 2- Organic farming; Scenario 3- Integrated nutrient management; Scenario 4- Conservation agriculture practices.

the CVL fraction had the highest proportion (0.26), followed by CNL (0.09), CL (0.10), and CLL (0.06). In Scenario 4, the proportion of CVL was highest (0.38), followed by CNL (0.10), CLL (0.03), and CL (0.03) (Figure 4).

This study showed that different management scenarios significantly affected the distribution of SOC fractions in the soil. The organic farming (Scenario 2) had the highest proportion of easily oxidizable SOC, consistent with previous studies showing that organic management practices can increase the amount of labile C in the soil (Chen et al., 2019). This suggests organic management practices can promote SOC turnover and improve soil fertility. The conservation agriculture scenario (Scenario 4) also had a high proportion of easily oxidizable SOC, possibly due to cover crops and reduced tillage, which can enhance SOM (García-Orenes et al., 2013; Mishra et al., 2022b). Although it is generally acknowledged that soil organic matter is primarily concentrated in the top 30 cm of the soil, there is mounting evidence that, despite the concentrations in the subsoil, deeper soil horizons have the ability to sequester significant amounts of SOC. The standard fixed depth of approximately 1 m is typically regarded appropriate in routine soil surveys, which is one factor contributing to the uncertainty. In light of this, it is still unsure how much the worldwide SOC budget has been underestimated.

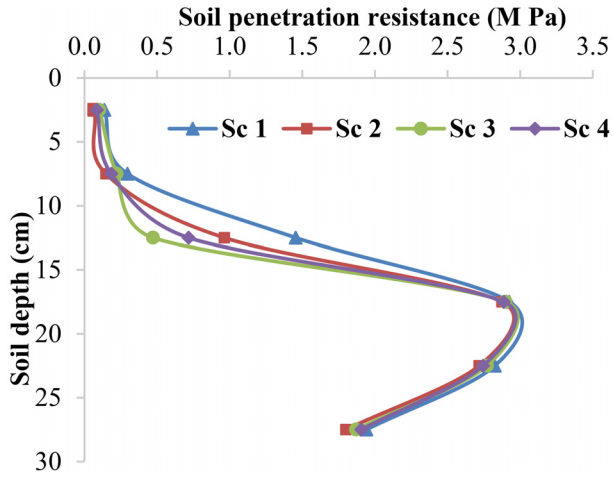

FIGURE 3
Resistances to soil penetration (M Pa) with depth increase (0-30) under different scenarios.

Further, this research is of relatively short duration (2020-2022). While our research provides important insights into the immediate and short-term effects of various farming practices on soil health and carbon dynamics, these findings may not fully capture the long-term implications. Soil processes, especially those related to carbon sequestration and microbial community shifts, often require extended periods to manifest significant and sustained changes. Future research focused on long-term studies to better understand the enduring effects of these agricultural practices on soil health, carbon storage, and overall ecosystem resilience is needed. This will help to validate the findings presented here, providing a more comprehensive understanding and benefits of sustainable farming practices over time.

3.4 Correlation matrix among all soil physicochemical and biological properties

Significant coefficients of correlations ($p \leq 0.01$ and $p \leq 0.05$) were observed among most soil physicochemical and biological properties, irrespective of different farming scenarios. Based on the correlation coefficients listed in Figure 5, it can be inferred that there are strong correlations between some of the variables.

There is a strong negative correlation (- 0.577) between BD and SOC (%). This suggests that as BD increases, SOC decreases, and vice versa. Similarly, a strong negative correlation exists between SOC and soil pH (- 0.485) indicating that as pH decreases, SOC tends to increase. There is also a strong positive correlation (0.889) between available P (Av. P) and available K (Av. K). This suggests that as the concentration of one nutrient increases, the concentration of the other also tends to increase.

There are strong positive correlations between some soil biological properties, such as bacteria and actinomycetes (r = 0.660), and between bacteria and fungi counts (r = 0.763). These correlations suggest that these microorganisms tend to coexist and influence each other's populations in the soil. Additionally, there is a strong positive correlation (0.662) between total glomalin-related soil protein (TGRSP) and soil respiration (SR), which suggests that TGRSP may be contributing to soil respiration the ecosystem (Figure 5).

3.5 Crop yield and rice equivalent system yield

Table 7 presents the crop yield data from different agricultural practices during the 2020-21 and 2021-22 periods. In the Kharif season of 2020-21, the highest rice yields were obtained from Scenario 3 (4.55 ± 0.20 t ha^{-1}), closely followed by Scenario 1 (4.35 ± 0.26 t ha^{-1}), while Scenario 2 (2.88 ± 0.21 t ha^{-1}) exhibited the lowest yield. Similarly, during the Rabi season, Scenario 3 (3.66 ± 0.19 t ha^{-1}) and Scenario 1 (4.03 ± 0.17 t ha^{-1}) showed comparable yields, while Scenario 2 (3.00 ± 0.17 t ha^{-1}) lagged. When considering the system yield (system productivity), which represents the overall productivity across all seasons, Scenario 4 (10.95 ± 0.49 t ha^{-1}) emerged as the most

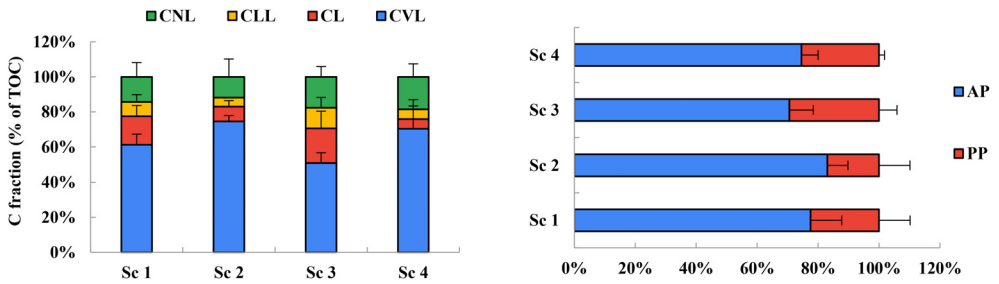

FIGURE 4
Distribution of soil organic carbon fractions of different lability (as % of total organic C) in different farming practices under rice-based cropping system. (Where; Scenario 1- Conventional farming, Scenario 2- Organic farming, Scenario 3- Integrated nutrient management, Scenario 4- Conservation agriculture practices; CVL- Very Labile; CL- Labile; CLL- Less Labile and CNL- Non-Labile).

productive approach, significantly outperforming the other scenarios. It was followed by Scenario 1 (8.54 ± 0.44 t ha^{-1}) and Scenario 3 (8.35 ± 0.40 t ha^{-1}), while Scenario 2 (7.08 ± 0.42 t ha^{-1}) exhibited the lowest overall yield.

These results suggest that conservation agriculture, characterized by practices such as reduced tillage and soil cover, can significantly enhance crop productivity (Kumar et al., 2021). The observed variations in crop yields can be attributed to multiple factors, including differences in soil health, nutrient availability, pest management (Mishra et al., 2015; Kumar et al., 2022), and overall management practices associated with each farming approach.

Use of organic fertilizers as opposed to chemical fertilizers can effectively mitigate soil erosion and minimize the potential for aquatic ecotoxicity. Moreover, the implementation of organic farming practices has been found to have a positive impact on soil biodiversity and the presence of both macro and microorganisms. This, in turn, leads to increased income per hectare. However, it is important to note that the yield of crops may be lower when employing OF practices, with a reduction of up to 22%. As per the existing literature, empirical evidence suggests that application of organic fertilizers may result in a decrease in crop yields per hectare. Notably, studies have consistently demonstrated reductions of

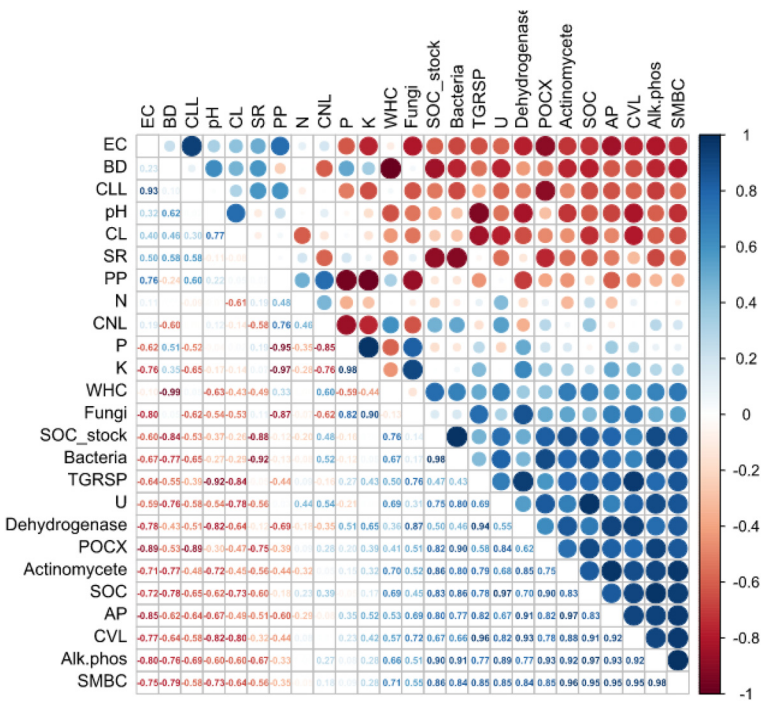

FIGURE 5
Correlation coefficients (r) among different soil physiochemical and biological properties across all the treatments. (*Values in bold are different from 0 with a significance level alpha ≤ 0.05*) Where; BD, Bulk density; pH, Potential of hydrogen; EC, Electric conductivity; WHC, Water holding capacity; SOC, Soil organic carbon; N, Available nitrogen; K, Available potassium; P, Available phosphorus; SMBC, Soil microbial biomass carbon; Alk.phos, Alkaline phosphatase activity; U, Urease activity; TGRSP, Total glomalin related soil protein; POXC, Permanganate oxidizable carbon; CVL, Carbon very labile; CL, Carbon labile; CLL, Carbon less labile; CNL, Carbon non-labile; AP, Active pool; PP, Passive pool; SR, Soil respiration.

10.3389/fpls.2024.1408515

TABLE 7 In the year 2020-22, pooled yield data (mean ± SD) and system yield (t ha^{-1}) as affected by different farming practices followed in four scenarios.

Scenarios[1] \Season	2020-21				2021-22			
	Kharif	Rabi	Zaid	Rice equivalent system yield** (t ha^{-1})	Kharif	Rabi	Zaid	Rice equivalent system yield** (t ha^{-1})
	Rice yield (t ha^{-1})	Wheat yield (t ha^{-1})	Mung bean yield (t ha^{-1})		Rice yield (t ha^{-1})	Wheat yield (t ha^{-1})	Mung bean yield (t ha^{-1})	
Scenario 1 (CF)*	4.35 ± 0.26^{a}	4.03 ± 0.17^{a}	-	08.54 ± 0.44^{a}	5.97 ± 0.36^{a}	4.12 ± 0.20^{a}	-	10.25 ± 0.57^{a}
Scenario 2 (OF)*	2.88 ± 0.21^{b}	3.00 ± 0.17^{b}	0.29 ± 0.01^{a}	07.08 ± 0.42^{b}	2.98 ± 0.18^{b}	3.12 ± 0.16^{b}	0.30 ± 0.02^{a}	07.33 ± 0.42^{b}
Scenario 3 (INM)*	4.55 ± 0.20^{ab}	3.66 ± 0.19^{ab}	–	08.35 ± 0.40^{b}	4.54 ± 0.24^{ab}	3.68 ± 0.22^{ab}	–	08.36 ± 0.47^{b}
Scenario 4 (CA)*	4.09 ± 0.19^{ab}	3.72 ± 0.18^{ab}	0.80 ± 0.03^{a}	10.95 ± 0.49^{a}	4.17 ± 0.21^{ab}	4.05 ± 0.17^{ab}	0.85 ± 0.04^{a}	11.56 ± 0.54^{a}

Where, * Scenario 1- Conventional farming; Scenario 2- Organic farming; Scenario 3- Integrated nutrient management; Scenario 4- Conservation agriculture practices.
1 For Scenario details refer to Table 1.
Different small letters denote significant differences among the value of mean an individual year, across the scenarios.
(The MSP for rice in 2021–22 was 1940 INR/quintal, mung bean MSP was 7275 INR/quintal, and wheat MSP was 2015 INR/ha).

approximately 20-25% and 50% in yields when comparing OF to conventional fertilizers showed the potential benefits associated with the integration of innovative plant breeding technologies, such as CRISPR/Cas9, within the framework of organic farming practices. Whereas, application of chemical fertilizers has been widely recognized for its positive impact on crop production. However, it is important to acknowledge that the use of chemical fertilizers can also have detrimental effects on soil physicochemical properties and subsequently influence the composition and functioning of soil microbiomes.

3.6 Principal component analysis

In the PCA of 21 variables, three principal components were extracted with eigenvalues> 0.9 and these explained 91.18% of the

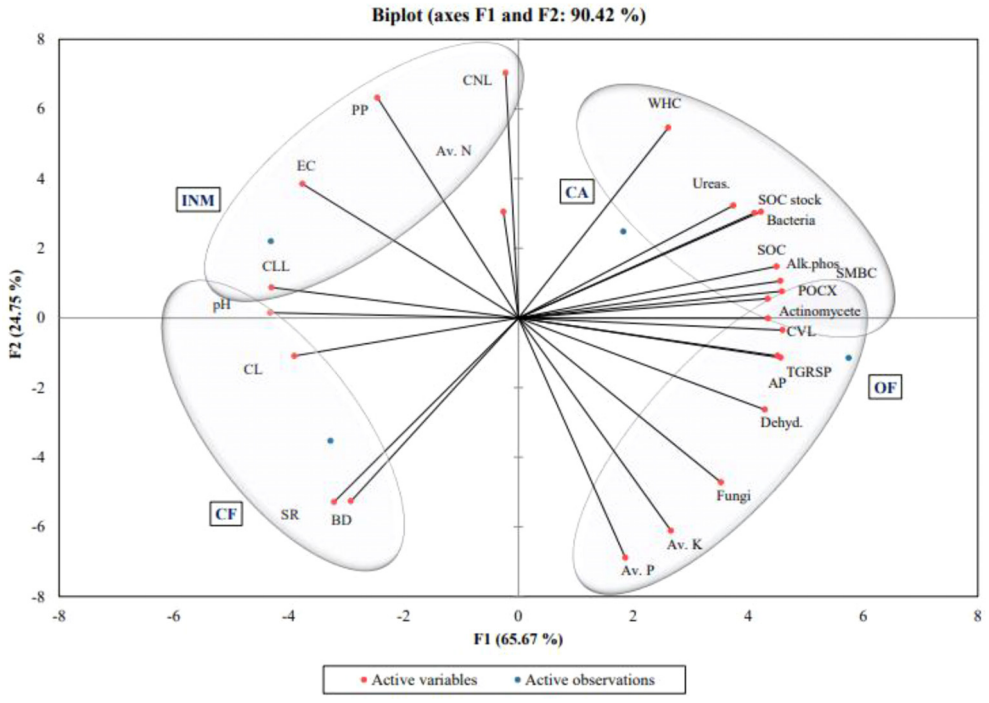

FIGURE 6
Under various agricultural techniques, the principal component analysis of the soil's physical-chemical characteristics, enzyme activity, and microbiological parameters.

variance. A correlation study (Pearson's correlation) was performed for all the variables (Figure 6). One of the most significant indicators of changes in soil quality was found to be the biomass of soil microbes (Stenberg, 1999). Correlations exist between microbial activity in the soil, microbial biomass, enzyme activity and SOM contents (Chaer et al., 2009). All soil microbial characteristics significantly ($p>0.05$) correlated with MBC but not with SOM. Soil MBC was found to be a reliable indicator for determining soil quality. DHA was removed from the MDS to reduce redundancy because it is closely connected to MBC. As a result, the MDS continued to use APA.

Based on PCA, most of the microbiome parameters in organic farming were selected to predict the optimum soil quality by different agricultural practices and qualified as key indicators of soil quality. In the present study, all the indicators except BD, available N, pH, (high and low) labile pool of carbon that were retained in the minimum data set were considered good and when in increasing order, these were scored as "more is better". In contrast, chemical parameters were scored as "less is better".

4 Conclusion and future prospects

The interrelationship between soil characteristics, carbon input, carbon pools, and the soil biome in a Vertisols was found improved in organic and conservation agriculture. Significant effects of the farming scenarios were observed on soil chemical properties, with variations in soil organic carbon, available nitrogen, potassium, and phosphorus. Organic farming exhibited higher soil organic carbon content, while conservation agriculture had the highest soil organic carbon stock. It was also revealed that variations in soil biological properties under organic farming promoted a more active and diverse microbial community. Correlation analysis showed relationships between soil physicochemical and biological properties. The findings highlight the importance of organic farming and conservation agriculture in improving soil quality, nutrient availability, and microbial activity. Conservation agriculture resulted in the highest crop yield, highlighting the efficacy of sustainable practices. As these are the agriculture field based data, findings support for policy development and implementation for large holding farmers for sustainable soil management and production. Further research is needed to understand the underlying mechanisms and develop effective management strategies for enhancing soil health and productivity. To realize the benefits of sustainable production as an integrated strategy, a comprehensive, site-specific framework must be established and scaled.

Data availability statement

The original contributions presented in the study are included in the article/supplementary material. Further inquiries can be directed to the corresponding author.

Author contributions

SS: Conceptualization, Funding acquisition, Investigation, Project administration, Resources, Supervision, Visualization, Writing – original draft, Writing – review & editing. AM: Conceptualization, Data curation, Investigation, Methodology, Writing – original draft, Writing – review & editing. PM: Data curation, Writing – review & editing.

Funding

The author(s) declare financial support was received for the research, authorship, and/or publication of this article. The authors are thankful to International Rice Research Institute (IRRI) for providing the funding and resources that made this research possible.

Acknowledgments

We like to thank our colleagues at IRRI for their support and advice throughout the research process.

Conflict of interest

The authors declare that the research was conducted in the absence of any commercial or financial relationships that could be construed as a potential conflict of interest.

Publisher's note

References

Babu, S., Das, A., Singh, R., Mohapatra, K. P., Kumar, S., Rathore, S. S., et al. (2023). Designing an energy efficient, economically feasible, and environmentally robust integrated farming system model for sustainable food production in the Indian Himalayas. *Sustain. Food Technol.* 1, 126–142. doi: 10.1039/D2FB00016D

Bastida, F., Torres, I. F., Moreno, J. L., Baldrian, P., Ondoño, S., Ruiz-Navarro, A., et al. (2016). The active microbial diversity drives ecosystem multifunctionality and is physiologically related to carbon availability in Mediterranean semi-arid soils. *Mol. Ecol.* 25, 4660–4673. doi: 10.1111/mec.2016.25.issue-18

Bentsen, N. S., Felby, C., and Thorsen, B. J. (2014). Agricultural residue production and potentials for energy and materials services. *Prog. Energy combustion Sci.* 40, 59–73. doi: 10.1016/j.pecs.2013.09.003

Blake, G. R., and Hartge, K. H. (1986). "Bulk density," in *Methods of Soil Analysis*. Ed. A. Klute (ASA and SSSA), 363–375.

Chaer, G., Fernandes, M., Myrold, D., and Bottomley, P. (2009). Comparative resistance and resilience of soil microbial communities and enzyme activities in adjacent native forest and agricultural soils. *Microbial Ecol.* 58, 414–424. doi: 10.1007/s00248-009-9508-x

Chen, Y., Cao, J., Zhao, J., Wu, J., Zou, X., Fu, S., et al. (2019). Labile C dynamics reflect soil organic carbon sequestration capacity: Understory plants drive topsoil C process in subtropical forests. *Ecosphere* 10, e02784. doi: 10.1002/ecs2.2019.10.issue-6

Cheng, H., Yuan, M., Duan, Q., Sun, R., Shen, Y., Yu, Q., et al. (2020). Influence of phosphorus fertilization patterns on the bacterial community in upland farmland. *Ind. Crops Products* 155, 112761. doi: 10.1016/j.indcrop.2020.112761

Das, A., Datta, D., Samajdar, T., Idapuganti, R. G., Islam, M., Choudhury, B. U., et al. (2021). Livelihood security of small holder farmers in eastern Himalayas, India: pond based integrated farming system a sustainable approach. *Curr. Res. Environ. Sustainability* 3, 100076. doi: 10.1016/j.crsust.2021.100076

Datta, A., Basak, N., Chaudhari, S. K., and Sharma, D. K. (2015). Soil properties and organic carbon distribution under different land uses in reclaimed sodic soils of North-West India. *Geoderma Regional* 4, 134–146. doi: 10.1016/j.geodrs.2015.01.006

Dick, R. P., Breakwell, D. P., Turco, R. F., Doran, J. W., and Jones, A. J. (1996). "Soil enzyme activities and biodiversity measurements as integrative microbiological indicators," in *Methods for Assessing Soil Quality*, 247–271.

FAO (2019). "The state of food and agriculture 2019," in *Moving forward on food loss and waste reduction* (Licence, Rome). CC BY-NC-SA 3.0 IGO.

García-Orenes, F., Morugán-Coronado, A., Zornoza, R., and Scow, K. (2013). Changes in soil microbial community structure influenced by agricultural management practices in a Mediterranean agro-ecosystem. *PloS One* 8, e80522. doi: 10.1371/journal.pone.0080522

Gielen, D., Gorini, R., Wagner, N., Leme, R., Gutierrez, L., Prakash, G., et al. (2019). Global energy transformation: a roadmap to 2050.

HiMedia Manual (2009). *HiMedia manual for microbiology laboratory practice* (HiMedia Laboratories Pvt. Ltd).

Hinz, R., Sulser, T. B., Hüfner, R., Mason-D'Croz, D., Dunston, S., Nautiyal, S., et al. (2020). Agricultural development and land use change in India: A scenario analysis of trade-offs between UN Sustainable Development Goals (SDGs). *Earth's Future* 8, e2019EF001287. doi: 10.1029/2019EF001287

Jackson, M. L. (1967). *Soil chemical analysis* (Prentice Hall International Inc).

Kpan, W. H., Bongoua-D., A. J., Kouadio, K.-K. H., Kone, B., and Bahan, F. M. L. (2023). Response of lowland rice to phosphate amendments in three acidics agroecological zones of Côte d'Ivoire: Man-Gagnoa-Bouaké. *Int. J. Environment Agric. Biotechnol.* 8, 135–144. doi: 10.22161/ijeab.85.18

Kumar, P., Chaudhari, S. K., Singh, A., Singh, R., Mishra, A. K., Singh, K., et al. (2021). Effect of tillage and residue management in rice-wheat system. *Indian J. Agric. Sci.* 91, 283–286. doi: 10.56093/ijas.v91i2.111638

Kumar, P., Mishra, A. K., Chaudhari, S. K., Singh, R., Yadav, K., Rai, P., et al. (2022). Conservation agriculture influences crop yield, soil carbon content and nutrient availability in the rice–wheat system of north-west India. *Soil Res.* 60, 624–635. doi: 10.1071/SR21121

Kumar, A., Nayak, A. K., Das, B. S., Panigrahi, N., Dasgupta, P., Mohanty, S., et al. (2019). Effects of water deficit stress on agronomic and physiological responses of rice and greenhouse gas emission from rice soil under elevated atmospheric CO2. *Sci. Total Environ.* 650, 2032–2050. doi: 10.1016/j.scitotenv.2018.09.332

Lal, R. (2004). Soil carbon sequestration to mitigate climate change. *Geoderma* 123, 1–22. doi: 10.1016/j.geoderma.2004.01.032

Lal, R. (2020). "Soil quality and sustainability," in *Methods for assessment of soil degradation* (CRC Press), 17–30.

Lazcano, C., Gomez-Brandon, M., Revilla, P., and Dominguez, J. (2013). Short-term effects of organic and inorganic fertilizers on soil microbial community structure and function. *Biol. Fertility Soils* 49, 723–733. doi: 10.1007/s00374-012-0761-7

Li, C., Zhou, K., Qin, W., Tian, C., Qi, M., Yan, X., et al. (2019). A review on heavy metals contamination in soil: effects, sources, and remediation techniques. *Soil Sediment Contamination: Int. J.* 28, 380–394. doi: 10.1080/15320383.2019.1592108

Liang, Q., Chen, H., Gong, Y., Yang, H., Fan, M., and Kuzyakov, Y. (2014). Effects of 15 years of manure and mineral fertilizers on enzyme activities in particle-size fractions in a North China Plain soil. *Eur. J. Soil Biol.* 60, 112–119. doi: 10.1016/j.ejsobi.2013.11.009

Liu, H., Li, S., Qiang, R., Lu, E., Li, C., and Zhang J and Gao, Q. (2022). Response of soil microbial community structure to phosphate fertilizer reduction and combinations of microbial fertilizer. *Front. Environ. Sci.* 10. doi: 10.3389/fenvs.2022.899727

Martin, J. P. (1950). Use of acid, rosebengal and streptomycin in the plate method for estimating soil fungi. *Soil Sci.* 69, 215–232. doi: 10.1097/00010694-195003000-00006

Mishra, U., Lal, R., Slater, B., Calhoun, F., Liu, D., and Van Meirvenne, M. (2009). Predicting soil organic carbon stock using profile depth distribution functions and ordinary kriging. *Soil Sci. Soc. America J.* 73, 614–621. doi: 10.2136/sssaj2007.0410

Mishra, A. K., Mahinda, A. J., Shinjo, H., Jat, M. L., Singh, A., and Funakawa, S. (2018). Role of conservation agriculture in mitigating soil salinity in indo-gangetic plains of India. *Eng. Pract. Manage. Soil Salin. Apple Acad. Press*, 129–147.

Mishra, A. K., Shinjo, H., Jat, H. S., Jat, M. L., Jat, R. K., Funakawa, S., et al. (2022a). Farmers' perspectives as determinants for adoption of conservation agriculture practices in Indo-Gangetic Plains of India. *Resources Conserv. Recycling Adv.* 15, 200105. doi: 10.1016/j.rcradv.2022.200105

Mishra, A. K., Sinha, D. D., Grover, D., Roohi,, Mishra, S., Tyagi, R., et al. (2022b). "Regenerative agriculture as climate smart solution to improve soil health and crop productivity thereby catalysing farmers' Livelihood and sustainability," in *Towards Sustainable Natural Resources: Monitoring and Managing Ecosystem Biodiversity* (Springer International Publishing, Cham), 295–309.

Mohanram, S., and Kumar, P. (2019). Rhizosphere microbiome: revisiting the synergy of plant microbe interactions. *Ann. Microbiology;* 69, 307–320. doi: 10.1007/s13213-019-01448-9

Olsen, S. R., Cole, C. V., Watenale, F. S., and Dean, L. A. (1954). *Estimation of available Phosphorus in Soil by Extraction with Sodium Bicarbonate* (Washington, DC: Circ. 939 USDA).

Pahalvi, H. N., Rafiya, L., Rashid, S., Nisar, B., and Kamili, A. N. (2021). "Chemical fertilizers and their impact on soil health," in *Microbiota and Biofertilizers*, vol. 2 . Eds. G. H. Dar, R. A. Bhat, M. A. Mehmood and K. R. Hakeem (Springer, Cham, Switzerland), 1–20.

Poonam,, Srivastava, S., Pathare, V., and Suprasanna, P. (2017). Physiological and molecular insights into rice-arbuscular mycorrhizal interactions under arsenic stress. *Plant Gene* 11, 232–237. doi: 10.1016/j.plgene.2017.03.004

Ren, B., Hu, Y., Chen, B., Zhang, Y., Thiele, J., Shi, R., et al. (2018). Soil pH and plant diversity shape soil bacterial community structure in the active layer across the latitudinal gradients in continuous permafrost region of Northeastern China. *Scientific. Rep.* 8, 5619. doi: 10.1038/s41598-018-24040-8

Ren, N., Wang, Y., Ye, Y., Zhao, Y., Huang, Y., Fu, W., et al. (2020). Effects of continuous nitrogen fertilizer application on the diversity and composition of rhizosphere soil bacteria. *Front. Microbiol.* 11. doi: 10.3389/fmicb.2020.01948

Richards, M. B., Butterbach-Bahl, K., Jat, M. L., Ortiz Monasterio, I., Sapkota, T. B., and Lipinski, B. (2015). Site-specific nutrient management: Implementation guidance for policymakers and investors. *CSA Pract. Brief.*

Samal, S. K., Rao, K. K., Poonia, S. P., Kumar, R., Mishra, J. S., Prakash, V., et al. (2017). Evaluation of long-term conservation agriculture and crop intensification in rice-wheat rotation of Indo-Gangetic Plains of South Asia: Carbon dynamics and productivity. *Eur. J. Agron.* 90, 198–208. doi: 10.1016/j.eja.2017.08.006

Shelef, O., Fernández-Bayo, J. D., Sher, Y., Ancona, V., Slinn, H., and Achmon, Y. (2018). "Elucidating local food production to identify the principles and challenges of sustainable agriculture," in *Sustainable Food Systems from Agriculture to Industry* (Academic Press), 47–81.

Singh, S., Singh, R., Mishra, A. K., Updhayay, S., Singh, H., and Rahgubanshi, A. S. (2018). Ecological perspectives of crop residue retention under the conservation agriculture systems. *Trop. Ecol.* 59, 589–604.

Sivojiene, D., Kacergius, A., Baksiene, E., Maseviciene, A., and Zickiene, L. (2021). The Influence of organic fertilizers on the abundance of soil microorganism communities, agrochemical indicators, and yield in east Lithuanian light soils. *Plants* 10, 2648. doi: 10.3390/plants10122648

Six, J., Conant, R. T., Paul, E. A., and Paustian, K. (2002). Stabilization mechanisms of soil organic matter: implications for C-saturation of soils. *Plant Soil* 241, 155–176. doi: 10.1023/A:1016125726789

Smith, P., Martino, D., Cai, X., Gwary, D., Janzen, H., Kumar, P., et al. (2016). "Agriculture, forestry and other land use (AFOLU)," in *Climate change 2014: Mitigation of climate change. Contribution of Working Group III to the Fifth Assessment Report of the Intergovernmental Panel on Climate Change* (Cambridge University Press), 499–572.

Stenberg, B. (1999). Monitoring soil quality of arable land: microbiological indicators. *Acta Agriculturae Scandinavica Section B-plant Soil Sci.* 49, 1–24. doi: 10.1080/09064719950135669

Subbiah, B. V., and Asija, G. L. (1956). A rapid procedure for the estimation of available nitrogen in soils. *Curr. Sci.* 25, 259–260. doi: 10.5555/19571900070

Taylor, J. P., Wilson, B., Mills, M. S., and Burns, R. G. (2002). Comparison of microbial numbers and enzymatic activities in surface soils and subsoils using various techniques. *Soil. Biol. Biochem.* 34, 387–401. doi: 10.1016/S0038-0717(01)00199-7

Upadhyay, M. K., Yadav, P., Shukla, A., and Srivastava, S. (2018). Utilizing the potential of microorganisms for managing arsenic contamination: a feasible and sustainable approach. *Front. Environ. Sci.* 6, 24. doi: 10.3389/fenvs.2018.00024

Vance, F., Brookes, P., and Jenkinson, D. (1987). Microbial biomass measurements in forest soil: the use of the chloroform fumigation incubation method in strongly acid soils. *Soil Biol. Biochem.* 19, 697–702. doi: 10.1016/0038-0717(87)90051-4

Wang, R., Bicharanloo, B., Hou, E., Jiang, Y., and Dijkstra, F. A. (2022). Phosphorus supply increases nitrogen transformation rates and retention in soil: A global meta-analysis. *Earth's Future* 10, e2021EF002479. doi: 10.1029/2021EF002479

Wang, L., Yuan, X., Liu, C., Li, Z., Chen, F., Li, S., et al. (2019). Soil C and N dynamics and hydrological processes in a maize-wheat rotation field subjected to different tillage and straw management practices. *Agric. Ecosyst. Environ.* 285, 106616. doi: 10.1016/j.agee.2019.106616

Wang, C., Zheng, M., Song, W., Wen, S., Wang, B., Zhu, C., et al. (2017). Impact of 25 years of inorganic fertilization on diazotrophic abundance and community structure in an acidic soil in southern China. *Soil Biol. Biochem.* 113, 240–249. doi: 10.1016/j.soilbio.2017.06.019

Wu, J., Sha, C., Wang, M., Ye, C., Li, P., and Huang, S. (2021). Effect of organic fertilizer on soil bacteria in maize fields. *Land* 10, 328. doi: 10.3390/land10030328

Xu, C., Li, Y., Hu, X., Zang, Q., Zhuang, H., and Huang, L. (2022). The influence of organic and conventional cultivation patterns on physicochemical property, enzyme activity and microbial community characteristics of paddy soil. *Agriculture* 12, 121. doi: 10.3390/agriculture12010121

Yadav, A. K., Gaurav, K., Kishor, R., and Suman, S. K. (2017). Stabilization of alluvial soil for subgrade using rice husk ash, sugarcane bagasse ash and cow dung ash for rural roads. *Int. J. Pavement Res. Technol.* 10, 254–261. doi: 10.1016/j.ijprt.2017.02.001

Zhang, D., Yang, X., Wang, Y., Zong, J., Ma, J., and Li, C. (2020). Changes in soil organic carbon fractions and bacterial community composition under different tillage and organic fertiliser application in a maize–wheat rotation system. *Acta Agriculturae Scandinavica Section B — Soil Plant Sci.* 70, 457–466. doi: 10.1080/09064710.2019.1700301

Zuberer, D. A. (1994). "Recovery and enumeration of viable bacteria," in *Methods of Soil Analysis: Part 2— Microbiological and Biochemical Properties*. Eds. R. W. Weaver, S. Angle, P. Bottomley, D. Bezdicek, S. Smith, A. Tabatabai, A. Wollum and S. H. Mickelson (SSSA, Madison, Wis.), 119–144.

frontiers | Frontiers in Plant Science

TYPE Review
PUBLISHED 06 December 2024
DOI 10.3389/fpls.2024.1444560

OPEN ACCESS

EDITED BY
Laichao Luo,
Anhui Agricultural University, China

REVIEWED BY
Alexandra Velasco,
Militar University of New Granada, Colombia
Ravi Sharma,
Dr. B. R. Ambedkar National Institute of Technology Jalandhar, India
Beppe Benedetto Consentino,
University of Palermo, Italy

*CORRESPONDENCE
Xiukang Wang
wangxiukang@126.com

RECEIVED 05 June 2024
ACCEPTED 18 November 2024
PUBLISHED 06 December 2024

CITATION
Xing Y and Wang X (2024) Precise application of water and fertilizer to crops: challenges and opportunities.
Front. Plant Sci. 15:1444560.
doi: 10.3389/fpls.2024.1444560

Precise application of water and fertilizer to crops: challenges and opportunities

Yingying Xing and Xiukang Wang*

Key Laboratory of Applied Ecology of Loess Plateau, College of Life Science, Yan'an University, Yan'an, Shaanxi, China

Precision water and fertilizer application technologies have emerged as crucial innovations in sustainable agriculture, addressing the pressing need to enhance crop yield and quality while optimizing resource use and minimizing environmental impacts. This review systematically explores the latest advancements in precision water and fertilizer application technologies. It examines the integration of advanced sensors, remote sensing, and machine learning algorithms in precision agriculture, assessing their roles in optimizing irrigation and nutrient management. The study evaluates various precision techniques, including micro-irrigation systems, variable rate technology (VRT), and predictive modeling, along with their implementation in diverse agricultural settings. Furthermore, the review addresses the challenges posed by soil environmental heterogeneity and emphasizes the necessity for a scientific index system to guide precise applications. Advanced irrigation methods, such as subsurface drip irrigation and micro-sprinkling, improve water-use efficiency and reduce salinity levels, while precision fertilization techniques optimize nutrient uptake and minimize leaching. The integration of machine learning and remote sensing facilitates real-time monitoring and adaptive management, resulting in increased resource use efficiency and reduced environmental pollution. However, the effectiveness of these technologies is contingent upon addressing soil heterogeneity and developing standardized application indices. This review highlights the novel combination of advanced sensing technologies and data analytics in precision agriculture, enabling targeted interventions tailored to specific field conditions. It underscores the importance of integrating soil microbial community dynamics and biochemical indicators with precision management practices to enhance soil fertility and crop performance. Furthermore, the development of predictive models and time series analysis tools represents a significant advancement in anticipating and responding to changing environmental conditions. Precision water and fertilizer application technologies offer substantial benefits for sustainable agricultural practices by improving crop yields, enhancing resource efficiency, and mitigating environmental impacts. The strategic integration of these technologies with tailored agricultural practices and robust monitoring systems is essential for optimizing nutrient cycling and maintaining soil health. Addressing existing challenges through interdisciplinary research and collaborative efforts will further advance the implementation of precision agriculture, contributing to long-term soil sustainability and global food security.

KEYWORDS

precision agriculture, water and fertilizer management, crop quality, soil regulation, intelligent equipment

1 Introduction

The advancement of agricultural science and technology, coupled with the urgent need for global food security, has brought the precise application of water and fertilizers to the forefront of sustainable agricultural development. Traditional farmland management often faces challenges such as excessive fertilization, inadequate irrigation, imbalanced water–fertilizer coupling, resource wastage, and environmental pollution (Chojnacka and Moustakas, 2024). Therefore, investigating the conditions for precise water and fertilizer application, as well as the mechanisms that enhance crop quality, increase yield, and regulate soil, is essential for promoting green agricultural development (Xing and Wang, 2024a).

Improving crop quality and yield involves optimizing nutrient supply and soil management to enhance crop performance while maintaining stable yields (Dhaliwal et al., 2022). Soil nutrient supply is a fundamental pillar of agricultural production, crucial for crop growth and development (Brown et al., 2022). However, traditional practices often lead to inefficient monitoring and application techniques, resulting in low fertilizer utilization, significant nutrient loss, and compromised crop quality and yield (Zhang et al., 2011). Thus, studying the technical conditions for precise water and fertilizer application is vital for achieving improvements in both crop quality and yield.

The mechanism of soil regulation encompasses the manipulation of the physical, chemical, and biological properties of soil to control nutrient supply and release, thereby enhancing soil fertility and crop yield. Understanding soil characteristics and nutrient transformation processes is crucial for precise nutrient regulation (Wei et al., 2024). By adjusting soil moisture content, aeration, and water-holding capacity, an optimal growth environment can be created that facilitates root development and nutrient uptake (Laghari et al., 2016). The incorporation of organic matter and microbial fertilizers can improve soil texture and structure, enhancing its capacity for water and fertilizer retention, ultimately increasing crop yield (Shu et al., 2022).

Research on precise water and fertilizer application conditions, alongside mechanisms that enhance crop quality, yield, and soil regulation, significantly promotes sustainable agricultural development (Peng et al., 2023). With global agriculture facing challenges such as limited land resources and water scarcity, improving the efficiency of water and fertilizer use and optimizing the soil ecological environment is a top priority (Wang, 2022). Furthermore, as consumer demand for high-quality agricultural products rises, the traditional model of prioritizing high yield and high fertilizer usage is becoming increasingly unsustainable (Yu et al., 2023).

2 Effects of combined application of water and fertilizer on crop quality

2.1 Analysis of crop growth characteristics

Optimizing irrigation practices is essential for maximizing banana production. Maintaining moderate soil water deficits promotes extensive root development and preserves fruit quality. The crop's water demand varies significantly—from 1,200 to 2,690 mm per year—depending on the cultivar, developmental stage, and environmental conditions. Additionally, considering the unique ratooning cycle of bananas is crucial for maximizing water productivity and minimizing environmental impacts (Panigrahi et al., 2021).

Understanding crop growth cycles—which typically include germination, vegetative growth, flowering, fruiting, and maturity—is vital for effective agricultural management. Monitoring development across these stages provides valuable insights into growth patterns. During germination, evaluating germination rates and related indicators assesses a crop's initial viability. Observations during vegetative growth help determine adaptability and growth vigor in response to environmental factors. In the flowering stage, tracking the development of floral organs and the duration of flowering allows for the measurement of key indicators such as flower bud count, flowering rate, and fruit set rate. Notably, despite claims of pollinator independence, the "Independence" almond variety exhibited a 60% increase in fruit set and a 20% enhancement in kernel yield when pollinated by bees, highlighting the critical role of pollinators even in self-fertile varieties (Sáez et al., 2020). Such detailed observations at various growth stages provide scientific evidence for precise water and fertilizer management aimed at improving crop quality and yield.

Crop biomass is a critical indicator for evaluating growth and potential yield. Accurate measurement of biomass offers insights into the status, growth rate, and total productivity of crops (Justes et al., 2021). Selecting optimal measurement methods tailored to specific circumstances ensures accurate assessments (Abbasi et al., 2020). Integrating biomass data with geographic and meteorological information enables comprehensive analyses of mechanisms to enhance crop quality and soil regulation (Liang et al., 2023). Continued research into the mechanisms and strategies of synchronized application will provide valuable insights and support sustainable agricultural development (Figure 1).

Accurate crop yield statistics are essential for assessing the effects of water and fertilizer management on agricultural output (Lobell et al., 2020). Given the variability in crops and treatments, statistical analyses are necessary to determine the significance of yield differences (Ye et al., 2020). Techniques such as variance analysis, regression analysis, and correlation analysis facilitate the identification of significant differences and the exploration of underlying mechanisms. Considering crop growth periods in statistical analyses is crucial, as yield patterns fluctuate throughout these phases (Wagg et al., 2021). Implementing standardized management practices during data collection ensures comparability and accuracy of results (Li et al., 2021b).

2.2 Evaluation of water and fertilizer application effects

Optimizing irrigation and fertilization strategies is crucial for enhancing crop yield, quality, and resource use efficiency. In the xerothermic regions of southwest China, Sun et al. (2022) identified an optimal schedule for mango cultivation that involves applying

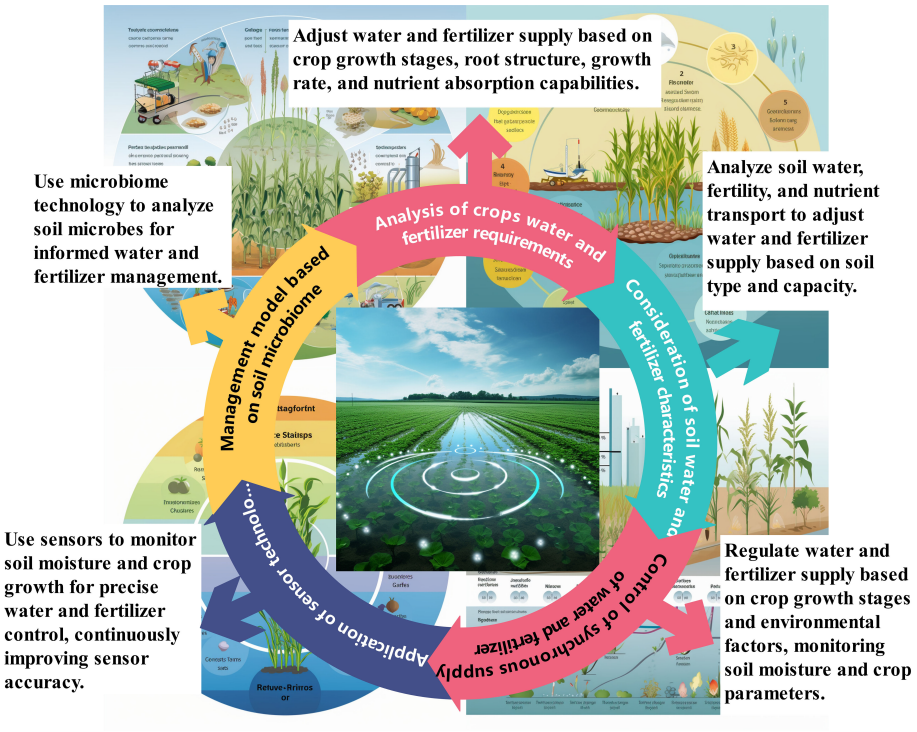

FIGURE 1
Mechanism of precise application of water and fertilizer on crop growth.

75% of the crop evapotranspiration, along with sequential fertilization of 50, 75, and 25 kg ha^{-1} at the flowering, fruit expansion, and fruit ripening stages, respectively. This strategy not only achieves high yield and quality but also significantly improves water use efficiency (WUE) and partial factor productivity (PFP) by 20% and 25%, respectively, compared to full irrigation.

Several factors influence WUE and nutrient use efficiency (NUE), including soil fertility, application methods, crop variety, cultivation management, and climatic conditions (Alkharabsheh et al., 2021). Implementing controlled-release urea at 150 kg N ha^{-1} for rice and 120 kg N ha^{-1} for other crops, in conjunction with common urea (30 kg N ha^{-1}) and straw incorporation, has been shown to enhance NUE and improve grain quality and soil fertility. Although this approach resulted in a yield reduction of up to 29.8% compared to local farming practices, it offers a sustainable compromise for agriculture in southern China (Liu et al., 2021a). The use of biofertilizers, such as phosphorus-solubilizing bacteria (PSBs), can further improve crop growth and soil nutrient availability. Inoculation with PSBs HRP2, SSP2, and JRP22 significantly enhanced the growth of Chinese fir, increasing plant height by 1.26-fold, stem diameter by 40.69%, and root, stem, and leaf biomass by 21.28%, 29.09%, and 20.78%, respectively (Chen et al., 2021a). These findings highlight the potential of PSBs as eco-friendly biofertilizers that enhance soil nutrient content and uptake.

Examining both traditional and precision management techniques is essential for assessing potential yield improvements. Fertilization methods affect nutrient supply and the crop growth environment, thereby influencing yield outcomes (Toksha et al., 2021). For instance, an optimal fertilization regime comprising 315 kg N ha^{-1}, 210 kg P_2O_s $ha^{-};^{1}$, and 285 kg K_gO ha^{-1} resulted in a lettuce yield increase of up to 42.42% and improved quality traits. Notably, nitrate content was directly proportional to the nitrogen rate, while soluble sugar and vitamin C levels showed positive correlations with nitrogen and phosphorus applications, respectively (Hong et al., 2022). These findings underscore the significant impact of balanced nutrient management on crop performance. Innovative analytical methods contribute to agricultural efficiency by enabling precise monitoring of nutrient and contaminant levels. A novel technique employing a platinum-coated tungsten-coil atom trap for lead analysis demonstrated a 32.5-fold increase in sensitivity compared to graphite furnace atomic absorption spectroscopy, achieving a limit of quantification of 11.0 ng L^{-1} and a precision of 2.3% relative standard deviation (Atasoy, 2023).

The System of Rice Intensification (SRI), when integrated with nutrient management practices such as integrated nutrient management (INM) or organic fertilization, consistently outperforms conventional methods. This approach led to grain yield increases of up to 43.8% and improved nutrient uptake (Thakur et al., 2020). Enhanced root growth and physiological functioning contributed to superior grain formation, yield, and nutritional content, including elevated levels of nitrogen (N), phosphorus (P), potassium (K), iron (Fe), manganese (Mn), copper (Cu), and zinc (Zn). Quality indicators such as grain moisture, sugar, and protein content can be assessed through chemical analysis and microscopy to evaluate crop quality under various management treatments (Padilla et al., 2020).

Effective phosphorus management is also critical for minimizing environmental impact. The application of spring-

applied phosphorus fertilizer resulted in a 19% reduction in total phosphorus losses and a 33% reduction in dissolved reactive phosphorus (DRP) losses compared to fall broadcasting. However, the effects of cover crops on total phosphorus loss were inconsistent; they were associated with increased DRP loss in 75% of observed years (Carver et al., 2022). These findings emphasize the importance of phosphorus fertilizer management and highlight the mixed effects of cover crops on phosphorus loss mitigation, despite their consistent effectiveness in reducing sediment loss. In the context of precise water and fertilizer application, selecting appropriate evaluation indicators significantly influences the results (Figure 2). Innovations in analytical methods and a deeper understanding of nutrient dynamics further support sustainable agricultural practices.

2.3 Regularity of crop quality change

Quality indicators are essential for evaluating agricultural products, as they directly influence standards, market demand, and consumer preferences. Nutrient content, including proteins, fats, vitamins, and minerals, is critical. For instance, protein content serves as a key indicator of rice quality (Gaikwad et al., 2020), aligning with human nutritional requirements (Zhou et al., 2020). Appearance characteristics, such as color, shape, and size, significantly affect consumer purchasing decisions and market competitiveness (Chen et al., 2021b). Flavor quality, which encompasses taste, aroma, and texture, is vital for consumer satisfaction, particularly in fruits where sweetness, acidity, and texture are of paramount importance (Yun et al., 2022). The implementation of precise water and fertilizer applications can enhance these quality indicators, thereby increasing both market appeal and consumer satisfaction (Yan et al., 2024).

Under precise water and fertilizer management, various factors significantly influence crop quality. Systematic screening is necessary to identify key determinants. Soil characteristics, including nutrient content, pH, and texture, play a critical role (Milošević and Milošević, 2020). Investigating crop quality across different soil types can elucidate these influences. Additionally, climatic factors such as temperature, precipitation, and sunlight affect both growth and quality, underscoring the need to examine how these conditions impact crops. Furthermore, different crop types and varieties may respond variably to management practices, highlighting the importance of tailored approaches. For instance, a 50% reduction in urea and phosphate fertilizers in Region 3, identified as the primary source of pollution, resulted in an 18.1% decrease in nitrate leaching and an 8.35% reduction in phosphate leaching into the Aras River (Badrzadeh et al., 2022).

Time series analysis is a powerful method for examining and modeling data over time (Figure 3), facilitating the identification of trends and patterns that are essential for optimizing crop management (Aphalo and Sadras, 2022). A bibliometric analysis of 290 articles published between 1991 and 2022 revealed a significant positive correlation (R^2 = 0.937) between annual citations and the number of publications, indicating a growing interest in soil nitrogen losses associated with drip irrigation (Wei et al., 2024). Time series models can predict future trends in crop quality, enabling adjustments in water and fertilizer applications based on anticipated changes. For example, spring-applied phosphorus fertilizer resulted in a 19% reduction in total phosphorus losses and a 33% reduction in DRP losses compared to fall broadcasting (Carver et al., 2022). Conversely, the effect of cover crops on total phosphorus loss was inconsistent, with an increase in DRP loss observed in 75% of the years analyzed.

Climate change factors, including a temperature increase of 1.2°C and a water depletion of approximately 29 mm m^{-2}, have counteracted the 7% yield increase associated with rising CO_2 levels

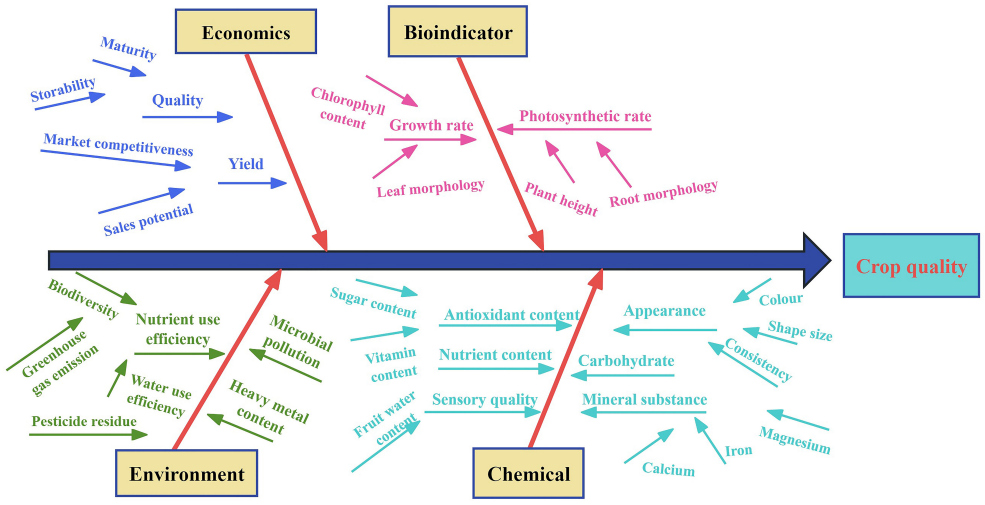

FIGURE 2
Crop quality evaluation index under precise combined application of water and fertilizer.

(approximately 98 μmol mol^{-1}) in major wheat-producing countries over the past six decades. Notably, Germany and France have experienced net yield losses of 3.1%, while yields in China and the former Soviet Union are 5.5% lower than anticipated (Helman and Bonfil, 2022). These trends underscore the significance of predictive models and time series analyses in adapting agricultural practices to changing environmental conditions. Advanced modeling techniques, such as artificial neural networks, provide precise predictions for agricultural management. A developed neural network model accurately predicted sodium hazard levels in groundwater for irrigation in the Pratapgarh district of Southern Rajasthan, achieving a correlation coefficient of 1 and a root mean square error (RMSE) of 0.14 (Gautam et al., 2023). This model enabled the comparison of various nitrogen, phosphorus, and potassium ratios to identify the most effective application strategy. In conclusion, time series analysis and precise management practices are crucial for studying crop quality improvement and soil regulation. They facilitate the identification of patterns, optimization of application schemes, and prediction of future quality trends, providing valuable guidance for enhancing crop quality and yield efficiency (Kang et al., 2021).

2.4 Key factors affecting crop quality

Water and fertilizer management critically determines crop quality by directly influencing nutrient supply (Han et al., 2021). An optimal combination of irrigation (653.7 m^3 ha^{-1}), nitrogen (1,141.9 kg ha^{-1}), and magnesium (422.1 kg ha^{-1}) fertilizers resulted in a cucumber yield of 88,412.6 kg ha^{-1}, increasing reducing sugars by 19.0% and free amino acids by 9.8%, while enhancing nitrogen use efficiency (Li et al., 2023b). The integration of organic and chemical fertilizers, especially with 60% cattle manure, significantly enhanced soil enzymatic activities and increased microbial biomass carbon and nitrogen by up to 62.2% and 54.5%, respectively (Iqbal et al., 2022). This approach yielded higher rice production compared to the exclusive use of chemical fertilizers, demonstrating a sustainable strategy for enhancing soil functionality and crop productivity.

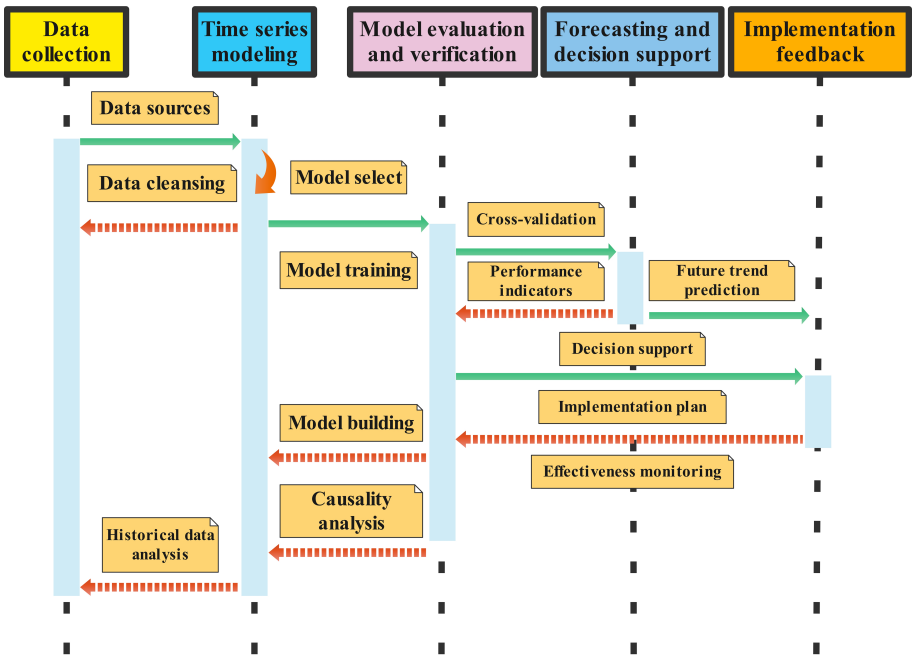

FIGURE 3
Application of time series analysis in the study of crop quality and soil control mechanism under the condition of precise combination of water and fertilizer. Data sources collect historical data on crop quality, including but not limited to growing environment data (e.g., temperature, rainfall, and light intensity), soil data (moisture, nutrient content), field management data (fertilization, irrigation records), and crop quality data (e.g., sugar content, protein content, yield, etc.). Data cleaning deals with missing values and outliers, standardizing data formats to ensure data accuracy and consistency. Historical data analysis (Growth stage) determines the changes in water and fertilizer requirements of crops at different growth stages and then optimizes the timing of fertilization and irrigation; (Climate impact) Analysis of crop quality changes under different climatic conditions, so as to adjust the water and fertilizer distribution strategy under specific climatic conditions. Model selection selects appropriate time series models according to data characteristics, such as the ARIMA model (autoregressive integral moving average model), the SARIMA model (seasonal ARIMA), and LSTM (long short-term memory neural network). Model training uses historical data to train models and adjust model parameters to improve prediction accuracy. In Model building, ARIMA (autoregressive integral moving average model), SARIMA (seasonal ARIMA model), LSTM (long short-term memory network), and other models were used for prediction and analysis. Causality analysis uses Granger causality test and other methods to determine the causal relationship between water and fertilizer distribution and crop quality change. In Cross-validation, the predictive power of the model is evaluated by cross-validation methods to avoid overfitting. In Performance indicators, mean square error (MSE), root mean square error (RMSE), and other indicators were used to evaluate the model performance. Future trend prediction uses trained models to predict trends in crop quality over a period of time. Decision support adjusts farmland management measures based on the forecast results, such as optimizing water and fertilizer application schemes to prevent possible quality degradation in advance. For Implementation plan, according to the forecast results and optimization plan, it is actually applied to farmland management. Effectiveness monitoring continuously monitors crop quality and yield, collects feedback data, and further optimizes models and management measures.

Effective water management is vital for healthy crop growth and has a significant impact on overall quality (Li et al., 2021a). By optimizing irrigation practices according to growth stages and soil moisture levels, losses can be minimized, and efficiency can be improved, ultimately enhancing crop quality (Zhang et al., 2021a). Amending soil with a combination of biochar and straw has been shown to significantly enhance soil aggregate stability, achieving a Granular Stability Index of up to 98.74, while also improving water-holding capacity (field capacity, FC = 0.317 cm^3 cm^{-3}). Furthermore, this amendment increases dissolved organic carbon content to 272.828 mg kg^{-1} and stabilizes air permeability under freeze–thaw cycles (Xue et al., 2022). Adjusting soil pH, organic matter, and trace elements within a combined management framework further promotes crop quality (Niu et al., 2021).

Maintaining optimal soil pH levels is crucial for enhancing crop quality, which includes improved vitamin content and increased disease resistance (Tripathi et al., 2022). A suitable pH establishes a favorable growth environment, facilitating better nutrient and water absorption (Antonangelo et al., 2021). Additionally, climate factors such as temperature, sunlight, and humidity play critical roles in crop growth (Malhi et al., 2021). For example, peanuts exhibit improved fruit color and taste at elevated temperatures, while tomatoes achieve higher nutritional content with adequate sunlight (Waraich et al., 2011). Therefore, regulating climate conditions is essential for enhancing crop quality. Appropriate levels of trace elements can also enhance plant metabolism and disease resistance (Kaur et al., 2023). The addition of selenium to soil improves wheat quality by increasing antioxidant levels and enhancing dough fermentation (He et al., 2023).

Analyzing the interaction between water and fertilizer under precise application conditions is essential for understanding improvements in crop quality and soil regulation. An adequate water supply maintains soil moisture, enhances nutrient absorption, and increases nutrient availability (Brouder and Volenec, 2008). Appropriate fertilizer application, including nitrogen, phosphorus, and potassium, provides essential nutrients that promote growth and quality (Yahaya et al., 2023). Key factors influencing these interactions include soil type, climate conditions, crop variety, and fertilization levels (Wang et al., 2019b). Climate factors such as rainfall and temperature also influence the decomposition and absorption of water and fertilizers (Maharajan et al., 2021). By simulating crop growth and nutrient processes, we can predict how these interactions affect crop quality (López-Pérez et al., 2018). A thorough understanding of these dynamics is essential for optimizing water and fertilizer management to enhance crop quality.

The interactive effects between water and fertilizer represent a critical mechanism influencing crop quality improvement and soil regulation under precise application conditions. Understanding these effects and the factors that influence them is vital for optimizing application schemes, enhancing crop quality, and efficiently utilizing soil nutrients. Consequently, future research should further investigate the mechanisms underlying water and fertilizer interactions to effectively improve crop quality and soil management.

3 Effects of physical and chemical properties of soil

3.1 Soil structure changes

Changes in soil structure play a crucial role in enhancing crop quality and optimizing soil conditions under precise water and fertilizer management. Applying organic amendments, particularly compost at 10 t ha^{-1}, significantly improves soil structure by enhancing aggregate stability, evidenced by a reduction in packing density (PAD) to 55% (Dong et al., 2022). Porosity also increases, with air-filled porosity reaching 0.29 cm^3 cm^{-3} and soil organic matter (SOM) levels rising to 24 g kg^{-1}, contributing to enhanced hydraulic conductivity and gas diffusivity. These improvements promote soil health and facilitate increased crop growth.

Precise management mitigates soil compaction (Rivier et al., 2022) and improves soil structure, thereby enhancing crop quality and yield compared to traditional agricultural practices (Lin et al., 2024). Traditional practices often lead to uneven fertilization and excessive water use, resulting in nutrient leaching, compaction, and soil degradation (Huang and Hartemink, 2020). In contrast, precise management tailors nutrient and water provision to the specific requirements of the soil, preventing waste and avoiding salinization and acidification, which further enhances soil structure (Hopmans et al., 2021).

Precise water and fertilizer management increases SOM content and enhances soil structure stability (Cen et al., 2021). Excessive use of chemical fertilizers in traditional agriculture, such as NPK, can reduce soil organic carbon by 14% and destabilize soil structure. Conversely, organic amendments like vermicompost can increase soil organic carbon by 16% and improve soil microstructure, enhancing overall soil functionality (Rivera-Uria et al., 2024). The integration of 20 t ha^{-1} of bio-organic fertilizer, coupled with a 20% reduction in chemical fertilizer, resulted in a decrease in soil bulk density by up to 0.22 g cm^{-3}, an increase in total porosity by up to 8.30%, and an optimal cucumber yield of 23.45 t ha^{-1} (Chen et al., 2022a). This demonstrates that the strategic use of organic amendments significantly enhances both soil physical properties and crop productivity in continuous cropping systems.

Land degradation drivers such as nitrogen enrichment and vegetation loss significantly reduce SOM decomposition rates. This reduction is mediated by changes in the alpha and beta diversities of rare soil bacteria and fungi, accounting for 33% of the variance in decomposition rates (Wu et al., 2021), underscoring the critical role of these rare microbial taxa in maintaining soil ecosystem functions. Traditional practices have led to a decline in soil microbial diversity and abundance, undermining soil stability (Hartmann and Six, 2023). In contrast, precise management creates a more favorable environment for microorganisms by limiting the use of chemical fertilizers and promoting organic applications, thus enhancing soil structure (Bamdad et al., 2022).

Effective water and fertilizer management is essential for enhancing soil structure, which, in turn, improves crop quality and yield. These practices reduce soil compaction, increase organic matter content, enhance microbial activity, and improve soil

aeration, permeability, and water retention (Usharani et al., 2019). Collectively, these factors create a more favorable growing environment for crops, leading to increased yields and improved quality. Therefore, regulating soil structure through precise management is crucial for optimizing the soil environment and promoting sustainable agriculture (Figure 4).

3.2 Soil pH and nutrient dynamics

Soil pH has emerged as a primary factor influencing bacterial communities and their functions in agricultural soils. It exhibits significant positive correlations with both bacterial abundance and α-diversity ($p < 0.05$) and plays a crucial role in determining the distribution of key functional groups, including chemoheterotrophs (27.66% and 26.14%) and nitrifiers (6.87%) (Wang et al., 2019a). Changes in soil pH directly affect nutrient availability: low pH in acidic soils can increase the solubility of iron and manganese to potentially toxic levels, while high pH in alkaline soils reduces the availability of phosphorus, zinc, and copper (Barrow and Hartemink, 2023). Proper pH adjustments enhance nutrient uptake, thereby improving crop yield and quality (Briat et al., 2020). Acidic conditions inhibit beneficial microorganisms, thereby reducing nutrient supply (Dotaniya and Meena, 2015), whereas alkaline conditions adversely affect organic matter degradation and nutrient mineralization (Fatima et al., 2021). Adjusting soil pH fosters microbial activity and nutrient transformations, ultimately benefiting crop growth (Das et al., 2022). Additionally, low pH accelerates nutrient leaching (Ren et al., 2023), while high pH increases nutrient fixation, leading to deficiencies (Gu et al., 2023). Therefore, regulating soil pH is crucial for enhancing nutrient efficiency and overall soil fertility (Singh et al., 2021).

The application of poultry manure (5 t ha^{-1}) in conjunction with biochar (5 t ha^{-1}) resulted in significant yield increases for maize and black gram, with increases of 73% and 169%, respectively. This combination also led to a remarkable enhancement of net returns by up to 313%, underscoring the effectiveness of organic amendments in enhancing crop productivity and profitability within fully organic production systems (Das et al., 2024). Furthermore, organic amendments promote microbial activity and nutrient transformations, thereby improving soil fertility (Xu et al., 2021). Consequently, investigating the relationship between soil pH and nutrient dynamics is essential for optimizing water and fertilizer management, as well as for enhancing crop yield and quality.

3.3 Monitoring of soil heavy metal content

Monitoring soil heavy metal content is essential for understanding the regulatory mechanisms governing soil health. Heavy metal pollution has emerged as a significant environmental issue, adversely impacting farmland ecosystems and compromising crop safety (Qin et al., 2021). Consequently, accurate monitoring of heavy metals is crucial for safeguarding ecological environments and enhancing crop quality. The initial step in this process involves selecting appropriate monitoring methods, including chemical analysis, spectroscopy, and electrochemical analysis (Akhtar et al., 2021). Chemical analysis, the most widely employed method, entails soil sample collection, acid extraction, and atomic absorption spectroscopy to quantify heavy metal concentrations.

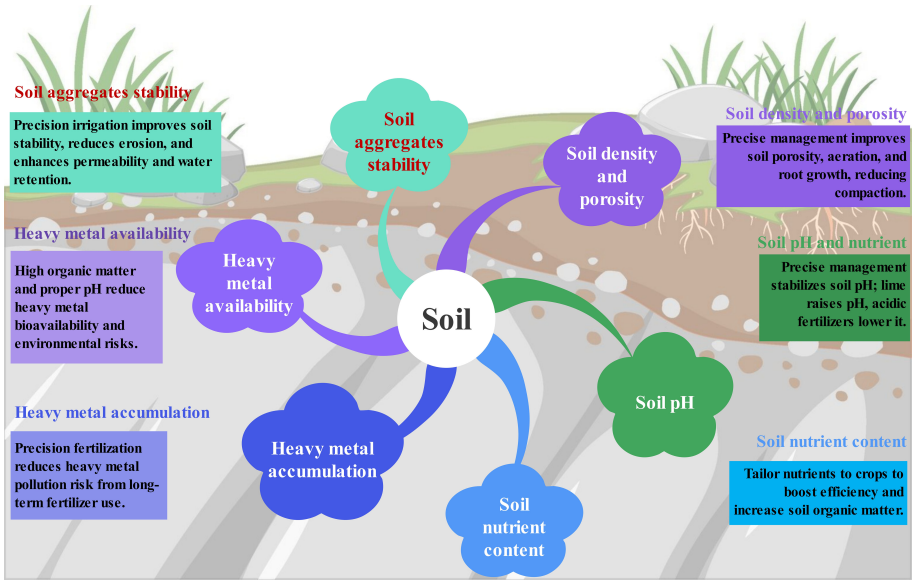

FIGURE 4
Response of soil structure, soil nutrients, and soil heavy metal content to precise application of water and fertilizer in farmland.

Spectroscopy evaluates heavy metal content by exposing samples to specific wavelengths and measuring light absorption, scattering, and fluorescence. Electrochemical analysis identifies the presence of heavy metals by detecting variations in current.

Identifying target heavy metals is essential for monitoring soil contamination. Common targets include lead, cadmium, mercury, chromium, and zinc (Balali-Mood et al., 2021). Each metal possesses distinct toxicity and accumulation properties; therefore, the selection of targets should align with research objectives and the characteristics of the soil (Dhaliwal et al., 2020). Representative sampling points must be carefully chosen to prevent contamination during collection. Soil samples should undergo appropriate treatment, including the removal of impurities and drying, to ensure accurate results. Analyzing and interpreting monitoring data is critical, with statistical methods and geographic information systems aiding in the identification of temporal and spatial patterns as well as factors influencing soil heavy metal content.

Monitoring soil heavy metal content is a vital component of research aimed at enhancing crop quality and yield through precise water and fertilizer management, as well as effective soil regulation mechanisms. The careful selection of monitoring methods, identification of target metals, accurate sampling and processing, and rigorous scientific data analysis and interpretation provide a crucial scientific foundation for preventing soil heavy metal pollution and safeguarding the ecological integrity of farmland.

4 Effects of soil biological characteristics

4.1 Microbial community structure

The microbial community structure is a fundamental aspect of soil biology, encompassing the diversity, abundance, distribution, and interactions of microorganisms. Soil pH, which ranges from 3.47 to 7.47, serves as the primary edaphic factor influencing bacterial communities following mining disturbances (Xiao et al., 2021). It affects the availability of nutrients and metal(loid)s, significantly impacting microbial diversity, taxonomic composition, and functional gene enrichment. These changes, in turn, shape essential physiological, ecological, and geochemical soil processes. A 7:3 ratio of organic to chemical fertilizer optimally enhances the yield and quality of Euryales Semen by improving soil fertility, microbial diversity, and enzyme activity. This ratio accounts for 90.80% of the variance in both yield and metabolome, thereby establishing a strong foundation for the sustainable and high-yield cultivation of Euryales Semen (Li et al., 2023a).

Environmental factors such as soil pH, moisture, and temperature significantly influence microbial community structure (Fan et al., 2022). The development of glycerol-based media incorporating zinc ions effectively facilitates the isolation of acidophilic sulfate-reducing bacteria (aSRB) from acidic environments (Ňancucheo et al., 2016). This method enhances the detection and cultivation of aSRB by converting harmful hydrogen sulfide into insoluble zinc sulfide, thereby enabling colony differentiation based on metal sulfide deposition (Suzuki et al., 2021). Additionally, the type and concentration of organic matter significantly affect microbial composition, leading to the enrichment of various microbial taxa (Wang et al., 2021). Crop types and planting methods also modify the rhizosphere environment, consequently impacting microbial communities (Gong et al., 2023). The integration of cellulolytic nitrogen-fixing bacteria into lignocellulosic crop residue composting processes accelerates decomposition, enhances compost quality and nutrient content, and promotes sustainable agriculture by improving soil fertility and crop yields (Harindintwali et al., 2020). Conversely, nitrate-reducing bacteria are more prevalent in waterlogged crops such as rice (Lin et al., 2018). Furthermore, farmland management practices play a crucial role; the application of organic fertilizers enhances microbial diversity, while excessive use of chemical fertilizers and pesticides diminishes and alters microbial communities (Xing et al., 2024).

The structure of microbial communities critically influences soil biological characteristics and crop yield. In-depth research on the changes and regulatory mechanisms of microbial community structure under precise water and fertilizer management conditions can optimize farmland practices, promote sustainable agricultural development, and enhance both crop quality and yield.

4.2 Changes in microbial activity

Precise water and fertilizer management in farmland has led to significant changes in soil microbial activity. Microorganisms are essential to soil biology and play a crucial role in influencing soil health. This management approach notably enhances microbial populations by meeting the moisture and nutrient requirements of crops, thereby creating a more favorable environment for microorganisms (Liu et al., 2021b). Continuous cropping significantly disrupts the structure of soil microbial communities, leading to reduced crop yields and quality (Chen et al., 2022c). However, the application of synthetic microbiology, along with the optimization of living conditions, can effectively restore microbial balance and improve soil health.

The combination of biochar addition with daily fertigation significantly enhances soil quality and microbial activity, resulting in improved water and nutrient retention. This synergistic approach maximizes cucumber yield and water–fertilizer productivity in the alkaline soils of semi-arid regions (Zhang et al., 2020). This improvement leads to greater efficiency in microbial utilization of water and nutrients, more active metabolic processes, and enhanced physiological functions (Bargaz et al., 2018). Furthermore, this management approach promotes microbial diversity by stabilizing the soil environment, which creates more favorable conditions for various microorganisms. Consequently, microbial species both compete and cooperate, positively influencing soil functions (Philippot et al., 2024). Overall, precise management increases the number, activity, and diversity of soil microorganisms, thereby supporting improved crop yield and quality (Sabir et al., 2021). Investigating the mechanisms underlying these changes is essential for optimizing soil management strategies and enhancing the efficiency of water and fertilizer use in agricultural settings.

4.3 Enzyme activity impact

Low tillage frequency combined with the application of liquid dairy manure enhances soil organic carbon by up to 31% and nitrogen by up to 21%, and increases the activities of key enzymes such as N-acetyl-β-D-glucosaminidase (NAG) and phosphomonoesterase (PME). Conversely, it reduces the activities of phosphatase (PO) and protease (PP), indicating a shift in carbon cycling and improved nitrogen and phosphorus availability (Uwituze et al., 2022). Variations in enzyme activity reflect changes in microbial metabolism, organic matter decomposition, and nutrient availability (Xu et al., 2015). Enzyme activity is influenced by soil type, nutrient levels, and seasonal fluctuations. Different forest types across varying climates significantly impact soil microbial communities and enzyme activities, with soil moisture and organic matter content being critical factors. For instance, Ponderosa Pine and Mountain Hemlock forests experience extreme moisture and temperature conditions, resulting in specialized enzyme profiles (Brockett et al., 2012). Nutrient-rich soils enhance microbial activity, leading to increased enzyme activity (Zhang et al., 2022). In temperate hardwood forest soils, seasonal variations in temperature and moisture significantly enhance microbial and enzyme activity; approximately 63% to 69% of total annual enzyme activity occurs during the warm months, highlighting the critical role of climatic factors in organic matter decomposition and ecosystem functioning (Baldrian et al., 2013).

Enzyme activity plays a crucial role in crop growth by facilitating the decomposition of organic matter and the release of nutrients, supplying essential nutrition to plants (Fageria and Moreira, 2011). It also influences microbial metabolism, promoting the production of growth factors, including plant hormones (Mitra et al., 2022), which enhance disease resistance and stress tolerance (Govind et al., 2016). Therefore, regulating soil enzyme activity can improve soil conditions and support crop growth and development.

Regulating soil enzyme activity is essential for enhancing both crop yield and quality. Appropriate fertilization increases nutrient levels, promoting microbial and enzyme activity (Zhang et al., 2016). In subtropical paddy soils, combining organic and inorganic phosphorus sources is necessary to sustain soil microbial activity and minimize environmental impacts. Total phosphorus application should not exceed 44 kg P ha^{-1} per year, as higher rates decrease acid phosphatase activity and pH levels (Zhang et al., 2015). Additionally, adjusting soil moisture and temperature can positively affect enzyme activity and microbial metabolism. By considering soil type, nutrient status, and environmental conditions, it is possible to effectively regulate soil enzyme activity to improve crop yield and quality.

Under precise water and fertilizer management conditions, investigating the impact of soil enzyme activity provides theoretical support for scientifically regulating soil environments and enhancing soil fertility. Effectively managing soil enzyme activity increases the soil's nutrient supply capacity, improving crop growth and achieving the goals of precise water and fertilizer management. Therefore, in-depth research into the mechanisms and regulatory pathways of enzyme activity is essential for promoting sustainable agricultural development.

5 Soil–crop system interaction

5.1 Nutrient absorption and transformation

Nutrient absorption and transformation are critical processes within the soil–crop system. Nutrient absorption involves the active uptake of water-soluble inorganic ions by plant roots from the soil (Tianqian et al., 2024). This process is primarily facilitated by root activities, such as the production of root hairs, which expand the absorption area and enhance efficiency (Chen et al., 2022b). The growth of root hairs significantly influences the adsorption of nutrient ions in the soil (Ganther et al., 2022). Ion selectivity enables root hairs to preferentially absorb the most beneficial nutrient ions essential for plant growth and development (Meychik et al., 2021). However, factors such as root tip aging can affect nutrient absorption efficiency. Environmental contaminants can also impact root function. For instance, photoaged PVC microplastics significantly impair the root growth and architecture of wheat seedlings. Particles aged for 108 h reduce root length by 3.56% to 7.45% and induce substantial oxidative stress. This highlights the pronounced ecotoxicity of leached additives, such as Irgafos 168-ox and Irganox 1076, which warrant greater consideration in environmental impact assessments (Wang et al., 2024).

Nutrient transformation refers to the biochemical conversion of absorbed inorganic ions into organic substances, primarily occurring in the chloroplasts and cytoplasm of plants. Photosynthesis is a key process in this transformation, converting light energy into chemical energy through pigments located in the chloroplasts. This energy facilitates the synthesis of organic compounds from carbon dioxide and water (Stirbet et al., 2020). The products of photosynthesis, including glucose, sucrose, and starch, serve as essential nutrients for plant growth (Aluko et al., 2021). Additionally, plants convert inorganic nutrients into organic compounds such as amino acids, nucleic acids, and sulfate esters through the metabolism of nitrogen, phosphorus, and sulfur (Narayan et al., 2023).

Several factors influence nutrient absorption and transformation. An increase in soil nutrient content enhances a plant's ability to absorb and convert these nutrients (Elbasiouny et al., 2022). Soil pH and temperature play crucial roles; optimal conditions facilitate root growth and nutrient uptake processes (Lyu et al., 2024). The dynamics of nutrients and water also influence the effectiveness of root traits in nutrient acquisition. For instance, in durum wheat, root angle traits affect phosphorus uptake. The "Narrow" genotype (41°) enhances deep soil exploration and phosphorus acquisition from deeper layers, whereas the "Wide" genotype (82°) is more effective in acquiring phosphorus from the topsoil (Van Der Bom et al., 2023). Understanding these interactions—which encompass root activities, ion selectivity for absorption, and the biochemical transformation of inorganic nutrients into organic substances—is essential for optimizing NUE (Li et al., 2024).

5.2 The relationship between soil and root growth

The relationship between root growth and soil is crucial for understanding the mechanisms of soil regulation. Roots play an

essential role in enabling crops to absorb nutrients and water, which directly influences their development and yield (Gregory and Wojciechowski, 2020). However, soil conditions can constrain root morphology and function (Schneider and Lynch, 2020). Different soil textures significantly impact root growth. Clayey soils retain more water and nutrients but provide poor aeration, which can slow root development (Russo et al., 2020). The magnesium-based biochar-modified hydrogel slow-release fertilizer demonstrates a 47.12% increase in water absorption capacity, achieving a maximum of 1,395.12 ± 35.45 g g^{-1}. This notable enhancement in soil water retention and maize seedling growth offers a promising solution for sustainable agriculture in arid regions, as it diminishes irrigation needs and improves nutrient efficiency (Lang et al., 2023). Soil nutrients, particularly nitrogen, are vital for crop growth. Both insufficient and excessive nitrogen levels can adversely affect root development; the appropriate amount fosters growth, while an excess can inhibit it (Xu et al., 2023). Consequently, proper fertilization is essential for regulating nutrient supply and promoting root growth.

SOM plays a crucial role in enhancing soil structure, improving water and nutrient retention, and promoting root development (Xing and Wang, 2024b). Research indicates that increased organic matter content correlates with more robust and extensive root growth in crops (Sokol et al., 2019). Consequently, the application of organic fertilizers can effectively increase SOM and stimulate root development (Wei et al., 2016). Root hairs significantly enhance nutrient uptake and shoot growth in *Zea mays*, with their effects being more pronounced in loamy soils than in sandy soils. This finding underscores the critical roles of soil texture and root trait plasticity in nutrient acquisition and overall plant development (Vetterlein et al., 2022). Therefore, effective soil management requires scientific adjustments to these conditions to create an optimal growth environment for roots, ultimately enhancing crop quality and yield.

5.3 Water and crop growth interactions

Water is essential for crop growth and yield formation, with its interaction intricately linked to crop development. Effective regulation of water use is crucial for enhancing crop quality and yield, particularly under conditions of precise water and fertilizer application (Kang et al., 2017). Crop water requirements vary by growth stage, with increased demands during the seedling and flowering phases, while the demand decreases at maturity (Dietz et al., 2021). Timely water supply during these critical stages is vital for maximizing yields (Jin et al., 2020). In the soil–crop system, the supply of water is closely related to the water absorption capacity of roots (Zhang et al., 2023). Adequate water availability promotes root growth, enhances the absorption area, and supports nutrient transport (Cai and Ahmed, 2022). Proper water levels regulate crop temperature and create favorable conditions for photosynthesis and other physiological processes, thereby boosting growth and yield (Morales et al., 2020). Furthermore, water supply influences nutrient release and transformation in the soil, which, in turn, affects nutrient absorption efficiency (Zhang et al., 2021b). Sufficient water facilitates the transformation of nutrients such as nitrogen, phosphorus, and potassium, thereby enhancing their availability for crops (Sardans and Peñuelas, 2021). Conversely, inadequate or excessive water can impede nutrient release and conversion, diminishing their effectiveness and adversely affecting nutrient absorption (Palansooriya et al., 2023).

6 Opportunities and challenges of water and fertilizer precise application technology

6.1 Precision agriculture and sustainable soil management: enhancing efficiency and crop yields

Precision agriculture is a transformative approach that enhances resource efficiency and crop yields through advanced technologies. By integrating remote sensing, GPS guidance, and data analytics, farmers make informed, localized decisions. This optimizes inputs like water, fertilizers, and pesticides, reducing waste and environmental impact. Targeted interventions, such as variable rate application, address specific field needs, leading to increased yields and improved crop quality. Real-time monitoring of crop health and environmental conditions allows farmers to respond swiftly to changes, enhancing resilience to climate variability. Key technologies include remote sensing tools like satellite imagery and aerial photography, which provide detailed data on crop health, soil conditions, and environmental factors. Data analytics processes this information to identify patterns and optimize production practices. Leveraging these advancements, farmers manage operations more efficiently, sustainably, and profitably. Despite its benefits, implementing precision agriculture faces challenges. High initial costs for equipment and technology are significant barriers, especially in resource-constrained regions. Effective use requires technical expertise in data analysis, necessitating training and support. Managing and storing large data volumes poses difficulties, requiring robust data management strategies. Nevertheless, the long-term advantages—such as increased productivity, reduced environmental impact, and enhanced profitability—make it a valuable investment in sustainable farming.

Sustainable soil management is crucial for improving crop quality and yield through precise water and fertilizer application. Since soil is the foundation of crops, its sustainable use is essential. Strategies for sustainable soil utilization optimize water and fertilizer use, enhance yields, and protect the environment. Regulating soil physical properties through practices like deep plowing, loosening, and drainage improves soil structure and water and nutrient retention, and promotes root development. Regulating soil chemical properties is equally important. Rational fertilization, tailored to crop nutrient demands, prevents excesses and deficiencies, improving yield and quality. Fertilization plans that consider growth stages and balance nitrogen, phosphorus, and potassium are essential for optimal performance. Leveraging soil

biological resources further enhances sustainability. Beneficial microorganisms and earthworms play vital roles in the soil ecosystem. Protecting and promoting soil biodiversity improves nutrient transformation, enhances crop resistance to pests and diseases, and reduces reliance on chemical pesticides, supporting sustainable agricultural ecosystems.

6.2 Integration and application of water and fertilizer precise application technology

Optimizing precision water and fertilizer application plans requires a thorough investigation and analysis of soil to evaluate nutrient status and crop requirements. Since different crops have unique nutrient needs, it is essential to scientifically determine the appropriate nutrient ratios based on crop characteristics and growth stages to meet these requirements and improve both yield and quality (Krouk and Kiba, 2020). Additionally, refining the application plan is vital for enhancing soil fertility and overall crop production capacity, which plays a significant role in promoting sustainable agricultural development and ensuring food security.

The design of control system integration is crucial for precision water and fertilizer application technologies. A comprehensive control system that leverages modern information technology is essential for the accurate application and regulation of water and fertilizers. The design of the control system integration should be based on modern information technology (Figure 5). Sensor technology, remote sensing, and geographic information systems can monitor soil moisture, soil fertility, and crop growth in real time, thereby providing vital data support for precision application. Furthermore, internet and Internet of Things technologies enable remote communication and data transmission, facilitating real-time monitoring and management by farmers.

The design of control system integration for precision water and fertilizer application technology must consider the specific conditions of the fields, including soil types, water and fertilizer management practices, and crop planting conditions. Furthermore, it should account for the operational capacity and economic feasibility for farmers. By leveraging modern information technology and integrating with environmental monitoring systems, while also addressing the actual conditions and needs of the fields, it is possible to develop efficient, user-friendly, and cost-effective control systems. These systems can optimize water and fertilizer usage, minimize waste and pollution, and contribute to the protection of the ecological environment, thereby supporting the sustainable development of agriculture.

Precision fertilization technology optimizes the use of water and fertilizers in agriculture, thereby enhancing production efficiency while minimizing pollution (Ladha et al., 2020). Analyzing soil nutrient content is essential for assessing fertility and developing a targeted fertilization plan. Determining the appropriate amounts of fertilizer based on crop needs and soil conditions ensures maximum efficiency. Furthermore, fertilization should align with the crop's growth cycle, taking into account the varying nutrient requirements at different stages. In some instances, multiple applications or zone-specific methods may be necessary, tailored to the unique characteristics of both the crop and the soil.

6.3 Problems in the application of technology

Key issues in the application of precision water–fertilizer technology include low fertilization precision, challenges in integrating water and fertilizer, and the variability of crop nutrient requirements. The low precision often arises from traditional methods that rely on fixed ratios and timings, which inadequately address the diverse needs of various soils. Some soils may possess excess nutrients, while others may be deficient, underscoring the necessity for accurate soil nutrient assessment to enable effective integration. Although existing soil testing and rapid nutrient measurement techniques can enhance precision, further optimization remains essential.

The integration of water and fertilizer poses a challenge due to the varying requirements of crops for water and nutrients, complicating the determination of optimal ratios. Additionally, soil moisture conditions significantly impact this integration, as arid regions require more water than humid areas. Therefore, it is essential to establish water–fertilizer ratios that are tailored to specific soil and crop characteristics. While advancements in irrigation and fertilization technologies can improve the precision of this integration, further research and practical application are necessary.

The varying crop requirements for water and fertilizer present significant challenges in the application of precision water–fertilizer technology. Different crops exhibit unique nutrient needs; for instance, some require high nitrogen levels but low phosphorus, while others necessitate the opposite. Therefore, accurately determining the appropriate water–fertilizer ratios and timing based on these specific requirements is crucial for enhancing both yield and quality. Current research on crop growth and nutrient absorption can facilitate the optimization of this integration; however, further in-depth studies are essential.

Addressing the issues of low fertilization precision, integration difficulties, and diverse crop requirements necessitates the refinement of precision technology, improvements in soil testing, and comprehensive research into crop demands. Optimizing fertilization methods and ratios is imperative (Figure 6). Only through scientific and technological advancements can effective water–fertilizer integration be achieved, ultimately improving crop yield and quality while ensuring sustainable agricultural development.

6.4 Analysis of environmental and economic benefits

Evaluating the environmental and economic benefits of precision water and fertilizer application technology is essential for its successful implementation in agriculture. This technology

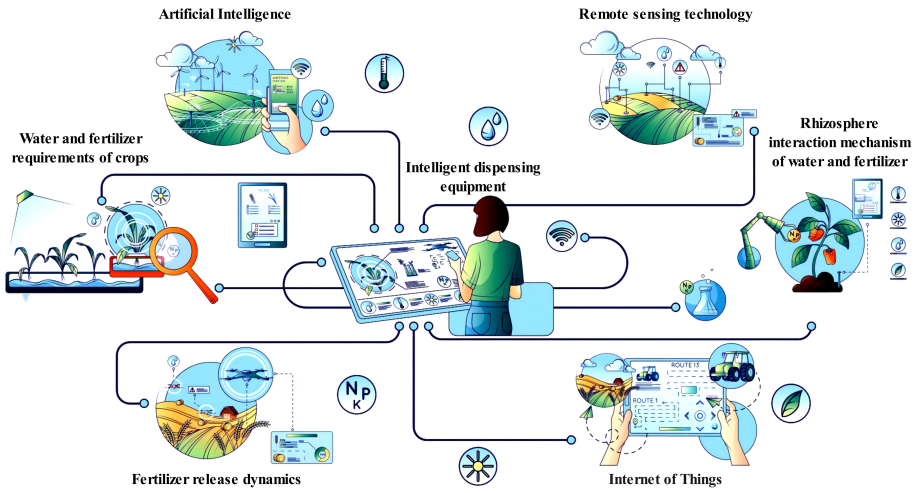

FIGURE 5
Through the intelligent distribution equipment assisted by the Internet of Things, remote sensing, and artificial intelligence, the law of crop water and fertilizer demand, the dynamic release of fertilizer, and the interaction mechanism of rhizosphere water and fertilizer are analyzed to implement precision agriculture. Intelligent dispensing equipment: automation equipment, control system, and feedback mechanism. Internet of Things: sensor, networked device, real-time monitoring, and data storage. Remote sensing technology: satellite remote sensing, UAV remote sensing, and ground remote sensing. Artificial Intelligence (AI): data processing and analysis, machine learning algorithm, prediction model, and decision support system. Water and fertilizer requirements of crops: water demand rule and fertilizer requirement rule. Fertilizer release dynamics: fertilizer type, release mechanism, and release model. Rhizosphere interaction mechanism of water and fertilizer: rhizosphere environment and interaction of water and fertilizer.

plays a significant role in promoting environmental protection and sustainable development. Firstly, it accurately assesses the water and fertilizer requirements of plants, thereby minimizing resource waste. Secondly, it helps reduce agricultural pollution; excessive fertilizer application can result in soil acidification and water contamination, but precision application effectively mitigates these issues, thereby safeguarding soil and water quality.

The application of precision water and fertilizer technology enhances agricultural production and promotes sustainable development. By accurately calculating the water and fertilizer requirements of plants, this technology minimizes resource waste, improves fertilizer efficiency, and reduces production costs. Furthermore, it decreases agricultural inputs and alleviates environmental pressure, thereby underscoring its economic benefits. Additionally, this technology improves soil quality and fosters crop growth by preventing nutrient accumulation or loss. It aids in regulating soil pH, enhancing soil structure, increasing organic matter content, and boosting water and nutrient retention, all of which collectively enhance soil fertility and create a more favorable environment for crops.

Precision water and fertilizer application technology provides substantial environmental benefits by reducing agricultural pollutant emissions, lowering greenhouse gas emissions, and mitigating climate change. Additionally, it decreases non-point source pollution, enhances water and soil quality, and safeguards the ecological environment. This technology not only improves environmental outcomes but also boosts economic performance by accurately determining the water and fertilizer requirements of plants, preventing over-application, and promoting resource efficiency while ensuring environmental protection. Economically, it reduces production costs and increases efficiency. Therefore, the adoption of this technology in agriculture presents promising prospects for future development.

6.5 Difficulties faced and countermeasures

Despite the significant achievements of precision water and fertilizer application technologies in enhancing crop yields and conserving resources, several challenges persist. A primary challenge is the establishment of a scientific index system for precise application, as controversies remain regarding the specific needs of different crops at various growth stages. Further research is necessary to develop a suitable index system that accommodates diverse farmland conditions and crop types, thereby improving both quality and production. Another challenge involves addressing the heterogeneity of soil environments, which is influenced by geographical factors, soil types, and texture. Effective application must account for this variability to adequately meet crop needs under differing conditions. Additionally, further study and optimization of soil improvement technologies are essential for enhancing soil quality and increasing the efficiency of fertilizer use by crops.

Implementing precision water and fertilizer technology requires a thorough understanding of various influencing factors, which presents a challenge for systematic research and evaluation. Current studies primarily rely on small-scale experiments, thereby limiting their applicability to broader agricultural contexts. To improve practical applications, it is essential to foster collaboration among scientists, farmers, and government entities to develop a systematic research and evaluation framework.

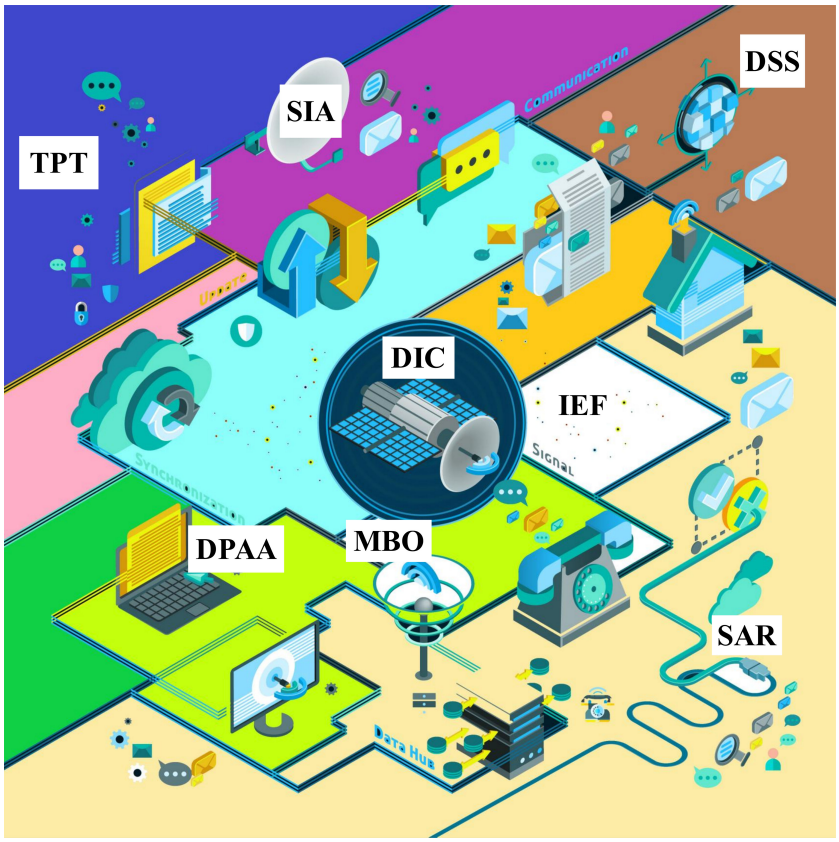

FIGURE 6
Intelligent distribution equipment to achieve accurate distribution of water and fertilizer need to solve scientific problems. SAR, sensor accuracy and reliability; DIC, data integration and consistency; DPAA, data processing and analysis algorithm; MBO, model building and optimization; IEF, impact of environmental factors; DSS, decision support system; SIA, system integration and application; TPT, technology popularization and training.

Precision water and fertilizer application technology is crucial for enhancing crop quality, increasing production, and managing soil conditions. However, challenges remain in its practical implementation. Addressing these challenges requires further research to establish a scientific index system, address soil environmental heterogeneity, and develop a systematic framework for research and evaluation. By undertaking these efforts, we can fully leverage the benefits of this technology, thus achieving sustainable farmland development alongside improved crop quality and yield.

6.6 Challenges in different agricultural regions

Water scarcity in arid regions presents significant challenges to agricultural productivity. Limited rainfall and high evaporation rates exacerbate this issue, highlighting the necessity for efficient irrigation practices to optimize water utilization. Advanced irrigation technologies, such as drip and subsurface irrigation, minimize water loss by delivering water directly to the root zone of crops. Additionally, moisture sensors enhance water efficiency by monitoring soil moisture levels and adjusting irrigation schedules accordingly. Furthermore, rainwater harvesting techniques and the cultivation of drought-tolerant crop varieties can play a crucial role in mitigating water stress. By implementing these strategies, arid regions can enhance agricultural sustainability and adapt to the challenges posed by water scarcity.

In humid regions, excessive rainfall poses several challenges, including waterlogging, nutrient leaching, and soil erosion. Waterlogged soils arise when saturation limits oxygen availability to plant roots, thereby hindering crop growth and potentially leading to reduced yields and increased susceptibility to diseases. Nutrient leaching is another significant concern, as heavy rainfall can wash away essential nutrients from the soil profile, depleting soil fertility and potentially contaminating water bodies. Furthermore, intense rainfall events can lead to substantial soil erosion, stripping away topsoil and degrading land productivity. To mitigate these challenges, farmers in humid regions can implement drainage systems to manage waterlogging, adopt cover cropping practices to prevent soil erosion, and utilize controlled irrigation methods to minimize nutrient leaching. By addressing these issues, agricultural productivity in humid regions can be sustained while also reducing environmental impacts.

Saline-alkali areas pose significant challenges to agricultural production due to the accumulation of salts and the poor structure of the soil. Elevated salt concentrations can hinder root growth and diminish the uptake of essential nutrients by plants, resulting in

stunted growth and reduced yields. Furthermore, the suboptimal structure of saline-alkali soils, typically characterized by compaction and low organic matter content, further limits root penetration and water infiltration. These adverse conditions create a harsh environment for crop production, thereby constraining plant growth and productivity. To mitigate these challenges, farmers in saline-alkali regions can adopt strategies such as applying soil amendments to enhance soil structure, implementing leaching practices to decrease salt accumulation, and selecting salt-tolerant crop varieties. By addressing the specific limitations posed by saline-alkali soils, agricultural productivity can be improved, and sustainable land management practices can be established.

7 Summary and prospect

Precise fertilizer application enhances soil nutrient status and microbial activity, which subsequently improves crop yield and quality. Intelligent systems equipped with sensor technology facilitate real-time monitoring and regulation of water and fertilizer, thereby supporting these advancements. However, the review lacks a comprehensive analysis of the mechanisms underlying soil regulation. Future research should focus on soil microorganisms and nutrient cycling, employing molecular biology and ecological methods to investigate how precise applications influence microbial diversity and nutrient cycling. Additionally, advancements in implementation technology are crucial.

Future studies should incorporate advanced sensor technology and smart agricultural equipment to achieve more accurate and efficient management of water and fertilizer. Significant challenges persist in understanding the mechanisms that enhance crop quality and regulate soil health. Future research should prioritize experimental design, data collection, and the exploration of regulatory mechanisms involving soil microorganisms and nutrient cycling. The integration of relevant technologies will enhance and expand research efforts, contributing to increased yield, improved quality, and sustainable development in the precise application of agricultural water and fertilizer.

Author contributions

YX: Formal Analysis, Funding acquisition, Investigation, Resources, Writing – original draft. XW: Formal Analysis, Funding acquisition, Investigation, Resources, Writing – original draft, Conceptualization, Data curation, Methodology, Project administration, Software, Supervision, Validation, Visualization, Writing – review & editing.

Funding

The author(s) declare that financial support was received for the research, authorship, and/or publication of this article. This research was funded by the Shanxi Province Key Special Project for the Fusion of "Two Chains", Grant No. 2023LLRH-01; the Key Research and Development of Shaanxi Province (2022NY-192) and the Shaanxi Provincial Department of Education Youth innovation team construction research project, Grant Nos. 21JP141, 22JP101, and 23JP189.

Conflict of interest

The authors declare that the research was conducted in the absence of any commercial or financial relationships that could be construed as a potential conflict of interest.

Publisher's note

References

Abbasi, M., Pishvaee, M. S., and Bairamzadeh, S. (2020). Land suitability assessment for Paulownia cultivation using combined GIS and Z-number DEA: A case study. *Comput. Electron. Agric.* 176, 105666. doi: 10.1016/j.compag.2020.105666

Akhtar, M. N., Shaikh, A. J., Khan, A., Awais, H., Bakar, E. A., and Othman, A. R. (2021). Smart sensing with edge computing in precision agriculture for soil assessment and heavy metal monitoring: A review. *Agriculture* 11, 475. doi: 10.3390/agriculture11060475

Alkharabsheh, H. M., Seleiman, M. F., Battaglia, M. L., Shami, A., Jalal, R. S., Alhammad, B. A., et al. (2021). Biochar and its broad impacts in soil quality and fertility, nutrient leaching and crop productivity: A review. *Agronomy* 11, 993. doi: 10.3390/agronomy11050993

Aluko, O. O., Li, C., Wang, Q., and Liu, H. (2021). Sucrose utilization for improved crop yields: A review article. *Int. J. Mol. Sci.* 22, 4704. doi: 10.3390/ijms22094704

Antonangelo, J. A., Sun, X., and Zhang, H. (2021). The roles of co-composted biochar (COMBI) in improving soil quality, crop productivity, and toxic metal amelioration. *J. Environ. Manage.* 277, 111443. doi: 10.1016/j.jenvman.2020.111443

Aphalo, P. J., and Sadras, V. O. (2022). Explaining pre-emptive acclimation by linking information to plant phenotype. *J. Exp. Bot.* 73, 5213–5234. doi: 10.1093/jxb/erab537

Atasoy, M. (2023). Development of a new sensitive method for lead determination by platinum-coated tungsten-coil hydride generation atomic absorption spectrometry. *ACS omega* 8, 22866–22875. doi: 10.1021/acsomega.3c01856

Badrzadeh, N., Samani, J. M. V., Mazaheri, M., and Kuriqi, A. (2022). Evaluation of management practices on agricultural nonpoint source pollution discharges into the rivers under climate change effects. *Sci. Total Environ.* 838, 156643. doi: 10.1016/j.scitotenv.2022.156643

Balali-Mood, M., Naseri, K., Tahergorabi, Z., Khazdair, M. R., and Sadeghi, M. (2021). Toxic mechanisms of five heavy metals: mercury, lead, chromium, cadmium, and arsenic. *Front. Pharmacol.* 12, 643972. doi: 10.3389/fphar.2021.643972

Baldrian, P., Šnajdr, J., Merhautová, V., Dobiášová, P., Cajthaml, T., and Valášková, V. (2013). Responses of the extracellular enzyme activities in hardwood forest to soil temperature and seasonality and the potential effects of climate change. *Soil Biol. Biochem.* 56, 60–68. doi: 10.1016/j.soilbio.2012.01.020

Bamdad, H., Papari, S., Lazarovits, G., and Berruti, F. (2022). Soil amendments for sustainable agriculture: Microbial organic fertilizers. *Soil Use Manage.* 38, 94–120. doi: 10.1111/sum.12762

Bargaz, A., Lyamlouli, K., Chtouki, M., Zeroual, Y., and Dhiba, D. (2018). Soil microbial resources for improving fertilizers efficiency in an integrated plant nutrient management system. *Front. Microbiol.* 9, 1606. doi: 10.3389/fmicb.2018.01606

Barrow, N., and Hartemink, A. E. (2023). The effects of pH on nutrient availability depend on both soils and plants. *Plant Soil* 487, 21–37. doi: 10.1007/s11104-023-05960-5

Briat, J.-F., Gojon, A., Plassard, C., Rouached, H., and Lemaire, G. (2020). Reappraisal of the central role of soil nutrient availability in nutrient management in light of recent advances in plant nutrition at crop and molecular levels. *Eur. J. Agron.* 116, 126069. doi: 10.1016/j.eja.2020.126069

Brockett, B. F., Prescott, C. E., and Grayston, S. J. (2012). Soil moisture is the major factor influencing microbial community structure and enzyme activities across seven biogeoclimatic zones in western Canada. *Soil Biol. Biochem.* 44, 9–20. doi: 10.1016/j.soilbio.2011.09.003

Brouder, S. M., and Volenec, J. J. (2008). Impact of climate change on crop nutrient and water use efficiencies. *Physiologia Plantarum* 133, 705–724. doi: 10.1111/j.1399-3054.2008.01136.x

Brown, P. H., Zhao, F.-J., and Dobermann, A. (2022). What is a plant nutrient? Changing definitions to advance science and innovation in plant nutrition. *Plant Soil* 476, 11–23. doi: 10.1007/s11104-021-05171-w

Cai, G., and Ahmed, M. A. (2022). The role of root hairs in water uptake: recent advances and future perspectives. *J. Exp. Bot.* 73, 3330–3338. doi: 10.1093/jxb/erac114

Carver, R. E., Nelson, N. O., Roozeboom, K. L., Kluitenberg, G. J., Tomlinson, P. J., Kang, Q., et al. (2022). Cover crop and phosphorus fertilizer management impacts on surface water quality from a no-till corn-soybean rotation. *J. Environ. Manage.* 301, 113818. doi: 10.1016/j.jenvman.2021.113818

Cen, R., Feng, W., Yang, F., Wu, W., Liao, H., and Qu, Z. (2021). Effect mechanism of biochar application on soil structure and organic matter in semi-arid areas. *J. Environ. Manage.* 286, 112198. doi: 10.1016/j.jenvman.2021.112198

Chen, W., Chen, Y., Siddique, K. H., and Li, S. (2022b). Root penetration ability and plant growth in agroecosystems. *Plant Physiol. Biochem.* 183, 160–168. doi: 10.1016/j.plaphy.2022.04.024

Chen, Y., Du, J., Li, Y., Tang, H., Yin, Z., Yang, L., et al. (2022c). Evolutions and managements of soil microbial community structure drove by continuous cropping. *Front. Microbiol.* 13, 839494. doi: 10.3389/fmicb.2022.839494

Chen, L., Halepoto, H., Liu, C., Kumari, N., Yan, X., Du, Q., et al. (2021b). Relationship analysis among apparel brand image, self-congruity, and consumers' purchase intention. *Sustainability* 13, 12770. doi: 10.3390/su132212770

Chen, C., Lv, Q., and Tang, Q. (2022a). Impact of bio-organic fertilizer and reduced chemical fertilizer application on physical and hydraulic properties of cucumber continuous cropping soil. *Biomass Conversion Biorefinery* 14, 921-930. doi: 10.1007/s13399-021-02294-z

Chen, J., Zhao, G., Wei, Y., Dong, Y., Hou, L., and Jiao, R. (2021a). Isolation and screening of multifunctional phosphate solubilizing bacteria and its growth-promoting effect on Chinese fir seedlings. *Sci. Rep.* 11, 9081. doi: 10.1038/s41598-021-88635-4

Chojnacka, K., and Moustakas, K. (2024). Anaerobic digestate management for carbon neutrality and fertilizer use: A review of current practices and future opportunities. *Biomass Bioenergy* 180, 106991. doi: 10.1016/j.biombioe.2023.106991

Das, S. K., Ghosh, G. K., Choudhury, B., Hazarika, S., and Mishra, V. (2024). Developing biochar and organic nutrient packages/technology as soil policy for enhancing yield and nutrient uptake in maize-black gram cropping system to maintain soil health. *Biomass Conversion Biorefinery* 14, 2515–2527. doi: 10.1007/s13399-022-02300-y

Das, P. P., Singh, K. R., Nagpure, G., Mansoori, A., Singh, R. P., Ghazi, I. A., et al. (2022). Plant-soil-microbes: A tripartite interaction for nutrient acquisition and better plant growth for sustainable agricultural practices. *Environ. Res.* 214, 113821. doi: 10.1016/j.envres.2022.113821

Dhaliwal, S. S., Sharma, V., and Shukla, A. K. (2022). Impact of micronutrients in mitigation of abiotic stresses in soils and plants—A progressive step toward crop security and nutritional quality. *Adv. Agron.* 173, 1–78. doi: 10.1016/bs.agron.2022.02.001

Dhaliwal, S. S., Singh, J., Taneja, P. K., and Mandal, A. (2020). Remediation techniques for removal of heavy metals from the soil contaminated through different sources: a review. *Environ. Sci. pollut. Res.* 27, 1319–1333. doi: 10.1007/s11356-019-06967-1

Dietz, K. J., Zörb, C., and Geilfus, C. M. (2021). Drought and crop yield. *Plant Biol.* 23, 881–893. doi: 10.1111/plb.13304

Dong, L., Zhang, W., Xiong, Y., Zou, J., Huang, Q., Xu, X., et al. (2022). Impact of short-term organic amendments incorporation on soil structure and hydrology in semiarid agricultural lands. *Int. Soil Water Conserv. Res.* 10, 457–469. doi: 10.1016/j.iswcr.2021.10.003

Dotaniya, M., and Meena, V. (2015). Rhizosphere effect on nutrient availability in soil and its uptake by plants: a review. *Proc. Natl. Acad. Sciences India Section B: Biol. Sci.* 85, 1–12. doi: 10.1007/s40011-013-0297-0

Elbasiouny, H., El-Ramady, H., Elbehiry, F., Rajput, V. D., Minkina, T., and Mandzhieva, S. (2022). Plant nutrition under climate change and soil carbon sequestration. *Sustainability* 14, 914. doi: 10.3390/su14020914

Fageria, N. K., and Moreira, A. (2011). The role of mineral nutrition on root growth of crop plants. *Adv. Agron.* 110, 251–331. doi: 10.1016/B978-0-12-385531-2.00004-9

Fan, S., Qin, J., Sun, H., Jia, Z., and Chen, Y. (2022). Alpine soil microbial community structure and diversity are largely influenced by moisture content in the Zoige wetland. *Int. J. Environ. Sci. Technol.* 19, 4369–4378. doi: 10.1007/s13762-021-03287-1

Fatima, S., Riaz, M., Al-Wabel, M. I., Arif, M. S., Yasmeen, T., Hussain, Q., et al. (2021). Higher biochar rate strongly reduced decomposition of soil organic matter to enhance C and N sequestration in nutrient-poor alkaline calcareous soil. *J. Soils Sediments* 21, 148–162. doi: 10.1007/s11368-020-02753-6

Gaikwad, K. B., Rani, S., Kumar, M., Gupta, V., Babu, P. H., Bainsla, N. K., et al. (2020). Enhancing the nutritional quality of major food crops through conventional and genomics-assisted breeding. *Front. Nutr.* 7, 533453. doi: 10.3389/fnut.2020.533453

Ganther, M., Lippold, E., Bienert, M. D., Bouffaud, M.-L., Bauer, M., Baumann, L., et al. (2022). Plant age and soil texture rather than the presence of root hairs cause differences in maize resource allocation and root gene expression in the field. *Plants* 11, 2883. doi: 10.3390/plants11212883

Gautam, V. K., Pande, C. B., Moharir, K. N., Varade, A. M., Rane, N. L., Egbueri, J. C., et al. (2023). Prediction of sodium hazard of irrigation purpose using artificial neural network modelling. *Sustainability* 15, 7593. doi: 10.3390/su15097593

Gong, X., Feng, Y., Dang, K., Jiang, Y., Qi, H., and Feng, B. (2023). Linkages of microbial community structure and root exudates: Evidence from microbial nitrogen limitation in soils of crop families. *Sci. Total Environ.* 881, 163536. doi: 10.1016/j.scitotenv.2023.163536

Govind, S. R., Jogaiah, S., Abdelrahman, M., Shetty, H. S., and Tran, L.-S. P. (2016). Exogenous trehalose treatment enhances the activities of defense-related enzymes and triggers resistance against downy mildew disease of pearl millet. *Front. Plant Sci.* 7, 1593. doi: 10.3389/fpls.2016.01593

Gregory, P. J., and Wojciechowski, T. (2020). Root systems of major tropical root and tuber crops: Root architecture, size, and growth and initiation of storage organs. *Adv. Agron.* 161, 1–25. doi: 10.1016/bs.agron.2020.01.001

Gu, X., Zhang, F., Xie, X., Cheng, Y., and Xu, X. (2023). Effects of N and P addition on nutrient and stoichiometry of rhizosphere and non-rhizosphere soils of alfalfa in alkaline soil. *Sci. Rep.* 13, 12119. doi: 10.1038/s41598-023-39030-8

Han, J., Xin, Z., Han, F., Xu, B., Wang, L., Zhang, C., et al. (2021). Source contribution analysis of nutrient pollution in a P-rich watershed: Implications for integrated water quality management. *Environ. pollut.* 279, 116885. doi: 10.1016/j.envpol.2021.116885

Harindintwali, J. D., Zhou, J., and Yu, X. (2020). Lignocellulosic crop residue composting by cellulolytic nitrogen-fixing bacteria: a novel tool for environmental sustainability. *Sci. Total Environ.* 715, 136912. doi: 10.1016/j.scitotenv.2020.136912

Hartmann, M., and Six, J. (2023). Soil structure and microbiome functions in agroecosystems. *Nat. Rev. Earth Environ.* 4, 4–18. doi: 10.1038/s43017-022-00366-w

He, P., Zhang, M., Zhang, Y., Wu, H., and Zhang, X. (2023). Effects of selenium enrichment on dough fermentation characteristics of Baker's Yeast. *Foods* 12, 2343. doi: 10.3390/foods12122343

Helman, D., and Bonfil, D. J. (2022). Six decades of warming and drought in the world's top wheat-producing countries offset the benefits of rising CO2 to yield. *Sci. Rep.* 12, 7921. doi: 10.1038/s41598-022-11423-1

Hong, J., Xu, F., Chen, G., Huang, X., Wang, S., Du, L., et al. (2022). Evaluation of the effects of nitrogen, phosphorus, and potassium applications on the growth, yield, and quality of lettuce (Lactuca sativa L.). *Agronomy* 12, 2477. doi: 10.3390/agronomy12102477

Hopmans, J. W., Qureshi, A., Kisekka, I., Munns, R., Grattan, S., Rengasamy, P., et al. (2021). Critical knowledge gaps and research priorities in global soil salinity. *Adv. Agron.* 169, 1–191. doi: 10.1016/bs.agron.2021.03.001

Huang, J., and Hartemink, A. E. (2020). Soil and environmental issues in sandy soils. *Earth-Science Rev.* 208, 103295. doi: 10.1016/j.earscirev.2020.103295

Iqbal, A., Liang, H., Mcbride, S. G., Yuan, P., Ali, I., Zaman, M., et al. (2022). Manure applications combined with chemical fertilizer improves soil functionality, microbial biomass and rice production in a paddy field. *Agron. J.* 114, 1431–1446. doi: 10.1002/agj2.v114.2

Jin, N., He, J., Fang, Q., Chen, C., Ren, Q., He, L., et al. (2020). The responses of maize yield and water use to growth stage-based irrigation on the loess plateau in China. *Int. J. Plant Production* 14, 621–633. doi: 10.1007/s42106-020-00105-5

Justes, E., Bedoussac, L., Dordas, C., Frak, E., Louarn, G., Boudsocq, S., et al. (2021). The 4C approach as a way to understand species interactions determining intercropping productivity. *Front. Agric. Sci. Eng.* 8, 3.

Kang, S., Hao, X., Du, T., Tong, L., Su, X., Lu, H., et al. (2017). Improving agricultural water productivity to ensure food security in China under changing environment: From research to practice. *Agric. Water Manage.* 179, 5–17. doi: 10.1016/j.agwat.2016.05.007

Kang, J., Hao, X., Zhou, H., and Ding, R. (2021). An integrated strategy for improving water use efficiency by understanding physiological mechanisms of crops responding to water deficit: Present and prospect. *Agric. Water Manage.* 255, 107008. doi: 10.1016/j.agwat.2021.107008

Kaur, H., Kaur, H., Kaur, H., and Srivastava, S. (2023). The beneficial roles of trace and ultratrace elements in plants. *Plant Growth Regul.* 100, 219–236. doi: 10.1007/s10725-022-00837-6

Krouk, G., and Kiba, T. (2020). Nitrogen and phosphorus interactions in plants: from agronomic to physiological and molecular insights. *Curr. Opin. Plant Biol.* 57, 104–109. doi: 10.1016/j.pbi.2020.07.002

Ladha, J. K., Jat, M. L., Stirling, C. M., Chakraborty, D., Pradhan, P., Krupnik, T. J., et al. (2020). Achieving the sustainable development goals in agriculture: The crucial role of nitrogen in cereal-based systems. *Adv. Agron.* 163, 39–116. doi: 10.1016/bs.agron.2020.05.006

Laghari, M., Naidu, R., Xiao, B., Hu, Z., Mirjat, M. S., Hu, M., et al. (2016). Recent developments in biochar as an effective tool for agricultural soil management: a review. *J. Sci. Food Agric.* 96, 4840–4849. doi: 10.1002/jsfa.2016.96.issue-15

Lang, Z., Yan, S., and Zhu, Q. (2023). Water retention and sustained release of magnesium-based biochar modified hydrogel composite materials. *J. Environ. Chem. Eng.* 11, 111380. doi: 10.1016/j.jece.2023.111380

Li, H., Li, J., Jiao, X., Jiang, H., Liu, Y., Wang, X., et al. (2024). The fate and challenges of the main nutrients in returned straw: A basic review. *Agronomy* 14, 698. doi: 10.3390/agronomy14040698

Li, H., Liu, H., Gong, X., Li, S., Pang, J., Chen, Z., et al. (2021a). Optimizing irrigation and nitrogen management strategy to trade off yield, crop water productivity, nitrogen use efficiency and fruit quality of greenhouse grown tomato. *Agric. Water Manage.* 245, 106570. doi: 10.1016/j.agwat.2020.106570

Li, H., Mei, X., Wang, J., Huang, F., Hao, W., and Li, B. (2021b). Drip fertigation significantly increased crop yield, water productivity and nitrogen use efficiency with respect to traditional irrigation and fertilization practices: A meta-analysis in China. *Agric. Water Manage.* 244, 106534. doi: 10.1016/j.agwat.2020.106534

Li, D., Qu, C., Cheng, X., Chen, Y., Yan, H., and Wu, Q. (2023a). Effect of different fertilization strategies on the yield, quality of Euryales Semen and soil microbial community. *Front. Microbiol.* 14, 1310366. doi: 10.3389/fmicb.2023.1310366

Li, J., Yang, X., Zhang, M., Li, D., Jiang, Y., Yao, W., et al. (2023b). Yield, quality, and water and fertilizer partial productivity of cucumber as influenced by the interaction of water, nitrogen, and magnesium. *Agronomy* 13, 772. doi: 10.3390/agronomy13030772

Liang, X., Jin, X., Liu, J., Yin, Y., Gu, Z., Zhang, J., et al. (2023). Formation mechanism and sustainable productivity impacts of non-grain croplands: Evidence from Sichuan Province, China. *Land Degradation Dev.* 34, 1120–1132. doi: 10.1002/ldr.v34.4

Lin, S., Wang, Q., Wei, K., Sun, Y., Shao, F., Lei, Q., et al. (2024). Enhancing pakchoi (Brassica chinensis L.) agriculture with magnetized-ionized brackish water and organic fertilizers: A sustainable approach to soil quality and crop yield optimization. *J. Cleaner Production* 450, 141935. doi: 10.1016/j.jclepro.2024.141935

Lin, Z., Wang, X., Wu, X., Liu, D., Yin, Y., Zhang, Y., et al. (2018). Nitrate reduced arsenic redox transformation and transfer in flooded paddy soil-rice system. *Environ. pollut.* 243, 1015–1025. doi: 10.1016/j.envpol.2018.09.054

Liu, C., Chen, F., Li, Z., Cocq, K. L., Liu, Y., and Wu, L. (2021a). Impacts of nitrogen practices on yield, grain quality, and nitrogen-use efficiency of crops and soil fertility in three paddy-upland cropping systems. *J. Sci. Food Agric.* 101, 2218–2226. doi: 10.1002/jsfa.v101.6

Liu, J., Shu, A., Song, W., Shi, W., Li, M., Zhang, W., et al. (2021b). Long-term organic fertilizer substitution increases rice yield by improving soil properties and regulating soil bacteria. *Geoderma* 404, 115287. doi: 10.1016/j.geoderma.2021.115287

Lobell, D. B., Azzari, G., Burke, M., Gourlay, S., Jin, Z., Kilic, T., et al. (2020). Eyes in the sky, boots on the ground: Assessing satellite-and ground-based approaches to crop yield measurement and analysis. *Am. J. Agric. Economics* 102, 202–219. doi: 10.1093/ajae/aaz051

López-Pérez, M. C., Pérez-Labrada, F., Ramírez-Pérez, L. J., Juárez-Maldonado, A., Morales-Díaz, A. B., González-Morales, S., et al. (2018). Dynamic modeling of silicon bioavailability, uptake, transport, and accumulation: applicability in improving the nutritional quality of tomato. *Front. Plant Sci.* 9, 647. doi: 10.3389/fpls.2018.00647

Lyu, H., Li, Y., Wang, Y., Wang, P., Shang, Y., Yang, X., et al. (2024). Drive soil nitrogen transformation and improve crop nitrogen absorption and utilization-a review of green manure applications. *Front. Plant Sci.* 14, 1305600. doi: 10.3389/fpls.2023.1305600

Maharajan, T., Ceasar, S. A., Krishna, T. P. A., and Ignacimuthu, S. (2021). Management of phosphorus nutrient amid climate change for sustainable agriculture. *J. Environ. Qual.* 50, 1303–1324. doi: 10.1002/jeq2.20292

Malhi, G. S., Kaur, M., and Kaushik, P. (2021). Impact of climate change on agriculture and its mitigation strategies: A review. *Sustainability* 13, 1318. doi: 10.3390/su13031318

Meychik, N., Nikolaeva, Y., and Kushunina, M. (2021). The significance of ion-exchange properties of plant root cell walls for nutrient and water uptake by plants. *Plant Physiol. Biochem.* 166, 140–147. doi: 10.1016/j.plaphy.2021.05.048

Milošević, T., and Milošević, N. (2020). Soil fertility: Plant nutrition vis-à-vis fruit yield and quality of stone fruits. *Fruit Crops* 41, 583–606. doi: 10.1016/B978-0-12-818732-6.00041-1

Mitra, D., Mondal, R., Khoshru, B., Senapati, A., Radha, T., Mahakur, B., et al. (2022). Actinobacteria-enhanced plant growth, nutrient acquisition, and crop protection: Advances in soil, plant, and microbial multifactorial interactions. *Pedosphere* 32, 149–170. doi: 10.1016/S1002-0160(21)60042-5

Morales, F., Ancín, M., Fakhet, D., González-Torralba, J., Gámez, A. L., Seminario, A., et al. (2020). Photosynthetic metabolism under stressful growth conditions as a bases for crop breeding and yield improvement. *Plants* 9, 88. doi: 10.3390/plants9010088

Ňancucheo, I., Rowe, O. F., Hedrich, S., and Johnson, D. B. (2016). Solid and liquid media for isolating and cultivating acidophilic and acid-tolerant sulfate-reducing bacteria. *FEMS Microbiol. Lett.* 363, fnw083. doi: 10.1093/femsle/fnw083

Narayan, O. P., Kumar, P., Yadav, B., Dua, M., and Johri, A. K. (2023). Sulfur nutrition and its role in plant growth and development. *Plant Signaling Behav.* 18, 2030082. doi: 10.1080/15592324.2022.2030082

Niu, J., Liu, C., Huang, M., Liu, K., and Yan, D. (2021). Effects of foliar fertilization: a review of current status and future perspectives. *J. Soil Sci. Plant Nutr.* 21, 104–118. doi: 10.1007/s42729-020-00346-3

Padilla, F. M., Farneselli, M., Gianquinto, G., Tei, F., and Thompson, R. B. (2020). Monitoring nitrogen status of vegetable crops and soils for optimal nitrogen management. *Agric. Water Manage.* 241, 106356. doi: 10.1016/j.agwat.2020.106356

Palansooriya, K. N., Dissanayake, P. D., Igalavithana, A. D., Tang, R., Cai, Y., and Chang, S. X. (2023). Converting food waste into soil amendments for improving soil sustainability and crop productivity: A review. *Sci. Total Environ.* 881, 163311. doi: 10.1016/j.scitotenv.2023.163311

Panigrahi, N., Thompson, A. J., Zubelzu, S., and Knox, J. W. (2021). Identifying opportunities to improve management of water stress in banana production. *Scientia Hortic.* 276, 109735. doi: 10.1016/j.scienta.2020.109735

Peng, Y., Fei, L., Liu, X., Sun, G., Hao, K., Cui, N., et al. (2023). Coupling of regulated deficit irrigation at maturity stage and moderate fertilization to improve soil quality, mango yield and water-fertilizer use efficiency. *Scientia Hortic.* 307, 111492. doi: 10.1016/j.scienta.2022.111492

Philippot, L., Chenu, C., Kappler, A., Rillig, M. C., and Fierer, N. (2024). The interplay between microbial communities and soil properties. *Nat. Rev. Microbiol.* 22, 226–239. doi: 10.1038/s41579-023-00980-5

Qin, G., Niu, Z., Yu, J., Li, Z., Ma, J., and Xiang, P. (2021). Soil heavy metal pollution and food safety in China: Effects, sources and removing technology. *Chemosphere* 267, 129205. doi: 10.1016/j.chemosphere.2020.129205

Ren, M., Li, C., Gao, X., Niu, H., Cai, Y., Wen, H., et al. (2023). High nutrients surplus led to deep soil nitrate accumulation and acidification after cropland conversion to apple orchards on the Loess Plateau, China. *Agriculture Ecosyst. Environ.* 351, 108482. doi: 10.1016/j.agee.2023.108482

Rivera-Uria, Y., Solleiro-Rebolledo, E., Beltrán-Paz, O., Martínez-Jardines, G., Nava-Arsola, E., Vázquez-Zacamitzin, G., et al. (2024). Short-term response on microstructure and soil organic matter characteristics after fertilization change in an Andic Anthrosol. *Soil Tillage Res.* 241, 106110. doi: 10.1016/j.still.2024.106110

Rivier, P.-A., Jamniczky, D., Nemes, A., Makó, A., Barna, G., Uzinger, N., et al. (2022). Short-term effects of compost amendments to soil on soil structure, hydraulic properties, and water regime. *J. Hydrology Hydromechanics* 70, 74–88. doi: 10.2478/johh-2022-0004

Russo, D., Laufer, A., and Bar-Tal, A. (2020). Improving water uptake by trees planted on a clayey soil and irrigated with low-quality water by various management means: A numerical study. *Agric. Water Manage.* 229, 105891. doi: 10.1016/j.agwat.2019.105891

Sabir, M. S., Shahzadi, F., Ali, F., Shakeela, Q., Niaz, Z., and Ahmed, S. (2021). Comparative effect of fertilization practices on soil microbial diversity and activity: an overview. *Curr. Microbiol.* 78, 3644–3655. doi: 10.1007/s00284-021-02634-2

Sáez, A., Aizen, M. A., Medici, S., Viel, M., Villalobos, E., and Negri, P. (2020). Bees increase crop yield in an alleged pollinator-independent almond variety. *Sci. Rep.* 10, 3177. doi: 10.1038/s41598-020-59995-0

Sardans, J., and Peñuelas, J. (2021). Potassium control of plant functions: Ecological and agricultural implications. *Plants* 10, 419. doi: 10.3390/plants10020419

Schneider, H. M., and Lynch, J. P. (2020). Should root plasticity be a crop breeding target? *Front. Plant Sci.* 11, 534260. doi: 10.3389/fpls.2020.00546

Shu, X., He, J., Zhou, Z., Xia, L., Hu, Y., Zhang, Y., et al. (2022). Organic amendments enhance soil microbial diversity, microbial functionality and crop yields: A meta-analysis. *Sci. Total Environ.* 829, 154627. doi: 10.1016/j.scitotenv.2022.154627

Singh, V. K., Gautam, P., Nanda, G., Dhaliwal, S. S., Pramanick, B., Meena, S. S., et al. (2021). Soil test based fertilizer application improves productivity, profitability and nutrient use efficiency of rice (Oryza sativa L.) under direct seeded condition. *Agronomy* 11, 1756.

Sokol, N. W., Sanderman, J., and Bradford, M. A. (2019). Pathways of mineral-associated soil organic matter formation: Integrating the role of plant carbon source, chemistry, and point of entry. *Global Change Biol.* 25, 12–24. doi: 10.1111/gcb.2019.25.issue-1

Stirbet, A., Lazár, D., Guo, Y., and Govindjee, G. (2020). Photosynthesis: basics, history and modelling. *Ann. Bot.* 126, 511–537. doi: 10.1093/aob/mcz171

Sun, G., Hu, T., Liu, X., Peng, Y., Leng, X., Li, Y., et al. (2022). Optimizing irrigation and fertilization at various growth stages to improve mango yield, fruit quality and water-fertilizer use efficiency in xerothermic regions. *Agric. Water Manage.* 260, 107296. doi: 10.1016/j.agwat.2021.107296

Suzuki, K., Kashiwa, N., Nomura, K., Asiloglu, R., and Harada, N. (2021). Impacts of application of calcium cyanamide and the consequent increase in soil pH on N 2 O

emissions and soil bacterial community compositions. *Biol. Fertility Soils* 57, 269–279. doi: 10.1007/s00374-020-01523-3

Thakur, A. K., Mandal, K. G., and Raychaudhuri, S. (2020). Impact of crop and nutrient management on crop growth and yield, nutrient uptake and content in rice. *Paddy Water Environ.* 18, 139–151. doi: 10.1007/s10333-019-00770-x

Tianqian, Z., Junli, W., Yuting, W., Xiaoru, F., Yuan, L., Huan, Z., et al. (2024). Mechanisms of cadmium absorption in Suaeda heteroptera roots. *Environ. Chem. Ecotoxicology* 6, 164-170. doi: 10.1016/j.enceco.2024.05.005

Toksha, B., Sonawale, V. A. M., Vanarase, A., Bornare, D., Tonde, S., Hazra, C., et al. (2021). Nanofertilizers: A review on synthesis and impact of their use on crop yield and environment. *Environ. Technol. Innovation* 24, 101986. doi: 10.1016/j.eti.2021.101986

Tripathi, R., Tewari, R., Singh, K., Keswani, C., Minkina, T., Srivastava, A. K., et al. (2022). Plant mineral nutrition and disease resistance: A significant linkage for sustainable crop protection. *Front. Plant Sci.* 13, 883970. doi: 10.3389/fpls.2022.883970

Usharani, K., Roopashree, K., and Naik, D. (2019). Role of soil physical, chemical and biological properties for soil health improvement and sustainable agriculture. *J. Pharmacognosy Phytochem.* 8, 1256–1267.

Uwituze, Y., Nyiraneza, J., Fraser, T. D., Dessureaut-Rompré, J., Ziadi, N., and Lafond, J. (2022). Carbon, nitrogen, phosphorus, and extracellular soil enzyme responses to different land use. *Front. Soil Sci.* 2, 814554. doi: 10.3389/fsoil.2022.814554

Van Der Bom, F. J., Williams, A., Raymond, N. S., Alahmad, S., Hickey, L. T., Singh, V., et al. (2023). Root angle, phosphorus, and water: Interactions and effects on durum wheat genotype performance in drought-prone environments. *Plant Soil* 500, 69-89. doi: 10.1007/s11104-023-05966-z

Vetterlein, D., Phalempin, M., Lippold, E., Schlüter, S., Schreiter, S., Ahmed, M. A., et al. (2022). Root hairs matter at field scale for maize shoot growth and nutrient uptake, but root trait plasticity is primarily triggered by texture and drought. *Plant Soil* 478, 119–141. doi: 10.1007/s11104-022-05434-0

Wagg, C., Hann, S., Kupriyanovich, Y., and Li, S. (2021). Timing of short period water stress determines potato plant growth, yield and tuber quality. *Agric. Water Manage.* 247, 106731. doi: 10.1016/j.agwat.2020.106731

Wang, X. (2022). Managing land carrying capacity: Key to achieving sustainable production systems for food security. *Land* 11, 484. doi: 10.3390/land11040484

Wang, X., Fan, J., Xing, Y., Xu, G., Wang, H., Deng, J., et al. (2019b). The effects of mulch and nitrogen fertilizer on the soil environment of crop plants. *Adv. Agron.* 153, 121–173. doi: 10.1016/bs.agron.2018.08.003

Wang, H., He, Y., Zheng, Q., Yang, Q., Wang, J., Zhu, J., et al. (2024). Toxicity of photoaged polyvinyl chloride microplastics to wheat seedling roots. *J. Hazardous Materials* 463, 132816. doi: 10.1016/j.jhazmat.2023.132816

Wang, Y., Zhang, G., Wang, H., Cheng, Y., Liu, H., Jiang, Z., et al. (2021). Effects of different dissolved organic matter on microbial communities and arsenic mobilization in aquifers. *J. Hazardous Materials* 411, 125146. doi: 10.1016/j.jhazmat.2021.125146

Wang, C.-Y., Zhou, X., Guo, D., Zhao, J.-H., Yan, L., Feng, G.-Z., et al. (2019a). Soil pH is the primary factor driving the distribution and function of microorganisms in farmland soils in northeastern China. *Ann. Microbiol.* 69, 1461–1473. doi: 10.1007/s13213-019-01529-9

Waraich, E. A., Ahmad, R., Ashraf, M. Y., Saifullah,, and Ahmad, M. (2011). Improving agricultural water use efficiency by nutrient management in crop plants. *Acta Agriculturae Scandinavica Section B-Soil Plant Sci.* 61, 291–304. doi: 10.1080/09064710.2010.491954

Wei, Q., Xu, J., Liu, Y., Wang, D., Chen, S., Qian, W., et al. (2024). Nitrogen losses from soil as affected by water and fertilizer management under drip irrigation: Development, hotspots and future perspectives. *Agric. Water Manage.* 296, 108791. doi: 10.1016/j.agwat.2024.108791

Wei, W., Yan, Y., Cao, J., Christie, P., Zhang, F., and Fan, M. (2016). Effects of combined application of organic amendments and fertilizers on crop yield and soil organic matter: An integrated analysis of long-term experiments. *Agriculture Ecosyst. Environ.* 225, 86–92. doi: 10.1016/j.agee.2016.04.004

Wu, Y., Chen, D., Saleem, M., Wang, B., Hu, S., Delgado-Baquerizo, M., et al. (2021). Rare soil microbial taxa regulate the negative effects of land degradation drivers on soil organic matter decomposition. *J. Appl. Ecol.* 58, 1658–1669. doi: 10.1111/1365-2664.13935

Xiao, E., Ning, Z., Xiao, T., Sun, W., and Jiang, S. (2021). Soil bacterial community functions and distribution after mining disturbance. *Soil Biol. Biochem.* 157, 108232. doi: 10.1016/j.soilbio.2021.108232

Xing, Y., and Wang, X. (2024a). Impact of agricultural activities on climate change: A review of greenhouse gas emission patterns in field crop systems. *Plants* 13, 2285. doi: 10.3390/plants13162285

Xing, Y., and Wang, X.. (2024b). Precision agriculture and water conservation strategies for sustainable crop production in Arid Regions[J]. *Plants* 13 (22), 3184. doi: 10.3390/plants13223184

Xing, Y., Zhang, X., and Wang, X.. (2024). Enhancing soil health and crop yields through water-fertilizer coupling technology. *Front. Sustain. Food Syst.* 8, 1494819. doi: 10.3389/fsufs.2024.1494819

Xu, Y., Ren, S., Liang, Y., Du, A., Li, C., Wang, Z., et al. (2021). Soil nutrient supply and tree species drive changes in soil microbial communities during the transformation of a multi-generation Eucalyptus plantation. *Appl. Soil Ecol.* 166, 103991. doi: 10.1016/j.apsoil.2021.103991

Xu, Z., Yu, G., Zhang, X., Ge, J., He, N., Wang, Q., et al. (2015). The variations in soil microbial communities, enzyme activities and their relationships with soil organic matter decomposition along the northern slope of Changbai Mountain. *Appl. Soil Ecol.* 86, 19–29. doi: 10.1016/j.apsoil.2014.09.015

Xu, X., Zhang, X., Liu, C., Qin, H., Sun, F., Liu, J., et al. (2023). Appropriate increasing potassium supply alleviates the inhibition of high nitrogen on root growth by regulating antioxidant system, hormone balance, carbon assimilation and transportation in apple. *Scientia Hortic.* 311, 111828. doi: 10.1016/j.scienta.2023.111828

Xue, P., Fu, Q., Li, T., Liu, D., Hou, R., Li, Q., et al. (2022). Effects of biochar and straw application on the soil structure and water-holding and gas transport capacities in seasonally frozen soil areas. *J. Environ. Manage.* 301, 113943. doi: 10.1016/j.jenvman.2021.113943

Yahaya, S. M., Mahmud, A. A., Abdullahi, M., and Haruna, A. (2023). Recent advances in the chemistry of nitrogen, phosphorus and potassium as fertilizers in soil: a review. *Pedosphere* 33, 385–406. doi: 10.1016/j.pedsph.2022.07.012

Yan, X., Muneer, M. A., Qin, M., Ou, J., Chen, X., He, Z., et al. (2024). Establishing quality evaluation standards for pomelo fruit: The role of harvesting time and appearance characteristic. *Postharvest Biol. Technol.* 212, 112863. doi: 10.1016/j.postharvbio.2024.112863

Ye, L., Camps-Arbestain, M., Shen, Q., Lehmann, J., Singh, B., and Sabir, M. (2020). Biochar effects on crop yields with and without fertilizer: A meta-analysis of field studies using separate controls. *Soil Use Manage.* 36, 2–18. doi: 10.1111/sum.12546

Yu, X., Schweikert, K., Li, Y., Ma, J., and Doluschitz, R. (2023). Farm size, farmers' perceptions and chemical fertilizer overuse in grain production: Evidence from maize farmers in northern China. *J. Environ. Manage.* 325, 116347. doi: 10.1016/j.jenvman.2022.116347

Yun, Z., Gao, H., and Jiang, Y. (2022). Insights into metabolomics in quality attributes of postharvest fruit. *Curr. Opin. Food Sci.* 45, 100836. doi: 10.1016/j.cofs.2022.100836

Zhang, P., Chen, X., Wei, T., Yang, Z., Jia, Z., Yang, B., et al. (2016). Effects of straw incorporation on the soil nutrient contents, enzyme activities, and crop yield in a semiarid region of China. *Soil Tillage Res.* 160, 65–72. doi: 10.1016/j.still.2016.02.006

Zhang, F., Cui, Z., Fan, M., Zhang, W., Chen, X., and Jiang, R. (2011). Integrated soil–crop system management: reducing environmental risk while increasing crop productivity and improving nutrient use efficiency in China. *J. Environ. Qual.* 40, 1051–1057. doi: 10.2134/jeq2010.0292

Zhang, X., Dong, W., Dai, X., Schaeffer, S., Yang, F., Radosevich, M., et al. (2015). Responses of absolute and specific soil enzyme activities to long term additions of organic and mineral fertilizer. *Sci. Total Environ.* 536, 59–67. doi: 10.1016/j.scitotenv.2015.07.043

Zhang, Y., Gao, M., Yu, C., Zhang, H., Yan, N., Wu, Q., et al. (2022). Soil nutrients, enzyme activities, and microbial communities differ among biocrust types and soil layers in a degraded karst ecosystem. *CATENA* 212, 106057. doi: 10.1016/j.catena.2022.106057

Zhang, P., Guo, Z., Ullah, S., Melagraki, G., Afantitis, A., and Lynch, I. (2021b). Nanotechnology and artificial intelligence to enable sustainable and precision agriculture. *Nat. Plants* 7, 864–876. doi: 10.1038/s41477-021-00946-6

Zhang, G., Mo, F., Shah, F., Meng, W., Liao, Y., and Han, J. (2021a). Ridge-furrow configuration significantly improves soil water availability, crop water use efficiency, and grain yield in dryland agroecosystems of the Loess Plateau. *Agric. Water Manage.* 245, 106657. doi: 10.1016/j.agwat.2020.106657

Zhang, X., Qu, J., Li, H., La, S., Tian, Y., and Gao, L. (2020). Biochar addition combined with daily fertigation improves overall soil quality and enhances water-fertilizer productivity of cucumber in alkaline soils of a semi-arid region. *Geoderma* 363, 114170. doi: 10.1016/j.geoderma.2019.114170

Zhang, H., Zhang, J., and Yang, J. (2023). Improving nitrogen use efficiency of rice crop through an optimized root system and agronomic practices. *Crop Environ.* 2(4), 192-201. doi: 10.1016/j.crope.2023.10.001

Zhou, H., Xia, D., and He, Y. (2020). Rice grain quality—traditional traits for high quality rice and health-plus substances. *Mol. Breed.* 40, 1–17. doi: 10.1007/s11032-019-1080-6

Frontiers in
Plant Science

Cultivates the science of plant biology and its applications

The most cited plant science journal, which advances our understanding of plant biology for sustainable food security, functional ecosystems and human health.

Discover the latest Research Topics

See more →

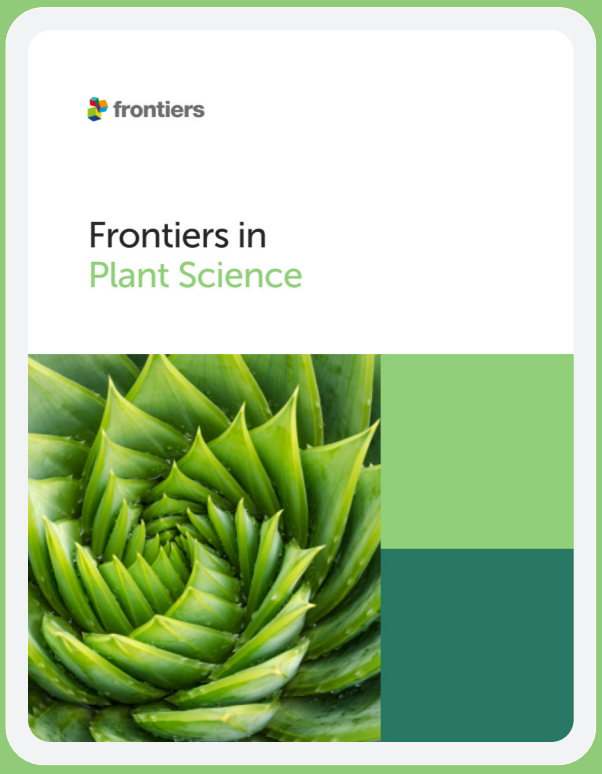

Frontiers

Avenue du Tribunal-Fédéral 34
1005 Lausanne, Switzerland
frontiersin.org

Contact us

+41 (0)21 510 17 00
frontiersin.org/about/contact